Bone Research Protocols

Edited by

Miep H. Helfrich, PhD
Stuart H. Ralston, MD

HUMANA PRESS

1

Human Osteoblast Culture

James A. Gallagher

1. Introduction

Osteoblasts are the cells responsible for the formation of bone; they synthesize almost all of the constituents of the bone matrix and direct its subsequent mineralization. Once a phase of active bone formation is completed the osteoblasts do not become senescent but instead redifferentiate into one of two other cell types: osteocytes and bone lining cells, both of which play a major role in the regulation of calcium homeostasis and bone remodeling.

Researchers have endeavored to culture osteoblasts from human bone for several reasons:

1. To investigate the biochemistry and physiology of bone formation.
2. To investigate the molecular and cellular basis of human bone disease.
3. To investigate the role of cells of the osteoblastic lineage in regulating bone resorption.
4. To screen for potential therapeutic agents.
5. To develop and test new biomaterials.
6. To use cell therapy in tissue engineering and bone transplantation.

The structure of bone tissue, the heterogeneity of cell types, the cross-linked extracellular matrix, and the mineral phase combine to make bone a difficult tissue from which to extract cells. Consequently, early attempts to culture osteoblasts avoided human tissue and instead relied on enzymatic digestion of poorly mineralized fetal or neonatal tissue from experimental animals. The first attempt to isolate cells from adult human bone, using demineralization and collagenase digestion, was reported by Bard and co-workers *(1)*. The cultured cells were low in alkaline phosphatase and collagen synthesis, which were then regarded as the best

markers of the osteoblastic phenotype. Although the cells remained viable for up to 2 wk they did not proliferate, and it was concluded that osteocytes were the predominant cell type present. Mills et al. used the alternative approach of explant culture and were successful in culturing cell populations that included parathyroid hormone (PTH) responsive and alkaline phosphatase positive cells *(2)*.

The first successful attempts to isolate large numbers of cells that expressed an osteoblastic phenotype from human bone were undertaken in Graham Russell's laboratory at the University of Sheffield in the early 1980s. The defining characteristics of these studies were (1) the use of explant cultures, which avoided the need for digestion of the tissue and (2) the availability of an appropriate phenotypic marker. Successful culture of any cell type can be achieved only if there is a specific marker of the phenotype that can be used to confirm the identity of the cells in vitro. In this case, the marker was the then recently discovered bone gla protein as measured by a radioimmunoassay developed by Jim Poser *(3,4)*. Nearly 20 yr later, bone gla protein, now known as osteocalcin, undoubtedly remains the most specific marker of the osteoblastic phenotype.

Although this culture system has been extensively modified by several groups of researchers (*see* **Note 1**), the vast majority of published reports on isolation of human osteoblasts still essentially use this simple but highly reproducible explant technique. This technique and its modifications have been described, compared, and reviewed elsewhere *(5,6)*. The aim of this chapter is to describe the basic methodology that is used in the author's laboratory. This is shown schematically in **Fig 1**. The nomenclature used by various research groups to describe the isolated cells includes "human bone cells," "human osteoblasts in vitro," "human osteoblastic cells," and "HOBS." We have preferred the conservative term "human bone derived cells" (HBDCs), and this is used throughout this chapter.

HBDCs have been widely used to investigate the biology of the human osteoblast, and their use has facilitated several major developments in our understanding of the hormonal regulation of human bone remodeling. These cells have also been used to investigate the cellular and molecular pathology of bone disease. The major milestones in the culture of human osteoblasts are summarized in **Table 1**. **Figure 2** shows the increase in the application of human osteoblast cultures since the initial reports in 1984.

Human bone cell culture is now becoming an important tool in tissue engineering to test the biocompatibility and osteogenicity of novel biomaterials and also for autologous transplantation of osteoblastic populations expanded in vitro.
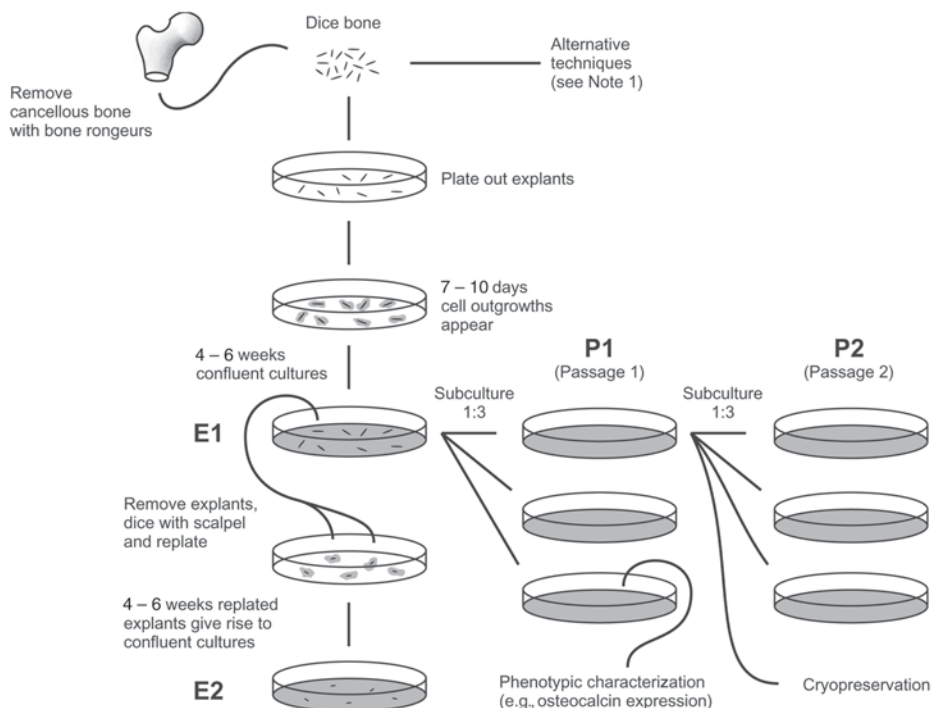
Fig. 1. Technique used to isolate cells expressing osteoblastic characteristics (HBDCs) from explanted cancellous bone. E1, explant 1; E2, explant 2.

2. Materials
2.1. Tissue-Culture Media and Supplements

1. Phosphate-buffered saline (PBS) without calcium and magnesium, pH 7.4 (Invitrogen).
2. Dulbecco's modification of minimum essential medium (DMEM) (Invitrogen) supplemented to a final concentration of 10% with fetal calf serum (FCS), 2 mM L-glutamine, 50 U/mL of penicillin, 50 μg/mL streptomycin. Freshly prepared 50 μg/mL of L-ascorbic acid should be added to cultures in which matrix synthesis or mineralization is being investigated (*see* **Note 2**).
3. Serum-free DMEM (SFM).
4. FCS (*see* **Note 3**).
5. Tissue culture flasks (75 cm^2) or Petri dishes (100-mm diameter) (*see* **Note 4**).

2.2. Preparation of Explants

1. Bone rongeurs from any surgical instrument supplier.
2. Solid stainless steel scalpels with integral handles (BDH Merck).

Table 1
Phenotypic Milestones in the Culture and Characterization
of Osteoblastic Cells (HBCDs) from Human Bone

Isolation of viable cells from human bone	Bard et al., 1972 *(1)*
Introduction of explant culture	Mills et al., 1979 *(2)*
Production of osteocalcin	Gallagher et al., 1984 *(3)*
	Beresford et al., 1984a *(4)*
High alkaline phosphatase activity	Gallagher et al., 1984 *(3)*
	Beresford et al., 1984 *(4)*
	Gehron-Robey and Termine 1985 *(7)*
	Auf'molk et al., 1985 *(8)*
Responsiveness to PTH	Beresford et al., 1984 *(4)*
	MacDonald et al., 1984 *(9)*
	Gehron-Robey and Termine 1985 *(7)*
	Auf'mkolk et al., 1985 *(8)*
	MacDonald et al., 1986 *(10)*
Synthesis of type I but not type III collagen	Beresford et al., 1986 *(11)*
Synthesis of other bone matrix proteins	Gehron-Robey and Termine 1985 *(7)*
	Fedarko et al., 1992 *(12)*
Response to cytokines	Beresford et al., 1984 *(13)*
	Gowen et al., 1985 *(14)*
Response to oestrogen	Vaishnav et al., 1984 *(15)*
	Eriksen et al 1988 *(16)*
Expression of purinoceptors	Schoefl et al., 1992 *(17)*
	Bowler et al., 1995 *(18)*
Production of nitric oxide	Ralston et al., 1994 *(19)*
Investigation of specific pathologies	Marie et al., 1988 *(20)*
	Walsh et al., 1995 *(21)*
Formation of mineralised nodules	Beresford et al., 1993 *(22)*
Formation of bone in vitro and in vivo	Gundle et al., 1995 *(23)*

2.3. Passaging and Secondary Culture

1. Trypsin–EDTA solution: 0.05% Trypsin and 0.02% EDTA in Ca^{2+}- and Mg^{2+}-free Hanks' balanced salt solution, pH 7.4 (Invitrogen).
2. 0.4% Trypan blue in 0.85% NaC1 (Sigma Aldrich).
3. 70-µm "Cell Strainer" (Becton Dickinson).
4. Neubauer hemocytometer (BDH Merck).
5. Collagenase (Sigma type VII from *Clostridium histolyticum*).
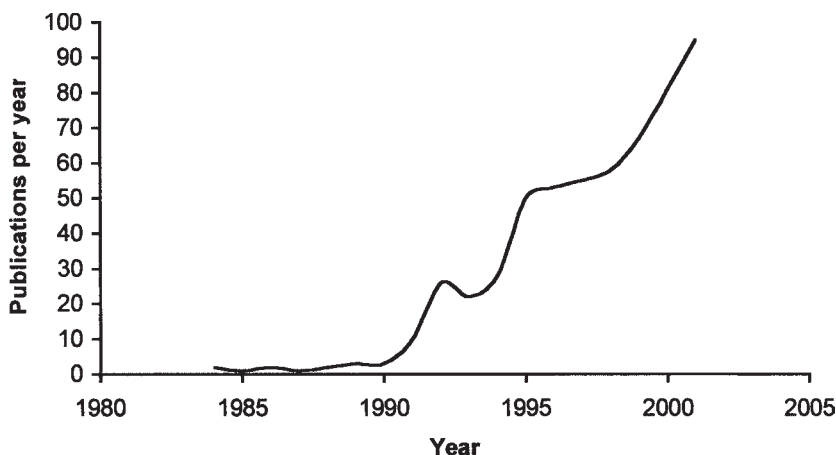6. DNase I (Sigma Aldrich).

Fig. 2. Graph showing the increase in the application of human osteoblast cultures since the initial reports in 1984.

2.4. Phenotypic Characterization

1. 1,25-Dihydroxyvitamin D_3 [1,25-$(OH)_2D_3$] (Leo Pharmaceuticals or Sigma Aldrich).
2. Menadione (vitamin K3) (Sigma Aldrich).
3. Alkaline phosphatase assay kit (Sigma Aldrich).
4. Staining Kit 86-R for alkaline phosphatase (Sigma Aldrich).
5. Osteocalcin radioimmunoassay (IDS Ltd., Boldon, UK) (*see* **Note 5**).
6. Polymerase chain reaction (PCR) primers and reagents for a panel of osteoblastic markers including osteocalcin (IDS Ltd., Boldon, UK).

2.5. In Vitro Mineralization

1. Dexamethasone (Sigma Aldrich).
2. Hematoxylin (BDH Merck).
3. L-Ascorbic acid (*see* **Note 2**).
4. Inorganic phosphate solution: Mix 500 mM solutions of Na_2HPO_4 and NaH_2PO_4 in a 4:1 (v/v) ratio. Sterile filter and store at 4°C prior to use.

2.6. Cryopreservation of Cells

1. Dimethyl sulfoxide (DMSO) (Sigma Aldrich).
2. Cryoampules.
3. Cell freezing container.

3. Methods

3.1. Establishing Primary Explant Cultures

A scheme outlining the culture technique is shown in **Fig. 1**.

1. Transfer tissue, removed at surgery or biopsy, into a sterile container with PBS or serum-free medium (SFM) for transport to the laboratory with minimal delay, preferably on the same day (*see* **Note 6**). An excellent source is the upper femur of patients undergoing total hip replacement surgery for osteoarthritis. Cancellous bone that would otherwise be discarded is removed from this site prior to the insertion of the femoral prosthesis. The tissue obtained is remote from the hip joint itself, and thus from the site of pathology, and is free of contaminating soft tissue (*see* **Note 7**).
2. Remove soft connective tissue from the outer surfaces of the bone by scraping with a sterile scalpel blade.
3. Rinse the tissue in sterile PBS and transfer to a sterile Petri dish containing a small volume of PBS (5–20 mL, depending on the size of the specimen). If the bone sample is a femoral head, remove cancellous bone directly from the open end using sterile bone rongeurs or a solid stainless steel blade with integral handle. Disposable scalpel blades may shatter during this process. With some bone samples (e.g., rib), it may be necessary to gain access to the cancellous bone by breaking through the cortex with the aid of the sterile surgical bone rongeurs.
4. Transfer the cancellous bone fragments to a clean Petri dish containing 2–3 mL of PBS and dice into pieces 3–5 mm in diameter. This can be achieved in two stages using a scalpel blade first, and then fine scissors.
5. Decant the PBS and transfer the bone chips to a sterile 30-mL "universal container" with 15–20 mL of PBS.
6. Vortex-mix the tube vigorously three times for 10 sec and then leave to stand for 30 sec to allow the bone fragments to settle. Carefully decant off the supernatant containing hematopoietic tissue and dislodged cells, add an additional 15–20 mL of PBS, and vortex-mix the bone fragments as before. Repeat this process a minimum of three times, or until no remaining hematopoietic marrow is visible and the bone fragments have assumed a white, ivory-like appearance.
7. Culture the washed bone fragments as explants at a density of 0.2–0.6 g of tissue/ 100-mm diameter Petri dish or 75-cm^2 flask (*see* **Note 4**) in 10 mL of medium at 37° in a humidified atmosphere of 95% air, 5% CO_2.
8. Leave the cultures undisturbed for 7 d, after which time replace the medium with an equal volume of fresh medium taking care not to dislodge the explants.
9. Check for outgrowth of cells at 7–10 d (*see* **Note 8**).
10. Replace the medium at 14 d and twice weekly thereafter until the desired cell density has been attained.

3.2. Passaging Cells and Establishing Secondary Cultures

1. Remove and discard the spent medium.
2. Gently wash the cell layers three times with 10 mL of PBS without Ca^{2+} and Mg^{2+}.

3. To each flask add 5 mL of freshly thawed trypsin–EDTA solution at room temperature (20°C) and incubate for 5 min at room temperature with gentle rocking every 30 sec to ensure that the entire surface area of the flask and explants is exposed to the trypsin–EDTA solution.

4. Remove and discard all but 2 mL of the trypsin–EDTA solution, and then incubate the cells for an additional 5 min at 37°C.

5. Remove the flasks from the incubator and examine under the microscope. Look for the presence of rounded, highly refractile cell bodies floating in the trypsin–EDTA solution. If none, or only a few, are visible tap the base of the flask sharply on the bench top in an effort to dislodge the cells. If this is without effect, incubate the cells for a further 5 min at 37°C.

6. When most of the cells have become detached from the culture substratum, transfer to a "universal container" with 5 mL of DMEM with 10% FCS to inhibit tryptic activity.

7. Wash the flask two to three times with 10 mL of SFM and pool the washings with the original cell isolate.

8. Centrifuge at 250g for 5 min to pellet the cells.

9. Remove and discard the supernatant, invert the tube, and allow the medium to drain briefly.

10. Resuspend the cell in 2 mL of SFM. If the cells are clumping *see* **Note 9**. If required, the cell suspension can be filtered through a 70-μm "Cell Strainer" (Becton Dickinson) to remove any bone spicules or remaining cell aggregates. For convenience and ease of handling the filters have been designed to fit into the neck of a 50-mL polypropylene tube. Wash the filter with 2–3 mL of SFM and add the filtrate to the cells.

11. Take 20 μL of the mixed cell suspension and dilute to 80 μL with SFM. Add 5 μL of trypan blue solution, mix, and leave for 1 min before counting viable (round and refractile) and nonviable (blue) cells in a Neubauer Hemocytometer. Using this procedure, typically $1–1.5 \times 10^6$ cells are harvested per 75-cm^2 flask, of which ≥75% are viable.

12. Plate the harvested cells at a cell density suitable for the intended analysis. We routinely subculture at $5 \times 10^3–10^4$ cells/cm^2 and achieve plating efficiencies measured after 24 h of ≥70% (*see* **Note 10**).

3.3. Phenotypic Characterization

The phenotypic characterization of HBDCs is described in detail in **ref. 5**. The simplest phenotypic marker to investigate is the enzyme alkaline phosphatase, a widely accepted marker of early osteogenic differentiation. Alkaline phosphatase can be measured by simple enzyme assay or by histochemical staining. Basal activity is initially low, but increases with increasing cell density. Treatment with $1,25\text{-}(OH)_2D_3$ increases alkaline phosphatase activity. The most specific phenotypic marker is osteocalcin. This is a protein of Mr 5800 containing residues of the vitamin K-dependent amino acid γ-carboxyglutamic

Table 2
PCR Primers for a Panel of Osteoblastic Markers

Osteoblastic phenotype marker	Primer pairs	T_m (°C)	Product size (bp)
Osteocalcin	5'-ccc tca cac tcc tcg ccc tat-3'		
	5'-tca gcc aac tcg tca cag tcc -3'	65	246
PTH receptor	5'-agg aac aga tct tcc tgc tgc a-3'		
	5'-tgc atg tgg atg tag ttg cgc gt-3'	55	571
Alkaline	5'-aag agc ttc aaa ccg aga tac aag-3'		
phosphatase	5'-ccg agg ttg gcc ccg at-3'	68	715
CBFA1	5'-ccc cac gac aac cgc acc-3'		
	5'-cac tcc ggc cca caa atc tc-3'	60	388
Osteoprotegerin	5'-ggg cgc tac ctt gag ata gag tt-3'		
	5'-gag tga cag ttt tgg gaa agt gg-3'	60	760
RANKL	5'-act att aat gcc acc gac atc-3'		
	5'-aaa aac tgg ggc tca atc ta-3'	54	462

acid. In humans its synthesis is restricted to mature cells of the osteoblast lineage. It is an excellent late stage markers for cells of this series despite the fact that its precise function in bone has yet to be established. Osteocalcin can be measured by one of the many commercially available kits. $1,25\text{-}(OH)_2D_3$ increases the production of osteocalcin in cultures of HBDCs, but not fibroblasts obtained from the same donors. More recently, researchers have adopted the use of reverse transcription (RT)-PCR to look at the expression of osteoblastic markers in HBDCs. PCR primers for a panel of osteoblastic markers including osteocalcin are shown in **Table 2**.

3.4. Phenotypic Stability in Culture

As a matter of routine we perform all of our studies on cells at first passage. Other investigators have studied the effects of repeated subculture on the phenotypic stability of HBDCs and found that they lose their osteoblast-like characteristics. In practical terms this presents real difficulties, as it is often desirable to obtain large numbers of HBDCs from a single donor. As an alternative to repeated subculture, trabecular explants can be replated at the end of primary culture into a new flask (*see* **Fig. 1**). Using this technique, it is possible to obtain additional cell populations that continue to express osteoblast-like characteristics, including the ability to mineralize their extracellular matrix, and maintain their cytokine expression profile *(6)*. Presumably, these cultures are seeded by cells that are situated close to the bone surfaces, and that retain

the capacity for extensive proliferation and differentiation. The continued survival of these cells may be related to the gradual release over time in culture of the cytokines and growth factors that are known to be present in the extracellular bone matrix, many of which are known to be produced by mature cells of the osteoblast lineage. The addition of 25 µ*M* L-ascorbic acid (50 µg/mL) (*see* **Note 2**) to HBDCs in secondary culture (E1P1) produces a sustained increase in the deposition of matrix due to an increase in the synthesis of collagen and noncollagenous protein and bone sialoprotein and osteocalcin.

3.5. Passaging Cells Cultured in the Continuous Presence of Ascorbate

Because of their synthesis and secretion of an extensive collagen-rich extracellular matrix, HBDCs cultured in the continuous presence of ascorbate cannot be subcultured using trypsin–EDTA alone. They can, however, be subcultured if first treated with purified collagenase. The basic procedure is as follows:

1. Rinse the cell layers twice with SFM (10 mL/75-cm^2 flask).
2. Incubate the cells for 2 h at 37°C in 10 mL of SFM containing 25 U/mL of purified collagenase (Sigma type VII) and 2 m*M* additional calcium (1:500 dilution of a filter-sterilized stock solution of 1 *M* CaCl$_2$).
3. Gently agitate the flask for 10–15 sec every 30 min.
4. Terminate the collagenase digestion by discarding the medium (check that there is no evidence of cell detachment at this stage).
5. Gently rinse the cell layer twice with 10 mL of Ca^{2+}- and Mg^{2+}-free PBS. To each flask add 5 mL of freshly thawed trypsin–EDTA solution, pH 7.4, at room temperature (20°C).
6. Typically this procedure yields ~3.5–4 × 10^6 cells/75-cm^2 flask after 28 d in primary culture. Cell viability is generally ≥90%.

3.6. Setting Up Mineralizing HBDC Cultures

The function of the mature osteoblast is to form bone. Despite the overwhelming evidence that cultures of HBDCs contain cells of the osteoblast lineage, initial attempts to demonstrate the presence of osteogenic (i.e., bone forming) cells proved unsuccessful. Subsequently, several authors reported that culture of HBDCs in the presence of ascorbate and millimolar concentrations of the organic phosphate ester β-glycerol phosphate (β-GP) led to the formation of mineralized structures resembling the nodules that form in cultures of fetal or embryonic animal bone derived cells (reviewed in **ref**. *22*). These have been extensively characterized and shown by a variety of morphological, biochemical, and immunochemical criteria to resemble embryonic/woven bone formed in vivo. An alternative to the use of β-GP is to provide levels of inor-

ganic phosphate sufficient to support the process of cell-mediated mineralization in vitro, and the preferred method when studying HBDCs, is supplementation of the culture medium with inorganic phosphate (Pi; *see* **Note 11**). The protocol for inducing matrix mineralization in cultures of HBDCs is as follows:

1. Prepare fragments of human trabecular bone as described in **Subheading 3.1., steps 1–6** (*see* **Note 12**).
2. Culture the washed bone fragments in medium supplemented with 100 μM L-ascorbic acid 2-phosphate and either 200 nM hydrocortisone or 10 nM dexamethasone.
3. Culture for 4–5 wk until the cells have attained confluence with medium changes twice weekly.
4. When the cells have synthesized a dense extracellular matrix, subculture using the sequential collagenase/trypsin–EDTA protocol and plate the cells in 25-cm^2 flasks at a density of 10^4 viable cells/cm^2.
5. After a further 14 d, supplement the medium with 0.01% phosphate solution (*see* **Subheading 2.5.4.**).
6. After 48–72 h, wash the cell layers two to three times with 10 mL of SFM.
7. Fix with 95% ethanol at 4°C (*see* **Note 13**).

3.7. Measuring Alkaline Phosphatase Activity

1. Add 2.5 mL of staining solution from the Sigma 86-R Staining Kit to each flask of cells (or enough to coat the surface).
2. Place specimens in a humidified chamber and incubate for 1 h at 20°C in the dark.
3. Wash under running tap water and counterstain the nuclei for 15 sec with hematoxylin.
4. Mineral deposits can be stained using a modification of von Kossa's technique.
5. Prior to examination, mount sections in DPX and cell layers in flasks covered with glycerol.

3.8. Cryopreservation of HBDC

If required, HBDCs can be stored frozen for extended periods in liquid nitrogen or in ultralow temperature (–135°) cell freezer banks. We use the following protocol:

1. Passage the cells using trypsin–ETDA as described in **Subheading 3.2., steps 1–5**.
2. Pellet the cells by centrifugation at 250g for 5 min and pour off the supernatant.
3. Resuspend the cell pellet in FCS, adjust to a density of 1–2 × 10^6 cells/mL in a volume of 900 μL and transfer to a cryoampule.
4. Swirl the ampule in an ice water bath.
5. Add 100 μL of DMSO gradually while holding the ampule in the iced water.
6. Close ampules tightly and freeze at 5°C/min to 4°C, followed by 1°C/min to –80°C in a cell freezing container.
7. Transfer the cells to liquid nitrogen for long-term storage.

3.9. Thawing Cells

1. Retrieve the cells from liquid nitrogen and place in a water bath set at 37°C.
2. Transfer the cells to a universal container to which at least 20 volumes of pre-heated culture medium has been added.
3. Centrifuge at 250g for 2 min to pellet the cells and pour off the supernatant.
4. Resuspend the cells in approx 10 mL of the medium and place into culture for 24 h.
5. Replace the medium after 24 h and culture for 2–3 wk.

4. Notes

1. Although most investigators have used the original explant method with only minor modifications, others have developed alternative techniques for the isolation and culture of HBDCs. Gehron-Robey and Termine used prior digestion of minced bone with clostridial collagenase and subsequent culture of explants in medium with reduced calcium concentrations *(7)*. In contrast, Wergedal and Baylink have used collagenase digestion to liberate cells directly *(24)*. Marie and co-workers have used a method in which explants are first cultured on a nylon mesh *(20)*. These alternative methods are described in greater detail in **ref. 5**.
2. Beresford and co-workers introduced the more stable analogue L-ascorbic acid 2-phsophate (Wako Pure Chemical Industries Ltd.) which does not have to be added daily (*see* **ref. 6** for details).
3. Batches of serum vary in their ability to support the growth of HBDCs. It is advisable to screen batches and reserve a large quantity of serum once a suitable batch has been identified. HBDCs will grow in autologous and heterologous human serum, but as yet no comprehensive studies have been performed to identify the effects on growth and differentiation.
4. The authors have obtained consistent results with plasticware from Sarstedt and Becton Dickinson. Smaller flasks or dishes can be used if the amount of bone available is <0.2 g.
5. Several other assays for osteocalcin are commercially available.
6. Bone can be stored for periods of up to 24 h at 4°C in PBS or SFM prior to culture without any deleterious effect on the ability of the tissue to give rise to populations of osteoblastic cells.
7. Bone cells have also been cultured successfully from many other anatomical sites including tibia, femur, rib, vertebra, patella, and digits.
8. With the exception of small numbers of isolated cells, which probably become detached from the bone surface during the dissection, the first evidence of cellular proliferation is observed on the surface of the explants, and this normally occurs within 5–7 d of plating. After 7–10 d, cells can be observed migrating from the explants onto the surface of the culture dish (*see* **Fig. 3**). If care is taken not to dislodge the explants when feeding, and they are left undisturbed between media changes, they rapidly become anchored to the substratum by the cellular outgrowths. The typical morphology of the cells is shown in **Fig. 4**, but cell shape varies between donors, from fibroblastic to cobblestone-like. Cultures generally attain confluence 4–6 wk post plating, and typically achieve a saturation density of 29,000 ± 9000 cells/cm^2 (mean + SD, N = 11 donors).
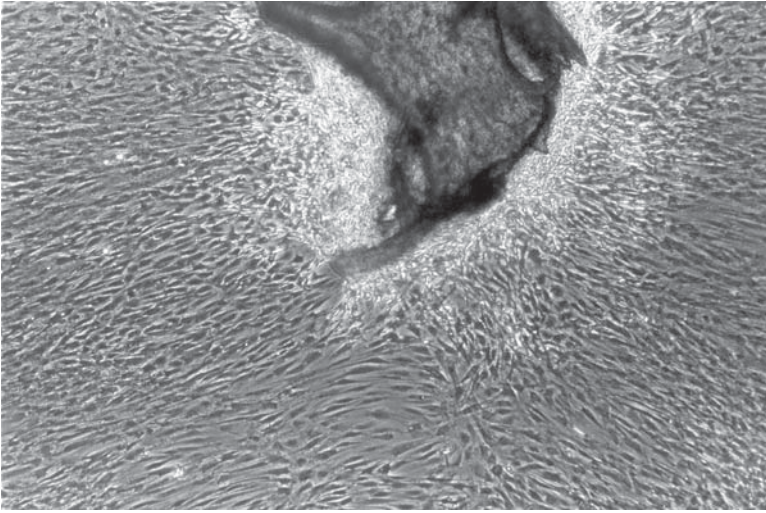
Fig. 3. Migration of cells expressing osteoblastic characteristics (HBDCs) from explanted cancellous bone.
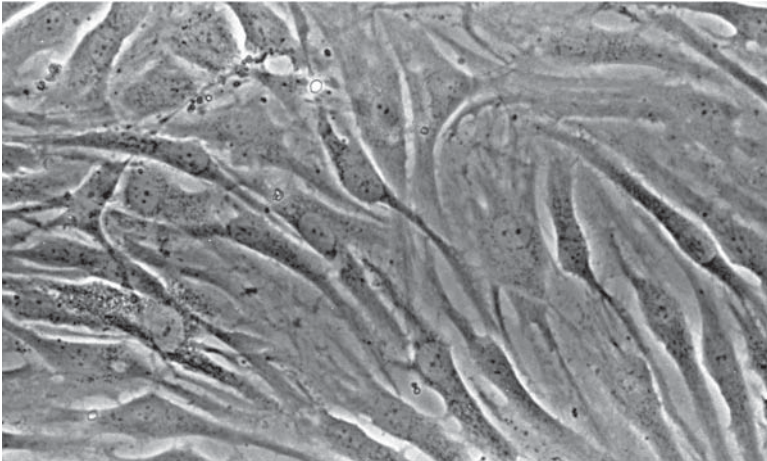

Fig. 4. Typical morphology of cells expressing osteoblastic characteristics (HBDCs) from explanted cancellous bone (*see* **Note 14**).

9. If the cells are clumping, resuspend in 2 mL of SFM containing 1 μg/mL of DNase I for each dish or flask treated with trypsin-EDTA, and using a narrow-bore 2-mL pipet, repeatedly aspirate and expel the medium to generate a cell suspension.

10. In our experience the minimum plating density for successful subculture is 3500 cells/cm^2. Below this the cells exhibit extended doubling times and often fail to grow to confluence. Note that cells can be passaged successfully onto a
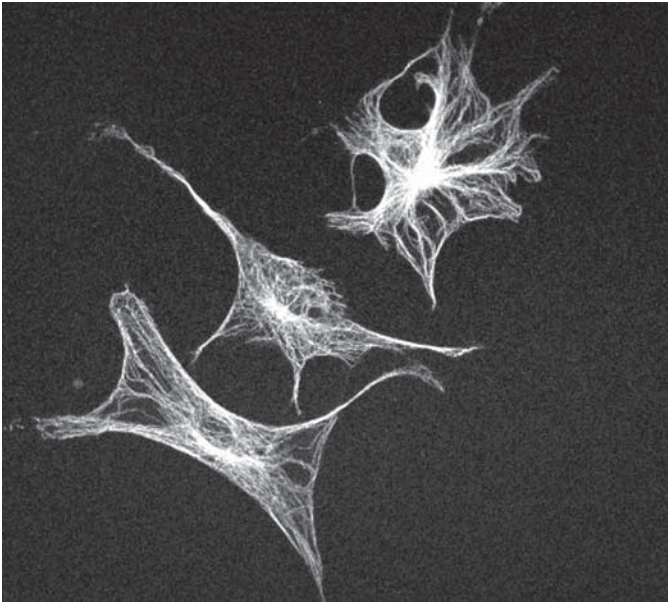
Fig. 5. Human primary derived osteoblasts cultured (7 d) on nanotopography textured titanium-coated silicon immunostained for β-tubulin to visualize the microtubles for specific orientations correlating to the stimulus of nanotopography. Image taken using a CLSM310 Zeiss confocal microscope. (J. M. Rice, J. A. Hunt and J. A. Gallagher, unpublished.)

range of substrates. Recently HBDC culture has been used to investigate biocompatibility and osteogenicity of novel biomaterials. **Figure 5** shows HBDCs passaged onto nanotopography textured titanium coated silicon and subsequently stained with antibodies specific for β-tubulin.

11. Mineralizing cultures: HBDCs cultured in the continuous presence of glucocorticoids and the long-acting ascorbate analogue produce a dense extracellular matrix that mineralizes extensively following the addition of Pi. This is the case for the original cell population (E1P1) and that obtained following replating of the trabecular explants (E2P1), which further attests to the phenotypic stability of the cultured cells. Cells cultured in the continuous presence of ascorbate and treated with glucocorticoids at first passage show only a localized and patchy pattern of mineralization, despite possessing similar amounts of extracellular matrix and alkaline phosphatase activity. Cells cultured without ascorbate, irrespective of the presence or absence of glucocorticoids, secrete little extracellular matrix, and do not mineralize. The ability of the cells to mineralize their extracellular matrix is dependent on ascorbate being present continuously in primary culture. The addition of ascorbate in secondary culture, even for extended periods, cannot compensate for its omission in primary culture. This finding provides further

evidence to support the hypothesis that maintenance of adequate levels of ascorbate during the early stages of explant culture is of critical importance for the survival of cells that retain the ability to proliferate extensively and give rise to precursors capable of undergoing osteogenic differentiation. HBDCs cultured continuously in the presence of ascorbate and glucocorticoids retain the ability to form bone when implanted in vivo within diffusion chambers in athymic mice *(23)*.

12. For studies of in vitro mineralization, it is preferable to obtain trabecular bone from sites containing hematopoietic marrow such as the upper femur or iliac crest.

13. Fixation of mineralized cultures: This can be done *in situ*, for viewing *en face*, or if sections are to be cut following detachment of the cell layer from the surface of the flask using a cell scraper. Great care is needed if the cell layer is to be harvested intact, particularly when mineralized.

14. The available evidence indicates that cultures of HBDCs contain cells of the osteogenic lineage at all stages of differentiation and maturation. This conclusion is consistent with the expression of both early (alkaline phosphatase) and late (osteocalcin, bone sialoprotein) stage markers of osteoblast differentiation. In addition, in ascorbate-treated cultures there is a small subpopulation (≤5%) of cells that express the epitope recognized by the monoclonal antibody (MAb) STRO-1 *(25)*, which is a cell-surface marker for clonogenic, multipotential marrow stromal precursors capable of giving rise to cells of the osteogenic lineage in vitro. The presence of other cell types, including endothelial cells and those derived from the hematopoietic stem cell, has been investigated using a large panel of MAbs and flow cytometry and/or immunocytochemistry. The results of these studies reveal that at first passage there are no detectable endothelial, lymphoid, or erythroid cells present. A consistent finding, however, is the presence of small numbers of cells (≤5%) expressing antigens present on cells of the monocyte/macrophage series. In the absence of added calcitriol, particularly in SFM or FCS that has been depleted of endogenous calcitriol by charcoal treatment, the amount of ostecalcin produced by HBDCs is below the limits of detection in most assays *(3,4)*. The same applies to the detection of steady-state levels of osteocalcin mRNA. An exception to this general rule is when HBDCs are cultured for extended periods in the presence of L-ascorbate or its stable analog, L-ascorbate-2-phosphate.

Acknowledgments

References

1. Bard, D. R., Dickens, M. J., Smith, A. U., and Zarek, J. M. (1972) Isolation of living cells from mature mammalian bone. *Nature* **236**, 314–315.

2. Mills, B. G., Singer, F. R., Weiner, L. P., and Hoist, P. A. (1979) Long term culture of cells from bone affected with Paget's disease. *Calcif. Tissue Int.* **29**, 79–87.

3. Gallagher, J. A., Beresford, J. N., McGuire, M. K. B., et al. (1984) Effects of glucocorticoids and anabolic steroids on cells derived from human skeletal and articular tissues in vitro. *Adv. Exp. Med. Biol.* **171**, 279–292.

4. Beresford, J. N., Gallagher, J. A., Poser, J. W., and Russell, R. G. G. (1984) Production of osteocalcin by human bone cells in vitro. Effects of 1,25(OH)2D3, parathyroid hormone and glucocorticoids. *Metab. Bone Dis. Rel. Res.* **5**, 229–234.

5. Gallagher, J. A., Gundle, R., and Beresford, J. N. (1996) Isolation and culture of bone forming cells (osteoblasts) from human bone, in *Human Cell Culture Protocols* (Jones, G. E., ed.), Humana Press Totowa, NJ.

6. Gundle, R., Stewart, K., Screen, J., and Beresford, J. N. (1998) Isolation and culture of human bone derived cells, in *Marrow Stromal Cell Culture* (Beresford, J. and Owen, M., eds.), Cambridge University Press, Cambridge, UK.

7. Gehron Robey, P. and Termine, J. D. (1985) Human bone cells in vitro. *Calcif. Tissue Int.* **37**, 453–460.

8. Auf'mkolk, B., Hauschka, P. V., and Schwartz, R. (1985) Characterisation of human bone cells in culture. *Calcif. Tissue Int.* **37**, 228–235.

9. MacDonald, B. R., Gallagher, J. A., Ahnfelt-Ronne, I., Beresford, J. N., Gowen, M., and Russell, R. G. G. (1984) Effects of bovine parathyroid hormone and 1,25(OH)2D3 on the production of prostaglandins by cells derived from human bone. *FEBS Lett.* **169**, 49–52.

10. MacDonald, B. R., Gallagher, J. A., and Russell, R. G. G. (1986) Parathyroid hormone stimulates the proliferation of cells derived from human bone. *Endocrinology* **118**, 2245–2449.

11. Beresford, J. N., Gallagher, J. A., and Russell, R. G. G. (1986) 1,25-Dihydroxy-vitamin D$_3$ and human bone derived cells in vitro: effects on alkaline phosphatase, type I collagen and proliferation. *Endocrinology* **119**, 1776–1785.

12. Fedarko, N. S., Vetter, U., Weinstein, S., and Robey, P. G. (1992) Age-related changes in hyaluronan, proteoglycan, collagen and osteonectin synthesis by human bone cells. *J. Cell Physiol.* **151**, 215–227.

13. Beresford, J. N., Gallagher, J.A., Gowen, M., et al. (1984) The effects of monocyte-conditioned medium and interleukin 1 on the synthesis of collagenous and non-collagenous proteins by mouse bone and human bone cells in vitro. *Biochim. Biophysica. Acta Gen. Subj.* **801**, 58–65.

14. Gowen, M., Wood, D. D., and Russell, R. G. (1985) Stimulation of the proliferation of human bone cells in vitro by human monocyte products with interleukin-1 activity in *J. Clin. Invest.* **4**, 1223–1229.

15. Vaishnav, R., Gallagher, J. A., Beresford, J. N., Poser, J. W., and Russell, R. G. G. (1984) Direct effects of stanozolol and oestrogen on human bone cells in culture, in *Osteoporosis. Proceedings of Copenhagen International Symposium*, pp. 485–488.

16. Eriksen, E. F., Colvard, D. S., Berg, N. J., et al. (1988) Evidence of estrogen receptors in normal human osteoblast-like cells. *Science* **241**, 84–86.

17. Schoefl, C., Cuthbertson, K. S. R., Walsh, C. A., et al. (1992) Evidence for P2-purinoceptors on osteoblast-like cells. *J. Bone Min. Res.* **7**, 485–591.

18. Bowler, W. B., Gallagher, J. A., and Bilbe, G. (1995) Identification and cloning of human P2U purinceptor present in osteoclastoma, bone and osteoblasts. *J. Bone Miner. Res.* **10**, 1137–1145.

19. Ralston, S. H., Todd, D., Helfrich, M., Benjamin, N., and Grabowski, P.S. (1994) Human osteoblast-like cells produce nitric oxide and express inducible nitric oxide synthase. *Endocrinology* **135**, 330–336.

20. Marie, P. J., Sabbagh, A., De Vernejoul, M. C., and Lomri, A. (1988) Osteocalcin and deoxyribonucleic acid synthesis in vitro and histomorphometric indices of bone formation in postmenopausal osteoporosis. *J. Clin. Invest.* **69**, 272–279.

21. Walsh, C. A., Birch, M. A., Fraser, W. D., et al. (1995) Expression and secretion of parathyroid hormone-related protein by human osteblasts in vitro: effects of glucocorticoids. *J. Bone Miner. Res.* **10**, 17–25.

22. Beresford, J. N., Graves, S. E., and Smoothy, C. A. (1993) Formation of mineralised nodules by bone derived cells in vitro: a model of bone formation? *Am. J. Med. Genet.* **45**, 163–178.

23. Gundle, R. G., Joyner, C. J., and Triffitt, J. T. (1995) Human bone tissue formation in diffusion chamber culture in vivo by bone derived cells and marrow stromal cells. *Bone* **16,** 597.

24. Wergedal, J. E. and Baylink, D. J. (1984) Characterisation of cells isolated and cultured from human trabecular bone. *Proc. Soc. Exp. Biol. Med.* **176**, 60–69.

25. Walsh, S., Jefferiss, C., Stewart, K., Jordan, G. R., Screen, J., and Beresford, J. N. (2000) Expression of the developmental markers STRO-1 and alkaline phosphatase in cultures of human marrow stromal cells: regulation by fibroblast growth factor (FGF)-2 and relationship to the expression of FGF receptors 1-4. *Bone* **27**, 185–195.

2

Osteoblast Isolation from Murine Calvariae and Long Bones

Astrid Bakker and Jenneke Klein-Nulend

1. Introduction

When conducting in vitro research on bone, a choice has to be made between using bone organ or bone cell cultures. When one decides to use the latter, the question is whether to use primary cells or cell lines. The advantage of using cell lines over freshly isolated cells lies in the ready availability of large numbers of cells, the homogeneity of the cell cultures, and the expected invariability of the phenotype. In the long run, however, cell lines appear unstable to some extent. In addition, their clonal selection has favored rapidly growing cells, but has not necessarily selected for the whole range of bone-specific gene expression characteristic of primary bone cells. This means that in certain experiments, the use of primary bone cells is preferred to the use of cell lines.

Peck and co-workers initiated the use of primary bone cell cultures in 1964 *(1)*. They isolated cells from frontal and parietal bones of fetal and neonatal rat calvariae by collagenase digestion of the uncalcified bone matrix. The isolated cells were viable, proliferated during culture, and exhibited high activity of the osteoblast marker alkaline phosphatase (ALP). The real nature of the cells, however, especially the amount of contamination with connective tissue fibro-blasts, could not be defined unambiguously *(1)*. Wong and Cohn (1974) tried to isolate a better defined and more homogeneous cell population by removing the outer layers of the periosteum with successive collagenase treatments *(2)*. Although this method led to cell cultures that were more osteoblastic in nature, these were not free from other cell types, such as osteoclast precursors, either *(3)*. Other investigators have tried to improve the osteoblastic character of the isolated bone cell populations by removing the fibroblastic outer periosteum before using enzymatic digestion to isolate the cells from the calvarium *(4,5)*.

This method resulted in two cell populations, one of which was still osteogenic after prolonged culture time (osteoblastic cells), and another one that was not (periosteal fibroblasts) *(6)*. These studies led to a broad range of methods for obtaining well-defined osteoblast-like cells in vitro, which are at present widely used as a tool to improve our knowledge of bone biology *(7–9)*.

This chapter describes the isolation of primary mouse bone cells from adult mouse calvariae and long bones, as well as the process of isolation of bone cells from neonatal mouse calvariae. Owing to their difference in origin and method of isolation, it is to be expected that each of the primary bone cell cultures described will have its own characteristics. For example, it has been shown that *neonatal* cells show a higher basal release of nitric oxide and a higher response to 1,25-dihydrogxyvitamin [D_3 1,25-$(OH)_2D_3$] treatment than bone cells obtained from *adult* bone *(10)*. Because vitamin D3 stimulates immature bone cell differentiation, this supports the notion that neonatal cell cultures contain more immature, rapidly growing cells than cultures from adult bone. Thus, for in vitro studies investigating the cellular behavior of adult bone, it seems advisable to use cells from adult bone fragments to reproduce best the inherent cellular properties of the adult tissue.

Another example relates to mechanosensitivity of bone cells. Because the prevailing mechanical strains in the skull are much lower than those in the axial and appendicular skeleton, the question has arisen whether cells from *calvariae* or *long bones* should be used in such studies. We addressed this issue by studying the nitric oxide production of the bone cells in response to mechanical stimulation in the form of fluid flow. We found no difference in the responsiveness of osteoblasts from adult mouse calvariae or adult mouse long bones *(12)*. These results suggest that the cellular mechanosensitivity of calvariae and long bone cells is not intrinsically different and that either cell culture can be used for these sorts of experiments.

2. Materials
2.1. Tissues
1. Cells are obtained from the long bones and the calvariae of adult (age 9 wk or older) mice, or the calvariae from neonatal mice pups (age 3–4 d).

2.2. Instruments
All of the following materials have to be sterile.

1. Polystyrene plate and needles for fixing the mice.
2. Scalpels (no. 10 and 11), scissors, tweezers, and curved forceps.
3. 5-mL and 10-mL syringes, 27G1/2 needles, disposable cell scrapers, and 0.2-µm disposable filter units.

4. 25-cm^2 tissue culture flasks (Nunc), six-well tissue plates (Costar), 94/16-mm cellstar Petri dishes (Greiner), and 145/20-mm cellstar (large) Petri dishes (Greiner).
5. 100 × 16 mm (10 mL) conical base test tubes with screw cap (Bibby Sterilin Ltd., Staffordshire, UK).

2.3. Media and Solutions

1. Phosphate-buffered saline (PBS): 137 mM NaCl, 1.5 mM KH$_2$PO$_4$, 2.7 mM KCl, and 8.1 mM Na$_2$HPO$_4$. Adjust the pH to 7.4.
2. Dulbecco's modified Eagle's medium (DMEM; Gibco, Paisley, UK): Add 2.2 g NaHCO$_3$/L; adjust the pH to 7.4.
3. Complete culture medium (cCM): DMEM, supplemented with 100 U/mL of penicillin (Sigma), 50 µg/mL of streptomycin sulfate (Gibco), 50 µg/mL of gentamycin (Gibco), 1.25 µg/mL of fungizone (Gibco), 100 µg/mL of ascorbate, and 10% fetal bovine serum (FBS) (Hyclone, Logan, UT, USA; *see* **Note 1**). Make fresh and filter sterilize.
4. Collagenase solution: 2 mg of collagenase II (Sigma) per milliliter of DMEM. Make fresh and filter sterilize.
5. Trypsin solution: 0.25% trypsin 1:250 (Difco, Detroit, MI, USA) and 0.10% EDTA in PBS; filter sterilize.
6. Digestion solution: Add 1 mL of trypsin solution and 3.2 mg of collagenase II to 4 mL of PBS. Make fresh.
7. Vitamin D medium (VDM): DMEM, supplemented with 100 U/mL of penicillin, 50 µg/mL of streptomycin sulfate, 50 µg/mL of gentamicin, 1.25 µg/mL of fungizone, 100 µg/mL of ascorbate, 0.2% bovine serum albumin (Sigma) and 10^{-8} M 1,25-(OH)$_2$D$_3$. Make fresh and shield away from direct light.
8. Vitamin D control medium (VDCM): Composition is the same as vitamin D medium, except that the 1,25-(OH)$_2$D$_3$ is replaced by an equal amount of vehicle.
9. BCA Protein Assay Reagent Kit (Pierce, Rockford, IL, USA).

3. Methods

Normal techniques for working under sterile conditions (use of sterile media and instruments and working in a flow cabinet) should be used to keep the cell cultures sterile.

3.1. Isolation and Culture of Primary Bone Cells from Adult Mouse Long Bones

1. Euthanize one or two adult mice by means of cervical dislocation.
2. Fix the mouse in a supine position on a polystyrene plate or in a large Petri dish, and clean the abdomen and extremities using 70% ethanol.
3. Make a single incision through the skin, starting at the top of the sternum and ending a few millimeters above the genitals, using a no. 10 scalpel. Make a second incision starting from the top of the first incision and ending at the wrist of

the upper left extremity. Repeat this procedure with the other paws. Carefully remove the skin from the abdomen with a blade.

4. Change your blade for a sterile no. 11 scalpel. Remove the muscles from the long bones in the limb (femur; tibia and fibula; or humerus, radius, and ulna), and scrape the bone with a scalpel until it is clean (*see* **Note 2**). Excise the long bone and place it in a Petri dish with PBS.

5. When all the long bones have been removed, cut off the epiphyses.

6. Flush out the bone marrow with PBS, using a 5-mL syringe and a 27-gauge needle.

7. Cut the clean diaphyses into small pieces of approx 1–2 mm^2 using scissors.

8. Wash the bone pieces with PBS, and incubate in 4 mL of collagenase solution at 37°C in a shaking water bath to remove all remaining soft tissue and adhering cells.

9. After approx 1 h, vigorously shake the solution by hand.

10. After 2 h, add 4 mL of cCM containing 10% FBS to inhibit further collagenase activity, and rinse the bone pieces three times with cCM.

11. Transfer the bone pieces to 25-cm^2 flasks, containing 5 mL of cCM, at a density of about 20–30 fragments per flask. Replace culture medium three times per week.

12. Adult mouse bone cells will start to migrate from the bone chips after 3–5 d. On average the cell monolayer growing from the bone fragments will reach confluency after 11–15 d.

13. To obtain more cells, trypsinize the monolayer by incubating the cells with 1 mL of trypsin solution at 37°C for 10 min.

14. Plate the cells at 25 × 10^3 cells per well in six-well culture dishes containing 3 mL of cCM per well.

15. Change medium three times per week, and after approx 7–10 d cells will reach subconfluency, upon which they can be used for experiments (*see* **Note 3** and **Subheading 3.4.**). The average number of cells thus obtained lies between 4 x 10^6 and 6 × 10^6 cells.

3.2. Isolation and Culture of Primary Bone Cells from Adult Mouse Calvariae

1. Euthanize two adult mice and fix them on a polystyrene plate, or in a large Petri dish.

2. Clean the head using 70% ethanol, and make a cut through the skin at the base of the skull, using scissors.

3. Make an incision starting at the nose bridge, and ending at the base of the skull. Remove the skin from the top of the head (*see* **Fig. 1**).

4. Use scissors to cut through the bone at the base of the neck. Cut the calvariae loose, while holding the head with curved forceps placed in the orbita.

5. Transfer the calvariae to a Petri dish with PBS and remove the soft tissues using tweezers or by scraping with a knife (*see* **Note 2**).

6. Remove the sutures, using scissors, and chop the remaining bone into small fragments of approx 1–2 mm^2.

7. Incubate the fragments for 30 min in 4 mL of collagenase solution at 37° in a shaking water bath.
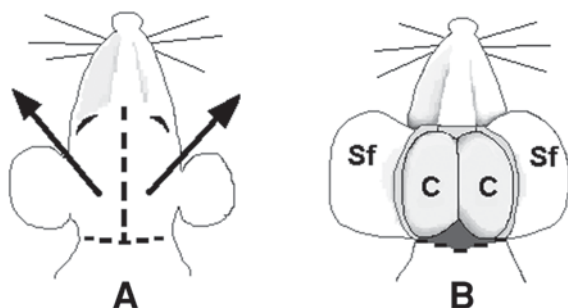
Fig. 1. Schematic presentation of mouse calvariae. **(A)** Make a cut through the skin at the base of the skull, using scissors (*short dashed line*). For adult tissue, make an incision starting at the nose bridge, ending at the base of the skull (*long dashed line*), and remove the skin from the top of the head (*arrows*). Use scissors to cut away the skin from the top of the neonatal mouse heads. **(B)** Dissect calvariae as indicated by area C and remove as much soft tissue as possible. Do not include the shaded area near the neck, as this will result in heavy fibroblast contamination of the cultures. Sf, Skin flap; C, Calvaria.

8. Remove the collagenase solution and replace with fresh collagenase solution. Incubate another 30 min, then replace the collagenase solution for trypsin solution.
9. Incubate in trypsin for 30 min. Replace by 4 mL of collagenase solution for the fourth and final incubation step of 30 min.
10. Add 4 mL of cCM to the collagenase to inhibit collagenase activity. Rinse the bone pieces three times with cCM.
11. Transfer the bone pieces to 25 cm^2 flasks, containing 5 mL of cCM, at a density of approx 20–30 fragments per flask.
12. Change the medium three times per week. Adult mouse bone cells will start to migrate from the bone chips after 3–5 d. On average the cell monolayer growing from the bone fragments will reach confluency after 11–15 d, upon which the monolayer is trypsinized by incubating the cells with 1 mL of trypsin solution at 37°C for 10 min.
13. Plate the cells at 25×10^3 cells per well in six-well culture dishes containing 3 mL of cCM per well.
14. After approx 7–10 d cells will reach subconfluency, upon which they can be used for experiments (*see* **Note 3** and **Subheading 3.4.**). The average number of cells thus obtained lies between 4×10^6 and 6×10^6 cells.

3.3. Isolation and Culture of Bone Cells from Neonatal Mouse Calvariae

1. Euthanize 20–30 neonatal mice pups (2–3 liters) by decapitation or halothane inhalation, and place the heads in a Petri dish with PBS (*see* **Note 4**).
2. Grasp the head by the nape of the neck, and cut the skin away using scissors.

3. Hold the head with curved forceps placed through the orbita, cut the calvariae loose along the edge, and place it in a Petri dish with PBS (*see* **Fig. 1** for a diagram illustrating how to dissect the calvariae).

4. Pin the calvariae down with tweezers and cut away the edges and sutures with a small scalpel. Transfer the calvariae halves to a 25-mL tube with PBS and wash twice with PBS.

5. Incubate the calvariae in 4 mL of digestion solution at 37°C in a shaking water bath. After 10 min shake the calvariae by hand for a few seconds.

6. Incubate for a total of 20 min, and then transfer the supernatant, containing cells, to a 10-mL tube. Add 700 μL of fetal calf serum (FCS) to the cell suspension to inhibit collagenase and trypsin activity.

7. Wash the calvariae with 3 mL of DMEM (without FBS!), shake well, and add the supernatant to the tube containing the cell suspension. This is population no. 1.

8. Add new digestion solution to the calvariae, and repeat the previous three steps to obtain population no. 2. During the 20 min that the calvariae have to incubate in the water bath, centrifuge cell population no. 1 for 5 min at 300g Discard the supernatant, resuspend the cell pellet in 1 mL of cCM, and add to 17 mL of cCM. Pipet in a six-well plate at 3 mL of cell suspension per well.

9. Repeat the entire procedure for a total of four times, to obtain population nos. 1–4.

10. The culture medium is changed 1 d after isolation of the bone cells.

11. Within approx 5 d cells will reach subconfluency, upon which they are trypsinized by incubation with 200 μL of trypsin solution per well, at 37°C for 10 min.

12. Population nos. 1 and 2, resembling osteoblast progenitor cells, are pooled, as well as population nos. 3 and 4. This latter pooled cell population is enriched with cells exhibiting biochemical characteristics associated with differentiated osteoblasts, such as high ALP activity and osteopontin expression. Both pooled populations can be used directly for experiments (*see* **Note 5**).

13. The number of cells obtained using this method varies between 6×10^6 and 10×10^6 cells. *see* **Note 5** for an alternative method for osteoblast isolation from neonatal calvariae.

3.4. Characterization of the Osteoblast Phenotype by Determination of ALP Activity

Primary bone cell cultures are not 100% pure and may contain some fibroblasts and other nonosteoblastic cell types. It is therefore advisable to check routinely the osteoblastic phenotype of the cultures. Because vitamin D_3 stimulates the differentiation of immature bone cells, leading to enhanced ALP activity *(11)*, the osteoblastic phenotype of the primary mouse bone cell cultures can be determined as follows:

1. Take a subconfluent cell culture in a six-well plate, wash the cells once with PBS, and replace the medium by 3 mL of either VDM or VDCM per well. After 3 d of incubation, remove the medium and wash the cell layer with PBS.

2. Put the cells on ice and add 1 mL of cold milliQ water to the cells. Harvest the cells with a cell scraper, and transfer the cell suspension to a 10-mL tube. Sonicate on ice for 10 min, and then centrifuge for 10 min at 500 *g*. Transfer the supernatants for determination of ALP activity and total protein content.

3. Determine ALP activity by using *p*-nitrophenyl phosphate as a substrate at pH 10.3, according to the method described by Lowry *(12)*. Read the absorbance at 405 nm.

4. Measure the protein content of the homogenate using a BCA Protein Assay Reagent Kit according to the manufacturer's protocol. Read the absorbance at 570 nm. On average the incubation of adult mouse bone cell cultures with 1,25-$(OH)_2D_3$ will result in a twofold induction of ALP production. In neonatal mouse calvarial cultures the induction of ALP production by 1,25-$(OH)_2D_3$ is on average sixfold.

4. Notes

1. Addition of serum to the medium is necessary for the survival and stimulation of proliferation of the primary mouse bone cells. "Serum" is not a constant and homogeneous product, however, and the growth rate of primary bone cells can vary considerably between several batches of serum. It is therefore recommended to test several batches of serum on their cell proliferative ability and continue to use the one that produces the best results.

2. Sometimes the primary bone cultures can contain fibroblasts, which grow faster than the bone cells and can quickly overgrow the primary bone cell cultures. If this problem occurs care should be taken to remove all soft tissues better by scraping the bones with a knife before starting the collagenase treatment. Also make sure the collagenase is not expired, and that the collagenase solution is made fresh every time.

3. The exact nature of the bone cells that are isolated from adult long bones and adult calvariae has not yet been determined. Because the cell isolation protocols involve removing the soft tissues and all adhering cells by means of incubation with collagenase, the cells that are isolated from the bones might represent osteocytes that reverted to proliferation after several days of exposure to fetal calf serum. The appearance of the isolated bone cells, however, is mostly osteoblastic (**Fig. 2**), and several osteoblast specific markers are expressed by these cells. Absence of staining for von Willebrand factor (factor VIII) shows that the bone cell cultures do not contain endothelial cells.

4. Smaller numbers of calvariae can be used successfully, leading to a proportionately lower yield of osteoblasts.

5. We prefer the use of collagenase type II; however, other groups have reported use of crude collagenase type IA (Sigma C9891), which is cheaper and intrinsically contains trypsin as a contaminant. An alternative protocol for isolation of osteoblasts from neonatal mouse calvariae, which uses alternate collagenase and EDTA incubations to remove as much mineralized matrix as possible and increase cellular yield, is given below in the following subheadings.
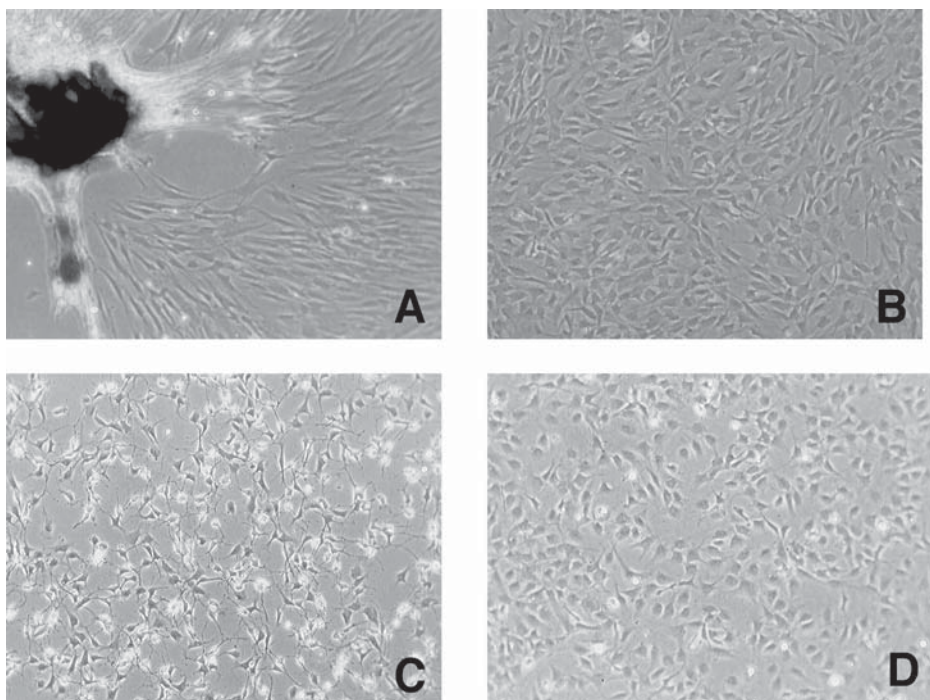
Fig. 2. Phase contrast microscopy of primary mouse bone cell cultures. **(A)** Adult mouse bone cells growing out of the bone chips, d 6 of culture. **(B)** Subconfluent layer of adult mouse bone cells, first passage. **(C)** Neonatal mouse calvarial cells, population nos. 1 and 2, d 3 of culture. **(D)** Neonatal mouse calvarial cells, population nos. 3 and 4, d 3 of culture. Note the cuboidal morphology of the osteoblasts.

Materials

1. Stock solution of collagenase type I at 10 mg/mL in Hanks' balanced salt solution (HBSS, Gibco). Filter sterilize and freeze aliquots for single use at –20°C. Dilute in HBSS to 1 mg/mL just before use. HBSS contains calcium, which increases the activity of the collagenase.
2. 4 mM EDTA in PBS without calcium and magnesium. Filter sterilize and store at 4°C.
3. Conical 15-mL centrifuge tubes (polypropylene, to reduce cell loss by minimizing adhesion to tube). Conical 25-mL centrifuge tubes for incubations. Sterile Petri dishes for dissection (ideally glass).
4. Sterile small curved forceps and spring bow scissors.

Method

1. Dissect calvariae as described in **Subheading 3.3.**, **steps 1–3** and collect them in HBSS.
2. All incubations are carried out in 3 mL of solution (making sure calvaria are completely covered) in a 25-mL centrifuge tube in a shaking water bath at 37°C.

3. Incubate calvariae in 1 mg/mL of collagenase for 10 min (fraction 1).
4. Replace the collagenase solution with fresh solution and discard fraction 1.
5. Incubate for 30 min in collagenase. Collect the cell suspension (fraction 2) and place in a conical centrifuge tube. Wash calvariae in 7 mL of PBS and add wash to fraction 2.
6. Add EDTA solution and incubate for 10 min. Collect the resulting cell suspension (fraction 3). Wash calvariae in 7 mL of HBSS and add wash to fraction 3.
7. Add collagenase and incubate for 30 min (fraction 4). Wash in HBSS and add wash to fraction 4.
8. Further fractions can be collected by repeating **steps 5** and **6**, but cell yields will be increasingly lower.
9. Centrifuge all fractions immediately after collection (250*g* for 5 min) and resuspend pellets in cCM (*see* **Subheading 2.3.3.**).
10. Plate out pooled or single fractions in 75-cm^2 culture flasks using cells derived from two or three animals per flask. Later fractions will contain the most differentiated cells. Cells isolated in this way (pooled fractions 2–4) have been used successfully in cocultures to generate osteoclasts (*see* Chapter 11 by van 't Hof, *this volume*).
11. Cultures will be confluent in 3–4 d. To minimize contamination by other adherent cell types, replace medium once cells have adhered (2–3 h after plating).

References

1. Peck, W. A., Birge, S.J., and Fedak, S. A (1964) Bone cells: biochemical and biological studies after enzymatic isolation. *Science* **146**, 1476–1477.
2. Wong G. L. and Cohn, D. V. (1974) Separation of parathyroid hormone and calcitonin-sensitive cells from non-responsive cells. *Nature* **252**, 713–715.
3. Burger, E. H., Boonekamp, P. M., and Nijweide, P. J. (1986) Osteoblast and osteoclast precursors in primary cultures of calvarial bone cells. *Anat. Rec.* **214**, 32–40.
4. Yagiela, J. A. and Woodbury, D. M. (1977) Enzymatic isolation of osteoblasts from fetal rat calvaria. *Anat. Rec.* **188**, 287–306.
5. Nijweide, P. J., van der Plas, A., and Scherft, P.J. (1981) Biochemical and histological studies on various bone cell preparations. *Calcif. Tissue Int.* **33**, 529–540.
6. Nijweide, P.J., van Iperen-van Gent, A.S., Kawilarang-de Haas, E. W. M., van der Plas, A., and Wassenaar, A.M. (1982) Bone formation and calcification by isolated osteoblast-like cells. *J. Cell Biol.* **93**, 318–323.
7. Klein-Nulend, J., Burger, E. H., Semeins, C. M., Raisz, L. G., and Pilbeam C. C. (1997) Pulsating fluid flow stimulates prostaglandin release and inducible prostaglandin G/H synthase mRNA expression in primary mouse bone cells. *J. Bone Miner. Res.* **12**, 45–51.
8. Klein-Nulend, J., Semeins, C. M., Ajubi, N. E., Nijweide, P. J., and Burger, E. H. (1995) Pulsating fluid flow increases nitric oxide (NO) synthesis by osteocytes but not periosteal fibroblasts: correlation with prostaglandin upregulation. *Biochem. Biophys. Res. Commun.* **217**, 640–648.

9. Bakker, A. D., Soejima, K., Klein-Nulend, J., and Burger, E. H. (2001) The pro-
   duction of nitric oxide and prostaglandin E2 by primary bone cells is shear stress
   dependent. *J. Biomech.* **34**, 671–677.
10. Soejima, K., Klein-Nulend, J., Semeins, C. M., and Burger, E. H. (2001) Differ-
    ent responsiveness of cells from adult and neonatal mouse bone to mechanical
    and biochemical challenge. *J. Cell Phys.* **186**, 366–370.
11. Auf 'mkolk, B., Hauschka, P. V., and Schwartz, E.R. (1985) Characterization of
    human bone cells in culture. *Calcif. Tissue Int.* **37**, 228–235.
12. Lowry, O. H. (1955) Micromethods for the assay of enzyme. II Specific pocedure.
    Alkaline phosphatase. *Methods Enzymol.* **4**, 371.

3

Mineralizing Fibroblast-Colony-Forming Assays

Andrew Scutt, Lynsey Reading, Nanette Scutt, and Karen Still

1. Introduction

Bone formation does not lend itself easily to investigation because bone tissue consists of various cell types embedded in a complex extracellular matrix. These cells interact with each other and with the extracellular matrix, and when cell populations are removed from the network they cease to function normally. In the past, bone cell differentiation was studied using histological methods in either whole embryos or organ cultures. Although this has provided much information regarding the temporal and spatial relationships of the various cells, the complexity of organ culture systems does not easily allow one to investigate the molecular mechanisms involved in bone development and mineralization. Cell culture techniques have given us much information regarding the mechanistic aspects of gene regulation and cell signaling in osteoblastic cells, but isolated osteoblasts do not respond to exogenous agents in a similar manner to that observed in vivo *(1)*. Recently a number of in vitro models have been established that re-create discrete elements of the cellular network present in the bone micro-environment. The advantage of these models is that they have reduced complexity compared with organ cultures yet retain osteoblasts and their progenitors at various stages of differentiation, allowing defined aspects of bone formation to be investigated at the cellular and molecular levels. These models are modifications of nodule cultures or fibroblast-colony-forming unit (CFU-f) cultures. In CFU-f cultures, bone marrow cells are cultured at relatively low densities under conditions that allow the individual CFU-f to adhere and proliferate to form colonies. Because of the low plating density, the colonies grow essentially in isolation. Each colony therefore represents the clonal expansion of one CFU-f and the assay is considered to be a measure of the number of CFU-f present in the original bone
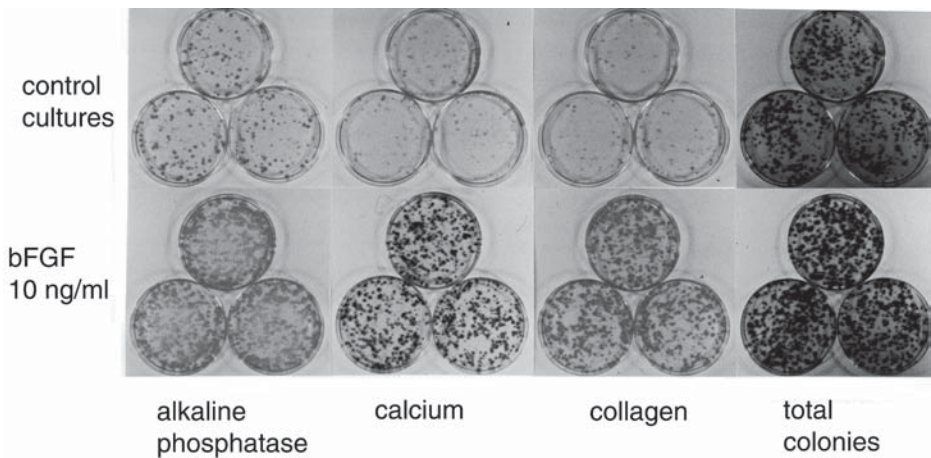
Fig. 1. Effect of bFGF on fibroblastic colony formation. By sequentially staining the cultures for alkaline phosphatase, calcium, collagen, and total colonies, it can be seen that bFGF stimulates not only colony formation but also the differentiation process. Analysis shows that the percentage of colonies positive for collagen and calcium increases from about 10% to 65% after treatment with 10 ng/mL of bFGF whereas the percentage ALP-positive colonies remains constant at about 80%.

marrow cell suspension (for review *see* **ref. 2**). Given the appropriate culture conditions, a proportion of these colonies will differentiate and develop osteoblastic characteristics such as the expression of alkaline phosphatase, collagen accumulation, and calcification. The colonies that have all three osteoblastic characteristics are considered to be derived from osteoprogenitor cells *(3)*. CFU-f cultures also respond to many agents that stimulate bone formation in vivo. For example, in **Fig. 1** it can be seen that 10 ng/mL of basic fibroblast growth factor (bFGF) stimulates not only total colony number but also the number of differentiated colonies. In nodule cultures the cells are plated at relatively high density, reach confluence, and subsequently form three-dimensional structures (nodules) that possess many bone-like characteristics *(4–6)*. Although the number of nodules has been shown to be dependent on the initial number of osteoblast progenitors *(7)*, there exists the possibility of considerable interaction between the various cell types in the cultures owing to the high cell density. This chapter deals exclusively with CFU-f cultures as these have been used with some success to elucidate the role of bone marrow osteoprogenitor cells in bone formation in vitro *(8–12)* and ex vivo *(13–20)*.

2. Materials
2.1. Isolation of Bone Marrow Cells

1. Assorted sterile dissection instruments including bone cutters, scissors, scalpels, and forceps.
2. Rotary saw or similar. In our laboratory we use a "Hobby drill" with a cutting wheel attachment.
3. Sterile 1.5-mL microfuge tubes.
4. Plastic supports cut from either pipet tips, 0.5-mL microfuge tubes, or hypodermic needle sleeves. These should be cut to size so that they fit inside the Eppendorf tubes and raise the bones 3–4 mm from the base of the tubes.

2.2. Tissue Culture Medium

Dulbecco's modified Eagle's medium (DMEM) containing 4500 mg/L of glucose, 1 mM of pyruvate, 2 mM Glutamax, 50 U/L of penicillin, 50 µg/L of streptomycin, 50 µg/mL of ascorbic acid, 10^{-8} M dexamethasone and 10% fetal calf serum (FCS) (*see* **Note 1**).

2.3. Staining and Destaining

1. Fixative: 70% ethanol (*see* **Note 2**).
2. Alkaline phosphatase (ALP) staining solution: 20 mM Tris, pH 7.5, containing 0.5 mg/mL of naphthol phosphate AS-BI and 1 mg/mL of fast red B. Prepare fresh before use (*see* **Note 3**).
3. ALP destaining solution: 100% Ethanol.
4. Alizarin red solution: To assess mineralization. 1 mg/mL of alizarin red in distilled water adjusted to pH 5.5 with ammonium hydroxide.
5. Alizarin red destaining solution: 5% perchloric acid in distilled water.
6. Collagen staining solution: To assess collagen production. Add 50 mg of sirius red to 50 mL of saturated picric acid.
7. Collagen destaining solution: 0.1 N NaOH mixed with methanol (50:50). Prepare fresh just before use.
8. Borate buffer. 10 mM boric acid; adjust pH to 8.8 with NaOH.
9. Total-colony staining solution: 1 mg/mL of methylene blue in 10 mM borate buffer, pH 8.8.

2.4. Colony Quantitation

1. Kodak DC50 digital camera or similar.
2. Good quality white light transilluminator.
3. Adobe Photoshop or similar image editing software.
4. Intelligent quantifier or similar colony counting software.

3. Methods
3.1. Isolation of Whole Bone Marrow Cells

1. Use four 125–200-g male Wistar rats and euthanize these by cervical dislocation (*see* **Note 4**).
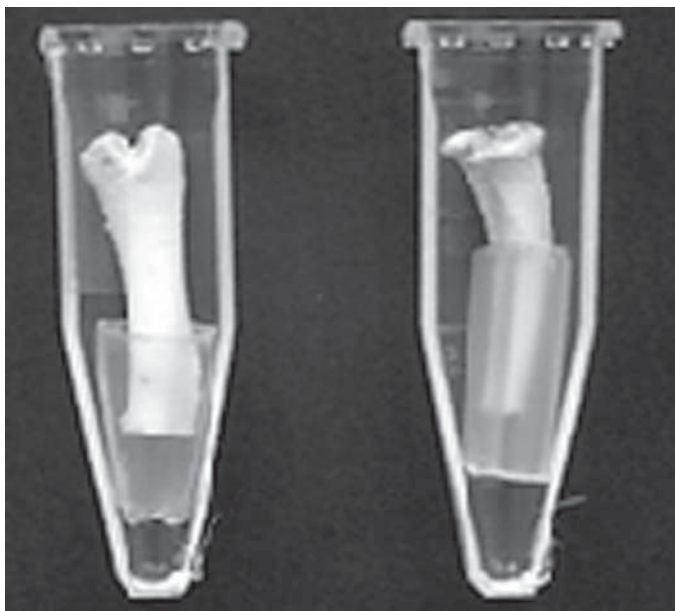
Fig. 2. Recovery of tibial and femoral bone marrow cells using a centrifugation method. Bone marrow cells are isolated using a brief centrifugation step. Excised and prepared bones are placed in 1.5-mL microfuge tubes supported by plastic inserts. The bone marrow cells are expelled by centrifuging the samples at 2000 rpm in a microfuge for 5 sec. The bone marrow pellet is then resuspended in 10 mL of culture medium as described in **Subheading 3.**

2. Remove the tibias and femurs from each animal under aseptic conditions and dissect away the soft tissues. For the tibia this can be best achieved by grasping the growth plate with bone cutters and tearing the growth plate off together with any attached musculature. The muscle can then be removed cleanly and the bone cut off at the junction of the tibia and fibula using a rotary saw. The condyle of the femur can be grasped and torn off in a similar manner. However, not all of the muscle will come off cleanly and will have to be removed carefully using either scissors or a scalpel. The bone can then be cut as close to the femoral neck as possible using a rotary saw.

3. Recover the bone marrow cells using the method of Dobson et al. *(21)* by placing the bones in 1.5-mL microfuge tubes supported by plastic inserts fabricated from either 0.5 mL microfuge tubes or hypodermic needle casings (**Fig. 2**). (*see* **Note 5**).

4. Centrifuge the tubes briefly at 900 *g* for 5 sec in a microfuge. The marrow cells will pellet at the bottom of the tube.

5. Resuspend the cell pellet in 1 mL of medium and create a single-cell suspension by aspirating through a 21-gauge needle.

6. Pool the cells from all bones and make up to 10–20 mL with medium (*see* **Note 6**).
7. Check the cell concentration using a hemocytometer (*see* **Note 7**).

3.2. Setting up the CFU-f assay

1. Plate 2×10^6 bone marrow cells out in 55-cm^2 Petri dishes in 10 mL of culture medium containing the required concentrations of the substance(s) to be tested.
2. Change the medium after 5 d and thereafter twice weekly for up to 18 d.
3. Terminate the cultures by washing with PBS and fix by adding cold 100% ethanol.

3.3. ALP Staining

1. Add enough ALP staining solution to cover the Petri dish (~5 mL) and allow to stand for 30 min at room temperature.
2. Wash the Petri dish under running tap water, and allow to dry.
3. Photograph the dishes to document the amount of ALP staining.
4. Destain the plates by gently shaking (approx 30 rpm) overnight with 100% ethanol on an orbital shaker.

3.4. Mineralization

1. Add enough alizarin red solution to cover each Petri dish (~5 mL) and allow to stand for 30 min at room temperature with gentle agitation.
2. Wash the Petri dishes under running tap water until the excess dye has washed off.
3. Allow to dry at room temperature.
4. Photograph the dishes to document the amount of mineralization.
5. Destain the dishes by gently shaking with 5% percholoric acid for 5 min.
6. Wash thoroughly with tap water.

3.5. Collagen

1. Add 5 mL of collagen staining solution to each dish and incubate for 18 h.
2. Wash the dishes under running tap water until the excess dye has washed off.
3. Allow to air-dry at room temperature.
4. Photograph the dishes to document the amount of staining.
5. Destain the dishes by gently shaking with collagen destaining solution.
6. Wash thoroughly with tap water.

3.6. Total Colonies

1. Wash the plates with borate buffer.
2. Cover the plates with borate buffer containing 1% methylene blue for 30 min.
3. Wash three times with borate buffer.
4. Allow the cultures air-dry at room temperature.
5. Photograph the dishes to document the numbers of methylene blue positive CFU-f.

3.7. Methods of Quantitating Colony Number and Size

Colony number and size distribution are best determined by image analysis *(22)*. It should be noted that the method described here is just one of a number

Fig. 3. A typical setup for the analysis of fibroblastic colonies. The stained cultures are photographed over a white-light transilluminator using a Kodak DC50 digital camera and the images downloaded to a computer. The images are then processed and analyzed.

of image analysis based methods of colony counting *(23–26)* all of which suffer from the weakness of being unable to resolve colonies at the periphery of the culture vessel and colonies that merge into each other. Automated methods perform considerably better than manual ones in that they are totally objective and do not suffer from operator fatigue. The system described here was chosen because much of the hardware is already in use in most laboratories and the software is freely available and relatively cheap.

3.8. Acquiring Images for Colony Quantitation

1. Place the Petri dishes in an appropriately sized template over a white light transilluminator.
2. Acquire the image using a Kodak DC50 digital camera mounted on a camera (**Fig. 3**; *see* **Note 8**).

3.9. Processing the Image

1. To analyze the images obtained with the digital camera (**Fig. 4A,E**) they first have to be converted to a format compatible with the IQ software using Photoshop 4.0.
2. Owing to the uneven surface of the individual colonies, the IQ software will recognize larger colonies as several distinct colonies. This is rectified by applying to the image a Gaussian blur with a radius of two pixels (**Fig. 4B,F**) and then a median filter with a radius of two pixels (**Fig. 4C,G**). This has the effect of
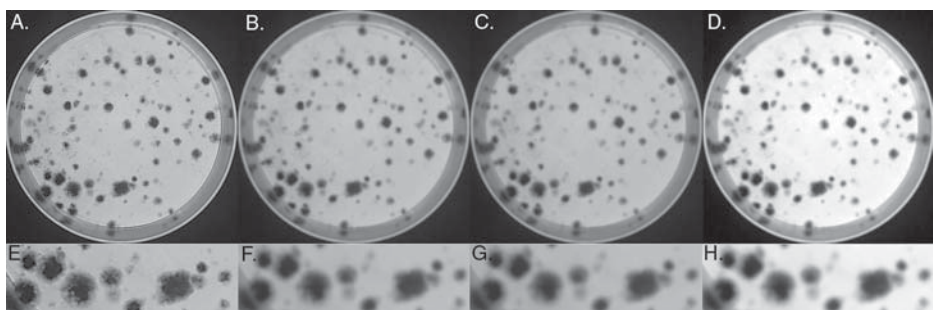
Fig. 4. Processing the acquired image. In the unprocessed images (**A**, **E**), the surface of the individual colonies is somewhat uneven and would be recognised as several distinct colonies. This is rectified by applying a gaussian blur with a radius of two pixels (**B**, **F**) and then a median filter with a radius of two pixels (**C**, **G**). This removes small variations in intensity and isolated pixels whose values differ from those of their surroundings. To make the analysis quantitative, the image levels are adjusted such that the background intensity is set to zero and black is set to 255 (**D**, **H**). The image is then converted to an 8-bit grayscale TIFF image, saved, and analyzed.

   removing small variations in intensity by evening out differences between adjacent pixels and also removing isolated pixels whose values differ from those of their surroundings. To make the analysis quantitative, adjust the image levels such that the background intensity is set to zero, and black (i.e., the area where the Petri dish is masked off) is set to 255 (**Fig. 4D,H**).

3. Lastly, convert the image to an 8-bit grayscale TIFF image and save it. The IQ software, like many image analysis packages, can analyze only grayscale images.

3.10. Analyzing the Image Using the IQ Program

   Import the 8-bit grayscale images into the IQ program (see **Note 9**). Mark the area of interest and analyze this using the colony counting mode. Colonies can be selected according to both their size and intensity. In the study shown in **Fig. 4**, colonies of at least 20 pixels (corresponding to 1 mm) in diameter and having an intensity of at least 20 gray levels above background (corresponding to approx 80 cells) were selected. The software then assigns an identity to each colony and calculates its coordinates, surface area, and intensity (**Table 1**).

4. Notes

1. Choice of medium: Other media can be used instead of DMEM, the main criterion being the presence of 4500 mg/L of glucose. α-MEM can also be used, although in pharmacological studies it is difficult to get an increase in colony number using bone anabolic drugs with this medium. It should be noted that the absence of phenol red leads to decreased colony number and differentiation. The reason for this is unknown and does not appear to be related to its estrogenic

Table 1
Extract from the Report Generated After Analysis of the Petri Dish Shown in Fig. 3

Bio Image Colony Data Report
Image: image1g.bio   Date: 22-MAY-101   Time: 11:56:25
Number of colonies: 130
Area: 4143.71
% Area: 8.96

Colony #	Colony x	Colony y	Int.	Bkgd.	Area	% Area	Add	Colony Name
1	257	45	0.51	0.02	6.09	0.15	N	
2	306	56	0.05	0.04	1.27	0.03	N	
3	341	68	0.30	0.04	2.08	0.05	N	
4	216	83	0.18	0.02	2.05	0.05	N	
5	85	108	0.27	0.04	1.27	0.03	N	
6	160	101	0.09	0.03	1.18	0.03	N	
7	189	107	0.14	0.02	1.74	0.04	N	
8	212	103	0.39	0.02	5.25	0.13	N	
9	277	105	0.35	0.01	4.91	0.12	N	
10	303	106	0.58	0.01	7.34	0.18	N	
11	344	97	0.33	0.01	1.90	0.05	N	
12	92	113	0.05	0.03	0.37	0.01	N	
13	91	124	0.05	0.03	0.93	0.02	N	
14	231	115	0.43	0.02	3.17	0.08	N	
15	316	125	0.33	0.01	4.32	0.10	N	

The data for the first 15 colonies is shown and it can be seen that a total of 130 colonies were detected and that these covered 8.96% of the area selected. The colony coordinates, intensity, and area are given for each colony and these data can be imported into packages such as Excel and analyzed statistically.

properties. For reasons that are unclear, some batches of FCS will not support collagen accumulation or calcification. This be rectified by using 5% FCS and 5% "serum supreme," a supplemented newborn calf serum. Some laboratories use ascorbate-2-phosphate in place of ascorbate but we have found that this leads to a nonspecific overcalcification.

2. Fixation: Industrial methylated spirit can be used instead of 70% ethanol.
3. Other methods of ALP staining: Other substrates and dyes can be used for ALP staining such as naphthol phosphate AS-MX, fast red TR, or fast blue B, but it is not possible to destain them adequately.
4. Methods of euthanasia and sex of animals: Other methods of euthanasia may also be used. It is best to use male rats, as the hormonal variations during the estrous cycle in female rats can have a pronounced effect on the colony number achieved. Surgery (e.g., orchidectomy, ovariectomy, and sham procedures) have dramatic effects on colony number that last several weeks.

5. Methods of harvesting bone marrow cells: The centrifugation method is optimized for use with rat bones; however, with very minor modifications it can be adapted for use with mouse bones and with human bone chips. Another method of harvesting is to flush the cells from the bone using a syringe but the variability of the yield will be greatly increased. This is of particular importance when performing ex vivo studies, in which the near 100% recovery of the centrifugation method improves reproducibility greatly.

6. Volumes of culture medium used to harvest cells: When carrying out ex vivo cultures, changes in the numbers of other bone marrow cell types can have a confounding effect on the frequency of CFU-f. For this reason, when carrying out these kinds of experiments the cells are recovered in a constant volume of culture medium (10 mL per bone for a 200-g rat) and 0.5 mL of the resultant suspension is used in the culture. In this way the number of CFU-f per bone can be calculated and is largely independent of changes in the overall bone marrow cell population.

7. The overall cell viability is between 70% and 80%.

8. Acquiring images for colony quantitation: Position the camera stand so that the Petri dish fills as much of the image as possible. With careful positioning, images from dishes that have been stained sequentially can be easily aligned. There are now a good selection of digital cameras suitable for this type of work. The main criteria are the size of the memory and the speed of downloading. We have found that increasing the resolution beyond 800 × 600 pixels is unnecessary.

9. Image analysis programs: The IQ Bioimage software program described here is no longer available. There are a number of other cheap packages available dedicated to colony counting such as MACE (Weiss Associates, Branford, CT, USA; www.colonycount.com) and a system is also being developed by The Gray Laboratory (Middlesex, UK; *see* **ref. *26***) which will soon be on the market. Alternatively, with some ingenuity, other software can be adapted to count colonies such as NIH image or the Leica Q Win software. There are also a number of dedicated colony counting systems on the market that, although designed to count bacterial colonies, will also count fibroblastic colonies. They are somewhat expensive, being of the order of £10,000 (approx $15,000) or more.

References

1. Mundy, G. R. (1995) No bones about fluoride. *Nat. Med.* **1**, 1130–1131.
2. Friedenstein, A. J. (1990) Osteogenic stem cells in the bone marrow. *Bone Miner. Res.* **7**, 243–272.
3. Maniatopoulos, C., Sodek, J., and Melcher, A. H. (1988) Bone formation in vitro by stromal cells obtained form bone marrow of young rats. *Cell Tissue Res.* **254**, 317–330.
4. Nefussi, J-R., Boy-Lefevre, M. L., Boolekbache, H., and Forest, N. (1985) Mineralization in vitro of matrix formed by osteoblasts isolated by collagenase digestion. *Differentiation* **29**, 160–168.
5. Bellows, C. G., Aubin, J. E., Heersche, J. N. M. and Antosz, M. E. (1986) Mineralised bone nodules formed in vitro from enzymatically released rat calvarial cell populations. *Calcif. Tissue Int.* **38**, 143–154.

6. Stein, G. S., Lian, J. B. and Owen, T. A. (1990) Relationship of cell growth to the regulation of tissue specific gene expression during osteoblast differentiation. *FASEB J.* **4**, 3111–3123.

7. Bellows, C. G. and Aubin, J. E. (1989) Determination of numbers of osteoprogenitors present in isolated fetal rat calvarial cells in vitro. *Dev. Biol.* **133**, 8–13.

8. Scutt, A. and Bertram, P. (1995) Bone marrow cells are targets for the anabolic actions of prostaglandin E_2 on bone: induction of a transition from non-adherent to adherent osteoblast precursors. *J. Bone Miner. Res.* **10**, 474–489.

9. Still, K. and Scutt, A. (2001) Stimulation of CFU-f formation by prostaglandin E_2 is mediated in part by its degradation product, prostaglandin A_2. *Prostaglandins* **65**, 21–31.

10. Pitaru, S., Kotov-Emeth, S., Noff, D., Kaffuler, S., and Savion, N. (1993) Effect of basic fibroblast growth factor on the growth and differentiation of adult stromal bone marrow cells: enhanced development of mineralized bone-like tissue in culture. *J. Bone Miner. Res.* **8**, 919–929.

11. Gronthos, S., Simmons, P. J., Graves, S. E., and Robey, P. G. (2001) Integrin-mediated interactions between human bone marrow stromal precursor cells and the extracellular matrix. *Bone* **28**, 174–81.

12. Walsh, S., Jordan, G. R., Jefferiss, C., Stewart, K., and Beresford, J. N. (2001) High concentrations of dexamethasone suppress the proliferation but not the differentiation or further maturation of human osteoblast precursors in vitro: relevance to glucocorticoid-induced osteoporosis. *Rheumatology* **40**, 74–83.

13. Scutt, A., Kollenkirchen, U., and Bertram P. (1996) The effect of age and ovariectomy on fibroblastic colony-forming unit numbers in rat bone marrow. *Calcif. Tissue Int.* **59**, 309–310.

14. Erben, R. G., Scutt, A. M., Miao, D., Kollenkirchen, U., and Haberey, M. (1997) Short-term treatment of rats with high-dose calcitriol stimulates bone formation in vivo and increases the number of osteoblast precursor cells in the bone marrow. *Endocrinology* **138**, 4629–4635.

15. Nishida, S., Yamaguchi, A., Tanizawa, T., et al. (1994) Increased bone formation by intermittent parathyroid hormone administration is due to the stimulation of proiliferation and differentiation of osteoprogenitor cells in the bone marrow. *Bone* **15**, 717–723.

16. Weinreb, M., Suponitzky, I., and Keila, S. (1997) Systemic administration of an anabolic dose of PGE2 in young rats increases the osteogenic capacity of bone marrow. *Bone* **20**, 521–526.

17. Jilka, R. L., Weinstein, R. S., Takahashi, K., Parfitt, A. M., and Manolagas, S. C. (1996) Linkage of decreased bone mass with impaired osteoblastogenesis in a murine model of accelerated senescence. *J. Clin. Invest.* **97**, 1732–1740.

18. Di Gregorio, G. B., Yamamoto. M., Ali, A. A., et al. (2001) Attenuation of the self-renewal of transit-amplifying osteoblast progenitors in the murine bone marrow by 17 beta-estradiol. *J. Clin. Invest.* **107**, 803–812.

19. Jilka, R. L., Takahashi, K., Munshi, M., Williams, D. C., Roberson, P. K., and Manolagas S. C. (1998) Loss of estrogen upregulates osteoblastogenesis in the murine bone marrow. Evidence for autonomy from factors released during bone resorption. *J. Clin. Invest.* **101**, 1942–1950.

20. Kajkenova, O., Lecka-Czernik, B., Gubrij, I., et al. (1997) Increased adipogenesis and myelopoiesis in the bone marrow of SAMP6, a murine model of defective osteoblastogenesis and low turnover osteopenia. *J. Bone Miner. Res.* **12**, 1772–1779.

21. Dobson, K. R., Reading, L., Haberey, M., Marine, X., and Scutt, A. (1999) Centrifugal isolation of bone marrow from bone: an improved method for the recovery and quantitation of bone marrow osteoprogenitor cells from rat tibiae and femurae. *Calcif. Tissue Int.* **65**, 411–413.

22. Dobson, K., Reading, L., and Scutt, A. (1999) A cost effective method for the automatic quantitative analysis of fibroblastic-colony forming units with osteoblastic potential. *Calcif. Tissue Int.* **65**, 166–172.

23. Parry, R. L., Chin, T. W., and Donahoe, K. (1991) Computer-aided cell colony counting. *BioTechniques* **10**, 772–774.

24. Nefussi, J. R., Ollivier, A., Oboeuf, M., and Forest, N. (1997) Rapid nodule evaluation computer-aided image analysis procedure for bone nodule quantification. *Bone* **20**, 5–16.

25. Hoekstra, S. J., Tarka, D. K., Kringle, R. O., and Hincks, J. R. (1998) Development of an automated bone marrow colony counting system. *In Vitro Mol. Toxicol.* **11**, 207–213.

26. Barber, P. R., Vojnovic, B., Kelly, J., et al. (2001) Automated counting of mammalian colonies. *Phys. Med. Biol.* **46**, 63–76.

4

Osteocyte Isolation and Culture

Peter J. Nijweide, Arie van der Plas, Marcel J. Alblas, and Jenneke Klein-Nulend

1. Introduction

Osteocytes are the most abundant cells in bone. Although individual osteocytes are buried in an isolated position within bone matrix, they remain in contact with one another and with cells on the bone surface by long cell processes that run via small channels, termed canaliculi, through the bone matrix. Where the cell processes of two osteocytes meet in a shared canaliculus, gap junctions provide intracellular contact *(1)*. For a long time osteocytes were outside the mainstream of bone research. Increasing interest in the mechanoregulation of bone has changed this, and today there is a general consensus that osteocytes play a pivotal role as mechanosensors and effectors in bone *(2)*. Whether osteocytes have other functions remains to be elucidated.

The anatomical location of osteocytes deep within bone has proved to be a major obstacle in studying the role that osteocytes play in bone metabolism. Osteocytes depend for their activities and survival on the diffusion of oxygen, hormones, nutrients, and waste via the canaliculi. The bone tissue culture methods that have been used so successfully in the studies of osteoblast and osteoclast activity are therefore generally of little value in the evaluation of osteocyte function. Bone explants have to be very limited in size to allow sufficient transport of nutrients to and from the osteocytes, and in fetal bone tissues the osteocyte contribution to the cellular component is very small.

Direct isolation of osteocytes is therefore the method of choice to study osteocyte physiology *(3)*. Three major problems arise, however. First, how does one isolate live osteocytes from the bone matrix in sufficient numbers to study? Second, how can osteocytes be separated from other cells and how can the population be kept homogeneous? Third, how can osteocytes be recognized in

culture, as the cells tend to lose some of their morphological characteristics when they are removed from their three-dimensional tissue structure?

This chapter describes the isolation of osteocytes from 18-d-old fetal chicken calvariae. Calvariae of this age are used because at that developmental stage the calvariae are not yet too heavily calcified to allow collagenase to liberate matrix-entrapped cells. The isolation of these cells is facilitated by mild EDTA treatments alternating with collagenase treatments. The choice of fetal *chicken* calvariae is important because in this species the periostea from both calvaria surfaces can be dissected relatively easily, which results in the absence of most periosteal cells in the collagenase released cell population. Furthermore, fetal chicken calvariae have a much broader layer of osteoid on their surfaces than mouse or rat calvariae. Finally, the availability of a monoclonal antibody (MAb) that specifically recognizes osteocytes allows the purification of osteocytes from mixed cell populations (immunodissection). The MAb used in the separation procedure is also used to recognize osteocytes in cell cultures.

2. Materials

2.1. Fertilized Chicken Eggs

Incubate the eggs at 38.5°C in a humid air atmosphere for 18 d. The incubator should have a mechanism that turns the eggs regularly through 180°, about 10 times per hr. Fertilized eggs can be stored for 2–3 wk at 14–16°C before development of the embryo is started by incubation in the incubator.

2.2. Media and Solutions

1. Hanks' balanced salt solution (HBSS) from Gibco-BRL Life Technologies.
2. Phosphate-buffered salt solution (PBS): 137 mM NaCl, 2.7 mM KCl, 8.1 mM Na$_2$HPO$_4$ and 1.5 mM KH$_2$PO$_4$. Adjust to pH 7.4.
3. Isolation salt solution (ISS)*(4)*: 70 mM NaCl, 30 mM KCl, 1 mM CaCl$_2$, 10 mM NaHCO$_3$, 25 mM N-2-hydroxyethylpiperazine-N'-2-ethanesulfonic acid (HEPES), 5 mg/mL of glucose (Sigma), and 1 mg/mL of bovine serum albumin (BSA) (ICN Biomedicals Inc.). Adjust to pH 7.4 at 37°C.
4. Isolation medium: Add 7 μmoles/L of N^α-tosyl-L-lysyl-chloromethane hydrochloride (BDH Biochemicals) and 1 mg/mL of collagenase Type I (Sigma) to ISS. The N^α-tosyl-L-lysyl-chloromethane hydrochloride is added to inhibit proteases other than collagenase *(4)*.
5. EDTA solution: 4 mM EDTA in PBS. Adjust pH to 7.4.
6. Wash fluid: 10% Inactivated chicken serum (Sigma) in α-minimum essential medium (α-MEM) (Gibco). For inactivation, heat serum for 30 min at 56°C and centrifuge at 200g for 5 min.
7. Culture medium: α-MEM fortified with 2% inactivated chicken serum, 0.2 g/L of glutamine (Sigma), 0.05 g/L of ascorbic acid (Sigma), 0.05 g/L of gentamicin (Sigma) and 1 g/L of glucose.

8. Trypsin–EDTA (TE) solution: 0.05% Trypsin 1:250 (Sigma) and 0.27 m*M* EDTA in PBS.

9. Coated bead suspension: Mix DNA-conjugated beads (CELLection™ Pan Mouse IgG kit from DYNAL), with MAb OB7.3 IgG (*see* **Subheading 2.3.**) and PBS to a final concentration of 15 μg of IgG / 8×10^7 beads/mL. Two hundred and fifty microliters of this suspension is needed for the isolation of osteocytes from 40 calvariae. Incubate overnight at 4°C, gently shaking the suspension, and store at 4°C until use. Wash the beads shortly before use two times with 2% chicken serum in HBSS. For this the bead suspension is put in a holder next to a magnet (DYNAL) that attracts the magnetic beads to one side of the tube, allowing the removal of the suspension fluid. Finally, resuspend the IgG-coated beads in 250 μL of 2% chicken serum in HBSS.

10. Zinc fixative: Dissolve 0.5% zinc chloride and 0.5% zinc acetate in 0.1 *M* Tris-acetate buffer, pH 4.5.

2.3. MAb OB7.3

The antibody was originally raised according to standard procedures by injecting bone cells isolated from calvariae of 18-d-old fetal chickens into BALB/c mice *(5)*. In bone sections it recognizes only osteocytes embedded in osteoid or in calcified matrix (**Fig. 1A,B**). In cultures of cells enzymatically isolated from fetal chicken calvariae MAb OB7.3 stains a minority of the isolated cells. The positive cells show an osteocyte-like morphology in culture (**Fig. 1C,D** and **Fig. 2**). The antibody may be obtained from either Dr. J. Klein-Nulend (Deptartment of Oral Cell Biology, ACTA-Vrije Universiteit, Amsterdam, The Netherlands) or from Dr. K. E. de Rooij (Deptartment of Endocrinology and Metabolism, Leiden University Medical Center, Leiden, The Netherlands).

3. Methods
3.1. Tissue Dissection

1. Remove the eggs from the incubator after 18 d. Keep one of the eggs with the blunt side upwards where the air chamber is located. Crack the top of the shell and peel the shell off to the edge of the air chamber with a pair of sterile tweezers. Stab one leg of a second pair of tweezers underneath the white shell membrane and the chorioallantoic membrane. Close the tweezers and peel both membranes off in one movement.

2. Grasp the embryo under its head with a curved forceps, lift it a little above the egg, and decapitate underneath the forceps. The body of the embryo will fall back into the egg. Transfer the head to a Petri dish with some HBSS placed on ice. Resterilize tweezers and forceps by dipping into ethanol (100%) and burning the ethanol off.

3. Make a cut in the back of the neck with a small pair of scissors. Hold the head by the bill with tweezers and tear the skin off in the direction of the bill. Cut the calvaria loose along the edge and cut it into two parts through the central suture.
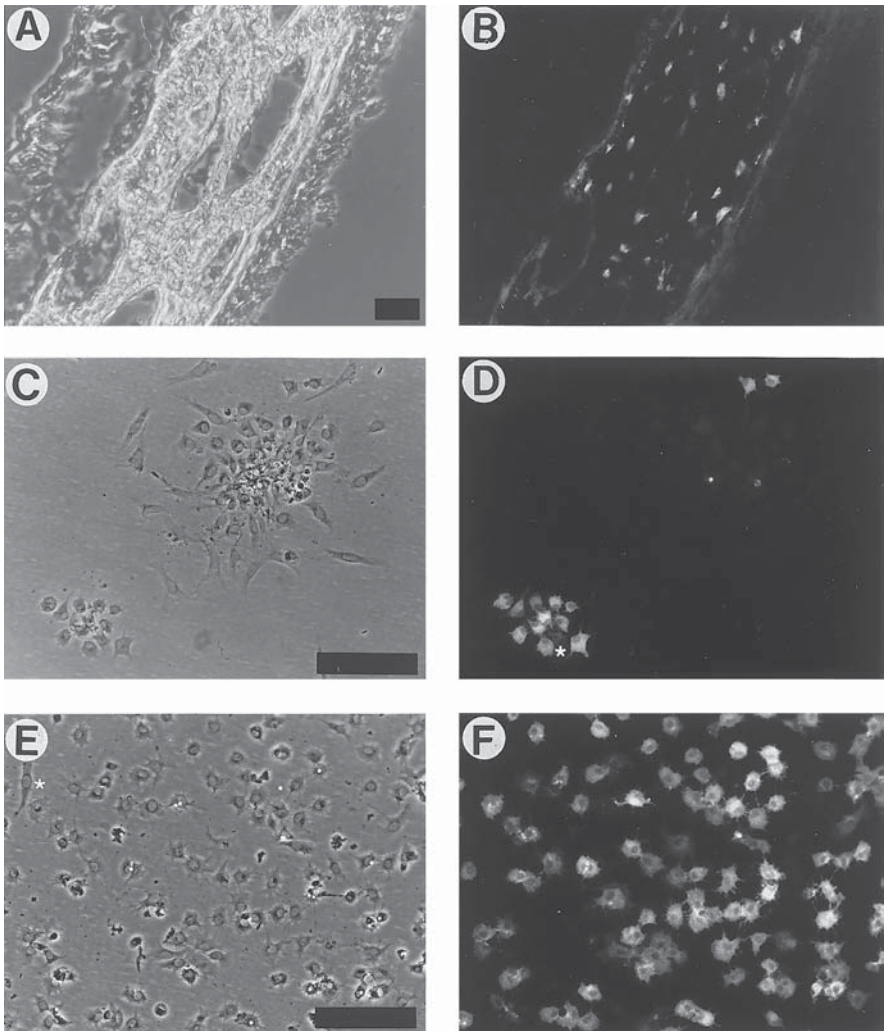
Fig. 1. Frozen section of a calvaria (**A, B**) and air-dried cell cultures (**C–F**) stained with MAb OB7.3. *Left side*: Phase contrast. *Right side:* Immunofluorescence. (**A,B**) Section of an 18-d-old fetal chicken calvaria. Note that only the osteocytes inside the bone matrix are stained. (**C,D**) OBmix after 1-d of culture. In the *lower left corner* a group of osteocytes with one MAb OB7.3-negative cell (*white asterisk*); in the *upper right corner* an osteoblast colony with two osteocytes. (**E,F**) Purified osteocyte population. Note the contaminating fibroblast-like cell in the *upper left corner (white asterisk)*. Scale bar = 100 μm. (Reproduced from *J. Bone Miner. Res.* 1992; **7**, 389–396 with permission of the American Society for Bone and Mineral Research.)

4. Put the calvaria halves in a droplet of sterile HBSS and remove the ectocranial and endocranial periostea under a dissecting microscope with small scalpels.
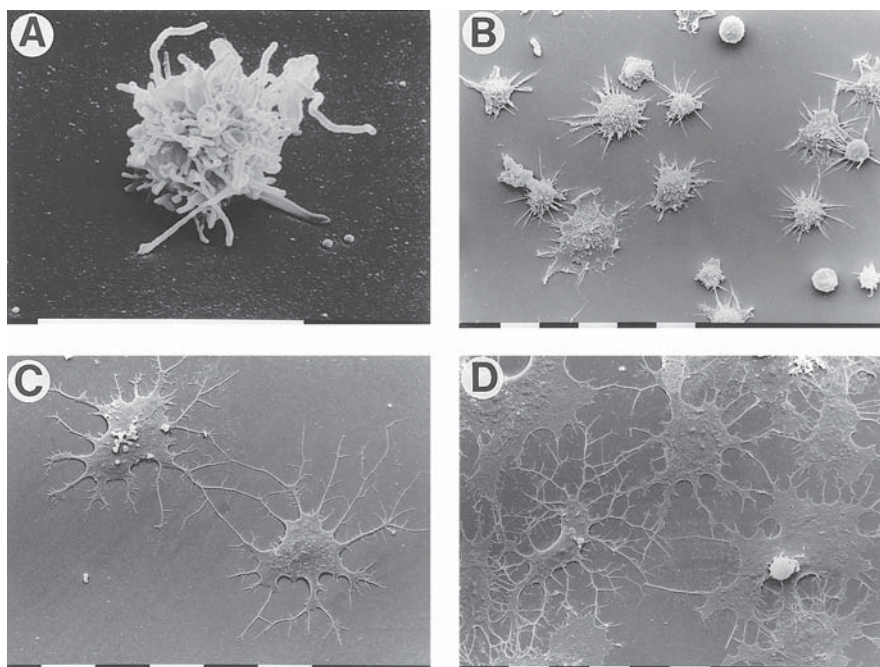
Fig. 2. Scanning electron micrographs of isolated osteocytes. (**A**) Osteocyte 5 min after seeding. The osteocyte is already attached and has formed finger-like projections in all directions. (**B**) Osteocytes 20 min after seeding. The cell processes in the plane of the support have elongated, whereas the processes perpendicular to the support have disappeared. Note the presence of two magnetic beads. (**C**) Two osteocytes have made contact with each other via their cell processes after 24 h of culture. (**D**) Extensive network of flattened osteocytes with many branched cell processes after 48 h of culture. Scale bar = 10 μm. (Reproduced from *J. Bone Miner. Res.* 1992; **7**, 389–396 with permission of the American Society for Bone and Mineral Research.)

Transfer the "bare" calvaria halves into a Petri dish with HBSS and keep on ice.
5. Repeat these actions for all eggs. Generally we use 40 eggs in one isolation session. Too many eggs would make the dissection procedure too long; a too small number of eggs is inefficient and relatively decreases the number of isolated osteocytes.

3.2. Isolation of OBmix

Perform all incubations in the steps below in a shaking water bath set at 37°C.

1. Transfer all calvaria halves to a small flask containing 3 mL of isolation medium diluted 10 times with ISS (final collagenase concentration: 0.1 mg/mL). Incubate for 10 min and discard the supernatant. Repeat this step once. (The discarded supernatants will contain primarily damaged cells and erythrocytes.)

2. Add 3 mL of isolation medium (final collagenase concentration: 1 mg/mL) to the calvariae. Incubate for 15 min and discard the supernatant. (This will contain primarily fibroblastic cells and some osteoblasts.) Wash calvariae three times with 2.5 mL of PBS each time; discard the PBS washings.

3. Add 4 mL of EDTA solution to the calvariae. Incubate for 10 min and remove the supernatant.

4. Centrifuge at 4°C for 3 min at 200g and resuspend the cell pellet in wash fluid. This cell suspension is termed fraction 1.

5. Wash the calvariae three times, once with 2 mL of PBS, and twice with 1 mL of ISS. Add the washings to fraction 1 from **step 4** and keep on ice.

6. Add 4 mL of isolation medium to the calvariae and incubate for 45 min. Remove the supernatant; centrifuge at 4°C for 3 min at 200g.

7. Resuspend the sedimented cells in wash fluid. This cell suspension is termed fraction 2.

8. Wash the calvariae three times with 1 mL of PBS. Add the washings to fraction 2 from **step 7**.

9. Combine fractions 1 and 2, centrifuge at 4°C for 3 min at 200g and resuspend the sedimented cells in culture medium. This is the OBmix population. It contains osteoblasts, 20–30% osteocytes, and a few fibroblasts (**Fig. 1C,D**).

10. Determine the cell concentration with, for example, a Burker-Türk hemocytometer and increase the volume of the cell suspension until a concentration of about 2×10^6 cells/mL is obtained.

11. Seed 0.5 mL of the cell suspension into small (50-mL) culture flasks containing 3 mL of culture medium per flask. Generally about four culture flasks (4×10^6 cells) will be needed.

12. Culture the cells for 24 h at 37°C in a humid atmosphere of 5% CO2 in air (*see* **Note 1**).

3.3. Isolation of Osteocytes

1. Remove the culture medium from the culture flasks on the next day, and rinse three times with PBS. Add 3 mL of TE solution per flask and incubate for 3 min at 37°C. Stop the trypsin activity by adding 0.3 mL of chicken serum per flask and hit the lab table three times with the flasks to loosen the OBmix cells from the bottom.

2. Disperse the cells by repeated pipetting over the surface bearing the cell layer.

3. Remove cell clumps by sieving the cell suspension through a nylon sieve of 30-μm mesh, sediment the cells at 200g for 3 min, discard the supernatant and resuspend the cells in 2 mL of cold (4°C) 2% chicken serum in HBSS. The sieving procedure is necessary to achieve a single cell suspension. OBmix cells, in particular the osteocytes, tend to form clumps of (probably) gap junction-coupled cells. These clumps will, however, contain not only osteocytes but also osteoblasts that will later quickly overgrow the nondividing osteocytes (*see* **Note 2**). Centrifuge the cell suspension (200g, 3 min) and resuspend the sedimented cells in 125 μL of HBSS–2% serum.

4. Add 125 μL of coated bead suspension, and incubate for 15 min in a rotator (60 rpm) at 4°C. Take good care during this step that beads and cells remain in suspension.

5. Separate the bead-bound osteocytes from the osteoblasts with the magnet. Wash the bead-bound osteocytes four times with 2% chicken serum in HBSS (using the magnet to collect the osteocytes) and finally resuspend the osteocytes in 200 μL of 2% chicken serum in HBSS.

6. Add a fresh batch of 125 μL of coated beads to the osteoblast fraction and repeat the separation procedure.

7. Combine both two bead-bound osteocyte fractions, separate the cells with the magnet, and resuspend them in 100 μL of culture medium. Count the number of cells per unit volume. The bead-bound osteocytes can now either be seeded and cultured or can be freed from their beads and cultured (*see* **Note 3**).

8. For immediate removal of the beads, wash the bead-bound osteocytes once with PBS–2% chicken serum, separate the cells with the magnet, and resuspend them in 100 μL of PBS–2% chicken serum.

9. Add 4 μL of releasing buffer containing 50 U of DNase/μL (CELLection™ Pan Mouse IgG kit) and incubate 15 min at 37°C in a shaking water bath.

10. Separate the beads from the osteocytes with the magnet. Wash the beads two times with PBS–2% chicken serum to remove all osteocytes from the beads and add the washings to the liberated osteocytes. Remove the last contaminating beads with the magnet.

11. Centrifuge the cell suspension, discard the supernatant, and resuspend the osteocyte pellet in culture medium.

12. If it is not necessary to use the isolated osteocytes immediately, it is much easier to seed the bead-bound osteocytes in culture medium in a Petri dish. The next day, the beads can simply be removed by washing the cell layer. DNase treatment is not needed. The osteocyte yield from 40 calvariae is generally approx 200,000 osteocytes (**Fig. 1E,F**).

13. Attached osteocytes can be removed from their support by a short treatment with TE solution. After washing and reseeding, the osteocytes reacquire their typical morphology of stellate cells in secondary culture (*see* **Note 4**).

4. Notes

1. Optimizing isolation of OBmix: The actual procedure one has to use depends heavily on the activity of the collagenase. If you start with a new batch of collagenase, you may have to adapt the procedure. For example, **step 2** may have to be shortened, if too many osteocytes are isolated in this step. If too many fibroblasts are still present in fraction 1, **step 2** should be repeated. **Steps 3–6** have to be repeated if many cells, in particular osteocytes, are isolated in these repeated steps. The yield of OBmix cells from 40 calvariae following the protocol in **Subheading 3.2.** is generally $3–4 \times 10^6$ cells. About 20–30 % of these cells are osteocytes (i.e., about 10^6 osteocytes). Most of the OBmix cells are, however, present in clumps of osteoblasts, osteocytes, or mixtures of osteoblasts and osteocytes.

Trying to isolate osteocytes from this population results primarily in the isolation of clumps of osteocytes often containing osteoblastic cells with high proliferative capacity. Sieving the original OBmix population (*see* **Subheading 3.2.**, **step 9**) before immuno-isolation of osteocytes results in a very low osteocyte yield. Culturing the OBmix population for 24 h allows the cells of the clumps to separate themselves from each other, increases the number of single cells after the trypsin–EDTA treatment and therefore increases the osteocyte yield.

2. Reducing numbers of contaminating cells: Generally, we use 2% or less chicken serum in the culture medium. Osteocytes are postmitotic cells. Because serum strongly stimulates cells capable of mitosis to proliferate, isolated osteocytes will therefore be quickly overgrown in the presence of serum by contaminating cells. A too low serum concentration will, however, deteriorate cell quality. In view of this, we recommend that osteocyte cultures be used for experimentation as soon as possible after isolation.

3. Purity of the osteocyte population. If the isolation procedure is used routinely, it is advisable to examine regularly the purity of the osteocyte populations. Contamination of the osteocyte isolate may be determined by seeding a small sample of the osteocyte suspension in a culture dish. Incubate until the cells are firmly attached (4–6 h), and immunostain the cells for the presence of MAb 7.3. Note that removal of the beads will not remove the antibody from the cell surface! At least 95% of the cells should be positive for the antibody **(Fig. 1E,F).**

4. Phenotypic characterization of osteocytes: In bone, osteocytes are fully defined by their location within the bone matrix. For isolated osteocytes other markers are needed to establish their identity.

   a. Stellate morphology. Avian osteocytes reacquire the stellate morphology of osteocytes in situ after isolation and attachment *(6)* (**Fig. 2**). This may be also the case for murine osteocytes *(7)*.

   b. Antibodies. Three osteocyte-specific MAbs have been described in the literature: MAb OB7.3 *(5)*, MAb OB37.11 *(8)*, and MAb SB5 *(9)*. All three are specific for avian osteocytes and do not cross-react with mammalian cells. The identities of the three antigens involved have not been reported, although that of MAb OB7.3 is recently elucidated *(10)*. So far, MAb OB7.3 is the only antibody used for osteocyte isolation. Other antibodies, but apparently less specific, are E11, a monoclonal antibody that reacts specifically with highly mature osteoblasts and with osteocytes in tissue sections of rat bone *(11)* and antibodies against fimbrin, an actin-bundling protein that is abundantly present in osteocytes *(12)*. The OB7.3 antigen is easily destroyed by harsh fixation procedures. For the immunostaining of osteocytes in tissues unfixed, air-dried, frozen sections are recommended (**Fig. 1A,B**). Cell cultures can be stained by incubating live cells with MAb OB7.3 in HBSS for 30–60 min at room temperature or by washing the cells with HBSS followed by air drying and incubation with the antibody (**Fig. 1C–F**). Also a short (10 min) fixation with 2–4% paraformaldehyde at 4°C will leave enough antigen intact for a reasonable staining. More recently, we have used zinc fixative successfully

for the fixation and immunostaining of cell cultures. Zinc fixative does not appear to damage the OB7.3 antigen. A further advantage of this fixative is that cell cultures can be kept in the fixative for a long time (days) without loss of immunoreactivity of the antigen. An osteocyte specific antibody similar to MAb OB7.3 but reacting with nonavian cells is as yet not reported. Mikuni-Takagaki et al. have used a repeated collagenase treatments of newborn rat calvariae. They describe that their last, seventh fraction contains many cells with an osteocyte-like morphology.

c. Protein products. Several proteins, such as osteocalcin and osteopontin, have been demonstrated in or around osteocytes in relatively high amounts *(13)*. Alkaline phosphatase, a cell surface bound enzyme, is generally low in osteocytes, in particular compared to the amounts present on osteoblasts. CD44, a membrane-bound glycoprotein that is involved in cell attachment to matrix proteins, is generally highly expressed in osteocytes *(14)*, but is also expressed by other cells in bone. The production and presence of these proteins is not specific for osteocytes but can be used as additional markers for osteocyte identification.

References

1. Doty, S. B. (1981) Morphological evidence of gap junctions between bone cells. *Calcif. Tissue Int.* **33**, 509–512.
2. Nijweide, P. J., Burger, E. H., Klein-Nulend, J., and van der Plas, A. (1996) The osteocyte, in Principles of Bone Biology (Bilezikian, J. P., Raisz, L. G., and Rodan, G. A., eds.), Academic Press, San Diego, pp. 115–126.
3. Van der Plas, A., Aarden, E. M., Feijen, J. H. M., et al. (1994) Characteristics and properties of osteocytes in culture. *J. Bone Miner. Res.* **9**, 1697–1704.
4. Hefley, T. J. (1987) Utilization of FPLC-purified bacterial collagenase for the isolation of cells from bone. *J. Bone Miner. Res.* **2**, 505–516.
5. Nijweide, P. J. and Mulder, R. J. P. (1986) Identification of osteocytes in osteoblast-like cell cultures using a monoclonal antibody specifically directed against osteocytes. *Histochemistry* **84**, 342–347.
6. Van der Plas, A. and Nijweide, P. J. (1992) Isolation and purification of osteocytes. *J. Bone Miner. Res.* **7**, 389–396.
7. Mikuni-Takagaki, Y., Kakai, Y., Satoyoshi, M., et al. (1995) Matrix mineralization and the differentiation of osteocyte-like cells in culture. *J. Bone Miner. Res.* **10**, 231–242.
8. Nijweide, P. J., van der Plas, A., and Olthof, A. A. (1988) Osteoblastic differentiation, in *Cell and Molecular Biology of Vertebrate Hard Tissues, Ciba Foundation Symposium 136* (Evered, D. and Harnett, S., eds.), John Wiley & Sons, Chichester, UK, pp. 61–77.
9. Bruder, S. P. and Caplan, A. I. (1990) Terminal differentiation of osteogenic cells in the embryonic chick tibia is revealed by a monoclonal antibody against osteocytes. *Bone* **11**, 189–198.
10. Westbroek, I., De Rooij, K. E., and Nijweide, P. J. (2002) Osteocyte-specific monoclonal antibody MAb OB7.3 is directed against Phex protein. *J. Bone Miner. Res.* **17,** 845–853.

11. Wetterwald, A., Hoffstetter, W., Cecchini, M. G., et al. (1996) Characterization and cloning of the E11 antigen, a marker expressed by rat osteoblasts and osteocytes. *Bone* **18**, 125–132.

12. Tanaka-Kamioka, K., Kamioka, H., Ris, H., and Lim, S. S. (1998) Osteocyte shape is dependent on actin filaments and osteocyte processes are unique actin-rich projections. *J. Bone Miner. Res.* **13**, 1555–1568.

13. Aarden, E. M., Wassenaar, A. M., Alblas, M. J., and Nijweide, P. J. (1996) Immunocytochemical demonstration of extracellular matrix proteins in isolated osteocytes. *Histochem. Cell Biol.* **106**, 495–501.

14. Nakamura, H. and Ozawa, H. (1996) Immunolocalization of CD44 and the ERM family in bone cells of mouse tibiae. *J. Bone Miner. Res.* **11**, 1715–1722.

5

Isolated Osteoclast Cultures

Astrid Hoebertz and Timothy R. Arnett

1. Introduction

Osteoclasts are large, multinucleated cells formed by the fusion of hemato-poietic, mononuclear progenitors of the monocyte/macrophage lineage, and are the cells responsible for resorbing bone. Osteoclasts are usually few in number relative to other cell types in bone and are difficult to isolate because they are contained in a hard tissue; in addition, they are at the end of their prolifera-tion and differentiation cycle, presenting problems for the creation of osteo-clast cell lines. However, with the development, almost 20 years ago, of in vitro resorption pit formation models, using isolated primary, mature osteo-clasts and mineralized bone or dentine matrix as a substrate *(1,2)*, considerable progress was made in our understanding of osteoclast biology. Data from such short term cultures complements that obtained from bone organ culture resorp-tion models and long-term cultures of osteoclast forming hematopoietic stem cells derived from marrow or peripheral blood.

Boyde, Jones, Chambers, and colleagues developed the disaggregated osteoclast resorption assay in 1984 *(1,2)*. Variants of these assays were then widely adopted to study osteoclasts isolated from neonatal rat, rabbit, or chick long bones *(4,17*; *see* chapters by Collin-Osdoby et al., Chapter 6, and Coxon et al., Chapter 7). The method used in each case is extremely simple: osteo-clasts are relatively abundant in the bones of neonatal animals (reflecting the requirement for rapid growth modeling) and can be released mechanically by fragmenting the bones in a suitable medium. This can be achieved by either mincing the bones or scraping the exposed endosteal surfaces of longitudinally split bones, and the resulting cell suspension is settled onto bone or dentine discs and, after rinsing in saline to remove non-adherent cells, cultured for about 24 h. Under suitable conditions, osteoclasts can then excavate resorption

lacunae. Although this model has several limitations in attempts to study the whole physiological cascade of bone resorption, it provides an excellent tool for detailed studies of the cellular mechanisms involved in the destruction of mineralized bone matrix, especially since the application of confocal microscopy to study osteoclasts cultured on bone or dentine slices. Because osteoclasts sediment or adhere somewhat more rapidly than other cell types present in the mixed cell population released from fragmented bones, "functionally purified" osteoclast populations may be generated by careful adjustment of settling times and washing methods. Clearly, one of the most important factors in this assay system is to obtain adequate basal levels of resorption. This is accomplished by the use of slightly acidified culture medium, as first described by Arnett and Dempster *(4)*.

Assessment of resorption is typically achieved by simply counting the number of multinuclear (more than three nuclei) osteoclasts, stained histochemically for tartrate-resistant acid phosphatase, and the number and/or area of resorption pits, using the technique of reflected light microscopy, after staining the discs with toluidine blue to visualize pits *(5,17)*. This replaced the more complicated use of scanning electronic microscopy (SEM) to study resorption pits. Measuring the volume of each individual pit rather than discrete pit number or resorbed area is a more accurate method of assessing resorption *(6)* but is clearly more time consuming.

This chapter describes the isolation and short-term culture of osteoclasts obtained from neonatal rat long bones, which in principle resembles the isolation of osteoclasts from rabbit and chick long bones. A special focus is on the role of extracellular pH in osteoclast cultures (*see* **Note 1**).

2. Materials

1. Tissue culture medium: Minimum essential medium (MEM) supplemented with Earle's salts, 10% fetal bovine serum, 2 m*M* L-glutamine, 100 U/mL of penicillin, 100 μg/mL of streptomycin, and 0.25 μg/mL of amphotericin (Gibco, Paisley, UK) for the isolation and maintenance of neonatal rat osteoclasts. To achieve a basal level of resorption, the medium should be acidified by adding approx 10 mEq/L of hydrogen ions. This can be achieved by adding 85 μL of concentrated HCl per 100 mL of medium, as described by Goldhaber and Rabadjija (1987) *(7)* (*see* **Note 1**).
2. Phosphate-buffered saline (PBS): For storing tissues prior to use and for removing non-adherent cells from dentine discs.
3. HCl: Concentrated 11.5 *M* HCl to alter the pH of the culture medium.
4. NaOH: 6 *M* NaOH to alter the pH of the culture medium.
5. Diamond saw: Buehler "Isomet" diamond saw to cut dentine slices.
6. Dentine slices: For bone resorption assay.
   a. Prepare the dentine slices by cutting 250-μm thick transverse wafers from a block of dentine (*see* **Note 2**) using a diamond saw operating at about 60% of maximum speed with a moderate blade weighting.

    b. Soak the slices for 2 h in distilled water to reduce brittleness; and cut 5-mm diameter discs from the wet wafers using a standard "Rexel" single-hole paper punch. These discs fit neatly into the wells of 96-multiwell plates.

    c. Wash the discs extensively by sonication in multiple changes of distilled water and store dry at room temperature.

    d. Before use, number the discs using a graphite pencil to aid identification and sterilize by immersing for 1 min in 100% ethanol.

    e. Allow the discs to air-dry inside a tissue culture flow cabinet (> 30 min) and rinse with sterile PBS.

7. Animals: The number of animals to be used depends on the number of treatment groups in the experiment. It should be borne in mind that variation within treatment groups is usually quite high in osteoclast resorption assays. Therefore, at least five or six replicate dentine discs should ideally be allowed for each treatment group. Generally, four rat pups, aged 2–4 d, are required for six treatment groups, and five animals for seven or eight groups. It is not recommended that more than five animals are used because the pooled, dissected bones need to be chopped very quickly (*see* **Subheading 3.1.**).

8. Fixative: 2% glutaraldehyde in PBS; prepare fresh before use.

9. Tartrate resistant acid phosphatase (TRAP) staining: leukocyte acid phosphatase kit (Sigma Kit 387-A).

10. Cell removal solution: 0.25 *M* ammonium hydroxide.

11. Resorption pit staining solution: 1% (w/v) Toluidine blue in 1% (w/v) sodium borate solution.

12. Microscopes: A transmitted light microscope is used to count TRAP-positive osteoclasts and total number of cells. Number and/or area of resorption pits are determined using brightfield reflected light microscopy *(5,8)*. We use a Nikon "Labophot" 2A microscope, with 100 W epi-illumination and metallurgical objectives.

3. Methods

3.1. Isolation of Osteoclast from Neonatal Rat Long Bones

1. Prior to obtaining the cells, place sterile dentine discs into the wells of a 96-well plate, numbered side facing down, and add 50 µL of culture medium to each well. Incubate for 30 min at 37°C.

2. Prepare 5 mL of culture medium containing test and control substances for each group and add to individual wells of a six-well plate. Place in an incubator at 5% CO_2–95% air at 37°C for at least 30 min.

3. Euthanize neonatal (2–4 d) rat pups by cervical dislocation or decapitation. Cut the arms and legs off and dissect the long bones dissected free of muscle, connective tissue, and cartilage.

4. Transfer the bones to a 6-cm diameter sterile plate (non-tissue-culture treated) containing 3 mL of medium. Chop the bones finely with a scalpel blade, using fine forceps to hold the bones steady.

5. Create a suspension by aspirating the minced bones 10–20 times through a wide-mouth polyethylene 3-mL transfer pipet with the tip cut back such that the opening is about 5 mm in diameter.

6. Transfer the suspension (including the remaining small bone pieces) to a sterile bijou container and vortex-mix for 30 sec.
7. Allow the mixture to settle for a few sec and—avoiding the bone fragments—transfer the supernatant to a fresh bijoux tube, using a 1-mL polyethylene pipet.
8. Wash the dish and remaining bone fragments with 2 mL of culture medium, and vortex-mix briefly. Aspirate the supernatant and combine with the cell suspension from **step 7**.
9. Quickly add 100 μL of cell suspension to each well of the 96-well plate and allow to settle for 45 min at 37°C (*see* **Note 3**).
10. Carefully remove the discs (containing adherent cells) from the 96-well plates using fine forceps or a 19-gauge needle and rinse by dipping with gentle agitation in two changes of sterile PBS.
11. Transfer to preequilibrated culture medium containing test substances or vehicle in a six-well plate, such that each test or control well contains 5 mL of MEM and five or six replicate dentine discs.
12. Incubate for 24–28 h in a humidified atmosphere of 5% CO_2–95% air.
13. At the end of the experiment, measure the medium pH and pCO_2 using a clinical blood gas analyser, with careful precautions to prevent CO_2 loss (*see* **Note 4**).

3.2. Fixation and Staining

1. On termination of the experiment, wash the dentine discs twice in PBS.
2. Transfer to fixative for 5 min.
3. Wash twice with PBS and leave to air-dry.
4. Stain the wafers for TRAP-positive cells and stromal cells by following the directions in the kit and count TRAP-postitive multinucleated osteoclasts (*see* **Note 5**).

3.3. Quantitation of Resorption

1. Remove cells from the discs by sonication for 5 min in 0.25 *M* ammonium hydroxide. (*see* **Note 6**).
2. Stain the resorption pits by immersing in resorption pit staining solution for 2 min and allowing to air-dry (*see* **Note 7**).
3. Count the pits by scanning the entire surface of each disc using reflected light microscopy and a × 20 objective.
4. Express the results as number of pits/osteoclast or area resorbed/osteoclast and as pits/dentine disc (or area resorbed/dentine disc). It is usually preferable to normalize resorption to osteoclast numbers, as the latter may vary quite markedly within and between treatment groups (*see* **Note 8**).

3.4. Statistics

Depending on the data we routinely use one-way analysis of variance (ANOVA) or nonparametric tests (Mann–Whitney) to analyze experiments. Although often neglected, adjustments for multiple comparisons between treatment groups (e.g., the Bonferroni correction) are frequently needed (*see* **Note 9**).

4. Notes

1. Importance of pH: Extracellular pH is a critical factor in all bone resorption experiments. Rat osteoclasts are maximally activated to form resorption pits at pH ~6.9 and resorption is essentially "switched off" above pH ~7.2 (**Fig. 1**) *(4,8)*. Similar responses to extracellular acidification have been observed in all bone resorption systems examined to date, using cells or tissues derived from murine, avian or human sources (**Fig. 1B**) *(9–12)*. The action of many bone resorbing agents including parathyroid hormone *(4)*, 1,25-dihydroxyvitamin D_3 [1,25-$(OH)_2D_3$] *(3)*, extracellular nucleotides such as ATP *(14)* and ADP *(3)*, receptor activator of nuclear factor NF-κB ligand (RANKL) *(15)* is enhanced by acidification. Examples of the effects of pH are shown for RANKL and ADP in **Fig. 2A,B**. Conversely, alkalinization attenuates the osteolytic action of parathyroid hormone, 1,25-$(OH)_2$-D_3 and prostaglandin E_2 *(12)*. These results indicate that a low pH is an essential requirement for the activation process; and once this activation has occurred, further stimulation by a wide range of bone resorbing agents can take place. Some tissue culture media (including MEM) are buffered to pH ~7.20 when fully equilibrated with 5% CO_2; this value corresponds to normal interstitial pH and is considerably more acidic than blood pH (7.35–7.40). Other media, such as DMEM, contain higher levels of bicarbonate and consequently are buffered to a higher pH (~7.5 for DMEM) when equilibriated with 5% CO_2.The metabolic activity of cells cultured in the medium will act to lower the pH further; when cell numbers are high relative to the volume of medium, this effect can be sufficient to acidify the medium quite rapidly, with resultant activation of resorption pit formation. To activate resorption in a more controlled manner, relatively large volumes (≥0.5 mL/dentine disc/24 h) of preacidified culture medium should be used. MEM should be acidified by the direct addition of small amounts of concentrated HCl, which has the advantage of being self-sterilizing *(7,8)*. This has the effect of reducing HCO_3^- concentration (i.e., "metabolic acidosis") and producing an operating pH close to 6.95 in a 5% CO_2 environment (*see* **Fig. 3**), which is optimal for resorption pit formation *(8)*. Further acidification in CO_2–HCO_3^--buffered media does not enhance resorption greatly and may ultimately reduce cell survival. Addition of HCl has the effect of increasing medium chloride concentration slightly, but this does not appear to affect bone cell function. Culture medium can also be acidified to give an operating pH close to 7.0 by increasing the concentration of CO_2 to 10% (equivalent to a partial pressure of 85 mmHg; "respiratory acidosis"), while HCO_3^- remains constant (*see* **Fig. 3**). In organ culture systems at least, CO_2 acidosis is a less effective activator of resorption than HCO_3^- acidosis *(12,16)*. However, in contrast to the stimulatory effect of pH on osteoclast activity, the formation of osteoclasts from hematopoietic precursors is optimal at ~ pH 7.35–7.4 *(15,17)*, and is inhibited at low pH. For osteoclast formation experiments using mouse marrow cocultures, we obtained best results when culture medium (MEM) was alkalinized to pH ~7.35 by the addition of 10 meq/L of NaOH for the first 10 d (to promote osteoclast recruitment), and then replaced
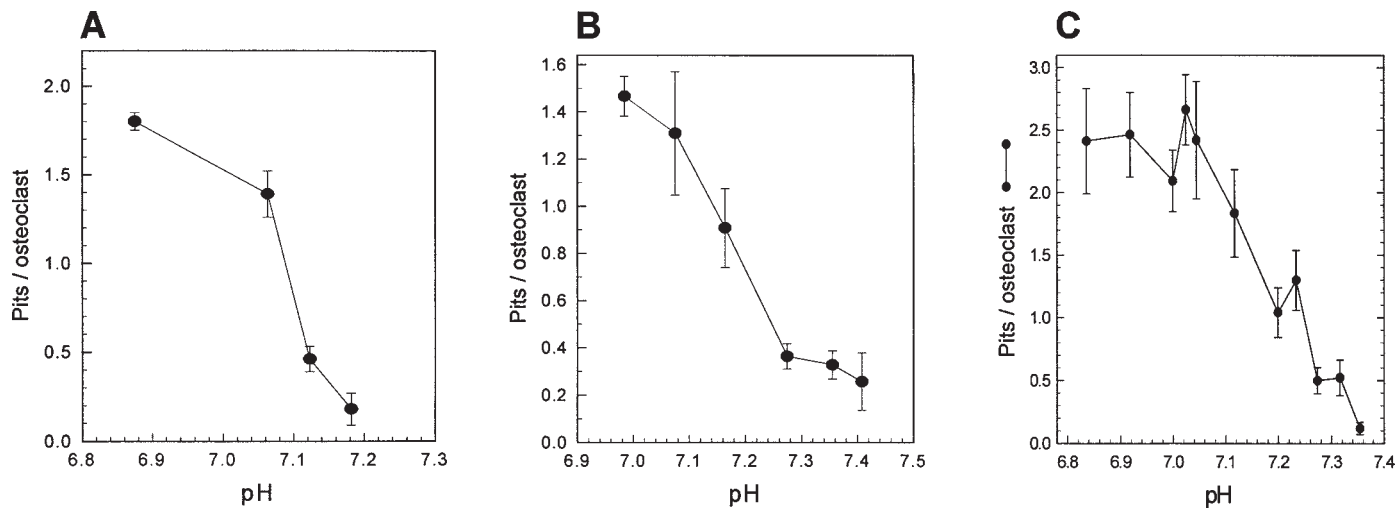
Fig. 1. Acid activation of rat (**A**), chick (**B**), and human osteoclastoma-derived osteoclasts (**C**). Culture medium pH was adjusted by addition of HCl or NaOH. Rat osteoclasts are essentially "switched off" above pH 7.2, whereas chick osteoclasts retain some resorptive activity even at pH 7.4; maximal acid-stimulation for osteoclasts occurs at pH ~6.9. Rat (and chick) osteoclasts were cultured as described in **Subheading 3.**; human osteoclasts were isolated from giant cell tumors by enzymatic and mechanical release and cultured under the same conditions. Values are means ± SEM (*n* = 5).
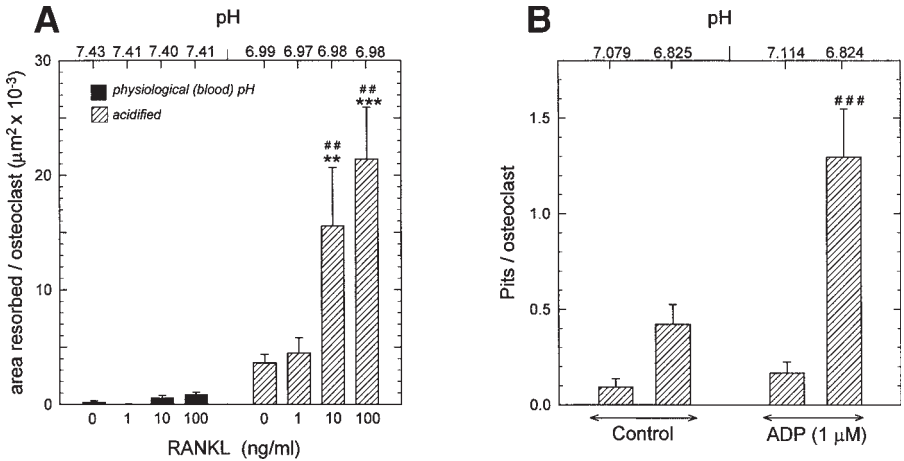
Fig. 2. Synergistic stimulatory effects of low pH and RANKL (**A**), and low pH and ADP (**B**) on osteoclastic resorption. (**A**) At physiological (blood) pH of ~7.4, basal resorption was very low and RANKL treatment caused small increases only. Combined treatment with RANKL (10 and 100 ng/mL) and low pH resulted in dramatic increases in resorption. (**B**) The stimulatory effect of ADP on resorption pit formation was observable clearly only when culture medium was acidified to a running pH of ~ 6.9. Addition of 1 μ*M* ADP resulted in a three-fold increase in number of pits/osteoclast compared to acidified control, and a 13-fold increase compared to nonacidified control, indicating synergism between the two stimuli *(3)*. Significantly different from control in the same pH group: # #, $p < 0.01$, # # # p, < 0.001. Significantly different from the same RANKL concentration at pH 7.4: ** p, < 0.01, ***, $p < 0.001$. Values are means ± SEM ($n = 5$).

for the last 4 d with MEM acidified to pH ~6.95 by addition of HCl to ensure resorptive activity (**Fig. 4**) *(10,18)*.

2. Sources of dentine: Dentine can sometimes be obtained in the form of confiscated elephant ivory or sperm whale teeth from customs or fisheries and wildlife agencies (e.g., in the United Kingdom or United States). Dentine is a convenient osteoclast substrate because it is uniform, easy to cut, and lacks features such as Haversian systems and osteocytes which make quantification of resorption difficult. If bone slices are being used, they should be prepared from defatted and washed cortical bone from bovine femora; the slices should be transversely cut to reduce the likelihood of confusing in vitro resorption with endogenous features. We find that cortical bone is usually too brittle to permit the fabrication of uniform discs using a hole punch. A number of thin layer synthetic substrates are also available. Some commercial preparations consist of hydroxyapatite sintered at high temperature onto silica discs; these have the advantage of being translucent (e.g., for electrophysiology or cell fluorescence work), but in our experience may impair osteoclast survival. Alternatively, mineralized collagen films can be prepared more
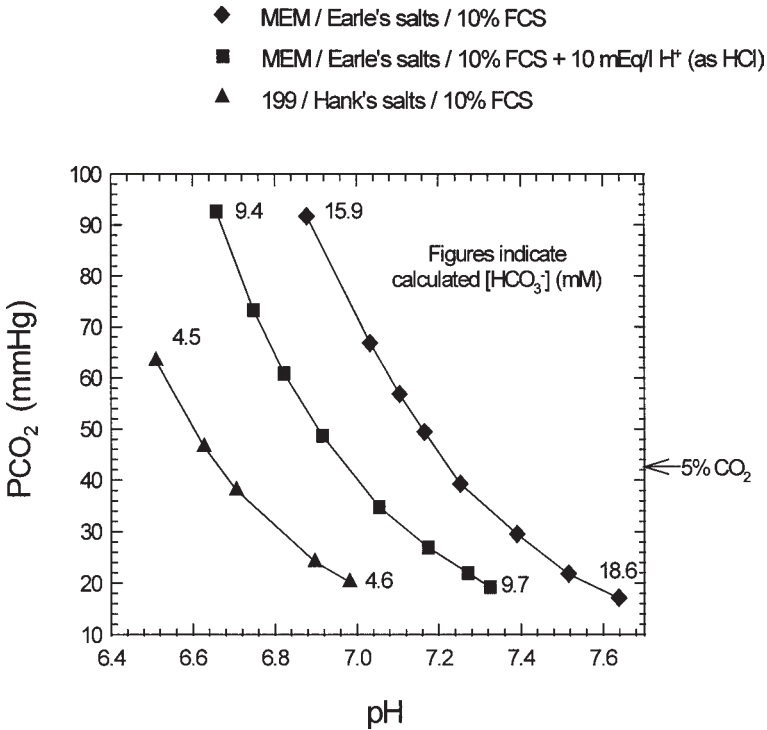
Fig. 3. Relationship between pH, pCO$_2$, and HCO$_3^-$ in tissue culture media.

cheaply using the method of Lees et al. *(19)*. The synthetic mineralized films also suffer from the disadvantage of disintegration and fragility in media acidified to pH 7.0 or below.

3. Technique for plating out cell suspension: A motorized 2.5-mL multidispensing pipet (Rainin) is ideal for plating out the cell suspension. Delays at this stage can cause problems, because the cells sediment rapidly from the suspension unless it is continuously agitated. Care should also be taken to ensure that dentine discs remain seated in the base of the wells and do not float up. To compensate for plating errors, the suspension should be dispensed sequentially *across* treatment groups, rather than dispensing to each treatment group in turn.

4. Measuring the medium pH: Accurate measurement of the operating pH of mammalian osteoclast cultures is necessary for meaningful comparison of results from different laboratories. For HCO$_3^-$–CO$_2$ buffered media, accurate pH measurements can be achieved only by the use of a properly standardized blood gas analyzer. We use a reconditioned Radiometer ABL 330 blood gas analyzer, which was obtained at low cost (Henderson Biomedical, Beckenham, Kent, UK). The blood gas analyzer uses a three-electrode system to measure pH, pCO$_2$ and pO$_2$ in a 200-μL injected sample (cycle time ~4 min). The first medium measurement,
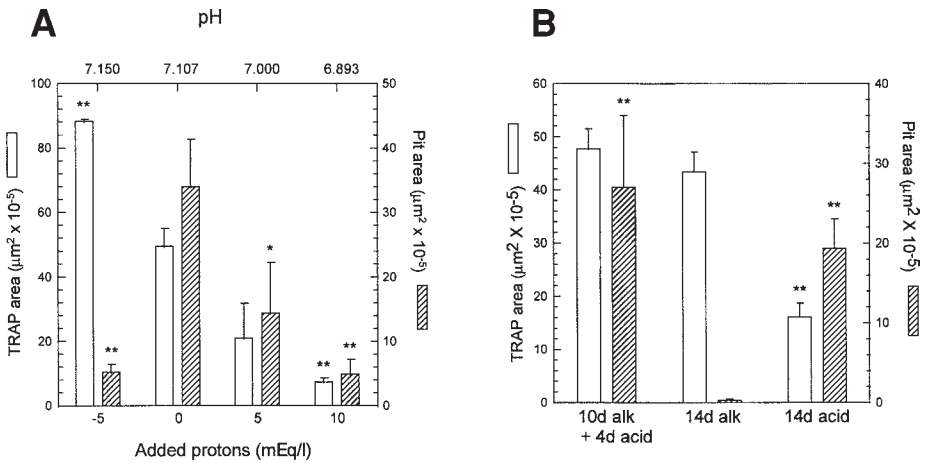
Fig. 4. Effects of pH variations on osteoclast formation and resorption in mouse marrow cultures. (**A**) Mouse marrow was cultured for 10 d; "-5 meq/L added protons" signifies the addition of 5 meq/L OH^- as NaOH. Increasing the final pH from 7.107 to 7.150 by addition of NaOH resulted in a two-fold increase in the area covered by TRAP-positive osteoclasts, but a seven-fold decrease in resorption area compared to control, whereas addition of 5 and 10 meq/L H^+ resulted in a reduction of osteoclast formation. (**B**) Incubation of mouse marrow cultures for 14 d at pH 7.41 resulted in abundant TRAP-positive multinucleated cell formation, but almost no resorption. In cultures maintained in alkaline medium for 10 d, followed by 4 d in acidified medium, formation of TRAP-positive osteoclasts was similar to 14 d at pH 7.41, but resorption pit formation was increased 93-fold. Continuous incubation in acidified media (pH 7.01) for 14 d reduced TRAP-positive multinucleate cell formation, but further increased the ratio of pit area/TRAP-positive area. (**A**) Significantly different from control: *, $p < 0.05$, **, $p < 0.01$. (**B**) Significantly different from 14-d alkaline medium: **, $p < 0.01$. (Reproduced by courtesy of Dr. M. Morrison.)

taken immediately after removing the culture plates from the incubator, is assumed to provide a pCO_2 value that is the same for all wells and that reflects the actual pCO_2 during the 24-h incubation. (It is worth noting that opening the door of the incubator during experiments, especially prior to termination, may cause perturbations in CO_2 levels that affect measured pH and pCO_2 values, and possibly osteoclast function). Measured pCO_2 typically drops for each subsequent reading from wells in a multiwell plate, causing pH values to rise accordingly. The pH readings for each well are then back-corrected to the pH value associated with the initially measured pCO_2 value, using calibration curves previously measured for culture medium with different bicarbonate concentrations (**Fig. 3**).

5. Counting cells: Numbers of TRAP-positive multinucleated osteoclasts (three or more nuclei) are assessed using transmitted light microscopy and a × 20 objec-
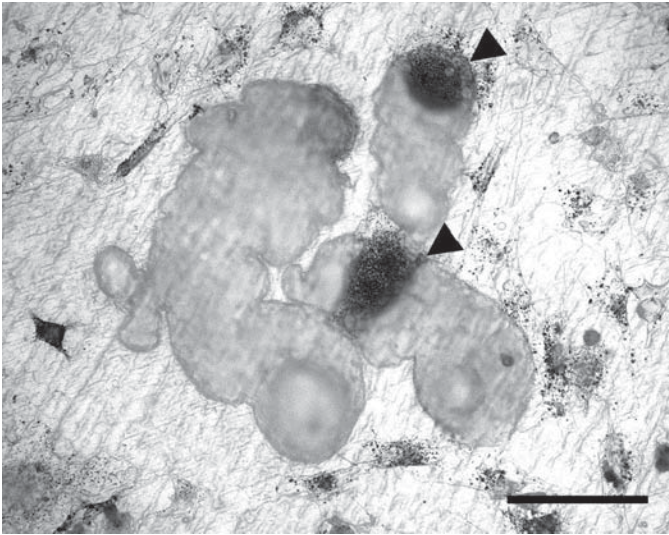
Fig. 5. Typical resorption pit complex with two osteoclasts (*arrowheads*), viewed by reflected light microscopy. Scale bar = 50 μm.

tive. Counting should ideally be performed "blind" to the treatment group. After counting osteoclasts, the numbers of mononuclear cells can be assessed using toluidine blue staining to ensure that cells were settled at similar densities onto the discs and that agents tested did not have a general cytotoxic effect. Cell counting should be performed in a "blinded" manner. Reducing the time allowed for bone cells to sediment onto the substrate reduces the number of cells that adhere. When cell density is low, the effects of substance being tested are more likely to be direct on osteoclasts, rather than mediated via other cell types. However, low cell numbers can result in high levels of variation between replicates and problematic statistics. Osteoclast counting on uniform substrates may be possible using semi-automated methods. Although this approach is not generally feasible using TRAP-stained preparations (because osteoclast cytoplasm is not uniformly demarcated), osteoclast preparations stained using the murine monoclonal antibody 23C6, directed against the vitronectin receptor, can show extremely clear cell definition and contrast. Our own studies have demonstrated that automated image analysis of low power digital images of entire 5 mm dentine discs, stained with antibody 23C6 to visualize human osteoclasts, is rapid and effective.

6. Removal of cells: Sonication can remove the graphite pencil markings. In view of this, discs should be sonicated in a known sequence, so that identification numbers can be rewritten if necessary.
7. Visualizing resorption pits: Although reflected light microscopy often yields adequate images of resorption pits on unstained specimens, image quality is improved greatly by staining because this has the effect of increasing reflectivity

(**Fig. 5**). Depending on the microscope system used, optimal reflected light images are obtained using either brightfield or darkfield modes. Pits that are completely separated by an area of unresorbed bone are counted individually, no matter how small; large, contiguous areas of resorption are also counted as single pits, as are extended "snail-trail" troughs. Although it may appear counterintuitive, the correlation between the number of discrete pits and the actual plan surface area resorbed is usually very close within treatment groups *(17)*. It is worth bearing in mind that biochemical analysis may be possible when high levels of resorption are achieved. For example, measurement of calcium release into culture medium using a standard colorimetric method or a sensitive electrode may be possible. Such methods are inherently more efficient than measuring anatomical resorption and should yield data that reflect closely the volume of matrix destroyed.

8. Assay variability: One of the most serious problems with this assay is the high variability between experiments. First, osteoclast number in some culture preparations can be low, even if the procedure is followed accurately. Second, the basal level of resorption can vary from experiment to experiment, perhaps reflecting alterations in ambient concentrations of bone resorbing agents such as growth factors and nucleotides. Thus, culture conditions should be kept as identical as possible (i.e., freshness and pH of the medium; serum batches; CO_2 concentration in the incubator; origin, washing, and sterilizing of the discs). If resorption fails to occur in cultures where authentic osteoclasts are clearly present, the problem can usually be rectified by acidification of the medium. To assess resorption area, we normally use a simple dot counting morphometry system: output from the reflected light microscope via a standard black and white or color video camera is displayed on a monitor, superimposed on which is an acetate sheet bearing a grid of dots. The dot grid is easily created by using a graph paper template that has been photocopied to the required magnification. Clearly, this process is more time consuming than simple pit counting and frequently it contributes little extra information. It is possible to measure the volume resorption pits using SEM or confocal microscopy *(6)*, but this requires specialized and expensive equipment. Pit volume can also be estimated by measuring pit depth and area, using reflected light microscopy (the fine focus control is usually calibrated in microns) and assuming that pits approximate to hemispheres; this method is not suited to determining the volume of individual pits to very high accuracy, but provides useful comparative data when multiple pits are measured.

9. Because of interassay variation, statistical comparisons should be performed only within one assay, and not between different assays. Variability within assays is likely to be high when cell numbers are low (e.g., < 10 osteoclasts/disc); the inherent "noise" in osteoclast resorption assays means that they are best suited for studying large, robust effects.

References

1. Boyde, A., Ali, N. N., and Jones, S. J. (1984) Resorption of dentine by isolated osteoclasts in vitro. *Br. Dent. J.* **156**, 216–220.

2. Chambers, T. J., Revell, P. A., Fuller, K., and Athanasou, N. (1984) Resorption of bone by isolated rabbit osteoclasts. *J. Cell Sci.* **66**, 383–399.

3. Hoebertz, A., Meghji, S., Burnstock, G., and Arnett, T. R. (2001) Extracellular ADP is a powerful stimulator of bone resorption: evidence for its signaling through the P2Y$_1$ receptor. *FASEB J.* **15**, 1139–1148.

4. Arnett, T. R. and Dempster, D. W. (1986) Effect of pH on bone resorption by rat osteoclasts in vitro. *Endocrinology* **119**, 119–124.

5. Walsh, C. A., Beresford, J. N., Birch, M. A., Boothroyd, B., and Gallagher, J. A. (1991) Application of reflected light microscopy to identify and quantitate resorption by isolated osteoclasts. *J. Bone Miner. Res.* **6**, 661–671.

6. Boyde, A. and Jones, S. J. (1991) Pitfalls in pit measurement. *Calcif. Tissue Int.* **49**, 65–70.

7. Goldhaber, P. and Rabadjija, L. (1987) H$^+$ stimulation of cell-mediated bone resorption in tissue culture. *Am. J. Physiol.* **253**, E90–E98.

8. Arnett, T. R. and Spowage, M. Modulation of resorptive activity of rat osteoclasts by small changes in extracellular pH near the physiological range. *Bone* **18**, 277–279.

9. Morrison, M. S. and Arnett, T. R. (1997) Effect of extracellular pH on resorption pit formation by chick osteoclasts. *J. Bone Miner. Res.* **12**, S290 (Abstr.).

10. Morrison, M. S. and Arnett, T. R. (1998) pH effects on osteoclast formation and activation. *Bone* **22**, 30S (Abstr.).

11. Hoebertz, A., Nesbitt, S. A., Horton, M. A., and Arnett, T. R. (1999) Acid activation of osteoclasts derived from human osteoclastoma. *J. Bone Min. Res.* **14**, S1049 (Abstr.).

12. Meghji, S., Morrison, M. S., Henderson, B., and Arnett, T. R. (2001) pH-dependence of bone resorption: mouse calvarial osteoclasts are activated by acidosis. *Am. J. Physiol.* **280**, E112–E119.

13. Murrills, R. J., Dempster, D. W., and Arnett, T. R. (1998) Isolation and culture of osteoclasts and osteoclast resorption assays, in *Methods in Bone Biology* (Arnett, T. R. and Henderson, B., eds.), Chapman and Hall, London, pp. 64–105.

14. Morrison, M. S., Turin, L., King, B. F., Burnstock, G., and Arnett, T.R. (1998) ATP is a potent stimulator of the activation and formation of rodent osteoclasts. *J. Physiol.* **511**, 495–500.

15. Zanellato, N., Hoebertz, A., and Arnett, T. R. (2000) Low pH is a key requirement for osteoclast stimulation by RANKL. *J. Bone Miner. Res.* **15**, S387 (Abstr.).

16. Bushinsky, D. A. (1987) Net calcium efflux from live bone during chronic metabolic, but not respiratory, acidosis. *Am. J. Physiol.* **256**, F836–F842.

17. Arnett, T. R. and Dempster, D. W. (1987) A comparative study of disaggregated chick and rat osteoclasts in vitro: effects of calcitonin and prostaglandins. *Endocrinology* **120**, 602–608.

18. Shibutani, T. and Heersche, J. N. (1993) Effect of medium pH on osteoclast activity and osteoclast formation in cultures of dispersed rabbit osteoclasts. *J. Bone Miner. Res.* **8**, 331–336.

19. Lees, R. L., Sabharwal, V. K., and Heersche, J. N. (2001) Resorptive state and cell size influence intracellular pH regulation in rabbit osteoclasts cultured on collagen–hydroxyapatite films. *Bone* **28**, 187–194.

6

Primary Isolation and Culture of Chicken Osteoclasts

Patricia Collin-Osdoby, Fred Anderson, and Philip Osdoby

1. Introduction

Bone is a dynamic tissue that is continually remodeled throughout life. Such remodeling is carried out by the coordinated actions of two bone cell types: bone-resorbing osteoclasts (OCs) which are uniquely capable of dissolving and removing a small volume of bone, and bone-forming osteoblasts that subsequently fill in these lacunae or pits with new bone tissue. Whereas osteoblasts originate from mesenchymal cell precursors, OCs derive from hematopoietic precursors related to monocytic cells that are present both in the bone marrow and peripheral circulation. In response to specific hormonal or local signals provided by osteoblasts, stromal cells, or other cells within the bone marrow microenvironment, OCs precursors fuse and differentiate into large multinucleated cells expressing characteristic morphological features, membrane polarization, adhesion molecules, ion pumps, enzyme activities, and antigenic profiles *(1–3)*. Most importantly, they develop a capacity for bone pit resorption, the unique and defining functional attribute of OCs. Bone resorption and formation are normally carefully balanced processes in adults. However, in various diseases or pathological conditions, an imbalance exists such that the number of OCs, number of resorption sites initiated, and/or rates of remodeling are altered, thereby resulting in either too much or too little bone turnover. Excessive bone loss occurs in many clinically relevant disorders that affect millions of people, including postmenopausal osteoporosis, rheumatoid arthritis, periodontal disease, tumor-associated osteolysis, and orthopedic implant loosening *(4–7)*. It is therefore important to decipher the complex signals that control OC bone resorption to further our understanding and provide a rational basis for the design of novel therapeutic or preventative strategies to combat

bone loss. In this regard, isolated primary cultures of in vivo formed OCs have proven to be an invaluable tool for investigating the characteristics, function, and regulation of OCs. In particular, many insights have been achieved through the use of avian OCs, cells that are highly active in their resorption of bone and are readily isolated in abundance from young chickens fed a low-calcium diet *(8)*. Following their enzymatic release from the bones harvested from such animals, OCs can be partially purified by density gradient (Percoll) sedimentation owing to their large size, and further enriched by rapid capture with magnetic beads precoupled with an antibody that specifically recognizes OCs *(9)*. OCs isolated via either procedure can be cultured and analyzed for biochemical, immunological, physiological, and functional properties, as well as modulator responses. Procedures for some of the most commonly used assays are presented.

2. Materials

2.1. Tissue Culture Medium, Solutions, and Supplies

All media and solutions should be prepared with glass distilled water.

1. Culture medium: Sterile α-mimimum essential medium (α-MEM) supplemented with 5% fetal bovine serum (FBS, Gibco) and 2.5% antibiotic/antimycotic (a/a, Gibco); store at 4°C and prewarm to 37°C for use with cells.
2. Hanks' balanced salt solution (HBSS, Gibco): Dissolve one packet in 990 mL of water, add 10 mL of a/a and 3.5 g of $NaHCO_3$, check that the pH is 7.2, sterile-filter one batch, and prepare another to store at 4°C without sterilization.
3. Moscona's low bicarbonate (MLB): Add 8 g of NaCl, 0.2 g of KCl, 50 mg of NaH_2PO_4, 0.2 g of $NaHCO_3$, 2 g of dextrose, 10 mL of a/a, and 990 mL of water; check that the pH is 7.2; and sterile-filter.
4. Moscona's low bicarbonate-EDTA (MLBE): Dissolve 1 g of EDTA in 15 mL of 1% KOH, add to 1 L of MLB, check that pH is 7.2, and sterile-filter.
5. Phosphate-buffered saline (PBS): Add 9 g of NaCl, 0.385 g of KH_2PO_4, and 1.25 g of $KHPO_4$ per liter of water (final volume); adjust pH to 7.2 using 10 *N* NaOH.
6. Collagenase: Prepare 0.5 mg/mL of stock solution in HBSS, store in aliquots at –20°C; dilute two parts of thawed stock solution with one part of MLB for use.
7. Trypsin: Prepare 1% stock (1 g in 100 mL) solution in MLB, store in aliquots at –20°C; dilute 11.25 mL of stock with 37.5 mL of MLBE and 201.5 mL of MLB for use.
8. Percoll: Dissolve one packet of HBSS powder (for 1 L) in 640 mL of water, add 0.35 g of $NaHCO_3$ and 10 mL of a/a, and sterile-filter. For 35% Percoll, mix 65 mL of this solution with 35 mL of Percoll (Pharmacia). For 6% Percoll, mix 83 mL of the HBSS solution with 17 mL of 35% Percoll–HBSS. Adjust the pH of the 35% and 6% Percoll solutions to 7.2 and sterile-filter.
9. Heparin: Sterile solution (1000 U/mL, Pharmacia, store at 4°C).
10. Trypan blue: Dissolve 0.4 g of trypan blue dye in 100 mL of water and sterile filter.

11. 1% Paraformaldehyde in HBSS (PF–HBSS): Preheat 100 mL of HBSS on a hot plate to 60°C in a Pyrex beaker (monitor with a thermometer), move the beaker to a stir plate, add 1 g of PF, cover with foil to contain the vapors (keep the thermometer in place and briefly move the beaker back to the hot plate if the temperature falls below 50°C), slowly stir with a magnetic bar, and add three or four drops of 10 *N* NaOH just to dissolve. Let cool, filter through Whatman no.1 paper into a brown glass bottle, and store at 4°C.

12. Protease inhibitor cocktail for cell pellet storage: Prepare an inhibitor stock solution A by dissolving 10 mg each of leupeptin, chymostatin, antipain, and pepstatin A in 1 mL of dimethyl sulfoxide, add 400 trypsin inhibitory units of aprotinin, and store this 1000× cocktail in 0.1-mL aliquots at –20°C. Mix 10 µL of this inhibitor stock solution A with 10 µL of a 1% stock solution of phenylmethylsulfonyl fluoride (PMSF) in ethanol (store at room temperature), 1.25 mg of *N*-ethylmaleimide (NEM), 1.56 mg of benzamidine, and 10 mL of HBSS to yield an inhibitor stock solution B. Store this at -80°C and overlay one drop (~50 µL) on top of each cell pellet to be stored frozen.

13. 350- and 110-µm Nitex filters: Sheets of Nitex (Tetko, Kansas City, MO) mesh are cut into squares larger (~50%) than the opening of a stackable plastic beaker, a filter square is stretched over the beaker, and the filter is secured in place by fitting in a ring (~1 inch deep) made from a second plastic stackable beaker whose lower three-quarter portion has been cut off (filter squares can be washed well and reused).

2.2. Preparation of Antibody-Conjugated Magnetic Beads

1. Magnetic polystyrene beads: 0.45 µm diameter, covalently conjugated with affinity purified sheep anti-mouse IgG (Dynal Inc., store at 4°C).
2. Mouse monoclonal antibody (MAb) to OC-specific antigen: *See* **Note 1**.
3. Rotary mixer: To fit microcentrifuge tubes.
4. Magnet: Dynal Inc. or other 20-lb pull magnet.

2.3. Fixation and TRAP Staining

Although not fully specific for OCs, high tartrate-resistant acid phosphatase (TRAP) activity is a characteristic of OCs that is upregulated in OC development and important for their resorption of bone *(10)*.

1. 1% paraformaldehyde in HBSS: *See* **Subheading 2.1.**, **step 11**.
2. For TRAP staining: Prepare the following stock solutions and mix just before use (or purchase a staining kit (cat. no. 386) from Sigma and follow the manufacturer's instructions; *see* **Note 2**).

   Solution A: Naphthol AS–BI phosphoric acid (12.5 mg/mL) in dimethyl formamide; store at –20°C.
   Solution B: 2.5 M acetate buffer, pH 5.2; store at 4°C.
   Solution C: 0.67 M tartrate solution, pH 5.2; store at 4°C.

a. Mix 0.4 mL of solution A, 0.4 mL of solution B, 0.4 mL of solution C, and 8.8 mL of deionized water (preheated to 37°C) in a 50-mL polypropylene tube and vortex-mix well. Wrap the tube in foil.

b. To this add 3 mg of Fast Garnet GBC salt, quickly vortex to mix well, and filter the solution through Whatman no.1 paper into a new foil-wrapped 50-mL polypropylene tube. Use immediately.

3. For a general stain: Use Difquik (eosin Y, azure A, and methylene blue, Criterion Sciences) as recommended by the manufacturer.

2.4. Fixation and Immunostaining

For immunostaining, prepare the following solutions:

1. Blocking solution: 1% Bovine serum albumin (BSA) and 10% horse serum in PBS.
2. Monoclonal (MAb) or polyclonal (PAb) antibodies: Directed against OC antigens and appropriately diluted (typically 1:100 to 1:500 of 1 mg/mL stocks) in blocking solution just prior to use.
3. Biotinylated secondary antibodies: Directed against the primary antibody and appropriately diluted (typically 1:200 to 1:500) in blocking solution just prior to use (*see* **Note 3**).
4. Glycerol-buffered mounting medium: For example, EM Sciences, 80% glycerol in PBS, Vectashield (Vector), or Citifluor; store at 4°C.

For fluorescence immunostaining:

5. Streptavidin conjugated with a fluorescent label (fluorescein isothiocyanate [FITC], Texas red, or similar): Appropriately diluted (typically 1:1000 or more) in PBS (without serum) just prior to use.
6. 4',6-Diamidino-2-phenylindole (DAPI): (Molecular Probes), prepare 100 μg/mL of stock solution in water, store at 4°C, and dilute stock 1:300 in HBSS for use in fluorescent nuclear staining.

For colorimetric immunostaining:

7. Streptavidin conjugated with β-galactosidase: Appropriately diluted (typically 1:100) in buffer A (*see* **step 8**).
8. Buffer A: 0.1 M Sodium phosphate, pH 7.2, containing 1.5 mM magnesium chloride, 2 mM β-mercaptoethanol, and 0.05% sodium azide; store at 4°C and warm to room temperature before use.
9. Buffer B: 10 mM Sodium phosphate, pH 7.2, containing 150 mM sodium chloride, 3 mM potassium ferricyanide, 3 mM potassium ferrocyanide, and 1 mM magnesium chloride; store at 4°C and warm to room temperature before use.
10. Substrate solution (0.42 mg/mL of X-gal in buffer B): Prepare a stock solution of X-gal (21 mg/mL) in dimethyl formamide to store at –20°C (e.g., in a parafilm sealed, foil wrapped glass tube), and dilute this stock solution 1:50 in buffer B to prepare the required fresh substrate solution.

2.5. Preparation of Devitalized Bone or Ivory Discs for Bone Pit Resorption Studies

1. Ivory is obtained either through donation from a local zoo or, in the United States, the Federal Department of Fish and Wildlife Services (or similar department in other countries; *see also* the chapter by Nesbitt and Horton, *this volume*). Bovine cortical bone is obtained from a local slaughterhouse. Segments of ivory and bovine cortical bone are thoroughly cleaned and washed (multiple HBSS and 70% ethanol rinses), sliced into small chunks, and then reduced to rectangular 0.4-mm thick sheets using a low-speed Isomet saw (Buehler, Lake Bluff, IL).
2. The sheets are rinsed three times with 70% ethanol, incubated in 70% ethanol overnight, and then washed for several hours in HBSS before circular discs are cut using a 5-mm paper punch.
3. The discs are soaked repeatedly in 70% ethanol in sterile 50-mL tubes (alcohol changes can be gently poured off because the discs tend to stick to the side of the tube), and stored in 70% ethanol at –20°C.
4. For experimental use, the required number of discs are removed from the tube using alcohol-presoaked tweezers (to maintain sterility) in a tissue culture hood, transferred to a fresh sterile 50-mL polypropylene tube, rinsed extensively by inversion and mild shaking at least three times with ~40 mL of sterile HBSS per wash, and the discs transferred using sterile tweezers into culture wells or dishes containing sterile HBSS for 3–24 h of preincubation in a tissue culture incubator prior to the plating of cells. HBSS is removed only immediately before the discs are to be used so that they do not dry prior to OC seeding.

2.6. Preparation of Gold-Coated Glass Coverslips for Phagokinetic Motility Studies (see Note 4)

This procedure is a modified version of the gold coverslip motility assay reported by Owens and Chambers *(11)*. Glass coverslips are precoated with a thin layer of gelatin to enhance attachment and homogeneous coverage of the gold coating. All steps are performed in a sterile hood, using sterile reagents and supplies, and more coverslips (10–50%, depending on the skill you develop for this procedure) should be coated than you expect to need in the experiment.

1. Place a 2% gelatin solution prepared in deionized water (which can be stored at room temperature) into a 37°C water bath.
2. Warm up two 24-well tissue culture dishes to 37°C (e.g., in an incubator).
3. Place glass coverslips, sterile tweezers, and one or two 100-mm Petri dishes containing a piece of Whatman filter paper into the hood.
4. Fill a single well of one prewarmed 24-well dish with warm 2% gelatin solution and dip each coverslip individually into the well using sterile tweezers.
5. Briefly drain each coverslip by touching it against the side of the well, and place it gelatin side up onto the filter paper in the open 100-mm dish to dry in the hood for at least 2 h.

6. Using tweezers, move each coverslip into one well of a sterile 24-well dish in the hood.

7. Prepare the gold coating solution (19.0 mL) in the hood by adding 11.0 mL of sterile deionized water, 4.44 mL of 0.2% gold chloride (in sterile water), and 3.36 mL of sterile 65.2 n*M* sodium carbonate into a 100-mL Pyrex beaker (foil covered and presterilized). Heat the solution on a hot plate (this can be performed outside the hood after the foil cover is replaced) just to boiling.

8. Place the hot beaker back into the hood and add 1.8 mL of a sterile solution of 0.1% paraformaldehyde in water.

9. Allow the gold solution to cool to 60°C in the hood. Monitor the temperature (this is critically important to achieve good gold coating) with an alcohol prewiped thermometer.

10. When the solution has cooled to 60°C, pipet 1 mL of the gold solution on top of each gelatin precoated coverslip and then place the 24-well dish into the refrigerator for 1 h.

11. Remove the excess solution, gently rinse the coverslips with HBSS twice, and place each coverslip onto filter paper in a 100-mm dish in the sterile hood to dry (several hours to overnight).

12. Repeat **steps 7–11** to ensure adequate and even coverage of the gold particles on the coverslips.

13. After the second gold coating, the coverslips are stored on the filter paper in a 100-mm dish in the hood for up to a few days prior to their experimental use. Check one or two coverslips the next day by placing into a 24-well dish with HBSS for at least 1 h to verify that the gold coating does not lift up and that it is sufficiently dark and evenly coated when viewed under the microscope (otherwise tracks produced by OCs will be hard to evaluate). If the coating lifts up, check a few other coverslips from that batch and discard them all if they fail this test. If the gold coating is too sparse, repeat **steps 7–11** for a third time.

14. Before use, preincubate all of the coverslips for at least 1 h in HBSS early on the day of cell plating and plan to use only those that exhibit a firm, even, and dark gold coating.

3. Methods

3.1. Isolation of Osteoclasts from Calcium-Deficient Chicks (see *Note 5*)

White Leghorn chick hatchlings are initially fed a normal diet for 4–6 d and then placed on a low calcium diet (0.15–0.25% calcium, analyzed before the feed is shipped from Purina) for at least 28 d *(8)*. Typically, 15 chicks are used for each OC preparation and three people assist in the dissection and initial steps of the protocol to minimize the time involved until the cells are isolated and plated (even an additional hour can affect the ultimate OC yield and viability; *see* **Note 6**). Animals are handled and euthanized in accordance with approved rules and procedures for the Institutional Animal Care and Use Com-

mittee and standards approved by the National Institutes of Health Guidelines for the Care and Use of Experimental Animals (or similar appropriate authority for countries other than the United States).

1. Just prior to dissection, forceps, tweezers, and scissors should be placed into beakers of 70% alcohol and all buffers prechilled on ice.
2. Readjust the pH of MLB if necessary.
3. Fill several ice containers and place two 100-mm Petri dishes with HBSS on ice.
4. Several people wearing alcohol-rinsed gloves should each remove a group of birds immediately after they are euthanized (do not delay), alcohol squirt the wings and legs of each bird just prior to its dissection, rapidly remove the tibiae and humeri using the alcohol-soaked scissors and forceps, clean off extraneous soft tissue without removing the bone ends (which are replete with OCs), and place the bones into one of the two HBSS-filled Petri dishes on ice.
5. When a number of bones have accumulated in the first HBSS dish on ice, this dish is given to one person to remove the marrow from the bones, while the other people continue to dissect bones from the remaining birds and place them into the second HBSS dish on ice.
6. Remove the marrow from each bone by gripping the bone with alcohol-soaked tweezers over another 100-mm dish containing MLB, poking several small holes in each end of the bone using a 3-mL syringe fitted with an 18-guage needle, and quickly flushing the marrow out by repeatedly inserting the tip of the syringe filled with MLB (from the dish) into the end of the bone and pushing this fluid through the marrow cavity into the lower dish (if the marrow is to be cultured, this step is done in a sterile tissue culture hood by one individual working on some of the bones while the others are dissecting more bones out of the birds).
7. Carefully flip the bone over and repeat **step 6** by flushing MLB several more times through holes poked into the other end of the bone. Place this bone back into the original (nonmarrow) dish of HBSS. Repeat for the next bone, each time flushing MLB through both ends of the bone before proceeding to the next bone.
8. After all of the marrow has been extruded from the bones, remove any remaining bits of extra tissue carefully from the bones and place the bones into eight 50-mL tubes each filled with 40 mL of HBSS. Shake gently by hand to wash the bones (~30 sec).
9. Divide and place the bones into two new dishes of HBSS on ice to split each bone lengthwise using sterile scissors while keeping the bones submersed in HBSS.
10. Transfer the split bones into eight 50-mL polypropylene tubes containing 40 mL of HBSS each, shake vigorously for 30 sec, and pass the supernatants sequentially through 350- and 110-μm Nitex filters fitted over plastic beakers set on ice (be sure the filters are tightly fitted so that the cell suspensions do not leak into the bottom beaker unfiltered).
11. Refill each of the eight tubes containing bones with 40 mL of MLB, shake, and filter these supernatants through the same 350- and 110-μm filters into the beakers containing the first filtrates on ice.

12. Dispense the final filtered solutions into 50-mL centrifuge tubes on ice and centrifuge at 210*g* for 10 min at 4°C. This pellet represents a crude fraction containing the majority of the nonviable OCs (which tend to be much larger in size on average than the surviving OCs) and a minor proportion of viable OCs. Because it provides a valuable source of OC material for enzyme-linked immunosorbentassay (ELISA), sodium dodecyl sulfate-polyacrylamide gel electrophoresis (SDS-PAGE), Western blotting, and other biochemical assays, it is routinely stored at -80°C as one or two cell pellets overlaid with a drop of protease inhibitor cocktail solution B.

13. To obtain the viable OC fraction for cell culture studies, incubate the bones in eight 50-mL tubes with 35 mL of 0.333 mg/mL of collagenase in HBSS–MLB for 30 min at 37°C (e.g., stationary in a water bath).

14. Gently shake the tubes by hand, and discard this solution. Then incubate the bones in eight tubes containing 35 mL of MLB each for 15 min to rinse, use tweezers to pick the bones out of these tubes and transfer them to eight tubes containing 35 mL of 0.045% trypsin in MLB–MLBE, and incubate for 30 min. at 37°C (stationary in a water bath) to detach viable OCs from the bone surfaces.

15. Shake the bones vigorously for 3 min., and pass the resulting cell suspension through a 350-μm Nitex filter into a plastic beaker on ice containing 1 mL of heparin (1000 U, to reduce clotting) and 5 mL of FBS (to inhibit further trypsin action).

16. Immediately refill the tubes containing the bones with 20 mL of MLB, shake vigorously for another 3 min., and filter this cell suspension through the 350-μm Nitex into the beaker on ice containing the first shaken suspension from **step 15**.

17. Again, refill the tubes containing the bones with 20 mL of MLB, shake vigorously for 1 min., and filter this solution through the 350-μm Nitex into the beaker on ice containing the first and second shaken cell suspensions.

18. Pour half of the filtered solution from **steps 15–17** through one 110-μm Nitex filter into a beaker on ice and the other half through another similar filter into a second beaker on ice (two filters, or sometimes three, are recommended because they get clogged easily). Dispense the filtrates into twelve 50-mL centrifuge tubes held on ice.

19. Centrifuge the filtered cell suspensions at 300*g* for 10 min at 4°C. Gently pour out the lipid pad and supernatant, and wipe out lipid and matrix material clinging to the side of the tube with a clean tissue before inverting each tube. Resuspend each pellet, using a 10-mL wide-bore pipet, in 2–5 mL of chilled MLB (*see* **Note 7**).

20. Transfer the OC suspension to six new 50-mL tubes, add 0.1 mL of heparin per tube, fill the tubes to 50 mL with chilled MLB, and invert to mix.

21. Centrifuge the cell suspensions again as in **step 19** to wash the cells.

22. Discard the supernatants and resuspend the cell pellets (*see* **Subheading 3.1.1.**). If OCs are to be cultured, sterile techniques and solutions should be initiated at this point for Percoll fractionations.

3.1.1. Percoll Purification of Osteoclasts

Use sterile solutions and techniques throughout.

1. Resuspend each of the six OC pellets in 5 mL of ice-cold 35% Percoll.
2. Combine the resuspended pellets into one new tube and add 0.6 mL of heparin.
3. Vortex-mix the tube briefly at low speed and divide the cell suspension into four 50-mL tubes.
4. Raise the volume of each tube to 10 mL with additional 35% Percoll.
5. Slowly overlay each tube with 3.0 mL of ice-cold HBSS (try not to deform the interface).
6. Centrifuge the tubes in a swinging bucket rotor at 440g for 20 min at 4°C.
7. Carefully remove the tubes without disturbing the gradients, and slowly withdraw the interface and top 5–8 mL with a pipet (*see* **Note 7**).
8. Transfer this interface/top solution into four new 50-mL tubes on ice containing 25 mL of HBSS, and then fill the tubes with additional ice-cold HBSS to 50 mL. Discard the tubes with remaining pellets.
9. Centrifuge at 300g for 10 min at 4°C, and discard the supernatant.
10. The 35% Percoll fractionated OC obtained can either be used for immunomagnetic purification (*see* **Subheading 3.1.2.**) or purified further by 6% Percoll fractionation as described in **steps 11–22**.
11. Set up four tubes containing 10 mL of 6% Percoll on ice.
12. Resuspend each of the four OCs pellets from the 35% Percoll separation thoroughly in 3 mL ice-cold HBSS using a 10-mL pipet.
13. Combine the suspensions and briefly vortex-mix (if clumping is a problem, add 0.12 mL of 1000 U/mL of heparin).
14. Slowly overlay 3–3.5 mL of this suspension on top of each of the four 6% Percoll gradient tubes.
15. These tubes are left undisturbed standing upright on ice for 1 h to allow OCs to penetrate the Percoll layer (under 1g).
16. Remove the top 4 mL from each tube and discard.
17. Combine the bottom fractions pairwise and dilute with ice-cold HBSS to 50 mL each.
18. Centrifuge the cell suspensions at 300g for 10 min at 4°C.
19. Resuspend each of the two OC pellets in 5 mL of α-MEM medium, combine, mix gently, and analyze by withdrawing 0.1 mL into a microcentrifuge tube containing 0.1 mL of 0.4% trypan blue to assess immediately OC yield, viability (unstained cells), and purity using a hemocytometer.
20. Meanwhile, centrifuge the OC suspension again at 300g for 10 min at 4°C. To culture, resuspend the OC pellet in prewarmed culture medium and disperse into sterile tissue culture dishes or wells.

Typically, enrichments of at least 40% on a per cell basis (>80% on a per nucleus basis) are routinely achieved for OCs after 35% Percoll fractionation, and yields of 1–3 million OCs exhibiting > 85% viability for OCs are obtained following 6% Percoll fractionation. Further enrichment of the 6% Percoll OCs population can be accomplished readily by allowing these cells to attach to bone or ivory in culture for 2.5–3 h, after which the unbound cells are removed and the adherent OCs are gently washed once or twice with fresh medium before further culture.

3.1.2. Immunomagnetic Purification of Osteoclasts (see **Note 8**)

   Partially purified OCs can be further enriched after the 35% or 6% Percoll fractionation step via immunomagnetic bead capture *(9)*. However, significantly higher OC yields are obtained if immunomagnetic capture is performed on 35%, rather than 6%, Percoll-separated populations. The last steps of bead preparation (**steps 1–4** *below*) should be timed so that the beads are ready to add as soon as the OCs have been separated on the 35% Percoll gradients.

1. Just before they are to be used for OC enrichment, magnetically sort the beads that have been coupled with an anti-OC MAb to remove the MAb coupling solution.
2. Wash the beads three times by gentle resuspension in PBS (~1 mL) and magnetic sorting.
3. Incubate the beads for 30 min. with 250 μL of sterile 1% FBS in PBS to block nonspecific attachment of the beads to the cells.
4. Wash the beads gently three times with PBS, and resuspend in 200 μL of PBS in preparation for addition to the 35% Percoll-fractionated OCs.
5. At this point, the four OC pellets from the 35% Percoll gradient (*see* **Subheading 3.1.1.**, **step 10**) are resuspended in a 50-mL polypropylene tube in a total volume of 6 mL of ice-cold HBSS.
6. Add the MAb-coupled magnetic beads from **step 4** (200 μL) and swirl the tube gently to mix cells and beads quickly (*see* **Note 9**).
7. Place the tube into a container (bucket) of ice at a ~45° angle with the bead–cell mixture clearly visible from the top.
8. Place the container with the bead–cell mixture on a rotary shaker and adjust the speed to mix the beads and cells slowly for 30 min (*see* **Note 9**).
9. Remove from the rotary shaker. Stand the tube upright in the ice container. Push a magnet down into the ice and tightly against the lower vertical portion of the tube. Let stand for ~5 min. to draw bead-bound OCs over to the magnet side of the tube. Using a pipet, slowly withdraw the unbound (nonbead) cell supernatant and transfer it to a new 50-mL tube on ice (this is resorted later to capture any lost beads bound with cells).
10. Move the tube away from the magnet. Resuspend the bead-bound cells in 40 mL of ice-cold sterile HBSS to wash, invert several times to mix gently, then place the tube back against the magnet in ice. Incubate undistrubed for 5 min. to capture bead-bound OCs and then remove the wash supernatant with a pipet to another tube (to resort later for lost beads).
11. Repeat **step 10** twice more to wash the bead-bound OCs a total of three times.
12. To recover any bead-bound OCs remaining in the original unbound cell supernatant (**step 9**) or lost during the wash steps (**steps 10** and **11**), incubate each of these tubes against the magnet for 5 min. on ice, remove and discard the supernatants, and resuspend any additional bead-bound OCs that were captured in a small volume of HBSS and add back to the main sample of bead-bound OCs.
13. Resuspend the final collection of bead-bound cells in 2–5 mL of HBSS, transfer 0.1 mL to a microcentrifuge tube, add 0.1 mL of 0.4% trypan blue to the

microcentrifuge tube, and immediately assess this sample for OC yield, viability (unstained cells), and purity in a hemocytometer.

14. Sort the remaining 2–5 mL of immunocaptured OCs with a magnet and either resuspend the cells in medium for culture, immediately extract RNA, prepare protein lysates, or use the cells in some similar fashion.

Typically, 5- to 10-fold greater OC purity is achieved with MAb 121F immunomagnetic affinity capture in comparison with 6% Percoll density gradient fractionation, and immunomagnetic OC enrichments of up to 90% on a per cell basis and over 98% on a per nucleus basis are achieved.

3.2. Osteoclast Culture

3.2.1. Percoll Purified OCs

1. Resuspend purified OCs from the 6% Percoll separation in 5 mL of culture medium and immediately plate out at:
   a. 0.5 mL per well (~100,000 OCs) in 10 wells of a 24-well dish, with or without a glass coverslip in the bottom of the well and/or two to four sterile discs of bone or ivory per well (*see* **Subheading 2.5.**), or
   b. 0.2 mL per well (~50,000 OCs) in 20 wells of a 48-well dish, with or without one sterile disc of bone or ivory (*see* **Note 10**).
2. To enrich further for OCs on bone or ivory, change the medium after 2–3 h of incubation, and then add modulators in fresh medium. Otherwise, change the medium after 16 h of incubation, and add modulators in fresh medium.
3. Culture for the designated period of time, typically 1–2 d (*see* **Note 11**).

3.2.2. Immunomagnetically Purified OCs (see **Note 8**)

Because the yield of OCs is lower following immunomagnetic purification than Percoll density gradient separation, highly purified immunomagnetic OC populations are considered most useful for confirming in a limited number of experiments that biochemical or functional effects observed using Percoll fractionated OCs can be directly attributed to OCs.

1. Culture immunomagnetically purified OCs on bone, ivory, glass, or plastic in the presence or absence of modulators for up to several d as described in **Subheading 3.2.1.** above.
2. Although the temperature is kept at or below 4°C to prevent OCs from phagocytosing the beads bound to their outer surface during immunomagnetic capture, these beads will be internalized within min once the cells are exposed to a higher temperature (*see* **Note 12**).

3.3. Assay Techniques

3.3.1. Morphology and Ultrastructure

Standard protocols can be used to evaluate the morphological and ultrastructural characteristics of isolated chick OCs. When viewed by light microscopy,
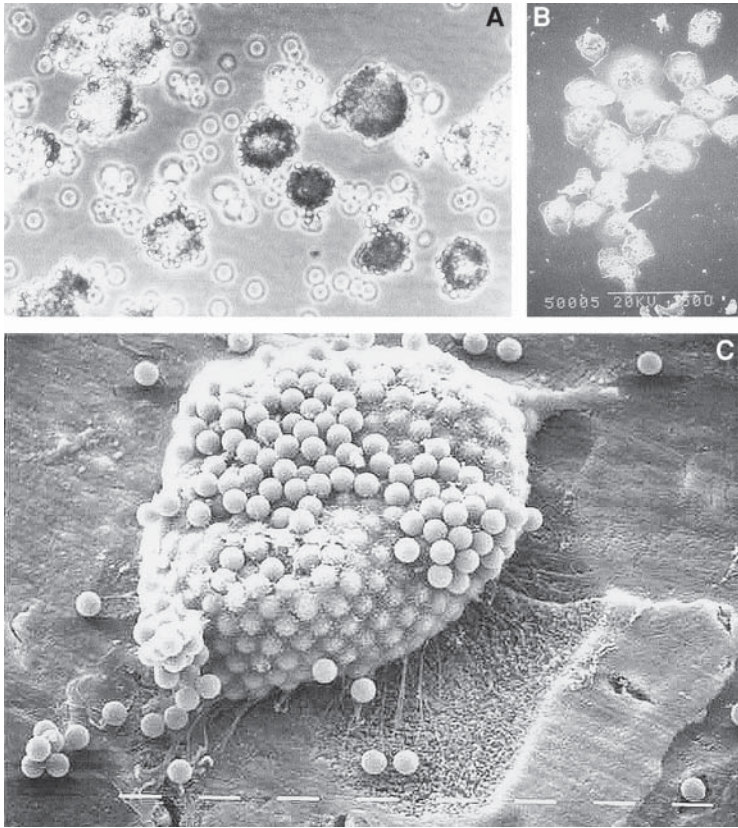
Fig. 1. Chick OC immunomagnetic purification and bone pit resorption. (**A**) Chick
OC from 35% Percoll preparations were affinity captured and purified via their bind-
ing to MAb 121F-coupled magnetic beads. Phase-contrast microscopy reveals numer-
ous beads avidly attached to and covering OC cell surfaces. (**B**) SEM appearance of
6% Percoll purified chick OC preparations cultured on plastic. Scale bar = 50 μm. (**C**)
SEM analysis of MAb 121F immunomagnetically isolated chick OC and an associated
resorption pit formed during culture on bone. Scale bar = 10 μm.

chick OCs appear as large multinucleated cells of varying sizes and shapes,
which have a grainy cast and frequently one or more pseudopodial extensions
per cell. Immunomagnetically isolated chick OCs are typically decorated with
multiple beads per cell and can be so thoroughly coated with MAb-conjugated
beads that they resemble a ball of beads (**Fig. 1A**). On culture of
immunomagnetically captured OCs on bone, ivory, glass, or plastic, the cells
spread out and internalize the beads, rather than shedding them as do
nonphagocytic cells.

OC morphology and ultrastructure can be analyzed in greater detail using transmission (TEM) or scanning (SEM) electron microscopy as detailed in other chapters of this volume. Features that are characteristic of OCs and should be evident by TEM include: multiple nuclei often clustered within the cell and varying in number between cells, abundant mitochondria, numerous vesicles, extensive vacuolation, well-developed perinuclear Golgi complexes, prominent rough endoplasmic reticulum, free polysomes, and ruffled border membrane and clear zone domains. By SEM, chick OCs cultured on plastic typically appear as large cells having a complex morphology with many fine filopodial projections, microvilli, and membrane blebs visible over the cell surface, and a peripheral cytoplasmic skirt (**Fig. 1B**). When cultured on bone or ivory, chick OCs appear by SEM either as large domed cells actively engaged in excavating a resorption cavity or as stretched inactive cells having a motile phenotype and characteristic leading and trailing membrane domains (**Fig. 2F**). OCs associated with resorption pits often exhibit membrane projections stretched back over a portion of the well-excavated lacuna that has exposed collagen fibrils (**Fig. 2F**). Resorption pits formed by cultured chick OCs are typified by multilobulated excavations or long resorption tracks (which also may be multilobulated) or, less often, as a unilobular cavity adjacent to or underlying an OC actively involved in resorption (**Fig. 2F**). Immunomagnetically isolated OCs may exhibit less pit resorbing activity (**Fig. 1C**). The morphology of resorption pit excavations can be examined more thoroughly by SEM following the removal of OCs from the bone or ivory substrate (either initially before a gold coating step or after viewing the sample and then recoating with gold to visualize the pits alone).

3.3.2. Cytochemical Staining

A quick and easy method for discriminating nuclear and cytoplasmic detail in cultured chick OCs is by use of the general differential stain Difquik, which is simply incubated with the fixed chick OCs for several min and then rinsed off. However, by far the most commonly used stain to visualize OCs is based on their high level of TRAP activity, which is upregulated early in OC development and is essential for their resorption of bone. Although TRAP activity is not completely specific for OCs alone, this cytochemical stain readily identifies OCs in bone tissue sections and in isolated OC preparations (**Fig. 3A,C**). In addition to detecting the relative levels of TRAP activity associated with individual OCs by staining, cell extracts can be quantitatively evaluated for TRAP activity levels using a microplate enzymatic assay and such activity normalized for cell extract protein *(12)*.

To stain for TRAP activity using freshly prepared staining solutions (*see* **Subheading 2.3.** and **Note 2**):
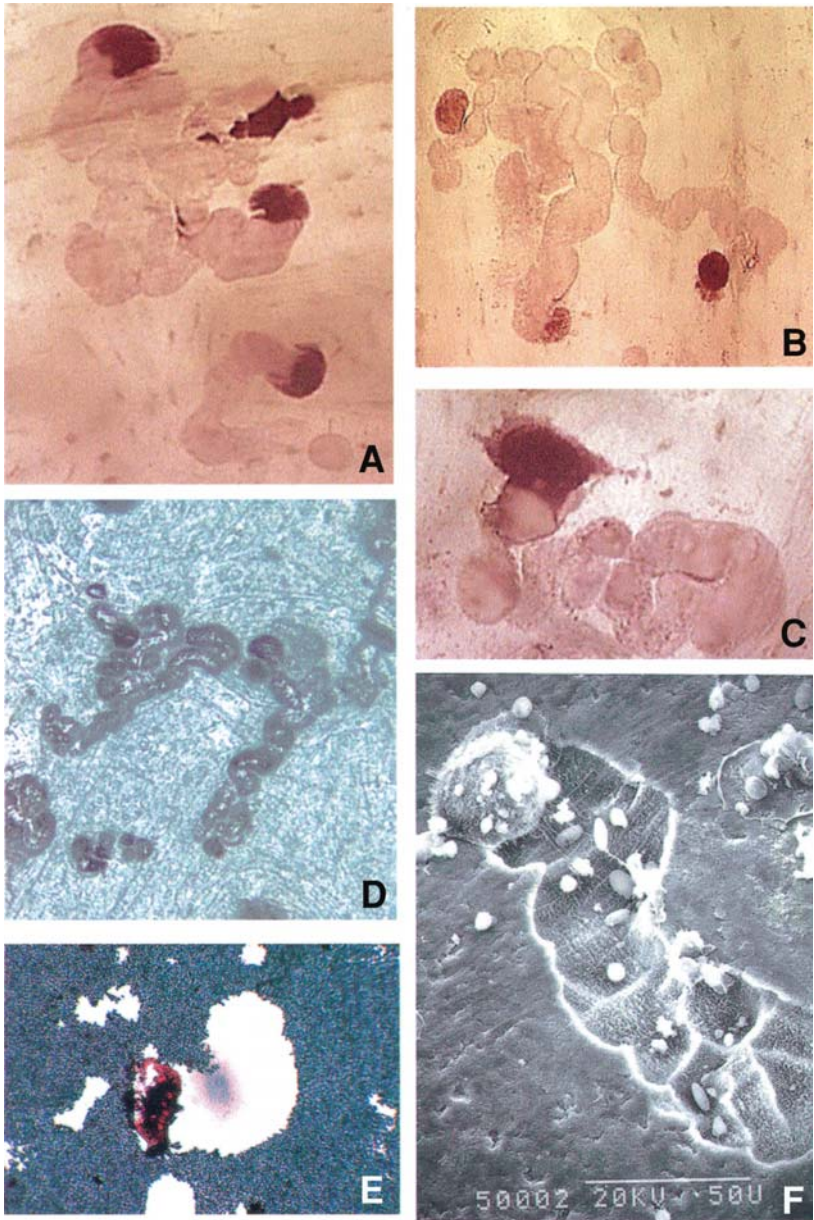
Fig. 2. Chick OCs form resorption pits on ivory and phagokinetic tracks on gold-coated coverslips. (**A–C**) 6% Percoll-purified chick OCs were cultured on ivory (2–3 d) and harvested for TRAP staining and resorption pit analysis. As viewed by light microscopy, OCs formed multilobulated resorption tracks that frequently were composed of connecting resorption lacunae. These represent periods of OC attachment

1. Remove the conditioned medium from the cells (and either discard or save for other analyses).
2. Rinse cells quickly three times with warm HBSS (tilt dish to add and remove solutions gently).
3. Add 1% PF–HBSS solution (~300 μL per 48-well, 500 μL per 24-well-plate) and fix cells for 15 min. at room temperature.
4. Remove the fixative and rinse three times with HBSS and once with deionized water.
5. Air-dry the samples overnight (to permeabilize the cells) or, alternatively, incubate in –20°C methanol for several min, followed by a rinse with water (there is no need then to air-dry).
6. Add enough staining solution to cover cells in the wells and incubate the dish or plate at 37°C for 1 h in the dark.
7. Remove the stain and rinse the samples several times with water.
8. Air-dry the samples (on the dish or ivory) or mount coverslips using fine tweezers to pick up a coverslip and invert it onto a drop of glycerol buffered-mounting medium spotted onto a glass slide (these should then be stored at 4°C and rewarmed before viewing in a microscope).

Alternatively, a commercially available staining kit (Sigma cat. no. 386) can be used as directed by the manufacturer (*see* **Note 2**).

3.3.3. Antigenic Profile

Together with specific morphological features and high TRAP activity levels, chick OCs exhibit various characteristic surface markers that are commonly monitored, as they are not expressed (or only at low levels) by related monocytes, macrophages, or macrophage polykaryons. These include expression of $\alpha v \beta 3$ integrin (vitronectin receptor), H^+-ATPase proton pump, carbonic anhydrase II, and a series of antigens recognized by anti-OC MAbs including the 121F MAb-reactive OC-specific membrane glycoprotein (**Fig. 3B,D,F,G**). Most, if not all, of these OC markers play an essential or important role in the bone resorptive function and/or survival of OCs. Using specific antibodies,

---

Fig. 2. *(continued)* and pit formation, followed by OC movement to an adjacent area of ivory for further resorption. (**D**) Resorption pits viewed by darkfield reflective light microscopy, as performed for quantifying the number and areas of resorption pits within the exact same fields evaluated for OC numbers. (**E**) 6% Percoll-purified chick OCs cultured on gold coated coverslips for 16 h and subsequently stained for TRAP activity. OCs phagocytose the gold particles and thereby clear a path during their movement across the gold-coated coverslip. The numbers and areas of such phagokinetic tracks are measured and expressed relative to the numbers of associated OCs. (**F**) SEM analysis of 6% Percoll-purified chick OCs engaged in bone pit resorption on ivory. Note the deep, well excavated lacunae that are typically formed by chick OCs. Scale bar = 50 μm.
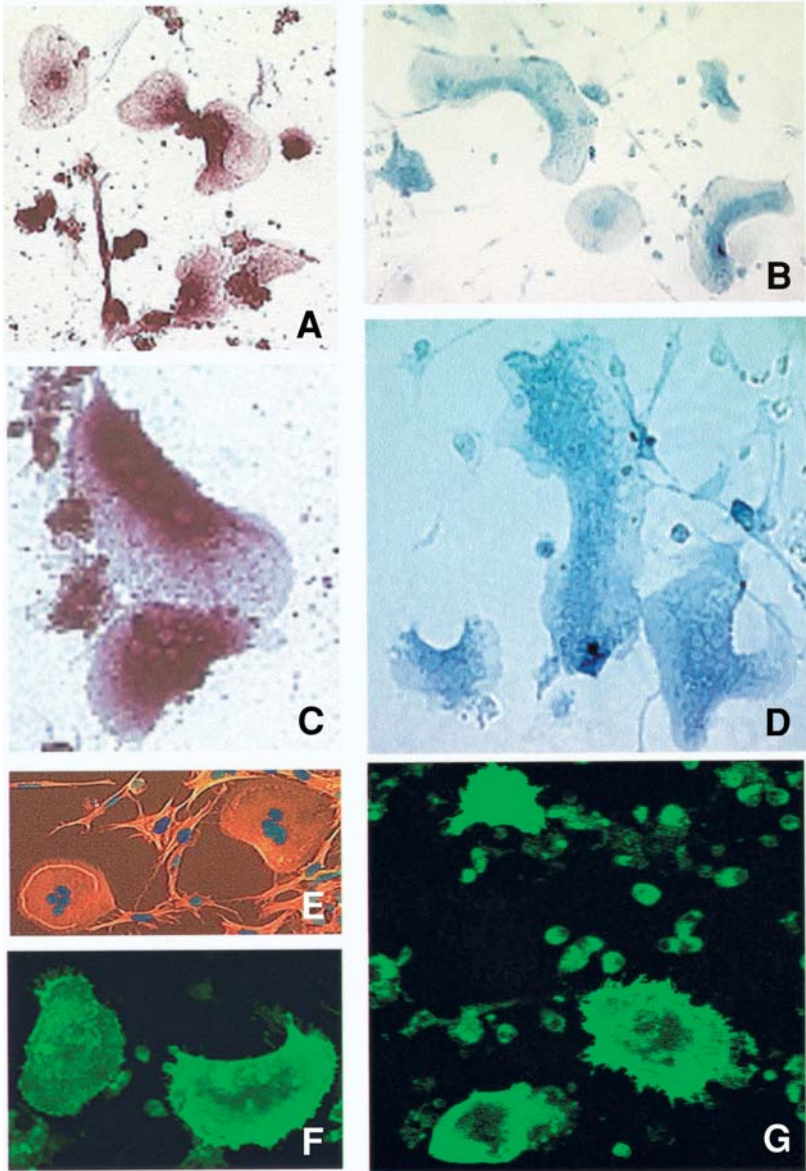
Fig. 3. Cytochemical and immunostaining analysis of 6% Percoll purified-chick OCs. (**A,C**) Chick OCs cultured on plastic (1–2 d) and stained for TRAP activity. (**B,D**) Chick OCs cultured on plastic and immunostained using a MAb to the vitronectin receptor, integrin αvβ3 (LM 609) and a biotin–streptavidin β-galactosidase detection system. (**E**) Chick OCs cultured on plastic, fixed and permeabilized (Triton X-100), and double stained with rhodamine phalloidin to label cytoskeletal F-

these markers can be detected on the surface of chick OCs cultured and fixed on bone, ivory, glass, or plastic via immunostaining, alone or in combination with TRAP staining, F-actin cytoskeletal staining (with rhodamine-labeled phalloidin), and/or DAPI nuclear labeling (**Fig. 3A–G**). The relative surface level expression of these protein markers can also be measured for chick OCs following their fixation (as whole cells) in 96-well microtiter dishes and quantitative analysis by ELISA as detailed elsewhere *(12)*. Alternatively, these markers may be monitored in total cell extracts or membrane lysates of chick OCs by ELISA, gel electrophoresis (with or without immunoprecipitation), or immunoblotting. OCs also express high intracellular levels of pp60$^{c\text{-src}}$, a critical signal molecule required for OC bone resorption. This cytoskeletally associated protein can be detected by immunostaining in permeabilized cells (e.g., incubate fixed OCs in 0.1% Triton X-100 for 30 min prior to blocking) or by immunoblotting of electrophoresed cell extracts, with or without probing for phosphorylation status. A general protocol for immunostaining is given here (use a minimum of 250 μL of reagent per well of a 24 well-plate):

1. After culture of OCs on coverslips, bone, or ivory, rinse the tissue culture wells gently and fix as for TRAP staining above (*see* **Subheading 3.3.2.**, **steps 1–4**).
2. Do NOT let the samples dry, but, instead, immediately process them for antibody staining.
3. Block nonspecific protein binding sites by incubating with blocking solution for 1 h at room temperature.
4. Incubate with appropriate dilutions of antibodies directed against OC antigens for 1 h at room temperature. Incubate one set of samples (representative of each test condition) in blocking solution alone (in place of antibody) to serve as negative controls for nonspecific background staining.
5. Rinse three times briefly and once for 10 min. with PBS.
6. Incubate with a secondary biotin-conjugated antibody directed against the primary antibody for 1 h at room temperature.
7. Rinse three times briefly and once for 10 min. with PBS.
8. Incubate for 30 min in the dark with streptavidin conjugated with FITC (or Texas red).
9. Rinse three times briefly and once for 10 min. with PBS.
10. Mount specimens onto glass slides with glycerol-buffered mounting medium (*see* **Subheading 3.2.2.**, **step 8**), store in the dark at 4°C, and rewarm slides before viewing in a microscope.

Fig. 3. *(continued)* actin (*red*) as well as DAPI to label multiple nuclei within OCs (*blue*). Note the peripheral actin ring formation characteristic of mature OCs. (**F,G**) Chick OCs cultured on plastic and immunostained with MAb 121F using a biotin–streptavidin FITC detection system. Both αvβ3 and the 121F antigen become highly expressed on the OC cell surface during their differentiation into bone-resorptive multinucleated cells, and each of these OC markers plays an important functional role in the resorption of bone by OCs.

11. If desired, OCs on coverslips can be briefly reacted with a membrane-permeable fluorescent dye to label the nuclei (bright blue) by incubation in a 1:300 dilution of DAPI in HBSS for 1 min, followed by two rinses in HBSS before mounting. Immunostained samples can also be stained for TRAP activity (after **step 9** above) before being mounted on glass slides.

Antigen detection on OCs adherent to bone or ivory is difficult to measure using a fluorescent system unless confocal microscopy is used (*see* the chapter by Nesbit and Horton, *this volume*). A histochemical detection method is more appropriate for this purpose, and this method also works well to immunostain OCs cultured on glass or plastic in place of the fluorescent system. We prefer to use antibodies coupled to β-galactosidase (which has negligible background problems and requires no specific blocking), but other enzymes (e.g., horseradish peroxidase) can also be used with good results if endogenous enzyme activities are quenched (*see* the chapter by Bord, *this volume*).

For β-galactosidase-based immunostaining, perform **steps 1–7** of the protocol given earlier in this subheading. Then continue as follows:

1. Incubate for 30 min with streptavidin conjugated with β-galactosidase in buffer A.
2. Rinse five times with buffer A over 30 min.
3. Incubate for 30 min (or longer, if necessary) in the dark with substrate solution.
4. Rinse five times over 30 min with PBS.
5. Store bone or ivory slices dry before viewing. (If using this protocol for cells on coverslips, do not dry but, instead, mount the coverslips onto glass slides as described in **step 10** earlier in this subheading).
6. OCs that have been immunostained by this method (on bone, ivory, glass or plastic) can also be subsequently double stained for TRAP activity (*see* **Subheading 3.3.2.**).

3.3.4. Molecular Profile

Both Percoll-fractionated and immunomagnetically purified chick OCs can serve as sources of RNA for analyzing the relative gene expression levels of various OC phenotypic and functional markers either in freshly isolated cells or following OC culture on plastic, bone, or ivory in the presence or absence of modulators. Although it can be difficult to obtain sufficient RNA to examine changes in mRNA expression in response to varying conditions by northern analysis, OC preparations readily provide sufficient RNA for more sensitive ribonuclease protection assay (RPA) or reverse transcription-polymerase chain reaction (RT-PCR) applications *(13)*. Typically, one well of a 24-well dish seeded with 200,000 viable chick OCs (in 250 μL of medium) yields 2–5 μg of total RNA, of which 100 ng–1 μg may be used per RT-PCR reaction, or up to 5 μg for a single RPA assay. Currently, chicken-specific primers for PCR amplification may be available only for a limited subset of chick OC markers,

however, it is sometimes possible to generate others as needed based on primers or sequences reported for OC genes cloned from human or mouse or other species. Thus, regions corresponding to high interspecies homology and gene specificity can be chosen for initial PCR attempts with chick OCs; any amplified products are then sequenced and optimal chicken-specific primers can then be designed based on the sequences obtained. Similarly, species homologous primers can be used to amplify chicken-specific genes and the PCR products cloned into appropriate vectors for the preparation of probes for RPA analyses of chicken OCs *(13)*. Methods for RNA preparation are given elsewhere in this volume (*see also* chapter by Stewart and Mann, *this volume*).

3.3.5. Motility (see **Note 4**)

Because OCs are very large and vary considerably in size (and number of nuclei), it can be difficult to perform classical chemotaxis/chemokinesis experiments through porous membranes to measure OC movement in response to various agents. However, OC movement can easily be monitored after culture on gold-coated coverslips, because OCs phagocytose the gold and thereby generate a cleared track in their wake *(10)*. To perform this assay, 6% Percoll-purified OCs are used (*see* **Subheading 3.1.1.**).

1. Resuspend the cells gently in 6–8 mL of culture medium.
2. Plate out 0.5 mL (~100,000 OCs) per well of a 24-well dish containing rinsed and prewetted gold coated coverslips (*see* **Subheading 2.6.**).
3. Culture the cells for 2–3 h to allow OCs to attach.
4. Remove the nonadherent cells and add fresh medium with or without modulators.
5. Culture the cells for 16–24 h.
6. Rinse gently three times with warm HBSS.
7. Fix the cells with 1% PF–HBSS for 15 min. at room temperature.
8. Rinse as in **step 6**.
9. Stain the cells for TRAP activity (*see* **Subheading 3.3.2.** and **Note 2**).
10. Determine the number of TRAP-stained OCs, the number of phagokinetic tracks, and the cleared area of each track within a constant number of random adjacent fields using a microscope fitted with an ocular reticle and computer linked to an image analysis system (**Fig. 2E**). Calculate the mean track area and the total area of gold cleared. Also present the data as normalized values representing the number of tracks per OC and the mean area cleared per OC.

3.3.6. Bone Resorption

OCs and other phagocytic cells can all resorb (ingest and degrade) small particles of bone in vitro or secrete acid that dissolves hydroxyapatite (e.g., on calcium phosphate coated dishes). However, only OCs are capable of excavating resorption pit lacunae on bone. This is therefore the key defining attribute and best assay for evaluating the bone resorptive function of fully developed

OCs. Because the number of new sites initiated and the rate of resorption by OCs are major parameters controlling bone remodeling in both normal and pathological states, the in vitro bone pit resorption assay has therefore become a very valuable investigational tool. The data obtained from this analysis reveals information about whether a modulator has altered the number of OCs on the bone or ivory (possibly reflecting effects on integrin-mediated attachment, cell survival, or development), the number of pits formed (reflecting the activation of OCs for initiating pit resorption), and the area of bone or ivory resorbed (overall or per pit, reflecting the amount and rate of resorption by OCs).

1. Culture chick OCs (6% Percoll purified) on bone or ivory in the presence or absence of modulators for 30–40 h (*see* **Note 13**).
2. Rinse, fix, and stain for TRAP activity as described in **Subheading 3.3.2.**
3. Evaluate resorption by using a microscope fitted with an ocular reticle and computer linked to an image analysis system (*see* Chapter 11 by van 't Hof et al. for a detailed description of a system) (**Fig. 2A–C**).
4. Count the number of TRAP-stained OCs within a constant number of random fields per bone slice, usually measured consecutively from an arbitrary starting location on the edge of the chip that is marked with a dot using a permanent ink marker. The number of fields chosen for analysis should encompass at least 100–300 OCs per bone chip (typically ~20 fields or half of the chip). To ensure that the exact same fields will subsequently be analyzed for resorption pits, mark or draw the fields that have been evaluated for each chip on a grid log sheet.
5. After all the bone chips have been analyzed for OC numbers (to ensure that no category has too few OCs), remove the OCs from the bone surface by soaking the chip for 1 min in 0.2 M NH_4OH, rubbing the entire surface with gloved fingers, repeating this treatment a second time, and then rinsing the chip in deionized water.
6. Quantify the number and planar area of each resorption pit contained within the fields evaluated for OC numbers in **step 4** using darkfield reflective light microsopy (**Fig. 2D**).
7. Express resorption measures as the mean number of OCs, number of pits, and total areas resorbed in this constant number of fields for each experimental condition. Also normalize the data to yield the mean number of pits per OC, area resorbed per OC, and area (size) per individual pit.
8. In general, several trials, with four to six replicates each for control and treated groups, should be performed to achieve statistically significant results.

4. Notes

1. OC-specific antibodies that can be used for this purpose include MAb 121F (available upon request from our laboratory) or antibodies to integrin αvβ3 (e.g., 23C6 or LM609; *see* the chapter by Coxon et al., *this volume*).
2. Cytochemical staining for TRAP activity is routinely performed using either reagents freshly prepared in the laboratory or a commercially available staining kit (Sigma cat. no. 386) as directed. Because the intensity of TRAP staining tends

to be stronger with the freshly prepared reagents, this protocol is preferred for tracking changes in OC TRAP activity (during development or in response to modulators), for discriminating OCs in quantitative resorption pit analyses, and for double staining of immunostained OCs.

3. Secondary antibodies may be directly conjugated with an enzymatic or fluorescent probe, but greater sensitivity is achieved if a biotinylated secondary antibody is used to amplify the primary antibody signal (e.g., biotinylated goat anti-mouse IgG for detecting a primary mouse MAb to an OC antigen).

4. We find that gelatin precoating enables the gold particles to remain more reliably adherent to the glass coverslips. BSA cannot substitute for gelatin, as the former interferes with chick OC movement on the gold-coated coverslips. It is important to avoid plating too many OCs on the gold-coated coverslips because the resultant overlapping tracks become difficult to analyze. Similarly, incubation times with chick OCs should not exceed 16–24 h generally because the phagokinetic tracks may become too long and convoluted (and therefore overlap significantly), migration differences in response to agents may become less apparent, and OCs may cease movement when overloaded with ingested gold particles.

5. Young posthatch growing chicks represent a highly abundant source of OCs, whose numbers are further increased by maintaining the chicks on a low-calcium feed diet. However, it is important that the level of calcium in this feed does not fall below 0.15% or the bones of the young chicks will become so soft and weak that the birds are unable to stand to walk, eat, or drink. The feed is prepared by special order (Purina) and can be stored at 4°C (kept dry to avoid mold) for up to 12 mo. In addition, the birds should have free access to tap water (not deionized water which makes them too weak when they are on the low calcium feed). As opposed to the millions of OCs that are obtained from chicks, more than 1000-fold fewer OCs are typically isolated from mouse, rat, or rabbit bone preparations, and only negligible OC numbers from most human bone tissue. Besides sharing all the morphological, phenotypic, and antigenic properties as well as most or all of the regulatory responses observed with OCs from other species, chick OCs are the most highly active and aggressive OC species for bone pit resorption. Consequently, chick OCs provide a particularly sensitive assay system to measure the regulatory influences of various agents (many of which typically act to suppress, rather than stimulate, OC activity) on OC-mediated bone resorption.

With the recent discovery of the RANKL–RANK–OPG regulatory pathway controlling OC development, resorption, and survival, some of the restrictions on studies with OCs from other species have been alleviated as it is now possible to generate OCs in vitro from OC precursors present in primary cell preparations (e.g., avian, mouse, or human bone marrow or circulating monocytes) or cell lines (murine RAW 264.7 cells). Details of such procedures are given in the chapters by Sabokbar and Athanasou, Flanagan amd Massey, and Collin-Osdoby et al.(Chapter 12).

Despite such advances, it will often still be necessary to compare the responses obtained with such in vitro generated OCs against those observed with isolated OCs formed in vivo for each agent under investigation.

6. OC viability is dependent on the total length of time that it takes from the removal and processing of the bones until the 6% Percoll fractionated or immunomagnetically isolated OCs are placed into culture. It is best if this time does not exceed 6–7 h, as each additional hour will negatively impact on the final OC viability obtained. If the bone marrow is to be used (e.g., for OC precursor studies) from these same chicks, one person should be designated to blow out the bone marrow in a sterile hood from a group of bones while other individuals are harvesting or cleaning the remaining bones, and the dishes should be passed back and forth until they are all completed. One person should then continue with the bone marrow cell preparation independently from those working on isolating OCs from the marrow stripped bones *(12)*.

7. Use only wide-bore pipets or tips for any work in isolating or manipulating OCs to avoid fragmenting these large multinucleated cells. Also, care should be taken to resuspend, mix, or vortex OC preparations gently and for as little time as necessary.

8. Immunomagnetic isolation of OCs provides a rapid and highly efficient way of purifying OCs from mixed cell populations. The magnetic beads coupled with 121F MAb are not species restricted and can therefore also effectively purify OCs from rat, rabbit, and human sources. Similarly, other anti-OC MAbs can also be coupled to such magnetic beads and used to purify OCs via this procedure (*see also* **Note 1**). The procedure is performed on ice to prevent ingestion of the beads by OCs. However, because MAb 121F (bivalent or Fab fragments) partially inhibits OC bone pit resorption *(14)*, and immunomagnetic yields of OCs are lower than with Percoll purifications, immunomagnetically isolated OCs are therefore considered most useful for: (1) obtaining highly purified OC samples for molecular or biochemical analysis and (2) confirming that responses observed in Percoll-purified OC preparations can be attributed to OC-specific effects.

9. For optimum OC immunomagnetic capture, it is important to avoid stirring the MAb-coupled beads with the cells either too fast (which interferes with their attachment) or too slow (which reduces their binding due to poor mixing). Best results are achieved with 35% Percoll-separated OC preparations used as the starting material as opposed to more crude preparations because the latter yields less pure OC populations and matrix reassembly is more problematic. Six percent Percoll preparations typically yield fewer immunomagnetically isolated OCs.

10. As an alternative to seeding OCs onto individual bone slices, OCs may be seeded in 2.5 mL of medium onto ~24 bone or ivory discs spread out to cover fully the bottom of a 35-mm dish. After allowing OCs to attach selectively to the bone or ivory pieces for 2.5–3 h, the nonadherent cells are removed, adherent OCs are gently washed with medium, and the discs are individually lifted out with sterile tweezers. Each disc is then placed into one well of a 48-well culture dish with 250 μL of fresh medium. Modulators are typically administered (diluted into 50 μL of medium) at this time (to yield a final volume of 300 μL in each well) and the cells are cultured for 30–40 h before harvest.

11. For resorption, OCs are routinely cultured for 30–40 h before harvest. For histochemical, enzymatic, or immunocytochemical analysis, OCs are cultured for 1

or 2 d before analysis. For molecular studies, RNA may be harvested directly from the Percoll-fractionated or immunomagnetically captured cells. Alternatively, RNA can be harvested from OCs cultured on bone, ivory, or plastic for up to 3 d in the presence or absence of modulators. OC survival is enhanced if the cells are cultured on bone or ivory (due to integrin-mediated survival signals) as opposed to glass or plastic, so experiments under the latter conditions should be limited to a few days at most. Although some studies have indicated that OCs resorb better under slightly acidic conditions, we find that chick (and human) OC performance is actually better in α-MEM supplemented with 5% FBS.

12. Immunomagnetically purified OCs can be cultured and will form resorption pits on bone or ivory, but because they will ingest beads rapidly at 37°C (rather than shed the beads during culture), it is important to consider that the antibody and/or bead engagement of the OCs cell surface could affect their physiology or resorptive function (**Fig. 1A,C**). It is possible to remove many, but not all, of the beads from the outer surface by physical (strong vortex-mixing) or biochemical (low pH, protease digestion) methods, performed at 4°C, although some cell damage may occur during these procedures *(9)*.

13. Because ethanol inhibits OC bone resorption, it is very important that the bone or ivory slices are well rinsed (and soaked for > 3 h) in HBSS before the cells are plated onto them. In general, resorption pit analysis using bone is somewhat more complicated than with ivory owing to the need to distinguish Haversian canals in the bone apart from the pits made by the cultured OCs. In our replicate studies using bone and ivory, no substrate-dependent differences have been noted to date in either basal or modulator evoked resorption parameters for isolated chicken OCs. Therefore, although ivory can be more difficult to obtain than bovine bone, it is preferable to use for quantitative resorption pit analysis.

Acknowledgments

References

1. Hall, T. and Chambers, T. (1996) Molecular aspects of osteoclast function. *Inflamm. Res.* **45**, 1–9.
2. Roodman, G. (1996) Advances in bone biology—the osteoclast. *Endoc. Rev.* **17**, 308–332.
3. Suda, T., Udagawa, N., Nakamura, I., Miyaura, C., and Takahashi, N. (1995) Modulation of osteoclast differentiation by local factors. *Bone* **17**, S87–S91.
4. Kanis, J. (1995) Bone and cancer: pathophysiology and treatment of metastases. *Bone* **17**, 101S–105S.
5. Mundy, G. (1993) Cytokines and growth factors in the regulation of bone remodeling. *J. Bone Miner. Res.* **8**, S505–S510.
6. Wiebe, S., Hafezi, M., Sandhu, H., Sims, S., and Dixon, S. (1996) Osteoclast activation in inflammatory periodontal diseases. *Oral Dis.* **2**, 167–180.

 7. Manolagas, S., Bellido T., and Jilka, R. (1995) New insights into the cellular, biochemical, and molecular basis of postmenopausal and senile osteoporosis: roles of IL-6 and gp130. *Int. J. Immunopharmacol.* **17**, 109–116.
 8. Oursler, M., Collin-Osdoby, P., Anderson, F., Li, L., Webber, D., and Osdoby, P. (1991) Isolation of avian osteoclasts: improved techniques to preferentially purify viable cells. *J. Bone Miner. Res.* **6**, 375–385.
 9. Collin-Osdoby, P., Oursler, M., Webber, D., and Osdoby, P. (1991) Osteoclast-specific monoclonal antibodies coupled to magnetic beads provide a rapid and efficient method of purifying avian osteoclasts. *J. Bone Miner. Res.* **6**, 1353–1365.
10. Minkin, C. (1982) Bone acid phosphatase: tartrate-resistant acid phosphatase as a marker of osteoclast function. *Calcif. Tissue. Int.* **34**, 285–290.
11. Owens, J. and Chambers, T. (1993) Macrophage colony-stimulating factor (M-CSF) induces migration in osteoclasts in vitro. *Biochem. Biophys. Res. Commun.* **195**, 1401–1407.
12. Collin-Osdoby, P., Oursler, M., Rothe, L., Webber, D., Anderson, F., and Osdoby, P. (1995) Osteoclast 121F antigen expression during osteoblast conditioned medium induction of osteoclast-like cells in vitro: relationship to calcitonin responsiveness, tartrate resistant acid phosphatase levels, and bone resorptive activity. *J. Bone Miner. Res.* **10**, 45–58.
13. Sunyer, T., Rothe, L., Kirsch, D., et al. (1997) Ca^{2+} or phorbol ester but not inflammatory stimuli elevate inducible nitric oxide synthase messenger ribonucleic acid and nitric oxide (NO) release in avian osteoclasts: autocrine NO mediates Ca^{2+}-inhibited bone resorption. *Endocrinology* **138**, 2148–2162.
14. Collin-Osdoby, P., Li, L., Rothe, L., et al. (1998) Inhibition of osteoclast bone resorption by monoclonal antibody 121F: a mechanism involving the osteoclast free radical system. *J. Bone Miner. Res.* **13**, 67–78.

7

Isolation and Purification of Rabbit Osteoclasts

**Fraser P. Coxon, Julie C. Frith, Helena L. Benford,
and Michael J. Rogers**

1. Introduction

Osteoclasts are notoriously hard to study because of the difficulty in obtaining pure populations of cells in large numbers for biochemical and molecular analyses. Unlike with other rodents (e.g., mice and rats), mature osteoclasts can be obtained from rabbits in relatively large numbers and can be purified easily. For some studies, such primary cultures of authentic osteoclasts may be preferable to osteoclast-like cells generated in vitro from bone marrow cultures. Isolated rabbit osteoclasts are capable of resorbing mineralized substrates in vitro and are therefore useful for assessing the effect of pharmacologic agents on osteoclast-mediated bone resorption *(1,2)*. We and others have also extracted protein or RNA from purified rabbit osteoclasts for studies on metabolic processes in osteoclasts, or molecular studies on osteoclast biology using Western blotting, enzyme assays or reverse transcriptase-polymerase chain reaction (RT-PCR) *(3–7)*.

We routinely isolate osteoclasts from the long bones of neonatal rabbits using a method adapted from that of Tezuka et al. *(8)* (*see* **Subheading 3.1.**). Isolated rabbit osteoclasts can then be cultured on plastic, glass, or mineralized substrates (such as bovine cortical bone, elephant ivory, or whale dentine). Culturing osteoclasts on glass coverslips (in multiwell plates) is useful for immunocytochemistry, as the coverslips can be mounted onto glass slides, enabling cells to be visualized using an upright microscope.

For some applications, such as preparation of osteoclast lysates for Western blot analysis, osteoclasts must be further purified from contaminating bone marrow cells. This can be done either by further washing culture dishes with phosphate-buffered saline (PBS), or by removing contaminating adherent cells
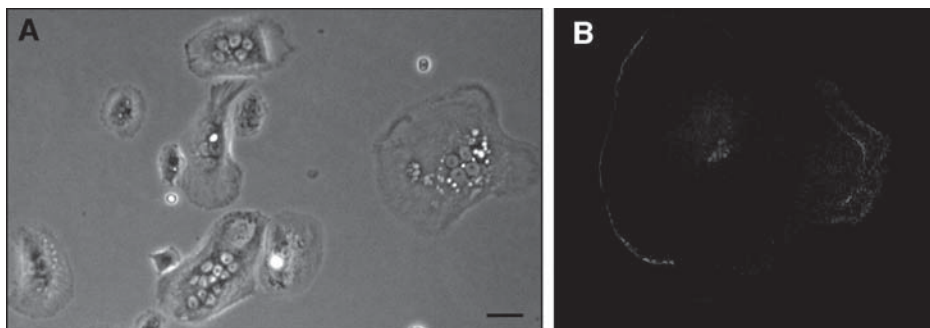
Fig. 1. **(A)** Phase-contrast photograph of multinucleated, rabbit osteoclasts cultured in a plastic Petri dish following purification with PBS. Scale bar = 25 μm. **(B)** A rabbit osteoclast showing VNR expression by fluorescence immunostaining.
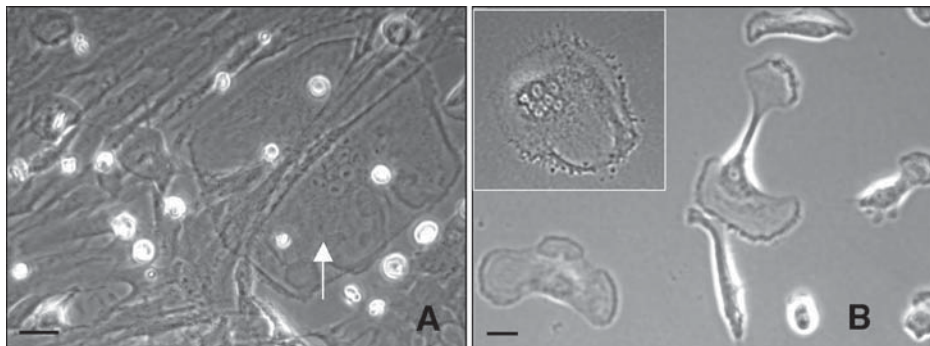

Fig. 2. Phase-contrast photographs of a rabbit bone marrow culture **(A)** after 7 d, showing a developing multinucleated, osteoclast-like cell *(arrow)* beneath the stromal cell layer; **(B)** following purification of osteoclast-like cells after 10 d (multinucleated cell shown in inset). Scale bars = 20 μm.

using a solution of pronase–EDTA (*see* **Subheading 3.2.**). This provides cultures of >95% pure, tartrate-resistant acid phosphatase (TRAP)-positive, multinucleated osteoclasts and mononuclear, prefusion osteoclasts (**Fig. 1A**).

When isolating mature osteoclasts we typically achieve a yield of approx 5×10^4 purified osteoclasts from each rabbit. It is also possible to generate larger numbers of osteoclast-like cells (TRAP-positive multinucleated cells, capable of resorption) without having to euthanize more rabbits. Indeed, from each rabbit it is possible to generate up to 16 semiconfluent 10-cm Petri dishes of osteoclast-like cells (**Fig. 2**). This is achieved by culturing the nonadherent cells in the presence of 1,25-dihydroxyvitamin D_3 [1,25-$(OH)_2D_3$] over a
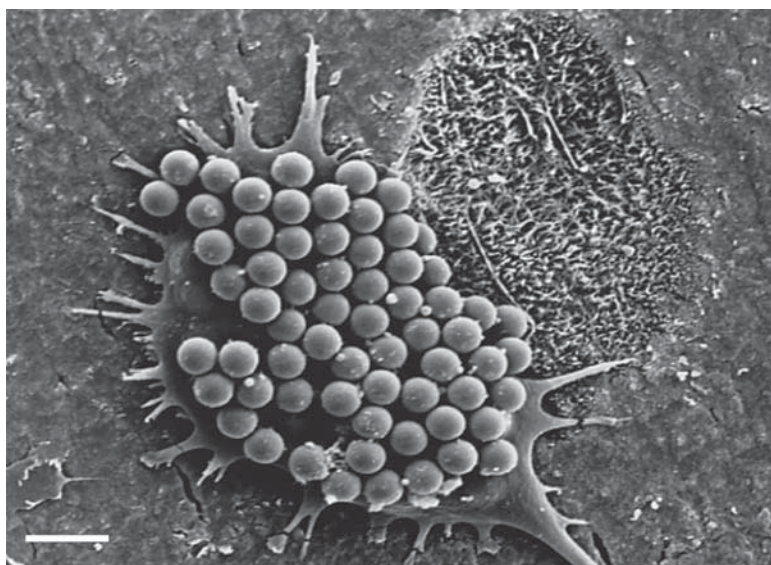
Fig. 3. Scanning electron micrograph of an immunomagnetically isolated rabbit osteoclast cultured on ivory. The osteoclast is associated with a resorption lacuna and still has magnetic beads attached. Scale bar = 10 μm.

period of 10 d, using a method modified from David et al. *(9)* (*see* **Subheading 3.3.**).

For in vitro applications, purification of osteoclasts on culture dishes by pronase–EDTA digestion is sufficient to provide pure osteoclasts for biochemical studies. However, a pure population of osteoclasts can also be isolated directly from rabbit bones, without prior cell culture in vitro. This is particularly useful when studying the effects of pharmacological agents on osteoclasts in vivo. We have modified a technique (*see* **Subheading 3.4.**) developed by Collin-Osdoby and colleagues *(10)*, that involves separation of osteoclasts from a mixed cell suspension using immunomagnetic beads and the 23C6 monoclonal antibody (**Fig 3**). The latter specifically recognizes the $\alpha_v\beta_3$/vitronectin receptor (VNR) integrin, which is highly expressed on osteoclasts *(11)* (**Fig. 1B**).

Rabbit osteoclasts in culture can be identified using markers that are highly abundant in these cells, for example, by staining for TRAP (*see* **Subheading 3.5.1.**) and immunological detection of the vitronectin receptor/$\alpha_v\beta_3$ integrin (**Fig. 1A**) (*see* **Subheading 3.5.2.**). Enzyme histochemical studies have shown that osteoclasts contain TRAP in abundance *(12)*; therefore, staining for activity of this enzyme is useful for enabling the number of osteoclasts in culture to be counted, particularly when the cells are cultured on a substrate, such as ivory,
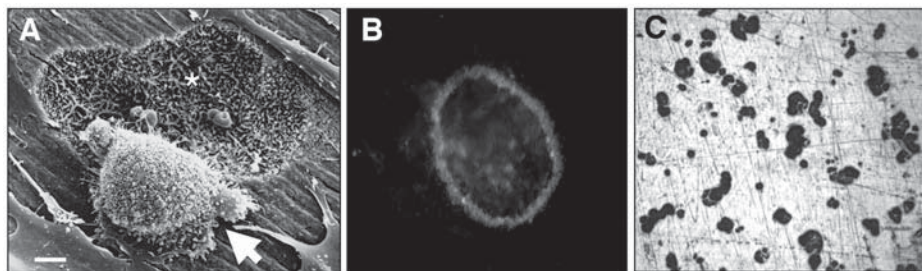
Fig. 4. Resorptive activity of rabbit osteoclasts cultured on ivory discs. **(A)** Scanning electron micrograph showing a cultured rabbit osteoclast **(arrow)** adjacent to a resorption pit **(asterisk)**. Scale Bar = 10 μm. **(B)** A rabbit osteoclast stained with TRITC–phalloidin, exhibiting a characteristic F-actin ring. **(C)** Reflected light photograph of resorption pits excavated by rabbit osteoclasts. (Reduced from original magnification, ×10).

on which cells cannot easily be seen by light microscopy. It should be noted, however, that this enzyme is not specific for osteoclasts and is present in other cell types, such as alveolar macrophages. To stain cells for TRAP activity we use a method adapted from that of van't Hof et al. *(13)*. When rabbit osteoclasts are cultures on a mineralized substrate such as ivory, actively resorbing osteoclasts can be identified by the presence of a characteristic ring of F-actin (*see* **Subheading 3.5.3.**) or by their ability of the osteoclasts to excavate resorption pits in the substrate (*see* **Subheading 3.5.4.**) (**Fig. 4**).

2. Materials
2.1. General Reagents

1. α-Minimum essential medium (α-MEM) supplemented with 100 U/mL of penicillin, 100 μg/mL streptomycin, and 1 m*M* glutamine.
2. Fetal calf serum (FCS).
3. PBS.
4. 4% Formaldehyde in PBS.

2.2 Isolation and Purification of Rabbit Osteoclasts

1. Sharp scissors.
2. Blunt-ended forceps.
3. Disposable scalpel (for removing tissue).
4. Autoclaved scalpel handle and disposable scalpel blade (for mincing bones).
5. 10-cm diameter glass Petri dishes.
6. PBS containing 0.001% (w/v) pronase, 0.002% (w/v) EDTA. Filter-sterilize (0.2-μm filter) before use. Pronase can be prepared as a concentrated stock solution in PBS and stored frozen as aliquots at –20°C, then diluted in PBS–EDTA before use.

2.3. Generation of Rabbit Osteoclast-Like Cells

1. 1,25-$(OH)_2D_3$ (Sigma, Poole, UK)

2.4. Isolation of Rabbit Osteoclasts Using Immunomagnetic Beads

1. 23C6 (Anti-$\alpha_v\beta_3$) monoclonal antibody (Mab) (Serotec, Oxford, UK).
2. 0.1% (w/v) Bovine serum albumin (BSA) in PBS.
3. Magnetic beads conjugated to rat anti-mouse IgG (e.g., Dynal, Lake Success, NY).
4. Magnet or magnetic particle concentrator.

2.5. Staining for TRAP

1. 10 mg/mL of Naphthol–AS–BI-phosphate substrate in dimethyl formamide (stable at 4°C for about 2 wk).
2. 4% (w/v) Sodium nitrite.
3. Pararosanilin: Add 1 g of pararosanilin to 20 mL of dH_2O then add 5 mL concentrated HCl. In a fume hood, heat the solution carefully with constant stirring in a water bath for 30 min, then filter after cooling (stable at 4°C for several months).
4. Veronal buffer: 11.7 g/L of anhydrous sodium acetate, 29.4 g/L of veronal (barbital) in dH_2O (toxic solution) (stable at 4°C for several months).
5. 0.1 N acetate buffer, pH 5.2: dissolve 0.82g of anhydrous sodium acetate in 100 mL of dH_2O. Adjust the pH of this solution to 5.2 using a solution of 0.6 mL of glacial acetic acid made up to 100 mL with dH_2O (stable at 4°C for several mon).
6. Acetate buffer plus tartrate: Add 2.3 g of sodium tartrate to 100 mL of acetate buffer, to give a stock solution of 100 mM tartrate (stable at 4°C for several mon).

2.6. Immunostaining for $\alpha_v\beta_3$ Integrin (VNR)

1. Monoclonal antibody 23c6 (anti-$\alpha_v\beta_3$).
2. Fluorescently conjugated secondary antibody (e.g., Alexa Fluor 594 goat anti-mouse IgG; Molecular Probes, OR, USA).
3. 0.5 µg/mL of 4',6-diamidino-2-phenylindole (DAPI).

2.7. Detection of F-Actin Rings

1. 0.5% (v/v) Triton X-100 in PBS.
2. Tetramethylrhodamine isothiocyanate (TRITC)–phalloidin (Sigma, Poole, UK).

2.8. Resorption Pit Assay

1. Ivory discs: Cut 200-µm sections of 1-cm^2 blocks of elephant ivory using a Beuhler low-speed saw with wafering blade. The surface of the slices is polished by rubbing vigorously with tissue paper, then the slices are punched into discs using a paper punch. The discs can be sterilized and stored in 95% ethanol.
2. 20% (w/v) Sodium hypochlorite solution.

3. Methods
3.1. Isolation and Culture of Rabbit Osteoclasts

1. Euthanize 2- to 4-d-old rabbits under halothane.
2. Remove all four limbs entirely, remove skin, and keep in PBS on ice.
3. In a glass Petri dish, remove all tissue from the femorae, tibulae, ulnae, and radii with a disposable scalpel. Transfer the bones to PBS as soon as they are dissected.
4. Create a mixed cell suspension in a glass Petri dish by mincing all isolated bones from one rabbit in α-MEM (approx 20 mL) using a scalpel. For the larger bones it is best to cut longitudinally first, then scrape out the marrow and the inside of the bones before mincing the remaining bone. It is important to perform this part of the procedure as quickly as possible, as the osteoclasts settle and adhere to the dish.
5. Transfer the cell suspension and bone fragments to a 50-mL conical tube and vortex-mix vigorously for three 10-s bursts. Allow the bone fragments to settle for 1 min and then decant the cell suspension to a fresh tube. Add α-MEM and supplement with FCS to a final concentration of 10% (v/v) in a final volume of 25 mL or 50 mL (*see* **Table 1**). This suspension should contain approx 1×10^8 total cells.
6. Plate out the mixed cell suspension into petri dishes (*see* **Notes 1** and **2**) or multiwell plates using the guidelines in **Table 1**.
7. Incubate cultures overnight in 5% CO_2 at 37°C, then remove nonadherent cells by washing gently in PBS using a sterile, wide-bore pasteur pipet. The remaining adherent cells are mainly osteoclasts, prefusion mononuclear cells, and stromal cells.

3.2. Purification of Rabbit Osteoclasts on Plastic

1. After overnight incubation of the bone marrow suspension as described in **Sub-heading 3.1.**, **step 7**, remove the medium containing nonadherent cells, then wash the plates gently with PBS using a sterile, plastic pasteur pipet. Three washes are usually sufficient to remove most of the nonosteoclastic cells (*see* **Notes 3** and **4**).
2. If significant numbers of contaminating cells remain, incubate the remaining adherent cells for 5–10 min (or until the nonosteoclastic cells are released) in prewarmed 0.001% (w/v) pronase, 0.002% EDTA in PBS, at 37°C.
3. Wash the plates four times in PBS and culture the remaining purified (typically >95% pure) osteoclasts and prefusion mononuclear cells in α-MEM supplemented with 10% (v/v) FCS. The purified osteoclast cultures are typically about 10–20% confluent, and each 10-cm Petri dish usually yields 100–200 μg of cellular protein following lysis (*see* **Note 5**).

3.3. Generating Large Numbers of Rabbit Osteoclast-Like Cells In Vitro

1. After allowing mature osteoclasts to adhere to culture dishes overnight, as described in **Subheading 3.1.**, remove the nonadherent bone marrow cells and pool with cells that have been removed by washing in PBS and pronase–EDTA digestion. Seed these cells into 10-cm diameter petri dishes (3×10^7 cells per

Table 1
Recommended Density of Bone Marrow Cells for Preparing Cultures of Rabbit Osteoclasts (*see* Note 2)

Culture vessel	Total volume of cell suspension	Volume per well (approx cell number)
10-cm Petri dish	50 mL	16 mL (3.2×10^7)
6-well plate	25 mL	2 mL (8×10^6)
24-well plate	25 mL	0.5 mL (2×10^6)
48-well plate	25 mL	0.3 mL (1.2×10^6)
96-well plate	25 mL	0.125 mL (0.5×10^6)

      dish) in α-MEM supplemented with 10% (v/v) FCS and containing 1×10^{-8} *M* 1,25-$(OH)_2D_3$.

2. Replace half of the medium [containing 1,25$(OH)_2D_3$] every 2 d.
3. After 10 d, remove the stromal layer by washing extensively with PBS. This usually yields >95% pure multinucleated, TRAP-positive osteoclast-like cells (capable of resorbing bone mineral when the marrow cells are cultured on ivory discs); therefore further purification using pronase–EDTA is not usually required.

3.4. Isolation of Rabbit Osteoclasts Using Immunomagnetic Beads

1. Prepare a mixed cell suspension from the long bones of a neonatal rabbit as described in **Subheading 3.1.**
2. Centrifuge the mixed cell suspension at 300*g* (10 min) and resuspend the cell pellet in 1.0 mL of undiluted 23C6 hybridoma supernatant for 30 min at 37°C.
3. Centrifuge the cells at 300*g* (5 min), then wash in 0.1% (w/v) BSA in PBS and resuspend in 0.1% (w/v) BSA in PBS containing 2×10^7 magnetic Dynal beads conjugated to rat anti-mouse IgG. Incubate at 4°C on a rotating mixer for 20 min.
4. Separate the VNR-positive from VNR-negative cells by placing in a Dynal magnetic particle concentrator for 5 min. Wash the VNR-positive cells (osteoclasts) four times in 0.1% (w/v) BSA in PBS, separating the bead-coated cells for 1 min after each wash. Finally, place the VNR-negative fraction into the magnet to retrieve any lost beads, wash these beads, and add to the VNR-positive fraction.
5. Count the number of purified osteoclasts using a hemocytometer. This technique typically yields approx 2×10^4 TRAP-positive multinucleated cells that are capable of resorption when cultured on a mineralized substrate (**Fig. 3**) (*see* **Note 6**).

3.5. Characterization of Rabbit Osteoclasts

3.5.1. Staining for TRAP

1. Osteoclast cultures should be rinsed with PBS then fixed with 4% (v/v) formaldehyde in PBS for 10 min prior to staining for TRAP. Fixed cells can then be stored at 4°C in PBS for up to 2 wk before staining for TRAP.

2. Prepare staining solution in glass vials by mixing solutions A and B described below (*see* **Note 7**). Once prepared, this staining solution should be used the same day.

    Solution A: 150 μL naphthol–AS–BI–phosphate stock, 750 μL of veronal buffer, pH 10.1; 0.45 mL of acetate buffer; 1.35 mL of acetate buffer–100 m*M* tartrate.

    Solution B: 120 μL of pararosanilin, 120 μL of sodium nitrite (4% w/v). Filter staining solution through a 0.2-μm filter before use.

3. Incubate osteoclasts in filtered staining solution at 37°C for 30–60 min. TRAP-positive cells metabolize the substrate to a red product that appears as granular staining throughout the cytoplasm of osteoclasts. Cells should be rinsed in PBS and can then stored in 70% (v/v) ethanol at 4°C for several weeks.

4. Count the number of osteoclasts (TRAP-positive, multinucleated cells with >2 nuclei) under bright field illumination at ×20 magnification. Because mono-nuclear prefusion osteoclasts are also TRAP positive it is important to verify the number of nuclei (easily distinguished by negative contrast as unstained areas) within each cell when counting

3.5.2. Fluorescence Immunostaining for $\alpha_v\beta_3$ Integrin (VNR)

1. Rinse cells in PBS, then fix in 4% formaldehyde for 10 min.
2. Incubate cells in 10% (v/v) FCS in PBS for 20 minutes.
3. Incubate cells in undiluted 23C6 (anti-VNR) hybridoma supernatant for 30 min at room temperature.
4. Wash three times in PBS containing 0.1% (v/v) FCS.
5. Incubate with fluorescently labeled, secondary antibody at a dilution of 1:80 (25 μg/mL) in PBS, for 30 min.
6. To identify multinucleated cells, nuclei can be fluorescently stained by incubating cells for 10 min with a 0.5 μg/mL solution of DAPI in PBS.
7. Rinse cells with PBS then visualize using a fluorescence microscope equipped with a 20× or 40× objective and appropriate filters (**Fig. 1B**).

3.5.3. Detection of F-actin Rings

1. Rinse cells in PBS then fix in 4% formaldehyde.
2. Permeabilize cells with 0.5% (v/v) Triton X-100 in PBS for 20 min.
3. Incubate with 0.5 μg/mL of TRITC–phalloidin in PBS for 30 min.
4. Rinse twice in PBS, then store in PBS at 4°C, protected from light.
5. Visualise actin rings using a fluorescence microscope with appropriate filters (**Fig. 4B**) (*see* **Note 8**).

3.5.4. Resorption Pit Assay

1. Prepare osteoclasts as described in **Subheading 3.1.** or **3.3.**, and seed onto mineral discs in 96-well plates.
2. Allow seeded osteoclasts to adhere to mineral discs for 2 h then gently rinse the discs in PBS to remove the nonadherent cells (*see* **Note 9**). At this stage, add any agents further agents (e.g., drugs or cytokines) into fresh α-MEM containing 10% (v/v) FCS.

3. At the end of the culture period (*see* **Note 10**), fix the cells on the discs in 4% (v/v) formaldehyde.
4. Immerse the discs in 20% (w/v) sodium hypochlorite solution, followed by vigorous wiping with a tissue to remove cells.
5. Visualize resorption pits using a reflected light microscope. Areas of resorption appear dark because the uneven surface of the disc scatters the light, whereas unresorbed, flat surfaces appear bright because they reflect light (**Fig. 4C**). Alternatively, pits can be visualized using a conventional light microscope after staining the discs with 0.5% (v/v) toluidine blue.
6. The area of resorbed mineral can be quantitated using image analysis software. We use a Leitz Q500MC image analysis system (Leitz, Milton Keynes, UK) with Aphelion-based software developed in house (*see* Chapter 11, Subheading 3.5.). The cultures prepared as described above usually result in 0.5–1 mm^2 of resorbed mineral per disc.

4. Notes

1. The source of Petri dishes appears to influence the yield of osteoclasts. In our hands, tissue-culture grade Falcon 10-cm diameter Petri dishes produce the best results.
2. It is difficult to obtain confluent monolayers of purified rabbit osteoclasts, as seeding the cells at higher densities than those indicated in **Table 1** prevents attachment of the osteoclasts to tissue culture dishes.
3. Extensive washing with PBS is often sufficient to remove contaminating stromal cells, which may lift off as a single layer. In these cases digestion with pronase–EDTA is unnecessary. However, cultures should be only gently rinsed with PBS using a wide-bore, plastic pasteur pipet, to avoid damaging the osteoclasts.
4. Rabbit osteoclasts have a relatively long life span when cultured in vitro, even following purification. Although cell number gradually declines, some rabbit osteoclasts remain viable after more than 1 wk in culture, without the addition of exogenous growth factors or supplements other than FCS.
5. Rabbit osteoclasts are extremely adherent to tissue culture plastic and difficult to remove enzymatically. Therefore, when preparing osteoclast lysates for Western blot analysis, we lyse the cells directly in the Petri dish. These lysates can be concentrated if necessary by centrifuging through a microconcentrator (we use 12-kDa molecular mass cutoff).
6. We typically use immunomagnetic separation to isolate osteoclasts for the preparation of cell lysates (e.g., for Western blot analysis) following in vivo administration of pharmacologic agents. Although the VNR-positive osteoclasts with magnetic beads attached can be cultured on ivory discs, the resorptive function of these cells is typically 20% of that of osteoclasts that have not been separated using magnetic beads.
7. A final tartrate concentration of 50 m*M* is used when staining for TRAP in rabbit osteoclast cultures, which is higher than that used for staining for TRAP in osteoclasts from other species, for example, mouse (use a final tartrate concentration of 30 m*M*).

8. F-actin-containing podosomes can also be observed in osteoclasts cultured on plastic or glass following staining with TRITC–phalloidin, but on these surfaces osteoclasts do not form a genuine "F-actin ring."

9. When seeding osteoclasts onto ivory discs to assess resorptive activity, it is important to wash off the nonadherent cells gently after seeding, as subsequent resorption appears to be greatly reduced in the presence of the nonadherent cells. The nonadherent cells can be removed as little as 1 h after seeding cells onto ivory discs. This will result in a purer population, but lower yield, of osteoclasts.

10. Rabbit osteoclasts adhere rapidly to ivory but, in our hands, do not begin to resorb until about 12 h after seeding. We routinely incubate cultures of rabbit osteoclasts for 48 h to assess resorptive activity. Only approx 25–50% of the TRAcP-positive, multinucleated osteoclasts seeded onto ivory discs are active (i.e., exhibit actin rings) at any one time.

References

1. Shakespeare, W., Yang, M., Bohacek, R., et al. (2000) Structure-based design of an osteoclast-selective, nonpeptide src homology 2 inhibitor with in vivo antiresorptive activity. *Proc. Natl. Acad. Sci. USA* **97,** 9373–9378.

2. Fisher, J. E., Rogers, M. J., Halasy, J. M., et al. (1999) Alendronate mechanism of action: geranylgeraniol, an intermediate in the mevalonate pathway, prevents inhibition of osteoclast formation, bone resorption and kinase activation in vitro. *Proc. Natl. Acad. Sci. USA* **96,** 133–138.

3. Coxon, F. P., Helfrich, M. H., van 't Hof, R. J., et al. (2000) Protein geranylgeranylation is required for osteoclast formation, function, and survival: inhibition by bisphosphonates and GGTI-298. *J. Bone Miner. Res.* **15,** 1467–1476.

4. Benford, H. L., McGowan, N. W., Helfrich, M. H., Nuttall, M. E., and Rogers, M.J. (2001) Visualization of bisphosphonate-induced caspase-3 activity in apoptotic osteoclasts in vitro. *Bone* **28,** 465–473.

5. Weidema, A. F., Dixon, S. J., and Sims, S. M. (2001) Activation of P2Y but not P2X(4) nucleotide receptors causes elevation of $[Ca^{2+}]_i$ in mammalian osteoclasts. *Am. J. Physiol. Cell Physiol.* **280,** C1531–C1539.

6. Lees, R. L., Sabharwal, V. K., and Heersche, J. N. (2001) Resorptive state and cell size influence intracellular pH regulation in rabbit osteoclasts cultured on collagen–hydroxyapatite films. *Bone* **28,** 187–194.

7. Chikazu, D., Hakeda, Y., Ogata, N., et al. (2000) Fibroblast growth factor (FGF)-2 directly stimulates mature osteoclast function through activation of FGF receptor 1 and p42/p44 MAP kinase. *J. Biol. Chem.* **275,** 31,444–31,450.

8. Tezuka, K., Sato, T., Kamioka, H., et al. (1992) Identification of osteopontin in isolated rabbit osteoclasts. *Biochem. Biophys. Res. Commun.* **186,** 911–917.

9. David, J. P., Neff, L., Chen, Y., Rincon, M., Horne, W. C., and Baron, R. (1998) A new method to isolate large numbers of rabbit osteoclasts and osteoclast-like cells: application to the characterization of serum response element binding proteins during osteoclast differentiation. *J. Bone Miner. Res.* **13,** 1730–1738.

10. Collin-Osdoby, P., Oursler, M. J., Webber, D., and Osdoby, P. (1991) Osteoclast-specific monoclonal antibodies coupled to magnetic beads provide a rapid and efficient method of purifying avian osteoclasts. *J. Bone Miner. Res.* **6,** 1353–1365.
11. Nesbitt, S., Nesbit, A., Helfrich, M., and Horton, M. (1993) Biochemical characterization of human osteoclast integrins. Osteoclasts express alpha v beta 3, alpha 2 beta 1, and alpha v beta 1 integrins. *J. Biol. Chem.* **268,** 16,737–16,745.
12. Minkin, C. (1982) Bone acid phosphatase: tartrate-resistant acid phosphatase as a marker of osteoclast function. *Calcif. Tissue Int.* **34,** 285–290.
13. Van 't Hof, R. J., Tuinenburg-Bol, R. A., and Nijweide, P.J. (1995) Induction of osteoclast characteristics in cultured avian blood monocytes; modulation by osteoblasts and 1,25-(OH)2 vitamin D3. *Int. J. Exp. Pathol.* **76,** 205–214.

8

Generating Human Osteoclasts from Peripheral Blood

Afsie Sabokbar and Nicholas S. Athanasou

1. Introduction
1.1. Historical Perspective

Osteoclasts are large multinucleated cells that are uniquely specialized for the function of lacunar bone resorption. For much of the previous century osteoclasts were thought to share a common progenitor cell with osteoblasts, bone-forming cells. Osteoclast formation occurring as a consequence of fusion of nonosteoblastic mononuclear precursor cells was suggested by a number of early investigators including Pommer (1883), Mallory (1912), La Coste (1923), and Hancock (1949) (for review *see* **ref. *1***). It was subsequently established by numerous studies that osteoclasts are derived from a hematopoietic marrow precursor *(2)*. These studies included parabiosis experiments in which normal and affected (osteopetrotic/radiation-treated) littermates are linked by a common circulation; these experiments established that the mononuclear osteoclast precursor is present in peripheral blood *(3,4)*.

Following establishment of the hematopoietic origin of osteoclasts, there was considerable controversy as to the precise nature of the mononuclear osteoclast precursor. Neither mitotic nor amitotic division has been seen in osteoclasts, and osteoclast formation is thought to occur as a consequence of fusion of mononuclear precursors. As monocytes and macrophages fuse to form polykaryons that morphologically resemble osteoclasts, and osteoclasts are known to be phagocytic cells, it was suggested that osteoclasts form part of the mononuclear phagocyte system and that monocytes or at least monocyte-like cells could represent osteoclast precursors *(5,6)*. There are numerous structural, functional, and immunophenotypic similarities between monocytes and osteoclasts. However, there are also significant differences, notably the inability of monocytes, macrophages, or their fused products, macrophage

polykaryons, to carry out lacunar resorption of a mineralized substrate, an essential functional defining characteristic of an osteoclast. On this basis, it was suggested that the osteoclast and its precursors could represent a unique type of phagocytic cell that was derived from a differentiation pathway that was distinct from that of monocytes and macrophages.

Some of the cellular and humoral requirements for osteoclast formation were identified in long-term hematopoietic (bone marrow or spleen) culture systems. In such cultures, it was found that osteoblasts or other specific bone-derived stromal cells are an absolute requirement for osteoclast precursors of hematopoietic origin to differentiate into functional osteoclasts *(7)*. In human bone marrow cultures it was noted that in the presence of 1,25-dihydroxyvitamin D_3 [1,25-$(OH)_2D_3$], osteoclast-like multinucleated cells formed from colony-forming units for granulocytes and macrophages *(8)*. It was subsequently shown that mouse monocytes and mononuclear phagocyte populations of extraskeletal tissue origin (alveolar macrophages) were found to be capable of osteoclast differentiation when these cells were cocultured with bone marrow stromal cells or osteoblast-like cell lines *(9,10)*. As these rodent cells produce macrophage colony-stimulating factor (M-CSF) that does not react with the human M-CSF receptor, it was found that in order to generate human osteoclasts from monocytes and tissue macrophage populations, human M-CSF had to be added to cocultures of human monocytes and bone-derived stromal cells in addition to 1,25-$(OH)_2D_3$ *(11)*.

The necessity for contact between circulating or marrow-derived osteoclast precursors and bone stromal cells to generate osteoclasts in vitro suggested that osteoclast formation involved a ligand–receptor interaction between these cell types. This hypothesis was confirmed by the discovery of the receptor activator for nuclear factor κB ligand (RANKL), which is expressed by bone stromal cells, and RANK, which is expressed by osteoclast precursors (including cells of the monocyte fraction) *(12,13)*. This permitted in vitro methods of human osteoclast formation to be devised in which cultures of peripheral blood mononuclear cells (or tissue macrophages) alone, in the presence of RANKL and M-CSF, can be used for osteoclast generation *(14,15)*.

Although M-CSF appears to be an absolute requirement for osteoclast formation, recent studies have shown that RANKL-induced osteoclast formation may not be the only means whereby bone-resorbing multinucleated cells are formed. It has been shown that cytokines (tumor necrosis factor-α[TNF-α] ± interleukin-α [IL-α]) can substitute for RANKL in generating osteoclasts from mouse marrow precursors under some circumstances *(16)*. We have recently shown that this RANKL-independent mechanism is also

capable of generating osteoclasts from human circulating precursors derived from the monocyte fraction *(17,18)*.

1.2. Defining Characteristics of Osteoclasts

In employing culture systems of peripheral blood mononuclear cells (or other tissues) to generate osteoclasts, it is important to establish the specific defining characteristics of osteoclasts. A number of ultrastructural, cytochemical, immunophenotypic, hormone receptor, and functional characteristics have been used to define a cell as an osteoclast *(5)*. It should be noted that some of these markers are not exclusively expressed by osteoclasts. Cytochemical markers such as tartrate-resistant acid-fast phosphatase (TRAP), which is not expressed by isolated monocytes, can be expressed by mononuclear and multinucleated cells that form in cultures of monocytes and macrophages; these cells do not possess the ability to carry out lacunar resorption and express phenotypic markers that are not found on osteoclasts, such as CD14, CD11/18, and HLA-DR. A useful osteoclast immunophenotypic marker is the vitronectin receptor CD51 (VNR) which is strongly (but not exclusively) expressed by osteoclasts *(19)*. Calcitonin receptors (CTRs) and inhibition of osteoclast resorption by calcitonin are also thought to be specific for osteoclasts *(20)*. Markers that have been used to identify osteoclasts are shown in **Table 1**. At the risk of stating the obvious, it should be noted that the only defining characteristic that permits a cell to be classified as an osteoclast is a functional one, that is, the ability of a cell to carry out lacunar resorption of a mineralized substrate. Monocytes, macrophages, and macrophage polykaryons are CTR negative and are not capable of lacunar resorption.

2. Materials

1. Ficoll–Hypaque (Pharmacia Biotech, UK).
2. Phosphate-buffered saline (PBS).
3. Acetic acid solution (5% [v/v] in H_2O).
4. Glass coverslips, 6-mm diameter.
5. MACS CD14 MicroBeads (Miltenyi Biotec).
6. $1,25\text{-}(OH)_2D_3$ (Solvay Dulpar, NL).
7. Dexamethasone (Sigma-Aldrich Chemicals).
8. Human M-CSF (R & D Systems Europe, Abingdon).
9. 30 ng/mL of soluble RANKL (PeproTech, UK).
10. TRAP kit (Sigma Aldrich Co., UK, Diagnostic Kit no. 386A).
11. 1 mg/mL collagenase type I (Sigma-Aldrich Chemicals, cat. no. C-0130).
12. 20 ng/mL of TNF-α (R & D Systems Europe, Abingdon).
13. 70-μm Cell strainer (Falcon, UK).
14. Minimum essential medium (MEM) (Gibco).
15. 10% Heat-inactivated fetal calf serum (FCS) (Gibco).

Table 1
Defining Criteria of Osteoclasts and Their Presumed Precursors

Morphological	Light microscopy: multinuclearity, location at resorbing sites
	Transmission electron microscopy[a]: ruffled borders, clear zones
Enzyme histochemistry	Expression of TRAP[b], tartrate-resistant tri-nucleotide phosphatase,[b] carbonic anhydrase isoenzyme type II,[b] cathepsin K[b].
Immunohistochemistry/ immunology	Expression of restricted range of leucocyte/ macrophage-associated antigens[b] (e.g., positive for CD13, CD15, CD45, CD68, CD51 [VNR]; negative for CD11/18, CD14, HLA-DR, Fc and C3b receptors)
	Calcitonin receptor expression[a]
Functional	Ability to form resorption lacunae on a bone substrate[a]
	Response to calcitonin/ability to bind calcitonin[a]
	F actin ring formation[a]

[a]Osteoclast-specific.
[b]Osteoclast-associated but not specific.

3. Methods

3.1. Isolation of Osteoclast Precursors from the Monocyte Population of PBMCs

Human peripheral blood mononuclear cells (PBMCs) are isolated by Ficoll–Hypaque sedimentation and adherence from the peripheral blood of human volunteers.

1. Collect blood in EDTA–citrate tubes and dilute 1:1 with culture media.
2. Layer over 5 mL of Ficoll–Hypaque and centrifuge at 510g for 20 min.
3. Remove the mononuclear cell rich layer at the interface and wash twice in culture medium.
4. Resuspend the pellet in culture medium containing 10% serum.
5. Lyse red cells using a 5% (v/v) acetic acid solution.
6. Count cells in the resulting suspension using a hemocytometer.
7. Add appropriate number of PBMCs (*see* either **Subheading 3.2.** or **Subheading 3.3.**) to a 96-well plate containing either 4-mm diameter dentine slices or 6-mm diameter glass coverslips in culture medium with 10% serum.
8. Ninety percent of the cells isolated from peripheral blood adhere to glass and are CD14-postitive monocytes (*see* **Note 1**).
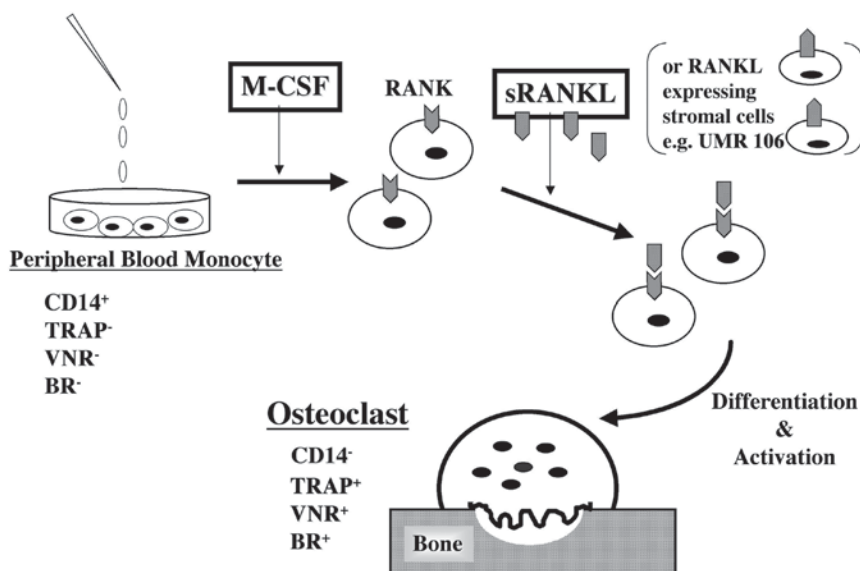
Fig. 1. Schematic representation of the technique used for generating human osteoclasts in vitro from peripheral blood mononuclear cells (PBMCs). M-CSF, macrophage colony stimulating factor; RANK, Receptor activator for nuclear factor-κB; RANKL, receptor activator for nuclear factor-κB ligand; sRANKL, soluble RANKL; TRAP, tartrate-resistant acid phosphatase; VNR, vitronectin receptor; BR, bone resorption.

3.2. Osteoclast Formation in Cocultures of Bone Stromal Cells and Monocytes (Fig. 1)

1. Place dentine slices (4-mm diameter) or glass coverslips (6-mm diameter) in 96-well tissue culture plates.
2. Add 2×10^4 UMR 106 cells (*see* **Note 2**) to each well and culture the cells on dentine slices and coverslips for 24 h in culture media containing serum.
3. Add 1×10^5 PBMCs to each well and incubate for 2 h.
4. Remove dentine slices and coverslips from the 6-mm wells, wash vigorously in culture medium to remove nonadherent cells, and place in a 24-well tissue culture plate containing 1 mL of culture media supplemented with 10^{-7} M 1,25-(OH)$_2$D$_3$, 10^{-8} M dexamethasone, and 25 ng/mL of M-CSF.
5. Maintain the cocultures for up to 21 d, during which time the medium (± added experimental factors, e.g., cytokines/growth factors) is replaced every 3 d.

3.3. Generation of Human Osteoclasts in the Absence of Stromal Cells (Fig. 1)

1. Add 5×10^5 PBMCs/well to wells of a 96-well tissue culture plate containing either dentine slices (4-mm diameter) or glass coverslips (6-mm diameter) as described in **Subheading 3.2., step 1**.

2. After 2 h of incubation, remove the dentine slices and coverslips from the wells and wash vigorously in culture medium to remove nonadherent cells.
3. Place slices or coverslips in 16-mm wells of a 24-well tissue culture plate containing 1 mL of culture medium containing serum supplemented with 30 ng/mL of soluble RANKL and 25 ng/mL of M-CSF ± 10^{-8} *M* dexamethasone (*see* **Notes 3** and **4**).
4. Incubate cultures for up to 21 d and replenish the culture medium containing the factors as in **step 3** every 3 d.

3.4. Assessment of Osteoclast Formation

3.4.1. Cytochemical Assessment of Osteoclast Formation

1. Carry out histochemical staining for TRAP, a marker of osteoclasts *(28)*, using a commercially available TRAP kit (Sigma, Diagnostic Kit no. 386A) and counterstain with hematoxylin.
2. Alternatively stain cell preparations on coverslips immunohistochemically using an indirect immunoperoxidase method, with the monoclonal antibody 23C6 (Serotec, Oxfordshire) to determine expression of VNR, an osteoclast-associated antigen.

3.4.2. Functional Assessment of Osteoclast Formation

Functional assessment of osteoclast formation is determined at the end of the culture period using a cortical bone or dentine slice resorption assay.

1. Place dentine slices in 1 *N* NH_4OH for 30 min and clean by ultrasonication to remove adherent cells.
2. Wash slices with distilled water.
3. Stain with 0.5% (v/v) toluidine blue for 3 min.
4. Let slices air-dry.
5. Examine by light microscopy for evidence of lacunar resorption.
6. The extent of resorption is determined either by counting the number of discrete pits on each dentine slice or by measuring the percentage surface area resorbed on each dentine slice using an image analysis system (*see* **Note 5**).

3.5. Preparation of Isolated Macrophages from Tissue Specimens

It is possible to isolate mononuclear phagocyte osteoclast precursors from tissue specimens in much the same way as from suspensions of peripheral blood mononuclear cells. This is particularly useful in studying osteoclast formation in tissues affected by inflammatory and neoplastic disorders that are associated with bone resorption such as rheumatoid arthritis, aseptic loosening, and bone tumors.

1. Wash tissue specimens thoroughly with PBS before cutting into small fragments.
2. Digest fragments in culture medium containing 1 mg/mL of collagenase type I for 30 min at 37°C.

3. Follow this by a further 1-h incubation in 0.25% trypsin (Sigma-Aldrich Chemicals).
4. Filter the digested tissue through a 70-μm cell strainer and pellet cells in the filtrate by centrifugation at 800g for 10 min.
5. Resuspend the cell pellet in culture medium containing 10% serum.
6. Lyse red blood cells using a 5% (v/v) acetic acid solution and count the number of leukocytes in a hemocytometer.
7. As there is a heterogeneous population of cells within each tissue specimen, add 1×10^5 CD14-postive-enriched cells (*see* **Note 1**) to 96-well plates containing either dentine slices or glass coverslips as described in **Subheadings 3.1.** and **3.2.**

3.6. Other Techniques of Osteoclast Generation from Peripheral Blood Mononuclear Cells, see Notes 6–8

3.7. Advantages and Disadvantages of Using PBMCs for Generating Osteoclasts

Generation of osteoclasts from PBMCs has distinct advantages.

1. Osteoclast precursors can be obtained readily without the use of invasive techniques.
2. The technique permits the role of osteoclast formation in systemic osteolytic disorders such as Paget's disease and osteoporosis to be studied directly.
3. It is possible to investigate the direct effect of cellular/humoral factors on an osteoclast or isolated population of osteoclast precursors. It is also possible to determine the role of other cell populations within peripheral blood mononuclear cell (e.g., T-cell subsets, granulocytes, etc.) on osteoclastogenesis (e.g., *see* the chapter by Flanagan and Massey, p. 113).

There are, however, a few disadvantages of generating osteoclasts from peripheral blood monocytes and these include:

1. The presence of relatively few mononuclear phagocyte osteoclast precursors cells in specimens of whole blood. Relatively large blood specimens are required to obtain adequate number of precursors for experiments (usually about 40–50 mL of whole blood).
2. There is individual and sex/age variability in the number of osteoclast precursors in peripheral blood; large numbers of specimens are required to carry out appropriate statistical analyses.
3. In vitro generation of human osteoclasts is time consuming and labor intensive, as each experiment is carried out over a period of 3 wk during which the culture media (plus added factors) need to be replenished twice weekly. Please note that our experiences here differ from those of some other workers who obtain osteoclast formation within 2 wk (*see* the chapter by Flanagan and Massey, *this volume*, p. 113). Each laboratory new to these techniques should try out the protocols given in this chapter and in the chapter by Flanagan and Massey and decide which culture period is best.

4. Notes

1. To increase the number of these cells and to ensure that osteoclasts are generated from the CD14-postive fraction of circulating cells, isolated PBMCs can be incubated with CD14 MicroBeads for 20 min at 4°C before being passed through a MACS magnetic cell separator *(21)* (*see* the chapter by Flanagan and Massey, p. 113, for full details).

2. Other stromal cells that have been shown to support osteoclast formation from marrow or circulating cells include the cell culture lines ST2, SAOS-2, MG63, and cultured calvarial osteoblasts and human trabecular bone-derived cells *(11,22–24)*.

3. Using the same methodology, Nicholson et al. *(25)* have recently shown that CD14-postive cells selected from human PBMCs can differentiate into active bone resorbing osteoclasts in vitro. They also noted that highly purified CD14-positive cells do not express mRNA for RANKL or OPG but express mRNA for NF-κB, whereas PBMCs expressed mRNAs for all three.

4. Although in this protocol RANKL is added throughout the culture, Nicholson et al. have recently described in detail the minimal exposure period for soluble RANKL required to generate osteoclasts from PBMC cultures *(26)*. Contrary to findings of Lam et al. *(27)*, their results suggested that early exposure of RANKL does not "prime" human PBMCs or enhance proliferation of RANKL responsive precursors. They have also shown that soluble RANKL is not required for each of the 3 wk of osteoclast formation, the second week of culture being the most crucial period of osteoclast generation from PBMCs. Moreover, they noted that incubation for as short as 1 h with soluble RANKL during the second week of a 3-wk culture can produce *bona fide* bone resorbing osteoclasts *(26)*.

5. Resorption pits are observed as either individual small pits or large multilocular areas. As such, it is necessary to define a resorption pit as an excavation of the dentine surface with a clear rim of unchanged original surface between neighboring excavations. Pit numbers are counted by a single blinded observer for all experiments. Measurement of the percentage area of resorption is a more accurate and reproducible method of quantifying the amount of lacunar resorption, particularly if this is extensive and there are numerous confluent areas of excavation on the dentine or bone slices. An image analysis method for measuring percentage resorption is described in detail in the chapter by van 't Hof, p. 145).

6. A RANKL-independent method of generating osteoclasts in vitro from human PBMCs has recently been described *(17,18)*. In this system, 1×10^6 human PBMCs are cultured on dentine slices and coverslips in the presence of 25 ng/mL of human M-CSF for 3 d after which time they are transferred to new wells containing M-CSF, 20 ng/mL of TNF-α, and 10 ng/mL of IL-1α for a further 17 d. This results in the formation of numerous TRAP-positive multinucleated cells (MNCs), some of which are capable of forming resorption pits that are generally smaller than those from PBMC cultures incubated with M-CSF and soluble RANKL.

7. Based on the fact that osteoclasts (and other cells of the monocyte-macrophage lineage) are generated from a pluripotent haemopoietic progenitor that is known

to express the antigen CD34, Matayoshi et al. *(29)* and Purton et al. *(30)* generated human osteoclasts from long-term cultures of CD34-positive cells in peripheral blood (this method is different from that described in the chapter by Flanagan and Massey, p. 113, where CD34-positive cells are directly isolated from blood marrow). As the percentage of CD34-positive cells in peripheral blood is very low (about 0.01–0.1%), each human donor was treated with granulocyte colony stimulating factor (G-CSF) for 3–5 d to mobilize the bone marrow CD34-positive cell population into the peripheral circulation. At the end of each treatment period, peripheral blood leucocytes were harvested by single leukapheresis using a Spectra Cell Separator. The CD34-positive-enriched cell population was purified by magnetic activated cell sorting, using the MiniMACS separation kit. CD34-positive cells (which did not express the stromal cell antigen, Stro-1) were seeded in 48-well culture plates and cultured in the presence of culture media containing GM-CSF, IL-1, IL-3, IL-6, and stem cell factor for 6 wk. At the end of the culture period MNCs were purified by serum gradient fractionation and immunomagnetic selection with the anti-osteoclast antibody 121F based on the methodology described in Chapter 6 by Collin-Osdoby et al., p. 65 *(31)*. Characterization of the purified osteoclasts was carried out as described in **Subheading 3.4.**

8. Faust et al. *(32)* have shown that when peripheral blood mononuclear cells are cultured at very high densities, these cells are capable of differentiating into bone resorbing osteoclasts in the absence of the addition of M-CSF or RANKL within 2 wk. These cultures consist of adherent cells having low nuclearity (mainly mono-, di-, trinuclear, ~10–20 μm in diameter). These preosteoclasts/osteoclasts were positive for TRAP, cathepsin K, VNR, and CTR and were capable of low level bone resorption. The authors suggest that cells express these osteoclast phenotypic features form from PBMCs in this way owing to the initial high cell density (1.5×10^6 cells/cm^2; 100-fold higher than other PBMC culture systems) used in their assay *(11,29)*. In this system it is likely that the essential differentiation factors required for osteoclast formation (such as M-CSF and RANKL) are supplied by other cell types present in peripheral blood, for example, monocytes and T and B lymphocytes.

References

1. Hancox, N. M. (1972) The osteoclast, in *The Biochemistry and Physiology of Bone*, (Bourne, G. H., ed.) Academy Press New York, pp. 45–67.
2. Marks, S. C., Jr and Popoff, S. N. (1988) Bone cell biology: the regulation of development, structure, and function in the skeleton. *Am. J. Anat.* **183,** 1–44.
3. Walker, D. G. (1973) Osteopetrosis cured by temporary parabiosis. *Science* **180,** 875.
4. Coccia, P. F., Krivit, W., Cervenka, J., et al. (1980) Successful bone-marrow transplantation for infantile malignant osteopetrosis. *N. Engl. J. Med.* **302,** 701–708.
5. Athanasou, N. A. (1996) Cellular biology of bone-resorbing cells. *J. Bone Joint Surg. Am.* **78,** 1096–1112.

 6. Chambers, T.J. (1985) The pathobiology of the osteoclast. *J. Clin. Pathol.* **38,** 241–252.
 7. Takahashi, N., Yamana, H., Yoshiki, S., et al. (1988) Osteoclast-like cell formation and its regulation by osteotropic hormones in mouse bone marrow cultures. *Endocrinology* **122,** 1373–1382.
 8. Kurihara, N., Chenu, C., Miller, M., Civin, C., and Roodman, G. D. (1990) Identification of committed mononuclear precursors for osteoclast-like cells formed in long term human marrow cultures. *Endocrinology* **126,** 2733–2741.
 9. Udagawa, N., Takahashi, N., Akatsu, T., et al. (1990) Origin of osteoclasts: mature monocytes and macrophages are capable of differentiating into osteoclasts under a suitable microenvironment prepared by bone marrow-derived stromal cells. *Proc. Natl. Acad. Sci. USA* **87** 7260–7264.
10. Quinn, J. M., McGee, J. O., and Athanasou, N. A. (1994) Cellular and hormonal factors influencing monocyte differentiation to osteoclastic bone-resorbing cells. *Endocrinology* **134,** 2416–2423.
11. Fujikawa, Y., Quinn, J. M. W., Sabokbar, A., McGee, J. O'D., and Athanasou, N. A. (1996) The human mononuclear osteoclast precursor circulates in the monocyte fraction. *Endocrinology* **139,** 4058–4060.
12. Lacey, D.L., Timms, E., Tan, H-L., et al. (1998) Osteoprotegerin ligand is a cytokine that regulates osteoclast differentiation and activation. *Cell* **93,** 165–176.
13. Yasuda, H., Shima, N., Nakagawa, N., et al. (1998) Osteoclast differentiation factor is a ligand for osteoprotegerin/osteoclastogenesis is identical to TRANCE/RANKL. *Proc. Natl. Acad. Sci. USA* **95,** 3597–3602.
14. Quinn, J.M.W., Elliott, J., Gillespie, M.T., and Martin, T.J. (1998) A combination of osteoclast differentiation factor and macrophage-colony stimulating factor is sufficient for both human and mouse osteoclast formation in vitro. *Endocrinology* **139,** 4424–4427.
15. Matsuzaki, K., Udagawa, N., Takahashi, N., et al. (1998). Osteoclast differentiation factor (ODF) induces osteoclast-like cell formation in human peripheral blood mononuclear cell cultures. *Biochem. Biophys. Res. Comm.* **246,** 199–204.
16. Kobayashi, K., Takahashi, N., Jimi, E., et al. (2000) Tumor necrosis factor alpha stimulates osteoclast differentiation by a mechanism independent of the ODF/RANKL-RANK interaction. *J. Exp. Med.* **191,** 275–286.
17. Hirayama, T., Sabokbar, A., and Athanasou, N.A. (2000) Humoral factors act directly on circulating osteoclast precursors to control osteoclast formation. *Calcif. Tissue Int.* **66** (Suppl 1), 212.
18. Kudo, O., Fujikawa, Y., Itonaga, I., Sabokbar, A., and Athanasou, N. A. (2002). Pro-inflammatory cytokine (TNFα/IL-1α) induction of human osteoclast formation. *J. Pathol.* **198,** 220–227.
19. Horton, M.A., Lewis, D., McNulty, K., Pringle, J.A.S., and Chambers, T.J. (1985) Monoclonal antibodies to osteoclastomas (giant cell bone tumours): definition of osteoclast specific cellular antigens. *Cancer Res.* **45,** 5663–5669.
20. Hattersley, G. and Chambers, T. J. (1989) Calcitonin receptors as markers for osteoclastic differentiation: correlation between generation of bone-resorptive

cells and cells that express calcitonin receptors in mouse bone marrow cultures. *Endocrinology* **125** 1606–1612.

21. Massey, H.M. and Flanagan, A.M. (1999) Human osteoclasts derive from CD14-positive monocytes. *Br. J. Haematol.* **106,** 167–170.

22. Blair, H.C., Sidonio, R.F., Friedberg, R.C., Khan, N.N., and Dong, S.S. (2000) Proteinase expression during differentiation of human osteoclasts in vitro. *J. Cell Biochem.* **78,** 627–637.

23. Neale, S.D., Fujikawa, Y., Sabokbar, A., et al. (2000) Human bone-derived cells support formation of human osteoclasts from arthroplasty-derived cells in vitro. *J. Bone Joint Surg.* **82B,** 892–900.

24. Itoh, K., Udagawa, N., Matsuzaki, K., et al. (2000) Importance of membrane- or matrix-associated forms of M-CSF and RANKL/ODF in osteoclastogenesis supported by SaOS-4/3 cells expressing recombinant PTH/PTHrP receptors. *J. Bone Miner. Res.* **15,** 1766–1775.

25. Nicholson, G.C., Malakellis, M., Collier, F.M., et al. (2000). Induction of osteoclasts from CD14-positive human peripheral blood mononuclear cells by receptor activator of nuclear factor kappaB ligand (RANKL). *Clin. Sci.* **99,** 133–140.

26. Nicholson, G. C., Aitken, C. J., Hodge, J. M., et al. (2001). Limited RANKL exposure in vitro induces osteoclastogenesis in human PBMC. *Bone* **28** (Suppl), S161.

27. Lam, J., Takeshita, S., Barker, J. E., Kanagawa, O., Ross, P. F., and Teitelbaum, S. L. (2000) TNF-alpha induces osteoclastogenesis by direct stimulation of macrophages exposed to permissive levels of RANK ligand. *J. Clin. Invest.* **106,** 1481–1488.

28. Minkin, C. (1982) Bone acid phosphatase: tartrate-resistant acid phosphatase as a marker of osteoclast function. *Calcif. Tissue Int.* **34,** 285–290.

29. Matayoshi, A., Brown, C., DiPersio, J.F., et al. (1996) Human blood-mobilized hematopoietic precursors differentiate into osteoclasts in the absence of stromal cells. *Proc. Natl. Acad. Sci. USA* **93,** 10,785–10,790.

30. Purton, L.E., Lee, M.Y., and Torok-Storb, B. (1996) Normal human peripheral blood mononuclear cells mobilized with granulocyte colony stimulating factor have increased osteoclastogenic potential compared to non-mobilized blood. *Blood* **87,** 1802–1808.

31. Collin-Osdoby, P., Oursler, M.J., Webber, D., and Osdoby, P. (1991) Osteoclast-specific monoclonal antibodies coupled to magnetic beads provide a rapid and efficient method of purifying avian osteoclasts. *J. Bone Miner. Res.* **6,** 1353–1365.

32. Faust, J., Lacey, D.L., Hunt, P., et al. (1999) Osteoclast markers accumulate on cells developing from human peripheral blood mononuclear precursors. *J. Cell Biochem.* **72,** 67–80.

9

Generating Human Osteoclasts In Vitro from Bone Marrow and Peripheral Blood

Adrienne M. Flanagan and Helen M. Massey

1. Introduction

Osteoclasts derive from macrophage colony-stimulating factor (M-CSF)-dependent hemopoietic precursors that develop into cells that express the $\alpha_v\beta_3$ subunit of the vitronectin receptor (VNR) and the calcitonin receptor (CTR). The extracellular degradative process, known as bone resorption, is the hallmark of the osteoclast, and includes removal of both the hydroxyapatite and organic components of the skeleton. For bone resorption to occur, osteoclasts form a subcellular space, referred to as an extracellular lysosome, into which they secrete acid and enzymes when they come into contact with either calcified bone or dentine but not with plastic or uncalcified collagen-based matrices. This subcellular space is dependent upon the formation of a "tight seal" by the osteoclast, a process involving rearrangement of the cytoskeleton into a characteristic F-actin ring structure (*see* the chapter by Nesbitt and Horton, *this volume*, for details).

This chapter addresses the various means by which human osteoclasts can be generated in vitro and describes the conditions that we have found optimal for generation of osteoclasts from both human peripheral blood mononuclear cells and bone marrow hemopoietic precursors. These conditions are not always similar to those required for murine osteoclast formation, and readers are directed to the chapter by Takahashi et al., *this volume*, for this information.

M-CSF-dependent precursors, capable of forming osteoclasts, exist in the bone marrow and peripheral and cord blood. From these hemopoietic sources, osteoclasts can be formed with relative ease and with good reproducibility provided a few crucial conditions are adhered to. The phenotypes of osteoclasts in these assays are largely similar to those of osteoclasts formed in vivo *(1,2)*, and

in only one circumstance have we identified a phenotypic difference in osteo-
clasts generated in vivo and in vitro *(2)*, (*see* **Table 1**). Using hemopoietic
precursors from different individuals, we have found that some variability is
observed in the number of osteoclasts generated in vitro. However, we have
not found that this prevents these osteoclast-forming in vitro assays from being
used as a means of testing responses to various agents. For example, we have
reproducibly found that: 17β-estradiol suppresses osteoclast formation gener-
ated from bone marrow cell cultures derived from post-menopausal women
and men, but not in bone-marrow cultures generated from premenopausal
women *(3)*; prostaglandins are essential for osteoclasts generated from human
bone marrow cell cultures *(4)*; transforming growth factor β (TGF-β) and
interleukin (IL)-4 and IL-13 enhance the osteoclast-forming potential of
peripheral blood hemopoietic precursors in a lymphocyte-rich microenviron-
ment *(5,6)*; and IL-4 and IL-13 consistently suppress osteoclast formation from
CD14-derived peripheral blood mononuclear cells (PBMNCs) *(6)*. Clearly, if
near maximal osteoclast formation occurs in a particular culture in the pres-
ence of M-CSF and the receptor activator for NFκB ligand (RANKL) (*see*
Note 1) it is impossible to detect enhancement of osteoclast formation or bone
resorption. This limitation of the human osteoclast forming in vitro assays is
difficult to overcome because it is not possible to predict in advance which
cultures give rise to small or large numbers of osteoclasts.

2. Materials
2.1. For Cell Isolation

1. Ficoll–Paque (Amersham Pharmacia Biotech, Little Chalfont, Buckinghamshire, UK).
2. Phosphate-buffered saline (PBS).
3. Various culture media are used successfully for the generation of human osteo-
   clasts including RPMI 1640, minimum essential medium (MEM) Eagle (Sigma-
   Aldrich Ltd., Gillingham, Dorset, UK), and MEM (Gibco Life Technologies,
   Paisley, Scotland, UK; *see* **Note 2**). The sera are supplemented with 10% batch-
   tested (*see* **Note 3**), heat-inactivated fetal or neonatal bovine serum (although
   15% of some sera are more effective at inducing osteoclast formation), 2 m*M* L-
   glutamine, 100 IU benzylpenicillin/mL, and 100 μg of streptomycin/mL (this is
   referred to hereafter as complete medium).
4. "Mister Frosty" vials (Nunc) or similar, for freezing cells. *See* **Note 7**.
5. DNase (Roche Diagnostics Ltd., Lewes, E. Sussex, UK). *See* **Note 28**.

2.2. For Osteoclast Cultures

1. UMR 106.01 cells (a gift from Professor T. J. Martin, Melbourne, Australia) are
   grown in MEM.
2. Devitalized bone slices or dentine discs (*see* **Note 4**).

Table 1
The Phenotype of the Osteoclast Precursor and Mature Resorbing
form as They Develop from Peripheral Blood and Bone Marrow Precursors

Blood	Tissue	
Osteoclast precursor →	→ Nonresorbing osteoclast →	→ Resorbing osteoclast
CTR –	CTR +	CTR +
VNR –	VNR +	VNR +
	F-actin ring –	F-actin ring +
CD11b +	CD11b +	CD11b –
CD11c +	CD11c +	CD11c +/–
	CD13 +	CD13 +
CD14 +	CD14 +	CD14 –
	CD16 –	CD16 –
	CD44 +	CD44 +
	CD54 +	CD54 +
	CD68 +	CD68 +

Peripheral blood mononuclear cells and bone marrow cells were plated on bone slices and cocultured with either UMR 106 cells in the presence of M-CSF or, in the absence of UMR 106 cells, with M-CSF and RANKL. The bone slices were removed from the cultures daily and assessed for the presence of cells simultaneously expressing the calcitonin receptor, using salmon ^{125}I-calcitonin and other markers. In addition, cells forming F-actin ring structures were assessed for coexpression of other markers. The immunophenotype of the osteoclast, as determined by the expression of the calcitonin receptor or the F-actin ring, was similar in vivo to that observed in vitro for all markers except when osteoclasts were generated in vitro in the presence of soluble RANKL *in the absence* of a stromal cell population. Under these conditions CD11c was expressed by virtually all CTR-positive F-acting-positive *resorbing* osteoclasts in vitro whereas in the presence of stroma CD11c is expressed only *transiently* by CTR-positive cells and its expression is lost when the F-actin ring is formed (*see* **refs.** *2* and *8*).

3. Cytokines/growth factors: TGF-β, IL-4, and IL-13 (R&D Systems). M-CSF was a gift from the Genetics Institute (Boston, MA) and RANKL was a gift from Amgen (CA, USA) (*see* **Note 5**). Hydrocortisone, prostaglandin E_2, and indomethacin were purchased from Sigma Aldrich Ltd. (Poole, Dorset, UK).

2.3. Immunomagnetic Cell Separation

1. Fluorescein isothiocyanate (FITC)-labeled monoclonal antibodies to CD3 and CD14, magnetic anti-FITC MicroBeads, CD34 Progenitor Cell Isolation Kit, positive selection columns, preseparation filters, and a magnet were all purchased from Miltenyi Biotec Ltd. (Bisley, Surrey, UK) FITC-labeled anti-CD19 was purchased from BD Biosciences (Oxfordshire, UK).
2. Cell separating buffer was used throughout the magnetic cell sorting procedure and made as directed by the manufacturer (Miltenyi Biotec Ltd.). PBS, pH 7.2, was supplemented with 0.5% heat-inactivated fetal or neonatal bovine serum and 2 m*M* ethylenediaminetetraacetic acid (EDTA; Sigma Aldrich Ltd.).

3. Methods
3.1. Preparation of Cells for Osteoclast Generation

1. As sources of osteoclast precursors use: peripheral blood (obtained from volunteers by venipuncture), cord blood (obtained with the consent of mothers from placentae postpartum, or bone marrow (aspirated from the posterior iliac crest of volunteers under either general or local anesthetic; *see* **Note 6**). Use heparin or EDTA to prevent coagulation.
2. Dilute the blood and bone marrow 1:1 in PBS. Additional heparin or EDTA is not required.
3. Separate mononuclear cells by centrifugation over Ficoll–Paque density gradients at room temperature following the manufacturer's instructions. Gently layer 35 mL of diluted peripheral blood or bone marrow over 15 mL of Ficoll–Paque and centrifuge at 1500 rpm for 30 min with the brake set "off." Keeping the same ratio, alter volume of blood and bone marrow to Ficoll–Paque as required.
4. Remove the mononuclear cell layer from the Ficoll–Paque/plasma interface and wash in 10 mL of PBS at 1500 rpm for 10 min. The brake can be set at "on" on this occasion. Either use the cells immediately, or alternatively freeze them (approx 1×10^7 cells in 1 mL of serum containing 10% dimethyl sulfoxide [DMSO]). Freeze in a controlled manner by placing vials at –80°C overnight in a "Mister Frosty" filled with isopropanol, and store in liquid nitrogen for use at a later time (*see* **Note 7**).
5. If the experiment is to be performed immediately, resuspend the pellet of cells in culture medium or cold cell-separating buffer for magnetic selection of mononuclear cell subpopulations as required.

3.2. Generation of Osteoclasts from Human Peripheral Blood Mononuclear Cells Using UMR 106.01 Cells as a Source of RANKL

This method is based on the original description of Fujikawa et al. *(7)*.

1. Plate 2×10^4 UMR 106.01 cells in 100 μL of RPMI medium on each bone slice present in a 96-well plate. Incubate overnight at 37°C in a humidified atmosphere of 3% CO_2/97% air (*see* **Notes 8** and **9**).
2. Sediment 1×10^5 PBMNCs/well (prepared as described in **Subheading 3.1.**) in 100 μL of RPMI medium on the UMR cells. After 2–4 h remove the bone slices, one by one, from the wells using sterile forceps and wash the bone slices in PBS (containing antibiotics but *not* serum). Transfer each bone slice to a fresh well of a 96 well plate containing 100 μl of RPMI medium/well (leaving behind the cells that have settled on the plastic). Add an additional 100 μL of medium/well containing 50 ng/mL of M-CSF (this gives a final concentration of 25 ng/mL). Incubate the cultures at 37°C in an incubator set to 3% CO_2/97% air. (*see* **Note 8** and **9**).
3. Feed the cultures twice per week (*see* **Note 11**) by removing half of the medium and adding 100 μL of fresh medium containing M-CSF (25 ng/mL). Terminate the cultures as required; osteoclasts should appear in small numbers by d 3 and large areas of bone resorption should be present by d 10–14 that are rarely significantly increased after d 14.

3.3. Generation of Human Osteoclasts from Washed PBMNCs in the Presence of M-CSF and RANKL (2,5,6) *(see Note 9)*

1. Prepare PBMNCs as described in **Subheading 3.1.**
2. Place bone slices in wells of a 96-well plate.
3. Plate 2×10^5 PBMNCs in 100 μL of MEM, without any added cytokines, on the bone slices. Incubate the cells at 37°C at 5%CO_2–95% air (*see* **Note 10**) for 2–4 h.
4. Remove the plate from the incubator. Remove the bone slices, one by one, from the wells using sterile forceps and wash the bone slices in PBS (containing antibiotics but *not* serum).
5. Place the washed bone slices in wells of a new 96-well plate containing 100 μL of MEM.
6. Add an additional 100 μL of medium (makes a total volume of 200 μL) containing 50 ng/mL of M-CSF (*see* **Note 11**) and 60 ng/mL of RANKL to each well.
7. Place the tissue culture plate in the incubator (d 1) at 37°C in a humidified atmosphere of 5% CO_2–95% air and remove for feeding on d 4 or 5 (feed 1; *see* **Note 12**). Feeding involves removing 100 μL of medium from each well and replacing this with 100 μL of fresh medium containing 25 ng/mL of M-CSF and 30 ng/mL of RANKL.
8. Feed the cultures again 3 or 4 d later (feed 2: d 7 or 8) as described in **step 7**.
9. Feed again 3 or 4 d later (feed 3: d 10 or 11) as described in **step 7**.
10. Stop the experiment on d 14 or as required (*see* **Notes 13** and **14**).

3.4. Generation of Human Osteoclasts from CD14-Positive Cells Selected from PBMNCs (8)

1. Prepare PBMNCs as in **Subheading 3.1.**
2. Select CD14-positive cells by adding 10 μL of anti-CD14-FITC to 1×10^7 PBMNCs resuspended in 100 μL of cell separating buffer. Cell separating buffer is used throughout the magnetic cell sorting procedure and is made as directed by the manufacturer (Miltenyi Biotec Ltd.). In brief, PBS, pH 7.2, is supplemented with 0.5% heat-inactivated fetal or neonatal bovine serum and 2 m*M* EDTA (Sigma Aldrich Ltd.). Mix the cells and antibody well using a pipet and then incubate the mixture in the dark for 10 min at 6°C. MiniMACS columns can separate 10^3–10^7 labeled cells from a total population of 2×10^8 cells but larger scale selections are possible with different columns.
3. Wash the labeled PBMNCs in cold cell-separating buffer and centrifuge at 1500 rpm for 10 min. Resuspend the pellet in the 10 μL of separating buffer. Add 10 μL of anti-FITC MicroBeads per 1×10^7 PBMNCs and incubate static for 15 minutes at 6°C in the dark.
4. Repeat the washing step, resuspend the cell pellet in 500–1000 μL of cell separating buffer, and pass the PBMNCs through a primed magnetic cell separation column. The CD14-positive cell fraction is held within the column, while the CD14-negative cells pass through. CD14-positive cells are then eluted from the

column on its removal from the magnetic field. The selected cells are expected to be at least 97% pure, and this can be assessed using a flow cytometer (*see* **Note 15**).

5. Place bone slices in wells of a 96-well plate.
6. Plate 5×10^4–1×10^5 CD14-positive PBMNCs in 100 μL of MEM medium on the bone slices.
7. Continue with the culture as described in **Subheading 3.3.**, **steps 6–10**.

3.5 Osteoclast Formation from Unwashed (Lymphocyte-Rich) Human PBMNC Cultures in the Presence of Either IL-4 or IL-13 (6) to Increase Osteoclast Formation (see Notes 16 and 20)

1. Isolate PBMNCs as described in **Subheading 3.1.**
2. Place bone slices in wells of a 96-well plate.
3. Plate 2×10^5 PBMNCs in 100 μL of MEM on the bone slices.
4. Add 100 μL of MEM containing 50 ng/mL of M-CSF and 2 ng/mL of IL-4 or 0.2 ng/mL of IL-13 to each well (*see* **Notes 17** and **18**).
5. Place the tissue culture plate in the incubator at 37°C in a humidified atmosphere of 5% CO_2–95% air (d 1) and remove for feeding on d 4 or 5 (feed 1; *see* **Note 12**). This involves removing 180 μL of medium and replacing this volume with fresh medium (*see* **Note 19**). This fresh medium contains 25 ng/mL of M-CSF and 30 ng/mL of RANKL. IL-4 or IL-13 is *not* added at this time; they are added only on d 1.
6. Feed the cultures again 3 or 4 d later (feed 2: d 7or 8) but this time remove only 100 μL of the medium and replace with 100 μL of fresh medium containing 25 ng/mL of M-CSF and 30 ng/mL of RANKL.
7. Feed again 3 or 4 d later (feed 3: d 10 or 11).

3.6. Osteoclast Formation from Unwashed (Lymphocyte-Rich) Human PBMNC Cultures in the Presence of TGF-β (5) (see Notes 20 and 21)

1. Isolate PBMNCs as described in **Subheading 3.1.** Place bone slices in wells of a 96-well plate.
2. Plate 2×10^5 PBMNCs in 100 μL of MEM medium on the bone slices.
3. Add 100 μL of MEM medium containing 50 ng/mL of M-CSF and 20 ng/mL of TGF-β to each well to give a final concentration of 25 ng/mL of M-CSF and 10 ng/mL of TGF-β. Do not add RANKL at this point (*see* **Notes 16** and **21**).
4. Place the tissue culture plate in an incubator at 37°C in a humidified atmosphere of 5% CO_2–95% air (d 1) and remove for feeding on d 4 or 5 (feed 1; *see* **Note 12**). This involves removing 100 μL of medium and replacing with 100 μL of fresh medium containing 25 ng/mL of M-CSF and 60 ng/mL of RANKL. Do not add TGF-β at this time; it is added only on d 1; (*see* **Note 21**).
5. Feed the cultures again 3 or 4 d later (feed 2: d 7 or 8). Remove 100 μL of the medium and replace with 100 μL of fresh medium containing 25 ng/mL of M-CSF and 30 ng/mL of RANKL.
6. Feed again 3 or 4 d later (feed 3: d 10 or 11) as described in **step 5**.
7. Stop the experiment on d 14 or as required (*see* **Notes 13** and **14**).

3.7. Generation of Osteoclasts from Human Bone Marrow, General Considerations

Generating osteoclasts from human bone marrow is extremely efficient, as marrow contains high numbers of early hemopoietic precursors. However, the effort of obtaining bone marrow on a regular basis in large volumes prohibits most research laboratories from using it frequently for the generation of human osteoclasts.

Three protocols are given below: one in which a stromal osteoblastic/fibro-blastic supporting cell layer is used as source of RANKL and in which no endogenous RANKL is added (two-phase culture system), a second in which osteoclasts are generated from nonadherent bone marrow M-CSF-dependent cells in the presence of recombinant human or murine RANKL, and a third in which purified early hemopoietic precursors (CD34-positive cells) are used to generate human osteoclasts in the presence of recombinant RANKL, M-CSF, and other cytokines.

3.8 Generating Human Osteoclasts from Whole Human Bone Marrow Without Addition of RANKL

This methodology was developed prior to the cloning of RANKL *(13)*. It had been anticipated for some time that an osteoclast differentiation factor existed and that it was membrane bound *(14)*. This method is reproducible but the draw-back is that osteoclast formation takes 3–4 wk. This was the first in vitro model in which 17β-estradiol was found to suppress osteoclast formation *(3,15)*.

1. Bone marrow is aspirated from the posterior iliac crest of volunteers under either local or general anesthetic (*see* **Note 6**).
2. Prepare bone marrow mononuclear cells over a Ficoll–Paque density gradient as described in **Subheading 3.1.**
3. Plate the cells in tissue culture flasks (10^5 cells/cm^2 of tissue culture flask) either in MEM or RPMI supplemented with M-CSF (final concentration 5 ng/mL) or in the absence of M-CSF (*see* **Note 22**).
4. Feed the cultures on d 5 and d 10 by removing half of the medium and replacing this with the same volume of fresh medium containing 5 ng/mL of M-CSF and 10^{-6} *M* of hydrocortisone. Replace the non-adherent cells removed when feeding; this is achieved by centrifuging the spent medium and resuspending the cellular pellet in the fresh medium being added to the flasks. 10^{-6} *M* of hydrocortisone is present throughout the whole culture period (phases I and II; *see* **Note 23**).
5. Maintain the culture until the cells become confluent; this occurs between d 9–14 (*see* **Note 24**).
6. Harvest the cells in the flasks using trypsin–EDTA. Centrifuge the cells to give a pellet and resuspend the cells in fresh medium and plate on bone slices (high density) at 10^5 cells/well in a 96-well plate. This is phase II of the culture.
7. Add M-CSF (final concentration 50 ng/mL) to the cultures (*see* **Note 22**).

8. Terminate the cultures as described in **Notes 13** and **14** for the PBMNC cultures. Osteoclasts and VNR- and CTR-positive cells appear on d 5–7, F-actin ring structures appear 48 h later, and bone resorption commences almost immediately thereafter (*see* **Note 25**).

3.9 Generation of Human Osteoclasts from M-CSF-Dependent NonAdherent Hemopoietic Precursors (see Note 26)

1. To obtain a M-CSF-dependent population, prepare the mononuclear cells over Ficoll–Paque as described in **Subheading 3.1.**
2. Remove the lymphocytes by magnetic selection using CD3 and CD19 antibodies, following the protocol described in **Subheading 3.4.** Test for remaining lymphocyte contamination using a flow cytometer (*see* **Note 15**).
3. Plate the bone marrow mononuclear cells overnight in medium in a tissue culture flask (75 cm^2). The cell density is not critical at this point but approx 10^7 cells are plated in a 75-cm^2 tissue flask
4. The next day harvest the nonadherent cells by centrifugation and resuspend the pellet in either complete MEM or RPMI medium. Discard the adherent cells.
5. Plate the nonadherent cells on bone slices (10^5 cells/well of a 96-well plate; *see* **Note 27**) in the presence of M-CSF and RANKL (final concentrations 25 ng/mL and 30 ng/mL, respectively). Do *not* add hydrocortisone.
6. Feed the cultures every 3–4 d (*see* **Note 12**) by removing half of the medium and replacing it with fresh medium and cytokines.
7. To ensure that the hemopoietic precursors are truly M-CSF-dependent (and not surviving because stromal cells are present), control cultures in the absence of M-CSF should also be included. After 10 d all of the cells in these control cultures should be dead.
8. Terminate the experiment at the time required (*see* **Note 13**); osteoclasts should be present on d 10 and extensive bone resorption by d 14 (*see* **Note 14**).

3.10 Generation of Osteoclasts from CD34-Positive Cells Selected from Bone Marrow

1. Aspirate bone marrow from volunteers into a heparinized container.
2. Dilute 1:1 with serum-free RPMI containing 100 U/mL of DNase and shake gently for 45 min at room temperature (*see* **Note 28**).
3. Separate the mononuclear cells from the red blood cells using Ficoll–Paque, as described in **Subheading 3.1**.
4. Select CD34-positive cells using the CD34 Progenitor Cell Isolation Kit, using the manufacturer's instructions (**steps 5–10** below).
5. Add 100 μL of FcR Blocking Reagent per 1×10^8 total cells in 300 μL of cell separating buffer C.
6. Label cells by adding 100 μL of CD34 MicroBeads per 1×10^8 total cells. Mix well and incubate for 30 min at 6°C.
7. Wash the cells in cell separating buffer at 1500 rpm for 10 min and resuspend the cell pellet in 500–1000 μL of buffer.

8. Pass the mononuclear cells through a magnetic cell separation column via a 30-μm filter to remove any clumps. This filtering process is used only when separating CD34-positive cells from bone marrow. The CD34-positive fraction is held within the column, while the CD34-negative cells pass through.

9. Elute the CD34-positive cells from the column by removing it from the magnetic field.

10. The purity of the selected cells can be tested by incubating 1×10^6 selected cells with an anti-CD34 monoclonal antibody labeled with phycoerythrin (PE) (Miltenyi Biotec Ltd.) and analyzed using a flow cytometer (*see* **Note 15).**

11. Place bone slices in wells of a 96-well plate.

12. Plate 2×10^4 CD34-positive mononuclear cells in 100 μL of complete MEM or RPMI medium on the bone slices.

13. Add 100 μL of MEM–RPMI medium containing 50 ng/mL of M-CSF and 60 ng/mL of RANKL to each well (*see* **Note 29**).

14. Proceed as described in **Subheading 3.3.**, **steps 7–10**.

4. Notes

1. We define maximal osteoclast formation as resorption of 80–100% of the bone slices (3 × 3 mm). This equates to approx 600 VNR-positive cells which generally occurs on d 10–14 of culture.

2. The presence or absence of phenol red appears to make no significant difference to the outcome of peripheral blood or bone marrow experiments.

3. The serum should be batch-tested (companies will hold sera batches for you for several weeks). A large order for the serum of your choice should then be placed. In this way, it is necessary only to batch-test sera approx every 2–3 yr.

4. Devitalized bovine bone and dentine can be used as a substrate for human osteoclast resorption. The preparation details of dentine slices are described in Chapter 11 by van 't Hof, *this volume*. Bone slices are prepared from bovine cortical bone; the bone is purchased fresh from the local butcher. It should be frozen at –20°C if not prepared immediately. Preparing the bone involves removing all of the adherent soft tissue with a sharp knife. The bone is cut transversely on a band saw and the fatty marrow is then removed. Subsequently, the rings of bone are cut into three or four segments that can be placed on the diamond blade bone saw from which wafers (1 mm thick) can be sectioned. Square bone slices (3 × 3 mm^2) can be cut from the wafers using a scalpel or sharp, fine scissors. Dentine can be processed in the same way. Bone or dentine slices can be sterilized by UV light (in tissue culture hood cabinet, minimum of 30 min), or by storage in 75% ethanol. Rehydrate slices in PBS before use. The advantage of using *square* slices of substrate means that it is possible to visualize the cells on the plastic surrounding the bone or dentine during the experiment; this cannot be done if discs of the substrate are employed as they fill the well. Plating cells in some additional wells without substrate overcomes this problem.

5. M-CSF is synthesized in membrane-associated and secreted forms and can either be added to the osteoclast-forming cultures as a recombinant soluble molecule or can be present endogenously in the cultures *(16)*. M-CSF is essential for human

osteoclast formation, but *murine* M-CSF does not mediate an effect on human cells *(7,13)*. In contrast, *human* M-CSF induces osteoclast formation from *murine* hemopoietic precursors. There have been reports that vascular endothelial growth factor (VEGF) can substitute for M-CSF. However, we have been unable to reproduce this work. In our studies, we have used human M-CSF gifted from Genetics Institute (Boston, MA, USA), but human recombinant M-CSF is also commercially available from several companies, in particular R & D Systems and Peprotech (both in the UK).

RANKL is a membrane-bound molecule, now available as a recombinant soluble molecule (for review *see* **ref. 14**). It induces osteoclast differentiation from M-CSF-dependent precursors. It also enhances osteoclast activity, thereby increasing bone resorption *(17)*. However, this function is difficult to assess in recruitment assays because osteoclast formation continues throughout most of the experiment. RANKL is not species specific. In our work, we have used recombinant human RANKL, obtained as a gift from Amgen: however, RANKL is also commercially available from several companies, in particular Peprotech and Insight Biotechnology. It is advisable to batch-test and titrate different lots for biological activity. If large numbers of experiments are to be carried out, it is recommended that a large quantity is ordered, as this allows for considerable cost savings to be achieved.

6. Local ethical committee approval should be obtained before human blood or bone marrow is taken and used in experiments. Informed consent should be obtained from all individual donors and from mothers before obtaining cord blood. Approximately 10^7–2×10^7 PBMNCs is generally obtained following Ficoll density separation of 10 mL of peripheral blood. The number of mononuclear cells obtained from a bone marrow aspirate is considerably more variable and ranges between 10^7 and 10^8 mononuclear cells from a 10-mL aspirate. To obtain large numbers of PBMNCs ($>10^8$) it may be possible to obtain "blood packs," that is, the buffy coat from a single blood donation from an individual. Most blood transfusions are now given with leukocyte-depleted blood and many blood transfusion services will make excess or outdated blood packs available for research. Cells should be prepared over Ficoll-Paque as described in **Subheading 3.1.** This large volume of cells is useful for titration studies and experiments in which many different factors are tested. It is important to note that all cells are derived from an individual donor

7. Up to 20% of the frozen sample of bone marrow and peripheral blood does not survive the freezing process. Apart from this initial loss, however, osteoclasts are formed in the normal fashion. To maximize cell viability it is important to thaw frozen cell samples quickly in warm water and immediately wash in culture medium.

8. In the original description of the method of generating osteoclasts from peripheral blood *(7)*, bone slices on which cells were plated were cultured in wells of a 24-well plate in an incubator set at $p\mathrm{CO_2}$ of 5%. This procedure permitted the UMR cells to continue to grow and provided ample medium for these highly metabolic cells. We suspect that as a result of having a large volume of medium

in the wells of 24-well plates, the pH of the medium remains sufficiently high (alkaline) to permit osteoclast formation. However, we made minor modifications to this initial protocol. We found that if the bone slices bearing the plated mononuclear cells were transferred from a 96 well plated into *fresh wells of a 96-well plate*, instead of a 24-well plate, and the cultures were maintained in an incubator set at a pCO_2 of 3%, osteoclasts formed efficiently *(8)*. The reason for doing this was to prevent acidification of the medium, as it is well documented that osteoclast formation requires alkaline conditions (*see* the chapter by Hoebertz and Arnett, *this volume*). Ninety-six-well plates were chosen over 24-well plates, as fewer reagents are used and this reduces the cost of the experiments, and second, we find that microorganism contamination of the cultures occurs less frequently in 96-well plates. Our study and manipulation of the pCO_2 underscores the importance of pH in osteoclast formation. *See also* **Note 10**.

9. Osteoclasts can be generated by culturing unfractionated PBMNCs in the presence of M-CSF and RANKL. However, removal of the nonadherent population (mainly lymphocytes) by washing the bone slices 2–4 h (even up to 24 h) after the cells have been plated results in enhanced osteoclast formation *(5,6)*. This washing procedure is tedious and is associated with increased risk of microorganism contamination. We have found that the addition of IL-4 or TGF-β to lymphocyte-rich PBMNC osteoclast-forming cultures eliminates the need to remove nonadherent PBMNCs (*see* **Subheadings 3.5.** and **3.6.**) *(5,6)*. However, the particular procedure that is chosen for generating human osteoclasts will depend on the question being investigated.

10. The pH of the culture medium is critical for both osteoclast formation and bone resorption. *This point cannot be overemphasized:* Osteoclasts will not form or, if they form, they will not resorb, irrespective of the starting population of M-CSF-dependent cells and the concentrations of M-CSF and RANKL if the pH of the medium is not optimized. Arnett and co-workers have reported on this in detail using murine cultures (*this volume*). To date, no such detailed analysis of pH has been reported using human cultures. However, consistent with the fact that pH is determined by cell density (the higher the cell density, the more acidic the medium becomes) and the concentration of CO_2, we have found that these two parameters are crucial for the success of the human osteoclast-generating in vitro models described in this chapter. Also, ensure that there is sufficient water in the incubator at all times as failure to do so will alter the pCO_2. Unlike the procedure described by Hoebertz and Arnett, *this volume*, we do not acidify our human osteoclast cultures by adding HCl, because we find that the pH of the medium becomes reduced sufficiently during the culture period to activate the osteoclasts to resorb. Regular monitoring of the concentration of the pCO_2 (twice per week) in the culture incubators is performed using a Bacharach Fyrite (Leec Ltd., Nottingham, Nottinghamshire, UK). In all of our cultures, unless otherwise stated (**Subheading 3.2., Note 8**), the CO_2 concentration in the incubator is 5%.

11. The final concentration of M-CSF in human osteoclast forming experiments is 25 ng/mL, although this may depend on the source of the product. Titration

experiments may need to be performed to assess biological activity when a new batch or supplier is used (*see also* **Note 5**). When 100 μL of medium containing M-CSF is first added to the cultures the concentration of M-CSF is 50 ng/mL because it is diluted in 100 μL of medium already present in the culture wells. On feeding, 100 μL of medium is removed from the wells of a 96 well plate and 100 μL is replaced; this 100 μL of fresh medium contains 25 ng/mL of M-CSF (not 50 ng/mL) because it is considered that the cytokine in the medium that has not been removed will not have degraded significantly. This same presumption is made for other cytokines.

12. The medium in osteoclast forming cultures is replaced every 3–4 d. As a rule, if an experiment is set up on Monday or Thursday it is fed on Thursdays and Mondays. If an experiment is set up on Tuesday or Friday it is fed on Fridays and Tuesdays. If an experiment is set up on Wednesday, it is first fed on Monday and subsequently on Thursdays and Mondays.

13. Experiments are stopped in different ways depending on which information is required. For assessment of osteoclast numbers using tartrate resistant acid phosphatase (TRAP) or the VNR as markers and for assessment of bone resorption, bone slices are removed from the culture medium, washed in PBS to remove cell debris, and then left to air-dry. Fixation can be deferred until the immunohistochemistry or enzyme histochemistry is to be performed. The cells are fixed in 10% formalin for TRAP staining and in cold acetone for labeling with antibody 23c6 (for VNR). Bone and dentine substrates and plastic discs can be stored frozen following drying if histochemistry cannot be performed immediately. Bone resorption can be visualized under reflected light or by scanning electron microscopy by either staining with toluidine blue or sputter-coating with gold, respectively. Fixation of cells for confocal microscopy requires that the cells are placed in fixative immediately. However, the type of fixation varies depending on the antibody being used and may require optimization for new untested antibodies. Details of these techniques are described in Chapter 11 by van 't Hof and Chapter 19 by Nesbitt and Horton, *this volume*.

14. In our experience, if large numbers of osteoclasts (approx 200 VNR-positive cells per bone slice) have not formed by d 10 and bone resorption has not occurred by d 14, the chance of successful generation of human osteoclasts is extremely low. However, occasionally osteoclasts can develop up to d 21 but this indicates that the conditions for osteoclast formation are suboptimal and it is therefore worth spending time optimizing the culture conditions.

15. This is achieved by selecting fluorescently labeled cells using a fluorochrome conjugated primary antibody, for example, HPCA-2 (Becton Dickinson Ltd.). The analysis must include negative controls, including unselected PBMNCs and/ or unselected PBMNCs previously incubated with a FITC-conjugated, isotype-matched control antibody (Dako Ltd., Ely, Cambridgeshire, UK).

16. The role of the immune system is intricately involved in the regulation of osteoclast formation *(9,10)*. We were interested in identifying which lymphocyte-produced molecule(s) might suppress osteoclast formation and the mechanism by

which this occurs and found that macrophage-deactivating molecules (TGF-β, indomethacin [unpublished data], IL-4, and IL-13) block the suppressive effect that lymphocytes exert on human osteoclast formation from PBMNCs *(5,6)*. The addition of these factors to the cultures results in reproducible enhancement of osteoclast formation and avoids the need to remove lymphocytes either by washing or obtaining a lymphocyte-free population by selection of CD14-positive cells. Interestingly, the mechanism by which TGF-β and IL-4/IL-13 mediate their effects appears to be different.

17. These concentrations give a final concentration of 25 ng/mL of M-CSF and 1 ng/mL of IL-4. 60 ng/mL of RANKL is added either at this time point (d 1) or can be added for the first time on d 4. Both protocols enhance osteoclast formation.

18. IL-13 (0.1 ng/mL final concentration) exerts a similar effect on osteoclast formation as IL-4.

19. 180 μL of medium are removed from these cultures in order to remove as much of the IL-4 as possible. The same volume of fresh medium is replaced containing 25 ng/mL of M-CSF and 30 ng/mL of RANKL. If IL-4 is present in the culture medium in the *absence* of lymphocytes (lymphocytes are for the most part dead after 4 d) it exerts a powerful inhibitory effect on osteoclast formation

20. There are major differences between the molecules that exert an osteoclast enhancing effect on murine precursors obtained from bone marrow (and spleen) and human precursors from peripheral blood. These differences may be due to the different sources of the osteoclast precursors. Alternatively, it may indicate that the molecules that regulate human and murine osteoclast formation are fundamentally different. For example, TGF-β exerts no direct effect on human CD14-positive PBMNCs. In contrast, TGF-β is a powerful direct enhancer of murine osteoclast formation, exerting its effect directly on the murine bone marrow M-CSF-dependent osteoclast precursor *(11,12)*.

21. If RANKL is added simultaneously with TGF-β, there is no enhancement of osteoclast formation from unwashed PBMNCs. TGF-β is added only on d 1 of the culture and there is no additional benefit to adding TGF-β after day 1. We speculate that this is because TGF-β and IL-4/IL-13 abrogate the osteoclast-inhibitory effect of the lymphocytes, possibly blocking the effect of an osteoclast inhibitory factor produced by lymphocytes. Because lymphocytes are largely dead by d 4 in our cultures, the presence of TGF-β exerts no effect except when present at the beginning of the cultures. Unlike the effect of IL-4 and IL-13, TGF-β does not suppress osteoclast formation if maintained throughout the cultures.

22. In phase II, even very high concentrations of M-CSF, up to 500 ng/mL, are not inhibitory to the process of osteoclast formation. In contrast, if high levels of M-CSF are added in phase I of the culture osteoclast formation is inhibited.

23. The requirement for glucococorticoids (hydrocortisone/dexamethasone) in human osteoclast formation is complicated and apparently discrepant results are published. Dexamethasone, being more potent than hydrocortisone, is used at 10–8 *M* whereas hydrocortisone is used at 10–6 *M*. There is evidence that steroid hormones exert different effects on formation and resorption. Tobias and Cham-

bers showed that steroid hormones suppress bone resorption by the mature osteo-
clast by inducing apoptosis *(18)* but there is also good evidence that steroid hor-
mones induce osteoclast formation in human cultures in which either RANKL is
provided endogenously by stromal cells or in human PBMNCs in which lympho-
cytes are present *(13)*. We have found, however, that steroid hormones are not
necessary for human osteoclast formation (generated from CD34-positive pro-
genitor cells, M-CSF-dependent precursors, or peripheral blood mononuclear
cells) performed in the presence of soluble RANKL and that hydrocortisone sup-
presses osteoclast formation in such cultures *(2)*. Others have found that dex-
amethasone enhances osteoclast formation from unwashed PBMNCs in which
lymphocytes are present, in the presence of RANKL *(19)*. Because, lympho-
cytes suppress osteoclast formation formed from PBMNCs, these results sug-
gest that steroid hormones abrogate the inhibitory effect of the lymphocytes.
However, the reports are complicated by the results from Athanasou's group,
who found that steroid hormones enhance osteoclast formation when lympho-
cytes are absent in osteoclast-forming PBMNCs (personal communication).
There is no clear explanation for these apparently discrepant results. However,
one possibility is that the effect of steroid hormones is determined by the batch
of serum used, as it is known that the concentration of steroid hormone in sera
varies considerably.

24. The purpose of phase I of the culture is to permit the osteoclast-supporting stro-
mal (osteoblast/fibroblast) population of cells to expand. These are the cells that
produce RANKL to promote osteoclast formation in phase II of the culture.

25. Detailed time course experiments have been reported regarding the acquisition
of the osteoclast phenotype *(2,8)*.

26. Osteoclast formation from this population of cells allows study of molecules that
exert a direct action on the osteoclast precursor as bone marrow stromal cells and
lymphocytes are removed from the cultures. It is clear that in the presence of
cells other than osteoclast precursors, molecules can exert different effects from
those seen if the precursors are present alone. For example, TGF-β exerts no
effect on human osteoclast formation generated from CD14-positive cells
whereas in a lymphocyte-rich environment TGF-β enhances osteoclast forma-
tion from PBMNCs *(5)*, but suppresses osteoclast formation in human bone mar-
row cultures in which there is a stromal population *(13)*. Another example is seen
in the generation of murine osteoclasts; TGF-β enhances murine osteoclast for-
mation by exerting a direct effect on the osteoclast precursor but suppresses
osteoclast formation when osteoclasts are generated in the presence of bone mar-
row stromal cells *(11)*.

27. It may be possible to plate the bone marrow precursors at a density of fewer than
10^5 cells per well and to stop these experiments earlier that 14 d, but this has not
been tested.

28. DNase is added to bone marrow samples to prevent cell clumping *(29)*. We have
attempted to improve the osteoclast-forming potential of this culture system by
treating the CD34-positive cells in various combinations of stem cell factor, flt3

ligand, IL-3, IL-11, and TGF-β in the presence of M-CSF prior to the addition of and simultaneously with RANKL. However, these treatments did not enhance osteoclast formation over that generated in cultures treated with M-CSF and RANKL from d 1.

References

1. Flanagan, A. M., Sarma, U., Steward, C. G., Vellodi, A., and Horton M. A. (2000) Study of the non-resorptive phenotype of osteoclast-like cells from patients with malignant osteopetrosis: a new approach to investigating pathogenesis. *J. Bone Miner. Res.* **15,** 1–9.
2. Lader, C. S., Scopes, J., Horton, M. A., and Flanagan, A. M. (2001) Generation of human osteoclasts in stromal cell-free and stromal cell-rich cultures: differences in osteoclast CD11c/CD18 integrin expression. *Br. J. Haematol.* **111,** 1210–1217.
3. Sarma, U., Edwards, M., Motoyoshi, K., and Flanagan, A. M. (1998) 17β-Estradiol inhibits human osteoclast formation in vitro. *J. Cell. Physiol.* **175,** 99–108.
4. Lader, C. S. and Flanagan, A. M. (1998) Prostaglandin E2, interleukin 1α and tumor necrosis factor α increase human osteoclast formation and bone resorption in vitro. *Endocrinology* **139,** 3157–3164.
5. Massey, H. M., Scopes, J., Horton, M. A., and Flanagan, A. M. (2001) Transforming growth factor-β 1 stimulates the osteoclast-forming potential of the haemopoietic precursor in peripheral blood cells in a lymphocyte-rich microenvironment. *Bone* **28,** 577–582.
6. Scopes, J., Massey, H. M., Ebrahim, H., Horton, M. A., and Flanagan, A. M. (2001) Interleukin-4: bidirectional effects on human osteoclast formation. *Bone* **29,** 203–208.
7. Fujikawa, Y., Quinn, J. M. W., Sabokbar, A., McGee, J. O. D., and Athanasou, N. A. (1996) The human osteoclast precursor circulates in the monocyte fraction. Endocrinology. 137, 4058-4060.
8. Massey, H. M. and Flanagan A. M. (1999) Human osteoclasts derive from CD14-positive monocytes. *Br. J. Haematol.* **106,** 167–170.
9. Kong, Y.-Y., Yoshida, H., Sarosi, I., et al. (1999) OPGL is a key regulator of osteoclastogenesis, lymphocyte development and lymph-node organogenesis. *Nature* **397,** 315–323.
10. Kong, Y. Y., Feige, U., Sarosi, L., et al. (1999) Activated T cells regulate bone loss and joint destruction in adjuvant arthritis through osteoprotegerin ligand. *Nature* **402,** 304–308.
11. Sells Galvin, R. J., Gatlin, C. L., Horn, J. W., and Fuson, T. R. (1999) TGF-β enhances osteoclast differentiation in hematopoietic cell cultures stimulated with RANKL and M-CSF. *Biochem. Biophys. Res. Commun.* **265,** 233–239.
12. Fuller, K., Lean, J. M., Bayley, K. E., Wani, M. R., and Chambers, T. J. (2000) A role for TGFβ(1) in osteoclast differentiation and survival. *J. Cell Sci.* **113,** 2445–2453.
13. Sarma, U. and Flanagan, A. M. (1996) Macrophage-colony stimulating factor (M-CSF) induces substantial osteoclast formation in human bone marrow cultures. *Blood* **88,** 2531–2540.

14. Suda, T., Takahashi, N., Udagawa, N., Jimi, E., Gillespie, M. T., and Martin, T. J. (1999) Modulation of osteoclast differentiation and function by the new members of the tumor necrosis factor receptor and ligand families. *Endocr. Rev.* **20,** 345–357.

15. Lea, C. K., Sarma, U., and Flanagan, A. M. (1999) Macrophage colony stimulating-factor transcripts are differentially regulated in rat bone-marrow by gender hormones. *Endocrinology* **140,** 273–279.

16. Flanagan, A. M. and Lader, C. S. (1998) Update on the biological effects of macrophage colony-stimulating factor. *Curr. Opin. Hematol.* **5,** 181–185.

17. Fuller, K., Wong, B., Fox, S., Choi, Y., and Chambers, T. C. (1998) TRANCE is necessary and sufficient for osteoblast-mediated activation of bone resorption in osteoclasts. *J. Exp. Med.* **188,** 997–1001.

18. Tobias, J. and Chambers, T. J. (1989) Glucocorticoids impair bone resorptive activity and viability of osteoclasts disaggregated from neonatal rat long bones. *Endocrinology* **125,** 1290–1295.

19. Matsukaki, K., Udagawa, N., Takahashi, N., et al. (1998) Osteoclast differentiation factor (ODF) induces osteoclast-like cell formation in human peripheral blood mononuclear cell cultures. *Biochem. Biophys. Res. Commun.* **246,** 199–204.

10

Generating Murine Osteoclasts from Bone Marrow

Naoyuki Takahashi, Nobuyuki Udagawa, Sakae Tanaka, and Tatsuo Suda

1. Introduction

Osteoclasts, the multinucleated giant cells that resorb bone, originate from hemopoietic cells of the monocyte–macrophage lineage *(1,2)*. We have developed a mouse bone marrow culture system, in which osteoclasts are formed in response to several bone-resorbing factors such as $1\alpha,25$-dihydroxyvitamin D_3 $[1\alpha,25\text{-}(OH)_2D_3]$, parathyroid hormone (PTH), prostaglandin E_2 (PGE_2) and interleukin-11 (IL-11) *(2,3)*. We also developed a mouse coculture system of primary osteoblasts and hemopoietic cells to examine the regulatory mechanism of osteoclastogenesis *(2,4)*. A series of experiments using the coculture system established the concept that osteoblasts/stromal cells have a key role in regulating osteoclast differentiation *(2)*. Macrophage colony-stimulating factor (M-CSF, also called CSF-1) produced by osteoblasts/stromal cells was shown to be an essential factor for differentiation of osteoclasts from osteoclast progenitors *(2,5)*. Recently, receptor activator of nuclear factor κB ligand (RANKL) was identified as another essential factor for osteoclastogenesis, which is expressed by osteoblasts/stromal cells in response to several bone-resorbing factors (*6,7*; *see* **Note 1**). Osteoclast precursors that possess RANK, a tumor necrosis factort (TNF) receptor family member, recognize RANKL through cell–cell interaction with osteoblasts/stromal cells, and differentiate into osteoclasts in the presence of M-CSF. Recent progress of molecular technology allows us to introduce foreign genes into mature osteoclasts for modulating their functions. Adenoviral vectors are quite useful for introducing foreign genes into osteoclasts *(8)*. We describe here the methods for osteoclast formation in mouse bone marrow cultures and for introduction of foreign genes into mature osteoclasts.

2. Materials

2.1. Mice and Cell Lines

1. ddY mice (*see* **Note 2**).
2. Mouse bone marrow derived stromal cell lines, ST2 and MC3T3-G2/PA6 (RIKEN Cell Bank, Tsukuba, Japan).
3. Human embryonic kidney cell line 293 (American Type Culture Collection, Manassas, VA).

2.2. Reagents

1. Recombinant human M-CSF (Leukoprol; Kyowa Hakko Kogyo Co.Tokyo, Japan, or R &D systems, Minneapolis, MN) (*see* **Note 3**).
2. Recombinant mouse TNF-α, and human IL-1α (R&D Systems).
3. 1α,25-$(OH)_2D_3$ and PGE_2 (Wako Pure Chemical Industries, Ltd., Osaka, Japan).
4. PTH (Peptide Institute, Inc., Osaka) and IL-11 (R&D Systems).
5. Human osteoprotegerin (OPG) and a soluble form of human RANKL (Pepro Tech EC Ltd., London, UK).
6. Synthetic analogue of eel calcitonin (Elcatonin, Asahi Chemical Industry Co. Tokyo, Japan).
7. ^{125}I-labeled human calcitonin (Amersham Inc., Buckinghamshire, UK).
8. NR–M2 emulsion (Konica Co., Tokyo).
9. Rendol developer (Fuji Photo Film Co., Tokyo).
10. Type I collagen gel solution (cell matrix type IA; Nitta Gelatin Co., Osaka) (*see* **Note 4**).
11. Bacterial collagenase (Wako Pure Chemical Industries, Ltd.).
12. Tissue culture plastics (Corning).
13. α-Modification of minimum essential medium α-MEM), Dulbecco's modified Eagle's medium (DMEM), and Ca^{2+}- and Mg^{2+}-free phosphate-buffered saline [PBS(–)] (Sigma Chemical Co., St. Louis, MO).
14. Fetal bovine serum (FBS) (JRH Biosciences, Lenexa, KS or Gibco BRL, Gaithersburg, MY).
15. Sterile instruments, syringes, and needles.
16. Other chemicals and reagents are of analytical grade.

2.3. Culture Media and Buffer Solutions

1. α-MEM containing 10% FBS for cultures of mouse bone marrow cells.
2. DMEM containing 10% FBS for cultures of 293 cells.
3. PBS(-) for washing cells.
4. α-MEM containing 0.2% bacterial collagenase for detachment of cells cultured on collagen gel coated dishes.
5. Trypsin–EDTA solution: PBS(-) containing 0.05% trypsin and 0.5 m*M* EDTA for detachment of cells from culture plates.
6. Pronase–EDTA solution: PBS(-) containing 0.001% pronase and 0.02% EDTA for removal of osteoblasts from cocultures. Pronase is dissolved in PBS(-) containing 0.02% EDTA just before use.

7. 0.1% Triton X-100 in PBS(-) for permeabilization of cells fixed with 3.7% formaldehyde in PBS(-).

8. Tartrate-resistant acid phosphatase (TRAP) staining solution: Five milligrams of naphthol AS–MX phosphate is dissolved in 0.5 mL of *N,N*-dimethyl formamide in a glass container. Thirty milligrams of fast red violet LB salt and 50 mL of 0.1 *M* sodium acetate buffer, pH 5.0, containing 50 m*M* sodium tartrate are added to the mixture. This solution is made up fresh before use. Further details on TRAP staining procedures can be found in Chapter 11 by van 't Hof and other chapters on osteoclast formation, *this volume*.

9. Type I collagen mixture for preparing collagen gelcoated dishes: Type I collagen solution (*see* **Subheading 3.3.**), 5× conc. α-MEM, and 200 m*M* *N*-2-hydroxyethylpiperazine-*N*'-2-ethanesulfonic acid (HEPES) buffer, pH 7.4, containing 2.2% $NaHCO_3$ (7:2:1, by vol) are quickly mixed at 4°C just before use.

10. 0.1 *M* cacodylate buffer, pH 7.4, containing 1% formaldehyde and 1% glutaraldehyde for fixation of cells for autoradiography.

3. Methods
3.1. Marrow Culture

The mouse bone marrow culture system was developed for examining effects of bone-resorbing factors on osteoclast formation *(3)*. Discovery of the RANKL–RANK interaction for osteoclastogenesis indicated that the growth of stromal cells is an essential step for osteoclast development in bone marrow cultures *(6,7)*.

1. Tibiae are removed aseptically from 7- to 9-wk-old male mice and the bone ends are cut off with scissors. The marrow cavities are flushed with 1 mL of α-MEM by injecting at one end of the bone using a sterile 27-gauge needle.

2. Bone marrow cells are washed once with α-MEM, suspended in α-MEM containing 10% FBS, and cultured at 1.0×10^6 cells/0.5 mL/well in 24-well plates (Corning, Corning, NY) in a humidified atmosphere of 5% CO_2. Cultures are fed every 2–3 d by replacing 0.4 mL of old medium with fresh medium *see* **Note 5**).

3. Osteotropic factors such as 10^{-8} *M* 1α,25-$(OH)_2D_3$, 100 ng/mL of PTH, 10^{-6} *M* PGE_2, and 10 ng/mL of IL-11 induce osteoclast formation in this marrow culture. These factors are usually added at the beginnning of culture and at each time of medium change.

4. Cells are fixed, and stained for TRAP (a marker enzyme of osteoclasts) as described in section **Subheading 3.5.1.**

TRAP-positive mononuclear cells appear on d 3–4 and multinucleated cells on d 4–5 in the presence of bone-resorbing factors. The number of TRAP-positive multinucleated cells reaches a maximum on d 6–8. TRAP-positive osteoclasts are formed only near the colonies of alkaline phosphatase (ALP)-positive osteoblasts in the culture treated with PTH (**Fig. 1A**,**B**; *see* **Note 6**). OPG completely inhibited the TRAP-positive cell formation induced by PTH
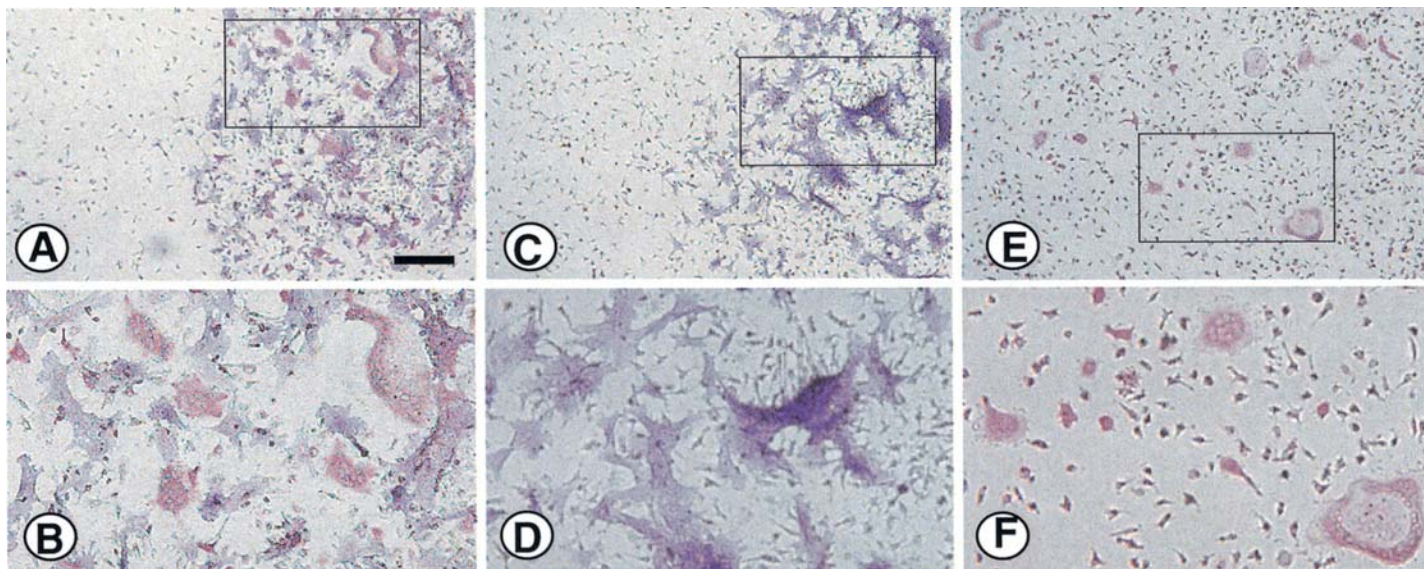
Fig. 1. Enzyme histochemistry for TRAP and ALP in mouse bone marrow cultures. Bone marrow cells of ddY mice were cultured for 7 d with 100 ng/mL of (**A**) PTH, 100 ng/mL of PTH plus 100 ng/mL of OPG (**C**), or 100 ng/mL of RANKL plus 50 ng/mL of M-CSF (**E**). Marrow cultures were then fixed and double-stained for TRAP and ALP. TRAP-positive cells appeared as red cells and ALP-positive cells as blue cells. (**B**), (**D**), and (**F**) show high power views of portions in (**A**), (**C**), and (**E**), respectively. Note that TRAP-positive cells formed in the culture are observed near or within the colonies of ALP-positive cells in the presence of PTH (**B**). In contrast, TRAP-positive cells are distributed uniformly on the culture dish in the presence of both RANKL and M-CSF (**F**). Adding OPG completely suppressed the formation of TRAP-positive cells induced by PTH (**D**). Scale bar = 200 μm.

in bone marrow cultures (**Fig. 1C**, **D**). Osteoclasts are also formed when mouse bone marrow cultures are treated with 50 ng/mL of M-CSF and 100 ng/mL of RANKL (**Fig. 1E**, **F**). In this culture, osteoclasts are formed uniformly all over the culture dish. Cocultures of primary osteoblasts with bone marrow cells produce more osteoclasts than bone marrow cultures alone do *(4)*. A protocol for osteoclast formation in coculture is given in Chapter 11 by van 't Hof, *this volume*.

3.2. Bone Marrow Macrophage Culture

Macrophages appearing in bone marrow cultures are the precursors of osteoclasts. We have modified the mouse bone marrow culture system to prepare highly purified osteoclast precursors *(9)*.

1. Bone marrow cells are treated with 100 ng/mL of M-CSF in αMEM containing 10% FBS in 48-well plates (3×10^5 cells/0.5 mL/well) (*see* **Note 7**).
2. Cells are cultured for 3 d, and nonadherent cells are completely removed from the culture by pipetting. Adherent cells strongly express macrophage specific antigens such as Mac-1, Moma-2, and F4/80. Therefore, adherent cells are called "M-CSF-dependent bone marrow macrophages (M-BMMφ)." Typically, 1×10^4 M-BMMφ are obtained when 1×10^5 bone marrow cells are cultured for 3 d in the presence of M-CSF.
3. When M-BMMφ are further cultured with 100 ng/mL of RANKL and 100 ng/mL of M-CSF, TRAP-positive mononuclear and multinucleated cells are formed within 3 d (**Fig. 2B**) (*see* **Note 7**).

3.3. Collagen Gel Culture

Osteoclasts formed on plastic culture dishes are very difficult to detach by the treatment with either trypsin–EDTA or bacterial collagenase. To obtain functionally active osteoclasts formed in cocultures with osteoblasts, a collagen gel culture is recommended *(10,11)*.

1. A 10-cm culture dish (Corning) is coated with 4 mL of the type I collagen mixture at 4°C. The dish is put in a CO_2 incubator for 10 min to make the aqueous type I collagen gelatinous at 37°C.
2. Primary osteoblasts (2×10^6 cells; *see* the chapter by Bakker and Klein-Nulend, *this volume*) and bone marrow cells (2×10^7 cells; *see* **Subheading 3.1.**) are cocultured on a collagen gel coated dish in 15 mL of α-MEM containing 10% FBS and 10^{-8} *M* 1α,25-(OH)$_2$D$_3$. The medium is changed every 2–3 d.
3. After culture for 7 d, the dish is treated with 4 mL of 0.2% collagenase solution for 20 min at 37°C in a shaking water bath (60 cycles/min). The culture dishes are carefully placed on a sheet of aluminum foil put on the water surface of the water bath to maintain the sterile condition of the dishes.
4. The cells released from the dish are collected by centrifugation at 250*g* for 5 min and suspended in 10 mL of α-MEM containing 10% FBS (the crude osteoclast preparation). Usually, 4×10^4–1×10^5 osteoclasts are recovered from a 10 cm

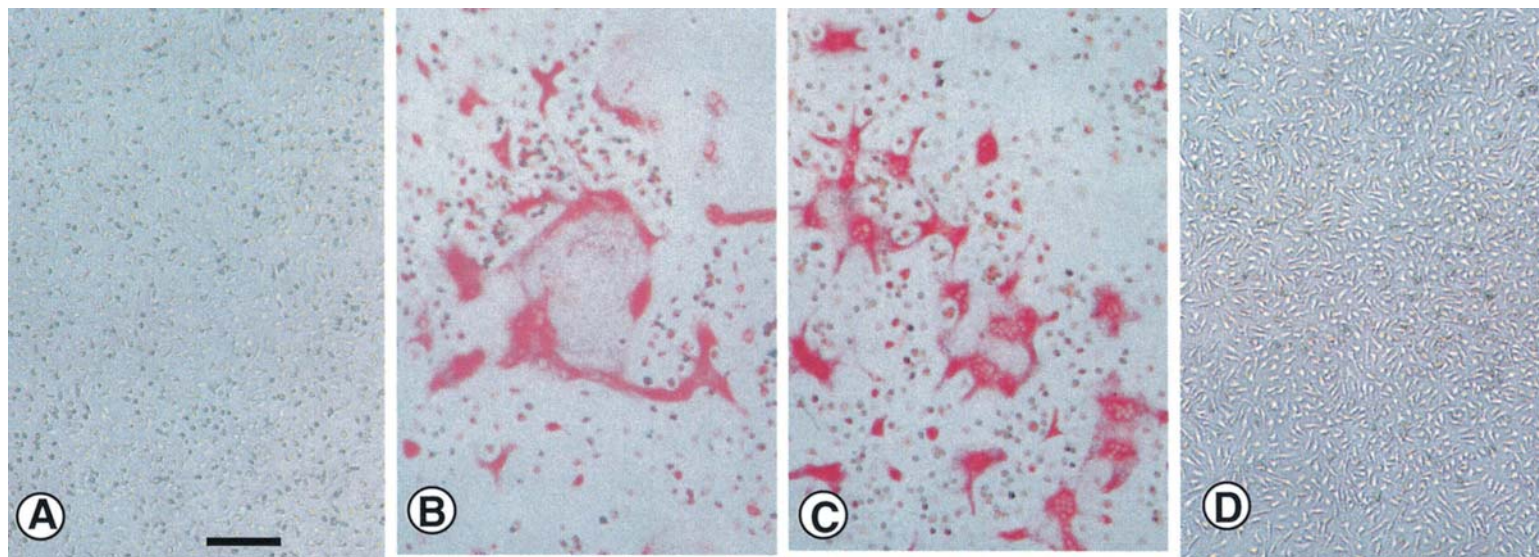Fig. 2. Effects of RANKL, mouse TNF-α , and IL-1 on TRAP-positive cell formation in M-BMMφ cultures. Bone marrow cells of ddY mice were cultured with M-CSF for 3 d to prepare M-BMMφ. M-BMMφ were further cultured for 3 d without (**A**) or with either 100 ng/mL of RANKL (**B**), 20 ng/mL of mouse TNF-α (**C**), or 10 ng/mL of human IL-1 (**D**) in the presence of 100 ng/mL of M-CSF. Cells were then fixed and stained for TRAP. Scale bar = 100 μm.

collagen gel coated dish, and the purity of osteoclasts is 2-3% in this crude preparation.
5. The crude osteoclast preparation is used for biological and biochemical studies of osteoclasts.

3.4. Purification of Osteoclasts Formed In Vitro

Because the purity of osteoclasts in the crude osteoclast preparation is only 2–3%, further purification is essential for biochemical studies of osteoclasts. Osteoclasts are easily purified from the crude osteoclast preparation placed on plastic dishes by treatment with pronase–EDTA solution *(12,13)*. This procedure is identical to that described in the chapter by Coxon et al. to obtain pure mature rabbit osteoclasts.

1. Ten milliliters of the crude osteoclast preparation is placed on a 10-cm culture dish (Corning) for 6–15 h in the presence of 10% FBS (**Fig. 3A**).
2. Adherent cells are washed with α-MEM, and treated with 8 mL of pronase–EDTA solution for 10 min.
3. Osteoblasts are then removed by gentle pipetting. More than 90% of the adherent cells on the dishes are TRAP-positive mononuclear and multinucleated cells (**Fig. 3B**).

Using the purified osteoclast preparation, we have shown that osteoclasts possess phosphatidylinositol-3 kinase *(14)*, *rho* p21 *(15)*, and p60[c-src] *(16)*. We have also reported that osteoclasts express IL-1 receptors *(17)*, TNF type I and type II receptors *(18)*, and RANK *(18)*, and they respond to cytokines through these receptors.

It is difficult to obtain a highly enriched preparation of functionally active osteoclasts (*see* Chapter 7 by Coxon et at. and Chapter 6 by Collin-Osdoby et al., *this volume*). Using the disintegrin "echistatin," highly purified mononuclear and binuclear prefusion osteoclasts (pOCs) can be obtained from the coculture of mouse bone marrow cells and mouse osteoblastic MB1.8 cells treated with $10^{-8} M$ 1α,25-(OH)$_2$D$_3$ *(19)*. The purity of pOCs in the preparation is about 95% as determined by staining for TRAP. We have shown that pOCs themselves fail to form resorption pits on dentine slices, but they form resorption pits in the presence of RANKL or IL-1 *(17,18)*.

3.5. Identification of Osteoclasts Formed In Vitro

3.5.1. TRAP staining (see **Note 8**)

Cytochemical staining for TRAP is widely used for identifying osteoclasts in vivo and in vitro *(2,7,13)*.

1. Cells are fixed with 3.7% (v/v) formaldehyde in PBS(-) for 10 min, fixed again with ethanol–acetone (50:50, v/v) for 1 min, and incubated with the TRAP-staining solution for 10 min at room temperature.
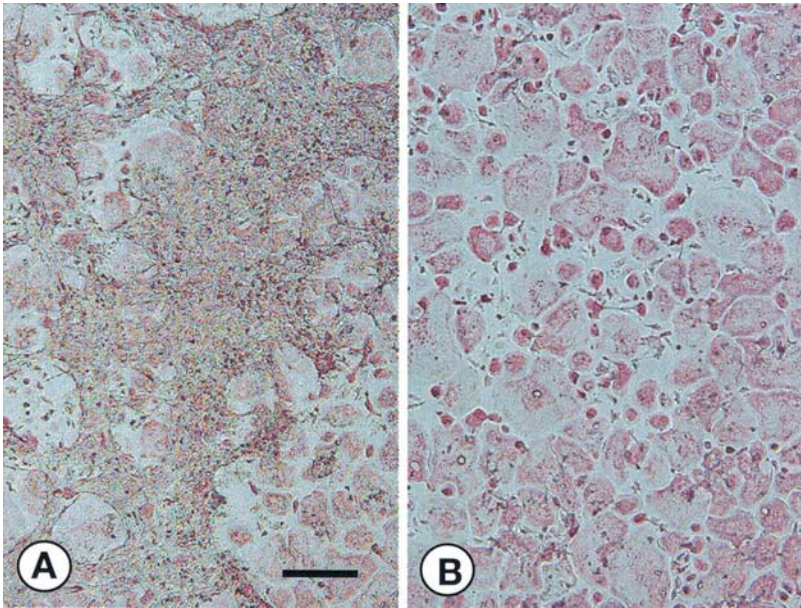
Fig. 3. Purified TRAP-positive osteoclasts formed in cocultures of mouse osteo-blasts and bone marrow cells. Primary osteoblasts (2×10^6 cells) and bone marrow cells (2×10^7 cells) were cocultured for 7 d on a collagen gel coated dish. The dish was then treated with 0.2% collagenase solution to recover all the cells from the dish. The cells released from the dish were collected by centrifugation and suspended in 10 mL of α-MEM containing 10% FBS (the crude osteoclast preparation). The crude osteo-clast preparation was placed on a 10-cm culture dish for 10 h in the presence of 10% FBS (**A**). The purity of osteoclasts in this crude preparation was only 2–3%. Adherent cells were washed with α-MEM, then treated for 10 min with 8 mL of pronase–EDTA solution. Osteoblasts were then removed by gentle pipetting. More than 90% of the adherent cells on the dish were TRAP-positive mononuclear and multinucleated cells (**B**). Scale bar = 200 μm.

2. TRAP-positive osteoclasts appear as red cells. An incubation period longer than 10 min should be avoided, since cells other than osteoclasts become weakly posi-tive with time.
3. After staining, cells are washed with distilled water, and TRAP-positive multi-nucleated cells having three or more nuclei are counted as osteoclasts under a microscope.

3.5.2. Autoradiography for Calcitonin Receptors

Osteoclasts have been shown to possess abundant calcitonin receptors *(13,20)*. Expression of calcitonin receptors is one of the most reliable markers

for identifying osteoclasts. Here we give a method for detection of calcitonin receptors by autoradiography, but immunocytochemical detection has been described also (*see* **Note 9**).

1. For autoradiography with ^{125}I-labeled human calcitonin, cultures are prepared on plastic coverslips (ϕ13.5 mm) placed in 24-well culture plates.
2. Cells grown on the coverslips are washed with α-MEM, and incubated with 0.2 n*M* ^{125}I-calcitonin in the presence or absence of 200 n*M* unlabeled salmon calcitonin in α-MEM containing 0.1% bovine serum albumin (BSA) for 1 h at 20°C.
3. Cells are washed three times with PBS(-) and fixed for 5 min with 0.1 *M* cacodylate buffer, pH 7.4, containing 1% formaldehyde and 1% glutaraldehyde.
4. The specimens are fixed again with ethanol–acetone for 1 min, and stained for TRAP.
5. The coverslips are then mounted on a glass slide, dipped in NR–M2 emulsion, and stored in a dark box at 4°C.
6. After incubation for 14 d, slides are developed in Rendol. Calcitonin receptors are identified by accumulation of dense grains due to ^{125}I-calcitonin binding, which disappear from the specimen when incubated with excess unlabeled calcitonin.

3.5.3. Pit Formation Assay

When osteoclasts are placed on dentine slices, they form resorption pits within 24 h. A reliable pit formation assay was established using the crude osteoclast preparation and dentine slices *(13,21)*.

1. Dentine slices (ϕ 4 mm, 200 μm thick) are prepared from ivory blocks using a band saw (BS-3000, Exakt, Germany) and a cutting punch.
2. Dentine slices are cleaned by ultrasonication in distilled water, sterilized using 70% ethanol, and dried under ultraviolet light.
3. Dentine slices are placed in 96-well plates containing 0.1 mL/well of α-MEM with 10% FBS (a slice/well). A 0.1-mL aliquot of the crude osteoclast preparation is transferred onto the slices.
4. After a setting period of 60 min at 37°C, slices are removed, and placed onto 24-well plates containing α-MEM with 10% FBS (0.5 mL/slice/well).
5. After incubation for 24–48 h, the medium is removed and 1 *M* NH_4OH (1 mL/well) is added to the wells for 30 min.
6. Dentine slices are then cleaned by ultrasonication, stained with Mayer's hematoxylin (Wako Pure Chemical Industries) for 35–45 s, and washed with distilled water.
7. Resorption pits are clearly visualized with Mayer's hematoxylin under transmitted light.
8. The number of resorption pits formed on dentine slices is counted under a light microscope. Alternatively, the resorbed area is measured using an image analysis system linked to the light microscope. For a detailed description of such a method using reflected light microscopy *see* Chapter 11 by van 't Hof, *this volume*.

3.6. Introduction of Foreign Genes into Osteoclasts (see *Note 10*)

3.6.1. Preparation of Adenovirus Vector

An adenoviral vector system is useful for introducing foreign genes into osteoclasts to study the regulation of osteoclast function *(8)*.

1. The recombinant adenovirus carrying a foreign gene under the control of the CAG (cytomegalovirus IE enhancer + chicken β-actin promoter + rabbit β-globin poly[A] signal) promoter is constructed by homologous recombination between the expression cosmid cassette and the parental virus genome in 293 cells *(22)*.
2. Titers of virus stocks are determined by an endpoint cytopathic effect assay with the following modifications. Fifty microliters of DME containing 10% FBS is dispensed into each well of a 96-well plate, then eight rows of threefold serial dilutions of the virus starting from 10^{-4} dilutions are prepared.
3. To each well 3×10^5 293 cells in 50 μL of DMEM containing 10% FBS is added. The plate is incubated at 37°C in 5% CO_2 in air, and 50 μL of DME containing 10% FBS is added to each well every 3 d.
4. After culture for 12 d, the endpoint of the cytopathic effect is determined by microscopy, and the 50% tissue culture infectious dose ($TCID_{50}$) is calculated. One $TCID_{50}$ approx corresponds to one plaque forming unit (PFU)/mL.
5. The efficiency of infection is affected not only by the concentration of viruses and cells, but also by the ratio of viruses to cells, the multiplicity of infection (MOI). MOI is expressed as a measure of titer how many PFU are added to each cell.

3.6.2. Infection of Adenovirus Carrying Foreign Genes to Osteoclasts

1. Incubate mouse cocultures on d 4, when osteoclasts begin to appear, with a small amount of α-MEM containing the recombinant adenoviruses for 1 h at 37°C at a suitable MOI. We usually employ an MOI of 100 in our experiments.
2. Wash the cells twice with PBS(-) and incubate further with α-MEM with 10% FBS at 37°C. Experiments are preformed 24 h after the infection.

Using recombinant adenovirus carrying the *lacZ* gene, we have shown that the adenovirus carrying the *lacZ* gene can effectively infect osteoclasts with no apparent morphological changes or cellular toxicity *(8)* (**Fig. 4**). A high level of β-galactosidase activity is observed in mouse osteoclasts infected with the recombinant adenovirus carrying the *lacZ* gene. The proportion of β-galactosidase-positive osteoclasts increases in an MOI dependent manner, and > 80% of osteoclasts are positively stained at 100 MOI (**Fig. 4**).

4. Notes

1. In 1997, osteoprotegerin (OPG) and osteoclastogenesis inhibitory factor (OCIF), which inhibit osteoclast development in vivo and in vitro, respectively, were cloned independently by two different research groups *(23,24)*. Incidentally, OPG and OCIF were the same protein molecule. OPG/OCIF is a member of the TNF
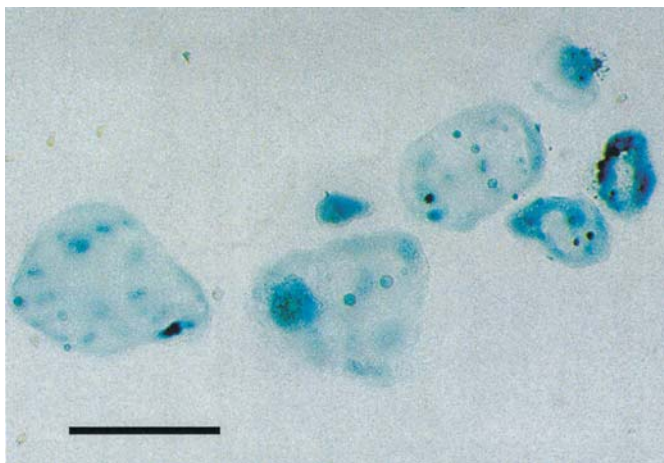
Fig. 4. An efficient adenovirus vector-mediated gene transfer to mouse osteoclasts as evidenced by cytochemical staining for β-galactosidase activity. Mouse cocultures on d 4 were incubated with a small amount of α-MEM containing the recombinant adenovirus vector encoding the *lacZ* gene (*AxCASLacZ*) for 1 h at 37°C at an MOI of 100. The cells were then washed twice with PBS(-) and further cultured for 2 d with α-MEM with 10% FBS at 37°C. Then, the cells were fixed for 10 min in 3.7% (v/v) formaldehyde in PBS(-) and washed in PBS(-). β-Galactosidase activity was detected by immersing the cells into a staining solution. Cells expressing β-galactosidase activity were stained as blue cells. More than 80% of multinucleated osteoclasts were transfected with the adenovirus carrying the *lacZ* gene at an MOI of 100. Scale bar = 100 μm.

receptor family, but it does not have a transmembrane domain, suggesting that OPG/OCIF functions as a circulating soluble factor. Subsequently, the cDNA encoding the binding molecule of OPG/OCIF was isolated from an expression library of the mouse stromal cell line ST2 and was named as osteoclast differentiation factor (ODF) *(25)*. A ligand for OPG/OCIF was also cloned from an expression library of the mouse myelomonocytic cell line 32D, and was named as OPG ligand (OPGL) *(26)*. OPGL was found to be identical to ODF. The binding molecule of OPG/OCIF was a membrane-associated protein of the TNF ligand family. ODF/OPGL was also identical to TNF-related activation-induced cytokine (TRANCE) *(27)* and RANKL *(28)*, which were independently cloned from mouse T cell hybridomas and mouse dendritic cells, respectively. RANK is the transmembrane receptor of ODF/OPGL/TRANCE/RANKL, which is expressed by osteoclast precursors and mature osteoclasts (**Fig. 5**). OPG/OCIF is a decoy receptor of ODF/OPGL/TRANCE/RANKL. Thus, ODF, OPGL, TRANCE, and RANKL are different names for the same protein, which is essential for the development and function of osteoclasts (**Fig. 5**). The terms "RANKL," "RANK," and "OPG" are used in this chapter according to the guide-
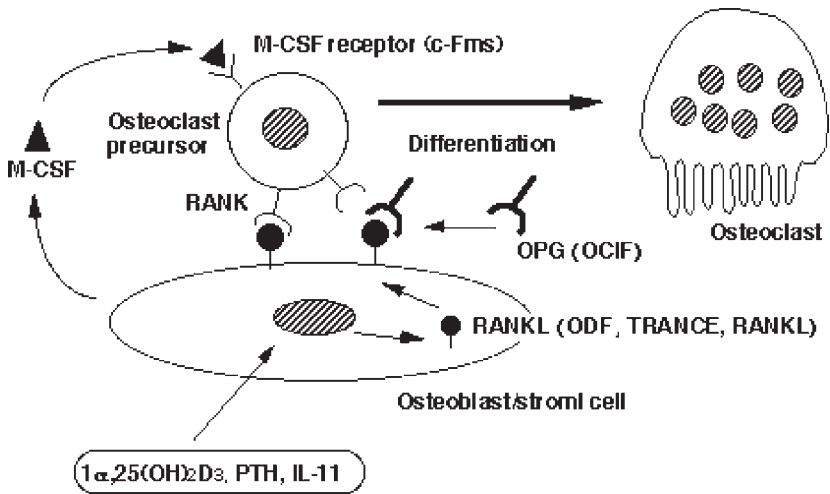
Fig. 5. Schematic representation of osteoclast differentiation regulated by osteo-blasts/stromal cells. Recent studies have revealed the role of new TNF receptor-ligand family members responsible for osteoclast formation. Osteotropic factors such as $1\alpha,25\text{-}(OH)_2D_3$, PTH, and IL-11 stimulate expression of RANKL in osteoblasts/stromal cells as a membrane-associated cytokine for induction of osteoclast differentiation in bone marrow cultures or in cocultures of osteoblasts and hemopoietic cells. OPG, a soluble decoy receptor of RANKL, is produced mainly by osteoblasts. OPG strongly inhibits the RANKL-induced differentiation of osteoclast precursors into osteoclasts. The terms "RANKL," "RANK," and "OPG" are used in this chapter according to the guideline of the American Society for Bone and Mineral Research (ASBMR) President's Committee on Nomenclature *(29)*.

line of the American Society for Bone and Mineral Research (ASBMR) President's Committee on Nomenclature *(29)*. When spleen cells are treated with RANKL in the presence of M-CSF, osteoclasts are formed even in the absence of osteoblasts. OPG completely inhibits osteoclast formation in bone marrow cultures treated with osteotropic factors. RANKL and OPG are expressed mainly by stromal cells in bone marrow cultures. Osteotropic factors stimulate the expression of RANKL and suppress OPG expression by stromal cells in mouse bone marrow cultures.

2. Other strains of mice such as BALB/c, C57BL, and ICR can also be used for mouse osteoclast formation.
3. Human M-CSF is effective in both human and murine cells, whereas murine M-CSF is effective in murine cells but not in human cells.
4. Only this type of collagen (cell matrix type IA; Nitta Gelatin Co.) is suitable for this procedure.
5. Because FBS is one of the important factors that affect osteoclast formation, careful batch testing of FBS is recommended.

6. Osteoclast development proceeds within a local microenvironment of bone. This process can be reproduced ex vivo in a coculture of mouse calvarial osteoblasts and hemopoietic cells. Some mouse stromal cell lines such as MC3T3-G2/PA6 and ST2 are capable of supporting osteoclastogenesis when cultured with mouse spleen cells *(2,30)*. In such cocultures, osteoclasts are formed in response to various osteotropic factors including $1\alpha,25$-$(OH)_2D_3$, PTH, PGE_2 and IL-11. Cell-to-cell contact between osteoblasts/stromal cells and osteoclast progenitors is required to induce osteoclastogenesis *(2,7)*. Subsequent experiments have established that the target cells of osteotropic factors for inducing osteoclast formation in vitro are osteoblasts/stromal cells *(2,7)*. In bone marrow culture, stromal cells present in bone marrow support osteoclast formation from the progenitors in response to osteotropic factors. Therefore, the growth of stromal cells is one of the determinants for osteoclast formation in bone marrow cultures *(2,7)*.

7. Treatment of bone marrow cells with a high concentration of M-CSF (100 ng/mL) for 3 d stimulates the proliferation of macrophages without growth of stromal cells. ALP-positive cells are seldom observed in the M-BMMϕ preparation. In the absence of M-CSF, most of the M-BMMϕ rapidly die within 3 d. No TRAP-positive cells are formed even in the presence of RANKL, when M-CSF is not added to the culture. Mouse TNF-α (20–100 ng/mL) also stimulates formation of osteoclasts from M-BMMϕ in the presence of M-CSF (**Fig. 2C**), but human TNF-α shows only weak activity in inducing TRAP-positive cell formation from M-BMMϕ even at a higher concentration (100 ng/mL). Osteotropic hormones and cytokines including $1\alpha,25$-$(OH)_2D_3$, PTH, PGE_2 and IL-1 (**Fig. 2D**) fail to induce osteoclast formation in M-BMMϕ cultures.

8. Various alternatives to the TRAP staining protocol given here are described in the other chapters on osteoclasts in this volume. All are equally useable.

9. Recently, Quinn et al. (*31*) developed a method for immunostaining of murine calcitonin receptors using polyclonal antibodies against rat calcitonin receptors. Osteoclasts (both mononuclear and multinucleated) formed in the coculture of mouse bone marrow cells and osteoblasts were specifically immunostained by the antibodies.

10. To investigate the molecular mechanism of osteoclast function, it is necessary to modulate gene expression in osteoclasts by introducing foreign genes into the cells. Adenovirus vectors have several advantages *(8)*. First, these vectors are capable of infecting a variety of terminally differentiated cells including neurons, hepatocytes, and osteoclasts. Second, recombinant adenovirus can be amplified easily to a very high titer in vitro. Third, adenovirus infection to the cells has been reported to require the interaction of the RGD sequence in the penton base of the virus with the cell surface of osteoclasts. We have successfully introduced such foreign genes into osteoclasts as epidermal growth factor receptor *(8)*, C-terminus Src family kinase (csk) *(32)*, dominant negative ras *(33)*, constitutively active MEK1 (MAP kinase kinase) *(33)*, dominant negative IκB kinase 2, and constitutively active IκB kinase 2 *(33)*.

Acknowledgments

References

1. Roodman, G. D. (1996) Advances in bone biology: the osteoclast. *Endocr. Rev.* **17**, 308–332.
2. Suda, T., Takahashi, N., and Martin, T. J. (1992) Modulation of osteoclast differentiation. *Endocr. Rev.* **13**, 66–80.
3. Takahashi, N., Yamana, H., Yoshiki, S., et al. (1988) Osteoclast-like cell formation and its regulation by osteotropic hormones in mouse bone marrow cultures. *Endocrinology* **122**, 1373–1382.
4. Takahashi, N., Akatsu, T., Udagawa, N., et al. (1988) Osteoblastic cells are involved in osteoclast formation. *Endocrinology* **123**, 2600–2602.
5. Yoshida, H., Hayashi, S., Kunisada, T., et al. (1990) The murine mutation osteopetrosis is in the coding region of the macrophage colony stimulating factor gene. *Nature* **345**, 442–444.
6. Yasuda, H,, Shima, N., Nakagawa, N., et al. (1999) A novel molecular mechanism modulating osteoclast differentiation and function. *Bone* **25**, 109–113.
7. Takahashi, N., Udagawa, N., and Suda, T. (1999) A new member of TNF ligand family, ODF/RANKL/TRANCE/OPGL, regulates osteoclast differentiation and function. *Biochem. Biophys. Res. Commun.* **256**, 449–455.
8. Tanaka, S., Takahashi, T., Takayanagi, H., et al. (1998) Modulation of osteoclast function by adenovirus vector-induced epidermal growth factor receptor. *J. Bone Miner. Res.* **13**, 1714–1720.
9. Kobayashi, K., Takahashi, N., Jimi, E., et al. (2000) Tumor necrosis factor α stimulates osteoclast differentiation by a mechanism independent of the ODF/RANKL-RANK interaction. *J. Exp. Med.* **191**, 275–286.
10. Akatsu, T., Tamura, T., Takahashi, N., et al. (1992) Preparation and characterization of a mouse multinucleated cell population. *J. Bone Miner. Res.* **7**, 1297–1306.
11. Suda, T., Nakamura, I., Jimi, E., and Takahashi, N. (1997) Regulation of osteoclast function. *J. Bone Miner. Res.* **12**, 869–879.
12. Jimi, E., Ikebe, T., Takahashi, N., Hirata, N., Suda, T., and Koga, T. (1996) Interleukin-1β activates an NF-κB-like factor in osteoclast-like cells. J. *Biol. Chem.* **271**, 4605–4608.
13. Suda, T., Jimi, E., Nakamura, I., and Takahashi, N. (1997) Role of 1α,25-dihydroxyvitamin D_3 in osteoclast differentiation and function. *Methods Enzymol.* **282**, 223–235.
14. Nakamura, I., Takahashi, N., Sasaki, T., et al. (1995) Wortmannin, a specific inhibitor of phosphatidylinositol-3 kinase, blocks osteoclastic bone resorption. *FEBS Lett.* **361**, 79–84.

15. Zhang, D., Udagawa, N., Nakamura, I., et al. (1995) The small GTP-binding protein, rho p21, is involved in bone resorption by regulating cytoskeletal organization in osteoclasts. *J. Cell Sci*. **108**, 2285–2292.

16. Tanaka, S., Takahashi, N., Udagawa, N., et al. (1992) Osteoclasts express high levels of p60$^{c\text{-}src}$, preferentially on ruffled border membranes. *FEBS Lett*. **313**, 85–89.

17. Jimi, E., Nakamura, I., Duong, L. T., et al. (1999) Interleukin 1 induces multinucleation and bone-resorbing activity of osteoclasts in the absence of osteoblasts/stromal cells. *Exp. Cell Res*. **247**, 84–93.

18. Jimi, E., Akiyama, S., Tsurukai, T., et al. (1999) Osteoclast differentiation factor acts as a multifunctional regulator in murine osteoclast differentiation and function. *J. Immunol*. **163**, 434–442.

19. Wesolowski, G., Duong, L. T., Lakkakorpi, P. T., et al. (1995) Isolation and characterization of highly enriched, prefusion mouse osteoclastic cells. *Exp. Cell Res*. **219**, 679–686.

20. Takahashi, N., Akatsu, T., Sasaki, T., et al. (1988) Induction of calcitonin receptors by 1α,25-dihydroxyvitamin D$_3$ in osteoclast-like multinucleated cells formed from mouse bone marrow cells. *Endocrinology* **123**, 1504–1510.

21. Tamura, T., Takahashi, N., Akatsu, T., et al. (1993) A new resorption assay with mouse osteoclast-like multinucleated cells formed in vitro. *J. Bone Miner. Res*. **8**, 953–960.

22. Miyake, S., Makimura, M., Kanegae, Y., et al. (1996) Efficient generation of recombinant adenoviruses using adenovirus DNA-terminal protein complex and a cosmid bearing the full-length virus genome. *Proc. Natl. Acad. Sci. USA* **93**, 1320–1324.

23. Simonet, W. S., Lacey, D. L., Dunstan, C. R., et al. (1997) Osteoprotegerin: a novel secreted protein involved in the regulation of bone density. *Cell* **89**, 309–319.

24. Tsuda, E., Goto, M., Mochizuki, S., et al. (1997) Isolation of a novel cytokine from human fibroblasts that specifically inhibits osteoclastogenesis. *Biochem. Biophys. Res. Commun*. **234**, 137–142.

25. Yasuda, H., Shima, N., Nakagawa, N., et al. (1998) Osteoclast differentiation factor is a ligand for osteoprotegerin/osteoclastogenesis-inhibitory factor and is identical to TRANCE/RANKL. *Proc. Natl. Acad. Sci. USA* **95**, 3597–3602.

26. Lacey, D. L., Timms, E., Tan, H. L., et al. (1998) Osteoprotegerin ligand is a cytokine that regulates osteoclast differentiation and activation. *Cell* **93**, 165–176.

27. Wong, B. R., Rho, J., Arron, J., et al. (1997) TRANCE is a novel ligand of the tumor necrosis factor receptor family that activates c-Jun N-terminal kinase in T cells. *J. Biol. Chem*. **272**, 25190–25194.

28. Anderson, D. M., Maraskovsky, E., Billingsley, W. L., et al. (1997) A homologue of the TNF receptor and its ligand enhance T-cell growth and dendritic-cell function. *Nature* **390**, 175–179.

29. The American Society for Bone and Mineral Research President's Committee on Nomenclature (2000) Proposed standard nomenclature for new tumor necrosis

factor family members involved in the regulation of bone resorption. *J. Bone Miner. Res.* **15**, 2293–2296.

30. Udagawa, N., Takahashi, N., Akatsu, T., et al. (1989) The bone marrow-derived stromal cell lines MC3T3-G2/PA6 and ST2 support osteoclast-like cell differentiation in cocultures with mouse spleen cells. *Endocrinology* **125**, 1805–1813.

31. Quinn, J. M., Morfis, M., Lam, M. H., et al. (1999) Calcitonin receptor antibodies in the identification of osteoclasts. *Bone* **25**, 1–8.

32. Miyazaki, T., Takayanagi, H., Isshiki, M., et al. (2000) In vitro and in vivo suppression of osteoclast function by adenovirus vector-induced csk gene. *J. Bone Miner. Res.* **15**, 41–51.

33. Miyazaki, T., Katagiri, H., Kanegae, Y., et al. (2000) Reciprocal role of ERK and NF-κB pathways in survival and activation of osteoclasts. *J. Cell Biol.* **148**, 333–342.

11

Osteoclast Formation in the Mouse Coculture Assay

Robert J. van 't Hof

1. Introduction

The murine coculture assay originally described by Takahashi et al. *(1)*, was the first culture system developed that generated genuine, bone-resorbing osteoclasts. In this assay, osteoblasts are stimulated with 1,25-dihydroxyvitamin D_3 (D3) to stimulate RANKL and macrophage colony-stimulating factor (M-CSF) expression. These factors then stimulate early osteoclast precursors present in the spleen or bone marrow cell populations to differentiate into mature osteoclasts. At the end of the culture, osteoclasts can be identified by tartrate-resistant acid phosphatase (TRAP) staining, and, when the cultures are performed on dentine slices, resorption activity can be measured as well. Even though today it is possible to generate osteoclasts from bone marrow cells alone by treating the cultures with RANKL and M-CSF, the coculture system is still a useful model for studying osteoblast–osteoclast interactions. It has been widely used to study the origin of the osteoclast *(2)* and the effects of growth factors and drugs on osteoclast formation *(3,4)*. In studies with osteopetrotic mice, the coculture assay has been used to determine whether the underlying mechanism was due to a defect in the osteoblasts or in the osteoclast precursors *(5)*.

2. Materials

2.1. General Reagents/Materials

1. Sterile instruments (scissors, forceps).
2. Sterile syringes and needles (19- and 25-gauge).
3. Ficoll.
4. Sterile Petri dishes.

5. Conical polypropylene centrifuge tubes.
6. 25-mL Centrifuge tubes.

2.2. Tissue Culture Reagents

1. Culture medium: α-Modification of minimum essential medium (α-MEM) supplemented with 10% fetal calf serum (FCS) and antibiotics.
2. Hanks' balanced salt solution (HBSS).
3. HBSS supplemented with 10% FCS.
4. 1000× stock 1,25-$(OH)_2D_3$ (10^{-5} M in ethanol, Sigma), further referred to as D3.
5. Dentine slices: The dentine we use is elephant ivory, cut into slices of approx 200 μm thickness using a Buehler Isomet low-speed saw with a diamond wafering blade (series 15 HC). Out of these slices we punch discs that fit the wells of a 96-well plate, using a paper puncher (*see* **Notes 1** and **2**).

2.3. TRAP Stain Reagents

Solutions 2–5 are stable for months if kept protected from light in a refrigerator.

1. Naphthol AS–BI-phosphate stock: 10 mg/mL of naphtol–AS–BI–phosphate in dimethyl formamide (Sigma). Stable ± 1 wk at 4°C.
2. Veronal buffer: 1.17 g of anhydrous sodium acetate, 2.94 g Veronal (sodium barbiturate). Dissolve in 100 mL of distilled water.
3. 0.1 N Acetate buffer, pH 5.2:
    a. Dissolve 0.82 g of anhydrous sodium acetate in 100 mL of distilled water.
    b. 0.6 mL of glacial acetic acid, make up to 100 mL with distilled water.
    Adjust the pH of solution a to pH 5.2 with solution b.
4. 100 mM Tartrate: Dissolve 2.3 g of sodium tartrate in 100 mL of acetate buffer.
5. Pararosanilin, acridinfrei: Add 1 g of Pararosanilin to 20 mL of distilled water and add 5 mL of concentrated hydrochloric acid; heat carefully for 15 min in a 95°C water bath while stirring and filter once the solution has cooled down.

3. Methods
3.1. Osteoblasts

The assay starts with the isolation of the cell populations needed. Although some people have reported good results with osteoblast-like cell lines, such as ST2 cells, we have not been very successful with these and use primary osteoblasts isolated from the calvaria of 2- to 3-d-old neonatal mice (*see* **Note 5** in the chapter by Bakker/Klein-Nulend, *this volume*). The osteoblasts are plated on plastic or dentine 1 d before the addition of the bone marrow cells (*see* **Note 1**).

3.2. Isolation of Bone Marrow Cells

Although the assay was originally described using spleen cells (*1*; *see* **Note 3**), we generally use bone marrow cells as the source of osteoclast progenitors. Furthermore, other people have successfully used certain hemopoietic stem cell lines, such as C2GM cells (*6*).

1. Dissect the femurs and tibia out of two or three mice (3–6 mo old).
2. Flush out the marrow using a 25-gauge needle and HBSS + 10% FCS.
3. Get a single-cell suspension by squeezing the cell suspension through needles of decreasing size (start with 19-gauge, end with 25-gauge).
4. Remove red blood cells by Ficoll density centrifugation ($600g$, 25 min, brake off).
5. Harvest the bone marrow cells from the interface and wash once in HBSS.
6. Resuspend in 1 mL of culture medium.
7. Keep the cells on ice until use (but try to place the cells into culture as soon as possible).

3.3. Setting Up the Coculture

The optimal number of bone marrow cells and osteoblasts per well may vary, as we have found that the optimal number depends on the mouse strain used. For the MF1 mouse strain we use, the following seeding densities give optimal numbers of osteoclasts.

In a 96-well plate:

1. On d 0, plate 8×10^3 osteoblasts in 100 μL of medium + 10 n*M* D3 per well. Because of problems with evaporation of culture medium do not use the wells at the edges of the plate, but fill them with sterile water.
2. On d 1, add 2×10^5 freshly isolated bone marrow cells in 50 μL of medium/well. The medium should contain 10 n*M* D3.
3. On day 6, refresh 50% of the medium as follows (*see* **Note 4**):
   a. Gently add 150 μL of fresh medium + 20 nM D3 per well.
   b. Allow the cells to settle for ±15 min.
   c. Remove 150 μL of medium from each well.
4. On d 10, fix the cultures in formalin and perform a TRAP stain.

The medium refresh needs to be done very carefully, because the confluent layer of osteoblasts can be quite easily disturbed, and come off (*see* **Note 4**). This would result in a total absence of osteoclasts. Usually the first osteoclasts and resorption pits appear on d 6 (*see* **Note 5**). Reasonable numbers of osteoclasts (*see* **Note 6**) are present between d 7 and 10 (**Fig. 1**).

3.4. TRAP Staining

Osteoclasts express very high levels of the enzyme TRAP and can therefore be easily visualized by staining for this enzyme as follows (*7*; *see* **Notes 7–10**). As an alternative to the protocol described here, a staining kit from Sigma (387-A, Leukocyte Acid Phosphatase staining kit) can be used. This kit uses fast garnet as the dye, and this leads to a very dark purple stain.

1. Rinse the cultures with PBS.
2. Fix the cells for 5 min with 4% formaldehyde.
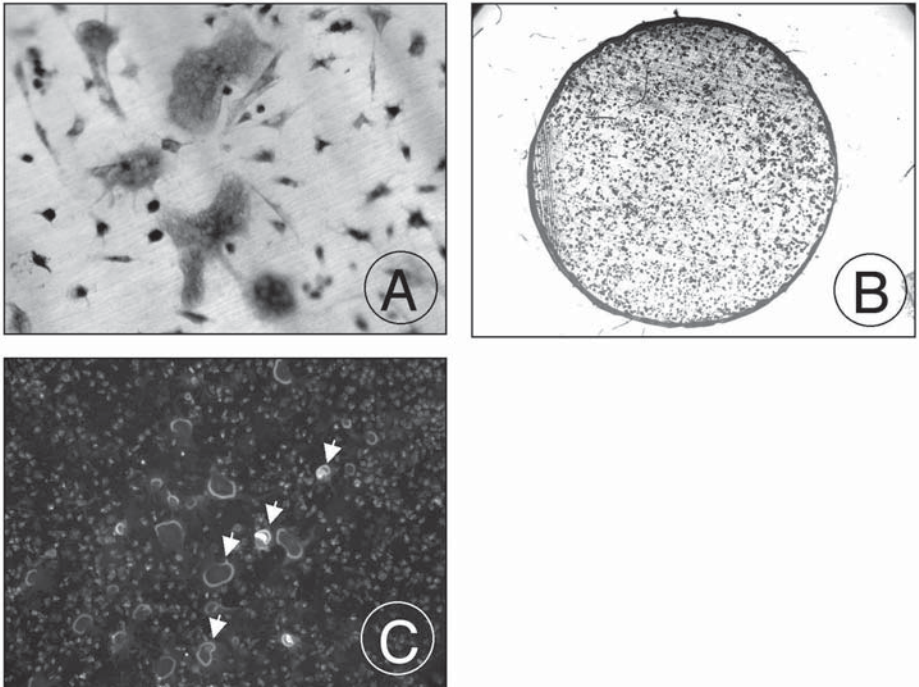3. Rinse with PBS.
4. Prepare staining solution:

Fig. 1. End result of a coculture. (**A**) Multinucleated osteoclasts identified by TRAP staining. (**B**) Resorption pits visualized by reflected light microscopy. The resorption pits stand out as dark objects. (**C**) Actin rings in the osteoclasts, visualized by phalloidin staining.

Solution 1:

   In a glass container, add 150 μL of naphthol AS–BI phosphate stock to 750 μL Veronal buffer pH 10.1. Then add 0.9 mL of acetate buffer. Add 0.9 mL of acetate buffer with 100 mM tartrate.

Solution 2:

   120 μL of Pararosanilin.

   120 μL of 4% NaNO$_2$.

Mix solutions 1 and 2, filter through a .45-μm filter and use immediately.

5. incubate the cells for 30–60 min at 37°C with staining solution (50–100 μL/well).
6. Rinse with distilled water.
7. Store in 70% ethanol.

Osteoclasts and mononuclear osteoclast precursors should be visible as bright red stained cells (*see* **Fig. 1A**).

3.5. Quantification of the Resorption Area

After the osteoclasts have been stained and counted, the slices are cleaned and the resorption pits can be visualized either by staining with dyes such as toluidine blue or Coomassie blue, by scanning electron microscopy, or by reflected light microscopy. We routinely use reflected light microscopy, because it is easy to perform, the slices need only thorough cleaning and no staining, and the image obtained can be fairly easily quantified using image analysis. Because the slices need to be completely flat for the reflected light microscopy, we glue them to glass slides under pressure of a 0.5-kg metal weight. We use a Zeiss Axiolab reflected light microscope, fitted with a × 2.5 lens, wide-field c-mount adapter, and Diagnostics Instruments Insight B/W large chip digital camera. This set up allows us to capture an entire bone slice in one image at sufficient resolution to identify and measure the resorption pits (**Fig. 1B**). We developed our own image analysis software package using the Aphelion ActiveX image analysis toolkit from ADCIS (ADCIS SA, Hérouville-Saint-Clair, France). The program prompts the user to focus the slice to be measured (**Fig. 2A**), captures the image, and identifies the dentine slice (**Fig. 2B**), so that any dark objects outside the dentine slice can be automatically removed. Next, the resorption pits are identified using gray level thresholding and selection by shape (**Fig. 2C**), and the resorption area is calculated. The entire process takes 2–3 min per slice.

4. Notes

1. Ivory is preferred to cortical bone for this assay, because it is very even and does not contain osteocyte lacunae, which interfere with the identification of the resorption pits.
2. As we use reflected light microscopy to visualize the resorption pits at the end of the culture, it is important that the surface of the slices is as smooth and shiny as possible. Therefore we polish the slices using brasso copper polish followed by cerium oxide polishing compound (Buehler) for fine polishing. Any remaining polish particles are removed by sonicating the dentine slices for ±15 min in 70% ethanol. The slices are stored in 70% ethanol until use.
3. Spleen cells can be used as an alternative to bone marrow cells in the coculture. The advantage is that they are easier to isolate than bone marrow cells. However, we generally get more consistent results using bone marrow. To use spleen cells, dissect the spleens out of two young adult mice. Use a bent 19-gauge needle to press the cells out of the spleen. Thoroughly resuspend the cells, load onto Ficoll and proceed as described in **Subheading 3.2.**, **step 4** using similar cell numbers.
4. The most common problem with the coculture is the osteoblast layer contracting and coming off the slice. This is usually due either to the plating density of the osteoblasts being too high or to the layer being disturbed during an over-vigorous medium refresh. Because of the last point, we do a 50% medium refresh and keep
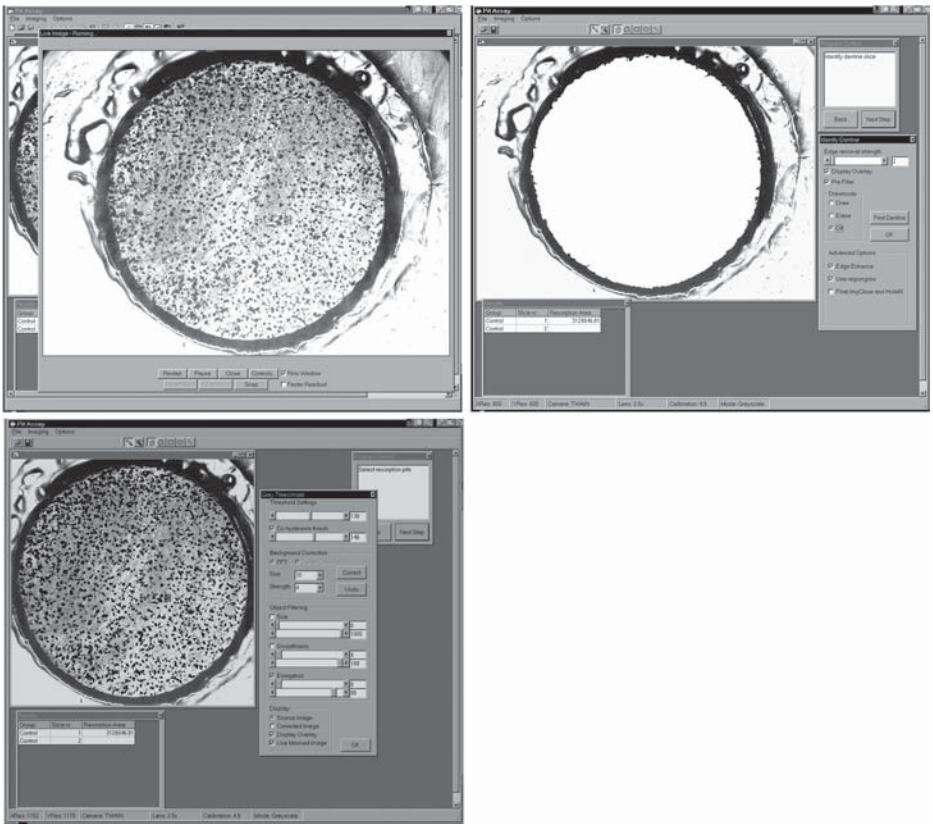
Fig. 2. Measurement of resorption pits. (**Top left**) An image of the dentine slice is captured using a digital camera. (**Top right**) The dentine slice is identified by the software. (**Bottom**) The resorption pits are detected using gray level thresholding.

the number of medium refreshes as low as possible. Once half way through the culture is sufficient. Make sure that the tip of the pipet does not touch the osteo-blast layer.

5. Any drugs or factors to be tested can be present during different parts of the coculture. To test effects on mature osteoclasts, drugs can be added during the last 2–3 d of the culture, whereas having the drugs present during the first 3–4 d gives an indication of effects on osteoclast precursors.

6. The usual yield of osteoclasts should be between 150 and 300 osteoclasts per slice. If the numbers are substantially lower, this may be due to nonoptimal seeding densities. Although the seeding densities mentioned in the preceding work well for cells from MF1 mice, other mouse strains may need different densities. It should be noted that numbers of osteoblasts and bone marrow cells that are

either too high or too low will both lead to a reduction of osteoclast numbers and a series of densities should be tested.

7. In this murine assay, the most convenient procedure is the TRAP stain. However, it should be noted that in long term cultures, macrophage polykaryons become TRAP positive as well *(8)*. These macrophage polykaryons can be distinguished from osteoclasts by their staining for the macrophage antigen F4/80. Furthermore, the TRAP stain as described here works fine for murine osteoclasts. However, when staining osteoclasts from different species, the concentration of tartrate may need to be changed. For human osteoclasts, for example, we use a final concentration of 100 m*M* tartrate.

8. In some species, osteoclasts can be identified easily by staining for the vitronectin receptor *(9)*. However, reagents for detection of vitronectin receptor in the mouse are not easily available.

9. Osteoclasts can also be identified by the presence of calcitonin receptors *(10)*. However, this procedure is too involved and time consuming for routine analysis, as it involves using radiolabeled calcitonin and autoradiography.

10. Osteoclasts that are actively resorbing display an actin ring, and this can be visualized by staining the actin with phalloidin coupled to rhodamine (Molecular Probes or Sigma). Comparing total number of TRAP-positive osteoclasts with the number of cells displaying the actin ring gives an indication of the fraction of osteoclasts actively resorbing bone.

References

1. Takahashi, N., Akatsu, T., Udagawa, N., et al. (1988) Osteoblastic cells are involved in osteoclast formation. *Endocrinology* **123**, 2600–2602.

2. Hagenaars, C. E., Kawilarang-De Haas, E. W., van der Kraan, A. A., Spooncer, E., Dexter, T. M., and Nijweide, P. J. (1991) Interleukin-3-dependent hematopoietic stem cell lines capable of osteoclast formation in vitro. *J. Bone. Miner. Res.* **6**, 947–954.

3. van 't Hof, R. J. and Ralston, S. H. (1997) Cytokine-induced nitric oxide inhibits bone resorption by inducing apoptosis of osteoclast progenitors and suppressing osteoclast activity. *J. Bone. Miner. Res* **12**, 1797–1804.

4. van 't Hof, R. J., Armour, K. J., Smith, L. M., et al. (2000) Requirement of the inducible nitric oxide synthase pathway for IL-1- induced osteoclastic bone resorption. *Proc. Natl. Acad. Sci. USA* **97**, 7993–7998.

5. Lowe, C., Yoneda, T., Boyce, B. F., Chen, H., Mundy, G. R., and Soriano, P. (1993) Osteopetrosis in Src-deficient mice is due to an autonomous defect of osteoclasts. *Proc. Natl. Acad. Sci. USA* **90**, 4485–4489.

6. De Grooth, R., Mieremet, R. H., Kawilarang-De Haas, E. W., and Nijweide, P. J. (1994) Murine macrophage precursor cell lines are unable to differentiate into osteoclasts: a possible implication for osteoclast ontogeny. *Int. J. Exp. Pathol.* **75**, 265–275.

7. Barka, T. and Anderson, P. J.(1962) Histochemical method for acid phosphatase using hexazonium pararosanilin as coupler. *J. Histochem. Cytochem.* **10**, 741–753.

8. Modderman, W. E., Tuinenburg-Bol Raap, A. C., and Nijweide, P. J. (1991) Tar-

trate-resistant acid phosphatase is not an exclusive marker for mouse osteoclasts in cell culture. *Bone* **12**, 81–87.

9. Horton, M. A., Taylor, M. L., Arnett, T. R., and Helfrich, M. H. (1991) Arg-Gly-Asp (RGD) peptides and the anti-vitronectin receptor antibody 23C6 inhibit dentine resorption and cell spreading by osteoclasts. *Exp. Cell Res.* **195**, 368–375.

10. Nicholson, G. C., Horton, M. A., Sexton, P. M., et al. (1987) Calcitonin receptors of human osteoclastoma. *Horm. Metab Res.* **19**, 585–589.

12

RANKL-Mediated Osteoclast Formation from Murine RAW 264.7 Cells

Patricia Collin-Osdoby, Xuefeng Yu, Hong Zheng, and Philip Osdoby

1. Introduction

Osteoclasts (OCs) are the cells uniquely responsible for dissolving both the organic and inorganic components of bone during bone development and remodeling throughout life. These cells originate from hematopoietic precursors of the monocyte/macrophage lineage that are present both in the bone marrow and peripheral circulation, and their numbers and/or activity are frequently increased in a wide array of clinical disorders that are associated with excessive bone loss and affect millions of people *(1)*. For many years, investigations into how OCs develop and function have been hampered by the considerable difficulties associated with isolating and culturing these normally rare cells. Whereas cell lines have frequently provided an invaluable research tool and are widely used to decipher mechanisms involved in osteoblast (OB) differentiation and bone formation, no immortalized cell lines for mature OCs exist and the few pre-OC cell lines that have been reported either do not undergo full OC differentiation *(2,3)* or involve coculture systems and cells that may not be readily available to all researchers *(4–6)*. To compound the problem further, it has proven difficult or impossible until recently to generate reliably bone-resorptive OCs expressing mature OC characteristics from primary bone marrow or circulating precursor cells in vitro. However, recent breakthroughs have now made the latter possible owing to the identification of the key signal, receptor activator of nuclear factor κB ligand (RANKL), that is responsible for the full development and activation of OCs both in vitro and in vivo *(7–9)*. During OB development or in response to specific hormonal or local signals, RANKL becomes highly expressed on the surface of OB/stromal

cells and directly interacts with a receptor, RANK, upregulated by macrophage colony-stimulating factor (M-CSF) on the surface of pre-OCs to stimulate their fusion, differentiation, and resorptive function. Many researchers now routinely form OCs in vitro through the exogenous addition of soluble recombinant RANKL (in combination with M-CSF to stimulate pre-OC proliferation, survival, and RANK expression) to cultures of primary bone marrow cells or peripheral blood monocytes derived from various species (e.g., human, mouse, rat, rabbit, or chicken). However, such procedures still necessitate the isolation of primary precursor populations and in sufficient numbers to provide enough in vitro generated OCs for experimentation or characterization.

In addition to primary cells, at least one pre-OC cell line, murine macrophage RAW 264.7 cells, responds to RANKL stimulation in vitro to generate bone pit resorptive multinucleated OCs (RAW-OCs) with the hallmark characteristics expected for fully differentiated OCs *(10–12)*. RAW cells have been extensively employed in macrophage studies for >20 yr and were originally established from the ascites of a tumor induced in a male mouse by intraperitoneal injection of Abelson leukemia virus (although RAW cells do not secrete detectable virus particles) *(13)*. RAW cells express the c-fms receptor for M-CSF *(14)* as well as M-CSF (our unpublished observations), perhaps explaining why they also express high levels of RANK *(10)* and do not require M-CSF as a permissive factor in their RANKL-induced formation into RAW-OCs. RAW cells are increasingly being used for studies of OC differentiation and function. There are many advantages of this system over the generation of OCs from primary cell populations, including the: (1) ready access (making it unnecessary to schedule studies around when primary cells may become available) and widespread availability of this cell line to most researchers; (2) easy culture and homogeneous nature of the pre-OC population (devoid of OBs, stromal, lymphocytes, or other cell types); (3) sensitive and very rapid RANKL-mediated formation of RAW-OCs (within d); (4) very large number of RAW-OCs that can be generated; and (5) high bone pit resorptive capability and expression of OC characteristics exhibited by RAW-OCs. In this chapter, we describe methods for the culture and RANKL-mediated differentiation of RAW cells into bone-resorptive RAW-OCs, the preparation of RAW-OC enriched populations by serum density gradient fractionation, and the culture and characterization of RAW-OCs. Such in vitro generated OCs can be analyzed using biochemical, immunological, physiological, molecular, or functional assays according to commonly employed procedures (*see* Chapter 6 by Collin-Osdoby, *this volume*).

2. Materials

2.1. Tissue Culture Medium, Solutions, and Supplies

All media and solutions should be prepared with glass-distilled water.

1. Culture medium: Mix 90 mL of sterile Dulbecco's modified Eagle medium (DMEM) supplemented with 4 m*M* L-glutamine, 1.5 g/L of sodium bicarbonate, 4.5 g/L of glucose, and 1.0 m*M* sodium pyruvate with 10 mL of fetal bovine serum (FBS, Gibco) and 1 mL of a 100× stock of antibiotic/antimycotic (a/a, Gibco); store at 4°C and prewarm to 37°C for use with cells.

2. Phosphate buffered saline (PBS): Add 9 g of NaCl, 0.385 g of KH_2PO_4, and 1.25 g of K_2HPO_4 per liter of water (final volume); adjust pH to 7.2 using 10 *N* NaOH.

3. RANKL (Alexis Biochemicals, Peprotech, Calbiochem, R & D Systems, or homemade): Reconstitute and store as a concentrated stock solution (typically 100 μg/mL in PBS) in small aliquots (~10–50 μL) at –80°C as recommended by the manufacturer, briefly thaw and dilute into culture medium (to 35 ng/mL final concentration for the homemade murine recombinant soluble RANKL) immediately before use with RAW cells, and refreeze remaining RANKL (and aim to thaw individual vials no more than three times to retain optimal bioactivity).

4. Moscona's high bicarbonate (MHB): Add 8 g of NaCl, 0.2 g of KCl, 50 mg of NaH_2PO_4, 1.0 g of $NaHCO_3$, 2 g of dextrose, 10 mL of a/a, 990 mL of water, check that the pH is 7.2, and sterile filter.

5. Hanks' balanced salt solution (HBSS, Gibco): Dissolve one packet in 990 mL of water, add 10 mL of a/a and 3.5 g of $NaHCO_3$, check that the pH is 7.2, and sterile filter.

6. Collagenase: Prepare 3% stock (3 g in 100 mL) solution in HBSS; store in aliquots (0.5–1.0 mL) at –20°C.

7. Trypsin: Prepare 1% stock (1 g in 100 mL) solution in HBSS; store in aliquots (1.0 mL) at –20°C.

8. Collagenase/trypsin digestion solution: Briefly thaw and add 71 μL of 3% collagenase solution and 141 μL of 1% trypsin solution to 3 mL of MHB (per dish) immediately before use with cells.

9. Protease (EC 3.4.24.31, Sigma P-8811): Prepare 0.1% (100 mg in 100 mL) stock solution in PBS, store at 4°C for up to several months or in aliquots (0.5 mL) at –20°C for long-term storage.

10. EDTA: Prepare 2% (2 g in 100 mL) stock solution (using EDTA sodium salt) in PBS, store at 4°C.

11. Protease–EDTA digestion solution: Briefly thaw and add 50 μL of 0.1% protease solution and 50 μL of 2% EDTA solution to 5 mL of PBS (per dish) immediately before use with cells.

12. Supplies: Sterile bottles, flasks, and tissue culture dishes; rubber cell scrapers (Fisher); hemocytometer.

2.2. Preparation of Devitalized Bone or Ivory Discs for Bone Pit Resorption Studies

1. Ivory is obtained either through donation from a local zoo or, in the United States, the Federal Department of Fish and Wildlife Services (or similar Department in other countries, *see also* the chapter by Nesbitt and Horton, *this volume*). Bovine cortical bone is obtained from a local slaughterhouse. Segments of ivory and

bovine cortical bone are thoroughly cleaned and washed (multiple HBSS and 70% ethanol rinses), sliced into small chunks, and then reduced to rectangular 0.4-mm thick sheets using a low-speed Isomet saw (Buehler, Lake Bluff, IL).

2. The sheets are rinsed three times with 70% ethanol, incubated in 70% ethanol overnight, and then washed for several h in HBSS before circular discs are cut using a 5-mm paper punch.

3. The discs are soaked repeatedly in 70% ethanol in sterile 50-mL tubes (alcohol changes can be gently poured off because the discs tend to stick to the side of the tube), and stored in 70% ethanol at –20°C.

4. For experimental use, the required number of discs are removed from the tube using alcohol-presoaked tweezers (to maintain sterility) in a tissue culture hood, transferred to a fresh sterile 50-mL polypropylene tube, rinsed extensively by inversion and mild shaking at least three times with ~40 mL sterile HBSS per wash, and the discs transferred using sterile tweezers into culture wells or dishes containing sterile HBSS for 3–24 h of preincubation in a tissue culture incubator prior to the plating of cells. HBSS is removed only immediately before the discs are to be used so that they do not dry prior to RAW cell or RAW-OC seeding.

3. Methods

3.1. RAW 264.7 Cell Culture

RAW 264.7 cells are obtained from the ATCC or similar cell repository. They represent a murine macrophage cell line that has the capability to be grown indefinitely as an OC precursor population or can be differentiated by treatment with RANKL into multinucleated bone pit resorptive OCs expressing the hallmark characteristics of in vivo formed OCs (*see* **Subheading 3.2.**).

All work should be performed in a sterile hood using sterile solutions and supplies.

1. If starting from a frozen (liquid nitrogen) vial of RAW cells, quickly (<1 min) thaw the vial (e.g., in a 37°C water bath or by rapidly rubbing between palms), resuspend the cells in a small amount (~0.5 mL) of culture medium, and add the cell suspension to a T25 tissue culture flask. Increase the volume in the flask to 10 mL with additional culture medium and place into a tissue culture incubator (d 0).

2. On d 3, withdraw the spent medium and refeed the cells with 10 mL of fresh medium.

3. Culture the cells until confluent (typically 4–5 d).

4. To subculture the confluent RAW cells, withdraw the spent medium, add 10 mL of fresh medium to the flask, and scrape the cell layer into this fresh medium using a rubber scraper (*see* **Note 1**).

5. Immediately add 0.01 mL of this cell suspension to 0.09 mL of fresh medium in a microcentrifuge tube, mix gently, and count the cells using a hemocytometer.

6. Calculate the number of cells per milliliter. Plate the 10-mL RAW cell suspension at 1.5×10^5 cells/cm^2 into tissue culture dishes of the desired size. Typically, one confluent T25 flask will provide a sufficient number of RAW cells to seed

two 100-mm dishes or 24-well dishes (*see* **Notes 2** and **3**). Increase these volumes with additional medium as needed to yield 8 mL per 100-mm dish or 0.5 (or 1.0) mL per well of a 24-well dish, and then place the cells into a tissue culture incubator.

7. To grow the RAW cells for an extended period of time, refeed the cultures every 2–3 d and subculture when they reach confluency as in **steps 4–6.**

3.2. RAW-OC Formation (see Note 4)

This method is based on the published procedure of Hsu et al. *(10)*.

1. Culture RAW cells to confluency (*see* **Subheading 3.1.**, **steps 1–3**).
2. Subculture confluent RAW cells into 24-well dishes as described in **Subheading 3.1.**, **steps 4–6** (*see* **Notes 2–5**). If the cells are to be used for cytochemical or immunological staining, replate the RAW cell suspension into 24-well dishes that contain a sterile glass coverslip in each well. If bone pit resorption is to be evaluated in parallel with OC development in the RAW cell cultures, replate the RAW cell suspension into 24-well dishes that contain two to four small discs of bone or ivory per well (with or without a glass coverslip under the discs).
3. Immediately add soluble recombinant RANKL to the dishes at a final concentration of 35 ng/mL to initiate OC development (d 0) and increase the volume in the wells to 0.5 (or 1.0) mL with additional culture medium (*see* **Note 6**).
4. Culture to d 3. Briefly examine the cells under a microscope for evidence that RAW cells are beginning to fuse into multinucleated RAW-OCs. Withdraw the spent medium, and add 0.5 (or 1.0) mL of fresh medium containing 35 ng/mL of RANKL to the developing RAW-OC cell cultures.
5. Culture until d 5 or 6 when many multinucleated RAW-OCs have formed but have not completely covered the dish (*see* **Note 7**). The d 5 or 6 RAW-OC populations may be immediately fixed and used for cytochemical or immunological staining, harvested for biochemical or molecular studies, or analyzed for bone pit resorption (*see* Chapter 6). Alternatively, RAW-OCs can be purified further by serum gradient density fractionation (*see* **Subheading 3.2.1.**).

3.2.1. Serum Gradient Purification of RAW-OC

Because not all RAW cells fuse into multinucleated RAW-OCs by d 5 or 6, those that have can be purified from the remaining mononuclear cells using serum density gradient fractionation (*see* **Note 8**). This procedure is a modification of the one we routinely use to purify in vitro formed OC or OC-like cells from chick or human origin *(17,18)*. Directions are provided for RAW-OCs formed on 100-mm tissue culture dishes. All steps are conducted at room temperature unless otherwise noted, and are performed in a sterile hood using sterile solutions and supplies.

1. Remove the spent culture medium from two 100-mm dishes of d 5 or 6 RANKL-generated RAW-OCs.

2. Gently add 10 mL of MHB to each 100-mm dish to wash the cells. Remove and discard the washes.
3. Repeat **step 2** to wash the RAW-OCs twice more with MHB.
4. Add 10 mL of MHB to each dish and place them into a tissue culture incubator at 37°C for 15 min.
5. Remove and discard the MHB solution from each dish.
6. Add 5 mL of freshly prepared collagenase–trypsin digestion solution to each dish and incubate at 37°C for 5 min.
7. Remove the dishes from the incubator and shake the plates gently by hand back and forth (e.g., slide the dish on a flat surface) for ~30 sec to detach and loosen the interaction of cells with extracellular matrix produced by the cells.
8. Completely remove the collagenase–trypsin solution containing the released matrix material from each dish and discard (*see* **Note 9**).
9. Gently wash the adherent cells on each dish by releasing 10 mL of PBS slowly against the side wall of the dish. Completely remove and discard the washes.
10. Repeat **step 9** to wash the cells on each dish with PBS twice more.
11. Add 5 mL of protease–EDTA digestion solution to each dish. Incubate at 37°C for 10–15 min (*see* **Note 10**).
12. Loosen the adherent cells on each dish by flushing the protease–EDTA incubation solution with a pipet gently over the surface of the cell layer to free the cells (*see* **Note 11**).
13. Transfer the cell suspensions from two 100-mm dishes into one 50-mL sterile centrifuge tube containing 1.0 mL of FBS (to inhibit further protease action).
14. Centrifuge the cells at 100g for 5 min.
15. Remove and discard the supernatant. Gently resuspend the cell pellet in 15 mL of MHB by repeatedly drawing up and releasing from a pipet (not too vigorously; *see* **Note 11**).
16. Prepare 16 mL of 70% FBS in MHB (11.2 mL of FBS plus 4.8 mL of MHB) in a 50-mL of centrifuge tube, and 16 mL of 40% FBS in MHB (6.4 mL of FBS plus 9.6 mL of MHB) in another 50-mL tube.
17. Prepare an FBS gradient in a 50-mL round-bottom centrifuge tube. To do this, carefully pipet 15 mL of the 70% FBS–MHB solution (from **step 16**) into the bottom of the tube. Very slowly overlay this with 15 mL of the 40% FBS–MHB solution (from **step 16**), using a pipet held at a 45° angle against the side of the tube just above the 70% FBS layer and slowly releasing the 40% FBS solution in a thin stream so as not to deform the surface of the 70% FBS layer.
18. Let the tube stand undisturbed for 30 min (at room temperature) to allow the larger multinucleated RAW-OCs to settle under normal gravity and penetrate the FBS layers (*see* **Note 12**).
19. Carefully pipet off the top 17 mL which contains mononuclear cells, and place into a 50-mL tube.
20. Then, remove the 16-mL middle layer, which contains primarily mononuclear cells and some small multinucleated RAW-OCs, and place into another 50-mL tube.
21. The bottom 12-mL fraction contains predominantly large multinucleated RAW-OCs.

22. Centrifuge the purified RAW-OC bottom fraction (and the other fractions if they are also to be cultured and/or analyzed) at 100*g* for 5 min.
23. Gently resuspend the RAW-OC pellet in culture medium, count an aliquot in a hemocytometer, and plate 1000–4000 cells per well of a 24-well dish. Typically, the purified RAW-OCs from two 100-mm dishes can be cultured in 2–10 wells of a 24-well dish (with 0.5–1.0 mL of medium per well) for 6–24 h (*see* **Note 13**). The top and middle fractions from the serum gradient fractionation are typically cultured in 20–40 wells and 15–30 wells of a 24-well dish, respectively. Alternatively, RAW-OCs (and the top and middle fractions, if desired) may be used immediately for analysis (*see* **Subheading 3.2.**, **step 5**).

Serum gradient fractionation routinely provides 4000–10,000 purified RAW-OCs from one 100-mm dish (this depends on the efficiency of one's technique and, more importantly, on the exact stage of RAW-OCs used to purify the cells; *see* **Notes 5**, **7**, **12**, and **13**). In unfractionated RANKL-generated RAW-OC cultures, multinucleated (more than three nuclei) RAW-OCs typically represent ~1% on a per cell basis and 25% on a per nuclear basis of the total cell population (**Fig. 1**, *left panel*). In contrast, serum gradient purified RAW-OCs (more than three nuclei) typically comprise 60–90% on a per cell basis and 96% on a per nuclear basis of the total cell population in the bottom serum fraction (**Fig. 1**, *lower right panel*). On average, RAW-OCs in this bottom serum fraction contain 15–30 nuclei per cell.

3.3. Assay Techniques

3.3.1. Phenotypic and Functional Characterization of RAW-OCs

Standard protocols can be used to evaluate the morphological (light, scanning electron microscope), ultrastructural (transmission electron microscope), histochemical (general or enzymatic activity stains), or immunocytochemical staining (e.g., for OC developmental markers) characteristics of RAW cells representing pre-OCs and in vitro RANKL-formed RAW-OCs (*see* Chapter 6 by Collin-Osdoby et al., *this volume*). Whereas untreated RAW cells do not stain for tartrate resistant acid phosphatase (TRAP) activity, a key marker and enzyme involved in OC bone pit resorption, RANKL-differentiated RAW cell cultures develop both TRAP+ mononuclear and multinucleated cells (**Fig. 2A,C**). The RAW-OCs formed by cell fusion contain multiple nuclei clustered together and the cells may appear either spread out or partially elongated when cultured on plastic (**Fig. 2A**). RAW-OCs cultured on bone or ivory (either during RANKL development or following replating of the differentiated cells) frequently display a more compact and highly motile elongated shape with numerous pseudopodial extensions (**Fig. 2C**). Resorption pits formed by RAW-OCs are typified by clusters of multilobulated excavation cavities or long resorption tracks (which may also be multilobulated) adjacent to or underlying
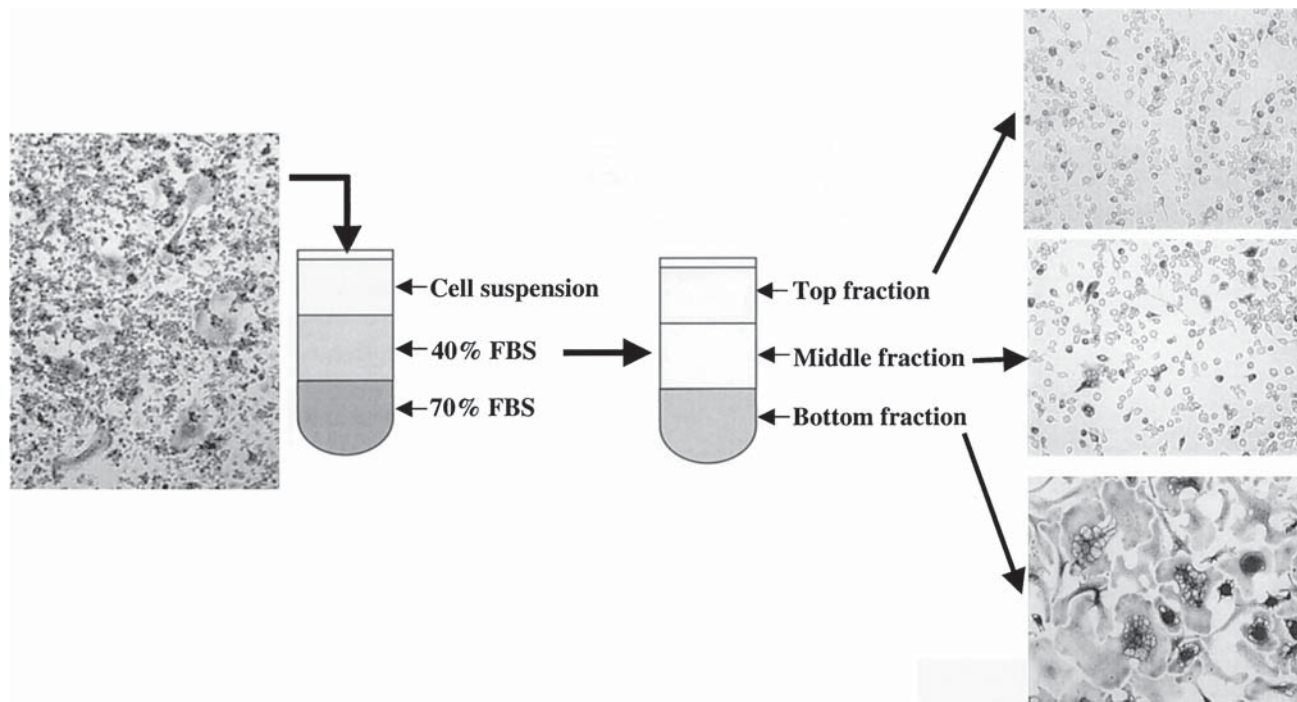
Fig. 1. RANKL-mediated RAW-OC formation and serum gradient purification. (**Left**) RAW cells were cultured with 35 ng/mL of murine recombinant RANKL for 6 d and then subjected to serum gradient fractionation. A well cultured in parallel was fixed and stained for TRAP activity to show the proportion of mononuclear and multinucleated TRAP+ cells that arise by d 6 in RANKL differentiated RAW cell cultures. The cells were viewed using a light microscope and images were captured with a computer-linked digital camera. (Reduced from original magnification, ×100.) (**Right**) The *top*, *middle*, and *bottom fractions* from the serum gradient fractionation were replated and cultured on plastic for several hours, after which the cells were fixed and stained for TRAP activity. (**Upper right**) The *top fraction* consists entirely of mononuclear cells, some of which are TRAP+ (in contrast to untreated RAW cells which are all TRAP-, not shown). (Reduced from original magnification, ×200.) (**Middle right**) The *middle fraction* primarily contains mononuclear cells, a
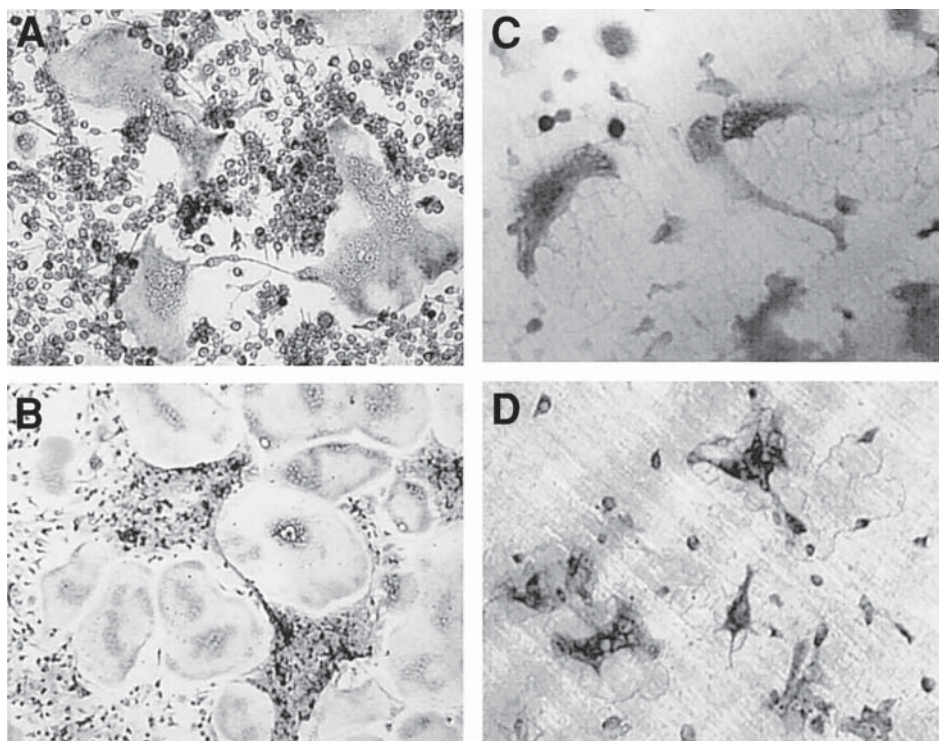
Fig. 2. RANKL-mediated RAW-OC or MA-OC formation and bone pit resorption. (**A**, **C**) RAW cells were cultured with 35 ng/mL of murine recombinant RANKL for 6 d on plastic (**A**) or ivory (**C**), and then fixed and stained for TRAP activity. Note the well spread morphology of RAW-OCs on plastic (**A**) compared with the more compact and motile phenotype of such cells actively engaged in bone resorption on ivory (**C**). Abundant resorption pits and tracks were evident that were frequently composed of connecting excavation cavities. These represent periods of RAW-OC attachment and pit formation, followed by RAW-OC movement to an adjacent area of ivory for further resorption. (**A**, **C** reduced from original magnification, ×200.) (**B**, **D**) Murine bone marrow cells were isolated and cultured at 5.6×10^5 cells per well of a 24-well dish (1.9 cm^2 per well) with 25 ng/mL of murine M-CSF and 35 ng/mL of murine RANKL for 6 d on plastic (**C**) or ivory (**D**), after which the cells (MA-OC) were fixed and stained for TRAP activity. Like RAW-OCs, the TRAP+ MA-OCs were well spread on plastic (**B**) and more compact on ivory (**D**). Resorption pits and tracks formed by MA-OCs (**D**) were indistinguishable from those formed by RAW-OCs (**B**). (**B**, **D** reduced from original magnification, ×200.)

Fig. 1. *(continued)* portion of which are TRAP+, and some small multinucleated RAW-OCs. (Reduced from magnification, ×200.) (**Lower right**) The *bottom fraction* consists primarily of large multinucleated RAW-OCs, although a few mononuclear cells may still be present. (Reduced from original magnification, ×100.)

RAW-OCs actively engaged in bone resorption (**Fig. 2C**). Molecular, immu-
nological, and/or biochemical analyses have shown that RAW-OCs express
hallmark properties of OCs including TRAP, calcitonin receptor, cathepsin K,
matrix metalloproteinase-9, integrin $\alpha v \beta 3$, and c-src (***10,18***, *our unpublished
data*). Both the phenotypic and functional characteristics of RANKL-differen-
tiated RAW-OCs resemble those of in vivo formed isolated murine OCs or
RANKL-differentiated OCs (MA-OCs) formed from murine bone marrow cells
in the presence of M-CSF (**Fig. 2B**, **D**). Thus, like RAW-OCs, TRAP + MA-
OCs exhibit a well spread morphology on plastic (**Fig. 2B**) and a more com-
pact, motile phenotype on bone or ivory (**Fig. 2D**). Multilobulated resorption
pits and tracks formed by MA-OCs (**Fig. 2C**) also resemble those formed by
RAW-OCs, with well defined margins and deep resorption lacunae (**Fig. 2D**).
Resorption pit formation by RAW-OCs, in the presence or absence of modula-
tors, can be quantified as for chicken or human OCs (*see* Chapter 6). In addi-
tion to these phenotypic and functional analyses, RAW-OCs provide sufficient
material (protein, RNA, etc.) for investigation of gene or protein expression
levels, receptors and signal transduction pathways, production of various fac-
tors (cytokines, growth factors, arachidonic acid metabolites), or the release of
other substances (free radicals, enzymatic activities) (*see* **Note 14**).

4. Notes

1. We find that a rubber-tipped cell scraper works best because it completely con-
   tacts the surface of the tissue culture flask (or dish) and causes the least cell
   damage.
2. In general, RAW cells should be subcultured at a ratio of 1:3 to 1:6.
3. If more cells will be needed than are provided by a reasonable number of T25
   flasks, the confluent RAW cells can be subcultured into T75 flasks (at a 1:3 to
   1:6 ratio) and then grown to confluency.
4. The number of RAW cell passages affects RANKL-mediated OC formation. In
   our hands, RAW-OCs will no longer form in response to RANKL stimulation
   once they have undergone 18–20 passages from the time that they were received
   from the ATCC repository. The reason for this is not yet clear, although other
   researchers have similarly noted that not all RAW 264.7 cell lines (or passages?)
   will form OCs after RANKL treatment. It is also possible that particular lots of
   FBS may differentially influence RANKL-mediated RAW-OC formation. There-
   fore, at least several different lots and sources of FBS should be tested if there are
   difficulties encountered in trying to form RAW-OCs.
5. The density of RAW cells plated affects the rate and yield of RAW-OC develop-
   ment, as well as the subsequent analysis of RAW-OCs formed. We find that too
   low a cell density (100–500 cells/cm^2) delays RAW-OC formation and decreases
   the final yield. For most purposes (e.g., testing the effects of various agents on
   RAW-OC development), the plating density for RAW cells should be in the range

of 10^3 to $3 \times 10^4/cm^2$ to facilitate counting or characterization of the RAW-OCs formed and still generate a sufficient number for analysis. If RAW-OCs are to be purified by serum density gradient fractionation, the initial plating density of RAW cells should be considerably higher ($1.5 \times 10^5/cm^2$) so that enough RAW-OCs are obtained following their purification (*see* **Subheadings 3.1.** and **3.2.**). However, too high a density of RAW cells (4.5 to $7.5 \times 10^5 / cm^2$) inhibits RAW-OC formation.

6. In our experience, the potency of recombinant soluble RANKL for inducing OC formation is largely dependent on its source (not only for RAW cells, but also for human monocyte, mouse bone marrow, or chicken bone marrow preparations). Thus, different commercial RANKL preparations vary significantly in the dose required, kinetics of OC formation, and final yield of bone pit resorptive OCs obtained. This is not strictly due to species compatibility issues because human or murine recombinant RANKL are similarly efficient for inducing OCs from murine RAW or bone marrow derived cells, chicken bone marrow cells, or human peripheral blood monocytes (although all but RAW cells require M-CSF costimulation). Although we have successfully used various commercial RANKL preparations, we now routinely prepare larger quantities of soluble recombinant mouse RANKL in our own lab that exhibits high osteoclastogenic activity with murine RAW or bone marrow cells, chicken bone marrow cells, or human monocytes. At 35 ng/mL, this mouse RANKL induces multinucleated TRAP+ cell formation that is first apparent on d 3–4 of RAW cell culture. Lower RANKL concentrations delay the kinetics and final yield of RAW-OC formation. Others have used recombinant RANKL preparations in the range of 20–100 ng/mL (depending on its source and bioactivity) to form multinucleated TRAP+ cells that usually first appear on d 3–4 of RAW cell culture *(11,15,16)*. However, certain recombinant mouse RANKL preparations appear to require an additional anti-RANKL antibody crosslinking step to induce osteoclastogenesis *(19)*. Therefore, it is recommended that pilot studies be performed with each new source and preparation of recombinant RANKL to ascertain an appropriate dose to achieve the level of RAW-OC formation needed.

7. In our model of RANKL-mediated RAW-OC development, TRAP+ cells first become apparent on d 2 of culture, and multinucleated TRAP+ cells appear on d 3–4 of culture and nearly reach a peak on d 5–6 of culture. It is important to either use the cells or subject them to serum gradient purification at this point (and not wait another d until the full peak of RAW-OC formation has occurred) because if the cells become overconfluent and overfused, they die very rapidly (<24 h) thereafter.

8. The mononuclear cells that remain in the RANKL-treated RAW cell cultures by d 5–6 can still fuse to form more RAW-OCs on further culture, even in the absence of any additional RANKL stimulation. Therefore, such cells represent an early stage in OC differentiation and are not equivalent to the original non-RANKL-treated RAW cells (in a number of characteristics). It is not advisable to simply culture the RANKL-treated RAW cell populations for any longer period of time than d 5–6 to encourage more of the mononuclear cells to fuse into multi-

nucleated RAW-OCs because continuing cell fusion (even one extra d) produces cells that are too large and fragile, and which undergo rapid and massive apoptosis in the cultures once such RAW-OCs have formed.

9. It is important to remove this released extracellular matrix completely, here and in the subsequent washes, or the cells will reattach to it and become extremely difficult to detach. At this point, the cells can be seen to have begun to pull up from the dish.

10. A rounding up from the dish becomes more obvious at this point for the RAW-OCs. The cells may appear somewhat shrunken, but should still appear bright and viable.

11. Use only wide-bore pipets or tips for any work in isolating or manipulating OCs to avoid fragmenting these large multinucleated cells. Also, care should be taken to resuspend, mix, or vortex OC preparations gently and for as little time as necessary.

12. The extent of RANKL-mediated RAW-OC formation impacts on this step as well. Therefore, if the RAW-OCs formed are relatively small (<10 nuclei per cell), they will be unable to settle effectively into the 70% portion of the serum gradient. However, if the RAW-OCs are too large (>30 nuclei per cell), they will be too fragile, prone to break, and die too quickly so that few viable RAW-OCs will be recovered following the serum gradient purification.

13. Even under controlled conditions of RANKL-mediated RAW-OC formation as discussed in this chapter, once such cells have formed they tend to apoptose very rapidly and the cells can be lost within 24 h if allowed to develop too long. Addition of 10 ng/mL of IL-1α to promote RAW-OCs survival on plastic slows the apoptotic process only slightly. Therefore, we typically use RAW-OCs formed in tissue culture dishes by d 5 or 6 for analysis within 6–24 h (e.g., staining, RNA or protein extraction, etc.). If RAW-OCs have been formed on bone or ivory, resorption pits are usually evident by d 4 and maximal by d 6; modulators can be added at appropriate times to observe stimulatory or inhibitory effects on resorption. When RAW-OCs are purified by serum gradient fractionation and replated onto tissue culture dishes, their viability is usually extended for an additional 24 h. Alternatively, purified RAW-OCs can be replated onto bone or ivory (~800 cells per well of a 48-well dish containing one piece of ivory or bone) and cultured with 35 ng/mL of RANKL and 10 ng/mL of interleukin-1α (IL-1α), in the presence or absence of other modulators, for 5–6 d to ascertain effects primarily on preformed RAW-OCs (although some additional RAW-OC development also occurs during this time period, as the 70% serum purified fraction still contains some mononuclear cells). Purified RAW-OCs typically do not exhibit pit formation within the first 24 h after replating onto bone or ivory.

14. Although many of the phenotypic and functional characteristics of RAW-OCs match those of RANKL-differentiated primary murine bone marrow-derived OCs or isolated in vivo formed murine OCs, this cannot automatically be assumed to be true for any particular property being evaluated. The most obvious difference is the requirement for M-CSF in RANKL-stimulated OC formation from bone

marrow cells (which have relatively low RANK prior to M-CSF exposure) but not for transformed RAW cells (which already make M-CSF and express high RANK levels). Therefore, it is important to consider that the property under study in the RAW-OC cell system may not necessarily reflect that of normal murine OCs. Because RAW cells are easier to obtain and culture than primary bone marrow cells, represent a relatively homogeneous population of pre-OCs (deficient in osteoblasts, stromal cells, lymphocytes, etc.), and provide abundant material for study, they provide a highly valuable resource for rapidly and efficiently screening and determining mechanisms underlying OC-related processes. However, we recommend that such studies are subsequently followed by at least a limited number of experiments using primary murine OCs (either isolated or RANKL-generated in vitro) to confirm that these processes are likewise observed in normal murine OCs and are not unique to transformed RAW cells or RAW-OCs.

Acknowledgments

References

1. Roodman, G. (1996) Advances in bone biology—the osteoclast. *Endoc. Rev.* **17**, 308–332.
2. Mancini, L., Moradi-Bidhendi, N., Brandi, M., Perretti, M., and MacIntyre, I. (2000) Modulation of the effects of osteoprotegerin (OPG) ligand in a human leukemic cell line by OPG and calcitonin. *Biochem. Biophys. Res. Commun.* **279**, 391–397.
3. Nagai, M., Kyakumoto, S., and Sato, N. (2000) Cancer cells responsible for humoral hypercalcemia express mRNA encoding a secreted form of ODF/TRANCE that induces osteoclast formation. *Biochem. Biophys. Res. Commun.* **269**, 532–536.
4. Hentunen, T., Reddy, S., Boyce, B., et al. (1998) Immortalization of osteoclast precursors by targeting Bcl-XL and Simian virus 40 large T antigen to the osteoclast lineage in transgenic mice. *J. Clin. Invest.* **102**, 88–97.
5. Chen, W. and Li, Y. (1998) Generation of mouse osteoclastogenic cell lines immortalized with SV40 large T antigen. *J. Bone Miner. Res.* **13**, 1112–1123.
6. Takeshita, S., Kaji, K., and Kudo, A. (2000) Identification and characterization of the new osteoclast progenitor with macrophage phenotypes being able to differentiate into mature osteoclasts. *J. Bone Miner. Res.* **15**, 1477–1488.
7. Takahashi, N., Udagawa, N., and Suda, T. (1999) A new member of tumor necrosis factor ligand family, ODF/OPGL/TRANCE/RANKL, regulates osteoclast differentiation and function. *Biochem. Biophys. Res. Commun.* **256**, 449–455.
8. Chambers, T. (2000) Regulation of the differentiation and function of osteoclasts. *J. Pathol.* **192**, 4–13.
9. Schoppet, M., Preissner, K., and Hofbauer, L. (2002) RANK ligand and osteoprotegerin. Paracrine regulators of bone metabolism and vascular function. *Arterioscler. Thromb. Vasc. Biol.* **22**, 549–553.

10. Hsu, H., Lacey, D., Dunstan, C., et al. (1999) Tumor necrosis factor receptor family member RANK mediates osteoclast differentiation and activation induced by osteoprotegerin ligand. *Proc. Natl. Acad. Sci. USA* **96**, 3540–3545.

11. Yamamoto, A., Miyazaki, T., Kadono, Y., et al. (2002) Possible involvement of IkappaB kinase 2 and MKK7 in osteoclastogenesis induced by receptor activator of nuclear factor kappaB ligand. *J. Bone Miner. Res.* **17**, 612–621.

12. Mizukami, J., Takaesu, G., Akatsuka, H., et al. (2002) Receptor activator of NF-kappaB ligand (RANKL) activates TAK1 mitogen-activated protein kinase kinase through a signaling complex containing RANK, TAB2, and TRAF6. *Mol. Cell. Biol.* **22**, 992–1000.

13. Raschke, W., Baird, S., Ralph, P., and Nakoinz, I. (1978) Functional macrophage cell lines transformed by Abelson leukemia virus. *Cell* **15**, 261–267.

14. Shadduck, R., Waheed, A., Mangan, K., and Rosenfeld, C. (1993) Preparation of a monoclonal antibody directed against the receptor for murine colony-stimulating factor-1. *Exp. Hematol.* **21**, 515–520.

15. Koseki, T., Gao, Y., Okahashi, N., et al. (2002) Role of TGF-beta family in osteoclastogenesis induced by RANKL. *Cell Signal* **14**, 31–36.

16. Shin, J., Kim, I., Lee, J., Koh, G., Lee, Z., and Kim, H. (2002) A novel zinc finger protein that inhibits osteoclastogenesis and the function of tumor necrosis factor receptor-associated factor 6. *J. Biol. Chem.* **277**, 8346–8353.

17. Sells-Galvin, R., Cullison, J, Avioli, L., and Osdoby, P. (1994) Influence of osteoclasts and osteoclast-like cells on osteoblast alkaline phosphatase activity and collagen synthesis. *J. Bone Miner. Res.* **9**, 1167–1178.

18. Yu, X., Collin-Osdoby, P., and Osdoby, P. (2003) SDF-1 increases recruitment of osteoclast precursors by upregulation of matrix metalloproteinase-9 activity. *Connect. Tissue Res.* **44 (Suppl. 1),** 1–6.

19. Cappellen, D., Luong-Nguyen, N., Bongiovanni, S., Grenet, O., Wanke, C., and Susa, M. (2002) Transcriptional program of mouse osteoclast differentiation governed by the macrophage colony-stimulating factor and the ligand for the receptor activator of NF-kappa B. *J. Biol. Chem.* **277**, 21,971–21,982.

13

Analysis of Osteoclast Function in Mouse Calvarial Cultures

Michael J. Marshall and Marit N. Rowlands

1. Introduction

Mouse calvarial organ cultures have been used for many years to study the basic mechanisms by which osteoclastic bone resorption is regulated. The most obvious advantage of organ cultures over in vivo studies is the absence of confounding factors such as hormonal and mechanical influences. Calvarial organ cultures have an advantage over isolated cell systems also, in that they preserve the interrelationships between the different cell types in the bone, and the relationship between these cells and bone matrix. Despite this, the mouse calvarial organ culture system has been used about half as frequently between 1995–2000 as during 1990–1995, as shown by a text word search of scientific publications. The main reason for this is that osteoclasts, the cells responsible for resorbing bone, can now be isolated from bone tissue of several species including rat *(1)*, chicken *(2)*, mouse *(3)*, rabbit *(4)*, and human *(5)*. More recently, techniques have been developed to generate osteoclasts in vitro *(6,7)* and then incubate these on bone slices to produce bone resorption. With these approaches, osteoclasts are defined by their ability to produce resorption pits on bone slices. However, this definition may not be sufficient. Other giant cells from nonosseous tissues can produce pits *(8)*, and two distinct morphologies of multinucleate tartrate-resistant acid phosphatase (TRAP)-positive osteoclast-like cells have been described with differing resorptive capacities *(9)*. Like the osteoclast, the foreign body giant cell is derived by fusion of monocytes, and if they share the same fusion mechanism then hybrid giant cells showing a range of phenotypes may be produced in cultures of bone marrow derived cells. The problem with studying osteoclasts in isolation is that this is not how they exist in vivo. Osteoclasts do not form in dead bone tissue, for instance, where a

fracture has damaged the blood supply *(10)*. They arise by fusion of monocyte precursors that arrive in the blood capillaries *(11)*. Osteoclast precursors must traverse the capillary endothelium and migrate to the bone surface, where they fuse to form multinucleated osteoclasts. They must be specifically activated to resorb bone in response to local or humoral stimulation *(12)* and they can be deactivated so that they detach from the bone surface *(13)*. Osteoclasts are essential to the process whereby bone is adapted to local mechanical stress *(14)* and this can occur only via local mechanisms. Osteoclasts possess a specific mechanism that recognizes a bone surface that is in need of remodeling *(12)*. When recognition is triggered the resorption mechanism is initiated. This ensures that previously resorbed bone is not further resorbed so that resorption proceeds only to a fixed depth. Also, osteoclasts have a short life span, about 4–12 d *(15,16)* and are responsive to apoptotic signals that bring about their orderly death *(17)*. There is abundant evidence that each of these steps is under the control of other cell types, including endothelial cells *(18,19)*, osteoblastic cells *(20,21)* and their descendants, the osteocyte and the bone lining cell *(22)*, and, under inflammatory conditions, cells of the immune system *(23)*. The clearest example of the control of osteoclasts by other cell types is the activation of the receptor activator of nuclear factor-κB (RANK) receptor by RANK ligand (RANKL) expressed on osteoblasts and bone marrow stromal cells *(24)*. In the absence of a resorptive stimulus, these cells default to the production of osteoprotegerin (OPG) which inhibits osteoclast activity and differentiation by binding and neutralizing RANKL *(25)*.

Bone organ cultures were pioneered by Dame Honor Fell *(26)* more than 50 yr ago and have been used by several investigators since *(27–30)*. Various types of bones have been used, including fetal long bones showing endochondral ossification and neonatal calvaria showing intramembranous ossification. Nutritional requirements differ in these two models because the different mechanisms of ossification produce different structures. The planar nature of the calvaria means that diffusion path lengths are short whereas the cylindrical nature of the long bone can lead to long path lengths, particularly in postnatal bones. This tends to restrict the use of long bones in organ culture to late fetal development, and this in turn means that it is modeling rather than remodeling of bone that is studied. A large number of effectors of bone resorption have been investigated including hormones, cytokines, growth factors, prostaglandins, drugs, and toxins *(27–30)* and the information obtained has in general been consistent with effects observed in vivo.

2. Materials
2.1. Dissection

1. Scalpel (no. 3 with curved blade no. 15).

2. Fine scissors (Vannas–Tubingen spring scissors, 8.5 cm long with a 5-mm cutting edge).
3. Scissors (Noyes spring scissors, 12 cm long with a 12-mm cutting edge).
4. Watchmakers' forceps (Dumont no. 5, 11 cm long).
5. Graefe forceps (10 cm long, curved, finely serrated) (Interfocus Ltd, Haverhill, UK).

2.2. Microscopy and Image Analysis

1. Dissecting microscope, Olympus with 0.7–4× zoom lens.
2. Inverted microscope: Nikon Diaphot-TMD for phase contrast and fluorescence.
3. Microscope: Leitz Dialux transmitted light and fluorescence microscope.
4. Digital Camera: Nikon Coolpix 990.

2.3. Media and Reagents

All reagents should be made up sterile or sterilized by passing through a 0.22-μm filter before use.

1. Radiolabeled calcium: Add 4 MBq/mL of $[^{45}Ca]$ calcium chloride to 0.9% saline.
2. Phosphate-buffered saline (PBS) with EDTA and heparin: Add 5 mM EDTA and 10 U/mL of heparin to PBS.
3. BGJb medium: Fitton Jackson modified BGJb medium supplemented with 10% heat inactivated fetal calf serum (FCS), 100 U/mL of benzylpenicillin, 100 μg/mL of streptomycin (Glaxo), and 10^{-6} M indomethacin. Used for preculture of calvarial explants (*see* **Note 1**).
4. BGJb medium pH 6.8: Add 150 μL of 1 M HCl to BGJb medium containing 10% heat-inactivated FCS, 100 U/mL of benzylpenicillin, and 100 μg/mL of streptomycin. Used for culture of calvarial explants (*see* **Note 2**).
5. Medium 199: Medium 199 medium, with 25 mM *N*-2-hydroxyethylpiperazine-*N*'-2-ethanesulfonic acid (HEPES), Hanks' balanced salt solution and 5% heat-inactivated FCS.
6. Tissue culture plates: Selection of 12-, 24-, and 96-well plates.
7. 1 M Hydrochloric acid to decalcify calvariae at the end of the culture period.
8. Scintillation cocktail: FluoranSafe XE Scintran.

2.4. TRAP Staining

1. TRAP fixative: 95% Ethanol, 5% glacial acetic acid.
2. TRAP staining reagent: 1 mM Naphthol AS–BI phosphate, 0.3 mg/mL of fast garnet GBC salt in 100 mM acetic acid and 26.8 mM L-(+)-tartaric acid. Adjust pH to 5.2 with NaOH and store at –20°C until use.
3. Glutaraldehyde in HCl: 12.5% Glutaraldehyde in 1 M HCl. Make up fresh before use.
4. PBS–EDTA: 10% EDTA in PBS, adjust to pH 6.6 with 1 M HCl.

2.5. Integrin Staining

1. Skim milk–Tris solution: 0.25% Skim milk in 0.1 M Tris-HCl, pH 7.4.
2. Anti-β_3 integrin antibody: Biotin-conjugated hamster IgG antimouse CD61 (integrin β_3 chain) monoclonal antibody (Cambridge Bioscience, Cambridge, UK).

3. Control antibody: Biotin-conjugated hamster IgG monoclonal (anti-trinitrophenol, Cambridge Bioscience, UK).
4. Avidin–peroxidase in skim milk–Tris: ExtrAvidin peroxidase (Sigma), 10 μg/mL in skim milk–Tris solution.
5. Peroxidase detection solution: 0.5 mg/mL of diaminobenzidene, 0.006% hydrogen peroxide, 1 m*M* nickel chloride, 1 m*M* cobaltous chloride, 24 m*M* citric acid in 100 m*M* disodium hydrogen phosphate, pH 6.4.

2.6. Bromodeoxyuridine Staining

1. Bromodeoxyuridine solution: 20 m*M* 5-Bromo-2'-deoxyuridine (BrdU) and 2 m*M* 5-fluoro-2'-deoxyuridine (FdU) in 0.9% saline. Sterile filter before use.
2. BGJb with BrdU and FdU. Add 50 μ*M* BrdU and 5 μ*M* FdU to BGJb medium.

3. Methods
3.1. Calvarial Explant Culture

1. Inject neonatal Balb/c neonatal mice (up to 2 d old) intraperitoneally with 10 μL of radiolabeled calcium. Inject enough mice to give four or five bones per treatment group in the experiment (*see* **Note 3**).
2. Euthanize the mice 5 d later by decapitation.
3. After exposing the calvaria and pinning back the skin, pipet 100 μL of PBS with EDTA and heparin onto the surface of the calvaria to prevent blood coagulation.
4. Carefully dissect out the parietal bones (**Fig. 1**; *see* **Note 4**).
5. Place the individual parietal bones into separate wells of a 12-well tissue culture plate containing 1 mL of medium 199 for 15 min.
6. Replace with 1 mL of BGJb medium and preincubate for 24 h at 37°C in 5% CO_2 and air.
7. Replace the medium with 1 mL of BGJb medium, pH 6.8, containing test substances or vehicle and incubate for 2 d at 37°C and in 5% CO_2 in air.
8. Aspirate the conditioned medium from each well into an 1.5-mL Eppendorf tube.
9. Removing the bone from each well using forceps, rinse briefly in PBS and put each bone into a scintillation vial containing 200 μL of HCl for 15 min.
10. Add 4 mL of scintillation cocktail to the dissolved bone, cap the scintillation vial, and mix well.
11. Add 200 μL conditioned medium from each well to a scintillation vial.
12. Add 4 mL of scintillation cocktail to the medium, cap the scintillation vial, and mix well.
13. Count the radioactivity in the bones and conditioned medium using a beta counter (*see* **Note 5**).
14. Calculate the percentage resorption from each bone by subtracting the background counts from the total counts released into the medium (i.e., medium counts × 5) divided by the sum of total counts in the medium and bone.
15. Calculate the treated control ratio, by dividing the percentage calcium released from treated bones with that released by control bones (bones cultured in medium/vehicle) (*see* **Note 6**).
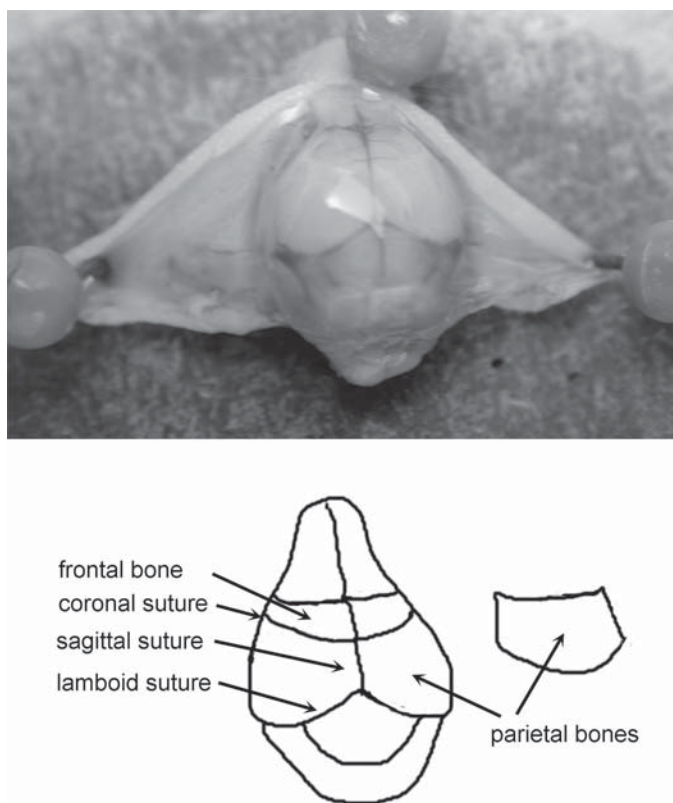
Fig. 1. The dorsal aspect of 7-d-old mouse calvaria and a diagram showing the suture lines. The initial incision is made with fine scissors posterior to and along the sagittal suture into the frontal bones. A cut is made along the full length of the lamboid suture, and then along the coronal suture which looks pale and is more difficult to see in this photograph. Flexing the parietal bone outwards, it hinges on the squamous suture, which is just out of sight on this photograph. Cut along the squamous suture to release the parietal bone.

3.2. Quantitating TRAP-Positive Osteoclasts in Calvarial Bones and the Endocranial Membrane

1. Eutahnize 7-d-old neonatal Balb/c mice by decapitation.
2. Isolate the parietal bones and place in culture as described in **Subheading 3.1.**, **steps 1–7**.
3. Terminate the culture after 48 h by aspirating the medium and transferring the bones to individual wells of a 96-well plate filled with TRAP fixative.
4. Transfer the bones, one at a time, to a Petri dish containing PBS and, with the aid of a dissecting microscope and watchmakers' fine forceps, strip the ectocranial membrane away and discard it (*see* **Note 7**).

5. Carefully peel the endocranial membrane back to the sagittal suture.
6. Transfer bones to individual wells of a 96-well plate containing 250 μL of PBS.
7. Stain the bone for TRAP activity by adding 100μL of TRAP reagent to each well. Incubate for 15 min at 37°C.
8. Wash each bone twice with 250 μL of PBS.
9. Fix and decalcify by adding 250 μL of glutaraldehyde in HCl to each well.
10. Wash each bone three times with 250 μL of PBS.
11. With the aid of a dissecting microscope, mount the bones, with endocranial side uppermost and the endocranial membrane spread out in Aquamount on a glass microscope slide (**Fig. 2a**).
12. Gently lower a coverslip onto the bone without disturbing the endocranial membrane.
13. Count TRAP-positive osteoclasts on each bone and membrane by transmitted light microscopy at ×100 magnification (*see* **Note 8**).

3.3. Immunolocalizing the Integrin β₃ Subunit in Calvarial Cultures

1. Set up the calvarial cultures as described in **Subheading 3.2.**, **steps 1–8**.
2. Wash the calvariae by adding 1 mL of PBS to each well.
3. Aspirate the PBS from each well.
4. Replace with 250 μL of PBS–EDTA and incubate at room temperature for 1 h.
5. Aspirate and replace with 250μL of fresh PBS–EDTA and incubate for a further 30 min.
6. Aspirate and add 250 μL of skim milk–Tris solution to each well. Incubate for 10 min.
7. Repeat **step 5** a total of three times.
8. Aspirate and add 25 μL of skim milk–Tris solution containing 10 μg/mL of anti-β₃ antibody or control antibody to each test well. Incubate at room temperature for 1 h.
9. Wash the bones three times with 200 μL of skim milk–Tris solution.
10. Add 25 μL of avidin peroxidase in skim milk–PBS to each well; incubate for 1 h.
11. Wash each bone three times with 200 μL of skim milk–Tris solution.
12. Add 200 μL of peroxidase detection solution to each well and incubate for 10 min at 37°C.
13. Wash each bone in 250 μL of PBS.
14. With the aid of a dissecting microscope, mount the bones, with endocranial side uppermost and the endocranial membrane spread out in Aquamount on microscope slides.
15. Gently lower a coverslip onto the bone without disturbing the endocranial membrane.
16. Count β₃-positive (brown staining) osteoclasts in the bone and endocranial membrane by transmitted light microscopy (**Fig. 3A,B**; *see* **Note 9**).

3.4. Analysis of Osteoclast Recruitment with BrdU in Mouse Calvarial Cultures

1. Weigh 5-d-old neonatal mice and inject each mouse intraperitoneally with 10 μL/g of BrdU solution.
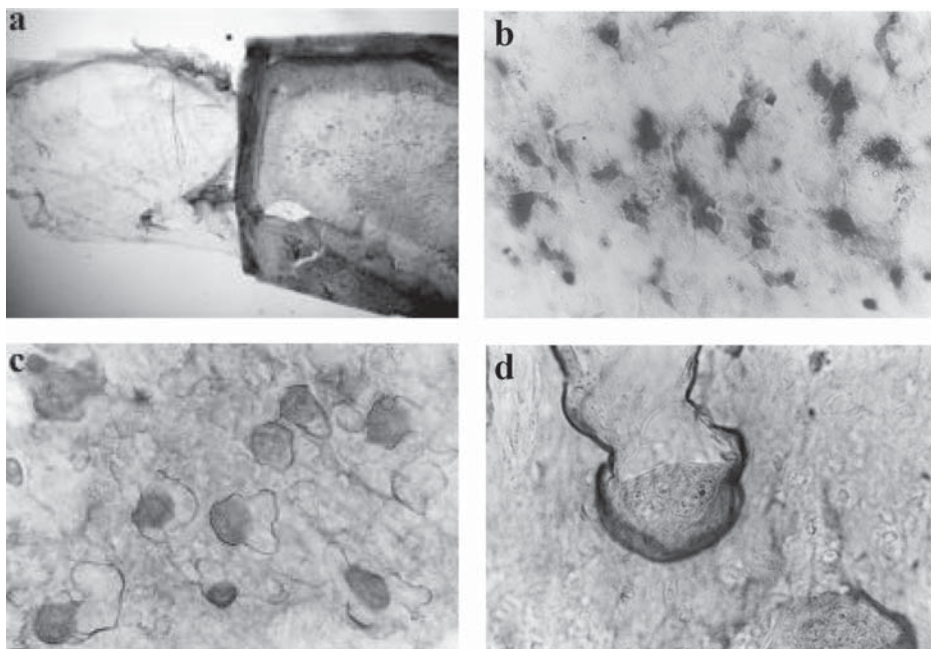
Fig. 2. (**a**) A freshly excised parietal bone showing the endocranial membrane peeled back to the sagittal suture and stained for TRAP. TRAP-positive osteoclasts are just visible on the bone surface on the right. (Reduced from original magnification, ×13.6.) (**b**) Irregular shaped TRAP-positive osteoclasts on the endocranial membrane of a parietal bone that has been incubated for 1 d in the presence of 10^{-6} M indomethacin. (Reduced from original magnification, ×175.) (**c**) TRAP-positive osteoclasts on the parietal bone surface after incubation for 1 d in the presence of 10^{-6} M indomethacin, then a further day in the presence of 10^{-6} M PGE$_2$. Resorption lacunae are visible in dark outline behind some of these darkly stained osteoclasts. (Reduced from original magnification, ×175.) (**d**) TRAP activity tends to be concentrated at the leading edge of rapidly resorbing osteoclasts and is also deposited at the borders of the resorption lacunae. Nuclei are visible in this osteoclast. (Reduced from original magnification, ×470.)

2. Euthanize by decapitation after 2 d.
3. Set up calvarial cultures as described in **Subheading 3.1.**, **steps 1–6**.
4. Incubate in BGJb with BrdU for 24 h.
5. Terminate the culture by transferring the bones to individual wells of 96-well plate filled with fixative.
6. Transfer the bones, one at a time, to a Petri dish containing PBS and, with the aid of a dissecting microscope and watchmakers' fine forceps, strip the ectocranial membrane away and discard it.
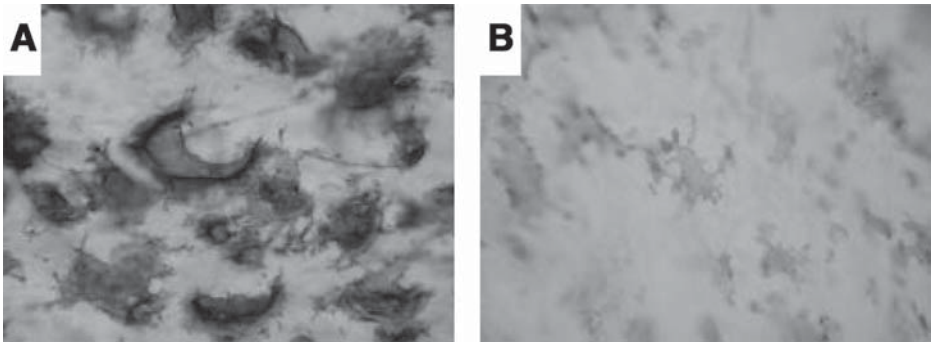
Fig. 3 (**A**) Immunolocalization of the β_3 subunit of the integrin $\alpha_v\beta_3$. A parietal bone was incubated for 1 d in the presence of 10^{-6} *M* indomethacin then a further day in the presence of 10^{-6} *M* PGE$_2$ and then stained for the β_3 subunit. Osteoclasts on the bone surface at about 12 h exhibit a pale brown concentric staining pattern which becomes more intense and crescent shaped at 24 h. (Reduced from original magnification, ×222.) (**B**) At the end of a 1-d incubation of parietal bones in the presence of indomethacin, osteoclasts can be seen on the peeled endocranial membrane but they are very palely stained for the β_3 subunit. (Reduced from original magnification, ×222.)

7. Carefully peel the endocranial membrane back to the sagittal suture.
8. Transfer bones to individual wells of a 96-well plate containing PBS.
9. Stain the bone for TRAP activity by adding 100 μL of TRAP reagent to each well. Incubate for 15 min at 37°C.
10. Wash each bone twice with 250 μL of PBS.
11. Fix and decalcify by adding 250 μL of HCl with glutaraldehyde to each well.
12. Wash each bone three times with 250 μL of PBS.
13. Add 200 μL of 1 *M* HCl to each well and incubate for 30 min at room temperature.
14. Wash three times with 250 μL of skim milk–Tris solution.
15. Add 25 μL of mouse monoclonal anti-BrdU antibody to each well. Incubate for 1 h at room temperature.
16. Wash three times in skim milk–Tris solution.
17. Add 25 μL of sheep anti-mouse IgG peroxidase conjugate to each well and incubate for 1 h.
18. With the aid of a dissecting microscope, mount the bones, with endocranial side uppermost and the endocranial membrane spread out in Aquamount on microscope slides.
19. Gently lower a coverslip onto the bone without disturbing the endocranial membrane.
20. Count BrdU-stained osteoclasts by transmitted light microscopy (*see* **Note 10**).

4. Notes

1. Role of preincubation: A 24-h preincubation period in BGJb medium with indomethacin is commonly employed to reduce spontaneous mineral mobiliza-

tion, which can occur at a high rate in some control cultures due to prostaglandin releases *(30)*. It is thought that prostaglandin release occurs as the result of tissue damage during dissection, emphasizing the importance of a careful dissection technique.

2. Optimal pH for bone resorption: HCl is added to culture medium during the experimental culture period because hydrogen ion concentration has a profound effect on the extent of bone resorption *(27)*. At a pH above 7.2 bone resorption is inhibited whereas at pH 6.8 it is about maximal in (BGJb) medium *(28)*.

3. Number of bones per group: We typically use five bones for each set of culture conditions. To determine the extent of non-cell-mediated calcium release, it is possible to culture an additional group of five bones that have been frozen and thawed three times in liquid nitrogen. We do not do this routinely because in our experience calcium release is fairly constant at about 7.5%. If frozen bones are used, however, the percentage resorption for this group should be subtracted from the values obtained for test and control bones to obtain the cell-mediated calcium release.

4. Use of half calvariae: Instead of using whole parietal bones it is possible to divide each parietal bone into two pieces and use half calvaria that contain the parietal bone and the frontal bone *(31,32)*. These are often cultured at the interface of the medium and the gas phase held in position by stainless steel mesh supports. We and others *(32)* have found no advantage in supporting parietal bones on mesh supports over immersion in culture media.

5. Alternative methods of assessing bone resorption: Calcium release may also be determined by the colorimetric analysis of calcium in the medium *(33)* instead of using radiolabeled calcium. This has the advantages of avoiding the use of radio-activity and the need to inject the mice. It may also result in a more precise measure of resorption than that obtained by ^{45}Ca release because all the released calcium is measured and not just the radioactive calcium which may be incorporated superficially within the bone. Assays are also available to measure products of bone degradation as an alternative to calcium measurements. They include measurements of the carboxy-terminal telopeptide fragments of rodent type I collagen, measurements of pyridinoline and deoxypyridinoline crosslinks, and measurements of hydroxyproline *(34–38)*. These are more expensive than calcium measurements and it is unclear if they offer any benefits over calcium determination.

6. Analysis of paired bones: For a more sensitive detection of differences between test and control substances it is possible to calculate the ratio of the percentage calcium released from test to control wells using paired parietal bones from a single mouse. This approach takes advantage of the fact that within mouse variation in parietal bone resorption is less than between mouse variation.

7. Identifying the endocranial membrane: To be able identify the endocranial surface during dissection, it is helpful to cut a small diagonal section of bone from the left corner opposite the sagittal suture, with the concave endocranial side and the sagittal suture toward the operator.

8. Distribution of TRAP-positive osteoclast in the bone and endocranial membrane: TRAP-positive osteoclasts can be counted using a conventional microscope by analyzing serial fields covering the entire bone and the endocranial membrane. Osteoclasts normally reside almost exclusively on the endocranial side of the bone in 7-d-old mice. After 1 d in culture in the presence of indomethacin, osteoclasts tend to detach from the bone surface *(39)* and instead are seen attached to the endocranial membrane (*13*; **Fig. 2B**). This change in osteoclast distribution and osteoclastic bone resorption can be reversed if the bones are incubated with prostaglandin E_2 (PGE_2), 1,25-dihydroxyvitamin D_3 (1,25-$(OH)_2D_3$) or parathyroid hormone (PTH; **Fig. 2C,D**).

9. After incubation with PGE_2 β-3 staining is confined to osteoclasts on the bone surface **Fig. 3A**). At the end of the incubation with indomethacin, which causes osteoclasts to detach from bone and attach to the endocranial membrane, very few osteoclasts showed any β 3 staining whether on the bone or on the endocranial membrane (**Fig. 3B**) *(40)*. Other controls will be needed to discover the source of the problem if staining is seen in the presence of control antibody. Omitting the primary or the secondary antibody (or enzyme conjugate) will distinguish between nonspecific binding of the primary antibody or enzyme conjugate. Nonspecific binding may be due to inadequate blocking or too high a concentration of antibody(ies). Incubation with a range of antibody concentrations will indicate the best conditions for specific antigen detection. Incubation time and temperature can be varied to alter sensitivity. Omitting both the primary and the secondary antibody will demonstrate enzyme activity that is endogenous to the parietal bone. Endogenous peroxidase activity can be eradicated by incubation with 0.3% hydrogen peroxide in methanol for 30 min. Endogenous biotin can be blocked by preincubation with avidin.

10. Studying the Kinetics of Osteoclast formation with BrdU. Multinucleate osteoclasts arise by the fusion of monocyte precursors. To study the kinetics of osteoclasts formation and osteoclast longevity we have developed a method for the detection of BrdU, an antigenic thymidine analogue, incorporated into the nuclei of monocytes that form osteoclasts on mouse parietal bones *(41)*. The major advantage of this method over [^{3}H]thymidine incorporation is that it does not require long exposure times for autoradiography. BrdU, along with FdU, can be injected into mice or added to culture medium without significant toxicity at the dose rates used. FdU increases the incorporation of BrdU into DNA by inhibiting endogenous thymidine synthesis *(42)*. When BrdU is injected into mice, labeled osteoclast nuclei appear in the parietal bone 1 d later (**Fig. 4**). The population of labeled osteoclast nuclei decayed with a half-life of approx 1.3 d *(41)*. When parietal bones were maintained in culture for up to 3 d in the presence of BrdU and FdU very few labeled osteoclast nuclei (fewer than four per bone) are seen. This suggests that there are very few osteoclast progenitors on mouse parietal bones of this age and therefore osteoclasts arise from postmitotic precursors that have arrived from the circulation. Other cell types in these parietal bones showed normal maintenance and labeling *(41)*. BrdU labeling of osteoclasts has been
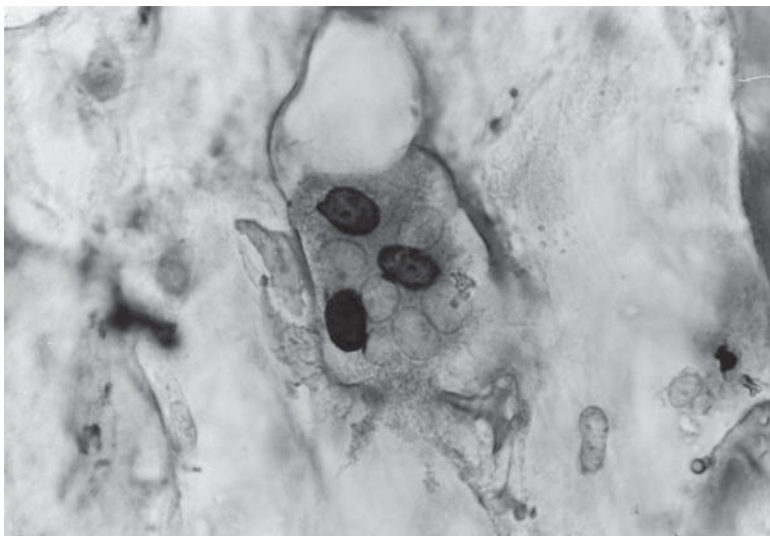
Fig. 4. BrdU incorporation into osteoclast nuclei. A 6-d-old mouse was injected with a saline solution containing BrdU and FdU, then 1 d later parietal bones were stained for TRAP and BrdU was immunolocalized. Three out of nine nuclei can be seen to be labeled with BrdU in this TRAP-positive osteoclast within a resorption lacuna. (Reduced from original magnification, ×708.)

used to examine the kinetics of osteoclast recruitment in mice in which bone resorption has been inhibited by the bis-phosphonate (3-amino-1-hydroxypropylidene)-1,1-bisphosphonate. In response to bisphosphonate, osteoclast recruitment is increased and they accumulated more nuclei than controls *(43)*. Osteoclasts appeared to show degenerative morphology and had a shorter life-span *(44)*. These observations are consistent with more recent observations suggesting that bisphosphonates act directly on osteoclasts to inhibit key enzymes *(45)* that cause apoptosis *(46)*.

References

1. Chambers, T. J. and Magnus, C. J. (1982) Calcitonin alters behaviour of isolated osteoclasts. *J. Pathol.* **136**, 27–39.
2. Jones, S. J., Ali, N. N., and Boyde, A. (1986) Survival and resorptive activity of chick osteoclasts in culture. *Anat. Embryol.* **174**, 265–275.
3. Takada, Y., Kasuda, M., Hiura, K. et al. (1992) A simple method to access osteoclast-mediated bone resorption using fractionated cells. *Bone Miner.* **17**, 347–359.
4. Chambers, T. J., Thomson, B. M., and Fuller, K. (1984) Effect of substrate composition on bone resorption by rabbit osteoclasts. *J. Cell Sci.* **70**, 61–71.

5. Murrills, R. J., Shane, E., Lindsay, R., and Dempster, D. W. (1989) Bone resorption by isolated human osteoclasts in vitro: effects of calcitonin. *J. Bone Miner. Res.* **4**, 259–268.

6. Takahashi, N., Akatsu, T., Uadagawa, N., et al. (1988) Osteoblastic cells are involved in osteoclast formation. *Endocrinology* **123**, 2600–2602.

7. Wani, M. R., Fuller, K., Kim, N. S., Choi, Y., and Chambers, T. (1999) Prostaglandin E_2 cooperates with TRANCE in osteoclast induction from hemopoietic precursors: synergistic activation of differentiation, cell spreading and fusion. *Endocrinology* **140**, 1927–1935.

8. Athanasou, N. A. and Quinn, J. M. (1992) Bone resorption by macrophage polykaryons of a pilar tumor of scalp. *Cancer* **70**, 469–475.

9. Hata, K., Kukita, T., Akamine, A., Kukita, A., and Kurisu, K. (1992) Trypsinized osteoclast-like multinucleated cells formed in rat bone marrow cultures efficiently form resorption lacunae on dentine. *Bone* **13**, 139–146.

10. Burger, E. H., van der Meer, J. W. M., and Nijweide, P. J. (1984) Osteoclast formation from mononuclear phagocytes: role of bone forming cells. *J. Cell Biol.* **99**, 1901–1906.

11. Fischman, D. A. and Hay, E. D. (1962) Origin of osteoclasts from mononuclear leucocytes in regenerating newt limbs. *Anat. Rec.* **143**, 329–338.

12. Suda, T., Nakamura, I., Jimi, E., and Takahashi, N. (1997) Regulation of osteoclast function. *J. Bone Miner. Res.* **12**, 869–879.

13. Marshall, M. J., Holt, I., and Davie, M. W. J. (1996) Inhibition of prostaglandin synthesis leads to a change in adherence of mouse osteoclasts from bone to periosteum. *Calcif. Tiss. Int.* **59**, 207–213.

14. Hillam, R. A. and Skerry, T. M. (1995) Inhibition of bone resorption and stimulation of formation by mechanical loading of the modeling rat ulna in vivo. *J. Bone Miner. Res.* **10**, 683–689.

15. Loutit, J. F. and Townsend, K. M. S. (1982) Longevity of osteoclasts in radiation chimaeras of beige and osteopetrotic microphthalmic mice. *Br. J. Exp. Pathol.* **63**, 214–220.

16. Marshall, M. J., Rees, J. A., Nisbet, N. W., and Wiseman, J. (1987) Reduced life span of the osteoclast in osteopetrotic (mi and mi[di]) mice. *Bone Miner.* **2**, 115–124.

17. Boyce, B. F., Hughes, D. E., and Wright, K. R. (1997) Methods for studying cell death in bone, in *Methods in Bone Biology* (Arnett, T.R. and Henderson, B., eds.), Chapman and Hall, London, pp. 127–148.

18. Soskolne, W. A. (1979) The osteoclast-endothelium interface during bone resorption in the femurs of young rabbits. *Cell Tissue Res.* **203**, 487–492.

19. Zaidi, M., Alam, A. S. M. T., Bax, B. E., et al. (1993) Role of the endothelial cell in osteoclast control: new perspectives. *Bone* **14**, 97–102.

20. McSheehy, P. M. J. and Chambers, T. J. (1987) 1,25-dihydroxyvitamin D_3 stimulates rat osteoblastic cells to release a soluble factor that increases osteoclastic bone resorption. *J. Clin. Invest.* **80**, 425–429.

21. Jimi, E., Nakamura, I., Amano, H., et al. (1996) Osteoclast function is activated by osteoblastic cells through a mechanism involving cell-to-cell contact. *Endocrinology* **137**, 2187-2190.

22. Lee, S., Harris, S. E., Roodman, et al. (2000) Chemotaxis: a potential mechanism whereby osteocytes target osteoclast precursors to bone. *J. Bone Miner. Res.* **15**, (*Suppl. 1*) Abstr. F082, S208.

23. Kong, Y., Felge, U., Sarosi, I., et al. (1999) Activated T cells regulate bone loss and joint destruction in adjuvant arthritis through osteoprotegerin ligand. *Nature* **402**, 304–309.

24. Lacey, D. L., Timms, E., Tan, H.-L., et al. (1998) Osteoprotegerin ligand is a cytokine that regulates osteoclast differentiation and activation. *Cell* **93**, 165–176.

25. Yasuda, H., Shima, N., Nakagawa, N., et al. (1998) Osteoclast differentiation factor is a ligand for osteoprotegerin/osteoclastogenesis-inhibitory factor and is identical to TRANCE/RANKL. *Proc. Natl. Acad. Sci. USA* **95**, 3597–3602.

26. Fell, H. B. and Mellanby, E. (1952) The effect of hypervitaminosis A on embryonic limb-bones cultivated in vitro. *J. Physiol.* **116**, 320–349.

27. Murrills, R. J., Dempster, D. W., and Arnett, T. R. (1997) Isolation and culture of osteoclasts and osteoclast resorption assays, in *Methods in Bone Biology* (Arnett, T. R and Henderson, B. eds.), Chapman and Hall, London, pp. 64–105.

28. Biggers, J. D., Gwatkin, R. B. L., and Heyner, S. (1961) Growth of embryonic avian and mammalian tibiae on a relatively simple chemically defined medium. *Exp. Cell Res.* **25**, 41–58.

29. Lerner, U. H. and Gustafson, G. T. (1979) Inhibitory effect of dibutyryl cyclic AMP on the release of calcium, inorganic phosphate and lysosmal enzymes from calvarial bones cultured for 24 hours. *Acta Endocrinol.* **91**, 730–742.

30. Lerner, U. H. (1987) Modifications of the mouse calvarial technique improve responsiveness to stimulators of bone resorption. *J. Bone Miner. Res.* **2**, 375–383.

31. Reynolds, J. J. (1976) Organ cultures of bone: studies on the physiology and pathology of resorption, in *Organ Culture in Biomedical Research* (Balls, M. and Monnickendam, M., eds.), Cambridge University Press, Cambridge, UK, pp. 355–366.

32. Ljunggren, O., Ransjo, M., and Lerner, U. H. (1991) In vitro studies on bone resorption in neonatal mouse cavariae using a modified dissection technique giving four samples of bone from each calvaria. *J. Bone Miner. Res.* **6**, 543–550.

33. Meghji, S. Sandy, J.R., Scutt, A., Harvey, W., and Harris, M. (1988) Stimulation of bone resorption by lipoxygenase metabolites of arachidonic acid. *Prostaglandins* **36**, 139–149.

34. Brown, S., Worsfold, M., and Sharp, C. (2001) Microplate assay for the measurement of hyroxyproline in acid-hydrolyzed tissue samples. *BioTechniques* **30**, 38–42.

35. Black, D., Duncan, A., and Robins, S. P. (1988) Quantitative analysis of the pyridinium crosslinks of collagen in urine using ion-paired reversed-phase high-performance liquid chromatography. *Analyt. Biochem.* **169**, 197–203.

36. Gineyts, E., Garnero, P., and Delmas, P. D. (2001) Urinary excretion of glucosylgalactosyl pyridinoline: a specific marker of synovium degradation. *Rheumatology* **40**, 315–323.

37. Brady, J. D. and Robins, S. P. (2001) Structural characterization of pyrrolic crosslinks in collagen using biotinylated Erlich's reagent. *J. Biol. Chem.* **276**, 18812-18818.

38. Robins, S. P. (1982) An enzyme-linked immunoassay for the collagen crosslink, pyridinoline. *Biochem. J.* **207**, 617–620.

39. Marshall, M. J., Holt, I., and Davie, M. W. J. (1995) The number of tartrate-resistant acid phosphatase-positive osteoclasts on neonatal mouse parietal bones is decreased when prostaglandin synthesis is inhibited and increased in response to prostaglandin E_2, parathyroid hormone and 1,25 dihydroxyvitamin D_3. *Calcif. Tissue Int.* **56**, 240–245.

40. Holt, I. and Marshall, M. J. (1998) Integrin subunit β3 plays a crucial role in the movement of osteoclasts from the periosteum to the bone surface. *J. Cell. Physiol.* **175**, 1–9.

41. Marshall, M. J. and Davie, M. W. J. (1991) An immunocytochemical method for studying the kinetics of osteoclast nuclei on intact mouse parietal bone. *Histochem. J.* **23**, 402–408.

42. Ellwart, J. and Dormer, P. (1985) Effect of 5-fluoro-2'-deoxyuridine (FdUrd) on 5-bromo-2'-deoxyuridine (BrdUrd) incorporation into DNA measured with a monoclonal BrdUrd antibody and by the BrdUrd/Hoechst quenching effect. *Cytometry* **6**, 513–520.

43. Marshall, M. J., Holt, I., and Davie, M. W. J. (1993) Osteoclast recruitment in mice is stimulated by (3-amino-1-hydroxypropylidene)-1,1-bisphosphonate. *Calcif. Tissue Int.* **52**, 21–25.

44. Holt, I., Marshall, M. J., and Davie, M. W. J. (1994) Pamidronate stimulates recruitment and decreases longevity of osteoclast nuclei in mice. *Semin. Arthrit. Rheum.* **23**, 263–264.

45. Coxon, F. P., Helfrich, M. H., van 't Hof, R., Sebti, S. et al. (2000) Protein geranylgeranylation is required for osteoclast formation, function, and survival: inhibition by bisphosphonates and GGTI-298. *J. Bone Miner. Res.* **15**, 1467–1476.

46. Reszka, A. A., Halasy-Nagy, J. M., Masarachia, P. J., and Rodan, G. A. (1999) Bisphosphonates act directly on the osteoclast to induce caspase cleavage of mst1 kinase during apoptosis. A link between inhibition of the mevalonate pathway and regulation of an apoptosis-promoting kinase. *J. Biol. Chem.* **274**, 34,967–34,973.

14

Assessing Bone Formation
Using Mouse Calvarial Organ Cultures

I. Ross Garrett

1. Introduction
1.1. Historical Aspects

The history of culturing bone explants goes back to the early 1920s, when Robinson reported that the enzyme alkaline phosphatase played an important role in bone mineralization based on studies of chick bone fragments. Subsequently, Reynolds used bone explants to study collagen synthesis in bone *(1)* and to investigate the effects of a wide variety of other agents on bone turnover such as vitamin A *(2)*, ascorbic acid *(3)*, calcitonin *(4,5)*, hydrocortisone *(6)* and bisphosphonates *(7)*. Others have used rodent calvarial and long bone explants to study the effects of cytokines on bone resorption *(8–12)* and bone formation *(13,14)*. This chapter focuses on the use of cultured neonatal calvariae as an assay for agents with anabolic activity *(13–19)* (*see* **Note 1**).

1.2. Overview of Assay

The assay is essentially divided into three parts as shown in **Fig. 1**: (A) isolating the calvariae from 4-d-old mouse pups, (B) culturing the calvariae in media containing factors or compounds and, (C) measuring new bone formation in treated calvariae by histological assessment of stained sections. The timelines for the assay are outlined in **Figs. 2** and **3**. For a 4-d assay (**Fig. 2**) the calvariae are dissected on day 0 and incubated with compounds or factors overnight. On the following day (d 1), the calvariae are placed into fresh media and the cultures returned to the incubator and allowed to remain undisturbed until d 4, at which time the experiment is ended. For a 7-d assay (**Fig. 3**), the protocol is similar except that the media are replaced again on d 4 and the cultures incubated for another 3 d until d 7. The calvariae can be incubated for up to 2 wk
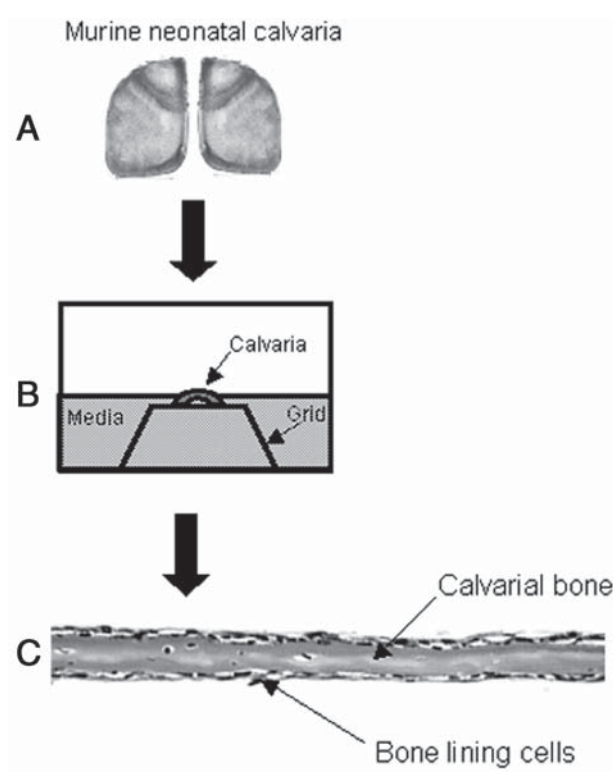
Fig. 1. Overview of the calvarial assay (**A**) Dissection of the calvaria. (**B**) Incubation in media on stainless steel grids. (**C**) Histological sections are cut to determine amount of new bone matrix formed.
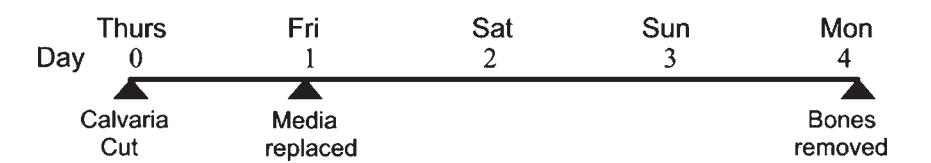

Fig. 2. Assay time line for 4-d assay. On d 0, calvariae are dissected and placed into media containing factors or compounds. On d 1, media are replaced with new media either with or without compounds and incubated. On d 4, calvarial bones are removed and histologically processed to determine the amount of new bone formation.

with evidence of continued bone formation (*see* **Note 2**). Following processing, cutting, and staining of the sections from the treated calvariae the area of new bone formation is measured by using image analysis techniques. This measures the total area of bone and the amount of original bone remaining, the number of cells lining the bone tissue, as well as the thickness of a suture area.
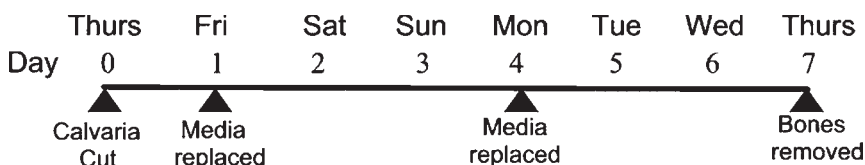
Fig. 3. Assay time line for 7-d assay. On d 0, calvaria are dissected and placed into media containing factors or compounds. On d 1, media are replaced with new media either with or without compounds and incubated. On d 4, media are replaced by fresh media with or without factors or compounds and incubated. On d 7, calvarial bones are removed and histologically processed to determine the amount of new bone formation.

The dissection, culturing, histological processing, and measurement usually requires 10–14 d to complete and offers the ability to determine statistically new bone growth, changes in bone cell numbers, as well as a visual representation of the bone formation occurring in the culture.

2. Materials
2.1. Animals

The assay is performed on bones dissected from 4-d-old mouse pups. These can be bred in house or purchased from an external supplier. We obtain the pups from pregnant Swiss white female mice, ordered to arrive on d 15 of gestation, but other strains of mice have been utilized for this assay with similar results. The mice usually give birth on the 18–19th day of gestation and produce litters of 10 or more pups. When the pups are 4 d old they are euthanized and the calvarial bones dissected out.

2.2. Culture Media

We use BGJ medium supplemented with 1 mg/mL of bovine serum albumin (Cohn fraction V), 100 U/mL each of penicillin/streptomycin, and 0.292 mg/mL of glutamine. If using powdered medium, make up fresh with distilled water, add supplements, adjust to pH 7.2, and sterile filter before use.

2.3.Preparation of Stainless Steel Grids

1. Prepare the grids by cutting rectangular 1 × 1.5 cm pieces of stainless steel mesh from the sheet (we use stainless steel no. 30 mesh; Small Parts Inc. CX-60).
2. Bend the ends of the mesh over using a sharp edge to make a bridge support (**Fig. 4**) so that the dissected calvariae sit at the air–liquid interface when 1 mL of medium has been added to the tissue culture well (**Fig. 5**). After each assay, wash the grids in detergent and rinse in 10% nitric acid. Wash the cleaned grids three times in distilled water to remove any residual detergent and nitric acid.
3. Dry the grids and heat sterilize in glass Petri dishes. Store sterile until use.

Fig. 4. Stainless steel grids measuring 1 cm × 1.5 cm are cut from mesh and both ends are bent to form a bridge to support the calvaria in culture. The mesh is bent at each end using a straight edge to make the bridge and adjusted to the height of 1 mL of medium.
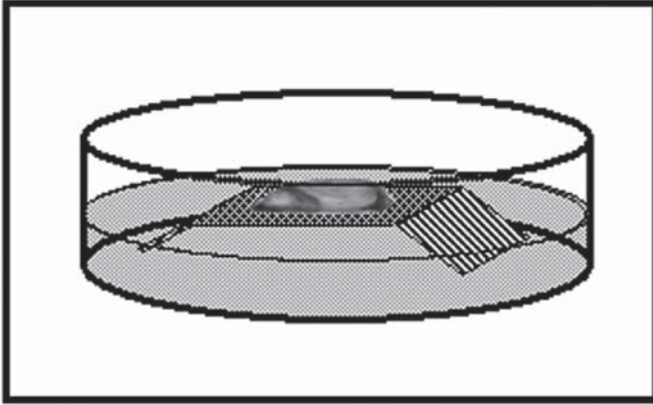

Fig. 5. Image of a half neonatal murine calvaria in culture with concave or cranial side down on the stainless steel grid in 1 mL of medium.

2.4. Staining Solutions

1. Harris hematoxylin with acetic acid: Dissolve 25 g of ammonium aluminum sulfate [AlNH$_4$(SO$_4$)$_2$ 12H$_2$O] in 225 mL of dH$_2$0. Dissolve 1.25 g of hematoxylin and 0.6 g of mercuric oxide in 15 mL of 95% ethanol and slowly add to the ammonium aluminum sulfate solution. Boil for 2 min and allow to cool. Store in the dark for at least 24 h. Immediately before use, filter the solution and add 8 mL of glacial acetic acid (*see* **Note 3**).
2. 0.6% Eosin Y: Add 6 g of eosin Y to 900 mL of absolute ethanol. Stir to dissolve and adjust pH to between 4.6 and 5.0 with glacial acetic acid.
3. 1% Phloxine B: Add 1 g of Phloxine B to 100 mL of dH$_2$.O
4. 2% Orange G: Add 2 g of Orange G, sodium salt to 100 mL of dH$_2$O.
5. Final eosin staining solution: Combine 6 mL of 2% Orange G with 6 mL of 1% Phloxine B and 238 mL of 0.6% eosin Y.
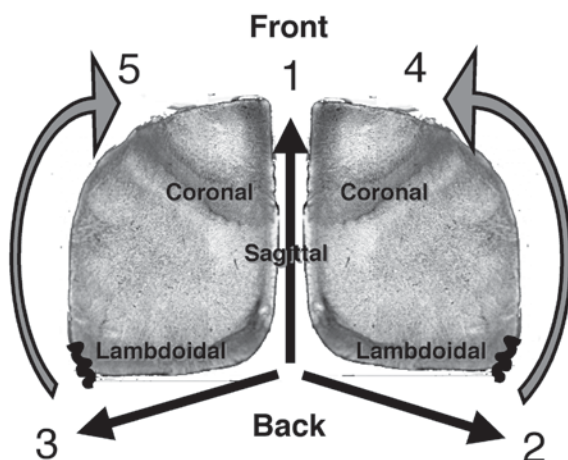
Fig. 6. Procedure and steps for dissecting half neonatal murine calvaria from mice. The calvaria are dissected using the five different cuts.

2.5. Fixation and Decalcification

1. Fixation solution: 10% Buffered formalin.
2. Decalcification solution: Prepare a solution of 14% EDTA in distilled water and adjust the pH to 7.2 by adding 9.5–10% NH_4OH.
3. Tissue processing: 75%, 95%, and 100% ethanol; xylene; paraffin wax.

2.6 Histomorphometry

1. We analyze the sections using a Nikon E400 microscope to which is attached an Optronics three-chip color video camera. The output is fed to a 266-mHz Pentium PC computer using a Pro-Series 128 Capture Kit frame grabber board to obtain images of the sectioned calvaria. The area of new bone is then measured using Image Pro Plus (Media Cybernetics L.P., Del Mar, California).

3. Methods

3.1. Dissection

Dissect the calvariae free from the skull using fine dissection scissors and curved fine point forceps as illustrated in **Fig. 6**.

1. Make sure the instruments used for dissection are clean and heat sterilized or autoclaved prior to dissection. The instruments must be kept sterile during the dissection procedure.
2. Using the scissors, cut the calvaria along the midline or sagittal suture from the rear to the front past the coronal suture (cut 1).
3. Make a second cut along the rear of the lambdoidal suture from the midline to a small capillary vessel above the ear (cut 2).
4. Repeat this on the other side (cut 3).

5. Dissect the calvariae free from the rest of the skull by cutting toward the front of the calvarial bones (cuts 4 and 5) and excising a half calvaria that contains both the frontal and parietal bones including the coronal suture.
6. Once removed, carefully wash the half calvariae in a Petri dish containing media.

3.2. Culture

1. Place one sterile grid into each well of a 12-well tisue culture plate.
2. Add 1 mL of culture medium to each well.
3. Place one half calvaria in each well concave side down on the grids so that the calvaria is resting at the air–medium interface (**Fig. 5**).
4. Incubate for 24 h at 37°C, in air–5% CO_2 in a humidified atmosphere.
5. Using fine curved forceps, carefully transfer the grids, complete with the calvarial bones, into a new 12-well plate containing media to which test substances have been added. Be careful not to disturb the calvariae during this process. Aim for at least four calvariae per treatment group.
6. Incubate the calvariae for up to 14 d with medium changes every 3 d.

3.3. Fixation

1. Fix the calvariae in 10% buffered formalin following termination of the cultures.
2. Place the fixed calvariae between two sponge mats in a Tissue-Tek processing cassette and immerse overnight in decalcifying solution.
3. The next day, process the demineralized calvaria overnight in a Shandon Hypercenter XP tissue-processing unit using the following protocol:
     70% Ethanol, 45 min.
     95% Ethanol, 45 min.
     95% Ethanol, 45 min.
     100% Ethanol, 45 min.
     100% Ethanol, 45 min.
     100% Ethanol, 45 min.
     100% Ethanol, 45 min.
     Xylene, 45 min.
     Xylene, 45 min.
     Paraffin, 45 min.
     Paraffin, 45 min.
4. Embed the processed calvariae in paraffin blocks using a Tissue-Tek embedding console with paraffin wax.
5. Orientate each calvaria with the midline suture down and each calvaria placed perpendicular to the plane of dissection and parallel to each other so that all calvariae from the same group are sectioned in the same orientation (**Fig. 7**; *see also* **Note 4**).

3.4. Sectioning

1. Trim the blocks to a depth of 800 μm to get past the remains of the midline suture.
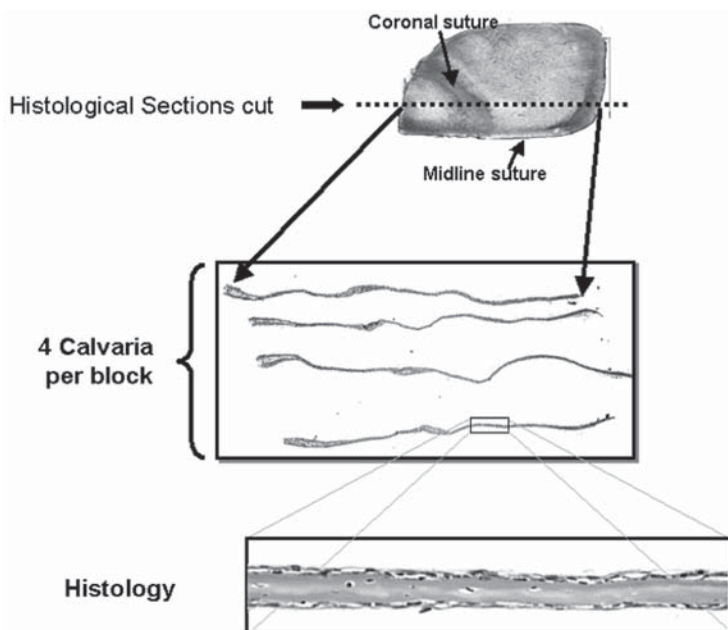
Fig. 7. Overview of the procedure of the histological sectioning of the half neonatal murine calvaria. Sections are cut parallel to the midline suture and include a cut through the coronal suture. Sections show both the front and parietal bones from the calvaria with the coronal suture area visible between the two bones.

2. Cut 5-μM thick sections.
3. Cut further 5-μm sections are taken at 400-μm and 800-μm depths.
4. Mount the sections onto treated glass microscope slides.
5. Air-dry in a 40°C oven overnight in preparation for staining.

3.5. Staining

Deparaffinize and stain the sections in the tissue processor using the following protocol:

1. Three changes in xylene, 2 min.
2. Three changes in 100% ethanol 1 min.
3. 95% Ethanol, 30 sec.
4. 80% Ethanol, 30 sec.
5. Deionized water, 3 min.
6. Hematoxylin solution, 1 min.
7. Rinse in deionized water until section is clear.
8. 0.5% Ammonia water, 10 sec.
9. Rinse in deionized water, 3 min.
10. 80% Ethanol, 30 sec.

11. 95% Ethanol, 30 sec.
12. Eosin solution, 3 min.
13. Four changes in 95% ethanol, dips.
14. Three changes in 100% ethanol, dips.
15. Coverslip with Cytoseal XYL.

3.6. Histomorphometry

1. The eosin Y differentially stains the original bone darker whereas the new bone matrix that is formed appears as a lighter color (**Fig. 8A**). The hematoxylin stains bone lining cells, active osteoblasts and osteocytes.
2. Using the imaging processing equipment (*see* **Subheading 2.6.**), capture several images along the bone surface of the bone sections in each group.
3. Outline the original bone using a pen-based drawing tablet attached to the computer (**Fig. 8B**; shaded area represents original bone present at the start of culture).
4. Measure the amount of old bone and total bone using the color recognition option of the Image Pro software.
5. Calculate the amount of new bone formed by subtracting the original bone from the total bone (*see* **Note 5**).
6. Quantitate the bone lining cells by counting the number of cells that lie on each side of the calvaria.
7. Measure the length of the bone represented by the image and calculate the number of cells/mm of bone by dividing the cell number by the section length.
8. Use a pen-based drawing tablet to measure the distance between the two outer edges of the suture. Suture width appears to increase with treatment anabolic agents that stimulate bone formation (**Fig. 13**; *see* **Note 6**).

4. Notes

1. Effects of growth factors in assay: We have investigated the anabolic effect of several growth factors in this assay (**Fig. 9–11**) . We find that BMP2, insulin, IGF-1, TGF-β, fibroblast growth factor-acidic (FGFa), fibroblast growth factor-basic (FGFb), leukemia inhibitory factor (LIF) (**Figs. 9** and **10**) and endothelin-1 (not shown here) all stimulate new bone formation over a 4-d period. We find that fibroblast growth factors increase bone resorption as well as increasing bone formation. Factors such as PDGFab, EGF, hMSP, bECGF, nerve growth factor (NGF), MIF, VEGF, and HGF (**Figs. 10** and **11**) did not stimulate bone formation in the assay. Prostaglandin E_2 (PGE_2) stimulates formation of new matrix but the major effect is to stimulate bone resorption.
2. Time course and duration of assay: Examples of time course experiments are shown in **Figs. 12** and **13**. The calvariae were treated with medium alone or with medium plus 1 μ*M* simvastatin and terminated at various times after the start of the assay. Images of the calvarial bones were obtained from both the coronal suture area (**Fig. 13**) and from bones distant from the coronal suture (**Fig. 12**). **Figure 13** illustrates the effect of either media alone (control) or simvastatin on
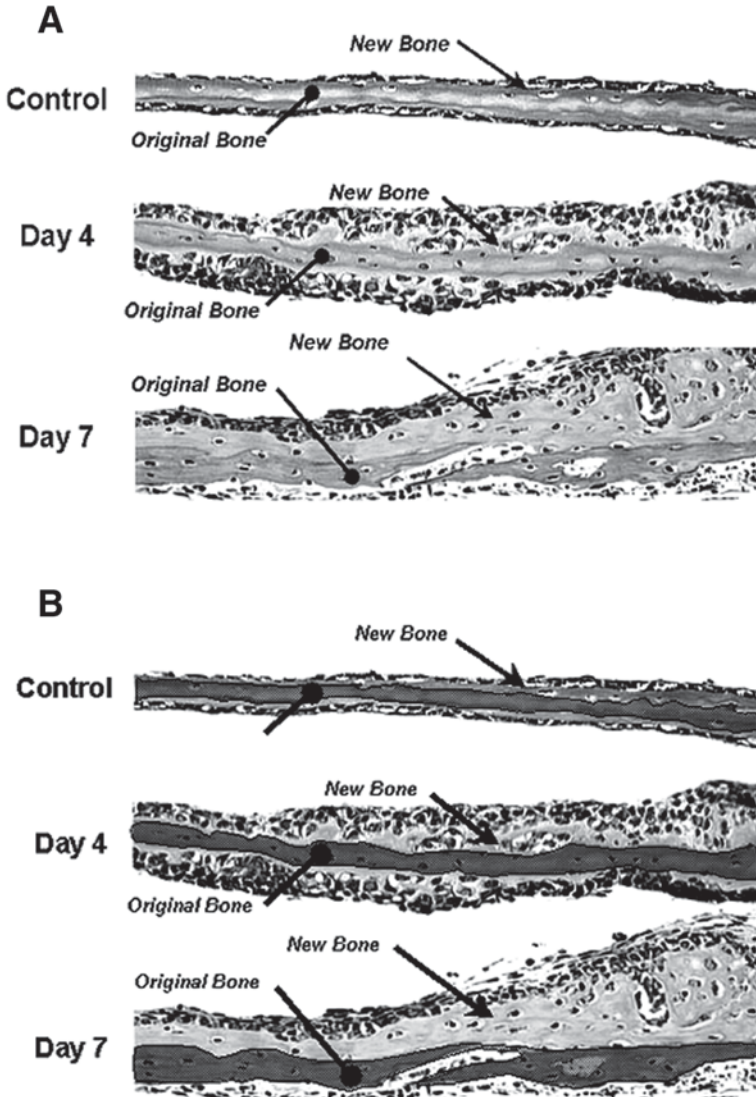
Fig. 8. Neonatal murine calvaria (**A**) treated with either vehicle (Control) or 1 μ*M* simvastatin for 4 d and 1 μ*M*simvastatin for 7 d. Note new bone growth and increased number of active osteoblasts in simvastatin treated bones. (**B**) The same sections outlined with *hatched areas* indicating the original bone from the start of the assay. This can be measured along with the total area of bone and the new bone area calculated.

bone at the coronal suture of the calvaria. The suture area, which is evident in these histological sections as two layers, increases in size progressively from d 2 to d 7 in control cultures. By d 7 the suture area appears to be relatively inactive.
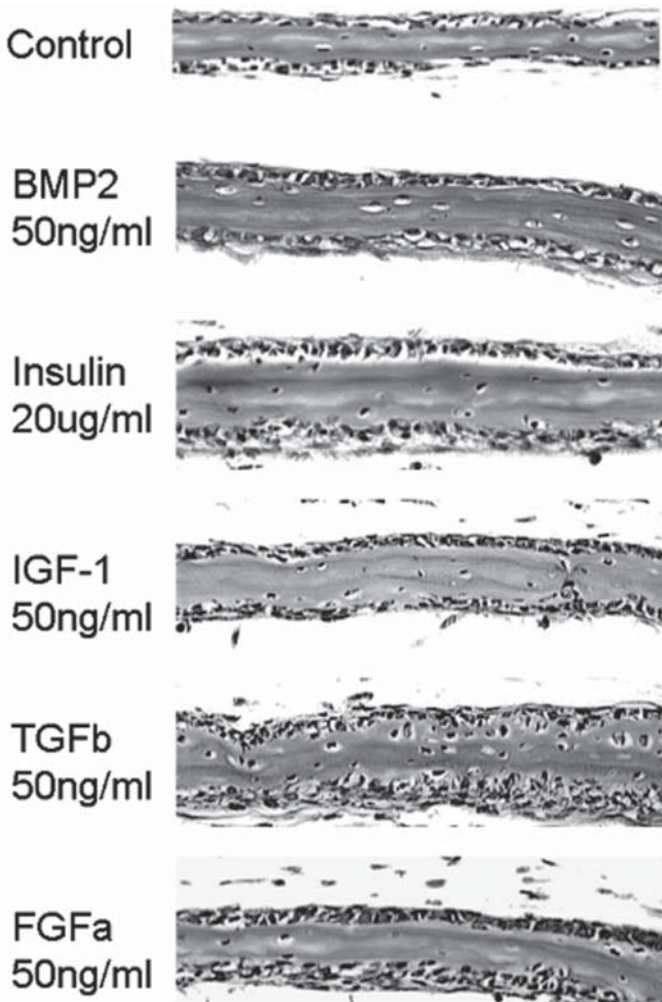
Fig. 9. Effects of various different growth factors on neonatal murine calvaria including 50 ng/mL of BMP2, 20 μg/mL of insulin, 50 ng/mL of IGF-1, 50 ng/mL of TGFβ, and 50 ng/mL of acidic FGF. All stimulated bone formation in these cultured neonatal calvaria.

In cultures treated with 1 μM simvastatin, marked stimulatory effects on cellularity can be observed as early as d 1. Thereafter, there is a progressive increase the thickness and cell content of the coronal suture. **Figure 12** compares the time course of cultures exposed to media alone with those exposed to simvastatin in the parietal bones distant from the coronal suture. The calvariae at this location are initially very thin pieces of bone that slowly increase in thickness over 7 d. You can see a small amount of new bone present in the control cultures by d 7.
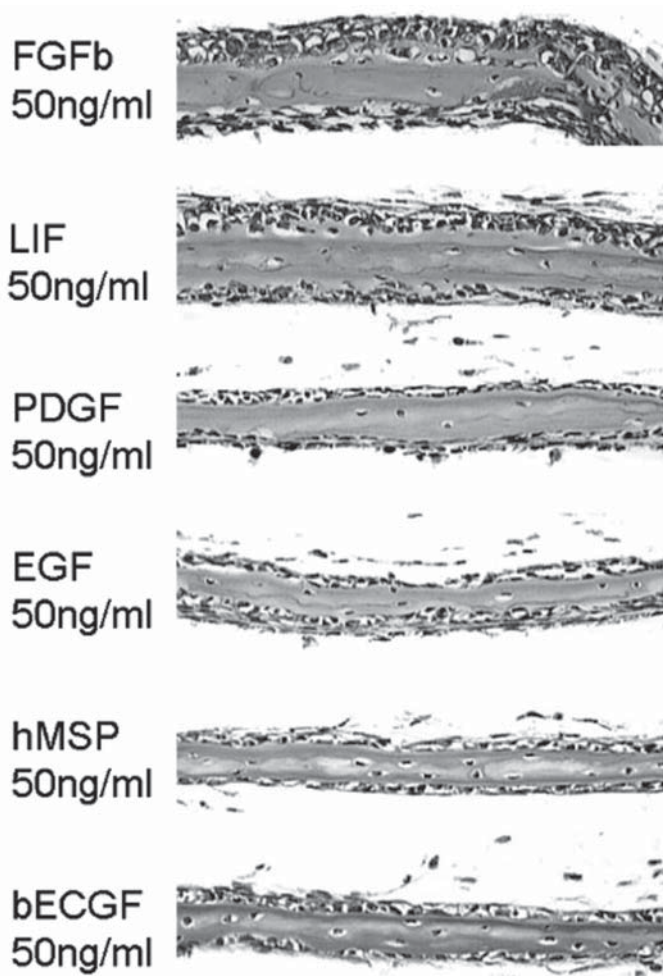
Fig. 10. Effects of various different growth factors on neonatal murine calvaria including 50 ng/mL of basic FGF, 50ng/mL of LIF, 50 ng/mL of PDGFab, 50 ng/mL of EGF, 50 ng/mL of hMSP, and 50 ng/mL of bECGF. Of these, only basic FGF and LIF were able to stimulate new bone formation in this assay.

When these calvariae are treated with an anabolic agent such as 1 μM simvastatin, marked changes can be observed over the 7-d period. Noticeable effects can be observed as early as d 2 (48 h after the initial exposure to the compounds). This effect becomes more pronounced by d 7, when there are substantial increases in the number of cells on the bone with a marked increase in new bone matrix. Measurements of new bone matrix formation, suture width, and numbers of cells along the bone surface in these calvarial bones for the assay described in the preceding are summarized in **Fig. 14**. Simvastatin treatment caused a significant
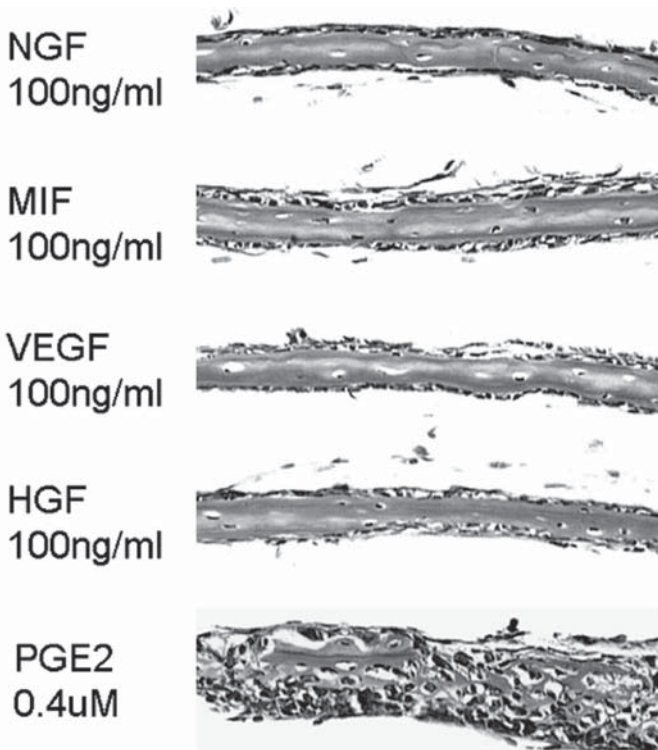
Fig. 11. Effects of various different growth factors on neonatal murine calvaria including 100 ng/mL of NGF, 100 ng/mL of MIF, 100 ng/mL of VEGF, 100 ng/mL of HGF, and 0.4 μM PGE$_2$. None of these stimulated bone formation. PGE$_2$ stimulated bone resorption in the cultured calvaria.

increase in the amount of new bone formed by d 4, which was further increased by d 7. There was also a progressive increase in the suture width as well as the number of cells lining the bone, with the most significant changes seen at d 4 and 7.

3. Storage of Harris hematoxylin: Do not keep the solution for more than 1 wk and filter each day before use.

4. Mounting and sectioning the calvariae: Orientation of the calvariae in the paraffin block is very important for consistent results. If several calvariae from a single experimental group are going to be placed into one block, they must be oriented so that they are all perpendicular to the plane of sectioning and parallel to each other. They should also be set at the same depth in the block. An alternative procedure is place only one calvaria per block. This is initially easier, but it creates much more work later during sectioning.

5. Measurement of alkaline phosphatase: Cells within the calvariae express alkaline phosphatase, and this can be measured in conditioned medium using standard assays to give a semiquantitative assessment of osteoblast activity.
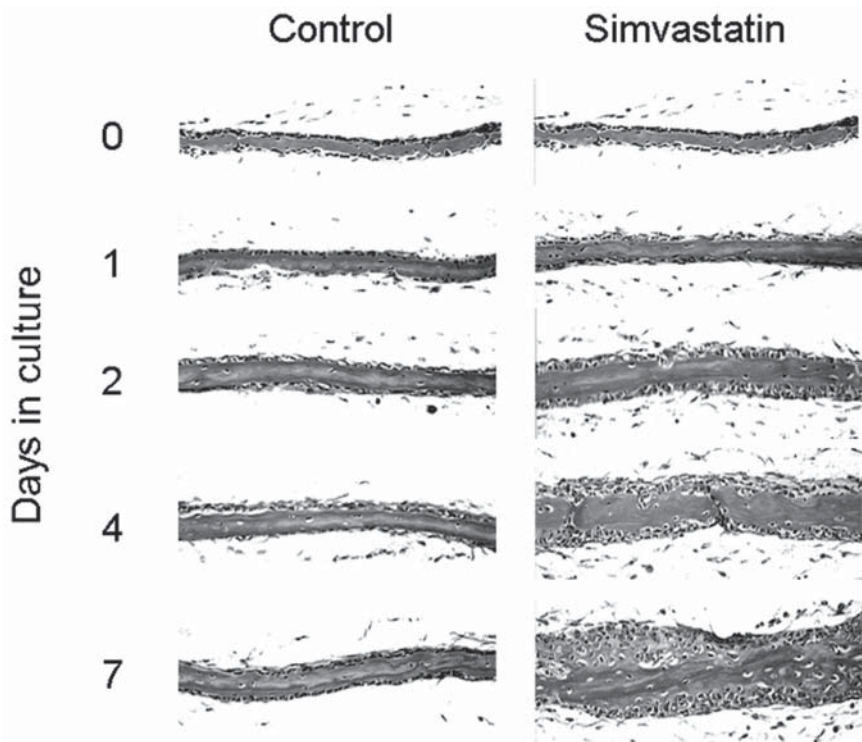
Fig. 12. Histological sections away from the coronal suture of neonatal murine calvaria cultured with or without 1 μ*M* simvastatin for different times from d 0 (day of dissection) to d 7. Simvastatin increased new bone matrix over the 7 d of culture.

6. Analysis of suture width: The suture appears to be important target for stimulation of new bone in this assay. It may contain a number of cells that are target cells for either growth factors or small molecular weight anabolic compounds.

References

1. Reynolds, J. J. (1967) The synthesis of collagen by chick bone rudiments in vitro. *Exp. Cell Res.* **47**,42–48.
2. Reynolds, J. J. (1968) Inhibition by calcitonin of bone resorption induced in vitro by   vitamin A. *Proc. R. Soc. Lond. B. Biol. Sci.* **170**, 61–69.
3. Reynolds, J. J. (1966) The effect of ascorbic acid on the growth of chick bone rudiments in chemically defined medium. *Exp. Cell Res.* **42**, 178–188.
4. Reynolds, J. J. and Dingle, J. T. (1968) Time course of action of calcitonin on resorbing mouse bones in vitro. *Nature.* **218**, 1178–1179.
5. Minkin C, Reynolds J. J., and Copp, D. H. (1971) Inhibitory effect of salmon and other calcitonins on calcium release from mouse bone in vitro. *Can. J. Physiol. Pharmacol.* **49**, 263–267.
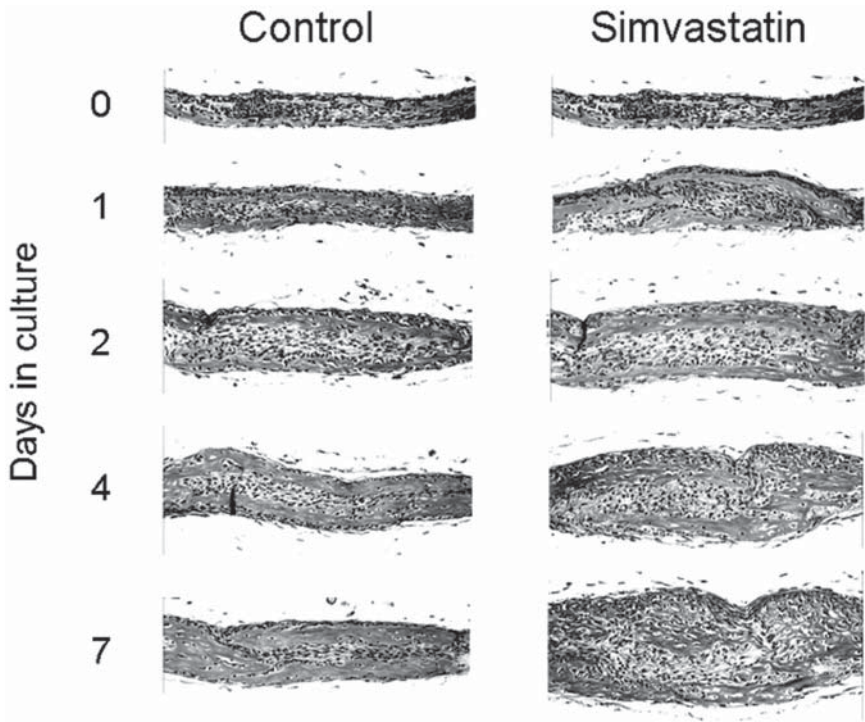
Fig. 13. Histological sections of the coronal suture of neonatal murine calvaria cultured with or without 1 μ*M* simvastatin for different times from d 0 (day of dissection) to d 7. Simvastatin increased the width of the suture over the 7 d of culture.

6. Reynolds, J. J. (1966) The effect of hydrocortisone on the growth of chick bone rudiments in chemically defined medium. *Exp. Cell Res.* **41**, 174–189.

7. Reynolds, J. J, Minkin, C., Morgan, D. B., Spycher, D., and Fleisch, H. (1972) The effect of two diphosphonates on the resorption of mouse calvaria in vitro. *Calcif. Tissue Res.* **10**, 302–313.

8. Gowen, M., Wood, D. D., Ihrie, E.J., McGuire, M. K., and Russell, R. G. (1983) An interleukin 1 like factor stimulates bone resorption in vitro. *Nature* **306**, 378–380.

9. Bertolini, D. R., Nedwin, G. E., Bringman, T. S., Smith, D. D., and Mundy, G. R. (1986) Stimulation of bone resorption and inhibition of bone formation in vitro by human tumor necrosis factors. *Nature* **319**, 516–518.

10. Lorenzo, J. A., Sousa, S. L., and Leahy, C. L. (1990) Leukemia inhibitory factor (LIF) inhibits basal bone resorption in fetal rat long bone cultures. *Cytokine* **2**, 266–271.

11. Reynolds, J. J. and Dingle, J. T. (1968) The induction and inhibition of bone resorption in vitro. *Calcif. Tissue Res.* (*Suppl*) 50-50a.
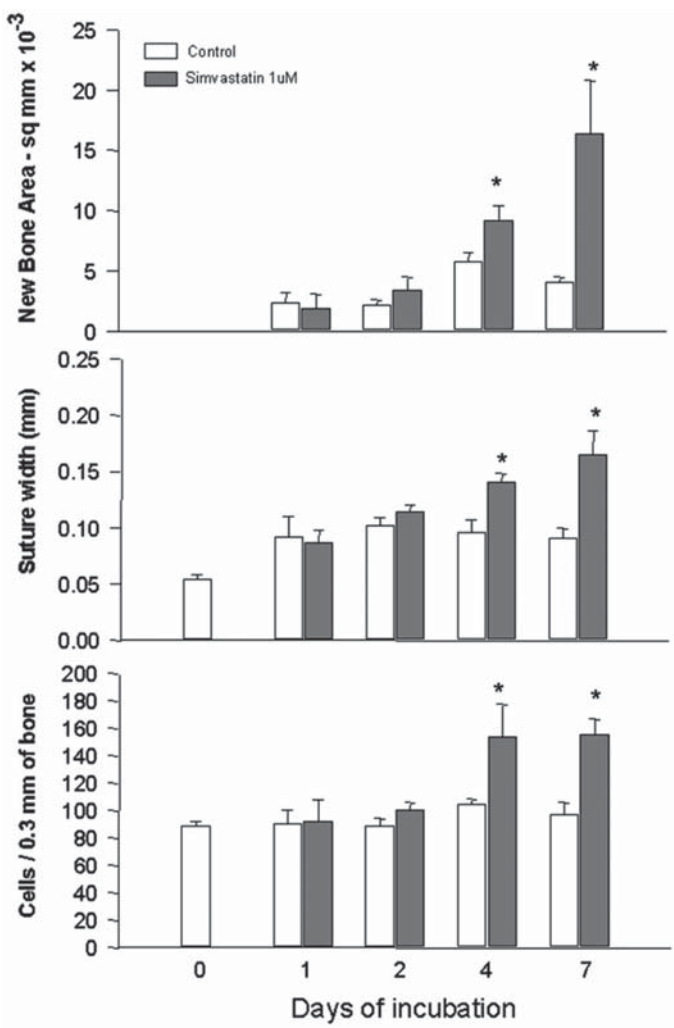
Fig. 14. Histomorphometric measurements of new bone area, suture width and numbers of cells in neonatal murine calvaria cultured with or without 1 μ*M* simvastatin for different times from d 0 (day of dissection) to d 7. Simvastatin significantly increased new bone matrix, numbers of cells/mm bone, as well as suture width, over the 7 d of culture.

12. Reynolds, J. J. and Dingle, J. T. (1970) A sensitive in vitro method for studying the induction and inhibition of bone resorption. *Calcif. Tissue Res.* **4**, 339–349.
13. Traianedes, K., Dallas, M. R., Garrett, I. R., Mundy, G. R., and Bonewald, L. F. (1998) 5-Lipoxygenase metabolites inhibit bone formation in vitro. *Endocrinology* **139**, 3178–3184.

14. Mundy, G, Garrett, R, Harris S, et al. (1999) Stimulation of bone formation in vitro and in rodents by statins. *Science* **286**, 1946–1949.

15. Garrett, I. R., Esparza, J., Chen, D., et al. (2000) Statins mediate their effects on osteoblasts by inhibition of HMG-CoA reductase and ultimately BMP-2. *J. Bone Miner. Res.* **15S**, 225.

16. Garrett, I. R., Chen, D., Zhao, M., et al. (2001) Statins mediate bone formation by enhancing BMP2 expression. *Bone* **28**, 75.

17. Yin, J. L., Grubbs, B. G., Cui, Y., et al. (2000) Endothelin A receptor blockade inhibits osteoblastic metastasis. *J. Bone Miner. Res.* **15S**, 201.

18. Garrett, I. R., Gutierrez, G., Chen, D., et al. (2000) Specific inhibitors of the chymotryptic component of the proteasome are potent anabolic agents in vivo. *J. Bone Miner. Res.* **15S**, 197.

19. Chen, D., Garrett, I.R., Qiao, M., et al. (2001) Proteasome inhibitors stimulate osteoblast differentiation and bone formation by inhibiting Gli3 degradation and enhancing BMP-2 expression. *Bone* **28**, 74.

15

In Situ Hybridization and *In Situ* Reverse Transcription Polymerase Chain Reaction in Human Bone Sections

Andrew P. Mee and Judith A. Hoyland

1. Introduction

Gene expression in bone can be assessed by several techniques such as reverse transcription polymerase chain reaction (RT–PCR), differential display PCR, subtractive hybridization, and microchip arrays. The problem with all of these techniques is that they do not allow cellular localization of the genes under investigation. *In situ* hybridization (ISH) circumvents this problem. It is possible to localize precisely sites of gene expression using ISH in intact cells and tissue sections, allowing one to build up a more complete picture of the processes occurring in the disease under investigation.

Although ISH is a very powerful technique for localizing expression of most targets, low levels of DNA or RNA (fewer than 20–40 copies per cell) cannot easily be detected (reviewed in **ref. *1***). In view of this, PCR has been developed to increase the sensitivity of ISH. For DNA targets, a PCR step is performed to increase the abundance of target, prior to its detection by ISH. This technique is termed *in situ* PCR (IS-PCR). For RNA targets, a reverse transcription step is performed prior to PCR-based amplification of the target molecule with final detection by ISH (IS-RT-PCR). The fact that amplification during IS-PCR and IS-RT-PCR occurs within the cells of interest reduces the possible problem of contamination associated with conventional PCR. IS-PCR has been used primarily to detect viral DNA *(2–5)* and single copy genes *(6)* within cells, whereas IS-RT-PCR has been used to detect expression of a variety of genes in bone and other tissues *(7–19)*. Although ISH and IS-RT-PCR are useful techniques, they are technically difficult and time-consuming. Here

we review the application of ISH and IS-RT-PCR to the detection of gene expression in bone.

2. Materials

2.1. Equipment

1. ThermoHybaid Omnislide system (**Fig. 1**): For thermal cycling in IS-RT-PCR.
2. ThermoHybaid Easiseals: To seal reactions during ISH-RT-PCR.
3. Tissue processor: For tissue processing.
4. Microtome: For tissue sectioning.
5. Small artist's paintbrush: For transferring sections to slides.
6. Microscope slides and coverslips.
7. Metal and plastic slide racks and glass slide troughs.
8. Lightproof slide box for autoradiography.
9. Developing tanks for autoradiography.
10. Plastic forceps for autoradiography.

2.2. Tissue Fixative

1. 10 mL of 37% formaldehyde in 90 mL of phosphate-buffered saline (PBS).

2.3. Decalcification Solution

1. 20% (w/v) Ethylenediaminetetraacetic (EDTA) acid in water. Adjust to pH 7.2 with Na OH.

2.4. DEPC Water

1. Add 1 mL of diethylpyrocarbonate (DEPC) (**Caution: This compound is carcinogenic.**) to 999 mL of distilled water. Incubate for 4 h at room temperature and autoclave to inactivate DEPC.

2.5. General Reagents

1. 0.5 M EDTA, pH 8.0: Add 93.05 g of EDTA to 300 mL of DEPC-treated water and adjust pH to 8.0 with 10 M NaOH. Make up to 500 mL with DEPC-treated water. Autoclave to sterilize.
2. 1 M DTT: Add 3.09 g of dithiothreitol (DTT) to 20 mL of DEPC-treated water. sterile filter and store in 1-mL aliquots at –20°C until use.
3. 1 M Tris-HCl, pH 8.0: Add 121 g of Tris base to 800 mL of DEPC-treated water; adjust to pH 8.0 with concentrated HCl. Make up to 1 L with DEPC-treated water and autoclave to sterilize.
4. 20× Saline sodium citrate (SSC) buffer: Add 175.3 g of NaCl and 88.2 g of sodium citrate·H_2O to 800 mL of DEPC-treated water. Adjust the pH to 7.0 with 1 M HCl, and make up to 1 L with DEPC-treated water. Autoclave to sterilize.
5. STE buffer: 0.1 M of NaCl, 10 mM Tris-HCl, pH 8.0, 1 mM ETDA, pH 8.0.
6. NTE buffer: 0.5 M NaCl, 10 mM Tris-HCl, pH 8.0, and 1 mM EDTA, pH 8.0.
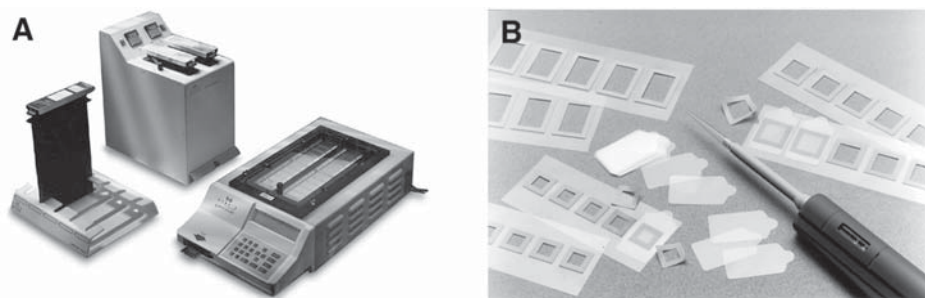
Fig. 1. Omnislide™ system and Easiseals. (**A**) The Omnislide is a flat-block system that holds 20 slides in a plastic slide rack. Hence, all slides can be manipulated at once, thus making handling much easier. Further, many of the incubations can be carried out by pipetting solutions directly onto the slides, without the need for coverslips. The system includes wash sleeves, an ambient sleeve rack, and a heated module for performing stringency washes within the wash sleeves. (**B**) Easiseals shown in a variety of sizes. The Easiseal consists of a plastic frame that is adherent on both sides, and a clear plastic cover that is laid over the frame on a slide to form an airtight seal.

7. 3 *M* Sodium acetate: Add 401.8 g of NaAc. 3H$_2$O to 800 mL of DEPC-treated water. Adjust pH to 5.2 with glacial acetic acid and make up to 1 L with DEPC-treated water. Autoclave to sterilize.
8. 50× Denhardt's solution: Dissolve 5 g of Ficoll, 5 g of polyvinylpyrrolidine, and 5 g of bovine serum albumin into 500 mL of DEPC-treated water. Filter sterilize and store frozen in aliquots of 1–5 mL.
9. 50× Modified Denhardt's solution: Dissolve 5 g of Ficoll, 5 g of polyvinylpyrrolidine, and 25 g of bovine serum albumin into 500 mL of DEPC-treated water. Filter sterilize and store frozen in aliquots of 1–5 mL.

2.6. Materials for Tissue Embedding, Sectioning, and Slide Preparation

1. Ethanols: 50%, 70%, 90%, 99%, and 100%.
2. Xylene.
3. APES solution: γ-Aminopropyltriethoxysilane (APES) diluted to 3% in acetone.
4. Acetone.
5. Industrial methylated spirits (IMS).
6. 1 *M* HCl.
7. 5% Dimethyldichlorosilane in xylene: Add 5 mL of dimethyldichlorosilane to 95 mL of xylene.

2.7 Preparation of Radioactive cDNA Probes

1. Amersham Megaprime™ kit.
2. [^{35}S] dCTP.
3. EDTA stop buffer: 0.2 *M* EDTA, pH 8.0.

2.8 Preparation of Digoxigenin(DIG)-Labeled cDNA Probes

1. DIG High Prime DNA labeling and detection starter kit II (Roche Molecular Biochemicals).
2. EDTA stop buffer: 0.2 M EDTA, pH 8.0.

2.9. Preparation of Radioactive Riboprobes

1. Riboprobe labeling kit (Promega).

2.10. Preparation of DIG-labeled Riboprobes

1. DIG RNA labeling Kit (SP6/T7) (Roche).

2.11. Quantification and detection of DIG-Labeled Probes

1. DIG quantification test strips (Roche).
2. DIG control test strips (Roche).
3. Dilution buffer: 50 μg/mL of herring sperm DNA in 10 mM Tris-HCl, pH 8.0.
4. Maleic acid Buffer: 0.1 M Maleic acid, 0.15 M NaCl, pH 7.5.
5. Blocking buffer: Dilute blocking solution 1:10 with maleic acid buffer.
6. Detection Buffer: 0.1 M Tris-HCl, 0.1 M NaCl, 50 mM MgCl$_2$, pH 9.5.
7. Anti-DIG AP antibody solution: Dilute antibody stock 1:2000 in maleic acid buffer.
8. Substrate solution: Add 40 μL nitroblue tetrazolium/5-bromo-4-chloro-3-indolylphosphate (NBT/BCIP) stock solution to 2 mL of detection buffer.

2.12. Sephadex Mini-Spin Columns

To separate unincorporated nucleotides from cDNA probes:

1. Plug a 1-mL syringe with glass wool.
2. Fill the plugged syringe with Sephadex G-50 suspended in STE buffer.
3. Place the syringe in a 15-mL centrifuge tube and centrifuge at 1500 rpm for 1 min to pack the column.
4. Pour off the STE from the centrifuge tube.

2.13. cDNA Probe Hybridization Buffer

For 1 mL combine together in an Eppendorf tube:

a. 0.1 g of dextran sulfate
b. 100 μL of 10× modified Denhardt's solution.
c. 200 μL of 3 M NaCl.
d. 20 μL of 10 mg/mL salmon sperm DNA.
e. 10 μL of 1 M Tris-HCl, pH 7.4.
f. 1 μL of 0.5 M EDTA.
g. 10 μL of 1 M DTT.
h. 500 μL of deionized formamide.
i. RNase-free water to 1 mL.

Incubate at 37°C until the reagents have dissolved.

2.14. Riboprobe Hybridization Buffer

1. For 1 mL, combine together in an Eppendorf tube:
   a. 500 µL of deionized formamide.
   b. 60 µL of 5 M NaCl.
   c. 20 µL of 1 M Tris, pH 8.0.
   d. 10 µL of 0.5 M EDTA, pH 8.0.
   c. 10 µL of 1 M DTT.
2. Warm to 60°C and add:
   a. 100 mg of dextran sulfate.
   b. 20 µL of 50× Denhardt's solution.
   c. 100 µL of 10 mg/mL tRNA (*E. coli*).
   d. 230 µL of DEPC-treated water.

2.15. Alkaline Hydrolysis Buffer

1. For 1 mL combine 500 µL of 0.4 M NaHCO$_3$ and 500 µL of 0.6 M Na$_2$CO$_3$, pH 10.0.

2.16. Autoradiography and Counterstaining

1. Photographic emulsion: Ilford K5 emulsion.
2. Developer: Ilford D-19 developer.
3. Fixative: Ilford Hypam.
4. Filtered Harris' hematoxylin and 2% eosin.
5. Loctite UV adhesive (glass bond).

2.17. Indirect IS-RT-PCR

1. Random hexamer solution: Add 15 µg of random hexamers to 100 µL of DEPC-treated water.
2. AMV reverse transcription system (Promega).
3. PCR amplification mix: 5 U of *Taq* DNA polymerase; 5 µL of 10× *Taq* DNA polymerase buffer; 10 pmol of each primer; 0.2 mM each of dATP, dCTP, dGTP, and dTTP, distilled water to 50 µL.

2.18. Direct IS-RT-PCR

This can use the Tth enzyme *(20)*, which possesses both RT and DNA polymerase activity:

1. Reaction mix: 10 µL of 5× reaction buffer; 5 µL of 25 mM Mn(OAc)$_2$; 6 µL of 10 mM dNTP mix; 0.65 µL of 10 mM DIG dUTP; 0.5 pmol of each primer; 10 U of rTth enzyme; add sterile distilled water to 50 µL.

3. Methods

3.1. Fixation, Decalcification, and Embedding

In order to obtain satisfactory paraffin sections of bone, it is necessary to remove the mineral and then soften the tissue. This can be carried out with

acids or chelating agents. The chelating agent EDTA in the form of its diso-dium salt has minimal effect on mRNA retention, whereas acids greatly reduce mRNA *(21)* and should not be used.

1. Transport the sample to the laboratory within 30 min of retrieval and cut to a manageable size if necessary (*see* **Note 1**).
2. Immerse the sample in fixative in a universal container and incubate for 3–48 h at 4°C depending on the sample size (*see* **Note 2**).
3. Wash the sample in distilled water and transfer to EDTA for 10–14 d, with fresh changes of EDTA every 3 d (*see* **Note 3**).
4. Dehydrate the tissue, through a series of ethanols and xylene and embed in paraf-fin wax (*see* **Note 4**).

3.2. Tissue Sectioning

We usually cut bone sections of 7 μm thickness. If samples are fragile, we cut sections onto sellotape as described below, as this increases adherence of the section to the slide and is particularly suitable for calcified tissues.

1. Place a strip of adhesive tape onto the surface of the block and press down firmly, leaving a sufficient length of tape free in front of the block.
2. Raise this end above the level of the knife edge and cut a section in the usual manner. The tissue section will adhere to the tape.
3. Continue until sufficient sections are obtained.
4. Cut round the section and press down firmly onto a clean subbed slides using water.
5. Dry on hot plate (60°C) for 1–7 d.
6. Remove the tape by placing the slide in acetone for 1 min.
7. Remove adhesive by placing in chloroform for 20–30 min.

3.3. Subbing Slides

Slides are subbed to increase adherence of cells and tissue sections to the slides *(22)*.

1. Place slides in a metal rack and wrap in aluminum foil.
2. Bake at 250°C for 3 h.
3. Wearing gloves, unwrap the slides and allow them to cool slightly. Rinse in IMS and air-dry.
4. Immerse slides in APES solution for 5 min.
5. Immerse slides in acetone.
6. Rinse slides in DEPC-treated water.
7. Place in oven at 37°C overnight.
8. Store in dust-free conditions until use.

3.4. Mounting Sections on Slides

1. Float the sections onto DEPC-treated water at 50°C. Any wrinkles in the sections can be removed by gently pressing on the section with a small paintbrush.

2. Introduce a subbed microscope slide (*see* **Subheading 3.3.**) into the water underneath the floating section, at an angle of approx 45° and carefully lift the slide to the surface of the water so that the section adheres to the slide.
3. Place the slides on a hot plate (60°C) to dry overnight (for ISH; *see* **Note 5**) or up to 5 d (for IS-RT-PCR).

3.5. Silanation of Coverslips

Silanation of coverslips minimizes the amount of hybridization buffer needed during ISH. Such coverslips can be purchased commercially (Sigma Hybrislips), or prepared using the protocol below.

1. Place coverslips in metal coverslip racks.
2. In a fume cupboard wash the coverslips in IMS for 5 min.
3. Allow to air-dry.
4. Wash the coverslips in 1 *M* HCl for 20 min.
5. Rinse in DEPC-treated water.
6. Dry in a 60°C oven.
7. In a fume cupboard, immerse the coverslips in 5% dimethyldichlorosilane in xylene for 5 min.
8. Allow to air-dry in fume cupboard.
9. Bake in 200°C oven overnight.
10. Rinse in DEPC-treated water.
11. Dry in a 60°C oven.

3.6. Choice of Probes for ISH

Many different probes and labeling systems can be used for ISH, each with different advantages and drawbacks (*see* **Note 6**). The following protocols give details of making radioactively labeled and DIG-labeled cDNA probes and riboprobes.

3.7. Random-Primed Radioactive cDNA Probes

The labeling reaction described below (50 ng of probe) produces sufficient labeled probe to hybridize to 10 tissue sections.

1. Combine 50 ng of probe and 10 μL of a random hexamers mix in a 1.5 mL Eppendorf tube. Make up the reaction volume to 52 μL with sterile distilled water and pierce a hole in the lid of each Eppendorf tube.
2. Incubate at 100°C for 5 min to denature the double-stranded DNA probe. Allow the mixture to cool to room temperature.
3. Add the following reagents from the Megaprime kit to the tube:
    a. 10 μL of reaction buffer.
    b. 8 μL of each unlabeled dNTP.
    c. 10 μL of [^{35}S]-dCTP (50 μCi).
    d. 4 μL of Klenow fragment DNA polymerase.
4. Incubate at 37°C for 1 h and terminate the reaction by adding 5 μL of EDTA stop buffer to the tube.

5. Transfer the reaction to a Sephadex G-50 mini-spin column (*see* **Subheading 2.12**) and remove the unincorporated nucleotides by centrifuging at 10,000*g* in a microcentrifuge for 1 min.
6. Use the labeled probe immediately or freeze at –20°C for 24–48 h until use.

3.8. Nonradioactive (DIG) Random-Prime Labeling of cDNA Probes

1. To an Eppendorf tube containing 1 μg of cDNA probe, add sterile water to a final volume of 16 μL.
2. Pierce a hole in the lid of the Eppendorf tube and incubate at 100°C for 5 min to denature the DNA.
3. Place on ice and immediately add 4 μL of DIG high prime mix. Vortex to mix and centrifuge briefly.
4. Incubate overnight at 37°C.
5. Stop the labeling reaction by adding 2 μL of EDTA stop buffer.
6. Use immediately or store at –20°C for up to 12 mo.

3.9. Quantitating DIG Probe Concentration

It is important to quantify the amount of labeled probe that has been gener-ated when using DIG-labeled probes (*see* **Note 7**). Too much probe causes high background, whereas too little leads to a weak signal. The amount of probe can be estimated using test strips as described here:

1. Add 1 μL of labeled probe to 19 μL of DEPC-treated water to give a stock solu-tion of approx 1 ng/μL.
2. Make serial dilutions of this solution at 1:3; 1:10; 1:30; 1:100; and 1:300 using dilution buffer:
3. Dot 1 μL of each dilution on the DIG quantification test strip.
4. Place the test strips and the DIG control strip in blocking buffer for 2 min.
5. Transfer the strips to antibody solution for 3 min.
6. Transfer to blocking buffer for 1 min.
7. Transfer to maleic acid buffer for 1 min.
8. Transfer to detection buffer for 1 min.
9. Transfer to substrate and incubate in the dark, for 5–30 min, checking for color development to monitor progress of the reaction.
10. Estimate the amount of DIG-labeled probe present by comparing with the DIG control test strip.

3.10. Radioactive Labeling of Riboprobes

1. Add the following together in an Eppendorf tube:
   a. 1 μg of linearized plasmid template.
   b. 4 μL of 5× transcription buffer.
   c. 2 μL of 100 mM DTT.
   d. 1 μL each of rATP, rCTP, rGTP.

     e. 2.4 µL of 100 µM rUTP.

     f. 1 µL of RNasin.

     g. 5 µL (50 µCi) of [^{35}S]UTP.

     h. 1 µL SP6, T3, or T7 polymerase.

2. Incubate for 2 h at 37°C and stop the reaction by adding 2 µL of EDTA stop buffer.
3. Remove unincorporated nucleotides and plasmid DNA by adding 4 µL of DNase and 1.5 µL of RNasin to the tube and incubate at 37°C for 15 min.
4. Add 50 µL of 7.5 *M* ammonium acetate and 375 µL of cold 100% ethanol to the tube. Place at –20°C overnight or at –70°C for 2–4 h to precipitate the RNA.
5. Centrifuge at 10,000*g* for 20 min. Aspirate the ethanol with care and dispose of appropriately.
6. Wash the RNA pellet with 500 µL of 70% ethanol.
7. Centrifuge for 10 min at 10,000*g*. Remove ethanol and allow the pellet to dry.
8. Suspend the probe in 19 µL of 100 m*M* DTT and 1 µL of RNasin.
9. For riboprobes of > 500 basepairs (bp), proceed to limited alkaline hydrolysis (*see* **Subheading 3.12.**) before use (*see* **Note 8**).
10. Add 1 µL of probe to 3 mL of scintillation fluid and read counts on the scintillation counter. For satisfactory results, the probe should have ≥600,000 counts/µL.

3.11. Nonradioactive (DIG) Labeling of Riboprobes

1. To 1 µg of linearized DNA add 2µL of 10× buffer, 2 µL of NTP mix, 1 µL of RNase inhibitor, and 2 µL of the appropriate RNA polymerase (T7, T3, or SP6). Make the total volume up to 20 µL with DEPC-treated water.
2. Place the reaction in a microcentrifuge and pulse spin for 10 sec to ensure reagents are mixed.
3. Incubate at 37°C for 2 h.
4. Add 2 µL of DNase and 1 µL of RNasin and incubate at 37°C for another 15 min.
5. Stop the reaction by adding 2 µL of EDTA stop buffer.
6. If probes are longer than 500 bp, reduce to 500 bp by limited alkaline hydrolysis (*see* **Subheading 3.12.**).
7. Add 500 µL of cold ethanol to the tube, place at –20°C and leave overnight.
8. Spin the tube at 10,000*g* for 20 min in a microcentrifuge.
9. Remove the supernatant, taking care not to disturb the RNA pellet.
10. Leave to air-dry (approx 30–60 min).
11. Resuspend pellet in 19 µL of DEPC-treated water and 1 µL of RNasin.
12. Store at –20°C for up to 12 mo until use.

3.12. Alkaline Hydrolysis of RNA Probes

1. Resuspend the probe in 160 µL of DEPC-treated water.
2. Add 40 µL of hydrolysis buffer and incubate at 60°C for a time defined by the equation:

$$t = L_o - L_f / KL_oL_f$$

where t = time in min, L_o = initial probe length in kb, L_f = desired final probe length in kb and K = rate constant of hydrolysis = 0.11.

3. Stop the reaction by adding 6.6 μL of 3 *M* sodium acetate and 1.3 μL of glacial acetic acid.
4. Precipitate the reaction by adding 500 μL of ethanol and leave at -20°C for at least 2 h or overnight.
5. Centrifuge at 10,000*g* for 15 min, aspirate the supernatant, and allow pellet to dry.
6. Resuspend the probe in 19 μL of 100 m*M* DTT (for ^{35}S-labeled probes) or DEPC-treated water (for DIG-labeled probes) and 1 μL of RNasin.
7. Store at -20°C for up to 4 wk (^{35}S-labeled probes) or 12 mo (DIG-labeled probes) until use.

3.13. Prehybridization ISH and IS-RT-PCR

1. Dewax the sections by placing in xylene for 5 min. Repeat three times.
2. Transfer the sections to 95% IMS for 5 min. Repeat four times.
3. Wash the sections with DEPC-treated water.
4. Place the sections in 0.2 *M* HCl for 20 min at room temperature.
5. Wash in 2× SSC or water for 3 min. Repeat once.
6. Rinse in 0.05 *M* Tris HCl, pH 7.4 for 3 min.
7. Cover the section with 10 μg/mL of Proteinase K solution to cover the entire section.
8. For ISH, incubate the slides at 37°C for 1 h. For IS-RT-PCR, this time is reduced to 20 min (*see* **Note 9**).
9. Rinse slides in 0.2% glycine–PBS, for 3 min. Repeat once.
10. Rinse slides in PBS.
11. If required, prepare negative controls by incubating selected slides with 10 mg/mL of crude RNase for 60 min (*see* **Note 10**).
12. If required, postfix in 4% paraformaldehyde–PBS for 4 min at room temperature.
13. Rinse slides in PBS.
14. Immerse in freshly prepared 0.25% acetic anhydride, 0.1 *M* triethanolamine, pH 8.0, for 10 min (*see* **Note 11**).
15. Rinse in DEPC-treated water and then dehydrate by incubating in 90% IMS for 5 min.
16. Allow to air-dry and proceed to ISH (*see* **Note 12**).

3.14. ISH with Radioactive cDNA Probes

1. Make up 1 mL of hybridization buffer and combine with two labeling reactions. Incubate at 100°C for 5 min and cool by placing on ice.
2. Apply approx 50 μL of probe mix to each tissue section.
3. Cover sections with treated coverslips and incubate overnight at 37°C.

3.15. ISH with DIG-Labeled cDNA Probes

Follow the same protocol as described in **Subheading 3.14.**, using 500 ng of probe per milliliter of hybridization buffer. The amount of probe should be

estimated by the results of the DIG quantification test strips (*see* **Subheading 3.9.**).

3.16. ISH with Radioactive Riboprobes

1. Add sufficient quantity of probe (as determined by scintillation counting [*see* **Subheading 3.10**]) to riboprobe hybridization buffer (*see* **Subheading 2.14.**).
2. Heat probe to 60°C for 10 min and cool on ice.
3. Apply 20–50 μL (approx 0.1×10^6 dpm) probe mix per section (total counts required in 500 μL is 2.5×10^6 dpm).
4. Place siliconized coverslip over section and hybridize overnight at 50°C.

3.17. Non-radioactive Riboprobe Hybridization

Follow the same protocol as described in **Subheading 3.16.**, using 500 ng of probe per millilter of hybridization buffer. The amount of probe should be estimated by the results of the DIG quantification test strips (*see* **Subheading 3.9.**). Typical results of radioactive and nonradioactive ISH are shown in **Fig. 2**.

3.18. Post-hybridization Washes for cDNA Probes

The same protocol applies for both radioactive and nonradioactive probes. The temperature of the incubation in **step 5** depends on the length of the probe and the G/C content (*see* **Note 13**).

1. Remove the coverslips from the slides by soaking in 4× SSC for 5 min.
2. Incubate the slides in 0.5× SSC, 1 mM EDTA, and 10 mM DTT for 5 min. Repeat once.
3. Transfer to 0.5× SSC, 1 mM EDTA for 5 min. Repeat once.
4. Transfer to 50% formamide, 0.15 M NaCl, 5 mM Tris-HCl, pH 7.4; 0.5 mM EDTA, pH 8.0, and incubate for 10 min in a fume cupboard.
5. Transfer to 0.5× SSC at the probe T_m minus 10°C for 5 min. Repeat three times.
6. Transfer to 0.5× SSC and incubate at room temperature for 5 min.
7. Transfer to IMS and incubate at room temperature for 5 min.
8. Remove from IMS and allow to air-dry.

3.19. Post-hybridization Washes for Radioactive Riboprobes

1. Rinse slides in 2× SSC–1 mM DTT until coverslips come off.
2. Transfer to fresh 2× SSC and leave at room temperature for 60 min.
3. Transfer to wash buffer for 4 h at 50°C.
4. Transfer to NTE buffer for 2 min.
5. Transfer to fresh NTE buffer containing 20 μg/mL of RNase A and 100 U/mL of RNase T1 for 30 min at 37°C.
6. Transfer to NTE buffer and incubate for 30 min at 37°C.
7. Transfer to wash buffer and leave overnight at 50°C.
8. Transfer to 2× SSC and leave at room temperature for 30 min.
9. Transfer to 0.1× SSC and leave at room temperature for 30 min.
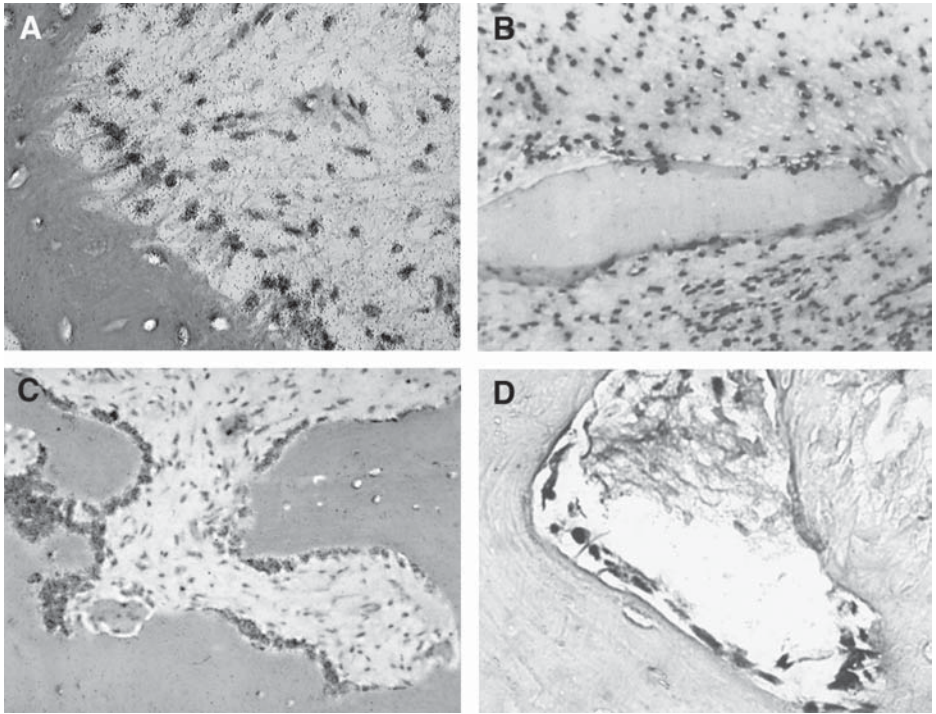
Fig. 2. Comparison of radioactive and nonradioactive ISH. (**A**) Transforming growth factor-β (TGF-β) mRNA demonstrated by autoradiography. (**B**) TGF-β mRNA demonstrated by digoxigenin—disclosed by NBT/BCIP (dark brown/blue stain). (**C**) Type I collagen mRNA demonstrated by autoradiography. (**D**) Type I collagen mRNA demonstrated by digoxigenin.

10. Transfer to IMS and incubate at room temperature for 5 min.
11. Remove from IMS and allow to air-dry.

3.20. Post-hybridization Washes for Nonradioactive Riboprobes

1. Immerse slides in 4× SSC until the coverslips come off.
2. Transfer to 50% deionized formamide in 1× SSC and incubate at 55°C for 20 min. Repeat for a total of three times.
3. Transfer to 1× SSC and incubate for 15 min at room temperature. Repeat once.

3.21. Autoradiography and Counterstaining

The following steps should be done in a dark room. Before beginning, make sure you have your slides to be dipped, along with blank clean slides, a dipping chamber, plastic slide racks, plastic forceps, a clean developing tank lined with

paper roll, and a water bath held at 40–45°C. Do not use metal objects—this will "stress" the emulsion and can produce false positive results.

1. Fill a universal container with 10 mL of distilled water and incubate at 40–45°C for 30 min.
2. Fill a universal container with approx 10 mL of K5 emulsion, using plastic forceps, and put the lid on. Place in a water bath at 40–45°C until it melts.
3. When the emulsion has melted add an equal volume of warm distilled water and invert slowly to mix.
4. Pour the diluted emulsion in a clean dipping chamber and dip a few blank slides to remove any air bubbles.
5. Dip the slides in the emulsion and allow them to drain upright on the side of the lined developing tank.
6. Put the slides upright onto plastic slide racks and allow to dry in a dark cupboard for 3–4 h.
7. When the slides are dry put them into a lightproof box, label, and seal the edges with tape.
8. Incubate slides at 4°C for 7–10 d if riboprobes are being used and for 10–14 d if cDNA probes are being used.
9. When the incubation is complete, take the slides to a darkroom, remove from the lightproof box, and transfer to a glass trough and cover with D-19 developer. Incubate for 5 min at 24°C.
10. Rinse slides in three changes of distilled water.
11. Cover slides with fixative and incubate for 5 min.
12. Wash once in distilled water.
13. Rinse in running tap water for 5 min.
14. Immerse in filtered Harris' Hematoxylin for 2 min.
15. Rinse in running tap water for 5 min.
16. Immerse in 2% eosin for 30 sec.
17. Rinse in water and allow to air-dry.
18. Add two drops of Loctite UV adhesive to each section and put on a coverslip.
19. Expose the slides to UV light using a UV transilluminator for 2 min.

3.22. Detection of DIG-Labeled cDNA Probes and Riboprobes

1. Place slides in maleic acid buffer for 5 min.
2. Place slides in a wet box and cover section with 0.5% Boerhinger Blocking Reagent (BBR). Incubate for 30 min at room temperature.
3. Tip off BBR from sections, and cover with a 1–500 dilution of anti-DIG (AP) in 0.5% BBR. Incubate for 2 h at room temperature.
4. Wash slides in maleic acid buffer.
5. Place slides in a wet box and equilibrate in detection buffer. Remove detection buffer and then cover section with substrate solution. Incubate in the dark and monitor the progress of the reaction over 1–12 h by looking for an appearance of staining.
6. Wash slides in distilled water and allow to air-dry.
7. Mount in Loctite UV adhesive as described in **Subheading 3.21.**, **steps 18** and **19**.
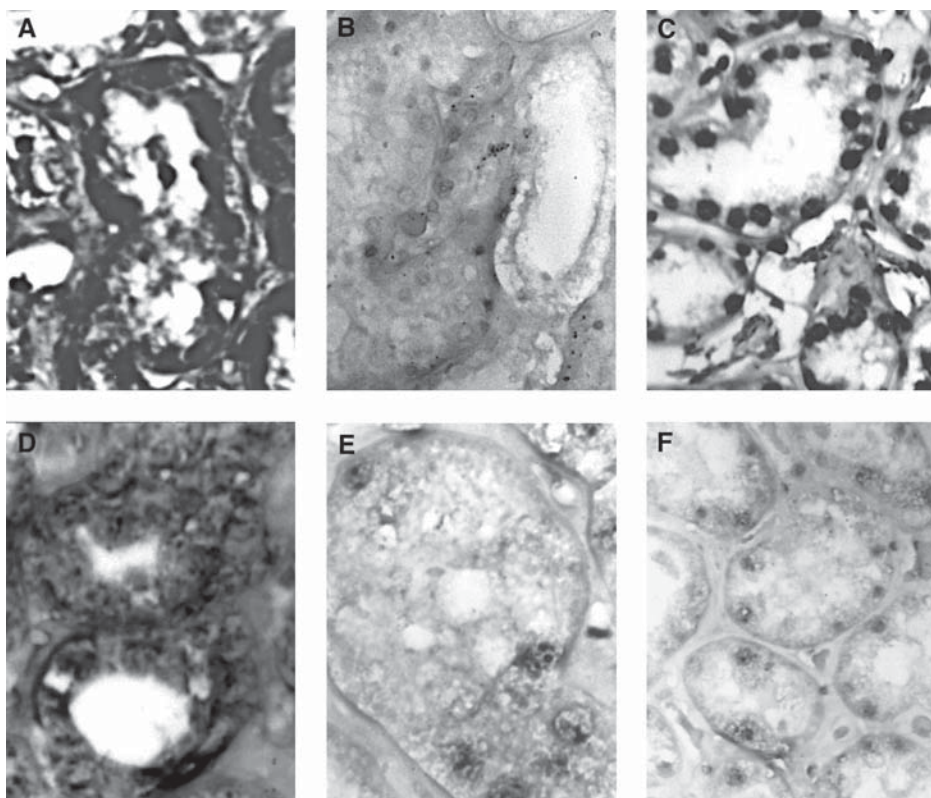
Fig. 3. Comparison of indirect and direct IS-RT-PCR. Note that these figures show sections of human kidney stained for the presence of vitamin D receptor (VDR) mRNA—we have never used the direct method on bone sections as it is such an unreliable technique. (**A**) Direct IS-RT-PCR, 20 cycles, positive staining in renal tubules. Note the poor morphology due to cycling for 20 times at 95°C. (**B**) Direct IS-RT-PCR, 20 cycles, negative control—omission of DNA polymerase. Note absence of staining (nuclei counterstained with methyl green). (**C**) Direct IS-RT-PCR, 20 cycles, negative control—omission of reverse transcriptase. Note presence of intense staining in all nuclei due to nonspecific DNA repair. It is also of note that the cytoplasm in (**C**) is not stained, hence the technique has worked in (**A**) (where the cytoplasm is also stained). However, the presence of staining in the nuclei means that this technique is unreliable. (**D**) Indirect IS-RT-PCR, five cycles, positive staining in renal tubules. Note the staining is less intense than in (**A**) (only five cycles compared with 20), but that the morphology is much better in (**D**). (**E**) Indirect IS-RT-PCR, five cycles, negative control—omission of DNA polymerase. Note absence of staining (nuclei counterstained with methyl green). (**F**) Indirect IS-RT-PCR, five cycles, negative control—omission of reverse transcriptase. Note absence of staining (nuclei counterstained with methyl green). Even if nonspecific DNA repair occurs, the VDR probe will not bind to the repaired DNA and hence there is no signal in the nuclei.

3.23. Reverse Transcription Step for Indirect IS-RT-PCR

The technique of IS-RT-PCR, can be performed using the direct or indirect methods. Since the direct method is extremely prone to false-positive results when working on sections (**Fig. 3**), we recommend the use of the indirect method.

1. Pre-hybridize the sections according to **Subheading 3.13.**, **steps 1–13** (**steps 14–16** follow in **Subheading 3.24.**).
2. Add 20 μL random primer mix to each section and incubate at 80°C for 5 min.
3. To each section, add 10 U of AMV RT; 1× RT buffer; 10 m*M* DTT; 2 m*M* sodium pyrophosphate; 15 U of RNasin; and 1 m*M* each of dATP, dCTP, dGTP, and dTTP in a final volume of 20 μL, and incubate the samples at 42°C for 2 h.
4. Wash twice in PBS or water.
5. Fix in 0.4% paraformaldehyde–PBS for 20 min at 4°C.
6. Dehydrate by incubating in 90% IMS for 5 min and allow to air-dry.

3.24. PCR Step for Indirect IS-RT-PCR

Annealing temperatures, Mg^{2+} concentration, cycling parameters (typically 5–10 cycles of amplication will be required; *see* **Note 14**) and extension times will vary with the particular mRNA under investigation.

1. Place an Easiseal around each sample.
2. Apply 50 μL of amplification solution to each section and cover the Easiseal.
3. Place the slides on the thermal cycler and start the reaction.
4. When the PCR has finished, wash the slides twice in PBS or water.
5. Transfer the slides to 0.4% paraformaldehyde–PBS and incubate for 20 min at 4°C.
6. The remaining pretreatments described in **Subheading 3.13.**, **steps 14–16** are now performed.

A comparison of radioactive and nonradioactive IS-RT-PCR is shown in **Fig. 4**. Indirect IS-RT-PCR in bone is shown in **Fig. 5**.

3.25. Stringency Washes and Autoradiography for Indirect IS-RT-PCR

1. Denature the samples at 95°C for 5 min, using the Omnislide™, prior to the addition of probe.
2. The hybridization conditions for IS-RT-PCR are exactly the same as those described for cDNA probes in **Subheading 3.14.**
3. The post-hybridization stringency washes are as described for cDNA probes in **Subheading 3.18.**
4. Autoradiography and counterstaining are performed as described in **Subheading 3.21.**
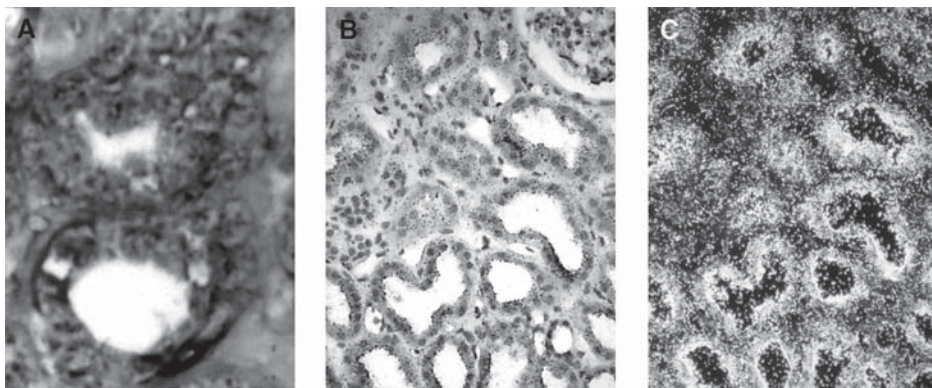
Fig. 4. Comparison of nonradioactive and radioactive indirect IS-RT-PCR. All sections are after five cycles of IS-RT-PCR, and are kidney sections demonstrating VDR mRNA. (**A**) Nonradioactive detection with DIG. (**B**) Lightfield view showing silver grains over renal tubules. (**C**) Darkfield view to highlight the signal—note the absence of signal in the glomeruli (*top right* of **B** and **C**).
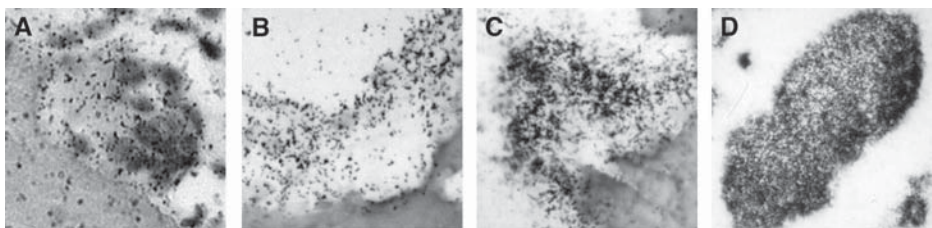
Fig. 5. VDR mRNA expression in osteoclasts. (**A**) Normal ISH of Pagetic osteoclast showing very low level of hybridization in this diseased tissue. (**B**) IS-RT-PCR, 10 cycles, normal bone. (**C**) IS-RT-PCR, 10 cycles, Pagetic bone. (**D**) IS-RT-PCR, 10 cycles, osteoclastoma.

3.26. Direct IS-RT-PCR

This procedure is not recommended for use on tissue sections—a variety of problems can cause false positive-results, but the most common problem is nonspecific DNA repair (**Fig. 3**). The protocol given below makes use of Tth enzyme *(22)*, which possesses both RT and DNA polymerase activity and can therefore be used in a one-step protocol:

1. Place Easiseal around sections.
2. Pipet 50 μL of reaction mixture onto each section.
3. Perform amplification steps: 60°C for 30 min (RT step), followed by 20 cycles of amplification (as appropriate to mRNA under investigation), followed by a 5-min incubation at 60°C.

3.27. Controls for ISH

Both negative and positive controls are absolutely essential when performing ISH. A specific reaction is of paramount importance. A false signal may arise from several causes, including sequence-independent binding of probe to nucleic acid; nonspecific binding to other tissue components; and artifacts of label visualization.

A number of strategies can be used to assess the specificity of hybridization:

1. Probe specificity: Check with Northern/Southern blots.
2. Pretreatment of tissue with RNase or DNase.
3. Hybridization with different fragments of specific sequence.
4. Use of heterologous (unrelated) probe with similar GC content.
5. Prehybridization of probe with specific cDNA or cRNA.
6. Hybridization with nonspecific vector sequences.
7. Reproducibility: Include tissue known to be positive or tissue with expressing and nonexpressing regions.
8. Correlation with immunohistochemistry.
9. If using riboprobes, a sense probe can be used as a further control. However, we and others have found that certain sense probes on certain tissues will produce positive staining. This staining is obviously not specific for the sequence being investigated by the antisense probe, hence many workers are now not using sense riboprobes as negative controls.

3.28. Controls for IS-RT-PCR (Fig. 6)

For IS-RT-PCR, the controls have to be even more rigorous. As with conventional ISH and IS-PCR a wide variety of control experiments must be performed to ensure that no false-negative or false-positive results are obtained.

1. Use known negative and positive control samples. These must be used if available to confirm that the reaction has occurred and that nonspecific amplification has not occurred. Another control within this category is to mix known numbers of positive and negative cells and check that the known negative cells show no positive signal following amplification. If more cells are apparently positive than should be, diffusion of amplification products has occurred.
2. Use of RNase or DNase: These tests are performed when examining tissues for the respective nucleic acids. For example, if examining for DNA (such as exogenous viral DNA) perform a DNase step to eliminate signal; if performing IS-RT-PCR, pretreat the sample with RNase to eliminate the signal.
3. Omission of DNA polymerase. This tests for nonspecific DNA repair. Nicks and gaps can occur in genomic DNA (and in the DNA generated during the amplification step), especially in fixed, paraffin-embedded sections. *Taq* DNA polymerase will repair this damage during the extension reaction. When using direct IS-RT-PCR, this nonspecific action will lead to incorporation of
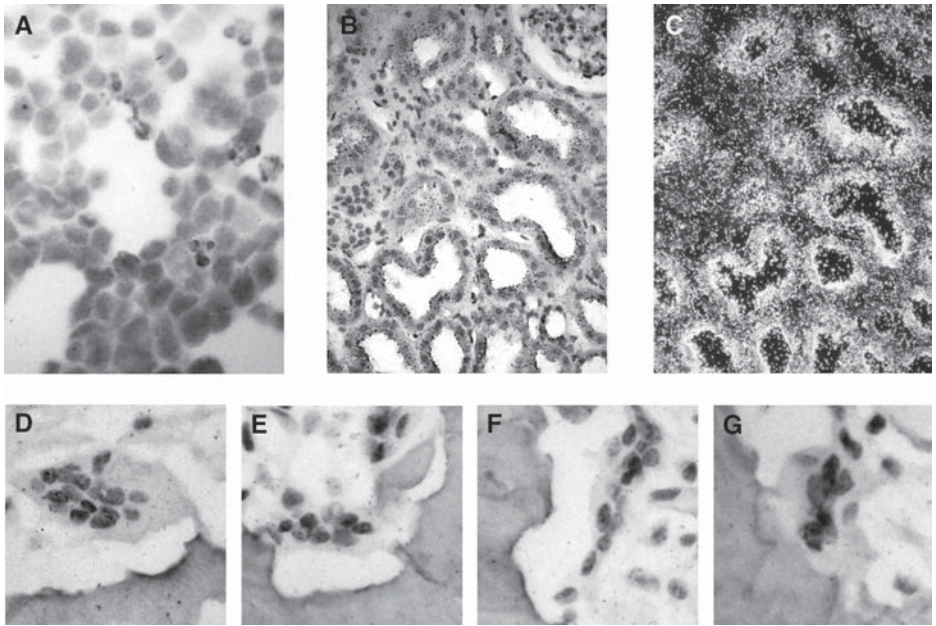
Fig. 6. Controls for IS-RT-PCR. All samples have been hybridized with a VDR probe. (**A**) Negative control tissue—small cell lung cancer cell line (NCIH82) that shows no expression of VDR with any technique (including conventional RT-PCR). (**B**) Lightfield and (**C**) darkfield views of positive control tissue—kidney sections showing positive hybridization for VDR. (**D**) Negative control—RNase pretreatment prior to hybridization. (**E**) Negative control—no RT enzyme in RT step. (**F**) Negative control—no DNA polymerase in PCR. (**G**) Negative control—no primers in PCR.

  labeled nucleotides within the repaired DNA, which will produce a false-positive result. A similar phenomenon can occur in cells that are undergoing necrosis or apoptosis.
4. Omission of primers. This test will ensure the specificity of the primers, particularly if higher Mg^{2+} concentrations have been used. The is also a further test to ensure that primer-independent nonspecific repair (as in the preceding) has not occurred. This control is particularly critical when performing direct IS-RT-PCR.
5. Omission of RT enzyme when performing IS-RT-PCR. As with the use of RNase, this test will confirm that RNA, and not genomic DNA, is being amplified.
6. Use of controls for the detection system. If using a nonradioactive detection system, these controls include omission of primary antibody. If using indirect IS-RT-PCR, a nonspecific probe (i.e., a probe that will not bind to the amplification product) can be used; alternatively, the probe can be left out altogether. A further test to ensure the specificity of the probe used for ISH is to perform the amplification reaction with a set of primers for a nucleic acid sequence that the probe should not hybridize with.

7. Extraction of amplification products from the sample. The DNA can be extracted from the sample and the size of the amplification product verified by agarose gel electrophoresis. Be aware that, if direct amplification has been carried out, the products will appear slightly larger than expected owing to the presence of label within the DNA.

4. Notes

1. Size of samples: If large samples are obtained then they should be cut into smaller pieces (less than 1–2 cm^3) prior to fixation.
2. Duration of fixation: Samples of less than 1 mm thickness can be fixed in 2–3 h; tissues up to 1 cm thickness should be fixed for 12–24 h; larger samples should be fixed for up to 48 h. Precipitating fixatives such as ethanol and acetic acid provide better probe penetration, but they may be associated with loss of RNA (up to 75% losses have been quoted) and the tissue morphology is not so good. In view of this we do not use these fixatives for the detection of RNA. Crosslinking fixatives such as paraformaldehyde, formaldehyde, and glutaraldehyde generally provide better RNA retention and tissue morphology, but probe penetration is less good. The merits and drawbacks of the fixatives most commonly used are shown in the table below:

Fixative	Characteristics
2% Glutaraldehyde	Best RNA retention, probe penetration poor
3% Formaldehyde	Provides a good balance between RNA retention and probe penetration. No permeabilization needed for oligonucleotide probes
4% Paraformaldehyde	Provides a good starting point—usually no permeabilization steps needed
10% Buffered formalin	Used routinely in our laboratories
Ethanol–acetic acid	Unsuitable for RNA work

3. Duration of decalcification: This is dependent on the sample size. Bone biopsies (8 mm trephine) usually take 10–14 d. Decalcification can be checked by placing the bone samples on top of a radiographic plate and exposing to X-rays for 5–8 sec at 30–45 KvP. By developing the radiographic plate you will be able to assess whether any mineralization remains. Agitation of the specimens will increase the rate of decalcification.
4. Embedding and processing tissues: Dehydration and embedding are best performed in a tissue processor. If this is not available in your own laboratory, embedding can be performed by most histopathology laboratories.
5. Any calcified tissues that contain a large amount of cartilage (e.g., healing fracture callus or metaphyseal areas in growing bones) are extremely difficult to deal with, as the cartilaginous areas easily become detached from the slide. Once the sections have been mounted onto APES slides, incubating at 60°C for longer periods (up to 5 d) can help with this problem.

6. Types of probe for ISH and IS-RT-PCR: Four types of probe are in common usage. These are double stranded complementary DNA (cDNA) probes; single stranded cDNA probes; RNA probes (riboprobe); and oligonucleotide probes. Each type of probe can be labeled using either radioactive or nonradioactive techniques. Radioactive labels include ^{32}P, ^{33}P, ^{35}S, and ^{3}H. Radioactive ISH gives more reproducible results and higher sensitivity than nonradioactive detection. Also, radioactive ISH is more readily quantifiable (silver grain counting). However, the disadvantages include safety, waste disposal and reduced stability of labeled probe, prolonged time required for autoradiography and poor spatial resolution. Nonradioactive labels include biotin, DIG, and fluorescein. Nonradioactive probes are safer to use and have much greater stability; however, the protocols are not easily reproduced and the sensitivity of nonradioactive detection is generally less than with radioactive probes, although many antibody detection systems have been developed that enhance the flexibility and sensitivity of the method.

7. Expected amounts of probe generated by DIG High Prime reaction: The product insert indicates that the DIG High Prime reaction yields approx 40 µg/mL of DIG-labeled DNA starting from 1 µg of template after 1 h of incubation, we have found that it is more typical to have 20 µg/mL of DIG-labeled DNA following an overnight incubation.

8. Size of riboprobes: RNA probes are most efficient when used as smaller fragments. The optimum size for ISH applications is generally 200–250 bases but should be determined empirically for each application. Probes <500 bp need not be hydrolyzed, but alkaline hydrolysis can be carried out for probes larger than this. The size of the probe can be checked by running an aliquot on a denaturing formaldehyde agarose gel.

9. Prehybridization conditions: Note that for both ISH and IS-RT-PCR, for all new probes and tissues the optimum concentration and time of the preincubation should be determined empirically by trial and error.

10. Negative control slides: Slides can be exposed to RNase during the prehybridization stage to provide a negative control. This tests specificity in providing a check that the probe is binding to RNA, rather than other cellular components. During this incubation, the test slides (not RNase treated) should be incubated in 2× SSC.

11. The immersion step in acetic anhydride–triethanolamine (*see* **Subheading 3.13.**, **step 14**) can be extended up to 30 min to help reduce excessive background levels of signal (*see* **Fig. 7**).

12. If background levels of staining are high, a prehybridization step can be included. This is merely an incubation for 60 min with all the components of the hybridization mix, except for the probe, performed at the normal temperature of hybridization (*see* **Fig. 7**).

13. Temperatures for post-hybridization washes: This is based on the probe T_m which depends on the length and G/C content of the probe. The T_m is calculated using the following equation:
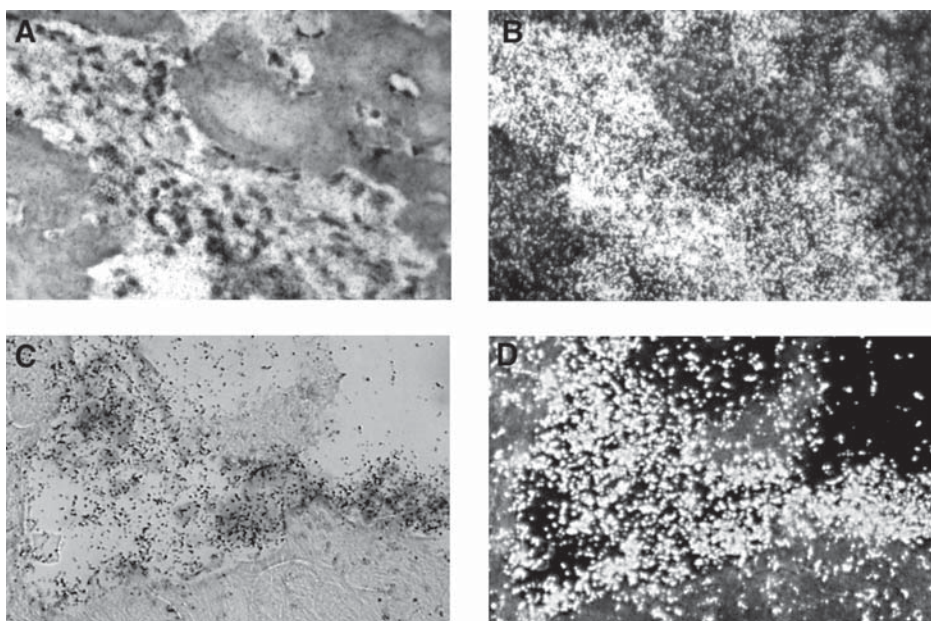
Fig. 7. Example of poor background staining and how to improve this. (**A**) Lightfield and (**B**) Darkfield views showing Bcl-2 expression in Pagetic bone. Note background signal over bone matrix and in clear areas within the marrow space. (**C**) Lightfield and (**D**) darkfield views showing the improvements seen by incorporating a prehybridization step and increasing the triethanolamine incubation to 30 min. Note a much cleaner signal over the osteoclasts.

$$T_m = 81.5°C + 16.61(\log M) + 0.41(\% \text{ GC}) - (820/L) - 0.6\% \text{ F} - 1-4\% \text{ (mismatch)}$$

where F = formamide concentration, $\log M$ = log molar salt concentration, %GC = % of guanine and cytosine, and L = length of probe.

When using cDNA probes, if high levels of background are still found, the formamide wash step can be performed at higher temperatures (up to 42°C)—this must be determined empirically for each probe and tissue. Similarly, the temperature of the 0.5 × SSC wash can also be increased to help reduce background.

14. IS-RT-PCR is inefficient—we have shown that amplification is at best linear (compared with exponential for conventional tube RT-PCR) *(16)*. This is important for two reasons; first, don't expect an exponential increase in signal, and second, criticism has been leveled at the technique owing to the fact that amplification has been used to generate a signal. The validity of results has hence been questioned by some authors owing to the "exponential increase" required to produce a positive result (i.e. authors have questioned whether positive IS-RT-PCR findings are demonstrative of relevant levels of mRNA in vivo). However, the

increase is clearly not exponential, hence this criticism is unfounded.

Too many cycles of IS-RT-PCR can actually reduce the level of signal. The reasons for this are unclear, although we have commented on the possibilities previously *(14)*. Nevertheless, when designing an IS-RT-PCR experiment, it is important to realize that only a few cycles of amplification will be needed (we have never gone above 10 cycles to get a positive result). This phenomenon appears to be related to the starting levels of mRNA, that is, the higher the original levels, the fewer cycles that will be needed; hence this phenomenon is especially important in positive control tissues that are used to optimize protocols. (We have never used more than five cycles for positive control tissues.)

References

1. Komminoth, P. and Long, A. A. (1993) In-situ polymerase chain reaction. An overview of methods, applications and limitations of a new molecular technique. *Virchows Arch. B* **64**, 67–73.

2. Haase, A. T., Retzel, E. F., and Staskus, K. A. (1990) Amplification and detection of Lentiviral DNA inside cells. *Proc. Natl. Acad. Sci. USA* **87**, 4971–4975.

3. Nuovo, G. J., Gallery, F., MacConnell, P., Becker, J., and Bloch, W. (1991) An improved technique for in situ detection of DNA after polymerase chain reaction amplification. *Am. J. of Pathol.* **139**, 1239–1244.

4. Bagasra, O., Hauptman, S. P., Lishner, H. W., Sachs, M., and Pomerantz, R. J. (1992) Detection of human immunodeficiency virus type 1 provirus in mononuclear cells by in situ polymerase chain reaction. *N. Engl. J. Med.* **326**, 1385–1391.

5. Zehbe, I., Hacker, G. W., Rylabder, E., Sallstrom, J., and Wilander, E. (1992) Detection of single HPV copies in SiHa cells by *in situ* polymerase chain reaction combined with immunoperoxidase and immunogold-silver staining techniques. *Anticancer Res.* **12**, 2165–2168.

6. Komminoth, P., Long, A., Ray, R., and Wolfe, H. (1992) *In situ* polymerase chain reaction detection of viral DNA, single copy genes and gene rearrangements in cell suspensions and cytospins. *Diagn. Mol. Pathol.* **1**, 85–97.

7. Embleton, M. J., Gorochov, G., Jones, P. T., and Winter, G. (1992) In-cell PCR from mRNA: amplifying and linking the rearranged immunoglobulin heavy and light chain V-genes within single cells. *Nucl. Acids Res.* **20**, 3831–3837.

8. Heniford, B. W., Shum-Siu, A., Leonberger, M., and Hendler, F. J. (1993) Variation in cellular EGF receptor mRNA expression demonstrated by in situ reverse transcriptase polymerase chain reaction. *Nucl. Acids Res.* **21**, 3159–3166.

9. Chen, R. H. and Fuggle, S. V. (1993) *In situ* cDNA polymerase chain reaction. A novel technique for detecting mRNA expression. *Am. J. Pathol.* **143**, 1527–1534.

10. Nuovo, G. J. (1994) Reverse transcriptase *in situ* PCR, in *PCR In Situ Hybridization. Protocols and Applications*, 2nd edit. Raven Press, New York, pp. 247–306.

11. Patel, V. G., Shum-Siu, A., Heniford, B. W., Wieman, T. J., and Hendler, F. J. (1994) Detection of epidermal growth factor receptor mRNA in tissue sections from biopsy specimens using *in situ* polymerase chain reaction. *Am. J. Pathol.* **144**, 7–14.

12. Martinez, A., Miller, M. J., Quinn, K., Unsworth, E. J., Ebina, M., and Cuttitta, F.

(1995) Non-radioactive localization of nucleic acids by direct in situ PCR and in situ RT-PCR in paraffin-embedded sections. *J. Histochem. Cytochem.* **43**, 739–747.

13. Martinez, A., Miller, M. J., Unsworth, E. J., Stegfried, J. M., and Cuttitta, F. (1995) Expression of adrenomedullin in normal human lung and in pulmonary tumours. *Endocrinology* **136**, 4099–4105.

14. Mee, A. P., Davenport, L. K., Hoyland, J. A., Davies, M., and Mawer, E. B. (1996) Novel and sensitive detection systems for the vitamin D receptor—*in situ*-reverse transcriptase-polymerase chain reaction and immunogold cytochemistry. *J. Mol. Endocrinol.* **16**, 183–195.

15. Mee, A. P., Hoyland, J. A., Braidman, I. P., Freemont, A. J., Davies, M., and Mawer, E. B. (1996) Demonstration of vitamin D receptor transcripts in actively resorbing osteoclasts in bone sections. *Bone* **18**, 295–299.

16. Mee, A. P., Denton, J., Hoyland, J. A., Davies, M., and Mawer, E. B. (1997) Quantification of vitamin D receptor mRNA in tissue sections demonstrates the relative limitations of in situ–reverse transcriptase–polymerase chain reaction. *J. Pathol.* **182**, 22–28.

17. Hoyland, J. A., Mee, A. P., Baird, P., Braidman, I. P., Mawer, E. B., and Freemont, A. J. (1997) Demonstration of oestrogen receptor mRNA in bone using in situ-reverse transcriptase-polymerase chain reaction. *Bone* **20**, 87–92.

18. Mee, A. P., Dixon, J. A., Hoyland, J. A., Davies, M., Selby, P. L., and Mawer, E. B. (1998) Detection of canine distemper virus in 100% of Paget's disease samples by *in situ*-reverse transcriptase-polymerase chain reaction. *Bone* **23**, 171–175.

19. Long, A. A., Komminoth, P., Lee, E., and Wolfe, H. J. (1993) Comparison of indirect and direct in situ polymerase chain reaction in cell preparations and tissue sections. *Histochemistry* **99**, 151–162.

20. Myers, T. W. and Gelfand, D. H. (1991) Reverse transcription and DNA amplification by a *Thermus thermophilus* DNA polymerase. *Biochemistry* **30**, 7661.

21. Walsh, L., Freemont, A. J., and Hoyland, J. A. (1993) The effect of tissue decalcification on mRNA retention within bone for in situ hybridization studies. *Int. J. Exp. Pathol.* **74**, 237–241.

22. Rentrop, M., Knapp, B., Winter, H., and Schweizer, J. (1986) Aminoalkylsilane-treated slides as support for in situ hybridization of keratin cDNAs to frozen sections under varying fixation and pretreatment conditions. *Histochem. J.* **18**, 271–276.

16

Techniques for the Study of Apoptosis in Bone

Brendon S. Noble and Hazel Y. Stevens

1. Introduction

Over the past five years there has been an explosion of interest in the process of apoptotic cell death. The fact that, in contrast to necrotic death, apoptosis constitutes a precisely regulated, energy-dependent form of death has led to interest in the potential to control this death process through an understanding of the molecular mechanisms involved in its initiation and occurrence. Early descriptions of apoptosis were based on morphological changes in cells (cell shrinkage, condensation and margination of chromatin nuclear fragmentation, and production of membrane-bound apoptotic bodies), and despite the more recent identification of a number of biochemical (e.g., ordered DNA fragmentation and activation of a range of caspase enzymes) and ultrastructural phenomena (e.g., externalization of phosphatidylserine molecules at the plasma membrane) specific to apoptosis, the morphological criteria are still often regarded as the "gold standard" *(1)*. Unfortunately, the use of morphological criteria to assess the apoptotic state in many cell types involves the use of high magnification microscopy (often electron microscopy), which precludes studying the high numbers of individual cells necessary for an assessment of apoptosis at a tissue level. We have attempted to address these difficulties by identifying more than one apoptotic characteristic at relatively low magnifications. Hence we assess (1) DNA fragmentation *in situ*, (2) cell loss, and (3) identification of internucleosomal sized increments of DNA, produced during DNA destruction (DNA ladders). The loss of cells through the energy-dependent, controlled mechanism of apoptosis has wide-ranging influence on the function of all body tissues and bone is no exception. The loss of bone cells by apoptosis occurs as an entirely normal component of the lifetime repertoire of these cells. It is thought to control the number of functional

osteoblasts at the bone surface *(2)*, and to play a role in endochondral bone formation by chondrocytes *(3)*; in addition, it deletes osteoclasts at the end of their resorption work cycle *(4)*. It has been suggested that in the osteocyte apoptotic death might play a role in the load and microdamage engendered targeting of bone resorption *(5)*. The importance of apoptosis in normal skeletal physiology is emphasized by recent evidence that apoptosis is perturbed or deregulated in a number of disease situations in bone *(6,7)*.

The study of cellular morphology in mineralized tissues is complicated by difficulties experienced in cutting thin sections of the tough, brittle mineral component of the bone and by the contrasting material properties of the mineralized bone and nonmineralized components, such as bone marrow and cartilage which are present within the same tissue. Sectioning of bone can be facilitated by the use of plasticized embedding materials such as methylmethacrylate to support the heterogeneous materials within bone tissue (*see* the chapter by van Leeuwen and Derkx, *this volume*). Unfortunately, the use of plastic embedding materials greatly hinders penetration of the tissue sections by enzymes, antibodies, and various other reagents necessary to detect apoptosis. Removal of embedding material with a deplasticizing step often results in loss of the small fragments of DNA associated with apoptosis, resulting in underestimates of apoptosis. Ideally, fresh frozen cryosections should be used to maximize the chances of identifying and quantifying enzymes or antigens in bone cells, as these methods avoid masking or changing conformation of the molecules studied. Using a tungsten carbide edged knife and a heavy-duty cryostat (ideally motorized Bright cryostat; *see* the chapter by Bord, *this volume*), it is possible to cut cryosections of bone.

2. Materials
2.1. Toluidine Blue Staining

1. Picric formalin: Mix 60 mL of formalin (40% aqueous formaldehyde), 500 mL of 95% ethanol, 40 mL of glacial acetic acid, and 400 mL of distilled water. The solution keeps for about 4 mo at room temperature (RT). Make a fresh batch as soon as a cloudy precipitate forms or the solution smells clearly of formic acid.
2. Toluidine blue (Gurr, Poole, UK).
3. *n*-Butyl alcohol (Sigma, Dorset, UK).
4. Citifluor (glycerol–PBS mix; Agar Scientific, Essex, UK).
5. Light green (Gurr).

2.2. LDH Assay

1. Gly-Gly powder (Sigma).
2. Polypep (40%). Weigh out 1.32 g Gly-Gly powder, add 100 mL of distilled water, then adjust pH to 8.0 by adding approx 34 mL of 0.1 *M* NaOH. Then add 80 g of

Polypep (Sigma). Leave stirring overnight. Make up to 200 mL with distilled water and store at 4°C (solidified stock solution keeps for 6–12 mo at this temperature).

3. Lactic acid (Sigma).
4. Nicotinamide adenine dinucleotide (NAD; BDH/Merk, Poole, Dorset, UK).
5. Nitroblue tetrazolium (NBT; Sigma).

2.3. Nick Translation

1. Paraformaldehyde (Sigma) dissolved in PBS (4% w/v) by gentle heating to 60°C. **Caution**: Do not boil! Ideally make fresh on day and do not shake before use.
2. Phosphate-buffered saline (PBS; Sigma).
3. Ethylenediaminetetraacetic acid (EDTA; BDH) 0.25 M in 50 mM Tris-HCl, pH 7.4 (stable for 1 yr).
4. Nucleotides: 100 mM of dGTP Li salt (cat. no.1051 466); 100 mM of dATP Li salt (cat. no. 1051 440); 100 mM of dCTP Li salt (cat. no. 1051 458) (all purchased from Roche Diagnostics). With all Roche products do not use beyond expiration date.
5. Polymerase buffer: 6.055g/L of 50 mM Tris-HCl, pH 7.5, 5 mM MgCl$_2$ (238 mg/500 mL), 0.1 mM dithiothreitol (7.7 mg/500 mL)]. Stable for 4 mo stored at 4°C.
6. Digoxigenin (DIG)-11-dUTP 25 μL of 25 nmol (Roche, cat. no. 157 3152).
7. 250 U (50 μL) of DNA polymerase 1 (Roche, cat. no. 0 642 711).
8. Anti-DIG-fluorescein (FITC) Fab fragments (200 μg) (Roche, cat. no. 1 207 741).
9. Normal sheep serum (Sigma).
10. Positive control DNase 1 (Sigma, cat. no. D4263). Do not use after expiration date.
11. Propidium iodide (PI; Sigma). Make up a stock solution of 100 μg/mL in distilled water. Stable for 6 mo at 4°C, stored in the dark. The working solution is 10 μL of PI stock solution in 10 mL of distilled water.

2.4. DNA Gel Electrophoresis

1. Reagent B, sodium perchlorate, Nucleon silica (Nucleon Biosciences, Scotlab, Glasgow, UK). Do not use after expiration date.
2. Ribonuclease A (Sigma).
3. Chloroform (BDH), incubated at –20°C for the purification step.
4. TBE: 54 g of Tris base, 27.5 g of boric acid, 20 mL of 0.5 M EDTA pH 8.0. Stable for 6 mo at 4°C.
5. Agarose (gel electrophoresis grade; Gibco, Paisley, Scotland).
6. 6X Gel loading buffer (stored refrigerated at 4°C, stable for 6 mo): 0.025 g of bromophenol blue, 0.025 g of xylene cyanol FF, 3 mL of glycerol, 7 mL of water. All reagents purchased from Sigma. A commercially available loading buffer can be substituted.
7. 100-Basepair (bp) ladder (Gibco). Do not use after expiration date.
8. Horizontal gel electrophoresis tank (Bio-Rad) and power supply delivering up to 150 V.
9. UV transilluminator.

3. Methods

3.1. Morphological Evidence of Apoptosis by Toluidine Blue Staining

Apoptotic cells can be identified in sections of bone by toluidine blue staining. The procedure stains the nuclei blue and enables visualization of condensation, blebbing, or fragmentation of the nucleus prior to packaging of nuclear and cytoplasmic contents into apoptotic bodies.

1. Fix cryostat sections in picric–formalin for 10 min at RT.
2. Make up a 0.1% solution of toluidine blue (0.2 g in 200 mL of H_2O).
3. Stain the sections for 30 min.
4. Blot dry and place in buffer for resin sections or *n*-Butyl alcohol for frozen sections (*see* **Note 1**) for 2 min.
5. If a counterstain is required, use 1% light green in distilled H_2O for 2 min and rinse again with distilled water.
6. Mount in Citifluor. (The standard technique involves dehydration and mounting in DePeX which may or may not suit the material being stained. In general, bone material does not require this dehydration step.)

3.2. Cell Viability by LDH Assay

During most of the apoptotic time course cells maintain intact cell membranes and active metabolic processes. This is in distinct contrast to the necrotic death process in which cell membranes rupture and cellular activities rapidly decline. Hence, detection of DNA fragmentation in cells with intact membranes and active metabolic enzymes will indicate apoptosis rather than necrosis. Loss of cell viability also represents the final "outcome" of the apoptotic process and, in the case of the osteocytes, entombed within lacunae in bone, it will indicate the site of cell loss. To determine cell viability in cryosections we use histochemical detection of LDH enzyme activity at the cellular level. Rather than attempt to measure enzyme activities quantitatively, the technique is designed to be highly sensitive to enzyme activity to ensure that any active enzyme present is identified.

Because apoptosis occurs only in living cells it is important to use the LDH assay alongside DNA ladders to test which cells were alive when the tissue was prepared for sectioning. The method given is a modification of the methods of Wong et al. 1987 *(6)* and Farquharson et al. 1992 *(8)*. Purple staining indicates viable cells; absence of staining implies a dead cell or presence of an empty lacuna (*see* **Fig. 1**).

1. Generate cryostat sections (10 μm thick) on microscope slides and keep slides at –20°C until use.
2. When ready, defrost slides at RT for a few minutes.
3. Melt 40% Polypep in a jar surrounded by hot water and to 10 mL of Polypep add 44 μL of lactic acid (final conc. 60 m*M*), 17.5 mg of NAD (final conc. 1.75 mg/mL), then adjust pH to 8.0 with conc. NaOH before adding 30 mg NBT (final conc. 30 mg/mL).
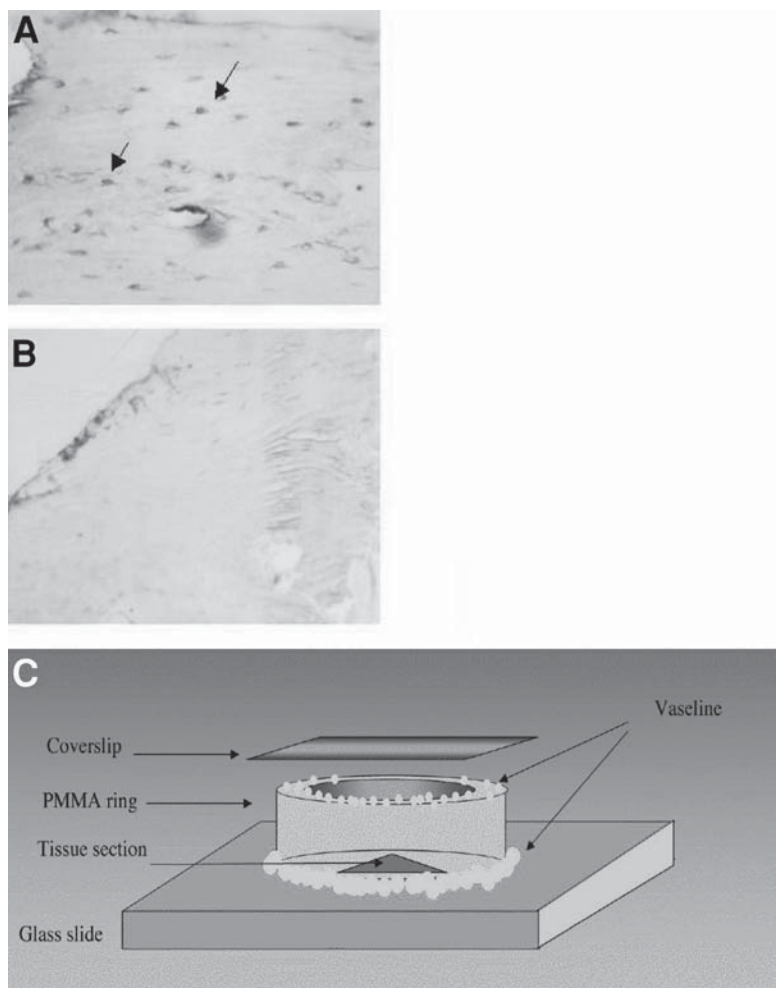
Fig. 1. Cell viability determined *in situ* using LDH activity as a marker. Cells in frozen sections are stained for lactate dehydrogenase activity and examined using light microscopy. **(A)** Live osteocytes stained (dark) for active lactate dehydrogenase. *Arrows* illustrate two examples of live cells. **(B)** Region of bone containing dead osteocytes showing no staining for LDH activity. Cells on bone surface stain positive. **(C)** Diagram illustrates the use of plastic rings for LDH staining. The reaction mix is placed in a plastic ring sealed at the base and top with vaseline to allow prolonged incubation at 37°C.

4. Adhere plastic rings (made from slices of polymethylmethacrylate [PMMA] tubing) over the specimens onto the slides using Vaseline, add the reaction mix into the ring excluding air bubbles and place coverslips on top to minimize evaporation.

5. Incubate for 3 h at 37°C in a humidified chamber.
6. Rinse in warm water (approx 50°C) to remove reaction medium.
7. Rinse in acetone (30 s) to remove soluble pink formazan.
8. Rinse in PBS and mount in Citifluor. Coverslips can be sealed with clear nail varnish if needed.

3.3. Nick Translation

In general, cells undergoing apoptosis cleave their DNA into internucleosomal sized increments (increments of 180–200 bp) so that, when the DNA from apoptotic cells is electrophoresed on an agarose gel, the DNA presents itself at regular intervals in the run giving the appearance of a "DNA ladder" (*see* **Subheading 3.4.**). The level of DNA fragmentation that occurs during apoptosis is extremely high, vastly in excess of that associated with normal DNA repair or during necrosis. The *in situ* nick translation technique described here uses the DNA polymerase I (Klenow fragment) driven incorporation of DIG-conjugated nucleotides into DNA strand breaks to identify cells in culture or in tissue sections that contain large amounts of highly fragmented DNA characteristic of apoptotic cells (*see* **Fig. 2**). The technique has been purposely designed to be relatively insensitive with regard to DNA fragment identification so that only cells with massive amounts of fragmented DNA will be identified. In this way the technique has an increased specificity for apoptotic cells *(7)*. We have found that when used on bone sections the technique provides a more accurate and consistent method of identification of apoptosis that the more commonly used TUNEL staining, which employs terminal deoxynucleotide transferase (TdT). The reasons for this are unknown but likely include the fact that TUNEL methods greatly amplify the fragmentation signal due to addition of multiple labeled (biotinylated) nucleotides at the 3'OH termini of a break (in a chain reaction) while nick translation applies only a single set of nucleotides. In addition, commercial kits for TUNEL often include a harsh proteinase K digestion step which probably introduces false positives.

While it is our experience that all bone cells tested so far (from various species) undergo this type of internucleosomal DNA fragmentation during apoptosis it is wise to always run a positive control (in which apoptosis has been positively identified by other means) to test the applicability of this technique to the specific tissue of interest.

DNA is susceptible to degradation by endonucleases. This means that all vessels, tips, and solutions should be sterile before use. In practice, the use of autoclaved microcentrifuge tubes, the wearing of gloves and sterile filtered stock solutions of buffer are usually sufficient to exclude exogenous endonuclease activity and enable the unambiguous use of the technique.
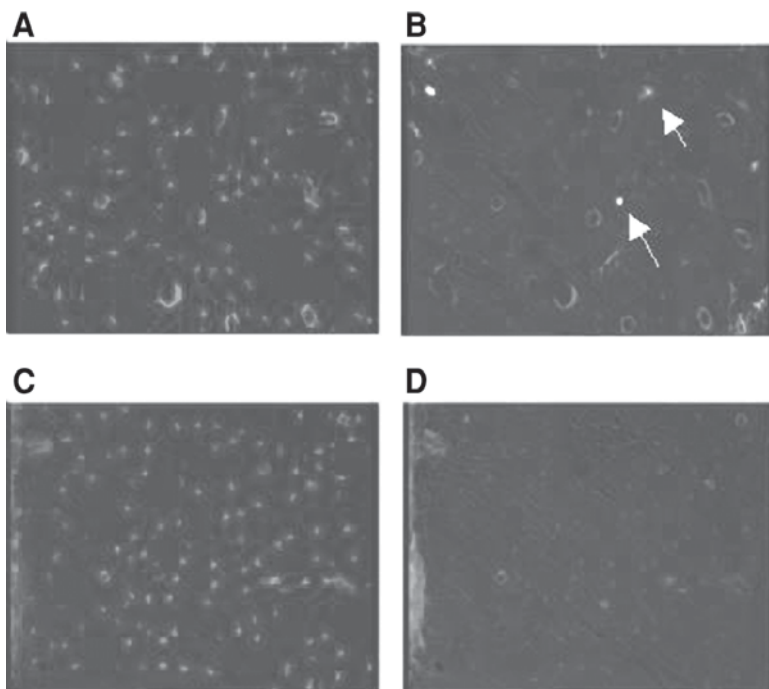
Fig. 2. Cells containing large amounts of highly fragmented DNA are labeled using a nick translation technique. Fragmented DNA in osteocytes resident in bone is identified after incorporation of labeled nucleotides using a nick translation reaction. **(A)** Propidium iodide staining of osteocyte nuclei. **(B)** Apoptotic osteocytes labeled positive for fragmented DNA (FITC). *Arrows* denote two example cells positive for fragmented DNA. **(C)** PI staining of osteocyte nuclei in the negative control (no polymerase enzyme). **(D)** Negative control (no polymerase enzyme) showing lack of FITC-labeled cells.

3.3.1. Preparing the Sections/Cells

1. Prepare *fresh* 7-μm cryostat sections of rat tibia or prepare bone cell cultures (*see* **Note 2**).
2. Fix in 4% paraformaldehyde in PBS for 10 min at RT.
3. Wash three times in PBS.
4. For sections, decalcify in 0.25 *M* EDTA in 50 m*M* Tris-HCl, pH 7.4, for 10 min. Cell cultures do not require any decalcification.
5. Wash three times in PBS.
6. Thoroughly air dry. Store at 4°C until ready to use.

3.3.2. Preparing the Nick Translation Mixture

The following recipe is based on an allocation of 50 μL of reaction mix per slide and is suitable for five slides plus a control slide (without polymerase enzyme).

1. Make up stock solutions of dGTP, dATP, and dCTP in three separate Eppendorf tubes by adding 1 μL of dGTP, dATP, and dCTP (from the 100 mmol/L stock) to 300 μL of polymerase buffer, resulting in working stocks of 0.3 mmol/L for each nucleotide.
2. Then add 3 μL of each of the working stocks of nucleotides into 300 μL of poly-merase buffer (= polymerase mix, containing 3 μM of each of nucleotides).
3. Add 1 μL of DIG-11-dUTP into the polymerase mix.
4. Take out 50 μL of polymerase mix for the negative control.
5. Then add 1.25 μL of DNA polymerase to the remaining 250 μL of polymerase mix (= nick translation mix) and vortex-mix well.
6. Use DNase I at 0.2 mg/mL in PBS as a positive control in a subset of sections (*see* **Subheading 3.3.3.**).

3.3.3. Nick Translation Technique

1. Treat one group of sections with DNase (positive control) for 1 h at 37°C to produce breaks in the DNA.
2. Incubate all other sections/cells in nick translation mix for 1 h at 37°C in a humidified chamber. Remember negative controls have no DNA polymerase in the mix.
3. Wash three times in PBS and keep moist at all times.
4. Incubate in 1:8 anti-DIG FITC Fab (300 μL of PBS, 37.5 μL of anti-DIG FITC Fab, 15 μL of sheep serum) for 1 h at RT.
5. Wash three times in PBS.
6. Counterstain in PI (10 μL of PI stock solution in 10 mL of distilled water) for 30 s (cells) and 2 min (sections).
7. Wash thoroughly in distilled water.
8. Mount in Citifluor, keep dark.
9. The sections/cells are examined under a fluorescent microscope to distinguish FITC stained (green) apoptotic cells from all cells (stained red with PI). Positive controls show a large number of cells (often approaching 100% of cells) with fragmented DNA (FITC positive) and negative controls should not show any FITC-positive cells, just a low background fluorescence of the bone.

3.4. DNA Ladders

Breaking DNA into internucleosomal sized increments during apoptosis (increments of 180–200 bp) leads to the production of a "DNA ladder" when the DNA is electrophoresed on an agarose gel *(9)*. A small number of cell types produce DNA fragments during apoptosis that are much larger (200–300 kbp and 30–50 kbp) and hence do not provide this ladder pattern *(10)*. It is thought

that the larger fragments are produced as a prelude to the production of oligonucleosomal fragments and that apoptotic cells not showing DNA ladders have stopped DNA fragmentation at this earlier stage in the process. It is possible to identify the larger fragments using pulse field electrophoresis (not covered in this chapter).

While it is our experience that all bone cells tested so far (from various species) undergo internucleosomal DNA fragmentation during apoptosis, it is again wise to always include a positive control (in which apoptosis has been positively induced, e.g., heating cell culture flask at 44°C for 30 min, or by using sections of material previously tested by nick translation) for the cell type under investigation to test the fragmentation pattern (*see* **Fig. 3** and **Note 4**). As for the nick translation assay, use autoclaved microcentrifuge tubes, wear gloves and use sterile filtered stock solutions of buffer to exclude exogenous endonuclease activity.

3.4.1. Preparation of Cells and Tissue

1. For a confluent T75 flask of bone cells (approx 4×10^6 cells), aspirate medium and wash the monolayer gently in PBS, aspirate to dryness, and place in freezer (–80°C) immediately.
2. Thaw by adding 1 mL of PBS and scrape cells off into a 1.5- to 2-mL Eppendorf tube.
3. Centrifuge at 600g, 4°C, 5 min.
4. For sections generated on a cryostat (15–20 at 10 µm thick; undecalcified tissue), collect these directly into a bijou/Eppendorf tube and store immediately at –80°C. Thaw when ready to use.

3.4.2. Isolation of DNA

The isolation of DNA uses a commercial kit, supplied by Nucleon Biosciences (*see* **Note 3**) and our protocol has been published in their scientific newsletter.

1. To the cell pellet or sections add 340 µL of Reagent B (SDS based). Vortex-mix. Leave for 40 min.
2. Centrifuge at 600g for 5 min. Decant the supernatant to another tube.
3. Digest RNA (optional) by addition of 2.5 µL of ribonuclease A (Sigma) to each tube (final conc. 50 µg/mL) and incubate for 30 min at RT.
4. Remove protein by adding 100 µL of sodium perchlorate per tube and mixing on a rotary mixer at 37°C for 20 min, followed by 20 min at 65°C.
5. Add 580 µL of chloroform (stored at –20°C). Place on rotary mixer for 20 min at RT.
6. Transfer the contents to a 2-mL Nucleon /Eppendorf tube. Nucleon tubes have a plastic division which makes separation of the organic and aqueous layers easier. Centrifuge at 1300g for 1 min.
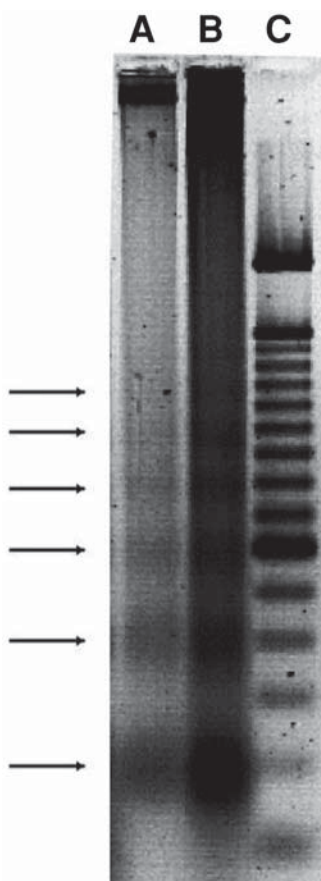
Fig. 3. DNA ladders indicative of apoptosis. DNA from apoptotic cells produces multiple bands of approx 180-bp increments when run on an agarose gel. *Lanes A*, *B*. DNA from apoptotic cells producing the characteristic "ladder" pattern. Individual bands are highlighted with *arrows*. *Lane C*, 1000-bp markers.

7. Add 45 µL of Nucleon silica suspension, then centrifuge at 1300*g* for 4 min.
8. Pour off (upper, aqueous) DNA phase into a fresh tube.
9. Centrifuge at 1300*g* for 30 s to pellet any silica.
10. Transfer supernatant to a fresh tube.
11. To precipitate DNA add 880 µL of absolute ethanol and invert the tube to mix.
12. Centrifuge at 4000*g* for 5 min to pellet DNA, discard the supernatant (or, optional, add 100 µL 3 *M* sodium acetate to the ethanol waste and leave at –20°C overnight to precipitate further DNA).

13. Wash the DNA pellet by adding 1 mL of 70% ethanol in distilled water at 4°C and place on a rotary mixer at RT for 20 min.
14. Centrifuge briefly at 4000*g* for 5 min. Remove ethanol and leave the pellet to air-dry (not to complete dryness). The samples are usually solubilized in TBE and run the same day. DNA can be stored in 70% ethanol at –20°C so that the procedure can be interrupted at **step 12**.

3.4.3 Agarose Gel Electrophoresis

1. Dissolve 1.5% (w/v) high-purity agarose in TBE (100 mL of 1X TBE for a 70-mL gel) in a 250-mL glass flask by microwaving at a medium wattage (500 W) for approx 3 min. To avoid overheating, take out the flask after 2 min with tongs and swirl the gel.
2. Pour the gel into a suitable container and let set for 45 min. Then hydrate gel with TBE.
3. Add 20 μL of TBE to pellets, incubate at 65°C for 3 min, cool, and add 4 μL of loading buffer (LB 6×).
4. Load approx 10 μg of DNA per lane, running approx 20 μL in each lane (*see* **Note 3**)
5. Include one lane of a 100 bp-standard.
6. Run the gel at 20 V overnight, until the front marker is near the end of gel (*see* **Note 4**).
7. Soak the gel in 300 mL of 1× TBE with 15 μL of ethidium bromide (final concentration 0.5 μg/mL) for 45 min.
8. Visualize using UV Transilluminator (*see* **Note 5**).

4. Notes

1. Resin-embedded sections should be washed in buffer rather than in *n*-butyl alcohol after toluidine blue staining to avoid shrinkage and crinkling of the section.
2. It is crucially important for the nick translation technique always to use freshly cut and fixed sections. Storage of frozen sections induces damage of DNA upon defrost and results in false-positive results.
3. We have most experience with the Nucleon kit; however, any commercial kit to isolate small quantities of DNA would probably suffice.
4. The amount of DNA that may be loaded on a gel depends on several factors:
   a. Well volume.
   b. Fragment size. The capacity of the gel drops sharply as the fragment size increases, especially over a few kilobases.
   c. Distribution of fragment sizes
   d. Voltage gradient. Higher voltage gradients are better suited to DNA fragments under 1 kb; lower voltages are better suited to fragments over 1 kb.
   The least amount of DNA in a single band that can be reliably detected with ethidium bromide is approx 10 ng and about 60 pg with SYBR® Green I stain. The maximum amount of DNA that can be run as a sharp, clean band is about 100 ng. Overloaded DNA results in trailing and smearing, a problem that will become more severe as the size of DNA increases.

5. Using standard agarose gel electrophoresis, the *presence* of a ladder *is* a clear indication of apoptosis but the *absence* of a ladder is *not* proof that apoptosis has not occurred until you have established the way in which DNA fragmentation occurs in the cell type under investigation. In addition, it is important to verify the apoptotic state using multiple criteria if possible.

References

1. Wyllie, A. H., Kerr, J. F. R., and Currie, A. R. (1980) Cell death: the significance of apoptosis. *Int. Rev. Cytol.* **68,** 251–306.
2. Jilka, R. L., Weinstein, R. S., Bellido, T., Roberson, P., Parfitt, A. M., and Manolagas, S. C. (1999) Increased bone formation by prevention of osteoblast apoptosis with parathyroid hormone. *J. Clin. Invest.* **104,** 439–446.
3. Stevens, H.Y., Reeve, J., and Noble, B.S. (2000) Bcl-2, tissue transglutaminase and p53 protein expression in the apoptotic cascade in ribs of premature infants. *J. Anat.* **196,** 181–191.
4. Kameda, T., Ishikawa, H., and Tsutsui, T. (1995) Detection and characterisation of apoptosis in osteoclasts in vitro. *Biochem. Biophys. Res. Commun.* **207,** 753–760.
5. Verborgt, O., Gibson, G. J., and Schaffler, M. B. (2000) Loss of osteocyte integrity in association with microdamage and bone remodelling after fatigue in vivo. *J. Bone Miner. Res.* **15,** 60–67.
6. Wong, S. Y., Evans, R. A., Needs, C., Dunstan, R., Hills, E., and Garvan, J. (1987) The pathogenesis of osteoarthritis of the hip. Evidence for primary osteocyte death. *Clin. Orthop.* **214** 305–312.
7. Noble, B.S., Stevens, H., Loveridge, N., and Reeve, J. (1997) Identification of apoptotic changes in osteocytes in normal and pathological human bone. *Bone* **20,** 273–282.
8. Farquharson, C., Whitehead, C., Rennie, S., Thorp, B., and Loveridge, N. (1992) Cell proliferation and enzyme activities associated with the development of avian tibial dyschondroplasia: an in situ biochemical study. *Bone* **13,** 59–67.
9. Wyllie, A. H. (1980) Glucocorticoid-induced thymocyte apoptosis is associated with endogenous endonuclease activation. *Nature* **284,** 555–556.
10. Oberhammer, F., Wilson, J. W., Dive, C., et al. (1993) Apoptotic death in epithelial cells: Cleavage of DNA to 300 and/or 50 kb fragments prior to or in the absence of internucleosomal fragmentation. *EMBO J.* **12,** 3679–3684.

17

Protein Localization in Wax-Embedded and Frozen Sections of Bone Using Immunohistochemistry

Sharyn Bord

1. Introduction

Immunohistochemistry can provide valuable information regarding protein expression in different cell types at specific stages of differentiation during bone modeling and remodeling. By combining immunohistochemistry with other techniques, it is possible for the researcher to determine protein expression, in relation to mRNA production, enzyme activity and bone remodeling, on the same sample of bone. This chapter covers the localization of protein in human bone by immunohistochemistry using an indirect immunoperoxidase method, and considers both frozen and wax-embedded sections. Methods for immunostaining of plastic embedded tissue can be found in the chapter by Van Leeuwen and Derkx, *this volume*. Immunohistochemistry is based on incubating high-affinity antibodies on tissue sections to detect patterns of expression for specific antigens within the tissue. This can be achieved using either an immunofluorescence-based technique in which the antibody is conjugated with a fluorochrome, or an enzyme-labeled antibody method. The latter procedure has several advantages; it utilizes the same enzyme complexes for all primary antisera irrespective of its origin in different animal species; stained sections may be permanently mounted; and sections can be viewed using brightfield microscopy. Detection methods have increased the sensitivity of immunohistochemistry. There are now several ways that the signal of antibody–antigen binding can be amplified, thus allowing the use of only small amounts of antibody. The method of choice for this chapter is the avidin–biotinylated enzyme complex (ABC) method first described by Hsu et al. *(1)* for localization of antigens in the thyroid. Primary antibody binds to specific epitopes of the anti-
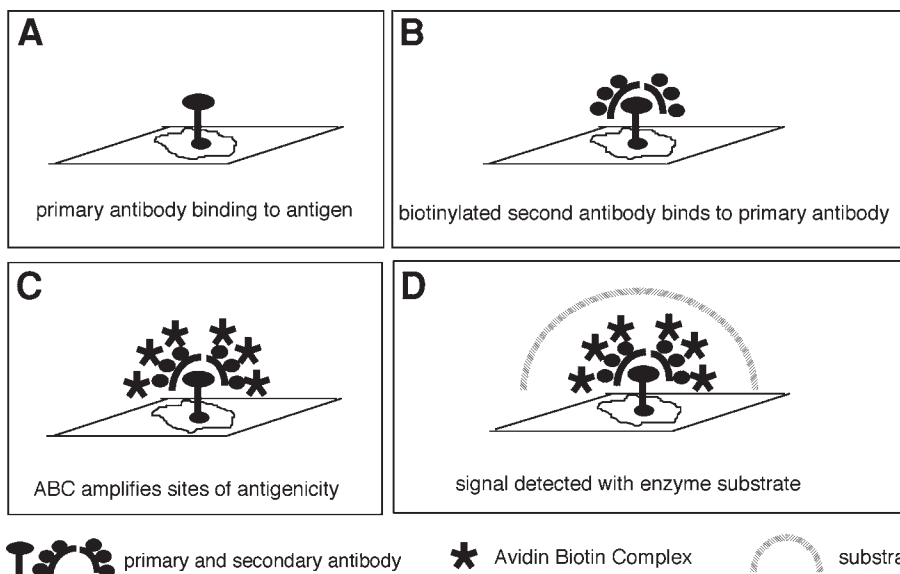
Fig. 1. Steps involved in the indirect immunoperoxidase system using an ABC amplification stage. (**A**) After fixation and blocking, the primary antibody is applied to the section. This binds specifically to the antigen. (**B**) A biotin-labeled second antibody binds to the primary antibody and introduces many biotins at this binding site. (**C**) The ABC enzyme binds to the biotinylated sites, thus increasing the signal. (**D**) The substrate reacts with the enzyme complex and gives a color reaction at sites of antigenicity.

gen within the section. A biotin-labeled secondary antibody is added that introduces many biotins at the sites of primary antibody binding. The next layer, ABC, binds to the biotin-labeled second antibody, amplifying the initial signal which is then visualized by addition of a substrate and chromogen to the enzyme. This produces a color reaction at sites of positive expression that can be assessed using brightfield microscopy (**Fig. 1**). We have successfully used this technique to detect various proteins in bone *(2,3)*.

2. Materials

Most general reagents can be obtained from Sigma.

1. Phosphate-buffered saline (PBS) 5× stock: Add 42.6 g of NaCl, 16.08 g of $Na_2HPO4·2H_2O$, and 0.78 g of NaH_2PO_4 to 900 mL distilled water. Adjust the pH to 7.4 with 6 *N* HCl and make up to 1 L. Store at room temperature and dilute 1: 5 with distilled water before use.
2. Buffered EDTA: Add 72.5 g of ethylenediamine tetraacetic acid disodium salt (EDTA) to 500 mL of distilled water and adjust to pH 7.4–7.6 with NaOH. Add five PBS tablets to the solution and mix thoroughly using stirrer.

3. Bovine serum albumin (BSA): Dissolve 1 mg of high-grade crystalline BSA in 1 mL of PBS to give a 0.1% solution.
4. Neutral buffered formalin (NBF): Add 5.2 g of $NaH_2PO_4·2H_2O$ and 6.4 g of Na_2HPO_4 (anhydrous) to 97 mL of 37% formaldehyde. Combine with in 900 mL of distilled water and adjust the pH to 7.2 with 6 *N* HCl. Make up to 1 L with distilled water.
5. 4% Paraformaldehyde fixative: Add 4 g of paraformaldehyde to 50 mL of PBS. Add a few drops of 2.5 *M* NaOH and stir on a hot plate in a fume hood until clear. Allow to cool and add 40 mL of PBS. Adjust pH to 7.3 with 1 *N* acetic acid. Make up to 100 mL with distilled water. Keep at 4°C, and use within after 1 wk. (Larger quantities can be aliquoted and stored at –20°C until use.)
6. 5% Polyvinyl alcohol (PVA): Dissolve 5 g of PVA in 100 mL of PBS. Store at 4°C.
7. 3-Aminopropyltriethoxysilane (APES)-coated slides: Place slides in racks and wash overnight in 10% decon-90. Wash in running hot water for 2 h. Dry overnight in oven at 50°C. Immerse slides in 2% solution of APES diluted in 100% alcohol for 10 min. Drain and wash in 100% alcohol for 10 min. Drain and wash in distilled water for 10 min. Repeat distilled water wash. Dry overnight in oven at 50°C. Store in clean boxes.
8. ImmunoPure peroxidase suppressor (Pierce and Warriner, Chester).
9. 3,3'-Diaminobenzidine (DAB) (Vector Laboratories).
10. Hematoxylin: Gills hematoxylin (Sigma) dilute 1:50 in distilled water before use.
11. Diff-Quik stain (Baxter-Dade AG).
12. Nikon 800 microscope equipped with a Basler digital camera and Lucia G image analysis software.

3. Methods

3.1. Choice of Bone Samples

Most of our studies have investigated protein expression in portions of human bone samples obtained from the iliac crest using a 8-mm trephine biopsy. Because adult bone is hard, brittle, and friable, bone samples are generally decalcified and wax embedded to obtain sections with the best morphology. Bone from younger patients is less brittle and therefore it is possible to use frozen sections, which with careful cutting can provide good morphology. Some antibodies will work only on frozen sections. Whatever method is used it is important to know the site from which the bone sample was obtained and, for comparative studies between patients, to use bone from the same anatomical site. The age of the donor and any prescribed drug regimen may also influence protein expression, and this should be considered when interpreting results.

3.2. Preparing Wax-Embedded Sections

1. Place the biopsy on ice immediately after removal.

2. If desired, divide biopsy into two halves to allow other types of analysis (*see* **Fig. 3** and **Note 1**).
3. Fix the biopsy by placing in NBF overnight at 4°C (*see* **Note 2**).
4. Remove the biopsy from NBF and wash in cold PBS for 2 h.
5. Decalcify the bone sample by incubating in 14.5% buffered EDTA for 3 wk, replacing the EDTA every week. (*see* **Note 3**).
6. Embed the biopsy in paraffin wax (*see* **Note 4**).

3.3. Preparing Frozen Sections

We usually prepare frozen sections in samples of neonatal ribs collected at postmortem from infants born at full term (30–40 wk).

1. Following removal, place the ribs immediately on ice. Trim the bone to an appropriate size and dip the sample in chilled PVA for 2 min.
2. Half fill a small plastic tray with chilled PVA and place the sample in the tray in the correct orientation for cryosectioning.
3. Carefully lower the tray into liquid nitrogen, ensuring that the PVA solidifies before it comes into contact with the liquid nitrogen (*see* **Note 5**).
4. Place the frozen sample in a 40-mL capped universal tube and store at –80°C.
5. When required for cryosectioning, transfer the sample from –80°C to dry ice and carefully remove the peelaway plastic tray.
6. Trim away excess PVA and mount on a suitable chuck for the cryostat (usually brass, 22-mm diameter).
7. Prepare a chilling bath containing a 12-mm deep cold slurry of alcohol in chips of dry ice. Stand the chuck in this bath and pipet a thin layer of PVA onto the top of the cold chuck.
8. Immediately place the bone sample (with the side to be sectioned uppermost) onto the PVA-covered surface of the chuck. More PVA can be added to ensure a tight bond between the PVA block containing the bone sample and the chuck.
9. Return the block and chuck to dry ice.

3.4. Sectioning Wax-Embedded Bone Samples

1. Cut 7-μm thick sections on a base sledge microtome, float out on water (45°C) and collect on APES-coated slides.
2. Dry the slides overnight at 45°C and store in dust-free boxes.
3. Immediately before performing immunohistochemistry, immerse the slides in xylene for 12 min. Replace with fresh xylene and incubate for another 12 min to dewax the sections.
4. Transfer the slides to 100% ethanol and incubate for 3 min.
5. Transfer the slides to 70% ethanol and incubate for 3 min.
6. Transfer the slides to 50% ethanol and incubate for 3 min.
7. Transfer the slides to PBS.

3.5. Cryosectioning Bone Samples

The sections should be cut on a good quality cryostat equipped with a slow drive, high-torque motor, and automatic speed control at a cabinet temperature of –30°C (*see* **Note 6**).

1. Cut 9-μm sections and transfer onto APES-coated glass slides by placing the slide over the section on the knife blade and applying slight thumb pressure to the back of the slide for about 5 s. This encourages the section to adhere well to the slide.
2. Air dry the slides for 10–20 min at room temperature.
3. Place the slides in a staining trough and fix by incubating in 4% paraformaldehyde for 30 min at room temperature.
4. Wash three times in PBS for 5 min per wash.

3.6. Immunohistochemistry Using an Indirect Immunoperoxidase Technique

The following procedure is suitable for both wax-embedded and frozen sections. Several factors influence the choice of antibody and even once an antibody is chosen, it is essential to establish the specificity of the immunoreaction to determine which control antibodies and which control tissues should be used to validate the procedure (*see* **Note 7**).

1. Draw around the sections with an ImmEdge™ pen (Vector) to provide a fluid barrier and thus minimize the amount of reagents needed.
2. Block endogenous peroxidase and nonspecific binding by incubation with ImmunoPure peroxidase suppressor (*see* **Note 8**). Carefully apply to the sections (about 100 μL/ section), taking care not to break over the hydrophobic ImmEdge™ pen barrier.
3. Place the slides in a humid chamber for 30 min to prevent "drying out."
4. Transfer slides to a staining trough and wash in PBS for 5 min with gentle shaking. Discard PBS by tipping the trough carefully so as not to dislodge sections from slides. Repeat the 5-min PBS wash two more times.
5. Incubate sections with 10–20% serum in PBS for 30 min in a humid chamber to block nonspecific binding (*see* **Note 9**).
6. Pour off the serum–PBS from the section, removing as much as possible.
7. Dilute the primary antibody to a working concentration in 0.1% BSA and add about 100 μL/section (*see* **Note 10**).
8. Incubate the slides in a humid chamber for either 90 min at room temperature or overnight at 4°C.
9. Remove the slides from chamber to a staining trough and wash three times in PBS for 5 min per wash to remove unbound antibody.
10. Remove the slides from PBS and apply the second antibody (3.5 μg/mL diluted in 0.1% BSA (*see* **Note 11**).
11. Incubate the slides in a humid chamber for 30 min at room temperature.
12. Prepare the ABC solution according to manufacturer's instructions and allow to stand for 30 min before use.

13. Wash the sections in three changes of PBS (5 min each, with gently shaking) to remove the unbound secondary antibody and drain slides.
14. Add ABC solution to the sections and incubate for 30 min at room temperature in a humid chamber.
15. Wash the sections in three changes of PBS (5 min each, with gently shaking) and drain slides.
16. Prepare the chromogenic substrate (DAB) according to the manufacturer's instructions (*see* **Note 12**).
17. Apply DAB to the section at timed intervals and then monitor microscopically for color development. Substrate action can be stopped by washing in distilled water and should be done at the same timed intervals as the application of the substrate.
18. Wash the slides in distilled water.
19. If required to detect nuclei and show general morphology, sections can be lightly counterstained with hematoxylin. Allow to blue in tap water for 10 min. Rinse in distilled water.
20. Dry sections at room temperature, add Vectamount (Vector Laboratories), and coverslip.
21. Analyze using brightfield microscopy.

3.7. Histological Staining

It is important to save one or two sections cut at the start and end of the tissue block for histological examination as this provides morphological detail upon which to interpret the immunolocalization findings. These sections can be conveniently stained using Diff-Quick using the following protocol:

1. Dip section in Diff-Quick solution A for 30 s.
2. Drain and transfer to Diff-Quick solution B for 1 min.
3. Drain and transfer to solution C for 1 min.
4. Drain and rinse in distilled water until water clears.
5. Allow to air-dry and mount with Vectormount.

3.8. Quantitation of Findings

1. Immunostained sections should be examined under low-power microscopy, compared to the Diff-Quick stained sections, and areas of positive and negative staining identified.
2. The sections should next be examined under high power, noting the type and distribution of staining (nuclear, cytoplasmic, matrix, etc.).
3. The results of the experiment can be analyzed and reported manually using a scoring system to denote the number of cells staining positively and/or the observed intensity of staining (e.g., +, ++, +++). Whenever possible, scoring should be carried out "blinded" to avoid reporter bias.
4. As an alternative to manual analysis, the extent and intensity of staining can be analyzed semi-quantitatively by image analysis (*see* **Note 13**).
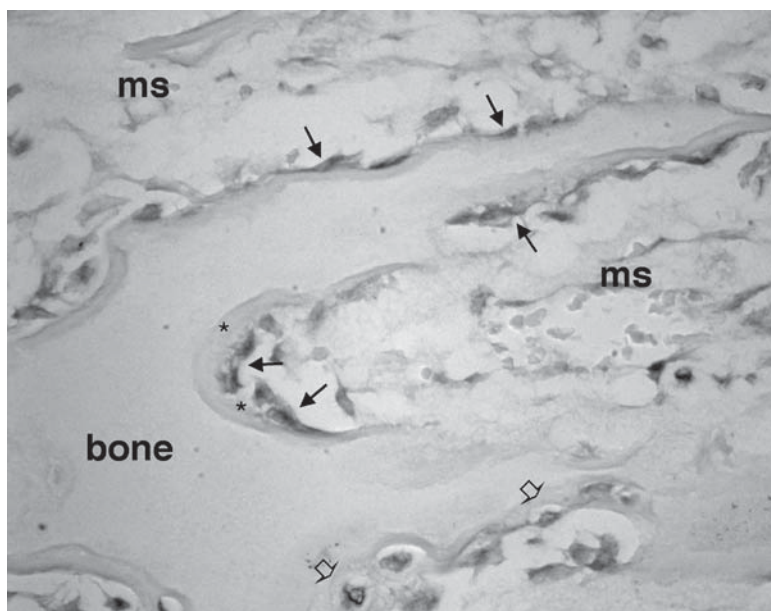
Fig. 2. Black-and-white photomicrograph demonstrating immunolocalization of ER-α by an indirect immunoperoxidase method with sites of antigenicity visualized with DAB (dark gray color). Positively stained osteoblasts *(arrows)*, often adjacent to nonmineralized osteoid (*), are apparent on bone surfaces. Newly incorporated osteocytes *(open arrows)* show ER immunoreactivity. Marrow space cells (MS) surround the cancellous bone (bone).

3.9 Practical Examples of Immunostaining in Bone Sections

We have successfully used the aforementioned procedures to immunolocalize estrogen receptors (ERs) in cryosections of human neonatal bone *(2)* and transforming growth factor-β (TGF-β) in sections from wax-embedded samples of adult human iliac crest bone *(3)*. The former study investigated the differential protein expression of ERα and ERβ in developing human rib (**Fig. 2**). Intense ER expression was observed in osteoblasts and osteocytes in cortical bone. In contrast, ER-β was seen to be most highly expressed in osteoblasts and osteocytes in cancellous bone. The latter study provided quantitative data on the expression of TGF-β, TGF-β receptors, platelet-derived growth factor (PDGF), and osteoclast activity in wax-embedded sections of adult human iliac crest bone samples. Bone sections from women treated with long-term high-dose estradiol were compared to those from women who had received no hormone replacement therapy. The results demonstrated that high-dose estrogen treatment is associated with increased TGF-β, TGF-βR, and PDGF synthesis

and decreased osteoclast activity, consistent with the hypothesis that these factors may mediate the actions of estrogen in bone. These two studies were quite different in their approach, using the various techniques outlined in this chapter, and posed very different questions. The former study was an observational study conducted on frozen tissue fixed in 4% paraformaldehyde after sectioning. The latter study utilized NBF-fixed wax-embedded tissue with quantitative results obtained by image analysis measurements. However, both studies used the same immunoperoxidase localization techniques, demonstrating the versatility and reliability of this method.

4. Notes

1. Dividing biopsies for multiple uses: The biopsy can be halved longitudinally by placing the biopsy in a cylindrical shaped jig fitted with a thumbscrew to hold the biopsy in place. A slot on each side allows a fine modelmaker's saw to cut the through the biopsy. The thumbscrew is released and the 2 pieces of biopsy carefully removed. One half can then be used for histomorphometry and the other half for histochemistry or RNA extraction (**Fig. 3**).

2. Choice of fixative and antigen retrieval techniques: A detailed description of the different fixatives that can be used and their modes of action can be found in textbooks of histochemistry and histopathology *(4,5)*. It is important to realize that the crosslinking action of fixatives may sometimes prevent access of antibodies to its antigen. There are many procedures available to unmask antigens (often referred to as "antigen retrieval"). Proteolytic digestion with enzymes such as trypsin, pronase, and pepsin is widely reported. We have successfully used Protease XXIV (dissolve 12.5 mg of Protease XXIV [Sigma] in 100 mL of PBS. Incubate sections for 30 min at 37°C prior to the ImmunoPure blocking step). Other methods of antigen retrieval use pressure, heat, and microwave irradiation with reported good results. However, it should be borne in mind that all these procedures may have deleterious effects on the adhesion of the section to the slide.

3. Decalcification: After 3 wk in EDTA most bone biopsy samples are fully decalcified; however, larger bone samples may require a longer time in EDTA. If desired, the extent of decalcification can be assessed radiographically.

4. Wax embedding: Wax-embedding procedures require specialist equipment, not normally available in research laboratories. Our samples are embedded by the histopathology department, a service provided by many hospitals. Wax blocks should be stored at 4°C.

5. Techniques for freezing samples: There are many methods of freezing tissue samples, critically reviewed by Chayen and Bitensky *(6)*. It is important to choose a method that avoids the introduction of ice crystals, prevents cracking during freezing, and avoids cell damage, which leads to denaturing of the cytoplasm and loss of membrane integrity. Embedding bone samples in PVA prevents the tissue desiccation associated with low-temperature storage.
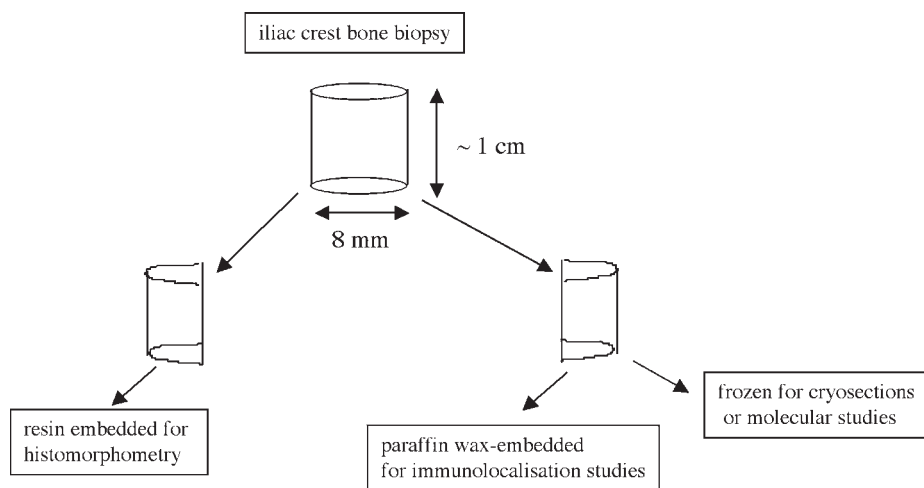
Fig. 3. Iliac crest bone biopsies can be cut longitudinally in a jig to provide two halves: one for resin-embedding for histomorphometry and one for either wax-embedding or freezing.

6. Cryosectioning techniques: We use a Bright Cryostat equipped with a highly polished tungsten carbide knife. The angle of the knife is important, and we generally set this to 19°C. The chuck and bone sample should be allowed to equilibrate to the temperature of the cryocabinet prior to cutting. Orient the block so that the smallest edge hits the knife first. Trim away carefully until full sections are obtained. Move the knife to expose the block to an unused cutting edge.

7. Choice of antibodies and control antibodies: Both monoclonal and polyclonal antibodies can be used successfully for immunostaining bone sections, provided that they bind specifically to the antigen, or epitope of interest. Monoclonal antibodies (MAbs) usually show high specificity and low background staining. They work well on frozen tissue fixed in acetone or paraformaldehyde but are not so reactive in tissue that have been subjected to long fixation times or decalcification. Antigen retrieval in such tissue may sometimes unmask the epitopes (*see* **Note 2**). Polyclonal antibodies usually give a strong staining signal as the antisera contain antibodies that react with different epitopes on the same antigen. Often they are associated with higher background staining than MAbs due to unknown reactivity of irrelevant antibodies from the immunized animal. Polyclonals usually work well in wax-embedded tissue despite some denaturation having taken place. The choice of control antibodies is dependent on the type of primary antibody used. With MAb it is possible to use another MAb directed against an antigen known to be absent from the tissue under investigation. We have successfully used a urease MAb as a control in our bone sections. With polyclonal antibodies it is usual to employ preimmune serum from an animal of the same species from which the primary antibody was generated. Care should be taken to ensure that

the control IgG concentration matches that used for the primary antibody. Further specificity checks can be made by using sections of tissue known to express and tissue known not to express the antigen under investigation. When carrying out these evaluations care should be taken to treat all tissue in the same manner, to minimize the chance of false negatives or positives. Some commercially available antibodies are now available with the appropriate immunizing peptide. Primary antibody is incubated with a 10-fold excess of immunizing peptide at room temperature for several hours prior to addition to the section. The antibody and immunizing peptide will complex, thus preventing binding to the antigen in the section, and give a negative signal. A positive signal would indicate that the primary antibody is binding nonspecifically.

8. Inhibiting endogenous peroxidase activity: Peroxidase enzymes present within the tissue can give false positive results. Hydrogen peroxide mixed in methanol or ethanol provides an efficient blocking agent but is very unstable at room temperature. We have therefore used Immunopure (store at 4°C) which is ready to use and stable at room temperature for the duration of this part of the experiment.

9. Blocking nonspecific binding: The serum used for blocking prior to addition of the primary antibody should be from the same species from which the second antibody has been generated. The optimal concentration can be determined by trial and error.

10. Optimization of primary antibody concentration: Most commercial antibodies are supplied with a data sheet that gives the recommended concentrations. Sometimes these work well without further adjustment, but more often than not, the antibody concentration needs to be optimized for a particular tissue. This can be achieved by carrying out the procedure with a range of antibody concentrations. Staining should decrease with decreasing concentrations of applied antibody. If inappropriate staining occurs or the signal does not decrease at the lowest concentrations of primary antibody it is essential to determine the cause. To ascertain the cause of nonspecific staining the procedure should be repeated with omission of specific components of the staining assay. To achieve this, four sections should be set up; to tissue section 1 add only substrate. To section 2 add ABC and substrate. To section 3 add second antibody, ABC, and substrate. To section 4 add primary antibody, second antibody, ABC, and substrate. Only section 4 should show staining. If staining occurs on the other slides it is necessary to add further blocking steps to eliminate this inappropriate staining at the problem stage. If sections 1–3 are negative but section 4 shows too much signal, decrease the primary antibody concentration. It may also be necessary to increase the concentration of the blocking serum if decreasing the primary antibody does not give the desired results. Too little or weak staining may indicate loss of antigenicity of the primary antibody. This can be checked by repeating the procedure on a tissue known to express the antigen. Other problems should also be considered. The activity of the substrate can be confirmed by mixing a few of the enzyme (ABC) with some substrate. An immediate color change should occur. Too high a concentration of second antibody can diminish signal. A different

fixative can be tried (e.g., acetone), as certain fixatives may mask epitopes, necessitating the use of antigen retrieval techniques.

11. Choice of second antibody: The second antibody should be raised against the species from which the primary antibody is generated. Data sheets will indicate the concentration at which the antibody should be used. If nonspecific staining is a problem, 1% serum from the same species as the tissue being studied can be added to the second antibody as an additional blocking agent.

12. Choice of chromogen: Several chromogens are available for immunoperoxidase procedures but DAB is the one we use as the brown color reaction provides a good contrast to the gray color of bone sections. Also, slides may be permanently mounted using this substrate. **Caution**: Care must be taken when handling DAB as it is a known carcinogen, but the hazards of using the compound are reduced when used in the kit supplied from Vector Laboratories.

13. Image analysis software packages are becoming more widely available and have the advantage of removing the subjective nature of manual scoring. However, care should be taken to ensure that all color thresholds are determined and reflect accurately the positive signal. These thresholds should be used for all measurements within each experiment. All sections should be measured in a similar manner. Comparisons between experiments and between antibodies are to be avoided. Antibodies have different binding affinities, and therefore it would be inaccurate to say that one antigen is more highly expressed than another without other extensive studies. When making comparisons between different samples it is important that these samples should be analyzed in a single run with the same reagents. Particular care must be taken to ensure that all samples within the experiment receive the same incubation and development times.

References

1. Hsu, S. M., Rainem L., and Fangerm H. (1981) A comparative study of the peroxidase–antiperoxidase method and an avidin–biotin complex method for studying polypeptide hormones with radioimmunoassay antibodies. *Am. J. Clin. Pathol.* **75,** 734–738.

2. Bord, S., Horner, A., Beavan, S. R., and Compston, J. E. (2001) Estrogen receptors α and β are differentially expressed in developing human bone. *J. Clin. Endocrinol. Metab.* **86,** 2309–2314.

3. Bord, S., Beavan, S., Ireland, D., Horner, A., and Compston, J. E. (2001) Mechanisms by which high-dose estrogen therapy produces anabolic skeletal effects in postmenopausal women: the role of locally produced growth factors. *Bone* **29,** 216–222.

4. Hopwood, D. (1980) Fixation and fixatives, in *Theory of Histological Techniques*, 2nd ed. (Bancroft, J. D. and Stevens, J., eds.), Churchill Livingstone, London, pp. 20–40.

5. Pearse, A. G. E., ed. (1968) Chemistry of fixation, in *Histochemistry, Theoretical and Applied*, vol. 1. Little, Brown, Boston, pp. 70–105.

6. Chayen, J. and Bitensky, L., eds. (1991) *Practical Histochemistry* 2nd ed. John Wiley & Sons, London.

18

Detection of Noncollagenous Bone Proteins in Methylmethacrylate-Embedded Human Bone Sections

Johannes P. T. M. van Leeuwen and Pieter Derkx

1. Introduction

The organic matrix of bone is a well-organized network of proteins. The main constituent is type I collagen. The noncollagenous proteins (NCPs) comprise about 10% of the total bone protein content. A variety of NCPs has been identified, including osteocalcin, osteopontin, osteonectin, bone sialoprotein, decorin, and biglycan. Of this group only osteocalcin and bone sialoprotein are specific for bone, whereas the other proteins are also present in other, noncalcifying, tissues. The knowledge of their role in and their effects on bone metabolism is limited. It is thought that these proteins play a role in the regulation of mineralization, in the attachment of osteoblasts and osteoclasts to the bone matrix, and/or attraction of cells to the bone matrix. In addition, a second group of proteins can be considered as noncollagenous bone matrix proteins, consisting of so-called growth factors "stored" in the bone matrix and may be released during bone resorption. Of these proteins, distinct cellular effects have been described, for example, regulation of growth and differentiation of cells. They probably do not play a direct role in the initiation of crystal formation of progress and termination of the mineralization process but may play a role in the coupling between resorption and formation. Examples of this second group are transforming growth factor beta (TGFß), insulin-like growth factors, and bone morphogenetic proteins.

So far it appears that both groups of NCPs are involved in bone modeling during development and growth and in adult bone remodeling and fracture healing. It is likely that for an optimal regulation of bone metabolism they act in concert. To achieve this, a coordinated synthesis and localization in the bone

matrix would be essential. To understand the role of the NCPs in bone metabolism and bone diseases it is important to assess their precise localization and quantity and preferably to monitor changes in localization and quantity in aging and disease states. A few studies have examined the localization of noncollagenous bone matrix proteins in animals and in adult human bone.

Immunolocalization studies in combination with standard bone histomorphometry *(1)* will allow the study of the relationship between NCPs and active osteoclasts/osteoblasts, mineralization front, osteoid seams, and so forth. In addition, these combined analyses will provide data on the localization of these proteins in patients with metabolic bone diseases and may add to the knowledge on the function of these proteins. The protocol was set up to be able to perform immunohistochemical analyses to localize and quantify NCPs in adult human bone, in combination with bone histomorphometry. For this the focus was to set up a technique that can also be applied on bone specimens previously embedded in plastic (methylmethacrylate [MMA]) and used for bone histomorphometry.

2. Materials
2.1. Plastic Embedding (see Note 1)

1. MMA monomer (Merck).
2. 0.4 g of Lucidol CH 50-L (a catalyst of polymerization active at –17°C; AKZO Chemicals, The Netherlands).
3. Plastoid N or dibutylphthalate.
4. Benzoylperoxide.
5. Plastoid N or dibutylphthalate.
6. *N,N*-dimethyl toluidine (Merck, accelerator of polymerizaton; *see* **Note 2**).
7. Technovit (Kulzer, Germany) (powder A and solution B: mix A:B = 2:1).
8. Thymol crystals (BDH).

2.2. Preparation of MMA Mixture for –17°C Embedding

Mix the following components in this order:

1. 40 mL of stabilized MMA monomer.
2. 0.4 g of Lucidol CH 50-L.
3. 10 mL of Plastoid N or dibutylphthalate.

2.3. Preparation of MMA Mixture for 37°C Embedding

Mix the following components in this order:

1. 40 mL of stabilized MMA monomer (Merck).
2. 1.4 g of dried benzoyl peroxide (initiator of polymerization active at 37°C). Remove explosive-inhibiting moistness by placing a few grams of powder overnight at 37°C.
3. 10 mL of Plastoid N or dibutylphthalate.

2.4. Technovit Mixture

Mix powder A and solution B: A:B = 2:1.

2.5. Immunostaining

1. Primary antibodies of choice (*see* **Note 3**).
2. 0.1% TPBS: phosphate buffered saline (PBS), pH 7.4, with 0.1% Triton X-100.
3. 10% Normal goat serum (DAKO PATTS, Denmark) in 0.02% TPBS containing 1.5% bovine serum albumin (BSA).
4. Linker and label of the Biogenex Stravigen Multilink HRP kit (San Ramon, CA, USA) (*see* **Note 4**).
5. 3-Amino-9-ethylcarbazole (AEC) (Sigma Chemical, St. Louis, MO, USA).
6. 0.01% H_2O_2 in 0.2 *M* of sodium acetate buffer pH 4.6.
7. 0.2 *M* of sodium acetate buffer, pH 4.6: 13.3 g of sodium acetate trihydrate extra pure (Merck) in 1000 mL of distilled water; add 5.8 mL of glacial acetic acid, 5 mL of Tween 20, and stir for a few min.
8. 1% AEC stock solution: 1 g of 3-amino-9-ethylcarbazole (**Caution**: carcinogen) in 100 mL of *N*,*N*-dimethyl formamide (use a glass container).
9. 1% AEC working solution (prepare fresh): Add 5 mL of AEC working solution to 95 mL of 0.2 *M* of sodium acetate buffer. Filter (wide-pore filter) and add 100 μL of 30% H_2O_2 just before use.
10. Methyl green staining solution: Dissolve 1.65 g of methyl green powder (Nustain) in 250 mL of hot distilled water. Cool at room temperature. Remove purple color (= methyl violet component) by eight washes in 500 mL of chloroform.
11. Thionin stock solution: Heat 0.275 g of Thionin-M3 (C.I. 52000 Waldeck GmbH & Co. Division CHROMA Germany. www.chroma.de) in 100 mL of distilled water at 60°C for 20 min. The powder should be completely dissolved. Cool. The solution can be kept at 4°C for 4 wk.
12. Citrate buffer: Add 1.25 g of anhydrous disodium hydrogen phosphate in 100 mL of distilled water to 0.63 g of citric acid in 300 mL of distilled water until pH 5.8 is reached. A few drops of 2% sodium azide (toxic) should be added it stabilize the solution. This solution can be kept for 2–3 mo at 4°C).
13. Thionin working solution: Mix one part thionin stock solution with five parts of citrate buffer. Heat to 37°C. The pH should be 5.8. Solution can be used for only 1 d.
14. Light green staining solution: Mix 0.3 g of light green with 150 mL of distilled water, add 0.3 mL of glacial acetic acid, pH 2.9. Can be kept for 3 wk at room temperature.

3. Methods
3.1. Bone Biopsy Preparation

1. Bone material can be obtained from various origins. This procedure originally was set up to be applied on human bone but it is anticipated that it is applicable to bone tissue of other species. Osteoporotic iliac crest biopsies, a knee bone fragments (stress fracture), bone biopsies from a distal radius, and normal iliac crest biopsies from adult individuals were used.

3.2. Fixation

1. Fix biopsies at room temperature for 24 h under vacuum (-0.85 bar) in either one of the following fixatives (*see* **Note 5**):
    a. 80% Alcohol.
    b. 4% Phosphate-buffered formaldehyde, pH 6.9.
    c. Burkhardt fixative, pH 7.4.

3.3. Dehydration

Dehydrate and impregnate fixed bone specimens either manually or using an automatic tissue processor according to the following scheme:

1. 80% Ethanol, 1 h.
2. Two times 96% ethanol, 1 h each.
3. Two times 100% ethanol, 1 h each.
4. 100% Ethanol, 10 h.
5. Two times MMA (monomer), 1 h each.
6. MMA (monomer), 7 h (at least).

3.4. Embedding in MMA at –17°C

Here we describe embedding done at –17°C, our current method, but we have in the past performed embedding at 37°C successfully (as described in **Subheading 3.4.**) (*see* **Note 6**).

1. Add specimen and 15 mL of MMA mixture to a 20-mL glass vial (Packard) and place it under vacuum (–0.85 bar) for 1 h.
2. Replace the MMA mixture with 15 mL of fresh MMA mixture and place again under vacuum (–0.85 bar) for 1 h.
3. Cap vial, place it in a box with 70% ethanol and place the box at –17°C.
4. After 1 h take the vial and add 150 μL of *N*,*N*-dimethyl toluidine (accelerator of polymerization) to the 15 mL of cold MMA mixture and shake gently, cap vial, and place it immediately in the 70% ethanol box at –17°C and leave overnight.
5. The next day, first check whether polymerization is complete. If not, leave it longer at –17°C.
6. When polymerization is complete, uncap the vial and discard the remaining liquid. To prevent breaking of the glass vial proceed carefully with the steps that follow.
7. Place capped vial in the 70% ethanol bath and place this in a refrigerator at 4°C for 1 h.
8. Place it at room temperature for at least 1 h, followed by placing bath and vials at room temperature for at least 1 h.
9. Uncap vial and cover sticky MMA upper layer by pouring a few milliliters of freshly prepared Technovit 3040 in the vial. This mixture will polymerize within 15 min at room temperature.

3.5. Embedding in MMA at 37°C

1. Add specimen and 15 mL of MMA mixture to a 20-mL glass vial (Packard) and place it under vacuum (-0.85 bar) for 1 h.
2. Cap the vial and place it in a box with water and place this in an oven at 37°C for at least one night, until polymerization has been completed.
3. Uncap the vial and cover sticky MMA upper layer by pouring a few milliliters of freshly prepared Technovit 3040 in the vial, this mixture will polymerize within 15 min at room temperature.

3.6. Sectioning

1. Carefully remove embedded tissue from the glass vial by wrapping the cooled vial in a tissue and breaking the glass with a small hammer.
2. Cut moistened sections on a Reichert–Jung Polycut S sliding microtome equipped with a Reichert–Jung tungsten carbide knife at an angle of 40°.
3. Mount sections on gelatine–chromium–alum coated slides (*see* **Subheading 3.8.**) using a mixture of egg whites and glycerin (*see* **Subheading 3.7.**).
4. For "immuno" slides: Stretch the sections with a 2:3 mixture of ethylene glycol monbutyl ether and 30% ethanol on a hot plate at 40°C (*see* **Note 7**).
5. For "histomorphometrical" slides: Stretch the sections with 30% ethanol on a hot plate at 70–80°C or use the "immuno" slides preparation described in **step 4** (*see* **Subheading 3.14.**).

3.7. Preparation of Egg White–Glycerin Solution

1. Take a fresh egg, break it, and separate white of egg from the yolk.
2. Put white of egg in a glass and measure volume (will be approx 15–25 mL).
3. Mix egg white until it is stiff (manual mixer).
4. Add an equal part of glycerin and mix again (± 30 sec).
5. Add some Thymol crystals as antibacterial agent and stir again.
6. Cover glass with parafilm and place solution at 4°C overnight.
7. The next day, collect 15–30 mL of the yellow liquid into a small bottle (use a funnel) and store at 4°C. This solution keeps for several months.

3.8. Mounting on Gelatin–Chromium–Alum-Coated Slides

1. Set heating plate to 40°C for immunoslides, to 70–80°C for histomorphometrical slides (*see* **Subheading 3.6.**).
2. Place one drop of egg white–glycerin on a coated slide and rub out with a tissue.
3. Dip section in 30% ethanol and put it down on the slide.
4. Add some drops of 30% ethanol for immunoslides or a 2:3 mixture of ethylene glycol monobutyl ether and 30% ethanol for histomorphometrical slides: "swimming section" (*see* **Subheading 3.6.**).
5. Put slide on heating plate, stretch with two dissection needles by rolling the needle from the middle of the section toward the left and right direction (removing air bubbles and flattening). *It is very important to keep the slide moist!*

6. Cut a strip of transparent cling film to the slide dimension (use the cheapest variety, *see* **Note 8**) and put it on the slide.
7. Pour off the excess ethanol carefully.
8. Put the slide back on the heating plate.
9. Flatten the section by rubbing off with filter paper using thumb or fingers.
10. Place slides between two 5-mm pieces of wood.
11. Clamp under light pressure for one night in a 45°C oven. Place one clamp in the center and or two clamps, one at either end.

3.9. Removal of MMA (see Note 9)

1. Remove MMA from bone sections with a 1:1 mixture of xylene and chloroform for 30 min under constant stirring (important) in a setup as shown in **Fig. 1**.
2. After 30 min place slides in xylene for 1 min.
3. Wash slides three times in 100% ethanol, 20 sec each.
4. Wash slides two times in 96% ethanol, 20 sec each.
5. Wash slides two times in 70% ethanol, 20 sec each.
6. Wash slides in 50% ethanol, 20 sec.
7. Wash slides in distilled water, 20 sec.

3.10. Decalcification (see Note 10)

1. Sections are decalcified by incubation for 10 min in 1% acetic acid in the device shown in **Fig. 1** under constant stirring.
2. Rinse slides twice with distilled water.

3.11. Immunochemistry

The protocol for immunostaining given here works for a range of antibodies *(2)*. All incubation steps (blocking, antibody incubation, and detection) should be carried out in a closed humidity chamber with the glass slides placed horizontally. The volumes used per section are 100–200 µL. Capillary incubation systems (such as Techmate) in our hands result in lower staining intensity.

1. Inhibit endogenous peroxidase activity by incubating the sections in a 10:1 mixture of methanol and 30% H_2O_2 for 25 min at room temperature.
2. Wash slides two times in distilled water.
3. Rinse slides in 0.1% TPBS (*see* **Note 11**).
4. Block with 10% normal goat serum in 0.02% TPBS containing 1.5% BSA (*see* **Note 12**).
5. Remove excessive liquid by placing the edge of the glass slide on a tissue.
6. Incubate with primary antibody in 0.02% TPBS containing 1.5% BSA overnight at 4°C.
7. The next day, wash sections for 5 min with three changes of 0.1% TPBS.
8. Incubate sections with 1:50 diluted Linker in 0.02% TPBS + 1.5% BSA for 45 min.
9. Wash three times with 0.1% TPBS, 5 min each.
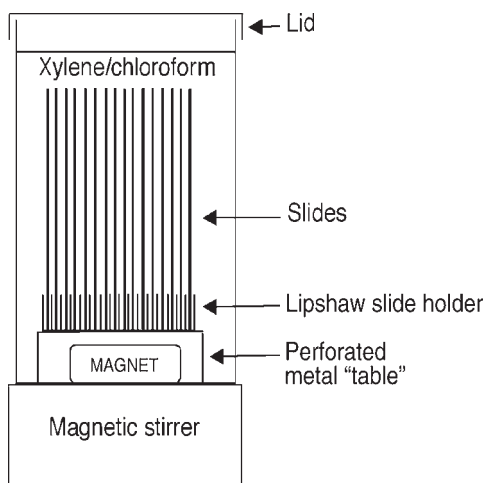
Fig. 1. Device for removal of MMA and decalcification.

10. Incubate with 1:50 diluted label in 0.02% TPBS + 1.5% BSA for 45 min (Label = peroxidase-conjugated biotin streptavidin).
11. Wash sections for 30 min with 0.2 mol/L of sodium acetate.
12. Incubate with 0.05% AEC and 0.01% H_2O_2 in 0.2 mol/L of sodium acetate trihydrate buffer, pH 4.6, for at least 15 min and check staining intensity under microscope (*see* **Notes 13** and **14**).
13. Rinse sections with 0.2 mol/L of sodium acetate trihydrate buffer for 10 min.
14. Rinse with running tap water followed by distilled water.
15. Counterstain with methyl green, 15 sec.
16. Rinse in distilled water, two times, 10 sec each.
17. Remove excessive liquid by placing the edge of the glass slide on a tissue, for a few seconds.
18. Mount in glycerin immediately.
19. Seal glass edges with nail polish or hot wax.

3.12. Modification of Staining Protocol for Quantitative Analyses

When quantitative analysis is required use the staining protocol below *(3)*:

1. After **step 14** in **Subheading 3.11.** continue as follows:
2. Incubate slides in thionin for 2 min.
3. Rinse shortly with distilled water.
4. Dip the sections for 3 s in 0.2% light green solution.
5. Rinse shortly with distilled water.
6. Remove excessive liquid by placing the edge of the glass slide on a tissue, for a few seconds.

7. Mount in glycerin.
8. Seal glass edges with nail polish or hot wax.

3.13. Digital Quantitative Analyses

After staining the sections can be digitized and quantitatively analyzed. The given protocol and equipment has been shown to be successful. However, other microscopes, cameras, and software platforms might also be applicable (*see* for example Chapter 24 by van 't Hof, *this volume*).

1. Digital images of immunostained samples are captured by a three-chip color charge-coupled device (CCD) camera, 512 × 512 pixels (Sony) mounted on a Zeiss Axioplan microscope (Zeiss, Oberkochen) with a ×20 objective.
2. The KS-400 (version 1.2) digital image analysis system (Kontron) is used for the analysis of images of 30 trabecular and 20 cortical bone areas in each of four 5-μm sections cut at steps of 100 μm in the same bone biopsy.
3. For determining the area of the mineralized matrix (green) and NCPs (red/brown), thresholds are set on the green and red channel. The thresholds are determined interactively on the basis of three different images. Then, the determined threshold is used to analyze automatically all recorded images of all sections that are stained in the same staining session.
4. The area of the mineralized matrix is calculated by counting pixels and eventually expressed as μm^2.
5. The same procedure is used to estimate immunostained areas. The ratio of the area of immunostained regions and the area of the mineralized matrix are calculated in each microscopic field. Analysis with osteopontin and osteonectin demonstrates that the measurements are more or less stable when the number of microscopic fields exceeds 50 *(2)*.

3.14. Histomorphometry

For histomorphometry in combination with immunolocalization, parallel sections are stained with Goldner *(3)*, a modified von Kossa *(4)* or tartrate-resistant acid phosphatase. Details of these staining procedures can also be found in the chapter by Everts et al. and Chapter 24 by van 't Hof et al., *this volume*.

4. Notes

1. All resin mixtures should be prepared just before use. Care should be taken when handling plastic monomers, wear gloves and work in a fume hood as much as possible. Dispose of waste carefully and in compliance with local rules.
2. Dimethyl toluidine can be used instead of dimethyl aniline.
3. We have used the protocol described successfully with the following antibodies: Rabbit polyclonal antibodies LF-7 to osteopontin, LF-32 to osteocalcin, BON-1 to osteonectin, LF-83 to bone sialoprotein, LF-51 to biglycan, and LF-30 to decorin. These were a generous gift of Dr. L.W. Fisher, National

Institutes of Health, Bethesda, MD, USA *(5)*. We have also used rabbit polyclonal antibodies against human transforming growth factor β_2 and β from Santa Cruz Biotechnology (Santa Cruz, CA, USA) and antibodies against human insulin-like growth factor-I from GroPep (Adelaide, Australia). This protocol therefore has proven to be applicable for detection of a range of antigens in mineralized bone *(2)*.

4. Linker contains a mixture of biotinylated goat anti-immunoglobulin antibodies and reacts with mouse, rat, rabbit, and guinea pig immunoglobulins. Other species-specific detection systems will also be applicable.

5. Satisfactory results can be obtained with all three types of fixatives.

6. Immunohistochemical analysis of NCPs can be performed after both procedures of embedding. At present, we routinely embed at -17°C but we have previously performed successful immunostaining of NCPs in bone fixed in Burkhardt and embedded at 37°C, 30 yr ago.

7. To obtain good immunosignal it is important that slides are stretched at maximal 40°C because at higher temperatures the efficiency of the antigen detection is reduced.

8. The cheaper types of cling film are best because they do not stick to the sections/slides.

9. The major advantage of MMA is that after sectioning it can be completely removed. This provides optimal penetration of the antibodies and chemicals necessary for immunostaining and histochemical staining. In addition, there is no background staining of plastic remains. With nondeacrylated sections staining of the bone matrix was much weaker and no cellular staining is observed.

10. Decalcification generally yields better immunostaining.

11. For some antibodies it might be advantageous to pretreat the sections before blocking with 0.1% saponin (0.1 g of saponin in 100 mL of distilled water, prepare just before use) for 30 min at room temperature. After saponin treatment generally lower concentrations of antibody can be used.

12. To avoid background staining preincubation with normal goat serum is essential.

13. AEC staining requires mounting in glycerin, which does not prevent fading (within 1 wk) of the AEC signal and of dissolution of the thionin–light green stain. However, this period is long enough to digitize and store the images. Water-based polymers cannot be used because they result in disrupted trabeculae due to shrinkage.

14. 3,3'-Diaminobenzidine (DAB) can also be used but in general AEC gives a more intense staining, more contrast, and no background.

References

1. Recker, R., ed. (1983) *Bone histomorphometry, Techniques and Interpretation.* CRC Press, Boca Raton, FL, pp. 17–22.

2. Derkx, P., Nigg, A. L., Bosman, F. T., et al. (1998) Immunolocalization and quantification of noncollagenous bone matrix proteins in methylmethacrylated-embedded adult human bone in combination with histomorphometry. *Bone* **22**, 367–373.

3. Derkx, P. and Birkenhäger-Frenkel, D.H. (1995) A thionin stain for visualizing bone cells, mineralizing fronts, and cement lines in undecalcified bone sections. *Biotech. Histochem.* **70**, 70–74.

4. Birkenhäger-Frenkel, D. H., Grieten, P., and van der Heul, R. O. (1977) A new staining method for bone, osteoid, and cells in undecalcified bone sections. *Calcif. Tissue Int.* **24**, (*Suppl. 4*).
5. Fisher, L. W., Stubbs, J. T. III, and Young, M. F. (1995) Antisera and cDNA probes to human and certain animal model bone matrix noncollagenous proteins. *Acta Orthop. Scand.* **66**, 1–5.

19

Fluorescence Imaging of Bone-Resorbing Osteoclasts by Confocal Microscopy

Stephen A. Nesbitt and Michael A. Horton

1. Introduction

Osteoclasts are large multinucleate bone cells with the capacity to degrade bone by the process of bone resorption and, thus, participate in the homeostasis of bone and calcium in the body *(1)*. Imaging of osteoclasts can be performed by a variety of microscopy methods including light microscopy, electron microscopy, and atomic force microscopy (AFM) *(2,3)*. These techniques, together with histochemical and immunocytochemical stains, enable the researcher to analyze the cellular structure and function of this complex cell type both in vivo within bone tissues and isolated in vitro in primary cell cultures (see Part II, Culture of Osteoclasts).

Unlike electron microscopy and AFM, which require a high degree of technical expertise, methods for light microscopy, including laser scanning confocal microscopy (LSCM), are generally quick, easy to apply, and allow the screening of large numbers of cells. Furthermore, the combination of fluorescence immunostaining and LSCM has provided a powerful, "hands-on" system for cell imaging (**Fig. 1**) *(4)*. Today, the simplification of the LSCM user interface has made these systems accessible to many researchers and, to date, more than 10,000 publications have cited the application of LSCM.

An early application of fluorescence immunostaining and LSCM was that used by Lakakkorpi and colleagues in 1993 to assess cell adhesion sites in bone-resorbing osteoclasts *(5)*. From these studies, it was apparent that confocal microscopy was a technique that showed several advantages for cellular imaging in the field of bone cell biology. First, these techniques enabled sectional views of the resorption sites to be collected without the need to cut the specimens physically by tissue sectioning on a microtome. This is particularly
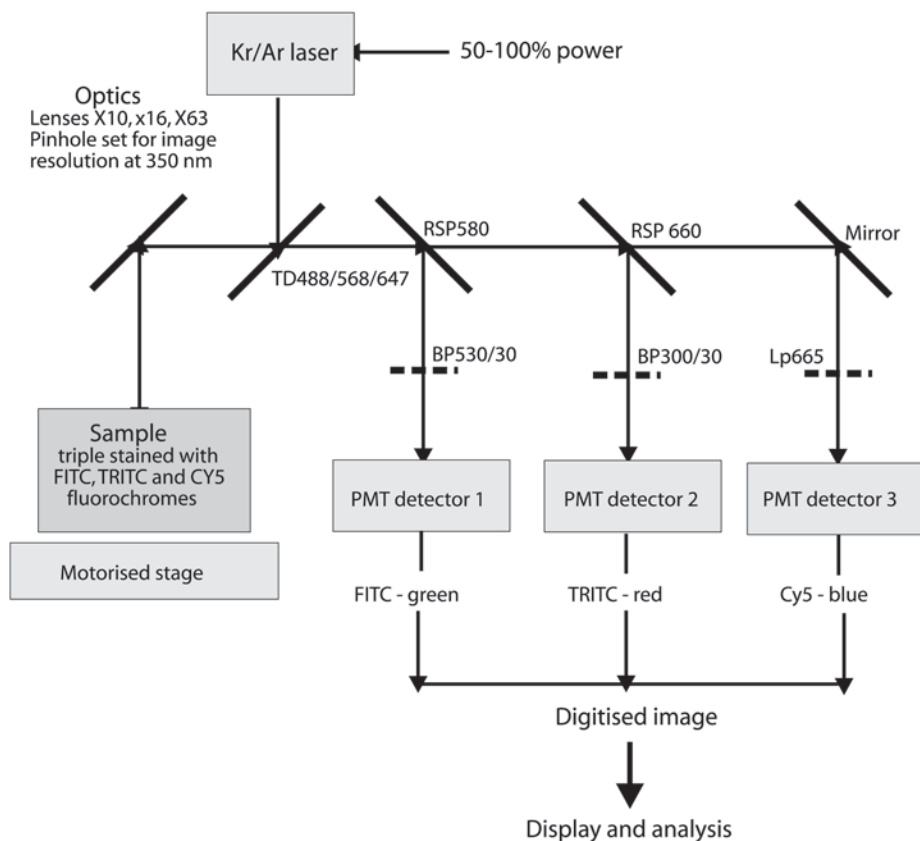
Fig. 1. Imaging of fluorescently labeled specimens by laser scanning confocal microscopy: a schematic diagram of protocols. A krypton–argon laser provides a bright light source of known wavelengths that illuminates the specimen in focus. It scans the sample to reduce the time it is exposed to the light source, and so minimizes the "bleaching" of the fluorescence stains. The tripled-stained sample is sequentially exposed to the laser light at wavelengths 488, 568, and 647 nm for excitation of the FITC, TRITC, and CY5 fluorochromes, respectively. Pinholes situated at the laser light source and detectors ensure that "out-of-focus" fluorescence is omitted and only light from the focal plane is collected within an optical section of 350-nm thickness. Mirrors target the emitted light form the FITC, TRITC, and CY5 fluorochromes (emission wavelengths 518, 576, and 670 nm, respectively) through a series of filters. The filtered light is collected by the detectors and converted into electrical signals and displayed as a digitized image. The specimen is mounted on a motorized stage and allows multiple optical sections to be sequentially collected at various depths throughout the specimen. The images can be viewed in both *xy* and *zx* planes and displayed in various formats: single fluorescence, intensity maps, merged for the analysis of colocalization of signals, or stacked to show a through focus view of the sample.

advantageous, as the procedures used to process bone samples prior to cutting (demineralization and tissue embedding methods) can destroy cell morphology and render protein epitopes inactive or inaccessible to a majority of antibody probes. Furthermore, imaging of osteoclasts in bone by conventional fluorescence microscopy can be limited by the excessive autofluorescence given by the mineralized matrix in bone, and by blurring of the object owing to its inherent thickness. The confocal microscope allows for these background signals to be assessed and removed and can penetrate, in focus, deep into a specimen; thus, it can provide clear images of osteoclasts and their subcellular structures.

Herein, the application of fluorescence immunostaining and LSCM methods are described for the imaging and functional analysis of bone-resorbing osteoclasts. An in vitro model of bone resorption of human osteoclasts isolated from human osteoclastoma (giant cell tumor of bone) tissue and seeded onto biotin-labeled dentine was used *(6)*. The cells were probed by triple fluorescence staining and visualized with LSCM. The osteoclasts were identified by the presence of characteristic rings or arcs of F-actin staining with phalloidin-tetramethylrhodamine isothiocyanate (TRITC) and the resorption sites were identified by a loss of the biotin label from the dentine surface with streptavidin–CY5. Primary antibody probes together with secondary-labeled anti-immunoglobulin fluorescein isothiocyanate (FITC) antibodies enabled proteins of interest to be examined for their localization within osteoclasts in the ruffled border, sealing zone, basolateral plasma membrane, within the cell body, and in the resorption pit. The resorption sites were imaged as cellular sections taken in *xy* (above view) and *zx* (lateral view) planes with single- and triple-color displays and reconstructed as views in two- and three-dimensional formats *(7)*. The lysosomal associated membrane protein (LAMP) *(8)*, the cell surface receptor $\alpha_v\beta_3$ integrin *(9)*, and the metalloproteinase MMP-9 *(10)* were used as example molecules to demonstrate the application of these osteoclast imaging techniques both in vitro in resorption cultures and also in vivo, in thick cryosections of osteoclastoma.

The application of these imaging techniques to functional analysis is further discussed and include the use of FITC labels to "track" the exogenous addition of compounds within the resorption cultures and measurement of resorption using fluorescence intensity profiles to quantify the amounts of degraded matrix endocytosed by osteoclasts during the bone resorption process *(6,11)*.

Fig. 1. *(continued)*Additional computation is required to convert the image stack into a 3D reconstruction. Image analysis can show fluorescence profiles and quantify fluorescence signals for the whole specimen or for discrete sites within the specimen.

2. Materials
2.1. Buffers and Solutions

1. Tissue culture media: Minimum essential medium (MEM), 10% fetal calf serum (FCS), 2% glutamine, penicillin, and streptomycin (GPS) at 100 U/mL (Gibco/Invitrogen).
2. Phosphate-buffered saline–Dulbecco A (PBS), pH 7.2 (Oxoid, UK).
3. Fixation buffer: 3.5% Paraformaldehyde, 2% sucrose in PBS (*see* the chapter by Everts et al., *this volume*, for details).
4. Wash solution: PBS, 5% normal calf serum (Gibco/Invitrogen), 0.05% sodium azide, pH 7.2.
5. Freezing buffer: PBS, 2.3 M sucrose, 0.05% sodium azide.
6. Biotin staining buffer: 230 mM NaCl, 50 mM NaHCO$_3$, pH to 8.2 with 1 M HCl.
7. Triton permeabilization buffer: 0.5% Triton X-100 (Pierce, UK), 20 mM N-2-hydroxyethylpiperazine-N'-2-ethanesulfonic acid (HEPES), 300 mM sucrose, 50 mM NaCl, 3 mM MgCl$_2$, 0.05% sodium azide, pH 7.0.
8. Saponin permeabilization buffer: 0.1% Saponin (Calbiochem, UK) in piperazine-N,N'-*bis* (2-ethanesulfonic acid) (PIPES) buffer, pH 6.8.

2.2. Reagents for Immunostaining and Protein Labeling

1. Primary antibodies of choice.
2. Secondary antibodies, for example, rabbit anti-mouse, swine anti-rabbit, or swine anti-goat immunoglobulin reagents (Dakopatts, Denmark).
3. Streptavidin–Cy5 (Amersham/Pharmacia, UK).
4. Phalloidin–rhodamine (Molecular Probes, Leiden, The Netherlands).
5. Antifade: PBS Citifluor (Canterbury University, UK).
6. Fluoro-Link reactive dye, FluoroX No. A28000 (Amersham, UK).
7. Centricon columns, 3-kDa cutoff (Millipore, UK).

2.3. Cells and Tissues

1. Elephant tusk (*see* **Note 1**).
2. Giant cell tumor of bone (osteoclastoma).

2.4. Equipment

1. ISOMET low-speed diamond saw (Buehler, USA).
2. Leica scanning laser confocal microscope, system TCS NT (Leica, Heidelberg, Germany) equipped with a multiline 750 mW Omnichrome krypton–argon laser (Chino, USA) and objective lenses ×10 (NA 0.30), –16 (NA 0.50), and ×63–water immersion (NA 1.20).
3. Silicon Graphics O$_2$ Workstation (SGI, Mountainview, CA, USA) and Imaris software for image analysis (Bitplane, Zurich, Switzerland).

3. Methods
3.1. Preparation of Dentine Discs

Dentine provides a suitable matrix substrate to study osteoclastic bone resorption in vitro *(12–14)* (*see* **Note 1**).

3.1.1. Cutting and Steriliation of Dentine

1. Using an electric bandsaw, cut the elephant tusk across its length at 5-cm intervals to give a series of large dentine discs. Rotate the discs 90°C and saw into four to eight equal segments (*see* **Note 2**).
2. Slice the segmented blocks of dentine into fine wafers (100 μm in thickness and a surface area 2–3 cm^2) with a water-cooled, ISOMET low-speed diamond saw (Buehler, USA); operate at speed no. 4 and weight the dentine block with 125 g to cut flat slices of dentine.
3. Rinse the wafers in distilled water and allow to soak for 1 h to soften the dentine before "hole punching" the wafers into 6-mm discs. Collect 200 discs.
4. Polish both sides of the dentine disks by rubbing onto 3MM paper, each for 10 s.
5. Mark the discs with a no. 2 pencil on one side. This assists to assess the orientation of the disc in future experiments; place the discs with the mark on the lower surface when manipulated or when in culture.
6. Wash in 50 mL of distilled water for 30 min on a roller mixer to remove debris. Repeat the washing procedure twice.
7. Sterilized the discs in 70% ethanol for 5 s, and rinse three times in sterile distilled water (*see* **Note 3**).
8. In a laminar flow tissue culture hood, dispense the discs into a large Petri dish (keep sterile) and allow them to dry. After 2 h, flip the discs and allow thorough drying for another 2 h before storing at room temperature (RT). This is a convenient stop point. Alternatively, to avoid drying the discs, leave out **step 8** and continue on to the biotinylation methods described in **Subheading 3.1.2.**

3.1.2. Surface Biotinyation of Dentine Discs

The surface mineral is partly stripped during dentine cutting and a proportion of the matrix proteins are exposed at the dentine surface. Biotin provides a suitable label for these exposed proteins including type I collagen, which comprises >90% of the organic matrix in bone and dentine *(6)*. Biotinylation products are stable and do not affect osteoclast resorption. Herein, the dentine proteins are quickly and easily labeled with a protein biotinylation kit using the biotinylation reagent biotinamidocaproate *N*-hydroxysuccinamide ester (*see* **Note 4).**

The ECL protein biotinylation kit (RPN 2202, Amersham/Pharmacia, UK) was primarily designed for biochemical applications, but in addition, it has proved useful for the surface labeling of dentine discs. The labeling should be performed under sterile conditions.

1. Place 200 dentine discs in a 30-mL universal container and rehydrate in 10 mL of distilled water on a roller mixer for 10 min. Discard the wash and repeat twice.
2. Add 10 mL of 50 m*M* NaHCO$_3$ buffer pH 8–8.5 (made fresh, from the 20× stock in the kit) and wash for 10 min. Discard the buffer and repeat the wash once. Resuspend in 10 mL of buffer.

3. Allow the biotinylation reagent to equilibrate at RT for 30 min. Add 50 μL of the biotinylation reagent, and gently invert/mix to resuspend the discs/buffer/label. Cover the universal container with foil to shield from direct light. Place on a roller mixer for 1 h and every 10 min gently invert/mix and return to the roller mixer (*see* **Note 5**).

4. Discard the buffer and transfer the discs to a 50-mL tube for thorough washing. Resuspend in 40 mL of distilled water and wash vigorously on roller mixer for 30 min. Discard the wash and repeat the washing five times.

5. Place the biotinylated discs into a large Petri dish and add 200 mL of PBS with 100 U/mL of penicillin–streptomycin and leave to soak overnight in a humidified incubator with 5% CO_2.

6. Remove the soaking solution and dry the biotinylated discs as described in **Subheading 3.1.1.**, **step 8** and store at 4°C in a dessicated box (*see* **Notes 6** and **7**).

3.2. Preparation of Osteoclasts from Giant Cell Tumours of Bone

Osteoclastomas (giant cell tumor of bone) are rare bone tumors, but provide an invaluable source of mature human osteoclasts that are otherwise difficult to extract from the hard matrix of bone. These cells are not the neoplastic cell type and have a normal phenotype and function *(15,16)*. The osteoclasts isolated from osteoclastoma are generally large (>50 μm) and this helps to image the bone-resorbing osteoclasts and their subcellular structures by LSCM.

The following method allows large numbers of viable osteoclasts to be extracted from osteoclastoma tissues by digestion of the collagenous extracellular matrix *(17)*. Typically, 2×10^6 osteoclasts can be obtained from 5 g of osteoclastoma tissue. The cells can be placed directly into tissue culture or frozen for long-term storage.

1. Perform all procedures in sterile conditions.

2. Take the osteoclastoma tissue immediately after surgical removal and place into MEM with 2% glutamine and penicillin–streptomycin at 100 U/mL (MEM–GPS) and leave on ice.

3. Dissect out the fat, connective, and necrotic tissues.

4. Place 5 g of osteoclastoma into 5 mL of ice-cold MEM–GPS and chop into a fine tissue suspension.

5. Add 10 mL of type I collagenase (Sigma, UK) at 3 mg/mL in MEM–GPS, mix, and incubate at 37°C for 30 min. Further mix to resuspend the tissue digest every 5 min. Prewarm the collagenase solution for 10 min at 37°C before use.

6. Pass the digested tissue through a sieve with a 100-μm mesh (Falcon, UK). Use the plunger from a 5-mL syringe and 30 mL of MEM–GPS at RT to mix and flush the osteoclastoma cells through the mesh. Discard the undigested tissue left in the sieve. (*see* **Note 8**).

7. Centrifuge the osteoclastoma cells at 200*g* for 10 min at RT.

8. Resuspend and wash the cell pellet in 50 mL of MEM–GPS with 10% FCS and repeat **step 7**. Finally, repeat **steps 8** and **7** at 4°C and place the cell pellet on ice.

9. Resuspend the cell pellet in tissue culture media (MEM–GPS and 10% FCS) and proceed with the resorption cultures in **Subheading 3.3.**
10. Alternatively, freeze the osteoclastoma cells at 2×10^4 osteoclasts per cryovial in 1 mL of MEM with 40% FCS and 10% dimethyl sulfoxide (DMSO). After rate freezing to –70°C, store the cells in liquid nitrogen.
11. To retrieve the cells from frozen stocks, reconstitute a vial of frozen cells with 10 mL of ice-cold MEM–GPS and repeat **step 7** at 4°C followed by **step 9**. The osteoclast viability is approx 50% after freezing the cells.

3.3. Resorption Cultures

In vitro models to study osteoclastic bone resorption were initially described by Boyde et al. and Chambers et al. in 1984 and Arnett and Dempster in 1986 *(12–14)*. Osteoclasts are cultured on the surfaces of bone and dentine and form resorption pits that are similar to resorption sites seen in vivo. The number and size of the pits provide a measure of resorption and these models can be used to screen compounds that regulate bone resorption *(18–20)*.

Herein, human osteoclasts isolated from osteoclastoma tissue are cultured on biotinylated dentine discs and are used to study cellular structure and function in bone-resorbing osteoclasts by fluorescence immunostaining and LSCM *(6)* (*see* **Note 9**).

1. Soak the biotinylated dentine discs in culture media (MEM–GPS and 10% FCS) for 30 min.
2. Remove the media and place the discs onto a sheet of sterilized parafilm in a Petri dish. Excess media remaining on the dentine surface can be removed by touching the edge of the disc on a flat sheet of tissue paper, but do not allow the discs to dry out, as this will inhibit cell attachment.
3. Resuspend the osteoclastoma cells in culture media. Between 1% and 5% of the osteoclastoma cells are osteoclasts. Apply 100–200 osteoclasts per disc. Use a 1-mL pastette (Jencons, UK) and place a droplet of cells onto each disc. The discs hold approx 40 µL and the droplets are held in position by the hydrophobicity of the parafilm.
4. Transfer the cells into tissue culture incubator, providing a humidified atmosphere of 5% CO_2 at 37°C for 2 h.
5. Rinse off nonadherent cells by shaking the discs in a bath of PBS at 37°C (*see* **Note 10**).
6. Place the discs and attached cells, which includes an enriched population of osteoclasts, into resorption media (MEM–GPS, 10% FCS, and 10 m*M* HCl to provide an operating pH of 6.9) and return to tissue culture for 22 h. Resorption is optimal under these conditions (*see* the chapter by Hoeberts and Arnett, *this volume*, for discussion of optimal pH for resorption). Use a 24-well tissue culture plate and place one to four discs per well with 1 mL of media (*see* **Note 11**).
7. To remove cytosolic components from the cells refer to **Subheading 3.4.** Alternatively, proceed onto **step 8**.

8. Quickly rinse the discs in MEM and immediately add to each well 1 mL of a 50:50 mixture of MEM with paraformaldehyde fixation buffer (3.5% paraform-aldehyde, 2% sucrose in PBS) at 37°C and leave for 10 min. Alternatively, fix the discs in ice-cold methanol for 6 min on ice *(21)* (*see* **Note 12**).
9. Rinse the discs three times in PBS and leave in wash (5% NCS, 0.05% sodium azide, and PBS) at 4°C.
10. Proceed to the cell staining methods described in **Subheading 3.5.** Alternatively, soak the discs in freezing buffer (2.3 *M* sucrose in PBS with 0.05% sodium azide) at 4°C for 4 h and store at –70°C. To retrieve the frozen discs, thaw at RT and repeat **step 9** (*see* **Note 13**).

3.4. Removal of Cytosolic Proteins from Osteoclasts During Cell Culture

Some cell proteins are expressed in high amounts in the cytosol compared to their membrane-associated forms. Thus, to see the membrane associated proteins it may be necessary to remove the cytosolic forms. This can be achieved by a temporary permeabilization of the cell membrane with saponin during tissue culture, with the cytosol being released into the media before cell fixation *(21,22)*. Previously, these procedures have been used in osteoclast cultures to visualize membrane bound annexins by fluorescence immunostaining and LSCM *(11,23)*.

1. Place the saponin permeabilization buffer (0.1% saponin, 80 m*M* disodium PIPES, pH 6.8) in a CO_2 incubator for 1 h.
2. Rinse the resorption culture discs in MEM at 37°C.
3. Add the prewarmed/pregassed saponin to the cells and return to tissue culture for 5 min.
4. Repeat **step 2** and fix the cells as described in **Subheading 3.3.**, **steps 8–10**.

3.5. Multicolor Labeling of Cells by Fluorescence Immunostaining

A variety of fluorescent probes are available to immunostain cells and sub-cellular structures and these include probes for the plasma membrane, nucleus, Golgi, mitochondria, lysosomes, and the cell's cytoskeleton (Molecular Probes, Holland; www.probes.com). Various combinations of these stains allow multiple cell types, cell structures, and cell proteins to be examined together.

3.5.1. Cell Permeabilization

Cell permeabilization is required after cell fixation with paraformaldehyde to allow intracellular access of the antibodies and fluorescence stains.

1. Select the number of cultured discs required for staining. Use a 24-well tissue culture plate and place a cultured disc into each well and add 1 mL of wash (5% NCS, 0.05% sodium azide, and PBS) and leave on ice.

2. Rinse the discs in PBS, and permeabilize the cells for 5 min in 1 mL of ice-cold Triton X-100 permeabilization buffer (20 mM HEPES, 300 mM sucrose, 50 mM NaCl, 3 mM MgCl$_2$, 0.5% Triton X-100, 0.05% sodium azide, in PBS at pH 7.0). Alternatively, use 0.1% saponin permeabilization buffer (0.1% saponin, 80 mM disodium PIPES, pH 6.8) for 30 min on ice.
3. Rinse the discs twice in PBS and soak in wash for 30 min (*see* **Note 14**).

3.5.2. Triple Fluorescence Immunostaining

Triple fluorescence immunostaining of the resorption cultures enables the resorption sites and resorbing osteoclasts to be identified and characterized within the mixed cell population of osteoclastoma cells. Resorbing osteoclasts are identified by their characteristic sealing zones and are stained for F-actin with a phalloidin–rhodamine conjugate. The biotinylated matrix proteins are probed with a streptavidin–CY5 conjugate and the resorption pits stain negative due to the loss of the biotinylated matrix from the resorption sites. Additional proteins are stained with specific primary antibodies and secondary labeled anti-immunoglobulin FITC antibodies.

Perform all subsequent cell rinsing/washing on ice in a 24-well tissue plate and the staining at RT in a wet box. Do not let the cells dry out at any stage of the staining procedure, as this will increase sample autofluorescence and elevate background signals in the LSCM analysis.

1. Take the permeabilized cells and drain off the excess wash from the surface of the disc by touching its edge onto tissue paper.
2. Place the discs on a sheet of parafilm in a wet box.
3. Add 100 µL of primary antibody (e.g., a mouse monoclonal, or a rabbit or goat polyclonal) in wash and probe for 30 min. The concentrations of the primary antibodies will vary, but generally, 5–10 µg/mL, or a 1:100 dilution of polyclonal sera is a good starting point.
4. Repeat **step 1** and rinse the discs twice in PBS and leave to soak in wash for 30 min.
5. Repeat **steps 1** and **2** and add 100 µL of FITC-conjugated secondary polyclonal antibody at a 1:40 dilution in wash and stain for 30 min.
6. Repeat **step 4**.
7. Repeat **step 1** and add 100 µL of streptavidin–CY5 at 10 µg/mL in biotin staining buffer (230 mM NaCl, 50 mM NaHCO$_3$, pH to 8.2) for 60 min.
8. Repeat **step 4**.
9. Repeat **step 1** and add 100 µL of phalloidin–rhodamine conjugate at 5 U/mL in wash and stain for 30 min.
10. Repeat **step 4**.
11. Stain additional discs for negative controls. Repeat **steps 1–11**, but omit staining with primary antibodies, **steps 3** and **4**.
12. Mount the triple-stained samples in PBS–antifade reagents and view by fluorescence microscopy and LSCM (*see* **Note 15**).

3.6. Laser Scanning Confocal Microscopy

A variety of confocal microscopes are available and include systems manufactured by Leica, Bio-Rad, Zeiss, and Olympus. Herein, a Leica TCS NT confocal microcope (Leica, Heidelberg, Germany) equipped with a multiline 750-mW Omnichrome krypton–argon laser (Chino, USA) was used to image osteoclasts after triple-color immunostaining *(6,7)*. Excitation of the fluorochomes FITC, TRITC, and rhodamine, and CY5 was performed at 488, 568, and 647 nm, respectively, and their optical images were collected, digitised, and displayed in pseudocolors of green, red, and blue, respectively (refer to **Fig. 1** for a schematic diagram of LSCM).

3.6.1. Setting up the Confocal Microscope

1. Go to the acquisition interface.
2. Adjust the filters for FITC, TRITC, and CY5 and activate their sequential collection.
3. Select the appropriate objective lens, ×16 or ×63. A ×16 objective lens is suitable for low-power overviews of the resorption sites and a ×63 enables high-power images of individual osteoclasts and resorption sites to be examined.
4. Set the mode to *xy* to collect optical sections in the horizontal plane.
5. Keep the pinhole setting at 1 for optimal image resolution (> 350 nm).
6. Set the collection speed to medium, the zoom to ×1, and image format to 512, the section number to 16, and the section accumulations to 2.
7. Adjust the laser to 50% power and photomultiplier tube voltage thresholds (PMT) to between 400 and 700 mV for channels 1 (FITC), 2 (TRITC). and 3 (CY5).

3.6.2. Image Collection

1. View the samples on the standard fluorescence microscope with the FITC and TRITC filters and light from the mercury UV lamp. Use a ×10 objective to screen the sample.
2. First check the negative controls samples for nonspecific staining.
3. Identify the resorbing osteoclasts by their F-actin rhodamine staining with the 568-nm filter (**Fig. 2A**).
4. Select a representative area of osteoclastic resorption and view with a ×16 objective.
5. Check the FITC staining with the 488-nm filter. Note, the CY5 647-nm wavelength is not visible with light from the mercury UV lamp and can be viewed only with the laser light source.
6. Scan the negative control sample with the confocal microscope and adjust the PMTs for each channel to gate out the background signals from nonspecific staining and autofluorescence from the cells and the dentine discs.
7. Repeat **steps 3–5** on the stained positive samples and scan. Lower the PMTs if the fluorescence signals for the images are too high and adjust to obtain a distinct staining pattern. Crosstalk between the channels may be visible on the scanned images, but is removed when the scan is, subsequently, operated in a series mode (**step 9**) (*see* **Note 16**).

Fig. 2. A low-power through focus overview of resorbing osteoclasts, cultured on labeled dentine. Human osteoclasts were cultured on biotinylated dentine for 24 h. The cells were fixed and permeabilized before fluorescent immunostaining and confocal microscopy (*see* **Subheadings 3.3–3.6.**)**.** The through focus images were compiled from 16 optical sections (each 350-nm in thickness) taken through the sites of resorption in the xy plane and are displayed in gray scale. The single fluorescent images in **(A)**, show F-actin; in **(B)**, lysosomal associated membrane proteins (LAMPS); and in **(C)**, the biotinylated dentine proteins. Examples of sealing zones and LAMPS in resorbing osteoclasts, and their resorption pits are arrowed in **(A)**, **(B)**, and **(C)**, respectively, and the broad arrow shows the directional path of resorption taken by an osteoclast. A colored overlay of these images is shown in **Fig. 5A**. (Reduced from original magnification, ×160.)

8. While scanning, adjust the *z*-position for the microscope stage and set the top position at the osteoclast's apex and the bottom position at the base of the resorption pit. Minimize the time of the scanning to reduce photobleaching of the sample by the laser light.

9. Start the series collection. The system automatically collects a series of 16 equidistant, optical sections from the cell's apex to the bottom of the resorption pit for each fluorescence channel in a sequential manner. Two accumulations are taken for each optical slice and averaged to reduce noise in the image.

10. Save the data. A typical file size is 12 MB for a stack of 16, triple-stained images.

11. View the stack of images as single- and triple-stained images (**Figs. 2–4**, and **5** and **6**, respectively) in gallery and quarter-tile formats. Select and display the images as described in **Subheading 3.6.3.**

12. Change the objective to ×63 and view the sample with water immersion.

13. Repeat **steps 6–11** and collect high-power images of individual sites of osteoclast resorption (**Figs. 3** and **5**).

14. Repeat **step 13** and adjust the laser to full power and collect 64 optical sections to obtain image data for three-dimensional analysis of the resorbing osteoclasts (*see* **Subheading 3.6.3.**, **step 11**) (**Fig. 6**). Photobleaching of the scanned area will be extensive and this area is not suitable for further imaging. Select other areas of the sample for more imaging.

15. Change the mode to *zx* (vertical) plane to observe the lateral view image. Repeat **steps 6–11** and collect lateral views of the resorption sites (**Figs. 3D** and **5C**). Imaging in the zx plane can cause "scan lines" from photobleaching. These "scan lines" will appear in subsequent imaging of the same cells in the *xy* plane, therefore, complete the *xy* imaging before scanning in the *zx* plane.

3.6.3. Image Display

1. Go to the view interface.

2. Display the single fluorescence images in gray scale (**Figs. 2–4**) and triple-stained images as pseudocolored overlays (**Fig. 5**).

3. View the low-magnification images (×160) in through focus for the entire image stack and to obtain an overview of the resorption sites (**Figs. 2A–C** and **5A**).

4. View the high-magnification images (×630) in each of the optical sections and analyze the osteoclast and its sub-celluar staining in detail in the *xy* plane (above view) (**Figs. 3A–C** and **5B,D**) and *zx* plane (lateral view) (**Figs. 3D, 5C**).

5. Note the localization and intensity of the stains in the resorption pit, along the resorption surface, in the resorbing osteoclasts at the cell's surface, ruffled border, sealing zone, cytoplasmic skirt, and in the basolateral cell body. In addition, examine the staining patterns in the surrounding stroma and in the nonresorbing osteoclasts (those osteoclasts without sealing zones and resident on the intact surface of dentine).

6. Identify colocalization of stains. For example, on merging the images green and red gives yellow to orange; green and blue gives pale blue and pale green; red and blue gives pink; and together green, red, and blue gives white (**Fig. 5**).
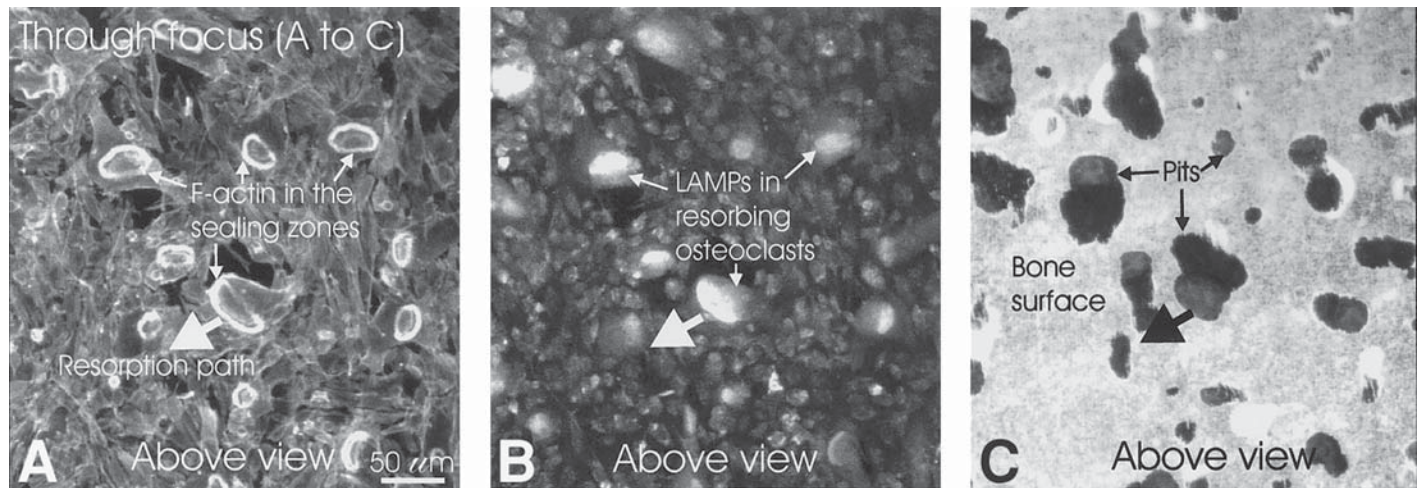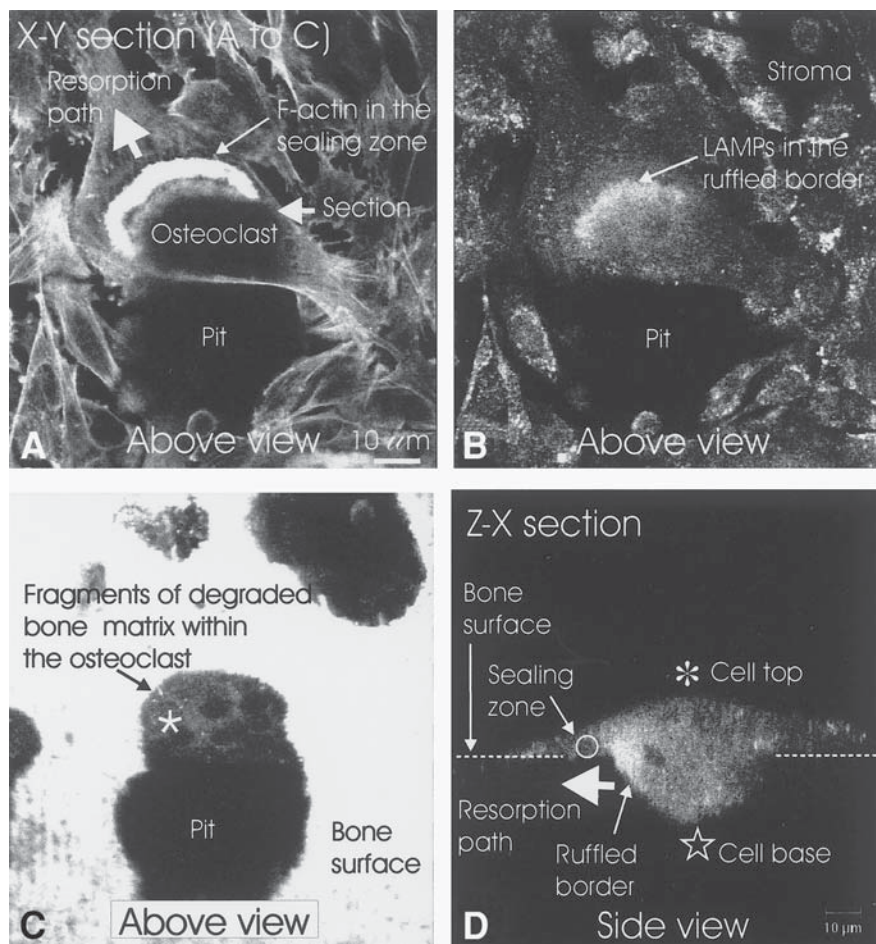
Fig. 3. High-power sectional views of a resorbing osteoclast cultured on labeled dentine. Human osteoclasts were cultured on biotinylated dentine for 24 h. The cells were fixed and permeabilized before fluorescent immunostaining and confocal microscopy (*see* **Subheadings 3.3–3.6.**). Optical sections (350-nm thick) for a resorption site were taken at the bone surface in the xy plane in **(A–C)** and through the center of the resorption site in the zx plane in **(D)** and are displayed in gray scale. The single fluorescent images in **(A)** show F-actin; in **(B, D)**, lysosomal associated proteins; and in **(C)**, the biotinylated dentine proteins. In **(A)** and **(D)** the resorption path is indicated by a broad arrow and the ruffled border is behind the broad arrow in **(D)**. The sealing zone, ruffled border, and degraded bone matrix in resorbing osteoclasts are arrowed in **(A)**, **(B)**, and **(C)**, respectively. The zx image in **(D)** was taken at the position identified by "Section" in **(A)**. In **(D)** the broken line, the open circle, and the open and closed stars show the position of the dentine surface, the sealing zone, the cell's apex, and cell base, respectively. A colored overlay of these images is shown in **Fig. 5B**, and **C**. (Reduced from original magnification, ×630.)
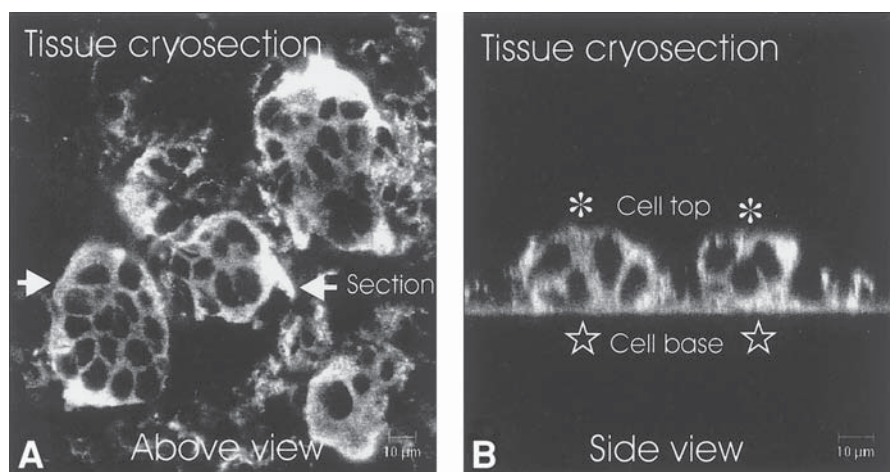
Fig. 4. High-power sectional views of osteoclasts in vivo in osteoclastoma tissue. A thick, 30-μm, cryosection of osteoclastoma tissue was fixed and permeabilized and processed by fluorescent immunostaining for the metalloproteinase MMP-9, before confocal microscopy (*see* **Subheading 3.8.**). Optical sections (350-nm thick) were taken through the tissue in the xy plane in **(A)** and in the zx plane in **(B)** and are displayed in gray scale. Cytoplasmic staining of MMP-9 is seen in the multinucleated osteoclasts in **(A)** and **(B)**. The zx image in **(B)** was taken at the position in the tissue identified by "Section" in **(A)**. Closed and open stars in **(B)** show the osteoclast's cell apex and cell base, respectively. A multicolored fluorescence intensity image of the zx section in **(B)** is shown in **Fig. 5F**. (Reduced from original magnification, ×630.)

Fig. 5. *(opposite page)* Multicolored imaging of osteoclasts by fluorescence immunostaining and laser scanning confocal microscopy. The cells were fixed and permeabilized before fluorescent immunostaining and confocal microscopy (*see* **Subheadings 3.3–3.6.**). In **(A)–(D)** human osteoclasts were cultured on biotinylated dentine for 24 h. The pseudocolors of fluorescence represented are green (lysosomal associated membrane proteins), red (F-actin), and blue (dentine matrix proteins). Low-power and high-power views of resorbing osteoclasts are shown in **(A**, and **B–D)**, respectively. In **(A)**, many resorbing osteoclasts are identified by their characteristic F-actin staining of the sealing zones and form ring/arc-shaped structures. The resorption sites are located by a loss of the dentine matrix proteins (*black*). In **(B),** optical sections of resorbing osteoclasts (350-nm thick) were taken at the bone surface in the xy plane **(B, D)** and through the center of the resorption site in the zx plane in **(C).** A pseudo-3D image in **(D)** shows the image in **(B),** rotated through 180° and tilted at an angle of 45°. The fluorescence intensity profile for the osteoclast in **(B–D)** is displayed in **(E),** for each of the 16 optical sections taken through the resorption site. In **(F),** a fluorescence intensity image shows the localization pattern of the metalloproteinase MMP-9. Two osteoclasts are viewed from a zx section taken
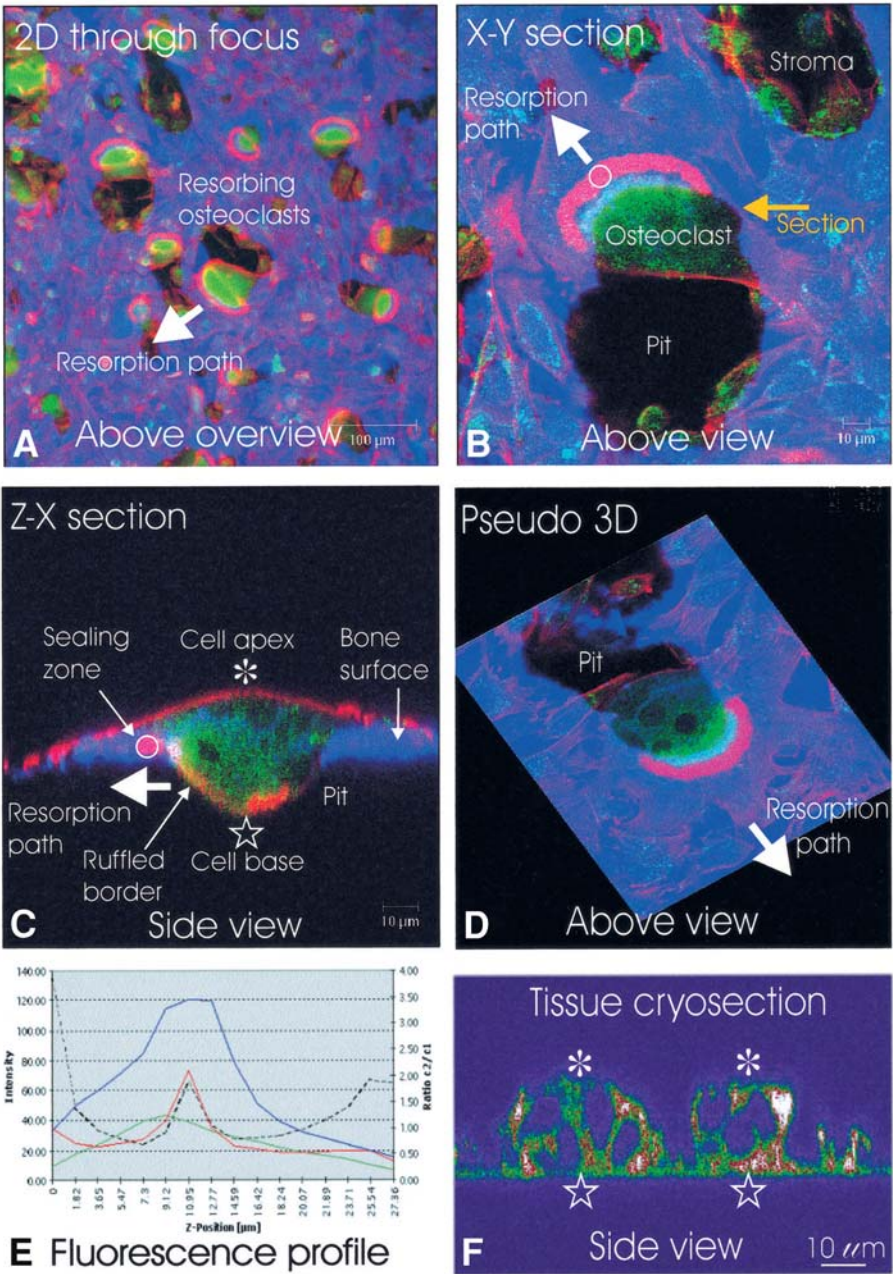
Fig. 5. *(continued)* through a thick cryosection of osteoclastoma tissue and show "hot spots" of MMP-9 colored white (colors white > red > yellow > green > blue > purple show the fluorescence intensities from high through to low).
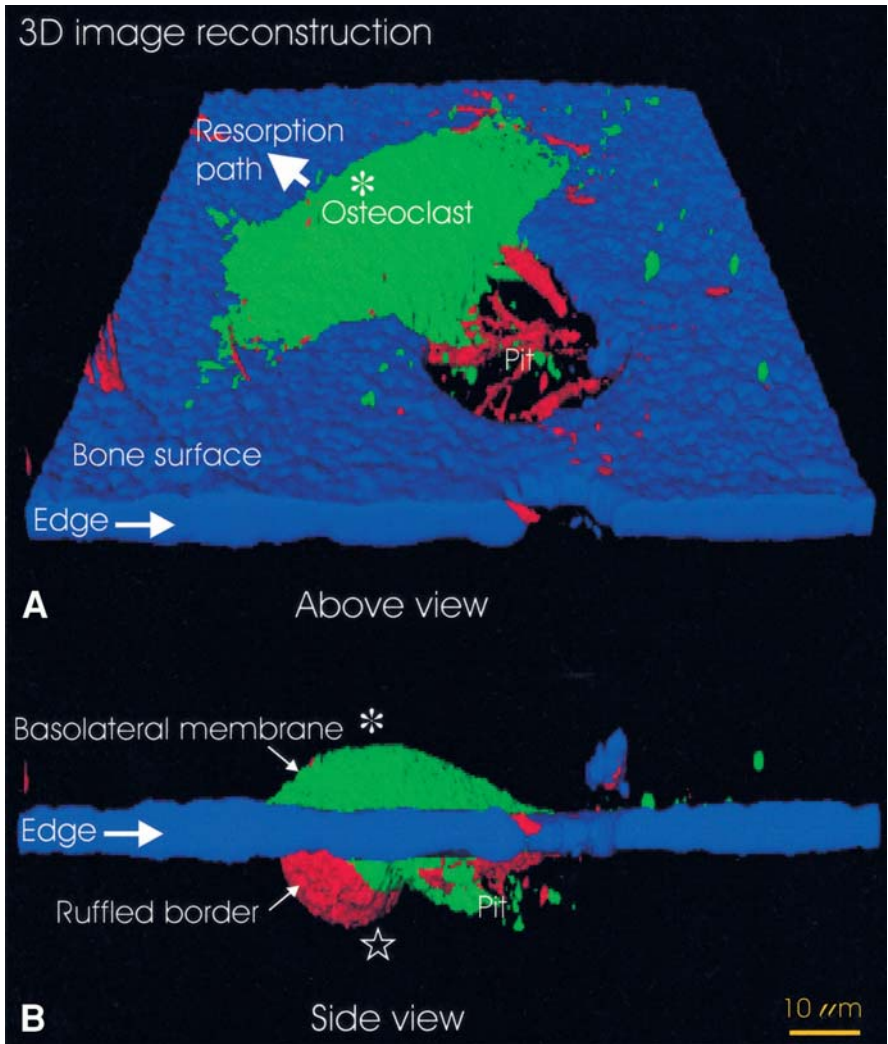
Fig. 6. Multicolored 3D imaging of bone-resorbing osteoclasts. Human osteoclasts were cultured on biotinylated dentine for 24 h. The cells were fixed before fluorescent immunostaining and confocal microscopy (*see* **Subheadings 3.3–3.6**.). The 3D isosurface images were reconstructed using Imaris software from 64 optical sections (each 350-nm thick) taken through a site of osteoclastic resorption in the xy plane. The pseudocolors of fluorescence represented are green (the integrin $\alpha_v\beta_3$, stained before cell permeabilization), red, and blue (F-actin and dentine matrix proteins, respectively, stained after cell permeabilization). The resorption path (broad arrow), the osteoclast's cell apex (closed star), and cell base (open star) and the edge of the bone surface (arrowed) are shown. In **(A)**, an above view of a resorption site tilted at an angle of 30° shows the extracellular face of the plasma membrane of a resorbing osteoclast (green)

7. Take the images from **steps 3** and **4** and display in a pseudo-3D format. Rotate and tilt the images and view from different perspectives (**Fig. 5D**).
8. Use the gamma correction to visualize weak staining. Avoid boosting the gamma correction beyond 20% as nonspecific signals may be given (diffuse and pixelated).
9. Convert single fluorescence stains into a multicolored fluorescence intensity images and locate "hot spots" of staining with the glow-over facility (Glut mode) (**Fig. 5F**).
10. Quantify the fluorescence stains. Map the area for analysis and measure the fluorescence intensity/μm^2 and display the fluorescence profile for the stack of images (**Fig. 5E**). Analysis of the fluorescence intensities can be used to assess the amount of the resorption by osteoclasts (*see* **Note 17**).
11. Finally, export the data from the 3D image collections (met**Subheading 3.6.2.**, **step 14**) into a Silicon Graphics O$_2$ Workstation (SGI, Mountainview, CA, USA) and generate 3D isosurface images using Imaris software (Bitplane, Zurich, Switzerland) *(7,24)*. View the 3D images of the osteoclasts and resorption sites from above, laterally, and below the dentine surface (**Fig. 6**).

3.7. Tracking of Exogenous Proteins in In Vitro Bone Resorption Assays

Many biological products, including peptides, proteins, and antibodies can be labeled effectively with a variety of fluorochromes and this allows them to be "traced" within live resorption cultures by fluorescence microscopy and LSCM *(11,25–27)*. Fluoro-Link reactive dyes (Amersham/Pharmacia, UK) are convenient for labeling proteins and are nontoxic and stable in resorption assays. The fluorescence from Fluoro-Link reactive dyes is not quenched in acidic conditions and is ideal for imaging compounds that target the resorption site. These dyes allow compounds to be identified within their target cells and subcellular structures, and in resorbing osteoclasts include the resorption pit, ruffled border, sealing zone, basolateral cell body, and cell apex.

3.7.1. Protein Labeling with FluorX

1. Reconstitute the protein in 1 mL of 50 mM NaHCO$_3$ buffer, pH 8-8.5 (made fresh) and add to a FluoroX reaction vial. Mix thoroughly and avoid foaming of the solution.
2. Cover the reaction vial with foil to shield from direct light and gently mix for 1 h at 4°C.
3. After protein conjugation, remove the unbound FluorX by membrane filtration using Centricon devices.
4. Aliquot and freeze the FluorX-labeled proteins at –70°C for long-term storage.

Fig. 6. *(continued)* and stromal cells (red) within the resorption pit (black) and the matrix surface (blue). In (**B**), a side view shows the resorption pit (under the surface of the matrix) together with the concealed ruffled border (red).

3.7.2. Cell Imaging with FluroX-Labeled Proteins

1. Add the desired concentration of the FluorX-conjugated proteins to the in vitro resorption cultures as described in **Subheading 3.3.**
2. Run a parallel culture and add an equivalent amount of unlabeled protein.
3. Fix and permeabilize the cell cultures as noted in **Subheading 3.3.**, **step 8**, and **Subheading 3.5.1.**
4. Fluorescently immunostain the cells for F-actin and matrix proteins described in **Subheading 3.5.2.** and omit **steps 3** and **5** for the primary and secondary antibody staining. Identify the resorbing osteoclasts and resorption pits.
5. Image the cells of interest by LSCM as noted in **Subheading 3.6.** View the FluoroX-labeled proteins using the FITC wavelength settings.
6. Quantify the labeled proteins in the cell images using fluorescence intensity profiles, **Subheading 3.6.3.**, **step 10**.
7. Analyze the effects on osteoclast resorption (*see* **Note 18**).
8. Repeat **steps 4–8** for the unlabeled protein and compare results with the FluoroX-conjugated protein. Establish if the results are specific to the exogenous protein and do not arise from any nonspecific effects of the label. If variations are seen, then repeat FluoroX labeling at lower concentrations and repeat the cell cultures and resorption analysis.

3.8 Fluorescence Immunostaining and LSCM of Other Cell Types and Tissues

In addition to the cells attached to bone and dentine discs, many other cell and tissue preparations can be studied by fluorescence immunostaining and LSCM techniques described in **Subheadings 3.3–3.7**. The cells can be seeded onto glass coverslips, or tissue cryostat sections can be attached onto glass slides. See, for example, the analysis of osteoclasts in vivo within a thick cryosection of osteoclastoma tissue probed for the metalloproteinase MMP-9 (**Figs. 4** and **5F**).

4. Notes

1. Typical sources of dentine include elephant tusk and sperm whale and hippopotamus teeth. Compared to bone, dentine lacks a Haversian system and is not remodeled. Its autofluorescence is low, which is very advantageous for cell imaging by fluorescence immunostaining and LSCM. Obviously this material is not routinely available, and legal sources need to be identified. In the UK, the Division of Customs and Excise (Heathrow Airport, London, UK) will make confiscated elephant tusk available for scientific research. Other sources to consider are natural history museums and zoos.
2. Correct orientation of the dentine cutting is essential. The dentine discs represent transverse cuts so that any tubules within the dentine do not appear longitudinally. Longitudinal channels weaken the discs and make them prone to breakage during handling. Bone, in comparison to dentine, has an extensive Haversian

system and less mineral content and requires thicker cuts (> 200 μm), and this elevates the autofluorescence. An increase in the background signals, in addition to osteoclasts being hidden from view within the channels, can severely restrict image analysis. Furthermore, discard unevenly cut dentine as "wedged-shaped" discs; these make high-quality image collection by LSCM difficult.

3. Alternative, quicker methods for cleaning and sterilizing dentine and bone have been described using sonication and UV light *(28)*. These procedures will degrade surface proteins on the dentine discs and may effect their subsequent biotin labeling and, moreover, may alter cell attachment and resorption in the osteoclast cultures.

4. Use biotinylation products that are stable, non-toxic, and utilize spacer arms to reduce steric hindrance. The biotinylation reagent biotinamidocaproate *N*-hydroxysuccinimide ester enables protein labeling via attachment to lysine or cysteine residues of amine groups with very low steric hindrance *(29,30)* and these labels do not effect cell attachment or resorption by osteoclasts *(6)*. Furthermore, the biotin label is resistant to extremes of pH (3.0–11.0). It is not degraded by the acidic conditions (pH 4) within the resorption site at the ruffled border *(31)* and, subsequently, binds to streptavidin-fluorochromes used to probe the resorption cultures in immunostaining and LSCM analysis.

5. A pH 8–8.5 provides optimal protein biotinylation and minimizes protein degradation of the dentine discs. The biotinylation reagent is susceptible to hydrolysis and is stored at 4°C; therefore leave the reagent at RT for 30 min before opening to avoid contamination with condensation. Discard the reagent 3 mo after opening.

6. The discs must be completely dry before storage and kept sterile to preserve the biotin label. The label is stable for several years when stored under these conditions.

7. Biotinylation methods are also suitable to surface label bone slices and enable the resorption sites to be imaged by fluorescence immunostaining and LSCM *(32)*.

8. The tissue digest can become gelatinous on cooling below RT and this can restrict the extraction of the osteoclastoma cells. If this occurs use more MEM–GPS to rinse the cells through the sieve, ensuring MEM–GPS is used at RT.

9. Osteoclasts from a variety of sources can be studied by the bone and dentine resorption slice assay and imaged by fluorescence immunostaining and LSCM *(5,6,20,25–27,32)*. The osteoclasts can be generated in in vitro cultures or isolated from the long bones of fetal and neonate limbs from human, rat, mouse, rabbit, and chick species (*see* Part II, Culture of Osteoclasts).

10. Keep the cells at 37°C when the samples are removed from tissue culture. Prewarm and pregas the washes and media and use gel "cold-packs" at 37°C to hold the tissue culture dishes. A constant temperature and pH will maintain osteoclast viability, attachment, and cell polarization of subcellular structures prior to cell fixation.

11. The osteoclasts can be cultured for 2 wk to achieve extensive resorption of the dentine matrix. The resorption media should be replaced every 2 d to maintain cell viability. The biotin label on the dentine discs is stable in long-term tissue culture for further biochemical analysis.

12. Paraformaldehyde and methanol are suitable cell fixatives for resorption cultures and preserve the actin cytoskeleton and tubulin networks, respectively *(5,21)*. The paraformaldehyde fixative contains sucrose to stop osmotic fluxes that may cause nonspecific endocytosis which would alter cell morphology during the fixation process. The MEM/fixation buffer mix stabilizes the localization of the cellular proteins that are calcium-dependent. Methanol fixatives also solubilize the cell lipids and puncture holes in the cell membranes and can cause some proteins to be lost from the cells.

13. The fixed samples can be conveniently stored in freezing buffer at –70°C and are stable for several years. Freezing the samples does not affect the cell or matrix morphology, or the subsequent analysis of the cells by fluorescence immmunostaining and LSCM.

14. The Triton X-100 detergent is used with an actin cytoskeleton stabilizing buffer at 4°C to preserve the cell's structure *(5)*. Saponin can be used as an alternative to Triton X-100; it creates pores within the cell membrane by altering the lipid structure. Generally, antibody access to the ruffled border and resorption site with saponin is less than that given with Triton X-100. Furthermore, 0.1% saponin is required in the subsequent antibody staining solutions and washes to maintain cell permeability.

15. Fluorescence antifade solutions are essential to minimize the photobleaching of the fluorochromes conjugates used to immunostain the cells. The exposure times to fluorescence are extended by > 10-fold in the presence of antifade reagents. Thus, the samples can be examined for several minutes before loss of the fluorescence signals. Use PBS–antifade mountants; the glycerol-based antifade mountants are not suitable for imaging osteoclasts on bone and dentine substrates.

16. Crosstalk can occur with FITC and TRITC, and TRITC and CY5 fluorochromes due, in part, to an overlapping of their emission spectra. Generally, this is noticeable when the fluorescence staining from one fluorochrome is significantly greater than the other. For example, crosstalk may occur form excessive staining of the sealing zone in resorbing osteoclasts with phalloidin–rhodamine. To avoid crosstalk, a laser beam splitter enables specific light excitation of each fluorochrome to be individually excited. This system functions during the series collection where optical slices are sequentially and separately gathered for each fluorescence stain.

17. Changes in the percentages of fluorescence intensities for the stained cells and subcellular structures can be measured and changes in their distribution noted, and related to cell function. The loss of the biotin-labeled matrix from the dentine surface is a measure of osteoclast resorption and can be quantified by image analysis *(6)*. In addition, the degraded matrix that is transported through the osteoclast during resorption can be stained with specific antibodies and quantified in the osteoclasts after LSCM and analysis of the fluorescence intensities *(11)*. Furthermore, the numbers of pits and osteoclasts (resorbing and non-resorbing types) may be counted by fluorescence microscopy *(33)*. After the LSCM analysis, histochemical staining for tartrate-resistant acid phosphatase (*see*

the chapter by Flanagan and Massey, *this volume*, for details) or staining for toludine blue may also be used to identify and count the osteoclasts and pits.

18. Methods to investigate bone-resorbing osteoclasts by live cell imaging techniques are under investigation. LSCM systems are required that provide high-resolution images while maintaining an environment in which the osteoclast retains its cell polarization and bone resorption activity. Generally, the rapid photobleaching of fluorochromes and the generation of hydrogen peroxide, caused by the scanning laser used in conventional confocal microscopy, reduces cell viability. Thus, these imaging systems are impractical for prolonged study of live osteoclasts in bone resorption cultures. Two-photon laser scanning microscopy (TPLSM) may circumvent these problems and operates with minimal photobleaching and phototoxicity *(34)*. TPLSM, together with the application of new fluorochrome labels for the bone matrix and the resorbing osteoclasts, will enable the dynamic process of bone resorption to be studied.

References

1. Teitelbaum, S. L. (2000) Bone-resorption by osteoclasts. *Science* **289,** 1504–1508.
2. McKee, M. D. and Nanci, A. (1996) Microscopy of bone. *Microsc. Res. Tech.* **33,** 92–239.
3. Lehenkari, P., Charras, G., Nesbitt, S., and Horton, M. (2000) New technologies in scanning probe microscopy for studying molecular interactions in cells. Expert Reviews. http://www-ermm.cbcu.cam.ac.uk/00001575h.htm.
4. Reynaud, K., Nogueira, R., Kurzawa, R., and Smitz, J. (2001) Confocal microscopy: principles and applications to the field of reproductive biology. *Folia Histochem. Cytobiol.* **39,** 75–85.
5. Lakkakorpi, P. T., Helfrich, M. H., Horton, M. A., and Väänänen, H. K. (1993) Spatial organization of microfilaments and vitronectin receptor, αvβ3, in osteoclasts. *J. Cell Sci.* **104,** 663–670.
6. Nesbitt, S. A. and Horton, M. A. (1997). Trafficking of matrix collagens through bone-resorbing osteoclasts. *Science* **276,** 266–269.
7. Nesbitt, S., Charras, G., Lehenkari, P., and Horton, M. (2000) Three-dimensional imaging of bone-resorbing osteoclasts: spatial analysis of matrix collagens, cathepsin K, MMP-9 and TRAP by confocal microscopy. *J. Bone Miner. Res.* **15,** 1219.
8. Baron, R., Neff, L., Brown, W., Courtoy, P., Louvard, D., and Farquhar, M. (1988) Polarised secretion of lysosomal enzymes: co-distribution of cation-independent mannose-6-phosphate receptors and lysosomal enzymes along the osteoclast exocytotic pathway. *J. Cell Biol.* **106,** 1863–1872.
9. Horton, M. A, Nesbitt S. A., Bennett, J. H., and Stenbeck, G. (2001) Integrins and other cell surface attachment molecules of bone cells, in *Principles of Bone Biology*, 2nd edit. (Bilezikian, J. P., Raisz, L. G., and Rodan G. A., eds.). Academic Press, San Diego.
10. Wucherpfennig, A., Li, Y., Stetler-Steveson, W., Rosenberg, A., and Stashenko P. (1994) Expression of 92 kD type IV collagenase/gelatinase B in human osteoclasts. *J. Bone Miner. Res.* **9,** 549–556.

11. Nesbitt, S. and Horton, M. (1999) Extracellular annexin II increases trafficking of matrix collagens through bone-resorbing osteoclasts to promote bone resorption. *Calcif. Tissue Int.* **64 (Suppl. 1),** S35.

12. Boyde, A., Ali, N. N., and Jones, S. J. (1984) Resorption of dentine by isolated osteoclasts in vitro. *Br. Dent. J.* **156,** 216–220.

13. Chambers, T. J., Revell, P. A., Fuller, K., and Athanasou, N. A. (1984) Resorption of bone by isolated rabbit osteoclasts. *J. Cell Sci.* **66,** 383–399.

14. Arnett, T. D. and Dempster, D. W. (1986) Effect of pH on bone resorption by rat osteoclasts in vitro. *Endocrinology* **119,** 119–124.

15. Horton, M. A., Rimmer, E. F., Lewis, D., Pringle, J., Fuller, K., and Chambers, T. J. (1984) Cell surface characterisation of the human osteoclast: phenotypic relationship to other bone marrow-derived cell types. *J. Pathol.* **144,** 282.

16. Atkins, G., Haynes, D., Graves, S., Evdokiou, S., Bouralexis, S., and Findlay, D. (2000) Expression of osteoclast differentiation signals by stromal elements of giant cell tumors. *J. Bone Miner. Res.* **15,** 640–649.

17. James, I., Lark, M., Zembryki, D., et al. (1999) Development and characterisation of a human in vitro resorption assay: Demonstration of utility using novel antiresorption agents. *J. Bone and Miner. Res.* **14,** 1562–1569.

18. Helfrich, M. H., Nesbitt, S. A., Dorey, E. L., and Horton, M. A. (1992). Rat osteoclasts adhere to a wide range of RGD (Arg-Gly-Asp) peptide-containing proteins, including the bone sialoproteins and fibronectin, via a β3 integrin. *J. Bone Min. Res.* **7,** 332–343.

19. Horton, M. A. (2001) Integrin antagonists as inhibitors of bone resorption: implications for treatment. *Proc. Nutr. Soc.* **60,** 275–281.

20. Helfrich, M. H., Nesbitt, S. A., Lakkakorpi, P. T., et al. (1996) β1 integrins and osteoclast function: involvement in collagen recognition and bone resorption. *Bone* **19,** 317–328.

21. Palokangas, H., Mulari, M., and Vannanen, K. (1997) Endocytotic pathway from the basal plasma membrane to the ruffled border membrane in bone-resorbing osteoclasts. *J. Cell Sci.* **110,** 1767–1780.

22. Chavrier, P., Parton, R. G., Hauri, H. P., Simons, K., and Zerial, M. (1990) Localization of low molecular weight GTP binding proteins to exocytotic and endocytotic compartments. *Cell* **62,** 317–329.

23. Horton, M. A, Townsend, P. A., and Nesbitt, S. A. (1996) Cell surface attachment molecules in bone, in, *Principles of Bone Biology* (Bilezikian, J. P., Raisz, L. G., and Rodan, G. A., eds.), pp. 217–230. Academic Press, San Diego.

24. Guilak, F. (1994) Volume and surface area measurement of viable chondrocytes in situ using geometric modelling of serial confocal sections. *J. Microsc.* **173,** 245–256.

25. Salo, J., Metsikkö, K., Palokangas, H., Lehenkari, P., and Väänänen, H. K. (1996) Bone-resorbing osteoclasts reveal a dynamic divison of basal plasma membrane into two different domains. *J. Cell Sci.* **109,** 301–307.

26. Townsend, P. A., Vilanoova, I., Teti, A., and Horton, M. A. (1999) β1 integrin antisense oligodeoxynucleotides: utility in controlling osteoclast function. *Eur. J. Cell Biol.* **78,** 448–496.

27. Stenbeck, G. and Horton, M. A. (2000) A new specialized cell-matrix interaction in actively resorbing osteoclasts. *J. Cell Sci.* **113,** 1577–1587.

28. Walsh, C. A., Carron, J. A., and Gallagher, J. A. (1996) Isolation of osteoclasts from human giant cell tumors and long-term marrow cultures, in *Methods in Molecular Medicine: Human Cell Culture Protocols* (Jones, G. E., ed.), Humana Press, Totowa, NJ.

29. Nesbitt, S. and Horton, M. (1992) A nonradioactive biochemical characterisation of membrane proteins using enhanced chemiluminescence. *Analyt. Biochem.* **206,** 267–272.

30. Hnatowitch, D. J., Virzi, F., and Rusckowski, M. (1987) Investigations of avidin and biotin for imaging applications. *J. Nucl. Med.* **28,** 1294–1302.

31. Silver, I. A., Murrills, R. J., and Etherington, D. J. (1988) Microelectrode studies on the acid microenvironment beneath adherent macrophages and osteoclasts. *Exp. Cell. Res.* **175,** 266–276.

32. Salo, J., Lehenkari, P., Mulari, M., Metsikkö, K., and Väänänen, H. K. (1997) Removal of osteoclast bone resorption products by transcytosis. *Science* **276,** 270–273.

33. Lader, C., Scopes, J., Horton, M. and Flanagen, A. (2001) Generation of human osteoclasts in stromal cell-free and stromal cell-rich cultures: differences in osteoclast CD11c/CD18 integrin expression. *Br. J. Haematol* **112,** 430–437.

34. Squirrell, J., Wokosin, D., White, J., and Bavister, B. (1999) Long-term two photon fluorescence imaging of mammalian embryos without compromising viability. *Nat. Biotechnol.* **17,** 763–767.

20

Bone Histomorphometry

Shobna Vedi and Juliet Compston

1. Introduction

Histomorphometric examination of bone biopsies provides information on bone turnover, remodeling, and structure, which cannot be obtained from other investigative approaches such as bone densitometry and biochemical markers of bone turnover. Recently, there have been significant advances in histomorphometric techniques with the use of computer-assisted analysis and the development of sophisticated approaches to assessment of microstructure of bone. The application of these techniques has been particularly valuable in analyzing the cellular pathophysiology of different forms of osteoporosis and in determining the mechanisms by which drugs affect bone. In this chapter we review current methodology used in the preparation and histomorphometric assessment of histological sections of bone, with particular reference to its application in humans.

2. Materials

2.1. Biopsy

1. Trephine biopsy needle with internal diameter of at least 6 mm.
2. Demeclotetracycline.
3. Sedative (e.g., 5–10 mg of Midazolam) and local anesthetic (20 mL of 1% Lignocaine).

2.2. Tissue Processing and Embedding

1. Heavy-duty microtome with tungsten carbide knife (Bright Instruments, Huntingdon).
2. Tissue processor (e.g., Shandon).
3. Ethanol series 70%, 80%, 90%, 100%.
4. LR White resin (store at 4°C).

5. DePeX.
6. XAM mountant (BDH, Poole).

2.3. Stains

1. Toluidine blue: Dissolve 20 mg of toluidine blue in 10 mL of McIlvane buffer (25 mL of 5 mM disodium hydrogen orthophosphate and 75 mL of 8 mM citric acid). Adjust to pH 4.2 with 1 M NaOH.
2. von Kossa: 2.5% Silver nitrate (store at 4°C protected from light).
3. van Gieson: Add 20 mL of 1% acid fuchsin in water to 80 mL of 1 M picric acid.

2.4. Analysis

We use a semi-automated system consisting of the following components:

1. Olympus BHS-BH2 microscope.
2. BH2-DA drawing attachment.
3. Digicad digitizing tablet with LED point light source (Kontron Ltd.).
4. HBO-100W/2 light source with EY-455 excitation filter for tetracycline labels.
5. CCD camera to capture images for analysis of cancellous bone structure *(1,2)*.

Manual analysis can be done with any good transmitted light microscope using a graticule attachment for eyepiece (e.g., Zeiss Integrationsplatte 1) (*see* **Note 1**).

3. Methods
3.1. Bone Biopsy

The iliac crest is the standard site for a bone biopsy in humans. A sample can be obtained using either a vertical or transverse approach, the latter being favored by most investigators since it provides a biopsy with two cortices and intervening cancellous bone. The vertical biopsy, by contrast, contains only one cortex. Transiliac biopsies are obtained approx 2.5 cm below and behind the anterior superior iliac spine of the crest. There are several specially designed trephines available on the market; ideally, for bone histomorphometry, a trephine with an internal diameter of at least 6 mm should be used.

Iliac crest biopsy is usually carried out as an outpatient procedure under mild sedation (e.g., 5–10 mg Midazolam) and local anesthesia (20 mL of 1% Lignocaine). It is associated with low morbidity; hematoma is the most common complication, occuring in <1% of cases.

Administration of two time-spaced doses of tetracycline prior to bone biopsy enables assessment of dynamic indices of bone turnover and should be performed whenever possible *(3)*. Various regimens have been described, involving a 10- to 14-d gap between the two administrations, bone biopsy being performed 3–5 d after the last dose. The regimen used in our laboratory is as follows:

Days 1 and 2: demeclotetracycline 300 mg twice daily.
Days 3–12: no demeclotetracycline.
Days 13 and 14: demeclotetracycline 300 mg twice daily.

The biopsy is performed 3–5 d after the last dose.

Side effects of demeclotetracycline are rare but include nausea and diarrhea. Skin rashes occasionally occur and, although usually mild, may be severe and exhibit photosensitivity. Different tetracycline compounds may differ with respect to the extent of their uptake at mineralizing fronts.

3.2. Fixation and Processing of Biopsy (see Note 2)

1. Fix the biopsy in 70% ethanol for a minimum of 48 h.
2. Dehydrate by placing the biopsy in 80% ethanol for 3 d in a polypropylene vial on a rock and roller machine.
3. Repeat using 90% ethanol for 3 d.
4. Repeat using 100% ethanol for 3 d.
5. Remove the biopsy from the ethanol, place centrally in the bottom of a rubber mold, and cover with approx 2 mL of LR White resin. Incubate at room temperature for 2 d.
6. Replace with 2 mL of fresh LR White resin and incubate for a further 2 d.
7. Replace with 2mL fresh LR White resin and incubate for 2 more days.
8. Place in an oven at 60°C for 2–3 h until the resin hardens.

3.3. Sectioning and Mounting

Sections should be cut using a heavy-duty microtome and tungsten carbide knife. For bone histomorphometry, sections of 8 μm and 15 μm thickness are cut every 200 μm at several levels throughout the biopsy, ensuring that each replicate section contains different trabeculae. The 15-μm sections should be mounted immediately in XAM for tetracycline label analysis. These sections remain unstained to be viewed under 365-nm UV light.

3.4. Staining

A number of different staining procedures may be used to demonstrate the histological features of bone:

a. Toluidine blue (1%, pH 4.2) is a metachromatic stain used for examination of bone cell morphology, identification of resorption cavities, mineralization fronts, and bone remodelling units. Polarized light microscopy can be used on toluidine blue stained sections for the measurement of wall width and for identification of resorption cavities (see below).
b. von Kossa with van Gieson counterstain is used to differentiate osteoid (red) from mineralized bone (black).
c. Solochrome cyanin R *(4)* is a red acid triphenylmethane dye used to stain basic and acidic proteins. It allows distinction between osteoid (orange) and mineralized bone (blue/grey) and the mineralization front (dark blue).

   d. Goldner's trichrome stain *(5)* can also be used to distinguis bhetween osteoid (red) and mineralized bone (green). Details can be found in Chapter 24 by van 't Hof et al.

   e. Villanueva stain *(6)* may be used for concomitant observation of osteoid and tetracycline labels.

Details of the toluidine blue and von Kossa staining procedures follow. All staining is performed on free floating sections.

1. Toluidine blue: Free float the 8-μm thick sections in the stain for 2 min and wash twice with distilled water. Place the stained section on a glass slide, trim off excess resin, and blot dry. Air-dry the section, clear with inhibisol, and mount in DePeX.

2. Von Kossa: Place the 8-μm thick sections in 2.5% silver nitrate solution in bright light for 3–4 h until they turn black. Wash twice in distilled water to remove all traces of silver nitrate. Fix in 2.5% sodium thiosulfate solution for 2 min and wash twice in distilled water. Immerse in van Gieson counter stain for 15 min and wash twice in distilled water. Flatten onto slides, air-dry and mount in DePeX.

3.5. Theoretical Basis of Histomorphometry

Bone histomorphometry has a number of limitations some of which are related to the restrictions imposed by a single-biopsy site and disease heterogeneity, whereas others reflect methodological problems and difficulties in identification of some key features of remodelling. The conventional histological sections on which bone histomorphometry is performed are viewed as 2D images in which profiles of 3D structures are seen. To extrapolate 2D data to 3D quantities, stereological formulae have to be applied. These are based on assumptions that sampling is unbiased and random and that the structure is isotropic (i.e. evenly dispersed and randomly oriented in space) *(7)*. However, in the case of bone, these conditions are not totally fulfilled and the expression of bone indices as 3D quantities is thus subject to some error. In practice, histomorphometric data may be reported either as 2D or 3D quantities; although there will be a difference in the absolute values and accuracy depending on which approach is taken, it will not influence comparisons between patient groups or the diagnostic value of histomorphometry, provided that the approach adopted is consistent.

3.6. Nomenclature

All histomorphometric measurements are described according to the standardized system proposed by ASBMR nomenclature committee *(8)*. **Table 1** shows the referents used in bone histomorphometry and **Tables 2** and **3** show the primary and derived indices of bone remodeling. All data are expressed in the format of source, the measurement, and the referent. The source is the structure on which the measurement is made, for example, bone tissue or bone sur-

Table 1
Referents Used in Bone Histomorphometry

Referent (3D/2D)	Abbreviation (3D/2D)
Bone surface/perimeter	BS/B.Pm
Bone volume/area	BV/B.Ar
Tissue volume/area	TV/T.Ar
Core volume/area	CV/C.Ar
Osteoid surface/perimeter	OS/O.Pm
Eroded surface/perimeter	ES/E.Pm
Mineralizing surface/perimeter	Md.S/Md.Pm
Osteoblast surface/perimeter	Ob.S/Ob.Pm
Osteoclast surface/perimeter	Oc.S/Oc.Pm

Table 2
Primary Histomorphometric Indices (Expressed as 2D Measurements)

Name	Abbreviation	Unit
Bone area	B.Ar/T.Ar	%
Osteoid area	O.Ar/T.Ar or O.Ar/B.Ar	%
Osteoid perimeter	O.Pm/B.Pm	%
Osteoid width	O.Wi	μm
Osteoblast perimeter	Ob.Pm/B.Pm	%
Wall width	W.Wi	μm
Mineralizing perimeter	M.Pm/B.Pm	%
Mineral apposition rate	MAR	μm/d
Eroded depth	E.De	μm
Eroded cavity area	E.Ar	$μm^2$
Eroded perimeter	E.Pm/B.Pm	%
Osteoclast perimeter	Oc.Pm/B.Pm	%
Erosion length	E.Le	μm
Cavity number	N.Cv/B.Pm or /T.Ar	No./mm or /mm^2
Osteoclast number	Oc/T.Ar	cells/mm^2

face. Measurements can either be primary or derived. The referent is area or perimeter in 2D and volume or surface in 3D terminology. Primary 2D measurements of perimeter, area, and number are expressed in terms of the amount of tissue examined and can be compared between subjects only when related to a common referent such as a clearly defined area or perimeter within a section. Absolute perimeter length and absolute area have no 3D equivalent but if 3D

Table 3
Derived Histomorphometric Indices of Bone Remodeling

Name	Abbreviation	Unit
Adjusted apposition rate	Aj.AR	μm/d
Mineralization lag time	Mlt	d
Osteoid maturation period	Omt	d
Bone formation rate	BFR/B.Pm or /B.Ar	$\mu m^2/\mu m/d$ or %/yr
Activation frequency	Ac.F	/y
Remodeling period	Rm.P	d
Formation period	FP	d
Active formation period	FP(a+)	d
Quiescent period	QP	d
Resorption period	RP	d
Reversal period	Rv.P	d
Total period	Tt.P	d
Trabecular width	Tb.Wi	μm
Trabecular number	Tb.N	/mm
Trabecular separation	Tb.Sp	μm or mm

terminology is used the quantities are referred to as volume and surface, the absolute values being identical. The fourth type of primary measurement is number, which cannot be extrapolated to 3D unless serial sections have been used.

Width measurements can be converted to thickness by dividing the width value by $4/\pi$ for isotropic structures. Values for width can be obtained by direct measurement or indirectly by calculation from area and perimeter.

Bone histomorphometry is most commonly applied to cancellous bone, which has a higher bone turnover than cortical bone. Cancellous bone may be divided into corticoendosteal and mid-cancellous regions; definition of these regions is somewhat arbitrary but a consistent approach should be used where possible, for example, using fixed distances from the outer periosteum. Cortical bone has been largely neglected by histomorphometrists despite its predominance in the skeleton and its importance as a determinant of bone strength and fracture risk. Nevertheless, application of histomorphometric techniques to cortical bone has been described in the rib, iliac crest, and femoral neck *(9–11)*.

3.7. Limitations of Histomorphometry

Measurement variance associated with bone histomorphometry arises from a number of factors including intraobserver, interobserver, intermethod, and sample variation *(12–14)*. Observer variation is mainly due to the subjective criteria used for identification of features such as osteoid seams, bone struc-

tural units, and resorption cavities. In addition, the criteria for corticomedullary differentiation, staining methods used and the magnification at which measurements are made all contribute to variation. Many of these sources of variance can be minimized by the standardization of staining methods, corticomedullary delineation, and magnification. In addition, standardization of the criteria used to identify histological features should be employed where possible; 3 μm is used as the lower limit for the recognition of an osteoid seam width *(15)* and resorption cavities are identified under polarized light by the presence of cut off collagen fibers at the edge of the cavity *(16)*. Measurement of the tetracycline-labeled perimeter is also subject to substantial variation between observers, especially if old labels are present as a result of tetracycline administration in the past. Current histomorphometric techniques are limited by the lack of reliable markers for activation and resorption. At present, indices related to these processes are used to calculate dynamic indices of bone turnover, based on the assumption that bone resorption and formation are coupled temporally and spatially and that bone remodeling is in a steady state; neither of these assumptions is likely to be tenable in the presence of treated or untreated osteoporosis *(17)*.

3.8. Primary Histomorphometric Indices

Primary measurements are summarized in **Table 2** and discussed individually below. These indices are measured directly and include area measurements (e.g., bone area), perimeter measurements (e.g., osteoid perimeter) and certain distance measurements (e.g., osteoid seam width and mean wall width) (*see* **Note 3**). In principle, all distance measurements can be measured either directly at multiple locations or by indirect calculation from area and perimeter measurements. The direct method is preferable *(15)* and provides a frequency distribution, standard deviation, and a mean value, which are necessary for reconstructing the remodeling sequence.

In our laboratory we perform the primary measurements of bone area, osteoid perimeter, and osteoid seam width on von Kossa stained secions on a minimum of 25 fields from three to six sections.

1. Bone area (B.Ar/T.Ar): Bone area is the percent area occupied by calcified bone in relation to the total area.
2. Osteoid area (O.Ar/T.Ar): Osteoid area is the percent area occupied by osteoid in relation to the total area.
3. Osteoid perimeter (O.Pm/B.Pm): Osteoid perimeter is the percent of the bone surface occupied by osteoid in relation to the total bone perimeter (*see* **Note 3**).
4. Osteoid width (O.Wi): Osteoid width is measured at four equidistant points or eight points on seams longer than 600 μm in length. A minimum of 20 seams per biopsy is measured on the same sections used for osteoid perimeter. All seams with a width of 3 μm or more are included.

5. Osteoblast perimeter (Ob/Pm/B.Pm): Osteoblast perimeter is the percent of the bone perimeter occupied by plump, cuboidal osteoblasts in relation to the total bone perimeter.

6. Wall width (W.Wi): The mean width of completed bone remodeling units is measured on toluidine blue stained sections viewed under polarized light at ×156 magnification. A minimum of 25 bone packets is measured on each biopsy from between three and eight sections.

7. Mineralizing perimeter (M.Pm/B.Pm): Mineralizing perimeter is assessed as the extent of bone perimeter that exhibits either single or double labels. Measurements are performed at ×156 magnification on a minimum of six 15-μm thick sections using fluorescence microscopy (*see* **Note 4**).

8. Mineral apposition rate (MAR). The mineral apposition rate is calculated as the mean distance between double labels divided by the time period between the administration of the two labels. Measurements are made at the midpoint of each label at approx four equidistant points along each double-labeled surface. A minimum of 20 labels from six sections is measured. The interlabel period is calculated as the number of d between the midpoints of the two labeling dose regimens of tetracycline. (*see* **Note 5**).

9. Maximum eroded depth (E.De.Max): This is defined as the maximum depth of eroded cavities measured interactively (*see* **Note 6**).

10. Mean eroded depth (E.De): This is defined as the mean depth derived from measurements made at four equidistant points along the resorption cavity (*see* **Note 6**).

11. Eroded cavity area (E.Ar): This is defined as the area of eroded cavities, measured automatically (*see* **Note 6**).

12. Eroded perimeter (E.pm): This is the percentage of bone perimeter occupied by eroded cavities (*see* **Note 6**).

13. Osteoclast perimeter: This is the percentage of bone perimeter covered by osteoclasts.

14. Erosion length: Mean length of the base of the eroded cavities drawn by using the cursor, measured interactively.

15. Cavity number: This is the number of cavities per millimeter of bone perimeter measured automatically (*see* **Note 6**).

16. Cavity count/mm^2: This is the number of cavities per square millimeter medullary area (trabecular bone + marrow) (*see* **Note 6**).

17. Osteoclast number: This is defined as the number of osteoclasts in relation to the total area of the section (*see* **Note 6**).

3.9. Calculation of Derived Indices

Derived indices and their measurement units are summarized in **Table 3** and discussed individually below.

1. Adjusted apposition rate (Aj.AR): This represents the mineral apposition rate or the bone formation rate averaged over the osteoid surface. In a steady state and in the absence of a mineralization defect, the adjusted apposition rate is the best estimate available for osteoid or matrix apposition rate, as it can be assumed that they occur at the same rate (although not synchronously). It is calculated as follows:

$$Aj.AR = MAR \times M.Pm / O.Pm$$

It is clear from above equation that Aj.AR is usually less than MAR and cannot exceed it.

2. Mineralization lag time (Mlt): The mineralization lag time is the interval between the deposition and mineralization of a given amount of osteoid, averaged over the life span of the osteoid seam. It is calculated as follows:

$$Mlt = O.Wi / Aj.AR$$

3. Osteoid maturation time (Omt): Osteoid maturation time represents the interval between the onset of deposition and onset of mineralization of a given amount of osteoid at each bone forming site. It results from processes such as collagen crosslinking which are necessary before mineralization can occur. In humans Omt is shorter than Mlt and never exceeds it. It is calculated as follows:

$$Omt = O.Wi / MAR$$

4. Bone formation rate (BFR): Bone formation rate can either be expressed in terms of osteoid perimeter (Aj.AR) or in terms of bone perimeter (tissue-based bone formation rate, BFR / B.Pm) or bone area. BFR expresses the rate of bone formation per unit of bone surface and is calculated as:

$$BFR / B.Pm = MAR \times M.Pm / B.Pm$$

5. Activation frequency (Ac.F): Activation frequency is a key determinant of bone mass in the adult skeleton and increased Ac.F is an important mechanism of bone loss in osteoporosis *(18)*. Ac.F is the frequency with which a given site on the bone surface will undergo new remodeling. At present there are no *in situ* markers of activation and so it has to be calculated indirectly, as the frequency with which a given site on the bone surface undergoes new remodeling, as follows:

$$Ac.F = (1/Tt.P) \text{ or } (BFR / B.Pm) / W.Wi)$$

6. Remodeling periods: The remodeling period is the average duration of a single cycle of bone remodelling at any point on the bone surface and is the sum of resorption, reversal, and formation periods. The formation period is the mean time required to build a new bone structural unit and is divided into the active (FPa+) and the inactive (FPa-) formation periods. FPa- is a measure of the "off-time," which accounts for the discrepancy between the osteoid and mineralising

perimeters that is not attributable to label escape. The formation period (FP) can be calculated as follows:

$$FP = W.Wi / Aj.AR$$

$$FPa+ = W.Wi / MAR$$

$$FPa- = FP - FPa+$$

Quiescent period (QP), erosion period (EP), and reversal period (Rv.P) are calculated as follows:

$$QP = Q.Pm/B.Pm \times FP$$

$$EP = E.Pm/B.Pm \times FP$$

$$Rv.P = Rv.Pm/B.Pm \times FP$$

The total period is defined as the time between the initiation of two successive remodeling cycles and is the sum of Rm.P and QP:

$$Tt.P = Rm.P + QP$$

3.10. Assessment of Bone Structure

Both cortical and cancellous bone structure are important determinants of bone strength. Cortical geometry, porosity, and width, together with cancellous bone size, shape, connectivity, and anisotropy, determine the mechanical strength of bone. A number of different approaches to the study of bone structure have been described, including direct measurement or calculation of trabecular width, separation and density *(19)*, strut analysis *(1)*, assessment of the trabecular bone pattern factor *(20)* and star volume *(21)*.

1. Trabecular width, separation and number: These indices can either be measured directly or calculated, as follows:
   a. Trabecular width (Tb.Wi) = $(2 \times B.Ar)/B.Pm$
   b. Trabecular number (Tb.N): Tb.N = $(B.Ar/T.Ar)/Tb.Wi$
   c. Trabecular separation (Tb.Sp): = $(1/Tb.N) - Tb.Wi$
2. Strut analysis: This method is based on the topological classification of struts and the definition of nodes and termini *(8)*. The bone section is viewed with a CCD camera mounted on a light box, allowing the whole section to appear within a single field of view (magnification ×9). Images of the whole bone sections are captured on the video screen and segmented to yield a gray-level image of the section. These binary images are interactively edited to remove "bone dust" at the edges of the section and rejoin torn trabeculae, referring to sections under the microscope. The right and left corticomedullary junctions are defined automatically. The upper and lower boundaries are defined by the operator and the images

are saved as "binim" files. These files are skeletonized to give a symmetric axis of the original bone profile. The computer automatically identifies trabecular nodes and termini and produces images with color-coded struts. The total length of all struts is calculated and the length of individual strut types is expressed as a percentage of the total length (*see* **Note 7**). The following indices are generated:

Tm./Tm: Number of struts joining free ends (termini).
Nd./Tm: Number of struts joining a node to a free end.
Nd./Nd: Number of struts joining two nodes.
Nd./ Lp: Number of struts forming part of a closed loop.
Cx./Tm: Number of struts joining a free end to the cortex.
Cx./Nd: Number of struts joining a node to the cortex.
Cx./Cx: Number of struts joining cortex to the same cortex.
Nd/Tm: Ratio of all nodes to free ends in a section.

3. Trabecular bone pattern factor: This index is based on the relationship between convex and concave surfaces *(30)*, convexity indicating poor connectivity and concavity being associated with a well-connected structure. Trabecular bone pattern factor (Tb.Pf) is assessed automatically by measuring the trabecular area and perimeter within the active region of the binary image before and after dilatation. Tb.Pf is calculated as follows:

$$Tb.Pf = (P1 - P2) / (A1 - A2)$$

Where P1 is the original perimeter, P2 is the dilated perimeter, A1 is the original area, and A2 is the dilated area. Values of Tb.Pf may be influenced by the computer-based smoothing technique, the degree of dilatation used, and the magnification at which the measurement is performed.

4. Star volume: The star volume is defined as the mean volume of all parts of an object that can be seen unobscured from a random point within the object *(22)* and can be applied to either the trabeculae (trabecular star volume) or the marrow (marrow space star volume). The application of this measurement was described by Vesterby using the vertical section technique and a cycloid test system, to assess trabecular structure in both vertebral *(23)* and iliac crest cancellous bone *(21)*. This method involves generation of intercepts from random sampling points, which in turn are used to measure the true Euclidean distance between the grid point and the intercept (l_n). This distance is measured using a simple computer algorithm and raised to the power of three (l_n^3). Marrow space star volume (mm^{-3}) is calculated as:

$$V^*_{\text{m.space}} = 4 \times (\pi/3) \times (l_n^3)$$

Values obtained for marrow space star volume are significantly influenced by biopsy size, especially in poorly connected cancellous bone.

3.11. Three-Dimensional Approaches

A number of approaches are now available for the generation of 3D images of bone, including reconstruction of serial sections *(24,25)*; scanning and ste-

reo microscopy; volumetric, high resolution, and microcomputed tomography and magnetic resonance imaging *(26,27)*. Although the in vivo application of these approaches is currently limited, they can provide information not available from histological sections, such as connectivity, anisotropy, and trabecular size and shape.

4. Notes

1. Histomorphometric measurements were originally accomplished by superimposing a set of lines and points, known as a grid or graticule, on the image. This was either inserted into the eyepiece of the microscope or drawn to a much larger scale on a flat surface onto which the image was projected. Several grids have been described. The Zeiss Integrationplatte 1 consists of 25 points arranged in a square array. The points are located at the crossings of short vertical lines with long horizontal lines. Random test line orientation can be achieved using alternative hemispherical lines, or a cycloid test grid for vertical sections *(28)*. Alternatively, random orientation of test lines may be achieved by random rotation of the graticule between each field of measurement *(29)*. Several commercial measuring systems are now available; alternatively, in-house systems can be designed using relatively simple hardware. The field area to be measured is defined using a square etched on the eyepiece graticule. The square is mapped to correspond with an active area on the table and an active drawing area on a video monitor. The system is calibrated for each magnification used. Computerized semi-automated methods for bone histomorphometry have now largely superseded the use of graticules, because they are less labor intensive and tedious for the operator and can perform complex measurements (e.g., strut analysis) that cannot easily be achieved by non computerized techniques. The method which we use combines a manually operated interactive drawing system and a computer for storing measurement data. Perimeter measurements are made by tracing with the cursor LED and distance measurements are made either by dotting with the cursor on either side of the structure at equally spaced points or by tracing the outline of the structure. For example, to measure a bone structural unit, the cement line and the outer mineralized bone surface are drawn separately using the cursor and the digitizing tablet. The distances between the two lines are calculated automatically at four equidistant points and stored as a mean of four measurements.

2. The preparation of high-quality histological sections is an essential prerequisite for bone histomorphometry. The specimens are embedded in a hard resin to allow preparation of undecalcified sections to assess mineralization of bone. The resins most commonly used are methylmethacrylate and LR White resin. In our laboratory we use LR White resin because of its lower toxicity and the shorter embedding time relative to methylmethacrylate.

3. Assessment of osteoid: Measurements of osteoid perimeter and osteoid seam width are strongly influenced by the magnification and the stain used. At low magnification it is difficult to differentiate between the thin endosteal membrane covering the quiescent bone surface and the osteoid seam. Therefore, all seams

less than one lamella (approx 3 μm) are excluded.

4. Interpretation of single tetracycline labels: The presence of single labels reflects the labeling escape phenomenon, caused by initiation of mineralization before the first label or its termination between administration of the two tetracycline doses *(30)*. If only double-labeled perimeters are considered, therefore, the actively mineralizing perimeter will be underestimated and thus the double plus half the single labels are included in this measurement.

$$Md.Pm/B.Pm\ (\%) = dL.Pm + (0.5 \times sL.Pm)/B.Pm$$

where

dL.Pm = double-labeled perimeter

sL.Pm = single-labeled perimeter

Single labels can also reflect the switch from an active to resting state in a minority of osteoid seams, that is, the "on/off" phenomenon. In cases where only single labels can be detected, it is suggested that the mineralising perimeter is expressed as half the single-labeled perimeter.

5. MAR is used to derive several indices of bone formation, and therefore an accurate measurement is of importance. In biopsies in which there is no uptake of tetracycline the MAR and the derived indices are treated as missing data. In cases where only single labels can be detected, the finite lower limit of 0.3 μm/d for MAR value is used *(31)*.

$$MAR\ (\mu m/day) = L.Wi/LP$$

where L.Wi is the interlabel distance and LP is the labeling period.

6. Assessment of bone resorption: Accurate measurement of resorption cavities is associated with a number of problems related to their identification and, in particular, characterization of cavities in which resorption has been completed. Problems related to identification of resorption can be resolved to a certain extent by using polarized light microscopy to demonstrate cut off lamellae at an angle to the bone whereas the presence of osteoid in the cavity *(16)* indicates that resorption has been completed. The presence of osteoclasts within the cavity may also aid identification, particularly when histochemical techniques are used to demonstrate the presence of tartrate resistant acid phosphatase (although this is not specific to osteoclasts) *(32,33)*. However, there is currently no certain method of distinguishing between completed cavities without osteoid and those cavities in which the process of resorption has been terminated prematurely ("arrested resorption") *(34)*. One method of direct measurement of resorption cavity size is to count the number of eroded lamellae beneath the trabecular surface in resorption cavities and to characterize the cavities according to the type of cells present *(35)*. This method enables measurement of completed resorption cavity size but is technically challenging and has not been widely adopted. The computerized method developed by Garrahan et al. *(36)* enables a relatively rapid and more widely applicable quantitative assessment of several resorption cavity characteristics including mean and maximum erosion depth, length, area, and number of cavities. This method involves reconstruction of the eroded bone surface by a curve fitting technique (cubic spline);

alternatively, reconstruction can be done manually *(37)*. Inclusion of all cavities in the measurements results in underestimation of the size of completed cavities but does provide information about the distribution of cavity indices and enables measurement of the eroded surface. Using this method, cavities are identified on toluidine blue stained sections, viewed under polarized light at ×156 magnification and measured at ×62.5, ×156, and ×312 magnification according to the size of the cavity. Cavities with a depth of >3 μm are included. A minimum of 20 resorption cavities is assessed per biopsy, from between two to six sections.

7. Analysis of struts: Struts at the border intersecting the upper and lower boundaries are not included in the analysis. Results can also be expressed as a percentage of tissue area, as the trabecular area is measured automatically at the same magnification.

References

1. Garrahan, N. J., Mellish, R. W. E., and Compston, J. E. (1986) A new method for the analysis of two-dimensional trabecular bone structure in human iliac crest biopsies. *J. Microsc.* **142**, 341–349.

2. Compston, J. E., Garrahan, N. J., Croucher, P. I., and Yamaguchi, K. (1993) Quantitative analysis of trabecular bone structure. *Bone* **14**, 187–192.

3. Frost, H. M. (1969) Tetracycline-based histological analysis of bone remodelling. *Calcif. Tissue Int.* **3**, 211–237.

4. Matrajt, H. and Hioco, D. (1996) Solochrome cyanin R as an indicator dye of bone morphology. *Stain Tech.* **41**, 97–99.

5. Goldner, J. (1938) A modification of the Masson trichrome technique for routine laboratory purposes. *Am. J. Pathol.* **14**, 237–243.

6. Villanueva, A. R., Kujawa, M., Mathews, C. H. E., and Parfitt A. M. (1983) Identification of the mineralization front: comparison of a modified toluidine blue stain with tetracycline fluorescence. *Metab. Bone Dis. Rel. Res.* **5**, 41–45.

7. Parfitt, A. M.(1983) The physiological and clinical significance of bone histomorphometric data, in *Bone Histomorphometry: Techniques and Interpretations* (Recker, R., ed.), CRC Press, Boca Raton, FL pp. 143–224.

8. Parfitt, A. M., Drezner, M. K., Glorieux, F. H., et al. (1987) Bone histomorphometry: standardization of nomenclature, symbols and units. *J. Bone Min. Res.* **2**, 595–610.

9. Frost, H. M. (1963) Mean formation time of human osteons. *Canad. J Biochem. Physiol.* **41**, 1307–1319.

10. Agerbaek, M. O., Eriksen, E. F., Kragstrup, J., Mosekilde, L., and Melsen, F. (1991) A reconstruction of the remodelling cycle in normal human iliac cortical bone. *Bone Miner.* **12**, 101–112.

11. Bell, K. L., Loveridge, N., Power, J., Garrahan, N. J., Meggitt, B. F., and Reeve, J. (1999) Regional differences in cortical porosity in the fractured femoral neck. *Bone* **24**, 57–64.

12. de Vernejoul, M. C., Belenguer-Prieto, R., Kuntz, D., et al. (1998) Bone histo-

logical heterogeneity in postmenopausal osteoporosis: a sequential histomorphometric study. *Bone* **8**, 339–342.

13. Chavassieux, P. M., Arlot, M. E., and Meunier, P. J. (1985) Intermethod variation in bone histomorphometry: comparison between manual and computerised methods applied to iliac bone biopsies. *Bone* **6**, 211–219.

14. Wright, C. D. P., Vedi, S., Garrahan, N. J., Stanton, M., Duffy, S., and Compston, J. E. (1992) Combined inter-observer and inter-method variation in bone histomorphometry. *Bone* **13**, 205–208.

15. Vedi, S. and Compston, J. E. (1984) Direct and indirect measurements of osteoid seam width in human iliac crest trabecular bone. *Metab. Bone Dis. Rel. Res.* **5**, 269–274.

16. Vedi, S., Tighe J. R., and Compston, J. E. (1984) Measurement of total resorption surface in iliac crest trabecular bone in man. *Metab. Bone Dis. Rel. Res.* **5**, 275–280.

17. Compston, J. E. and Croucher, P. I. (1991) Histomorphometric assessment of trabecular bone remodelling in osteoporosis. *Bone Miner.* **14**, 91–102.

18. Frost, H. M. (1985) The pathomechanics of osteoporosis. *Clin. Orthop. Rel. Res.* **200**, 198–225.

19. Parfitt, A. M., Mathews, C. H. E., Villanueva, A. R., Kleerekoper, M., Frame, B., and Rao, D. S. (1983) Relationship between surface volume and thickness of iliac trabecular bone in aging and in osteoporosis. Implications for the microanatomic and cellular mechanism of bone loss. *J. Clin. Invest.* **72**, 1396–1409.

20. Hahn, M., Vogel, M., Pompesius-Kempa, M., and Delling, G. (1992) Trabecular bone pattern factor—a new parameter for simple quantification of bone microarchitecture. *Bone* **13**, 327–330.

21. Vesterby, A. (1990) Star volume of marrow space and trabeculae in iliac crest: sampling procedure and correlation to star volume of 1st lumbar vertebra. *Bone* **11**, 149–155.

22. Serra, J. (1982) *Image Analysis and Mathematical Morphology*. Academic Press, London, UK.

23. Vesterby, A., Gundersen, H. J. G., and Melsen, F. (1989) Star volume of marrow space and trabeculae of first lumbar vertebra: sampling efficiency and biological variation. *Bone* **10**, 7–13.

24. Odgäard, A. and Gundersen, H. J. G (1993) Quantification of connectivity in cancellous bone, with special emphasis on 3-D reconstruction. *Bone* **14**, 173–182.

25. Gundersen, H. J. G., Boyce, R. W., Nyengäard, J. R., and Odgäard, A. (1993) The conneulor: unbiased estimation of connectivity using physical disectors under projection. *Bone* **14**, 217–222.

26. Majumdar, S. and Genant, H. K. (1995) A review of the recent advances in magnetic resonance imaging in the assessment of osteoporosis. *Osteoporos. Int.* **5**, 79–92.

27. Genant, H. K., Engelke, K., Fuerst, T., et al. (1996) Non invasive assessment of bone mineral and structure; state of the art. *J. Bone Miner. Res.* **11**, 707–730.

28. Vesterby, A., Kragstrup, J., Gundersen, H. J. G., and Melsen, F. (1987) Unbiased stereological estimation of surface density in bone using vertical sections. *Bone* **8**, 13–17.

29. Kragstrup, J., Melsen, F., and Mosekilde, L. (1982) Reduced wall thickness of

completed remodelling sites in iliac trabecular bone following anticonvulsant therapy. *Metab. Bone Dis. Rel. Res.* **4**, 181–185.

30. Frost, H.M. (1983) Bone histomorphometry: choice of marking agent and labelling schedule, in *Bone Histomorphometry: Techniques and Interpretation* (Recker, R., ed.), CRC Press, Boca Raton, FL, pp. 37–51.

31. Foldes, J., Shih, M. S., and Parfitt, A. M. (1990) Frequency distribution of tetracycline based measurements: implication for the interpretation of bone formation indices in the absence of double-labelled surfaces. *J. Bone Min. Res.* **5**, 1063–1067.

32. Evans, R. A., Dunstan, C. R., and Baylink, D. J. (1979) Histochemical identification of osteoclasts in undecalcified sections of human bone. *Miner. Electrolyte Metab.* **2**, 179–185.

33. Burstone, M. S.(1959) Histochemical demonstration of acid phosphatase activity in osteoclasts. *J. Histochem. Cytochem.* **7**, 39–41.

34. Croucher, P. I., Gilks, W., and Compston, J. E. (1995) Evidence for interrupted bone resorption in human iliac cancellous bone. *J Bone. Miner. Res.* **10**, 1537–1543.

35. Eriksen, E. F., Gundersen, H. J. G., Melsen, F., and Mosekilde, L. (1984) Reconstruction of the resorptive site in iliac trabecular bone; a kinetic model for bone resorption in 20 normal individuals. *Metab. Bone Dis. Rel. Res.* **5**, 235–242.

36. Garrahan, N. J., Croucher, P. I., and Compston, J. E. (1990) A computerised technique for the quantitative assessment of resorption cavities in trabecular bone. *Bone* **11**, 241–246.

37. Cohen-Solal, M. E., Shih, M-S., Lundy, M. W., and Parfitt, A. M. (1991) A new method for measuring cancellous bone erosion depth: application to the cellular mechanisms of bone loss in postmenopausal osteoporosis. *J. Bone. Miner. Res.* **6**, 1331–1338.

21

Transmission Electron Microscopy of Bone

Vincent Everts, Anneke Niehof, and Wouter Beertsen

1. Introduction

Ultrastructural analysis of bone and other mineralized tissues such as calci-fied cartilage and dentin is essential for the understanding of the cell–cell/cell–matrix interaction, composition, and three-dimensional organization of these tissues. A wide variety of techniques have been introduced to process such tissues. This chapter describes a few methods to process mineralized tissues obtained from different sources. In addition, attention is paid to processing of cultured bone explants for electron microscopic analysis.

2. Materials

Prepare all solutions containing fixative in a fume hood and use gloves. All compounds are very toxic and most are volatile.

2.1. Fixative

The fixative is 4% paraformaldehyde and 1% glutardialdehyde in 0.1 M sodium cacodylate buffer, pH 7.4) (*see* **Notes 1** and **2**).

1. Heat 200 mL of distilled water to 70°C.
2. Dissolve 40 g of paraformaldehyde and add approx 2.5 g of sodium hydroxide pellets. Allow the solution to cool (the solution should be clear).
3. Add 21.4 g of sodium cacodylate.
4. Add 40 mL of 25% glutardialdehyde and fill up to 800 mL with distilled water.
5. Adjust the pH to 7.4 with 1 N HCl and fill up to 1000 mL.
6. This solution should be stored at 4°C and new fixative should be prepared each week (*see* **Note 1**).

2.2. Osmium and Ferrocyanide Postfixative

The osmium and ferrocyanide postfixative consists of 1% osmium tetroxide and 1.5% potassium ferrocyanide $[K_4Fe(CN)_6].3H_2O]$ in 0.1 M sodium cacodylate buffer, pH 7.4. Stock solutions should be stored at 4°C (*see* **Note 3**).

1. 2% OsO_4 stock solution: Add 1 g of OsO_4 crystals (EMS, crystalline, highest purity 99.95%) to 50 mL of double-distilled water in a stoppered dark glass vial. Gently shake the solution until the crystals are dissolved. Store the solution in the tightly closed vial at 4°C. To avoid blackening of the solution the vial has to be thoroughly cleaned with acetone to remove lipids (osmium is an excellent fixative for lipids!), washed in double-distilled water, and dried. **Caution**: Use gloves and avoid any contact with the skin!
2. 0.2 M Sodium cacodylate buffer: Dissolve 42.8 g of sodium cacodylate in 900 mL of distilled water. Adjust the pH to 7.4 and add distilled water to a volume of 1000 mL.
3. 3% Ferrocyanide stock solution: Dissolve 3 g of potassium ferrocyanide in 0.2 M sodium cacodylate buffer.
4. Prior to use, mix one volume of 2% OsO_4 solution with one volume of 3% ferrocyanide solution.

2.3. Osmium and Cacodylate Postfixative

The osmium and cacodylate postfixative consists of 1% osmium tetroxide in 0.075 M sodium cacodylate buffer (*see* **Note 3**).

1. 4% Osmium tetroxide stock solution: Dissolve 1 g OsO_4 of crystals in 25 mL of distilled water according to the method described in **Subheading 2.2.**, **step 1**.
2. 0.1 M Sodium cacodylate buffer: Dissolve 21.4 g of sodium cacodylate in 900 mL of distilled water, adjust the pH to 7.4, and add distilled water to a volume of 1000 mL.
3. Prior to fixation, mix one volume of the 4% OsO_4 solution with three volumes of 0.1 M sodium cacodylate buffer.

2.4. Decalcification Solution

The decalcification solution consists of 1.9% glutaraldehyde and 0.15 M EDTA (Titriplex III, ethylenedinitrilotetraacetic acid disodium salt dihydrate) in 0.06 M sodium cacodylate buffer.

1. Dissolve 38.53 g of sodium cacodylate and 167.52 g of Titriplex III in 2 L of distilled water.
2. Stir the solution, and as soon as all Titriplex is dissolved (the solution should be clear) add 232 mL of 25% glutaraldehyde.
3. Adjust the pH to 7.4, first by adding approx 10 g of sodium hydroxide pellets followed by adding 2 N sodium hydroxide. Add distilled water to a volume of 3 L (*see* **Note 1**). This solution is stable for several mo at 4°C.

2.5. Goldner's Masson Trichrome

1. Dissolve 1.25 g of hematoxylin in 100 mL of 25% ethanol.
2. Dissolve 0.15 g of Light Green SF Yellowish and 0.2 mL of glacial acetic acid in 100 mL of distilled water.
3. Ponceau de Xylidine stock: Dissolve 1 g of Ponceau de Xylidine and 1 mL of glacial acetic acid in 100 mL of distilled water.
4. Acid fuchsin stock: Dissolve 1 g of acid fuchsin and 1 mL of glacial acetic acid in 100 mL of distilled water.
5. Ponceau–acid fuchsin stock: Two parts of Ponceau de Xylidine stock (**item 3**) with one part of acid fuchsin stock (**item 4**).
6. Orange G stock: Dissolve 1 g of Orange G in 100 mL of distilled water.
7. Ponceau–acid fuchsin staining solution: One part of Ponceau–acid fuchsin stock (**item 5**), one part of Orange G stock (**item 6**), and eight parts of distilled water.
8. Dissolve 0.5 g of phosphomolybdic acid hydrate in 100 mL of distilled water.
9. Dissolve 2.5 g of ferric chloride and 1 mL of concentrated HCl in 99 mL of distilled water.
10. Rinsing solution: 5.2 mL of 96% acetic acid in 1000 mL of distilled water.
11. All staining solutions are stable for months and are stored at room temperature.

2.6. Methylene Blue

1. Dissolve 2 g of methylene blue (Merck no. 1.15943) in 100 mL of distilled water (solution a).
2. Dissolve 0.5 g of Azure II (Merck no. 1.09211) in 50 mL of distilled water (solution b).
3. Dissolve 2 g of Borax (disodium tetraborat-10-hydrat) in 100 mL of distilled water (solution c).
4. Mix solutions a:b:c = 2:1:1, and store at 4°C. The staining solution is stable for months.
5. Filter just before use.

2.7. von Kossa

1. Dissolve 0.5 g of silver lactate in 100 mL of double distilled water.
2. Dissolve 0.5 g of hydrochinon in 100 mL of double distilled water.
3. Dissolve 5 g of sodium thiosulfate pentahydrate in 100 mL of distilled water.
4. All solutions are made fresh just before use.

2.8. Uranyl Acetate

1. Dissolve 0.35 g of uranyl acetate in 10 mL of double-distilled water. Store at 4°C.

2.9. Lead Nitrate

1. Boil and cool 50 mL of double-distilled water.
2. Dissolve 1.33 g of lead nitrate and 1.76 g of trisodium citrate dihydrate in 30 mL of water.
3. Shake vigorously for 1 min and then a few times during the following 30 min.
4. Add 8 mL of 1 N NaOH and boiled water to a volume of 50 mL. Store at 4°C.

2.10. Epoxy Resin

Use gloves and a fume hood when preparing the stock of epoxy resin.

1. Mix under continuous stirring the resin components (Ladd Res. Industries, Williston, VT), adding the next component when the previous one is completely dissolved. The components should be added in the following order: 100 g of LX-112 epoxy resin, 72.4 g of dodecenylsuccinic anhydride (DDSA), 40.4 g of nadicmethyl anhydride (NMA), and 3.9 g of 2,4,6-tri(dimethylamine-methyl) phenol (DMP-30).
2. Stir very well for another 30 min and collect the mixed resin in small, 10-mL plastic vials with cap.
3. Store these vials at –80°C. The frozen vials can be kept at this temperature for a very long time (at least for 1 yr).
4. Prior to embedding, warm an appropriate number of vials at ambient temperature. Open the dried vial only when the resin is at room temperature.

3. Methods
3.1. Perfusion Fixation of Animal Bones

1. Use a perfusion fixation system consisting of a perfusion pump or a bottle with a rubber cap hanging upside down at a height of approx 50 cm above the work area. If a pump is used, the tube is inserted in a bottle with fixative. If a hanging bottle is used, a needle (0.8 × 40 mm) is fixed to a tube and inserted into the rubber cap of the bottle. In addition, inserting a second tube with a needle into the cap makes an air inlet. The other end of this tube is fixed to the side of the bottle, with its opening above the fluid level in the bottle. To the tube used for fixation a hypodermic needle (0.6 × 30 mm for small animals [e.g., young mice], 0.8 × 40 mm for larger animals) is fixed for insertion into the heart. A valve should be placed somewhere along the length of the tube used for fixation.
2. Anesthetize the animal and fix it on its back on a plateau. Open the belly and cut the thorax left and right from the sternum. Reflect the skin and open the thorax, expose the heart, and cut the pericardium.
3. Fix the heart with two fingers (use well-fitting gloves) and insert the needle through the wall of the left ventricle. Open the tube valve (hanging bottle system) or switch on the perfusion pump (set to 2.5 mL/min). Wait a few seconds and cut the right atrium with a fine pair of scissors to let the perfusate escape.
4. The quality of fixation is checked by testing the stiffness of soft tissues such as the lip, the bleaching of the liver, and rigidness of the paws. After 5–10 min the perfusion is stopped and the tissues are collected and stored in fixative.

3.2. Immersion Fixation of Animal Bones

1. After euthanizing the animal and exposure of the bones of interest, dissect the bones and immerse them as quickly as possible in the fixative (4% paraformaldehyde and 1% glutaraldehyde in 0.1 M sodium cacodylate buffer, pH 7.4). If bones are collected from larger animals, the bones should be cut into smaller pieces. Cutting is preferably done in fixative. (Bones of young mice can be fixed without further cutting.)

2. Fix at ambient temperature for at least 4 h. After this the tissue samples can be left in fixative overnight at 4°C.
3. Transfer to postfixative for 1 h (*see* **Note 3**).
4. Wash the sample in 0.1 *M* sodium cacodylate buffer.
5. Proceed with the embedding protocol (*see* **Subheading 3.6.** and following).

3.3. Immersion Fixation of Human Bone Samples

Immersion fixation and processing of bone samples obtained from humans is similar to the protocol described in **Subheading 3.2.** It is essential that the samples are immersed into the fixative as quickly as possible and that the size of the fragments is small. Try to keep a maximal thickness of approx 3–5 mm. Cutting of the bones into smaller fragments has to be performed in fixative.

3.4. Immersion Fixation of Cultured Mineralized Tissues

1. Collect the bone explants after the preferred culture period and place in fixative (*see* **Note 4**).
2. Leave at ambient temperature for at least 4 h (after this period the fixed bones can be kept at 4°C for another day).
3. Process the bones further with or without decalcification (*see* **Subheading 3.5.**). Bones obtained from (very) young animals (e.g., mice <10 d) can be processed without the decalcification step.

3.5. Decalcification of Mineralized Tissues

1. Following fixation, immerse the bone samples in decalcification solution.
2. Place the samples at 4°C for 2–3 wk, replacing the decalcification solution weekly.
3. Check whether decalcification has been completed by X-ray photography.
4. Once decalcification is complete, proceed to embedding.

3.6. General Approach to Embedding and Analysis of Mineralized Tissues by TEM

Special care has to be taken in the embedment of calcified tissues, as epoxy resins do not easily penetrate such tissues. Bones and/or teeth obtained from very young animals can be easily embedded in resin without giving problems with cutting and/or staining. Special attention has to be paid to embedding of bones from older and larger animals or man.

3.7. Embedding of Small Tissue Samples

Tissue samples obtained from young animals (up to 1 wk old) of approx 3–5 mm in thickness are put into glass (plastic dissolves in propylene oxide!) vials that can be closed and they are embedded as follows:

1. Immerse the sample in 70% ethanol for 5 min. Repeat this three times.
2. Replace with 80% ethanol for 5 min. Repeat this three times.
3. Replace with 90% ethanol for 5 min. Repeat this three times.

4. Replace with 96% ethanol for 5 min. Repeat this three times.
5. Immerse the tissue in 100% ethanol and close the bottle. Incubate for 10 min. Repeat the 10 min incubation in 100% ethanol three times in total.
6. Replace the ethanol is replaced by propylene oxide. Incubate in a closed vial for 10 min. Change the propylene oxide and repeat once.
7. Dissolve the epoxy resin in propylene oxide at a 1:1 concentration. Immerse the tissue samples in the epoxy resin–propylene mixture, close the vials, and leave overnight with gentle shaking.
8. Replace with pure epoxy resin and with the vials left open, place on a shaker and leave gently shaking for 5 h.
9. Immerse the tissue samples in fresh epoxy resin in plastic molds, label, and leave overnight in an oven at 40°C.
10. Transfer to an oven set at 60°C to allow polymerization of the resin.

3.8. Embedding of Larger Bone Samples

It is possible to embed tissue samples of the size of a lower jaw of a full-grown mouse with good results. Larger samples have to be reduced in size or have to be cut in smaller pieces to obtain sufficient penetration of the epoxy resin.

1. Follow the procedure as indicated under **Subheading 3.7.** but increase the duration of each ethanol dehydration step to 10 min and each propylene oxide impregnation steps to 20 min.
2. Immerse the samples in propylene oxide–epoxy resin at a ratio of 3:1 for 3 h.
3. Immerse the samples in a 1:1 mixture of propylene oxide–epoxy resin for 3 h.
4. Immerse the samples in a 1:3 mixture of propylene oxide–epoxy resin overnight.
5. Immerse the samples in pure epoxy resin, with the vials open and shaking for 6 h.
6. Embed the samples in fresh epoxy resin and leave overnight in an oven at 40°C.
7. Proceed with polymerization as described in **Subheading 3.7.**, **step 10**.

3.9. Sectioning Mineralized Tissues

Sectioning of the tissue is best performed using diamond knives, which are available both for semithin and ultrathin sectioning (*see* **Notes 5** and **6**).

1. Use a glass knife to trim the block.
2. Proceed with semithin and ultrathin sectioning using a diamond knife with the cutting angle set at 6°.
3. Make sure the microtome to manually cut at a very low speed (1 mm/sec).
4. To avoid wetting of the surface of the tissue block, keep the water level of the trough as low as possible.

3.10. Methylene Blue Staining of Semithin Sections

The methylene blue staining solution stains most tissue components. It is an excellent stain for general purposes. Owing to its metachromatic properties, some components (e.g., cartilage and granules of mast cells) stain purple.

1. Cut semithin sections of approx 1–2 μm thickness.
2. Collect the sections on a drop of water on a glass slide and dry the sections on a heating plate (60–70°C); leave the sections on the plate for an hour or longer. To avoid wrinkles of sections of larger tissue samples sections are best dried on a plate at 50°C. Dry these sections overnight before staining.
3. When the sections are dry, add a drop of the filtered methylene blue staining solution to the section.
4. Leave the staining solution for approx 15 sec (depending on the type of tissue and thickness of the section).
5. Wash the section extensively with a jet of distilled water.
6. Dry the washed section and cover it with a drop of epoxy resin.
7. Cover the section with a cover glass and leave the section for several hours on a hot plate (or in a stove at 60°C) to polymerize the resin.

3.11. Modified Goldner's Masson Stain for Sections of Epoxy Resin

The Goldner stain *(1)* stains nonmineralized bone (e.g., osteoid) red, mineralized bone green, and calcified cartilage very light green. It also provides a very good staining for cells associated with bone and cartilage (**Fig. 1**). All staining procedures are carried out on a hot plate at 68–70°C.

1. Cut sections of approx 2.5 μm thickness.
2. Collect the sections on a coated (e.g., Vectabond, Vector Laboratories, #SP-1800) slide and dry them on a hot plate.
3. Wet the sections with distilled water and shake off excess of water.
4. Stain for 3 min with ferric chloride on hot plate.
5. Rinse quickly with warm tap water and dry on hot plate.
6. Stain for 25 sec with hematoxylin on hot plate.
7. Rinse quickly with warm tap water and dry on hot plate.
8. Stain for 8 min with Ponceau–acid fuchsin staining solution on hot plate.
9. Rinse quickly with 0.5% acetic acid.
10. Stain for 3 min with 0.5% phosphomolybdic acid on hot plate.
11. Rinse quickly with 0.5% acetic acid.
12. Stain for 3–5 min with Light Green SF Yellowish on hot plate.
13. Rinse quickly with 0.5% acetic acid.
14. Air-dry and cover the sections.

3.12. von Kossa

The von Kossa staining procedure *(2)* results in a black staining of mineralized tissue parts. If methylene blue is used as a counterstain, the other tissue components stain in different intensities of blue.

1. Cut sections of 2 μm thickness.
2. Collect the sections on coated slides (*see* **Subheading 3.11.**, **step 2**) and dry them on a hot plate.
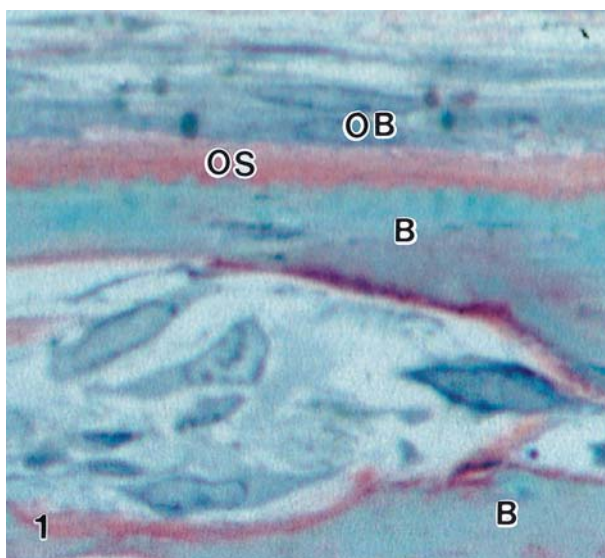
Fig. 1. Light micrograph of a section of mouse calvarial bone stained with the Goldner Masson's Trichrome staining. The mineralized bone (B) is green and the osteoid (OS) is red. Section was obtained from epoxy resin embedded undecalcified bone. Bone was fixed in 4% paraformaldehyde and 1% glutaraldehyde in 0.1 M sodium cacodylate buffer. OB,Osteoblast. (Reduced from original magnification, ×3000.)

3. Incubate the sections with 0.5% silver lactate for 20 min at ambient temp.
4. Rinse the sections with double-distilled water.
5. Incubate the sections with 0.5% hydrochinon for 2 min at ambient temperature.
6. Rinse the sections in double-distilled water.
7. Incubate the sections with 5% sodium thiosulfate pentahydrate for 2 min at ambient temperature.
8. Rinse the sections in double-distilled water.
9. Sections can be counterstained with methylene blue (*see* **Subheading 3.10.**).
10. Dry the sections and cover them.

3.13. Staining of Ultrathin Sections with Uranyl Acetate

1. Centrifuge the uranyl solution (10 min, 3000 rpm).
2. Put drops of uranyl acetate on a strip of parafilm.
3. Float the grids on top of the drops (sections facing the solution).
4. Stain the sections for 4–8 min in the dark.
5. Rinse the sections extensively with double-distilled water.
6. Air-dry the sections and stain them with lead nitrate.

3.14. Staining of Ultrathin Sections with Lead Nitrate (3)

1. Centrifuge the lead solution (10 min, 3000g).
2. Put drops of lead nitrate on a strip of parafilm.

3. Place a few sodium hydroxide pellets around the drops.
4. Float the grids on top of the drops of the lead solution.
5. Cover the drops and pellets with a cover of a Petri dish.
6. Stain the sections for 2–4 min.
7. Rinse the sections extensively with double-distilled water.
8. Air-dry the sections.

4. Notes

1. The fixatives mentioned in this chapter give reproducible and reliable results (**Figs. 2** and **3**). The recipes given are for large volumes. If your laboratory does not have a high throughput of samples, the amounts can be reduced appropriate to your needs. One of the advantages is that tissue samples can be stored for a very long time in the aldehyde mixture without noticeable loss of ultrastructural details. Essential is that the paraformaldehyde is not older than 1 wk before its use for the initial fixation of tissue samples.

2. Apart from the fixative mentioned in this chapter numerous others mentioned in the literature could be used that may give very good results. **Caution**: Whatever fixative used, it is crucial to avoid the use of phosphate buffer! Fixation carried out in phosphate-buffered fixatives, in particular if the fixative is somewhat older, results in formation and precipitation of mineral crystallites (**Fig. 4**). These crystallites are formed at the conjunction of mineral-containing tissue (e.g., bone) and the surrounding soft tissue but also within the cells, in particular in vacuoles and mitochondria. Owing to a relatively high calcium concentration at these sites calcium–phosphate crystals are rapidly formed.

3. Postfixation with osmium–ferrocyanide results in strongly contrasted plasma membranes. If this is not desired, postfixation should be carried out in osmium without ferrocyanide (*see* **Subheadings 2.2.** and **2.3.**).

4. Considerations mentioned under **Note 2** are also relevant for the choice of medium used to culture bone explants. Different commercially available culture media contain different concentrations of phosphate; the higher the concentration level the higher the chance for precipitation of crystals as soon as calcium is liberated. During our investigations on bone resorption, we have experienced this. We found that blocking the activity of certain proteolytic enzymes resulted in the occurrence of large areas of nondigested demineralized bone matrix adjacent to osteoclasts. This was clearly shown for bone explants cultured with M199 *(4)*. By using other media (e.g., BGJb medium) precipitation of crystals may occur at these sites.

5. A problem recognized for a long time is the loss of mineral due to handling and cutting of mineralized tissue. One has to be aware that during cutting of sections and their collection on water, mineral may easily dissolve. This is particularly the case if sections are collected on water with a low pH. Landis and co-workers *(5)* suggested using other techniques to overcome this problem.

6. Mineralized tissues are characterised by a high electron density in mineral-containing parts of the sections. Yet, quite often it appears as if mineral is absent due to the absence of a strong electron density in such sections (**Fig. 5**). This problem
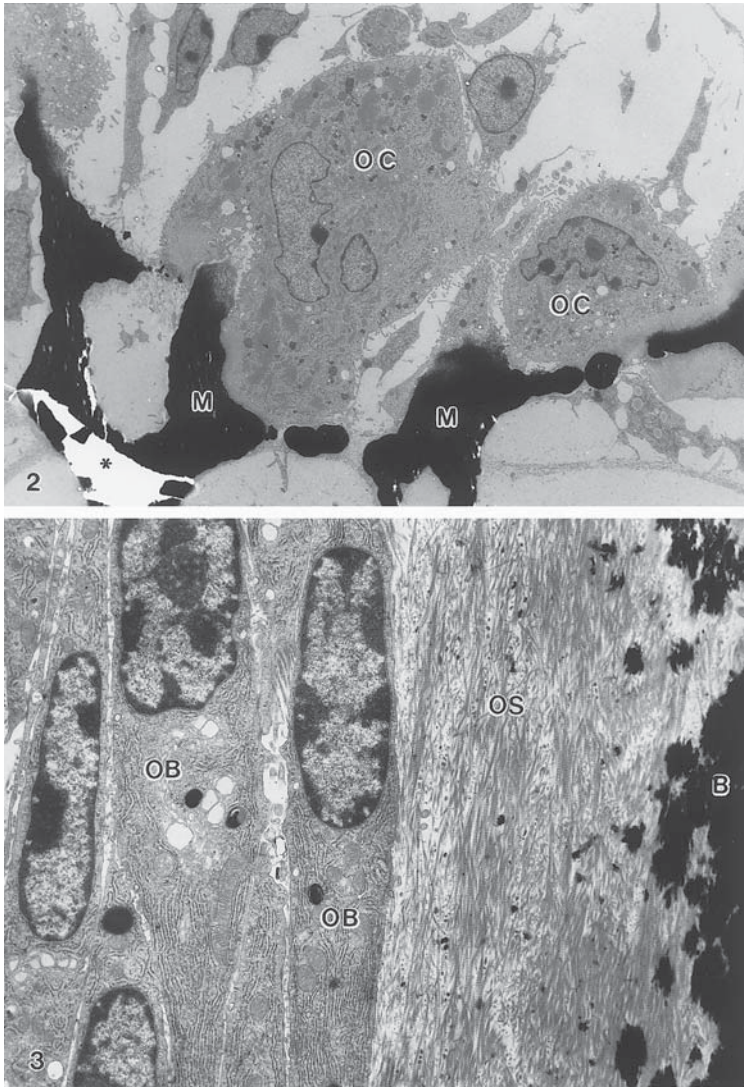
Fig. 2. Low-power electron micrograph of a mouse metatarsal fixed in 4% paraformaldehyde and 1% glutaraldehyde in 0.1 M sodium cacodylate buffer. OC, osteoclast; M, mineralized cartilage; *asterisk* indicates an area where the bone is absent due to ultrathin cutting of the mineralized matrix. (Reduced from original magnification, ×5,000.)

Fig. 3. Electron micrograph of osteoblasts (OB) separated from mineralized bone (B) by a layer of osteoid (OS). Calvarial bone of a 10-d-old mouse was fixed in 4% paraformaldehyde and 1% glutaraldehyde in 0.1 M sodium cacodylate buffer. Undecalcified bone. (Reduced from original magnification, ×16,000.)
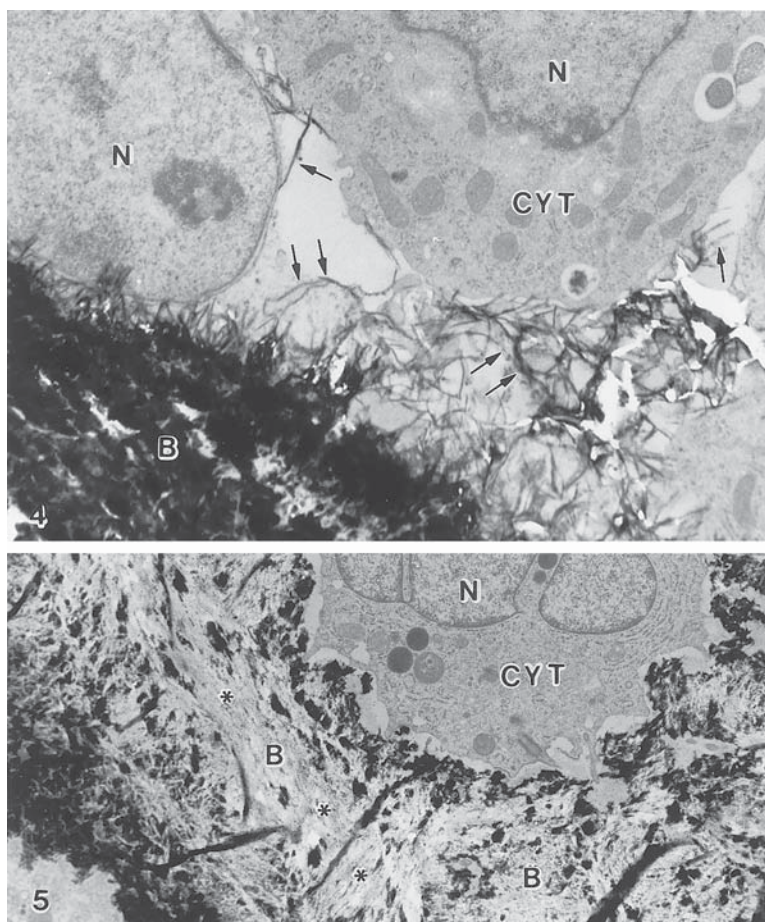
Fig. 4. Electron micrograph of a section of undecalcified bone obtained from a patient suffering from osteopetrosis. Note the presence of large crystallites *(arrows)* due to a phosphate-buffered fixative. Bone tissue was fixed in 4% paraformaldehyde and 1% glutaraldehyde in 0.1 *M* phosphate buffer. B, Bone; CYT, cytoplasm; N, nucleus. (Reduced from original magnification, ×26,500.)

Fig. 5. Electron micrograph of a section of undecalcified bone obtained from a control patient. Note the electron translucent area *(asterisks)* in the bone (B) part of the section. A high electron density (see area indicated by B in **Figs. 3–4**) characterizes a thicker section of the same area. Bone sample was fixed in 4% paraformaldehyde and 1% glutaraldehyde in 0.1 *M* sodium cacodylate buffer. N, Nucleus; CYT, cytoplasm. (Reduced from original magnification, ×15,500.)

is often due to the thickness of the section; the thinner the section the lower the electron density will be. If one wishes to compare the same area in a section with and without mineral, it is possible to decalcify ultrathin sections. To accomplish

this, sections collected on grids are floated on a drop of 0.1 *M* EDTA in buffer for 10 min. The sections are washed, counterstained, and examined. In sections thus treated most mineral is dissolved but decalcification of mineral enclosed by epoxy resin (e.g., free in vacuoles) proves to be very difficult.

References

1. Gruber, H. E. (1992) Adaptations of Goldner's Masson trichrome stain for the study of undecalcified plastic embedded bone. *Biotech. Histochem.* **67**, 30–34.
2. Rungby, J., Kassem, M., Eriksen, E. F., and Danscher, G. (1993) The von Kossa reaction for calcium deposits: silver lactate staining increases sensitivity and reduces background. *Histochem. J.* **25**, 446–451.
3. Reynolds, E. S. (1963) The use of lead nitrate at high pH as an electron opaque stain in electron microscopy. *J. Cell Biol.* **17**, 208.
4. Everts, V., Korper, W., Jansen, D. C., et al. (1999) Functional heterogeneity of osteoclasts: matrix metalloproteinases participate in osteoclastic resorption of calvarial bone but not in resorption of long bone. *FASEB J.* **13**, 1219–1230.
5. Landis, W. J., Paine, M. C., and Glimcher, M. J. (1978) Use of acrolein vapors for anhydrous preparation of bone tissue for electron microscopy. *J. Ultrastruct. Res.* **70**, 171–180.

22

Scanning Electron Microscopy of Bone

Deborah Marshall, Miep H. Helfrich, and Richard M. Aspden

1. Introduction

Scanning electron microscopy (SEM) is a technique whereby both structural and analytical information can be obtained from bone. Ways to use SEM to gain information on bone remodeling and bone pathology have been discussed in a number of comprehensive reviews *(1–4)*. In contrast to transmission EM, in which only very small pieces of tissue can be examined, the sample size for SEM is much less restrictive. Using SEM, a wide range of magnifications (10- to 10,000-fold) can be employed to obtain good overviews as well as detailed images.

SEM has been used extensively to analyze bone structure, to study bone resorption in vivo and in vitro, and to examine surface structures and cell–matrix interaction of bone cells with various substrates using standard secondary electron imaging *(5–8)*. Preparation techniques required are not different from those for nonmineralized tissues and a routine method is given in this chapter. SEM is very useful to obtain structural information about bone matrix. To examine the matrix, generally all cells and organic material are removed from the surface of the bone. Specimens can then be examined using secondary electron (SE) imaging, but use of backscattered electron (BSE) imaging has also been described and yields important additional qualitative information *(9)*.

BSE imaging has been used most extensively to obtain quantitative information *(9–13)*. To obtain quantitative information it is critical to embed specimens in resin and highly polish their surface. This ensures that differences in surface roughness do not contribute to the BSE signal obtained. Specimens can be rendered anorganic before embedding (using the procedure given in this chapter), but other publications *(11–13)* describe BSE imaging on routine pathological samples embedded in polymethylmethacrylate (PMMA).

Quantitative BSE imaging can yield detailed information on bone mineralization density distributions, which are independent of bone volume, and therefore provide additional information to traditional bone mineral density (BMD) measurements using dual energy X-ray absorptiometry (DXA) and bone histomorphometry. Description of the detailed analytical methods is beyond the scope of this chapter, which concentrates on specimen preparation techniques only, and the reader is referred to recent publications describing in detail the application of these methodologies to hard tissues *(10,11,13)*.

Quantitative information from bone can also be obtained using electron probe microanalysis, which measures local elemental composition with a spatial resolution of several cubic micrometers *(14)*. This allows, for example, the ratio of calcium to phosphorus to be measured in different sites *(9)*. Specimen preparation is as described for qualitative BSE imaging.

2. Materials

2.1. Equipment

1. 1-L Dewar flask.
2. Insulated forceps.
3. Sharpened chisel.
4. 60°C Oven.
5. 37°C Incubator.
6. Sputter Coater, for example, Baltec SCD 030.
7. Critial point dryer, for example, Baltec CPD 030.
8. Scanning electron microscope (we used Jeol 35 CF and Philips XL 20).
9. Aluminum stubs to hold specimen (Agar Aids).
10. Silver Dag adhesive (Agar Aids).
11. Double-sided carbon tape (Agar Aids).
12. Desiccator.
13. Bone saw, for example, Accutom 2 (Struers Ltd., Glasgow, UK), or Isomet (Buehler, Lake Buff, IL, USA).
14. Lapping machine for polishing bone slices (Struers).
15. Vacuum oven.

2.2. Reagents

1. 0.1 *M* Phosphate buffer, pH 7.2.
2. 0.089 *M* Phosphate buffer, containing 2.5 m*M* $MgCl_2$, pH 7.2.
3. Glutaraldehyde (25%, Agar Aids, or other).
4. Osmium tetroxide (Agar Aids).
5. Alcohol series (70% through to 100% dry ethanol).
6. Acetone.
7. 1 mg/mL of Proteinase K in 10% sodium dodecyl sulfate (SDS) solution in distilled water.

8. Diethyl ether.
9. Distilled water.
10. Liquid N_2.
11. LR White resin.

3. Methods
3.1. Cell Cultures

This is a method for the preparation of bone cell cultures on coverslips or bone/dentine slices used in resorption assays. Careful preparation results in excellent cell and bone surface morphology. The morphology and depth of the resorption pits can give important clues about the ability of osteoclasts to resorb under different conditions and pharmacological treatments (*see*, for example, **Fig. 1** and **ref. *8***). SEM was used extensively to quantify bone resorption in the pit assay before light microscopical systems were introduced (as described in Chapter 11 by van 't Hof, *this volume*). Quantification or examination of resorption pits is best performed on bone slices from which all cells have been removed, either manually by rubbing the slices between fingers, or by immersing slices in 0.2 M NH_4OH or 5% sodium hypochlorite (for 1 min or longer as necessary). Cells are usually removed after the fixation step (**step 2** below). Alternatively, slices are first examined with adherent cells after which cells are removed, slices recoated and reexamined to visualize the pits alone.

1. Rinse cell cultures on dentine/bone slices, or coverslips in phosphate buffer, pH 7.2 (*see* **Note 1**).
2. Fix in 2.5% glutaraldehyde, 2.5 mM magnesium chloride in 0.089 M phosphate buffer, pH 7.2 for 3 h.
3. Rinse in 0.1 M phosphate buffer.
4. Postfix in 1% osmium tetroxide for 1 h.
5. Wash in distilled water three times.
6. Dehydrate in a graded series of ethanol solutions (70% through to 100% dry ethanol).
7. Carefully remove dentine/bone slices, or coverslips from culture dishes using watchmaker's forceps.
8. Critical point dry from liquid CO_2.
9. Mount slices onto aluminum stubs using the silver adhesive and check that they are mounted the correct way up using a binocular microscope to observe cell surface.
10. Coat specimens with 20 nm of platinum (*see* **Note 2**).
11. Examine specimens in a scanning electron microscope at an accelerating voltage of 10 kV.
12. **Figure 1** shows and example of a bis-phosphonate treated osteoclast on a dentine slice, prepared using this method. Further examples can be found in the chapter by Coxon et al. and Chapter 6 by Collin-Osdoby et al., *this volume*.
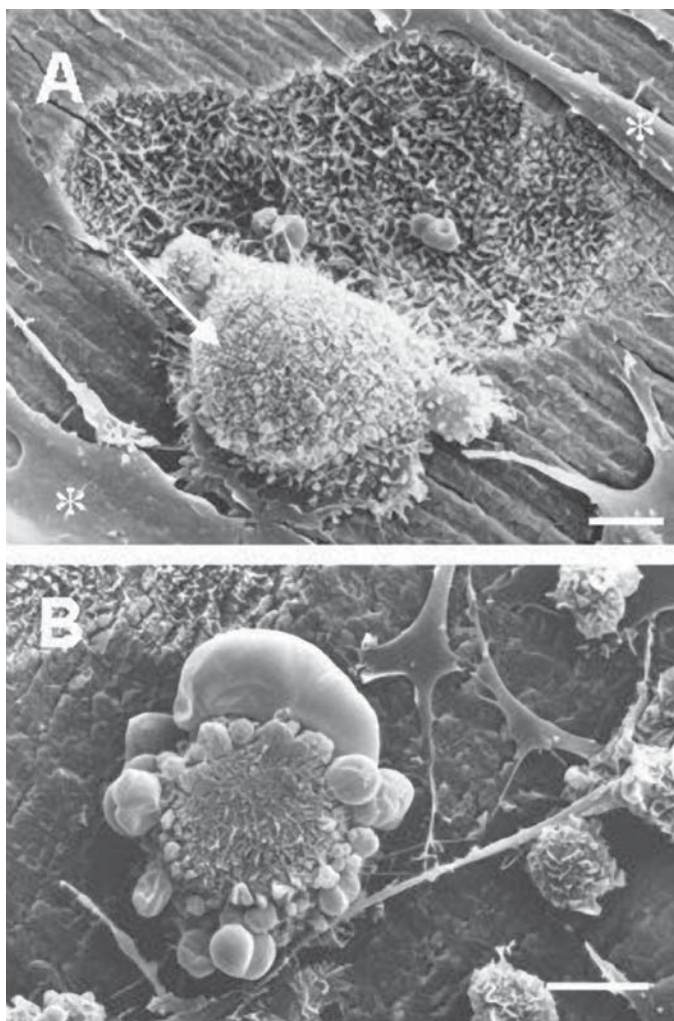
Fig. 1. **(A)** Control osteoclast *(arrow)* demonstrating typical surface morphology with numerous small microvilli, in contrast to the smooth surface of the fibroblasts *(asterisks)*. The osteoclast has just moved away from the resorption pit, which shows a characteristic fringe of demineralized collagen fibers. **(B)** Osteoclast treated with the bisphosphonate clodronate. Note the cell shows extensive surface blebs, indicative of apoptosis, and is not resorbing. Scale bar = 10 μm.

3.2 Preparation of Bone Cores/Bone Biopsies for SEM Using SE or BSE Imaging (see Note 3)

SEM is extremely useful to examine the bone matrix itself. An important difference from the method described in **Subheading 3.1.** is all organic material is removed from the specimen. Because there is no need to preserve the
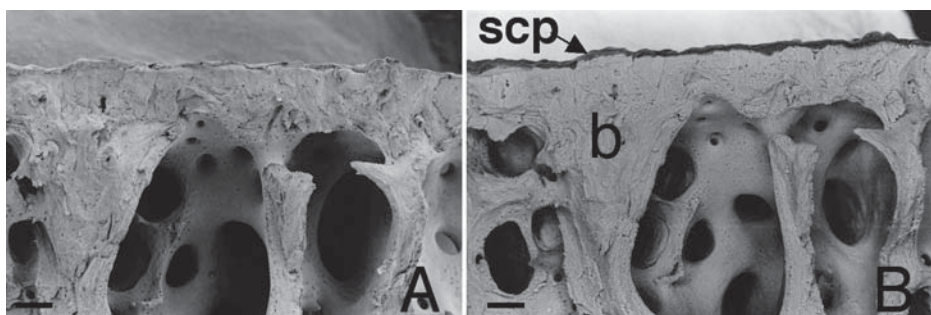
Fig. 2. Piece of subchondral bone from a femoral head of a patient with osteoarthritis. **(A)** All cells and organic surface material have been removed using the procedure described in **Subheading 3.2.** and the remaining mineralized bone was imaged using SE. **(B)** Same bone as in **(A)**, examined with BSE. Because contrast in BSE imaging is largely influenced by surface topography, only the surface area of the bone should be considered and compared with the same surface as seen in the SE. With BSE heavily mineralized areas appear white, whereas poorly mineralized areas appear dark. Note how the subchondral plate is poorly mineralized. Also note how this area is not specifically distinct in the SE image. scp, subchondral plate; b, bone. (Reproduced from: Li, B., Marshall, D., Roe, M., and Aspden, R. M. (1999) The electron microscope appearance of the subchondral bone plate in the human femoral head in osteoarthritis and osteoporosis. *J. Anat.* **195**, 101–110; with permission from Blackwell Science Ltd.)

integrity of the cellular component of bone, specimens do not have to be fixed and they may be stored frozen for considerable time (*see* **Note 4**). The method given here has been designed to be a nonaggressive means of removing all cellular and surface organic material from pieces of bone, to allow a detailed study of the bone structure, for example, the connectivity of trabecular bone, or the porosity of cortical bone. The resulting samples can be observed using conventional SE, or using qualitative BSE (**Fig. 2**). For quantitative analysis using BSE, the surface roughness of specimens should be minimal and embedding in plastic, followed by polishing the surface, is essential. A method for embedding bone in LR White is given here, but other methods, such as embedding in PMMA (*see* the chapter by van Leeuwen and Derkx, *this volume*), can also be used *(10–13)* and allow retrospective studies of routine pathological specimens.

3.2.1. Removal of Organic Material from Bone Samples

1. Obtain human samples of bone from orthopaedic surgery or postmortem examination, or from animal bone. For storage *see* **Note 4**.
2. There are a variety of methods to obtain samples of the required size (generally a few millimeters in any direction). For cancellous bone a dissecting knife or even a scalpel may be sufficient to cut through the tissue. Alternatively, a hacksaw

will produce rough samples. Precision cutting is done using a mineralogical saw fitted with either a diamond or an aluminum oxide cutoff wheel. We use an Accutom 2 (Struers) and a 125-mm aluminum oxide wheel (aluminum oxide in a medium-hard Bakelite bond) rotating at 600–800 rpm. Faster wheel speeds and slower specimen feed result in a better surface finish if this is required (*see* Note 2 of Chapter 27 by Aspden, *this volume*). Perhaps the most common saw cited in the bone literature is the Isomet (Buehler). These saws are precision machines and therefore have a limited capacity. Cutting specimens roughly to size first is essential. An alternative, which produces surfaces that may be indicative of material properties, is to freeze–fracture. To do this on subchondral bone plate samples about 1–2 mm thick, samples are immersed in liquid nitrogen using insulated forceps and then fractured by bending and snapping (*see* **Note 5** and **Fig. 2**).

3. To remove organic material, place bone fragments in a screw-topped container containing 1 mg/mL of proteinase K and 10 mg/mL of SDS in distilled water. Place in an incubator at 37°C and leave overnight with gentle agitation.
4. Change proteinase K–SDS solution and gently agitate by hand inversion after 3 h in the 37°C incubator.
5. After a total of 18 h at 37°C, discard the solution and gently shake any oil droplets from the samples.
6. Place bone samples in distilled water, invert several times, and discard the solution. Repeat three times to remove any debris from the samples.
7. Add fresh distilled water and leave for 3 h. Repeat this step once more for 3 h.
8. Discard water and add acetone for 2 h.
9. Replace acetone, invert the sample, and leave overnight.
10. Next morning, replace acetone, invert, and leave all day. At the end of the day replace acetone again and leave for 2–3 d.
11. Remove acetone and shake off excess from the trabecular pores of the sample.
12. Add diethyl ether and leave all day. In the evening replace diethyl ether and leave overnight.
13. Discard solution and gently shake the sample to remove any residue.
14. Place samples in a 60°C oven for 8 h on a glass dish to evaporate any residue.
15. Place samples under vacuum and leave overnight.
16. Mount samples on aluminum stubs using silver dag adhesive. Allow to dry overnight in a desiccator.
17. Coat samples with 20-nm platinum and examine in the scanning electron microscope at 10 kV to obtain a SE image.
18. Alternatively, coat the samples thinly with carbon and obtain a BSE image at 20–30 kV. If both a SE and BSE image are required from the same specimen *see* **Notes 6** and **7** and **Fig. 2**.

3.2.2. Embedding of Anorganic Samples in LR White and Processing for BSE Imaging

Resin embedding is a technique available in many EM laboratories and technical advice on the methods available locally should be obtained. The general steps are given below.

1. Prepare bone specimens as described in **Subheading 3.2.1.**, **steps 1–15**.
2. Embedding is done in a low-viscosity acrylic resin (LR White; *see* **Note 8**) under vacuum to ensure total impregnation. The resin is thermally cured without the need for a catalyst at a temperature of 55°C for 18–24 h.
3. After curing, each specimen must be sectioned using a diamond saw (*see* **Subheading 3.2.**, **step 2**) in a plane parallel with the surface to be examined.
4. The cut face must then be polished; a roughness of <1 μm is generally required for the highest quality work. This is done using a lapping machine using silicon carbide lapping plates and successively finer grades of diamond paste.
5. A slab containing the prepared surface, approx 5 mm thick, is then cut off, mounted on an SEM stub with carbon tape and carbon coated (*see* **Note 2**).
6. Examine the specimen using BSE at an accelerating voltage of 20–30 kV (*see* **Note 7** and **Fig. 3**).

4. Notes

1. To avoid formation of calcium phosphate crystals, fixation in cacodylate buffer should be considered (*see* the chapter by Everts et al., *this volume*). However, at lower magnifications, we find this not to be a significant problem and routinely use the nontoxic phosphate buffers.
2. Coating of the specimen is essential to make it electrically conductive. This can be done with gold–palladium, platinum, aluminum, or carbon. We routinely use platinum for SE imaging. A thin layer of carbon coating should be used for quantitative analyses using the BSE mode, as the heavy metals interfere with the BSE signal.
3. A traditional means for removing the organic component of bone is to use bleach (5% sodium hypochlorite). This is very effective. We prefer to use the combination of enzyme and detergent as it is less aggressive and the enzyme will target specifically the proteins while the detergent will help with their solubilization as well as that of most fats and carbohydrates. Collagen forming the structure of the bone will be protected by the mineralization and in any case is resistant to Proteinase K.
4. For storage for longer than a few d, samples are wrapped in several layers of gauze or tissue soaked in phosphate-buffered saline (PBS); double-bagged in evacuated, sealed plastic bags; and frozen at lower than -20°C. Short-term storage can be done in a refrigerator in PBS. If surface mineral content is important, then storage is best in a saturated calcium phosphate buffered solution as slow dissolution of surface calcium phosphate has been observed. We have used a calcium phosphate buffered 0.15 M saline solution (containing 0.2 mM $CaCl_2.2H_2O$, 0.2 mM Na_2HPO_4, 0.01 mM $Na_4P_2O_7.10H_2O$ and 0.4 g of sodium azide per liter as a bactericide/fungicide), as this has been shown to preserve the structure and composition of the bone *(15)*.
5. If freeze–fracturing is employed then the intention is normally to study the fracture surface. Clearly, any inspection of the surfaces that have been gripped is not advised and if this is done on cancellous bone then there is a distinct risk that
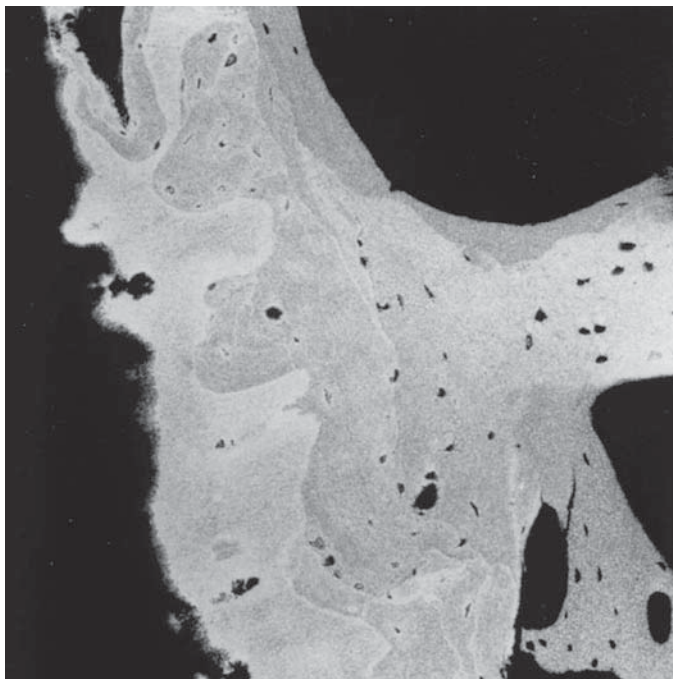
Fig. 3. BSE image of a resin-embedded bone slice. Note the clear distinction in brightness between different areas, indicative of differences in mineralization density.

some crushing of the specimen could occur. If BSE is used to examine the fractured surface remember that surface topography contributes substantially to the BSE signal and only the "flatter" surfaces will give interpretable results (*see* **Fig. 2**).

6. An accelerating voltage of 10 kV is routinely used. For BSE, an accelerating voltage of 20–30 kV is required. The carbon coating of the specimen for BSE should be thin to allow sufficient electrons to penetrate the specimen. If both and SE and BSE image from the same specimen are required, use carbon coating.

7. Quantitative BSE imaging uses detection of electrons backscattered in the top (0.5 μm) surface of the specimen. Contrast in the BSE image depends on the mean atomic number. Bone contains organic material and mineral with calcium being the constituent with the highest atomic number. Calcium therefore determines in largest part the intensity of the backscattered electrons. The BSE image appears brighter with increasing mineral density, which is related to bone turnover rate, with older bone having a higher density than newer bone *(1)*. The image obtained contains areas with different gray levels (**Fig. 3**)**.** By carefully calibrating the BSE signal with reference material of known atomic number, this gray scale can be used to obtain regional calcium concentrations. Different calibration procedures have been described *(11,16)* and the reader is referred to these original texts for analysis methods.

8. For quantitative analysis LR White may be less appropriate as it has a high chloride content and this needs to be corrected for *(9)*. Embedding in PMMA is a more common but more time consuming procedure. Addition of styrene to PMMA has been described to obtain resin that has improved stability under electron bombardment *(1,16)*. This modification further increases specimen preparation time and because this is not a routine procedure in pathology laboratories, may only be practical for research specimens. The choice of embedding material is therefore a trade off between what is best and what is practical. In most recent publications PMMA embedded material was examined. Generally, resin laboratories will be able to adapt their protocols for soft tissue to hard tissue requirements, essentially by increasing impregnation times. Very careful polymerization is also essential to avoid overheating leading to generation of air bubbles in blocks leading to holes and cracks in sections. Such blocks are not suitable for BSE analysis, because of their uneven surface and careful selection of archive material is necessary.

Acknowledgments

References

1. Boyde, A., Maconnachie, E., Reid, S. A., Delling, G., and Mundy, G. R. (1986) Scanning electron microscopy in bone pathology: review of methods, potential and applications. *Scan. Electr. Microsc.* **IV**, 1537–1554.
2. Boyde, A. and Jones, S. J. (1996). Scanning electron microscopy of bone: Instrument, specimen and issues. *Microsc. Res. Tech.* **33**, 92–120.
3. Goldman, H. M., Kindsvater, J., and Bromage, T. G. (1999) Correlative light and backscattered electron microscopy of bone—Part I: specimen preparation methods. *Scanning* **21**, 40–42.
4. Goldman, H. M., Blayvas, A., Boyde, A., Howell, P. G., Clement, J. G., and Bromage, T. G. (2000) Correlative light and backscattered electron microscopy of bone—Part II: automated image analysis. *Scanning* **22**, 337–344.
5. Abe, K., Kanno, T., and Schneider, G. B. (1983) Surface structure and osteoclasts of mouse parietal bones: a light and scanning electron microscopic study. *Arch. Histol. Jpn.* **46**, 663–667.
6. Chambers, T. J. and Fuller, K. (1985) Bone cells predispose bone surfaces to resorption by exposure of mineral to osteoclastic contact. *J. Cell Sci* **76**, 155–165.
7. Chambers, T. J., Revell, P. A., Fuller, K., and Athanasou, N. A. (1984) Resorption of bone by isolated rabbit osteoclasts. *J. Cell Sci.* **66**, 383–399.
8. Jones S. J., Boyde, A., and Ali, N. N. (1984) The resorption of biological and non-biological substrates by cultured avian and mammalian osteoclasts. *Anat. Embryol.* **170**, 247–256.
9. Li, B., Marshall, D., Roe, M., and Aspden, R. M. (1999) The electron microscope appearance of the subchondral bone plate in the human femoral head in osteoarthritis and osteoporosis. *J. Anat.* **195**, 101–110.

10. Roscher, P, Fratzl, P., Klaushofer, K., and Rodan, G. (1997) Mineralisation of cancellous bone after alendronate and sodium fluoride treatment: a quantitative backscattered electron imaging study on minipig ribs. *Bone* **20**, 393–397.

11. Roschger, P., Fratzl, P., Eschberger, J., and Klaushofer, K. (1998) Validation of quantitative backscattered electron imaging for the measurement of mineral density distribution in human bone biopsies. *Bone* **23**, 319–326.

12. Kingsmill, V. J. and Boyde, A. (1998) Mineralisation density of human mandibular bone: quantitative backscattered electron image analysis. *J. Anat.* **192**, 245–256.

13. Boyde, A., Travers, R., Glorieux, F. X., and Jones, S. J. (1999) The mineralization density of iliac crest bone from children with osteogenesis imperfecta. *Calcif. Tissue Int.* **64**, 185–190.

14. Friel, J. J. (1995). *X Ray and Image Analysis in Electron Microscopy*. Princeton Gamma Tech Inc., Princeton, NJ.

15. Lees, S. (1988) Sonic velocity and the ultrastructure of mineralised tissues, in *Calcified Tissues* (Hukins, D. W. L., ed.), Macmillan, London, UK, pp. 121–152.

16. Boyde, A., Jones, S. J., Aerssens, J., and Dequeker, J. (1995) Mineral density quantitation of the human cortical iliac crest by backscattered electron image analysis: variations with age, sex and degree of osteoarthritis. *Bone* **16**, 619–627.

23

Bone Measurements by Peripheral Quantitative Computed Tomography in Rodents

Jürg A. Gasser

1. Introduction

Quantitative computed tomography (QCT) is an established technique for the determination of bone mineral density (BMD) in the axial and appendicular skeleton *(1)*. QCT is unique amongst methods of bone mineral measurement in providing separate estimates of trabecular and cortical bone mineral density as a true volumetric mineral density value (g/cm^3) *(2)*. In addition, QCT can measure geometric properties of cortical bone with great accuracy *(3)* and predict some mechanical properties with remarkable precision *(4–6)*. Peripheral quantitative computed tomography (pQCT) is a special type of computed tomography in which scans of the appendicular skeleton are performed at a low radiation dosage. Bone and muscle development can be assessed noninvasively by pQCT at peripheral sites in studies of bone development, experimental models of bone loss, and in monitoring the effectiveness of therapeutic interventions. In addition, pQCT can be used to assess excised bones ex vivo from virtually any skeletal site.

The XCT 900 and XCT 960 series of pQCT scanners were developed at the University of Würzburg *(7)*, and brought into commercial clinical and preclinical application by Stratec Medizintechnik GmbH, Germany. The present chapter focuses entirely on the two most frequently used pQCT scanners which were adapted for use in small rodents, the XCT 960A and the XCT 2000. All pQCT scanners of the XCT-series work according to the translation–rotation principle. The photons emitted by the X-ray tube are detected by 6 (XCT 960A) or 12 (XCT 2000) semiconductor detectors which have a near 100% efficacy for X-rays of around 38.5 keV. The attenuation coefficients at each point of the cross-sectional image are reconstructed from the projected data (filtered back-

Table 1
Technical Data of the XCT Series

	XCT 960	XCT 960A	XCT 960M	XCT 2000
Slice thickness	2.2 mm	1.2 mm	1.0 mm	0.55 mm
High voltage	47 kV	49 kV	35 kV	45–49 kV
X-Ray energy	38 keV	38 keV	28 keV	38 keV
Matrix size	128*128	128*128	256*256	256*256
Resolution	590 μm	90–500 μm	70–500 μm	70–500 μm
No. of projections	72	72	90	90
Object size	Up to 85 mm	Up to 85 mm	Up to 85 mm	Up to 50 mm
Scan length	30 mm	30 mm	30 mm	30 mm
Radiation dose	0.01 mSv/h	<0.1 mSv/h	<0.1 mSv/h	<0.1 mSv/h

The XCT960 scanner was originally developed for clinical use. The machine was later adapted for use in rats, dogs, and primates (XCT960A) and mice (XCT960M and XCT2000) by changing the collimator to decrease slice thickness and obtain better resolution.

projection) *(8)*. Daily calibration of the system using a hydroxyapatite containing phantom allows one to calculate density values (mg/cm^3) from the attenuation coefficients. The XCT960A was the first commercially available dedicated animal pQCT scanner and in its technical aspects is closely related to the newer XCT Research SA. It was derived from the XCT 960 used in the clinic but provides a higher spatial resolution (100 μm) and smaller slice thickness (1.2 mm) to account for the reduced size of bones of small animals such as mice, rats, dogs, primates, and sheep (**Table 1**). All the rat data presented in this chapter were measured on the XCT 960A. The XCT2000 scanner evolved from the dedicated mouse scanner XCT 960M, which offered higher spatial resolution (70 μm), decreased slice thickness (0.55 mm), and better performance, and is closely related to the XCT Research M. The XCT2000 scanner was used for all the mouse data presented in this chapter. Most of the pQCT data reported in the literature is derived from measurements carried out in Sprague–Dawley or Wistar rats *(2–6,9,10)*. However, the increasing use of transgenic and KO animals in skeletal biology, with the aim of associating a skeletal phenotype with loss of function of a gene, receptor, or protein or with its overexpression, has increased our need to develop similar methods for mice *(11,12)*. Systems such as the XCT 2000 or XCT Research M fulfil these requirements. For general, more detailed information on the effects of ovariectomy (OVX) on the skeleton in rats the reader is referred to articles published elsewhere *(13–15)*.

2. Materials

1. XCT 960A and XCT 2000 scanners. Stratec Medizintechnik GmbH, Germany.

3. Methods

3.1. Number of Animals

The number of rats or mice per group, as a general rule, should be a minimum of 10 or higher to guarantee statistical significance for primary outcome parameters derived from pQCT measurements. This recommendation is based on the coefficient of variation obtained on the XCT 960A (rats) and on the XCT2000 (rats and mice) (**Table 2**). The coefficient of variation in percent was calculated using the formula (CV = STDEV/Mean * 100). Instrument precision ($CV_i\%$) was determined by repeating 10 measurements in the proximal tibia ex vivo, without repositioning of the bone at a distance of 5 mm from the proximal end of the bone. In vivo precision was calculated from 10 measurements with ($CV_r\%$) or without repositioning of the limb $CV_u\%$). Very comparable values for CV_r were obtained in rats and mice on the XCT2000. We recommend that users determine their own set of parameters, as these values are dependent on species, number of animals per group, age of animal, instrument type, scanning location, limb holder, and instrument setting. As a "rule of thumb" the difference between two measurements must be at least three times the value of the CV displayed in Table 2 for you to obtain statistically significant differences.

3.2. Age of Animals

Unless the focus of the study is on the evaluation of skeletal growth or factors influencing it, rats aged 6 mo (or, better, 9 mo) should be used for your experiments. The use of younger animals will inevitably confound disease- or drug- induced effects with those of skeletal growth. **Figure 1** clearly demonstrates that even though there is little change in cross-sectional bone area in aging 6- and 9-mo-old rats, periosteal modeling drifts are triggered by OVX in the younger, but not older animals. Fewer data are available from mice to make clear recommendations with regard to the ideal age range for studies. For C57BL/6J-mice, an age of 6 mo or older appears to be ideal.

3.3. Baseline Measurements and Other Controls

If you perform your measurements in vivo, the baseline value should be taken for every animal and changes induced by the disease or drug treatment measured against it. However, if you plan to carry out ex vivo measurements on excised bones such as lumbar vertebral bodies (which you cannot measure in vivo), or to carry out biomechanical tests or histomorphometric analyses of

Table 2
Coefficient of Variation (CV) Expressed in % Obtained in Rats on the XCT 960A and in Rats and Mice on the XCT2000

| | | | | | XCT2000 | |
| | | Rats: XCT 960A | | | Rat | Mouse |
Parameter	Unit	$CV_i\%$	$CV_v\%$	$CV_r\%$	$CV_r\%$	$CV_r\%$
Total bone mineral content	mg/mm	0.331	0.598	0.869	1.13	0.97
Total bone mineral density	mg/mm^3	0.116	0.170	0.273	0.36	0.25
Total bone area	mm^2	0.327	0.700	1.087	1.51	1.11
Trabecular bone mineral content	mg/mm	0.681	1.331	2.330	3.02	3.76
Trabecular bone mineral density	mg/mm^3	0.444	0.423	0.740	0.77	1.54
Trabecular bone area	mm^2	0.542	1.060	1.754	2.25	2.32
Cortical bone mineral content	mg/mm	0.456	0.576	0.856	0.44	0.79
Cortical bone mineral density	mg/mm^3	0.214	0.319	0.540	0.77	0.39
Cortical bone area	mm^2	0.605	0.849	1.353	0.90	1.03
Cortical thickness (circular ring nodel)	mm	0.585	0.688	1.152	0.42	0.97
Periosteal perimeter	mm	0.163	0.350	0.544	0.74	0.55
Endocortical perimeter	mm	0.283	0.528	0.867	1.11	1.26
Bone strength index	mm^4*g/cm^3	0.877	1.332	2.315	nd	nd

CV_i was determined from 10 measurements of the proximal tibia metaphysis carried out ex vivo, while CV_r and CV_v were determined in vivo with and without repositioning of the animal, respectively.

bone specimens, the addition of a baseline group (necropsy at baseline) is mandatory. Intervention studies may require additional control groups to collect bones prior to initiating active treatment.

In longitudinal studies, we recommend a baseline measurement and allocation of the animals to the various treatment groups based on their total cross-sectional BMD and their trabecular BMD. This should ensure homogeneity of variances between the groups. Assigning the animals to different groups on the basis of baseline measurements has advantages over random assignment. Most
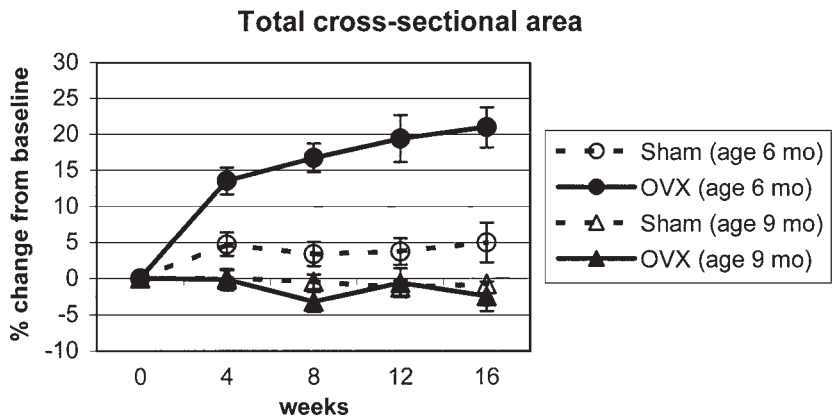
Total cross-sectional area

Fig. 1. Increase in cross-sectional area in the tibia of 6- and 9-mo-old rats. Sham-operated rats still show some growth-related increase in cross-sectional area up to age 7 mo. OVX-induces pronounced periosteal bone apposition in 6 but no longer in 9-mo-old rats.

interventions will induce bone loss (OVX, immobilization) or bone gain (anabolic agents such as parathryroid hormone [PTH], growth hormone [GH], prostaglandin E_2 [PGE_2]). Because the magnitude of the changes is in most cases proportional to the cancellous template, animals with different baseline BMD values will respond differently. Adjustment of groups to match for total cross-sectional BMD will also assure that animals are well matched in terms of biomechanical parameters.

3.4. Transgenic Animals

There are situations that do not allow a perfect protocol under consideration of **Subheadings 3.1.–3.3.** For example, transgenic or KO mice may show reduced survival in the postnatal period and it may be impossible to study their mature skeletal phenotype or to conduct longitudinal studies. Many investigators who interpret pQCT data derived from KO mice have not considered that the observed bone phenotype may derive from disturbances occurring during intrauterine skeletal morphogenesis, or changes in skeletal growth in the post natal period, concluding perhaps wrongly that the respective gene, receptor, or protein in question may represent an interesting target for the treatment of osteoporosis.

3.5. Selecting Regions of Interest

For in vivo monitoring of bone mass, density, and cortical architecture, pQCT measurements are restricted to locations in the appendicular skeleton and tail vertebra. In the past, most of these measurements were carried out in
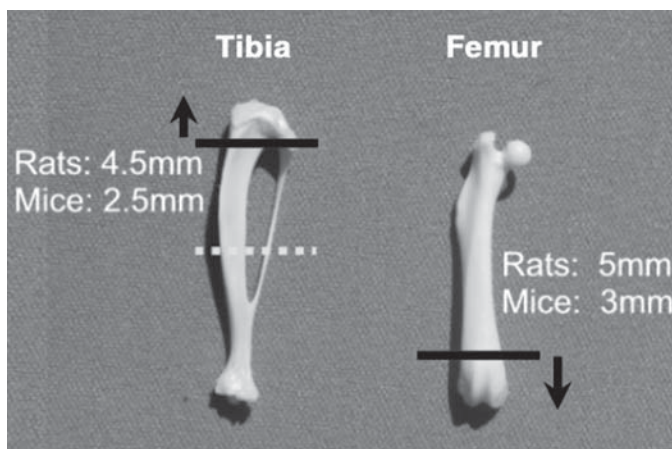
Fig. 2. Choice of region of interest in skeletally mature rats and mice. Indicated is the distance in millimeters from the joint space for the distal femur metaphysis and the proximal tibia metaphysis. A pure "cortical" bone site can be easily assessed in the mid-diaphysis of the tibia *(dotted line)*.

hindlimbs *(2–6,10)*. The proximal tibia metaphysis (PTM) has been the preferred site for various reasons (**Fig. 2**). This site is rich in cancellous bone and reacts with the greatest magnitude of change to interventions such as OVX *(2)*, immobilization, and bone anabolic therapies such as PTH. Another reason for choosing the PTM is the fact that it has been the most popular site for measuring structural and dynamic histomorphometric parameters. Serial scans carried out at various locations throughout the rat PTM showed that a section placed at a distance of 4.5–5 mm from the proximal end of the bone, a position in the secondary spongiosa, is most suited for skeletally mature animals (6 mo and older) (**Fig. 3**) *(3)*. The ideal "corresponding" site in mice is located 2.5mm from the proximal end of the tibia (**Fig. 2**). Not surprisingly, the magnitude of cancellous bone loss in rats decreases when the section is placed further away from the knee joint, because of the decreasing amount of spongy bone found, especially in older animals. Another ideal site to study cancellous and cortical bone is the distal femur metaphysis (DFM) even though the local strain pattern, which generates large forces in the direction of the patella, limits the magnitude of cancellous bone loss at this site *(2)*. For rats an ideal slice is placed at 5 mm from the distal end of the femur (3 mm in mice). In contrast, the distal tibia metaphysis (DTM) is only of limited use for pQCT scanning. Its crosssection is small and separating cancellous and cortical bone is in most cases not possible in rats and mice. Because of the inaccessibility of lumbar vertebral bodies (LVB) for in vivo monitoring, it is tempting to carry out mea-
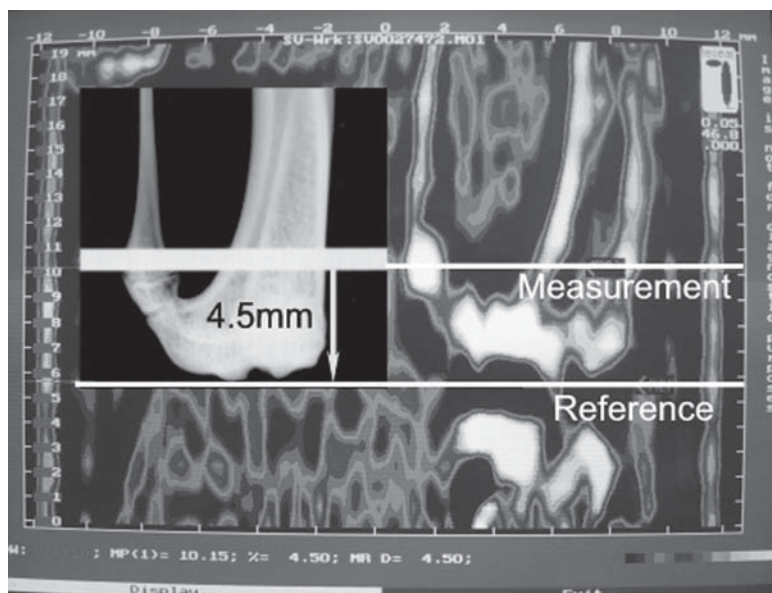
Fig. 3. Scout-scan of knee joint and positioning of ROI at the 4.5-mm distance in the proximal tibia metaphysis of the rat. For better visibility, the inserted picture shows an X-ray taken at the same location.

surements in tail vertebrae (TVB) instead, which are easy to position. Unfortunately the magnitude of bone loss in the TVB is considerably smaller than observed in PTM, DFM, and LVB, so that this site is only of limited use. The reasons for this "failure" are not clear but may include factors such as different cellularity (fatty marrow as opposed to red marrow), vascularity (metabolism), or protective local strain patterns. None of the scanner algorithms can separate cancellous and cortical bone in a perfect way. For this reason we recommend choosing a "pure" cortical bone site in addition to the PTM or DFM. One of the easiest sites to localize repeatedly with high precision in longitudinal studies is the mid-diaphysis (MDT) of the tibia. Bone length can be easily determined on a contact X-ray and the position calculated in growing as well as in skeletally mature rats and mice.

3.6. Quality Assurance

Before initiating your measurements in animals you must start the QA procedure (quality assurance procedure) by scanning the QA phantom provided by the vendor. This procedure has to be carried out once every day before the machine will allow you to collect data. The routine starts by initiating a Scout View scan (SV scan) followed by the collection of data from the phantom on

three different density values, all of which have to stay within the tolerated range of <1% of the true value.

3.7. Anesthesia and Limb Positioning

Accurate positioning of the limb is one of the crucially important factors to guarantee high-quality data in longitudinal studies. For this purpose we developed a special holder that guarantees exact positioning and does not allow movement of the limb in any direction, as well as preventing its rotation. For the measurement, the animal is placed on a plastic tray in a lateral position. The mouth and nose of the animal are placed in a hole to which a tube is plugged on to deliver the inhalation anesthetic, namely 2.5% Isofluran (Forene®, **Fig. 4**), which we deliver together with 0.8% oxygen and 0.8% air. Because the entire procedure of scanning normally requires < 6 min, this type of anesthesia is ideal. Rats and mice can be kept under anesthesia for prolonged periods if multiple slices are being assessed. Alternatively, anesthesia can be induced by intraperitoneal injection of 40 mg/kg Ketarom (1.2 mL of ketamine hydrochloride + 0.8 mL of rompun 2% + 8 mL of NaCl).

For proper positioning, the leg is placed into the tube at the other end of the holder with the foot sticking out (**Fig. 5**). The conical plug is then placed around the limb to hold the tibial muscle with the iron rod inserted into the lateral slit, thus preventing any rotation of the limb. Finally, the foot is kept from sliding back into the tube by placing the foot-holder around the ankle and securing it with adhesive tape (**Fig. 5**). The conical plug is available in three lengths and the right size is chosen by the operator depending on the size of the animal. This holder guarantees next to identical placement of the leg from one measurement to the next. The animal is now ready for the scout scan. Always give each animal a unique name (code) and keep this designation for all later time points. As soon as the code is typed in a second time, the software will recognize that it should compare the results of the upcoming SV scan with an earlier measurement from the same animal. This software-based automatic detection procedure is very able to place your measurement at the same location of any previous scan.

3.8. Setting up the Scanner

The numbers of possibilities for setting your instrument are virtually endless and it is beyond the scope of this guide to discuss all of them. We were operating software version 5.40 on both scanners. In **Table 3** you find our proposal for instrument setting for rats on the XCT960A and the XCT2000, as well as the settings for mice on the XCT2000. In our experience they work very well and give robust results of high quality for both cortical and cancellous parameters. We have chosen to use the same threshold based contour find-

Fig. 4. Animals are placed into a lateral position under inhalation anesthesia with 2.5% isoflurane (Forene®). Suction around the nose prevents spillage of fumes to the surrounding air. The overview shows the system with a special "flow through chamber" in which the next animal can be anesthetised while the limb of another rat is measured.
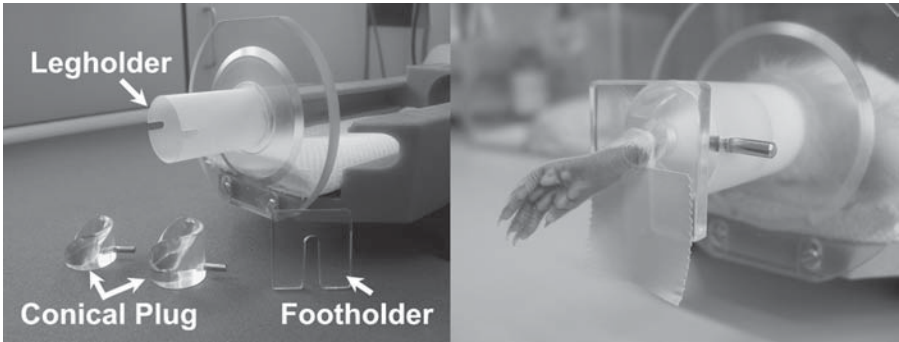
Fig. 5. Detailed view of the leg holder consisting of a tube, a conically shaped plug with a rod, and the foot holder. The function of the conical plug is to hold the tibial muscle preventing its rotation. The foot holder is placed around the ankle preventing its withdrawal into the tube.

ing for detection of both, the periosteal and the endocortical surface (CONTMODE 1, CORTMODE 2, PEELMODE 2) (**Fig. 6**). Some investigators prefer to define the cancellous bone area as a fixed value of 45% of the total bone area. This mode of analysis may have advantages in larger animals such as dogs, primates, and humans, where the cortical compartment is more difficult to separate from cancellous bone by threshold-based algorithms. For rodents we clearly prefer our threshold-based separation procedure as it gives

Table 3
Instrument Setting for Measurements in the Proximal Tibia Metaphysis
with the XCT 960A (Rats) and the XCT2000 (Rats and Mice)

	XCT960A (rats)	XCT2000 (rats)	XCT2000 (mice)
Collimator (diameter)	1.2 mm	1.0 mm	0.5 mm
Voxel size	$0.197 \times 0.197 \times 1.2$ mm	$0.2 \times 0.2 \times 1$ mm	$0.1 \times 0.1 \times 0.5$ mm
Scan speed:			
SV-scan	20 mm/s	20 mm/s	10 mm/s
Final scan	10 mm/s	10 mm/s	3mm/s
CONTMODE	1	1	1
PEELMODE	2	2	2
CORTMODE	2	2	2
Threshold	730 mg/cm^3	730 mg/cm^3	400 mg/cm^3
Threshold2	730 mg/cm^3	730 mg/cm^3	400 mg/cm^3

Threshold determines the outer contour in the CONTMODE part of scan-analysis while Threshold2 defines the cortical and cancellous bone compartment in CORTMODE.
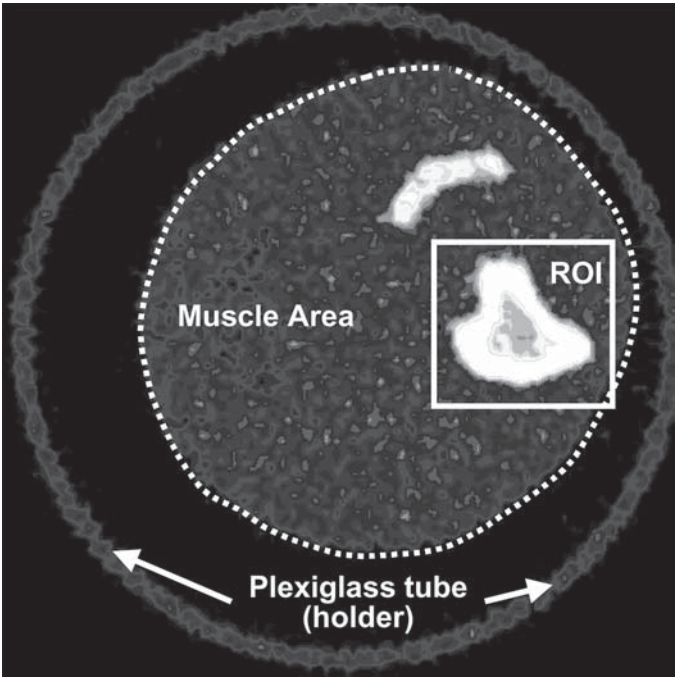

Fig. 6. Actual scan through the PTM at 4.5 mm from the knee joint taken on the XCT960A in a 9-mo-old rat. In most cases the software is able to define the ROI automatically on which the scan analysis is run. The *dotted line* delineates the contour of the muscle. Using a lower threshold, muscle area can be determined in all sections.

much more accurate information on the changes in cortical thickness and endocortical perimeter.

Our preferred setting for scan analysis is defined in the following subheadings.

3.8.1. CONTMODE 1

This parameter determines the separation of soft tissue from bone for delineation of the outer contour (periosteal perimeter). The threshold attenuation coefficient can be freely chosen by the operator and should be set to 610–730 mg/cm^3 in rats and 350–400 mg/cm^3 in mice.

3.8.2. CORTMODE 2

This algorithm separates trabecular from cortical bone at the endocortical surface. All voxels with a lower attenuation coefficient than the selected threshold are eliminated and counted as being part of the cancellous bone compartment. The voxels are then "proofed" by a 3 × 3 filter to ensure continuity. We recommend using the same threshold to define the inner contour of cortical bone as was used for detection of the outer contour (contour mode 1; 610–730 mg/cm^3 in rats and 350–400 mg/cm^3 in mice).

You may find it worthwhile to experiment with the instrument settings and find those which suit your purpose best (*see* **Subheading 3.10.**).

3.9. Data Analysis

The analytical part of the software generates a great number of parameters but luckily you do not require all of them. We find the 13 parameters listed in **Table 1** are sufficient for adequate interpretation of your data. In the following we will attempt to describe such an analytical process on a true data set. The 12-wk study was performed in 9-mo-old virgin Wistar rats. Ten animals per group were ovariectomized and treated daily p.o. with 0.3 mg/kg of 17α-ethinylestradiol dissolved in corn oil. Other groups of animals was injected twice weekly subcutaneously with 10 µg/kg alendronate or vehicle (corn oil). A sham-operated group was also measured to determine age-related changes with pQCT measurements being carried out in all groups at baseline, 4, 8, and 12 wk. Although it is possible to analyze absolute data in well-matched groups of animals, we recommend that you calculate the percent change for each parameter and time point of all animals from their own baseline value. The reasons for this is simple: You will find it virtually impossible to adjust the values of all treatment groups for all 13 parameters that you want to evaluate when allocating the animals to their groups at baseline. When looking at your graphs containing the data, always keep in mind the "rule of thumb" mentioned earlier. For any "effect" to be real, the percent change should be at least three times bigger than the respective CV$_r$ value displayed in **Table 2**.

Table 4
Definition of Most Relevant Parameters Required for Data Interpretation

Parameters	Definition	Unit
TOT_CNT	Total bone mineral content	mg
TOT_DEN	Volumetric total bone mineral density	mg/cm^3
TOT_A	Total bone mineral area	mm^2
CRT_CNT	Cortical bone mineral content	mg
CRT_DEN	Volumetric cortical bone mineral density	mg/cm^3
CRT_A	Cortical bone mineral area	mm^2
TRAB_CNT	Cancellous bone mineral content	mg
TRAB_DEN	Volumetric cancellous bone mineral density	mg/cm^3
TRAB_A	Cancellous bone mineral area	mm^2
PERI_C	Periosteal circumference	mm
ENDO_C	Endocortical circumference	mm
CRT_THK	Mean cortical thickness ring model	mm
xBSI	Axial bone strength Index (bending strength)	mm^4*g/cm^3
pBSI	Polar bone strength index (torsional strength)	mm^4*g/cm^3

Column 1 lists the parameters as denominated by the software and their unit is listed in column 3. Only the most relevant parameters required for interpretation of the data are listed.

We always start our analytical process by looking at the periosteal perimeter (PERI_C) or the total bone area (TOT_A) (**Table 4**). Both parameters describe the same feature of bone size. However, TOT_A, being an area measurement, shows a greater magnitude of change. Only an increase of 2% or greater in PERI_C or > 3% in TOT_A gives you an indication of a disease or drug-induced effect. Such changes are easily obtained during early skeletal growth up to the age of 6 mo in rats. Anabolic agents such as GH *(9,16,17)*, vitamin D *(18)*, and high dose PTH can induce them. In our example (**Fig. 7A**), none of the changes measured in PERI_C exceeded the 2% magnitude indicating that observed variations are within the precision of the measurement and therefore not real effects.

The next parameter we consider is the total cross-sectional BMC (TOT_CNT), which indicates whether there is an absolute gain or loss in bone mass caused by the intervention. Together with the previous parameter (PERI_C), we can learn whether this increase is happening entirely at the endosteal envelope (i.e., in the absence of changes in PERI_C) or connected to an increase in bone size (increase in PERI_C). In our simple example there was no change in bone size; therefore TOT_CNT gives the same information as the volumetric cross-sectional BMD (TOT_DEN) displayed in **Fig. 7B**. Our "rule of thumb" tells us that the sham OP and the alendronate group are stable and

A
Periosteal Perimeter (PERI_C)

B
Volumetric Cross-Sectional BMD (TOT_DEN)

C
Mean Cortical Thickness (CRT_THK)
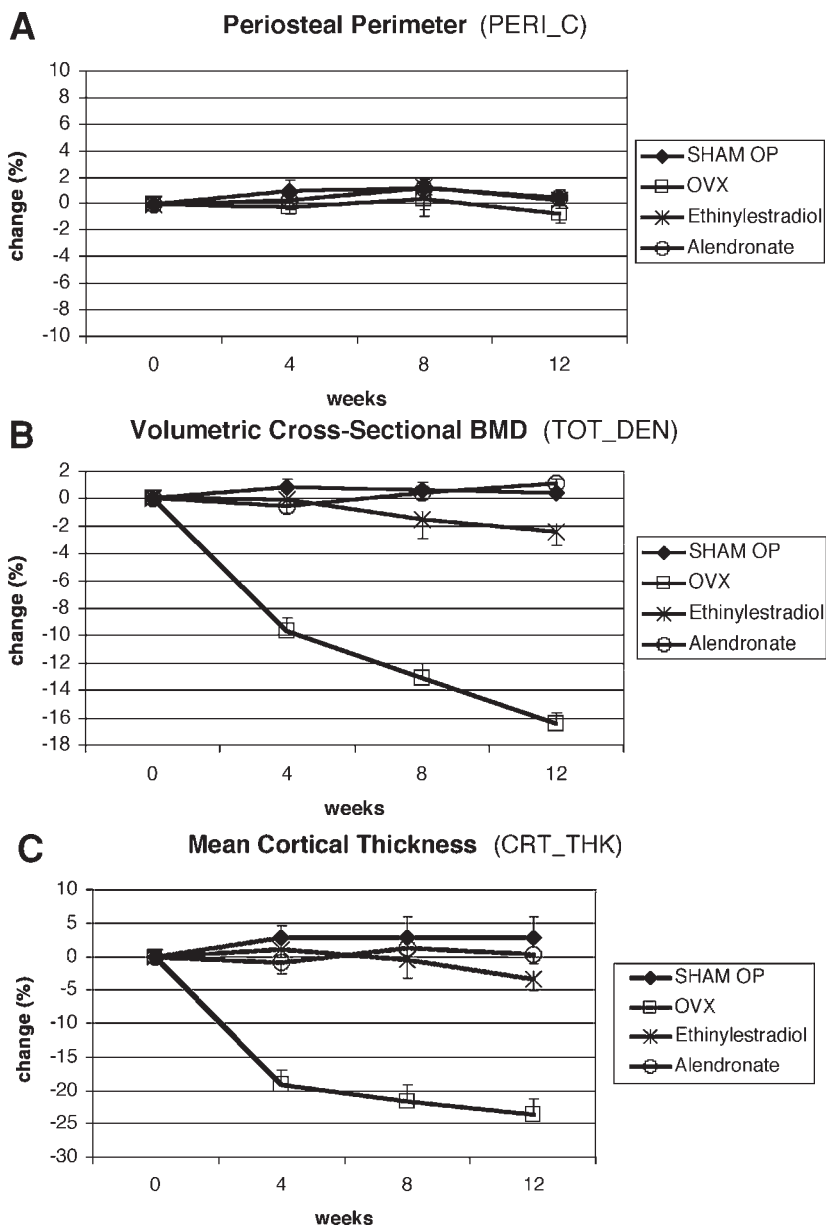
Fig. 7. **(A)** Change in periosteal perimeter (% from baseline) after OVX. **(B)** Change in volumetric cross-sectional BMD (% from baseline) after OVX. **(C)** Change in mean cortical thickness (% from baseline) after OVX.

not different from each other over time. However, the curve for the ethinylestradiol-treated rats drops off by more than three times the CV_r found

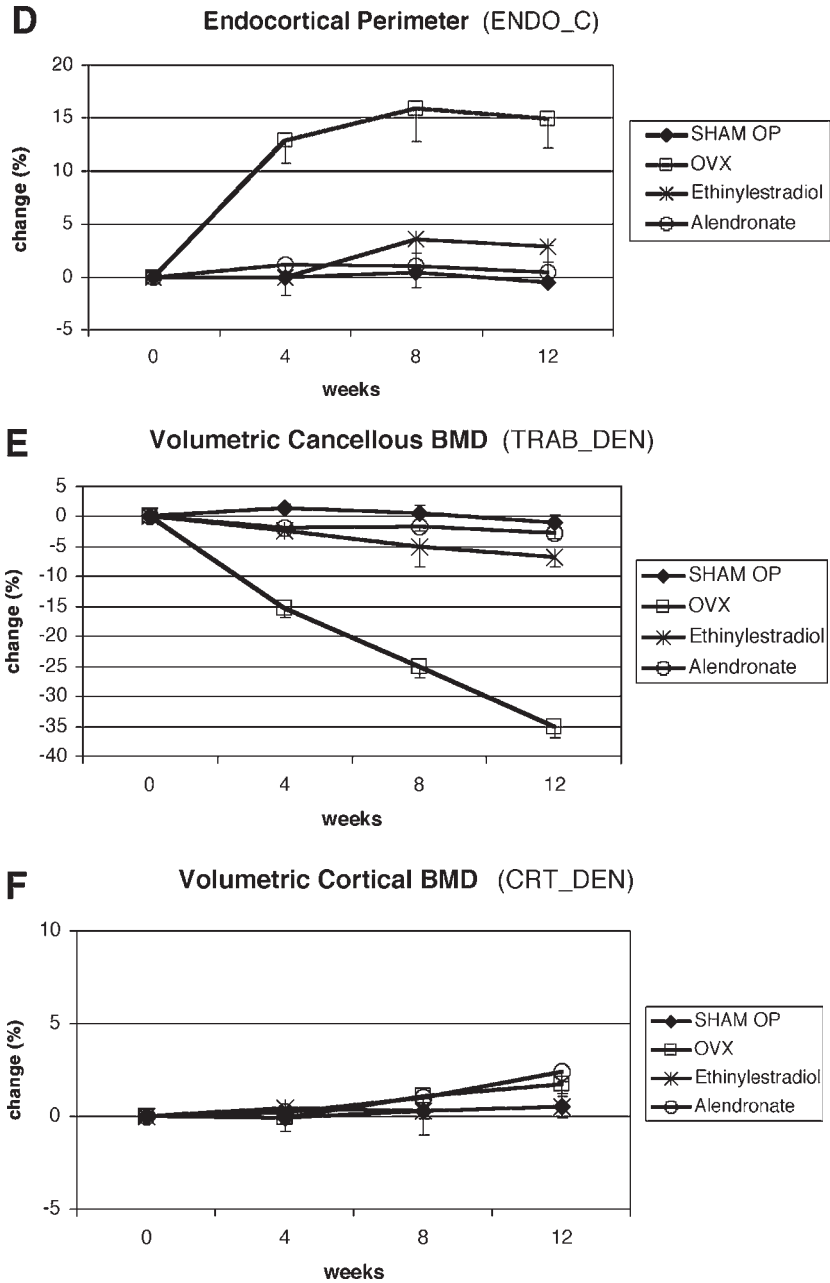**D**

E

F

Fig. 7. (**D**) Change in endocortical perimeter (% from baseline) after OVX. (**E**) Change in volumetric cancellous BMD (% from baseline) after OVX. (**F**) Change in volumetric cortical BMD (% from baseline) after OVX.

in **Table 2** (>0.8%), indicating that treatment is not 100% effective in preventing bone loss. OVX rats show highly significant changes in TOT_DEN already at 4 wk and this parameter can already give meaningful information at a 2-wk measurement point. In the absence of any change in bone size we can now also conclude that bone loss must have occurred entirely on the endosteal envelope (cancellous or endocortical bone resorption). Our analytical process should therefore try to distinguish between these two possibilities.

The best parameters available to address this question is to look for changes in mean cortical thickness (CRT_THK, **Fig. 7C**), and the threshold delineated endocortical perimeter (ENDO_C, **Fig. 7D**) or, alternatively, the cancellous bone area (TRAB_A). In our example, both the sham OP and alendronate-treated animals are stable over time in these three parameters. The ethinylestradiol-treated animals show changes that just about exceed three times the CV_r value for this parameter displayed in **Table 2** (>2.6%). This indicates that some cortical thinning through endocortical bone resorption has occurred. Apparently, this resorptive process is very fast and significant cortical thinning is observed in vehicle treated OVX rats as early as 4 wk after the operation (**Fig. 7C**). A decrease in CRT_THK in the absence of changes in bone size (PERI_C) indicates that all of the changes in CRT_THK are the result of endocortical bone resorption. Treatments that are known to increase cortical thickness through endocortical bone apposition are PTH *(2,19,20)* and PGE_2 (**21,22**). The magnitude of these changes (decrease in ENDO_C) is large and can easily be monitored after 4 wk or longer.

Next we would like to interpret the results on the trabecular compartment. Remember that we were using a threshold-based algorithm to separate cancellous from cortical bone. Also, our analysis shows that the marrow cavity is expanding through a strong endocortical resorption process. This ongoing endocortical erosion obviously lowers volumetric cortical density at the interface to such a degree, that it falls below the chosen threshold of 690 mg/cm^3 and as a consequence is counted as cancellous bone. Because of the constant increase in TRAB_A, just looking at cancellous BMC (TRAB_CNT) may give the misleading impression of an increase in cancellous bone mass even though rapid removal of cancellous bone structures is ongoing. We therefore recommend using the area-corrected volumetric cancellous BMD (TRAB_DEN, **Fig. 7E**) instead, which accounts for the expanding marrow cavity. This parameter clearly shows that cancellous bone is lost at even a greater rate than is observed in cortical thinning (CRT_THK, **Fig. 7C**). Again, alendronate appears to be fully protective while cancellous bone loss in ethinylestradiol-treated animals exceeds the threefold CV_r displayed in **Table 2**, indicating small but significant bone loss from this compartment.

Some of the known agents acting to increase cancellous bone in rats are PTH *(23,24)*, fibroblast Growth factor (FGF) *(25)*, PGE_2 *(21,22,26)*, vitamin D analogues *(27)*, and GH.

Volumetric cortical BMD (CRT_DEN) (**Fig. 7F**) is the only parameter, which indicates an intrinsic material property of bone. In contrast to TOT_DEN and TRAB_DEN, which in fact are nothing but projected area density measurements similar to those obtained by DXA, CRT_DEN is a true volumetric measurement of mineral density. Under most circumstances, this parameter changes very little over time but it may increase in long-term studies with bisphosphonates to indicate increased matrix mineralization (stiffer bone). Conversely, this parameter may decrease at least transiently during long-term treatment with bone anabolic agents such as PTH, because the newly formed endocortical bone is less densely mineralised and because secondary mineralization takes some time to catch up *(28)*. Volumetric CRT_DEN may also decrease in cases in which bone mineralisation is disturbed (vitamin D deficiency, osteogenesis imperfecta) *(29)* or in the presence of increased Haversian remodeling (only exceptionally in rodents). In our example there is indeed little change over time in CRT_DEN except for a trend to an increase in the alendronate and OVX group which, perhaps, could be indicative of increased matrix mineral content in bisphosphonate-treated animals.

In summary, our example shows rapid cancellous and endocortical bone loss, the latter resulting in cortical thinning. Cortical thinning is not counteracted by activation of a compensatory periosteal bone formation drift in these skeletally mature animals, in contrast to what would be seen in younger rats (*see* **Fig. 1**). The magnitude of bone loss is greater in the cancellous than the cortical bone compartment. None of the interventions has significant effects on matrix mineralisation as concluded from cortical BMD measurements but there is at least a trend toward an increase in alendronate-treated rats. It may be worthwhile to follow up such a trend with more sophisticated methods with better discriminatory power for matrix mineralisation such as backscattered electron imaging *(30,31)*.

3.10. Tips and Tricks on Instrument Setting

1. The settings you chose (especially the thresholds) vary with age of the animals. Younger animals often require lower thresholds than those displayed in **Table 1**. The same may be true for transgenic and KO mice with a severely osteopenic phenotype, animals that undergo heavy Haversian remodelling, or in situations in which mineralization is disturbed (vitamin D deficiency, osteogenesis imperfecta).
2. You should choose the highest possible threshold for contour finding to minimize the partial volume effect. The ideal threshold is 730 mg/cm^3, which corre-

sponds to an attenuation coefficient of 0.94 cm^{-1}. This high threshold only really works for rats 9 mo of age and older and may fail even in this age group at later measurement points, if the intervention results in substantial cortical bone loss.

3. If your cortical ring does not appear to be closed when running your chosen algorithm in the analytical part, your threshold is too high and you have to lower it, as the parameters describing cortical architecture would all be wrong!

4. Within one experiment you must choose the same peeling algorithms including the thresholds for each animal and each measurement point! If your chosen setup fails during later time points in your experiment you must go back and reanalyze all your earlier data points of the entire experiment using lower thresholds therefore.

5. We recommend to run the scan analysis loop always twice with two different thresholds (an ideal and a lower one). The two thresholds we routinely chose are 690 and 590 mg/cm^3, respectively, in skeletally mature rats, and 400 and 350 mg/cm^3 for skeletally mature mice. If your experimental conditions result in strong bone loss and your initially chosen "higher" threshold fails during later data acquisitions, you can choose to work with the data of the "lower," nonoptimal second threshold without having to reanalyze all your earlier time points.

References

1. Guglielmi, G., Glüer, C. C., Majumdar, S., Blunt, B. A., and Genant, H. K. (1995) Current methods and advances in bone densitometry. *Eur. Radiol.* **5,** 129–139.
2. Gasser, J. A. (1997) Quantitative assessment of bone mass and geometry by pQCT in rats in vivo and site specificity of changes at different skeletal sites. *J. Jpn. Soc. Bone Morphom.* **7,** 107–114.
3. Gasser, J. A. (1995) Assessing bone quantity by pQCT. *Bone* **17,** S145–S154.
4. Ferretti, J. L., Capozza, R. F., and Zanchetta, J. R. (1995) Mechanical validation of a tomographic (pQCT) index for non-invasive estimation of rat femur bending strength. *Bone* **17,** S145–S162.
5. Ferretti, J. L., Capozza, R. F., and Zanchetta, J. R. (1995) Mechanical validation of a non-invasive (pQCT) index of bending strength in rat femurs. *Bone* **18,** 97–102.
6. Ferretti, J. L. (1997) Non-invasive assessment of bone architecture and biomechanical properties in animals and humans employing pQCT technology. *J. Jpn. Soc. Bone Morphom.* **7,** 115–125.
7. Schneider, P. and Börner, W. (1991) Peripheral quantitative computed tomography for bone mineral measurements using a new special QCT-scanner: methodology, normal values, comparison with manifest osteoporosis. *Fortschr. Röntgenstr.* **154,** 292–299.
8. Hermann, G.T. (1980) *Image Reconstruction from Projections: The Fundamentals of Computerized Tomography*. Academic Press, Orlando.
9. Banu, M. J., Orhii, P. B., Mejia, W., et al. (1999) Analysis of the effects of growth hormone, voluntary exercise and food restriction on diaphyseal bone in female F344 rats. *Bone* **25,** 469–480.
10. Breen, S. A., Millest, A. J., Loveday, B. E., Johnstone, D., and Waterton, J. C. (1996) Regional analysis of bone mineral density in the distal femur and proximal

tibia using peripheral computed tomography in the rat in vivo. *Calcif. Tissue Int.* **58,** 449–453.

11. Beamer, W. G., Donahue, L. R., Rosen, C. J., and Baylink, D. J. (1996) Genetic variability in adult bone density among inbred strains of mice. *Bone* **18,** 397–403.

12. Graichen, H., Lochmüller, E. M., Wolf, E., et al. (1998) A non-destructive technique for a 3-D microstructural phenotypic characterisation of bones in genetically altered mice: preliminary data in growth hormone transgenic animals and normal controls. *Anat. Embryol.* **199,** 239–248.

13. Wronski, T. J., Dann, L. M., Scott, K. S., and Cintron, M. (1989) Long-term effects of ovariectomy and aging on the rat skeleton. *Calcif. Tissue Int.* **45,** 360–366.

14. Yamazaki, I. and Yamaguchi, H. (1989) Characteristics of an ovariectomized osteopenic rat model. *J. Bone Miner. Res.* **4,** 13–22

15. Kalu, D. N. (1991) The ovariectomized rat model of postmenopausal bone loss. *Bone Miner.* **15,** 175–192.

16. Andreassen, T. T., Jorgensen, P. H., Flyvbjerg, A., Orskov, A., and Oxlund, H. (1995) Growth hormone stimulates bone formation and strength of cortical bone in aged rats. *J. Bone Miner. Res.* **10,** 1057–1067.

17. Andreassen, T. T. and Oxlund, H. (2000) The influence of combined parathyroid hormone and growth hormone treatment on cortical bone in aged ovariectomized rats. *J. Bone Miner. Res.* **15,** 2266–2275.

18. Weber, K., Goldberg, M., Stangassinger, M., and Erben, R. G. (2001) 1α-hydroxyvitamin D_2 is less toxic but not bone selective relative to 1α-hydroxyvitamin D_3 in ovariectomized rats. *J. Bone Miner. Res.* **16,** 639–651.

19. Ejersted, C., Andreassen, T. T., Oxlund, H., et al. (1993) Human parathyroid hormone (1-34) and (1-84) increase the mechanical strength and thickness of cortical bone in rats. *J. Bone Miner. Res.* **8,** 1097–1101.

20. Ejersted, C., Andreassen, T. T., Nilsson, M. H., and Oxlund, H. (1994) Human parathyroid hormone (1-34) increases bone formation and strength of cortical bone in aged rats. *Eur. J. Endocrinol.* **130,** 201–207.

21. Jee, W. S. S., Mori, S., Li, X. J., and Chan, S. (1990) Prostaglandin E2 enhances cortical bone mass and activates intracortical bone remodeling in intact and ovariectomized female rats. *Bone* **11,** 253–266.

22. Jee, W. S. S., Ke, H. Z., and Li, X. J. (1991) Long-term anabolic effects of prostaglandin-E2 on tibial diaphyseal bone in male rats. *Bone Miner.* **15,** 33–55.

23. Gunness-Hey, M. and Hock, J. M. (1984) Increased trabecular bone mass in rats treated with synthetic parathyroid hormone. *Metab. Bone Rel. Dis.* **5,** 177–181.

24. Gunness-Hey, M. and Hock, J. M. (1993) Anabolic effect of parathyroid hormone on cancellous and cortical bone histology. *Bone* **14,** 277–281.

25. Pun, S., Dearden, R. L., Ratkus, A. M., Liang, H., and Wronski, T. J. (2001) Decreased bone anabolic effect of basic fibroblast growth factor at fatty marrow sites in ovariectomized rats. *Bone* **28,** 220–226.

26. Mori, S., Jee, W. S. S., and Li, X. J. (1992) Production of new trabecular bone in osteopenic ovariectomized rats by prostaglandin E2. *Calcif. Tissue Int.* **50,** 80–87.

27. Erben, R.G., Bromm, S., and Stangassinger, M. (1998) Therapeutic efficacy of 1α,25-hydroxyvitamin D3 and calcium in osteopenic ovariectomized rats: evidence for a direct anabolic effect of 1α,25-hydroxyvitamin D3 on bone. *Endocrinology* **139,** 4319–4328.

28. Kneissel, M., Boyde, A., and Gasser, J. A. (2001) Bone tissue and its mineralization in aged estrogen-depleted rats after long-term intermittent treatment with parathyroid hormone (PTH) analog SDZ PTS 893 or human PTH(1-34). *Bone* **28,** 237–250.

29. Boyde, A., Travers, R., Glorieux, F.H., and Jones, S.J. (1999) The mineralisation density of iliac crest bone from children with osteogenesis imperfecta. *Calcif. Tissue Int.* **64,** 185–190.

30. Boyde, A., Jones, S. J., Aerssens, J. and Dequeker, J. (1995) Mineral density quantification of the human cortical illiac crest by backscattered electron image analysis: Variations with age, sex, and degree of osteoarthritis. *Bone* **16,** 619–627.

31. Roschger, P., Plenk, H., Jr., Klaushofer, K., and Eschberger, J. (1995) A new scanning electron microscopy approach for the quantification of bone mineral distribution: Backscattered electron image grey levels correlated to calcium Kalpha-line intensities. *Scan Microsc.* **9,** 75–88.

24

Studies of Local Bone Remodeling

The Calvarial Injection Assay

Robert J. van 't Hof, Claire E. Clarkin, and Kenneth J. Armour

1. Introduction

There are several assays available to study the effects of cytokines, drugs, and hormones on bone cells in vitro. However, as the complex interactions between cells are disrupted, these in vitro assays do not always reflect what happens in vivo. The calvarial injection method, originally described by Boyce et al. *(1)*, is valuable for studying the effects of substances on bone metabolism in vivo. In this assay, the substance to be tested is injected subcutaneously over the calvarium of a mouse. At the end of the assay the animal is euthanized, and the calvarium dissected and analyzed by microscopy. Although the assay was originally used to study effects of cytokines on osteoclast formation and activity *(1,2)*, it has also been used to study the effects of drugs on bone formation *(3)*.

2. Materials
2.1. Injection

1. Recombinant murine interleukin-1α (IL-1α) (5 mg/mL; CN Biosciences [UK] Ltd., Nottingham, UK).
2. Hamilton syringe (Luer-lock type; Anachem Ltd, Luton, UK).

2.2. Tissue Processing

1. Histocryl (glycol methacrylate, TAAB).
2. Resin mix: Add 1.5 g of catalyst (benzoyl peroxide, comes with the histocryl) to 100 mL of histocryl; keep at 4°C.
3. Accelerator mix: 5 mL of polyethylene glycol 4000 (PEG 400), 5 mL dibutyl pthalate, and 240 μL of Histocryl accelerator.

4. Embedding mix: Add 175 μL of accelerator mix to 1 mL of resin mix (at 4°C) and use immediately.

2.3. Tartrate-Resistant Acid Phosphatase (TRAP)/von Kossa/Light Green Stain

1. 1.5% (w/v) Silver nitrate in dH$_2$O.
2. 0.1% (w/v) Hydroquinone.
3. 1% (w/v) Light green in dH$_2$O.
4. All the reagents for the TRAP stain are described in Chapter 11 by van 't Hof, *this volume*.

2.4. Goldner's Trichrome Stain

1. Weigert's hematoxylin:
   a. Solution A: Dissolve 10 g hematoxylin in 1000 mL of absolute alcohol. Ripen for at least 4 wk before use.
   b. Solution B: Dissolve 11.6 g of ferric chloride (hydrated) in 1000 mL of distilled water and add 10 mL of 2% HCl.
   Immediately before use mix equal parts of A and B. Do not keep working solution premade.
2. Ponceau de Xylidine–acid fuchsin: 1.5 g of Ponceau de Xylidine, 0.5 g of acid fuchsin, 2 mL of acetic acid (concentrated), and 98 mL of distilled water.
3. Azophloxine (working solution): 0.5 g of azophloxine, 0.6 mL of acetic acid (concentrated), and 99.4 mL of distilled water.
4. Ponceau de Xylidine–acid fuchsin–azophloxine (working solution): 12 mL of Ponceau de Xylidine–acid fuchsin, 8 mL of azophloxine, 80 mL 0.2% acetic acid; reuse the working solution.
5. Phosphomolybdic acid–orange G: 6 g of phosphomolybdic acid, 4 g of Orange G, and 1000 mL of distilled water.
6. Light green: 2 g of light green, 2 mL of acetic acid (concentrated), and 1000 mL of distilled water.

3. Methods
3.1. Injection Protocol (Resorption)

1. Inject the mice over the calvarial bones with 10 μL of recombinant murine IL-1α (5 mg/mL) or vehicle (sterile saline) using a 50-μL Hamilton syringe. Perform injections three times per day for 3 consecutive days (*see* **Notes 1–3**).
2. Euthanize the mice 4 d after the last injection.
3. Dissect out the calvarial bones and fix in 4% buffered formalin–saline, pH 7.4, for 1 h.
4. Rinse the calvaria in PBS and store in 70% alcohol.
5. Embed the undecalcified calvarial bones in glycol–methacrylate (GMA, *see* **Notes 4** and **5**) and cut 3-μm sections on a microtome (Jung, Heidelberg, Germany) using a glass knife (*see* **Subheading 3.2.** for embedding procedure).
6. Stain sections with von Kossa and TRAP, followed by counterstaining with light green. Alternatively, especially when one is interested in effects on osteoblasts,

the sections can be stained with Goldner's trichrome (*see* **Subheadings 3.3. and 3.4.** for staining protocols).

3.2. Tissue Processing

Cut out a strip of calvarial tissue from the center of the calvarium as illustrated in **Fig. 1**. The following steps are most easily performed using a tissue processor, but can also be performed manually. All the steps are performed at 4°C (*see* **Note 6**).

1. Transfer tissue strips to 96% ethanol for 1 h.
2. 1 h in 100% ethanol.
3. 1 h in a 1:1 mix of 100% ethanol and resin mix.
4. 1 h in resin mix.
5. 72 h in resin mix.
6. Transfer tissue to a mold placed in a crushed-ice slush, fill with embedding mix, seal with a stub, and leave to polymerize for 1 h.

3.3. TRAP/von Kossa/Light Green Staining of Mouse Calvariae

This method stains osteoclasts bright red, the mineralized bone black, and the remaining tissue green (**Fig. 2**). The von Kossa stain should be performed first because the TRAP staining solution (which is acidic) will dissolve much of the mineral from the section resulting in an unsatisfactory von Kossa stain.

1. Immerse sections in 1.5% silver nitrate (made up when required and filtered just before use) for 40 s.
2. Wash three times in water.
3. Develop the stain in 0.1% hydroquinone for 25–30 s (maximum). Check using a microscope at this point; mineralized bone should be black, not brown. If the bone looks brown, rinse in water and repeat the procedure.
4. Thoroughly rinse sections in running tap water for 10 min. Hydroquinone inhibits TRAP staining, and this step ensures that all the hydroquinone is washed off.
5. Perform the TRAP stain as described for cocultures in Chapter 11 by van 't Hof, *this volume*. Slides should be lying flat in plastic slide boxes with damp tissue lining the bottom. Boxes should then be covered to avoid drying of the staining solution.
6. Incubate at 37°C for 1.5 h. (Check staining after 1 h.)
7. Rinse off the TRAP staining solution with dH_2O.
8. Counterstain with 1% light green for 30–60 s. Wash off with dH_2O.
9. Air-dry.
10. Mount with aqueous mounting medium (e.g., Apathy's).
11. Store in cardboard slide trays and cover to prevent fading.

3.4. Goldner's Trichrome

This stain results in bright green stained calcified bone and good contrast of the cells. Although the osteoclasts do not stand out as well as with the TRAP
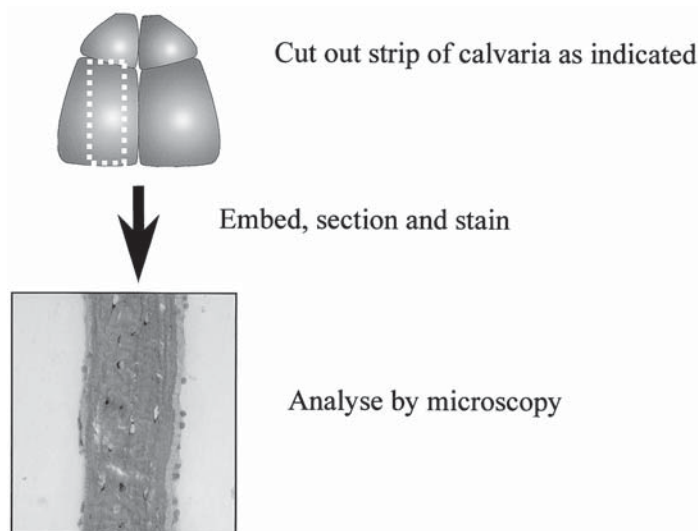
Fig. 1. A strip of tissue is cut out of the fixed calvarium and embedded for processing as indicated in this figure.

stain, this stain allows easy identification of osteoblasts. It is essential not to let the sections dry at any time during the staining protocol, as this leads to cracks in the mineralized bone.

1. Keep the sections in distilled water for at least 1 h (to prevent bubbling below the section; if this still persists keep the slides in water for a longer time).
2. Stain sections in Weigert's hematoxylin for 20 min (*see* **Note 7**).
3. Wash in water.
4. Differentiate with 0.5% acid alcohol.
5. Wash in water for 20 min.
6. Stain sections in Ponceau–acid fuchsin–azophloxine for 5 min.
7. Rinse in 1% acetic acid for 10 s.
8. Stain sections in phosphomolybdic acid–Orange G for 20 min.
9. Repeat **step 7**.
10. Stain sections in 0.2% light green for 5 min.
11. Rinse in water.
12. Blot dry.
13. Rinse in 100% alcohol.
14. Immerse the sections in xylene.
15. Wipe off xylene around section before mounting in DePeX.

This method stains cell nuclei blue/black, mineralized bone/muscle green and osteoid/collagen red (**Fig. 3**).
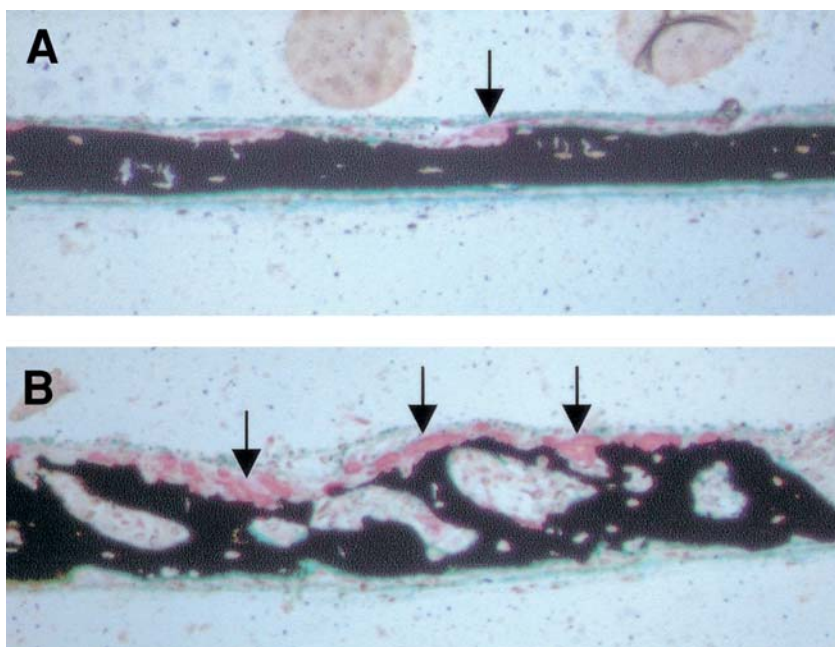
Fig. 2. Calvarial sections from neonatal mice treated with saline **(A)** or IL-1α **(B)** Stained by TRAP and von Kossa. Unlike the control section **(A)**, numerous TRAP-stained osteoclasts *(arrows)* are visible on the bone surface in **(B)** and extensive bone resorption is evident.
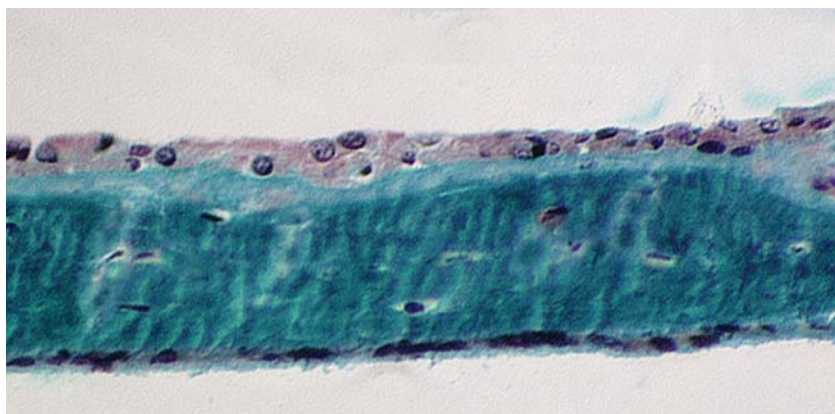
Fig. 3. Calvarial section, stained with Goldner's trichrome, from a neonatal mouse treated with bone morphologenic protein (BMP-2). Large activated osteoblasts and osteoid/collagen are clearly visible above the bone surface. (Reduced from original magnification, ×200.)

3.5. Analysis of Results

Although many qualitative conclusions can be drawn about the effects of test substances by simple microscopical observation, we usually perform a quantitative analysis using computer-assisted histomorphometry. Parameters of interest are numbers of osteoclasts and osteoblasts per bone surface, mineralized bone width, and bone formation and resorption surfaces. We use software developed using the Aphelion ActiveX image analysis toolkit from ADCIS (ADCIS SA, Hérouville-Saint-Clair, France) and a Zeiss Axioskop microscope fitted with a color camera. The program prompts the user to select and focus a field, captures the image, and identifies the part of the image that contains tissue. The bone is identified using color thresholding and the bone surface, volume, and width are calculated (*see* **Note 8**). Then the resorption and formation surfaces are drawn onto the image by the user and finally the user is prompted to enter the number of osteoclasts (*see* **Note 9**) and osteoblasts present in this field. We usually measure at least 10 fields from a representative area of a section, three sections at different levels (at least 100 μm apart) per animal and at least six animals per treatment group (*see* **Note 10**).

4. Notes

1. Mice aged from several days up to several months of age can be used for this assay. Neonates require smaller amounts of injection material (useful when using an expensive drug) and have the advantage that they are easier to handle.
2. The injection schedule needs to be optimized for each substance tested in this assay. One of the most important variables influencing this is the biological half-life of the substance tested. For example, when testing the effects of mevastatin we used a regimen of two injections (5 mg/kg) per day for 5 d and euthanize the animals 1 d or 7 d after the last injection.
3. It is essential that all injection solutions and syringes are sterile. Otherwise, the effects of a test drug could be masked easily by a localized immune response to the injection, which will invariably produce some localized bone loss in the calvarium.
4. Embedding in methyl methacrylate (MMA) plastic is not an alternative, as the TRAP stain does not work well on material embedded in this plastic. An alternative could be the embedding of decalcified calvariae in wax. However, the authors do not know of any stains for this material that will allow easy distinction between bone and the other tissues using simple color thresholding; consequently, the semi-automated analysis of these sections will be much more difficult.
5. We have found that the manufacturer's protocol, which uses only the histocryl accelerator, often leads to brittle blocks that are difficult to cut. Our variation, which uses an accelerator mix, produces blocks that are easier to cut.
6. It is essential to perform the embedding at low temperature. Especially the polymerization step. This step is best performed in a crushed ice slush that will optimally cool the polymerizing block.

7. Celestine Blue can be used as an alternative to hematoxylin if nuclei are not stained particularly well. Prepare the Celestine Blue as follows: 2.5 g of Celestine Blue B, 25 g of ferric ammonium sulfate, 70 mL of glycerin, and 500 mL of dH$_2$O. Dissolve the ferric ammonium sulfate in cold distilled water and stir well. Add Celestine Blue to this solution, then boil the mixture for a few minutes. After cooling, filter the stain and add the glycerin. Use the same staining time for Celestine Blue as for hematoxylin, that is, 20 min.

8. In many programs the calvarial width is determined by having the user draw lines across the mineralized bone at multiple sites. This method is fairly time consuming and not very reproducible owing to operator variability and bias. We use a mathematical method, whereby the calvarial bone is modeled as a rectangle and the width is calculated from the perimeter and the surface area of the bone according to the following formula:

$$\text{Width} = \text{Perimeter} - \sqrt{\text{Perimeter}^2 - (16 * \text{Area})}/4$$

To make this method work properly, all holes within the bone binary image should be closed (using an Image Holefill operator) and the outline should be smoothed by a Binary Close operator (or by an Image Dilate, followed by an Image Erode operator of the same size). The aforementioned operators are available in all image analysis packages that are currently on the market.

9. It can be difficult to get an accurate number of osteoclasts, as these cells are often present in clusters and not well separated visually. Furthermore, as osteoclasts are such large, irregularly shaped cells, what appear to be several osteoclasts close together in a section may actually be parts of the same osteoclast. For this reason it is good practice to analyze several histological sections, separated by at least 100 μm (*see* **Subheading 3.5.**).

10. To avoid possible artefacts introduced by the dissection procedure, do not take histomorphometric measurements at the calvarial ends.

References

1. Boyce, B. F., Aufdemorte, T. B., Garrett, I. R., Yates, A. J., and Mundy, G. R. (1989) Effects of interleukin-1 on bone turnover in normal mice. *Endocrinology* **125,** 1142–1150.
2. van't Hof, R. J., Armour, K. J., Smith, L. M., et al. (2000) Requirement of the inducible nitric oxide synthase pathway for IL-1- induced osteoclastic bone resorption. *Proc. Natl. Acad. Sci. USA* **97,** 7993–7998.
3. Mundy, G., Garrett, R., Harris, S., et al. (1999) Stimulation of bone formation in vitro and in rodents by statins. *Science* **286,** 1946–1949.

25

Inflammation-Induced Osteoporosis

The IMO Model

Kenneth J. Armour and Katharine E. Armour

1. Introduction

Generalized osteoporosis and an increased risk of fracture are commonly observed in chronic inflammatory diseases such as rheumatoid arthritis, ankylosing spondylitis, and inflammatory bowel disease *(1–4)*. Current evidence suggests that the osteoporosis developed during chronic inflammation may result from the inhibition of bone formation, and is associated with systemic overproduction of proinflammatory mediators, such as cytokines, nitric oxide (NO), and prostaglandins *(5–8)*.

The first animal model of generalized osteoporosis resulting from inflammation that closely resembled the chronic inflammatory bone loss seen in human patients was developed by Minne et al. *(9)* in the rat. The inflammation-mediated osteoporosis (IMO) model utilizes the subcutaneous injection of nonspecific irritants, such as talc or cotton wool, typically on the back of the rat at sites distant from the skeleton, to stimulate an acute phase response. Granulomatous reactions are noted at the injection sites along with the accumulation of chronic inflammatory cells. In the skeleton, at sites distant from the inflammatory lesions, loss of trabecular bone volume and significant decreases in osteoblast numbers are observed (**Fig. 1**). Subsequent studies have extended these observations to show that decreases in osteoblast numbers and bone formation are major features of the IMO model *(10–12)*. In growing rats, decreases in osteoprogenitor number and bone elongation are also observed *(12)*. Interestingly, osteoclast numbers and osteoclastic resorption are generally unchanged (or transiently decreased) in this model *(9–13)*, which also accords with the observations in humans with chronic nonosseous inflammation *(1–4)*.
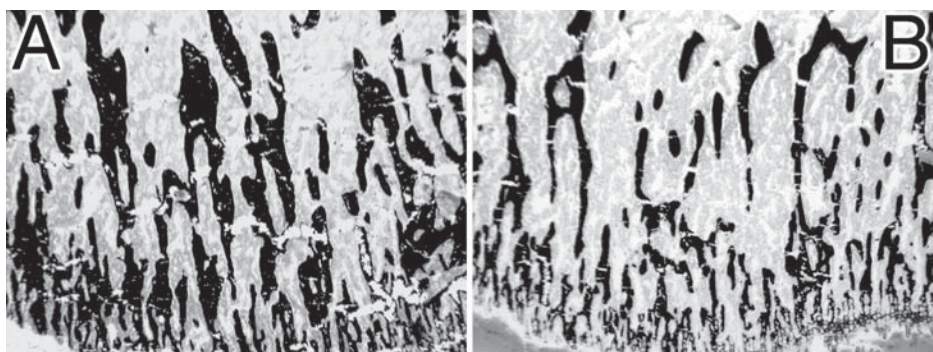
Fig. 1. Photomicrographs of distal femurs from rats 21 d after treatment with saline **(A)** or talc **(B)**. Trabecular thinning and lower numbers of trabeculae are evident in **(B)**. (Reduced from original magnification, ×25.)

Elevated tumour necrosis factor-α (TNF-α) levels have been shown to play a causal role in the bone loss seen in the IMO model and the effects of IMO can be neutralized with anti-TNF-α antibodies *(14)*. Furthermore, TNF-α is known to stimulate NO production. Recent work has shown that increased osteoblast apoptosis, associated with the production of high levels of NO synthesized by the inducible nitric oxide synthase (iNOS) pathway *(15,16)*, contributes to the pathogenesis of IMO.

This chapter describes a general protocol for the induction of IMO in rodents (rats and mice) using injections of talc and suggests suitable end points for the experimental investigations.

2. Materials

1. Sterile isotonic (0.9%) saline (Sigma, Poole, UK) for use as an injection vehicle. Phosphate-buffered saline or a balanced salt solution (such as Hanks') can be used as alternatives.
2. Talc (hydrous magnesium silicate; Sigma), sterilized by heating at 160°C for at least one hour *(17)*. After sterilization, aseptically prepare an 800 mg/mL suspension in sterile saline. Store at room temperature and use shortly after preparation. The talc suspension can be stored at 4°C for short periods but needs to be warmed to room temperature and mixed thoroughly before use.
3. Calcein (Sigma), prepared as a 4 mg /mL solution in sterile saline and adjusted to around neutral pH. Filter sterilize using a 0.2-μm filter (Acrodisc; Pall, Portsmouth, UK), then aliquot. Protect aliquots from light during storage, preferably at –20°C if stored for extended periods.
4. Vetalar (ketamine hydrochloride: 100 mg/mL; Pharmacia & Upjohn Ltd., Crawley, UK) and Rompun (xylazine: 2% solution; Bayer plc, Bury St. Edmonds, UK) for the induction of anesthesia.

5. 25-Gauge needles (BD UK Ltd., Cowley, UK).

3. Methods
3.1. Animals

1. Ideally, at least 10 mice or rats of the same sex should be used per group to ensure that any differences or changes measured reach statistical significance (*see* **Notes 1** and **2***).*

3.2. Inflammation-Mediated Osteoporosis

The following protocol describes a 21-d longitudinal study.

1. For urine collection, place animals in individual metabolic cages prior to the start of experiment and collect the urine samples into sterile containers over a 16–24-h period. Add a small volume of 5 *M* sodium hydroxide to each sample to prevent bacterial growth and freeze the samples immediately. Snap freezing in liquid nitrogen is preferable.
2. Weigh all the animals (to at least one decimal place for mice) (*see* **Note 3**).
3. Anesthetize animals with Vetalar (100 mg/kg of body weight) and Rompun (20 mg/kg body weight) by intraperitoneal (i.p.) injection (into the lower left quadrant of the abdomen). This will induce medium-depth anesthesia of sufficient duration to perform the subsequent two experimental steps (*see* **Notes 4** and **5**).
4. Using a 25-gauge needle, inject the talc suspension subcutaneously at four or more sites on the upper back and sides of the animal, to give a total talc dose of 16 mg/g body weight. Administer an equivalent volume of sterile saline to the controls. Avoid injecting directly over skeletal sites.
5. Scan the animals using bone densitometry. Dual-energy X-ray Absorptiometry (DXA) is useful for detecting bone mass changes over the whole skeleton, but peripheral quantitative computed tomography (pQCT) is preferable for assessing discrete changes in trabecular and cortical bone components (*see* the chapter by Gasser, *this volume*, for a full discussion of pQCT) (*see* **Notes 6** and **7**).
6. Administer calcein (40 mg/kg body weight) by i.p. injection at two or more time points during the IMO procedure to label bone fluorescently. In our laboratory we have obtained useful information from calcein injections on d 10 and d 17. The timing of the calcein injections is important and should be standardized to the same time of day on each of the injection days. Calcein is preferred over tetraxyclin in rodents.
7. Repeat experimental **step 1** on the penultimate day of the 21-d experimental period.
8. On the final day of the experiment repeat experimental **steps 2**, **3**, and **5**.
9. Euthanize the animals.
10. Remove the right and left hind leg bones (femorae and tibiae) and fix in preparation for bone histomorphometry (*see* **Table 1** and **Note 8**) (*see* the chapter by Vedi and Compston, *this volume*, for details).
11. Remove and weigh the spleens (*see* **Note 9**).

Table 1
Overview of the Pathophysiological Changes in Bone
Associated with Inflammation-Mediated Osteoporosis

Bone parameter	Response	References
Trabecular bone volume/density	⇓	*9,10,12–14,16,17,19,22,23*
Osteoprogenitor numbers	⇓	*12,17*
Osteoblast numbers	⇓	*9,10–12,14,16,19,23*
Osteoblast apoptosis	⇑	*16*
Bone formation	⇓	*10–12,16*
Bone elongation/growth	⇓	*11,12*
Osteoclast numbers	⇔ or ⇓ (transient)	*9–12,14,16,23*
Bone resorption	⇔ or ⇓ (transient)	*9,10,16*

4. Notes

1. Rats weighing 200 g or more and mice older than 14 wk of age are preferable. The potentially confounding effects of skeletal growth need to be accounted for when assessing the effects of IMO in younger animals.

2. Age matching is important, particularly when studying bone changes in transgenic mice, and the use of littermates is recommended.

3. It has been noted that talc-injected rats fed *ad libitum* consume less food and exhibit less weight gain (or even some weight loss) compared with saline-injected rats. For this reason it may be desirable to match and pair-feed controls with talc-injected rats to minimize any effect of lower caloric intake on bone *(11,12,14,17)*. Rats should be housed in individual cages to allow for this feeding regimen. We have not observed the same tendency to lower food consumption in mice following talc injection.

4. For anesthesia of mice, it is practical to prepare 1:10 dilutions of Vetalar and Rompun in sterile saline, using the same container for both dilutions to minimize the injection volume required. The administration of 0.1 mL/10 g of body weight provides the required dose (100 mg of Vetalar/kg body weight and 20 mg of Rompun/kg of body weight). In rats, 0.1 mL of each of the undiluted Vetalar and Rompun stocks should be used per 100 g of body weight to provide the correct dose for anesthesia. The solutions can be stored at 4°C.

5. It may be desirable to take *small* blood samples during the IMO experiment, for example, to measure circulating cytokine or electrolyte levels. In our hands, the use of a Vetalar–Rompun mix provides reliable and predictable anesthesia and is not associated with significant animal mortality. In practice, however, Vetalar–Rompun-induced anesthesia tends to decrease the amount of blood obtainable from sampling, and inhalation anesthesia using halothane is preferable in this situation. Induction of anesthesia using 3–4% halothane followed by the mainte-

nance of anesthesia using 1–2% halothane in the presence of an adequate flow of oxygen is effective for blood sampling. A 2-wk interval between blood samplings is generally recommended *(18)*, and samples taken at the start and end of the experiment are feasible when using a 21-d protocol. Blood withdrawal from the lateral vein of the tail is a minimally invasive method and recommended for small samples. Terminal blood samples at the end of the experiment can be also obtained by cardiac puncture, and inhalation anesthesia is again preferable for this. The use of inhalation anesthesia does not preclude the use of an injectable anesthetic and the latter may still be appropriate when subsequently undertaking densitometric measurements. *Note that only fully trained personnel, authorized by their relevant institutional and national authorities, should undertake procedures on animals.*

6. Longitudinal studies are clearly preferable to cross-sectional studies because of the additional experimental information they provide and the lower number of animals they require. However, if an end point only study is to be conducted, it is essential that an additional group of animals, killed at the start of the experiment, is included to provide baseline readings.

7. A 21-d period is ideal for demonstrating the osteoporosis that results from generalized inflammation and for investigating the bone-sparing effects of potential therapies. Although the magnitude of trabecular bone loss may be greater in longer experiments, studies of shorter duration have also been used successfully, with osteoblast insufficiency and some trabecular bone loss evident within 7 d of talc administration *(12,19)*.

8. It is good practice to obtain as much information as possible from each in vivo experiment and biomechanical and micro-CT analyses of bone (discussed in the chapters by Aspden and by Gasser, respectively, *this volume*) should be seriously considered as additional options when assessing the effects of experimentally induced bone loss. For biomechanical studies, freshly dissected bones should tested as soon as possible after dissection; alternatively, the bones should be wrapped in gauze or tissue paper soaked with sterile saline and frozen at –20°C in sterile containers until required.

9. As listed in **Table 1**, IMO is associated with marked pathological changes in bone that include decreased trabecular bone mass, osteoblast insufficiency, and decreased bone formation. In addition to pathological changes in bone, it is important to have bone-independent measures of the effectiveness of talc-induced inflammation. In this regard, the following indices may be applicable:

   a. Splenomegaly is a clear and useful indicator of an inflammatory response *(10)* and weighing a dissected spleen is simple to perform. A 400% increase in spleen weight in mice compared with controls is not uncommon *(16)*.

   b. Microscopic examination of the spleen may also be useful for describing the cellular changes associated with the acute phase response *(20)*. The spleens should be fixed or frozen in liquid nitrogen prior to immunohistological analysis.

   c. Urinary nitrate excretion is elevated during IMO as a result of increased NO production and the measurement of urinary NOx using the Griess reaction *(21)* is another useful and straightforward indicator of inflammation.

Table 2
Overview of the Pathophysiological Changes Associated with Inflammation-Mediated Osteoporosis

	Response	Citation
Serum components/trace elements		
Calcium	⇔	*9,17,19,22,23*
Phosphorus	⇑/⇔	*9,23/17,19*
Zinc	⇓	*14,17,19,23*
Iron	⇓	*14,17,19,23*
Copper	⇑	*14,17,19,23*
Magnesium	⇔	*17,19,23*
Creatinine	⇔	*9*
Serum proteins		
Albumin	⇓	*19,23*
Alkaline phosphatase (liver isoform)	⇑	*17,19,23*
C-reactive protein	⇑	*14*
α_1-, α_2-, and β-globulin	⇑	*19,23*
γ-Globulin	⇓	*19,23*
Hormones/growth factors		
Adrenocorticotropic hormone	⇑	*14,19,23*
Corticosterone	⇑	*19*
Parathyroid hormone	⇔	*9*
Calcitonin	⇔	*9*
1,25-Dihydroxyvitamin D_3	⇓ (transient)	*9*
Osteocalcin	⇓	*19,23*
TNF-α	⇑	*14*
Urinary excretion		
Creatinine	⇔	*13,15,16*
Nitrate/nitrite (NOx)	⇑	*15,16*
White blood cell counts		
Mononuclear cells	⇓	*19,20,23*
Polymorphonuclear cells	⇑	*19,20*

Table 2 lists numerous other humoral or cellular changes that have been reported in response to IMO, and many of these can be used as bone-independent indicators of the inflammatory response.

References

1. Deodhar, A. A. and Woolf, A. D. (1996) Bone mass measurement and bone metabolism in rheumatoid arthritis: a review. *Br. J. Rheumatol.* **35,** 309–322.
2. Andreassen, H., Rungby, J., Dahlerup, J. F., and Mosekilde, L. (1997) Inflammatory bowel disease and osteoporosis. *Scand. J. Gastroenterol.* **32,** 1247–1255.

3. Will, R., Palmer, R., Bhalla, A. K., Ring, F., and Calin, A. (1989) Osteoporosis in early ankylosing spondylitis: a primary pathological event? *Lancet* **2,** 1483–1485.

4. Ralston, S. H., Urquhart, G. D. K., Brzeski, M., and Sturrock, R.D. (1990) Prevalence of vertebral compression fractures due to osteoporosis in ankylosing spondylitis. *Br. Med. J.* **300,** 563–566.

5. Oudkerk, P. M., Bouma, G., Visser, J. J., et al. (1995) Serum nitrate levels in ulcerative colitis and Crohn's disease. *Scand. J. Gastroenterol.* **30,** 784–788.

6. Sakurai, H., Koshaka, H., Lui, M-F., et al. (1995) Nitric oxide production and inducible nitric oxide synthase expression in inflammatory arthritides. *J. Clin. Invest.* **96,** 2357–2363.

7. Dijkstra, G., Moshage, H., van Dullemen, H. M., et al. (1998) Expression of nitric oxide synthases and formation of nitrotyrosine and reactive oxygen species in inflammatory bowel disease. *J. Pathol.* **186,** 416–421.

8. Ralston, S.H. (1997) Nitric oxide and bone: what a gas! *Br. J. Rheumatol.* **36,** 831–838.

9. Minne, H. W., Pfeilschifter, J., Scharla, S., et al. (1984) Inflammation-mediated osteopenia in the rat: a new animal model for pathological loss of bone mass. *Endocrinology* **115,** 50–54.

10. Pfeilschifter, J., Wuster, C., Vogel, M., Enderes, B., Ziegler, R. and Minne, H. W. (1987) Inflammation-mediated osteopenia (IMO) during acute inflammation in rats is due to a transient inhibition of bone formation. *Calcif. Tissue Int.* **41,** 321–325.

11. Vukicevic, S., Marusic, A., Stavljenic, A., Cicak, N., Vogel, M., and Krempien, B. (1988) Talc granulomatosis in the rat: the relationship between osteoblast insufficiency and adjacent bone marrow hyperplasia. *Exp. Hematol.* **16,** 735–740.

12. Krempien, B., Vukicevic, S., Vogel, M., Stavljenic, A., and Buchele, R. (1988) Cellular basis of inflammation-induced osteopenia in growing rats. *J, Bone Miner. Res.* **3,** 573–582.

13. Lempert, U. G., Minne, H. W., Fleisch, H., Muhlbauer, R. C., Scharla, S. H., and Ziegler, R. (1991) Inflammation-mediated osteopenia (IMO): no change in bone resorption during its development. *Calcif. Tissue Int.* **48,** 291–292.

14. Vukicevic, S., Marusic, A., Stavljenic, A., Cesnjaj, M., and Ivankovic, D. (1994) The role of tumor necrosis factor-alpha in the generation of acute phase response and bone loss in rats and talc granulomatosis. *Lab. Invest.* **70,** 386–391.

15. Armour, K. E., van 't Hof, R. J., Grabowski, P. S., Reid, D. M. and Ralston, S. H. (1999) Evidence for a pathogenic role of nitric oxide in inflammation-induced osteoporosis. *J. Bone Miner. Res.* **14,** 2137–2142.

16. Armour, K. J., Armour, K. E., van 't Hof, R. J., et al. (2001) Activation of the inducible nitric oxide synthase pathway contributes to inflammation-induced osteoporosis by suppressing bone formation and causing osteoblast apoptosis. *Arthrit. Rheum.* **44,** 2790–2796.

17. Marusic, A., Kos, K., Stavljenic, A., and Vukicevic, S. (1991) Acute zinc deficiency and trabecular bone loss in rats with talc granulomatosis. *Biol. Trace. Elem. Res.* **29,** 165–173.

18. Waynforth, H. B. and Flecknell, P. A., eds. (1998) *Experimental and Surgical Techniques in the Rat*, 2nd edit. Academic Press, London.

19. Marusic, A., Kos, K., Stavljenic, A., and Vukicevic, S. (1990) Talc granulomato-
    sis in the rat. Involvement of bone in the acute-phase response. *Inflammation* **14,**
    205–216.
20. Radic, I., Vucak, I., Milosevic, J., Marusic, S., Vukicevic, S., and Marusic, M.
    (1988) Immunosuppression induced by talc granulomatosis in the rat. *Clin. Exp.
    Immunol.* **73,** 316–321.
21. Green, L. C., Wagner, D. A., Glogowski, J, Skipper, P. L., Wishnock, J. S., and
    Tannenbaum, S. R. (1982) Analysis of nitrate, nitrite and (15N) nitrate in biologi-
    cal fluids. *Analyt. Biochem.* **126,** 131–138.
22. Hadjidakis, D., Lempert, U. G., Minne, H. W. and Ziegler, R. (1993) Bone loss in
    experimental diabetes. Comparison with the model of inflammation mediated
    osteopenia. *Horm. Metab. Res.* **25,** 77–81.
23. Marusic, A., Kos, K., Stavljenic, A., and Vukicevic, S. (1993) Role of 1,25-
    dihydroxyvitamin D3 in the generation of the acute-phase response in rats with
    talc-induced granulomatosis. *Experientia* **49,** 693–698.

26

Ovariectomy and Estrogen Replacement in Rodents

Jade W. M. Chow

1. Introduction

Estrogen is known to be one of the major hormonal influences in bone remodeling and bone mass. Estrogen deficiency after the menopause is one of the leading causes of osteoporosis, and currently estrogen replacement is the first line management for postmenopausal osteoporosis. The bone loss associated with estrogen deficiency is due to increased bone resorption and a relative deficiency in bone formation. Although estrogen is thought to prevent bone loss mainly by suppressing bone resorption *(1,2)*, there is also recent evidence to suggest that estrogen may exert an anabolic effect in bone in humans *(3,4)*. Estrogen receptors (ER) are present in osteoblasts *(5)*, and oestradiol has been shown to increase type I collagen and alkaline phosphatase production by osteoblasts in vitro *(6)*. Animal models have proved invaluable in the study of the role of estrogen in bone metabolism. There is a large body of evidence that the cancellous bone of the secondary spongiosa of adult female rats has characteristics similar to that of humans. The secondary spongiosa undergoes bone remodeling and becomes osteopenic with disuse and estrogen deficiency. Ovariectomy induces increased bone resorption that in turn entrains increased bone formation. Resorption, formation and bone loss are all suppressed by estrogen, calcitonin, and bisphosphonates. Preliminary in vivo studies in the evaluation of new compounds directed at the estrogen receptor are generally performed in rats. For this reason, this chapter concentrates on ovariectomy and estrogen replacement in this species. With the development of transgenic and gene deletion animals, there is an increased demand for similar experiments in mice. While the bones of these animals behave in a similar manner to rats in many respects, its marked anabolic response to estrogen replacement is unusual and controversial *(7,8)*.

2. Materials

1. Estrogen: Prepare estradiol (Sigma) by sonication in a vehicle of 5% v/v benzyl (Sigma) and 95% v/v corn oil (Sigma). This may be stored for up to 4 wk at room temperature away from light.
2. Estrogen slow release pellets: 1µg and 10µg, Innovative Research of America, FL.
3. Dissecting Instruments. Selection of scissors, scalpels, and forceps.
4. Silk sutures (Ethicon).
5. Metal clips for wound closure (Brookwick ward, Fife, Scotland).
6. Mayer's hematoxylin and eosin: For staining vaginal smears (BDH, Poole).
7. Ethanol series: 25%, 50%, 75%, 90%, 100%. To dehydrate vaginal smear specimens.
8. Xylene. To dehydrate vaginal smear specimens.
9. DePeX mounting medium: For mounting vaginal smear specimens (BDH, Poole).

3. Methods

3.1. Ovariectomy

1. Anesthetize the animal with nitrous oxide and oxygen at 1 L/min and 2 L/min respectively and 2% v/v halothane (Sigma).
2. In rats, the dorsal aspect of each animal is first shaved. In mice, the fur of the dorsal surface is wetted by ethanol, and then gently parted to create a center line for the skin incision.
3. Make a midline dorsal incision (approx 2 cm in the rat) using a pair of sharp scissors. The subcutaneous connective tissue on either side can then be freed from underlying muscle by blunt dissection using a sterile pair of blunt artery forceps. A smaller incision (<1 cm in the rat) in the muscle layer on either side of this is then made to allow entry into the peritoneal cavity.
4. The ovaries can be identified in a fat pad adjacent to the perinephric region and should be excised as a whole. In mice, ovaries are sometimes visible even without the muscle incision because the muscle layer is quite thin. Removal of the fimbrial end of the fallopian tube may be done to ensure completeness of the ovariectomy.
5. Suture the muscle incision with silk, and close the skin incision with a metal clip.
6. Keep the animals under observation until they have recovered from the anesthetic and regained consciousness (*see* **Note 1**).
7. The same procedures are followed for sham operations except that the ovaries are identified but not removed.

3.2. Estrogen Injections

Prepare the estrogen as a stock solution so that the animal does not receive more than 1 mL/kg body weight to achieve the required amount of compound. The injections may be given daily, once, twice, or three times per week depending on the experimental design (*see* **Note 2**). For experiments that involve daily injections over prolonged periods, the injection sites should be rotated.

3.3. Estrogen Implants

Estrogen replacement and vehicle may also be given subcutaneously as slow release pellets. The pharmokinetics of the various forms of exogenous replacements are likely to be different, and this may need to be considered in the experimental design. They have not been studied in detail, however. (*see* **Note 2**).

3.4. Ovarian Transplantation

These may be done as renal capsule ovarian transplants or subcutaneous transplants *(9,10)* (*see* **Note 3**).

1. For renal ovarian transplants, adult (13 wk old) donor rats should be anesthetized and the ovaries exposed as described in **Subheading 3.1.**
2. Reflect the ovary onto a piece of sterile gauze and under a dissecting microscope, slit the ovarian bursa, and cut the hilum to release the ovary.
3. The recipient ovariectomized host animals should be simultaneously anesthetized.
4. For a renal capsule transplant, the left kidney is exposed through a dorsal skin and muscle incision and a small slit made in the renal capsule covering the kidney.
5. The donor ovary is cut into three segments to facilitate insertion and these are gently place these under the renal capsule and sutured in place using fine silk.
6. For subcutaneous transplantation, the ovarian segments are inserted into a subcutaneous pocket made using a skin incision followed by blunt dissection in the mid-scapular region.
7. When the transplant is complete, the skin incision should be closed with a metal clip.

3.5. Age of Animals and Duration of Follow-Up

This varies according to the study design and question being asked. However studies of ovariectomy induced bone loss in rats are typically carried out in 12–16-wk-old adult females, with follow-up for 6 wk, by which time there will have been significant bone loss which can be detected by histomorphometry (*see* the chapter by Vedi and Compston, *this volume*) or bone densitometry (*see* the chapter by Gasser, *this volume*). Experiments in mice are usually performed in 8–12-wk-old females with follow up for 3 wk.

3.6. Checking Efficacy of Ovarian Transplants Using Vaginal Smears

This is a simple and cheap method for testing the efficacy of ovarian transplants, and can be used in addition to monitoring estrogen and progesterone levels.

1. Moisten a small sterile cotton wool bud with normal saline solution, insert it into the vagina, and gently scrape the vaginal wall to obtain some cells.
2. Smear the cells onto a glass slide, air-dry, and fix with 70% ethanol.
3. Stain the cells for 5 min in Mayer's hematoxylin.
4. Wash in running water, and counterstain for 2 min in eosin. Rinse in running water.

Table 1
The Four stages of the Rat Estrous Cycle, Their Duration, and Associated Changes in Vaginal Cytology

Stage of cycle	Approximate duration (h)	Cytology		
		Epithelial cells	Cornified epithelial cells	Leukocytes
Pro-estrous	12–18	+++	+	±
Estrous	10–20	-	+++	-
Met-estrous	12	+	+	++
Di-estrous	48	+	-	+++

- None; ± occasional; + few; ++ many; +++ abundant. The laboratory rat has a regular estrous cycle of approx 4–5 d duration. The cycle is divided into four distinct stages based on microscopic examination of cell morphology of the vaginal smear.

5. Dehydrate the slides through graded ethanols (in the order of 25%, 50%, 75%, 90%, and 100%), for 5 min each.
6. Dip the slides in xylene and mount in DePeX.
7. Examine the slides microscopically for the presence of leucocytes, epithelial cells, and cornified epithelium. The four stages of the estrous cycle can be recognized by results of microscopic examination of the vaginal smear (**Table 1**).

4. Notes

1. The animals should be mobile and feed freely within 30 min.
2. The pharmacokinetics of a single subcutaneous injection of 40 µg/kg estradiol is such that peak serum levels are achieved after 2 h and the half-life is 8 h. Serum estrogen returns to near basal levels by 24 h after the injection *(11)*. The usual replacement dose of estradiol for rats is 5 µg/kg/d. Although this restores serum estradiol levels to those seen in intact cycling animals, and suppresses bone loss, the uterus weight tends to be lower than in normal animals, indicating that injections do not replicate the normal physiological state.
3. Both methods of ovarian transplantation are fully efficacious in restoring estrogen levels to that of sham-operated animals, but renal capsule ovarian transplantation is slightly more successful in restoring ovarian function if progesterone levels and number of normal oestrous cycles are also considered. This is due possibly to increased vascular supply associated with the renal capsule. For most bone studies, both methods are equivalent, as progesterone does not appear to play a major role in bone metabolism.

References

1. Vedi, S. and Compston, J. E. (1996) The effects of long-term hormone replacement therapy on bone remodeling in postmenopausal women. *Bone* **19**, 535–539.
2. Steiniche, T., Hasling, C., Charles, P., Eriksen, E. F., Mosekilde, L., and Melsen, F. (1989) A randomized study on the effects of estrogen/gestagen or high dose

oral calcium on trabecular bone remodeling in postmenopausal osteoporosis. *Bone* **10**, 313–320.

3. Khastgir, G., Studd, J., Holland, N., Alaghband-Zadeh, J., Fox, S., and Chow, J. (2001) Anabolic effect of estrogen replacement on bone in postmenopausal women with osteoporosis: histomorphometric evidence in a longitudinal study. *J. Clin. Endocrinol. Metab*. **86**, 289–295.

4. Vedi, S., Purdie, D. W., Ballard, P., Board, S., Cooper, A. C., and Compston, J. E. (1999) Bone remodeling and structure in postmenopausal women treated with long-term, high-dose estrogen therapy. *Osteoporosis Int*. **10**, 52–58.

5. Komm, B. S., Terpening, C. M., Benz, D. J., et al. (1988) Estrogenic binding, receptor mRNA, and biologic response in osteoblast-like osteosarcoma cells. *Science* **241**, 81–84.

6. Ernst, M., Heath, J. K., and Rodan, G. A. (1989) Estradiol effects on proliferation, messenger ribonucleic acid for collagen and insulin-like growth factor-I, and parathyroid hormone-stimulated adenylate cyclase activity in osteoblastic cells from calvariae and long bones. *Endocrinolog* **125**, 825–833.

7. Samuels, A., Perry, M. J., and Tobias, J. H. (1999) High-dose estrogen induces medullary bone formation in female mice. *J. Bone Miner. Res*. **14**, 178–186.

8. Turner, R. T. (1999) Mice, estrogen and postmenopausal osteoporosis. *J. Bone Miner. Res*. **14**, 187–191.

9. Parkes, A. S. (1956) Survival time of ovarian homografts in two strains of rats. *J. Endocrinol*. **13**, 201–210.

10. Felicio, L. S., Nelson, J. F., Gosden, R. G., and Finch, C. E. (1983) Restoration of ovulatory cycles by young ovarian grafts in aging mice: potentiation by long-term ovariectomy decreases with age. *Proc. Natl. Acad. Sci. USA* **80**, 6076–6080.

11. Jagger, C. J., Chow, J. W. M., and Chambers, T. J. (1996) Estrogen suppresses activation but enhances formation phase of osteogenic response to mechanical stimulation in rat bone. *J. Clin. Invest*. **98**, 2351–2357.

27

Mechanical Testing of Bone Ex Vivo

Richard M. Aspden

1. Introduction

The primary function of bone is to form the skeleton, which provides support for the body and protection for vital organs. These are primarily mechanical functions. To fulfil these, the bone matrix has to have the right combination of stiffness and strength to enable it to withstand the forces imposed upon it. These forces may be repetitive and moderate, such as those generated during walking, or high and transient, such as inflicted by a blow on the head. The structure and composition of bone can adapt over time to try match the mechanical properties of the bone to the prevailing demands being placed on it. How to measure some of these mechanical properties is the aim of this chapter.

There are two types of bone that are considered in this chapter: cortical, or dense, bone and cancellous, or trabecular, bone. Cortical bone is a solid, compact material that forms the diaphyses of long bones, and a shell around the metaphyses and the vertebrae. Cancellous bone has an open, porous structure comprising rods or plates. Hence it is less dense than cortical bone and also less stiff and strong. It makes up the center of the vertebrae and the metaphyses. However, the two materials in combination form structures that are strong and light and their properties *in situ* may differ considerably from those measured from tests on isolated samples *(1,2)*. In cancellous bone the distinction between material and structure is not always easy to define, and treating it as a cellular material has met with a considerable degree of success *(3,4)*.

Although conceptually relatively simple, the mechanical properties of these tissues are not easy to measure. If only a comparison is required between equivalent sites in different patient groups then careful use of the same technique on all samples will provide consistent relative values. If, however, absolute values are required then great care must be taken as bone is not isotropic or

homogeneous and its properties depend on the rate at which it is deformed. In addition, sample preparation can be difficult. Unlike engineering materials, which can be cut and machined to predetermined sizes for testing and for which there are officially recognized standards, bone samples are generally limited in size and shape by the site from which they are taken. The size of the sample being tested may affect the measurements being made.

This chapter describes methods of preparation and testing that can be applied to cortical and cancellous bone. Differences in approach that are required because of the different natures of the materials are noted. The descriptions are restricted to methods that can reasonably easily be applied by anyone having access to a materials testing machine. Researchers requiring more sophisticated techniques or more details of variations are referred to the recent book by Stephen Cowin *(5)* and to the original papers. Finally, a method is presented for testing whole bones, such as may be required to measure bone properties in genetically modified mice. These are so small that preparing and testing isolated samples of cortical or cancellous bone becomes very difficult and tests are generally performed on intact bones.

2. Materials

1. Phosphate-buffered saline (PBS) (Gibco): Used to keep specimens moist during preparation and testing (*see* **Note 1**).
2. Hacksaw: For cutting large bone samples to manageable sized pieces prior to precision cutting.
3. Mineralogical saw fitted with either a diamond or an aluminum oxide cutoff wheel. To precision cut bone samples (*see* **Note 2**).
4. Lathe or Milling machine: To mill bone samples to desired shape.
5. Coring bits, 5-mm and 9-mm internal diameter and break-off tools: Custom made by Bolton Surgical Ltd. (Sheffield, UK).
6. Materials testing machine: For mechanical testing of samples.
7. Software for calculation of biomechanical variables: Origin (OriginLab Corp., Northampton, MA, USA).

3. Methods

3.1. General Considerations for the Preparation of Bone Samples

All human tissue must be handled with due regard to health and safety because of the risk of infection. In addition to gloves and laboratory coat, a mask and eye shield are required because there is a risk of aerosols being generated during cutting, drilling, or machining. Samples must be kept moist at all times during the preparation procedure. Bones must be dissected free of soft tissues, taking care not to create notches in the bone that is going to be tested, as this will weaken it. General methods for the preparation of samples for testing are described in the following sections.

Fig. 1. Tensile test specimens are traditionally produced with a waist to ensure that failure consistently occurs in the center and not near the grips.

3.2. Preparing Prisms of Cortical Bone

1. Cut the bone into manageable sized pieces using a hacksaw or a junior hacksaw.
2. Precision cut the bone samples to the desired size using a mineralogical saw rotating at 600–800 rpm. For compression and bending tests the samples should be cut to give rectangular parallelepiped shaped specimens. For tensile testing, the specimens should be milled to give a waisted configuration (**Fig. 1**). If the samples are large enough, they should have cylindrical symmetry, but for thin specimens the waisting can be done in two dimensions. This is to ensure that fracture occurs consistently in the central part of the specimen away from the gripped ends. Water should be run over the sample at all times during sawing and machining.

3.3. Preparing Cancellous Bone Cores

1. Obtain the bone core by drilling through the bone sample with a coring bit (**Fig. 2**). To remove the core it either has to be drilled right through a piece of bone or broken off the underlying bone. Providing the core is not too deep, this can be done using the break-off tool shown in **Fig. 2**. This is made to the same specification as the coring bit except it does not require teeth and half of its circumference has been removed. This is inserted in place of the coring bit and, by levering on the end of it, the base of the core may be broken from the underlying tissue (*see* **Note 3**).
2. Trim the ends of the cores plane and parallel using a mineralogical saw. If the cores have been obtained from the articular surface of joints, they will have cartilage and subchondral bone at one end that needs to be removed using the saw.

Fig. 2. Coring bits and matching "break-off" devices. Unless cores can be drilled right through a piece of bone they will need to be removed from the underlying bone to which they are attached. Inserting the break-off device after drilling the core and levering it sideways generally successfully snaps the core at its base, after which it may be removed using forceps.

3.4. General Considerations for Mechanical Testing

1. Before testing it is important to decide what parameters are going to be measured. Most testing machines apply a deformation to a sample, which normally increases linearly with time. This deformation is commonly referred to as displacement. The operator can choose the rate at which the displacement occurs and the properties measured will depend on this rate as bone is viscoelastic. Choosing when to stop the test is also important depending on what is to be done next with the specimen. In tension or bending the machine can be set to stop automatically on fracture, as the load drops rapidly at this point. In compression, failure is not so easy to determine and various methods can be used. The applied load and displacement are recorded throughout the test. The load–displacement curve represents the extrinsic properties of the specimen under test and is therefore used to measure the properties of whole bones (**Fig. 3A**). These properties are important for understanding why bones fracture. For prepared samples of known dimensions what is commonly required are the intrinsic properties of the bone material itself. To obtain these, the load is divided by the cross-sectional area of the specimen to produce the stress, and the displacement is divided by the original length to give the strain. The stress–strain curve is then very similar to the load–displacement curve but refers now to the material not the structure (**Fig. 3B**).
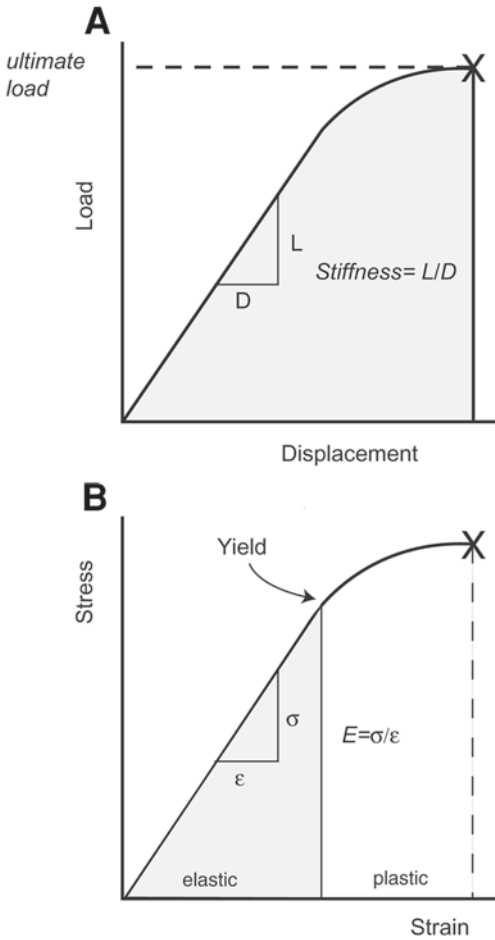
Fig. 3. A load–displacement curve **(a)** measures the extrinsic properties of a specimen, for example, an individual bone. The main parameters are stiffness, work to failure *(shaded)* and ultimate load and displacement. The stress–strain curve **(b)** is similar but, because it is normalized for the sample dimensions, measures the intrinsic properties of the material being tested. These are the elastic or Young's modulus (E), the yield stress and strain, the ultimate stress and strain, and the energies to yield and failure.

3.5. Repeating Tests on the Same Specimens

1. It has been found that if a test is repeated several times on the same specimen within a short period then the resulting load–displacement plots do not immediately coincide but appear to converge toward a stable curve. Because of this, many investigators apply up to five or six loading cycles to a specimen, often at a reduced load, before performing the actual test, a process called precondition-

ing. This is a point of some contention because it is not understood what happens during this process. It can be argued that what is finally being measured is not the natural property of the specimen but one that has somehow been modified by a series of cyclically applied loads. Does repeatability necessarily imply accuracy? We always apply a single test to a specimen.

3.6. Types of Mechanical Testing

There are four main types of test: tension, compression, bending, and torsion.

1. Tension and compression testing: These are most commonly done to measure the intrinsic properties of bone matrix. These tests use machined samples of known dimensions. Tension is generally used for cortical bone and compression is more common for cancellous bone because of the difficulty obtaining and mounting suitably sized specimens for tensile testing. Bending and torsion can be applied in this way but the interpretation of the results is more difficult. They are probably more commonly applied to whole bones. In this section, descriptions are given of tension and compression tests for machined specimens.
2. Bending: This is most commonly applied to whole long bones from rodents because of the difficulties of machining tensile or compressive specimens from such small bones. It is best for measuring extrinsic properties of the whole bone and therefore is very useful for studies comparing the effects of different drug therapies or genetic modifications. It is not easy to estimate intrinsic properties from this test for a variety of reasons, mainly related to the size and shape of the bone. More details are given by Turner and Burr *(8)*. There are two bending configurations, called three-point and four-point loading (**Fig. 4**). In three-point loading there is a significant shear stress generated at the midpoint of the beam. For this reason four-point loading is sometimes preferred because in a uniform specimen this is minimized and a pure bending moment is applied. However, in whole bones, the nonuniform cross section means that these assumptions do not apply. In addition, it is difficult to load all four points identically and test results will be subject to large errors. Three-point and four-point loading jigs can be bought or made to fit most materials testing machines. It is important to be able to adjust the span, the distance between the lower supports. For testing whole bones this means that the span may be matched to the length of the bone as this may differ between specimens. For machined specimens, testing at different spans enables extrapolation to be made for an infinite span *(9)*.

3.7. Tension Testing

1. Prepare the specimen as described in **Subheading 3.2.** or **3.3.** ensuring that it is at least 15–25 mm long and 5 mm across (*see* **Note 4**).
2. Keep the sample moist by lightly wrapping in cling film or moist tissue or gauze.
3. Fix the specimen in the testing machine. Most testing machines have grips for holding specimens in tension. These can be tightened on to the broader ends of the specimen and are adequate for testing cortical bone (*see* **Note 5**). If you are
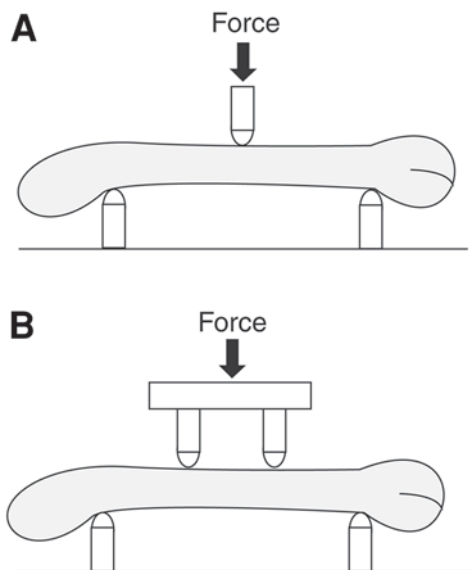
Fig. 4. Whole bones may be tested in either (**A**) three-point or (**B**) four-point load-ing configuration. Force is applied through the upper plate and the resulting displace-ment recorded. The span is the distance between the lower supports.

testing cancellous bone cores, set the ends into cups using dental or bone cement and the cups then held in the testing machine grips.

4. Set up the machine to apply the desired strain rate, and program in any predeter-mined limits on load, displacement, or fracture detection, and the rate of data recording. It is advisable to set the machine to stop as soon as fracture occurs because at this point the load falls to zero.
5. Start the testing machine.
6. After the test, transfer data from the instrument to a spreadsheet for further analy-sis if the instrument does not already have appropriate software.

3.8. Analyzing Data from Tension Testing

1. If intrinsic properties are required, and not already calculated, convert load val-ues to stress by dividing by the original cross-sectional area. (No account is taken of changes in the cross-sectional area which will occur during the test.)
2. Convert displacement values to strains by dividing by the unstretched distance between the points of attachment or reference marks of the displacement trans-ducer (*see* **Note 5**).
3. Plot stress as a function of strain. The elastic, or Young's, modulus, yield strength and strain, ultimate strength and strain, and energies to yield and failure may then be calculated.

4. Calculate the elastic modulus by estimating the gradient of the linear part of the curve. For linear relationships this is often calculated by the instrument software. If not, this can found crudely by hand calculation, better by fitting a straight line to the data or for nonlinear relationships, by differentiating the curve using software such as Origin.

5. Calculate the yield, by estimating when the elastic modulus starts to reduce. This is not always easy to define, but one way is to construct a line parallel with the linear part of the curve but offset along the strain axis by a small amount. The point at which this intersects the curve is defined as the offset yield point and the stress and strain at this point are the yield stress and strain.

6. Calculate the failure stress and strain from the point at which fracture occurs.

7. Integrate the curve, to either the yield point or failure point, to find the area beneath to estimate the energy needed to produce yield or failure, respectively, per unit volume of material. The energy to failure is often referred to as the modulus of toughness.

3.9. Compression Testing

1. Prepare a cylinder or rectangular parallelepiped of bone as described in **Subheading 3.2.** Try to ensure that the length of the specimen is about twice the diameter. (*see* **Note 6**).

2. Place the sample on the lower anvil of the testing machine. As in the case of tensile testing, a universal joint must be used in the loading path (*see* **Note 4**). Alternatively, a steel plate with small indentation containing a ball bearing between the specimen and the upper loading anvil can be used; this allows for any slight nonparallelism between the two faces.

3. Accurate measurements of strain requires the use of a displacement transducer, as for tension, but for most comparative studies the displacement of the crosshead is probably adequate (*see* **Note 5**).

4. Lower the crosshead of the machine until it is just in contact with the specimen.

5. Set the strain rate and any predetermined load or displacement limits as before.

6. Start the test and stop the test when the chosen criterion is met (*see* **Note 7**).

7. Calculate stress and strain and plot stress as a function of strain as described in the preceding. Where testing is done between two anvils there is often a region near the origin where the slope of the curve starts small and increases rapidly before becoming approx linear, resulting in a J-shaped curve. This toe region is an artefact of the method and is commonly found in this sort of testing both of natural and synthetic polymeric materials. Because it can be difficult to determine a straight portion of the curve or to fit a straight line to it, it is best to differentiate the curve to find the modulus as a function of strain. The elastic modulus can then be taken to be the peak value of this curve.

8. The yield stress may be defined as the stress at which the modulus starts to decrease. We used a reduction of 3% from its peak value to provide a defined reference point *(7)*.

9. Energy to yield is found by integration of the area under the stress–strain curve up to the yield stress. Strains are ill defined in this testing protocol because of the

toe region. Embedding the ends of longer specimens and gripping as for a tensile test can eliminate this problem. Failure cannot usually be defined in the same way as for tensile testing because progressive crushing of the material often occurs rather than a fracture.

3.10. Bending

Set the bending jig in the materials testing machine.

1. Adjust the spacing of the lower supports to be as close to the ends of the diaphysis as possible.
2. Lower the crosshead of the instrument so that the upper loading anvil is just in contact with the bone surface.
3. Set the displacement rate, any load or displacement limits, and the data collection rate.
4. Start the test.
5. The machine can be set to stop as soon as fracture occurs because at this point the load falls very rapidly, although not always to zero.
6. Load is plotted as a function of displacement and the stiffness, yield load and failure load, and energy to fracture may be found using the same criteria as used for stress–strain curves in the tensile and compression tests (*see* **Note 8**).

4. Notes

1. Storage of samples: Samples should be kept moist with phosphate-buffered saline (PBS) prior to mechanical testing; formalin and other fixatives must never be used as this affects the mechanical properties. If the samples are not being tested immediately (within 2–4 h), the specimens can be stored frozen at -20°C. They must be wrapped in tissue or gauze dampened with PBS and vacuum sealed into plastic freezer bags. A vacuum bag sealer can be obtained for this purpose.
2. Instruments for precision cutting: We use an Accutom 2 (Struers Ltd, Glasgow) and a 125-mm aluminum oxide wheel, but the most common saw cited in the bone literature is the Isomet (Buehler, Lake Bluff, IL, USA). Whatever saw is used, faster wheel speeds and slower specimen feed results in a better surface finish. Where samples of a predetermined size are required, it is important to know how much of the sample will be lost during the cutting procedure. Any saw will remove an amount of material corresponding to the width of the blade, termed the kerf. For an aluminum oxide wheel the kerf is about 0.5 mm compared with about 0.3 mm for a diamond blade. When the kerf is known it is possible to obtain samples of the desired size by adjusting the cutting position appropriately. It is possible to cut specimens 100–150 µm thick using an aluminum oxide wheel. Care must be taken to keep specimen feed speeds, that is, the rate at which the specimen is moved past the cutting wheel, fairly low, as aluminum oxide wheels are brittle and shatter easily and diamond wheels are thin and are easily bent. However, aluminum oxide wheels cost about £10 ($15), in contrast to about £200–£300 ($200–300) for a diamond cutter, depending on size.
3. Obtaining bone cores: When coring right through a block of tissue, the sample is commonly left in the coring bit. Occasionally this can happen, too, if a core snaps

off while being drilled. To be able to remove this core we have had the bits made with a hole from end to end so that a close fitting plunger may be inserted to push out the core. However, this can damage the top of the core if it is tightly wedged into the drill bit. For this reason we prefer not to drill right through and to use the break-off tool to snap the core from its base after the coring bit has been removed.

4. Tension testing: The specimen must be large enough to get consistent results; Keaveny's methods start with a specimen 40 mm long, which highlights the difficulties that may sometimes be encountered obtaining suitable specimens *(6)*. If the grips are not exactly in line or the specimen is not precisely machined then applying a tensile load will also result in a degree of bending. This will add uncertainty to the test data which will be different for each specimen and make accurate comparison between specimens impossible. A universal joint must be placed in the path of the load to ensure that only tensile forces are transmitted to the specimen. These are available from the instrument manufacturers.

5. Measuring strain during tension tests: An estimate of the strain can be calculated from the displacement of the crosshead recorded by the machine. However, for accurate studies a strain gauge or displacement transducer must be applied to the waisted part of the specimen. This can be done using either a clip-on device or video recording methods.

6. Shape of samples for compression testing: It is desirable for the length of the specimen to be twice the diameter. It is possible to conduct tests on samples in which the dimensions are roughly equal without too much of a problem and in many cases, this may be unavoidable due to anatomical considerations.

7. Setting limits for compression testing: Care needs to be taken when setting applied loads and limits into certain testing machines. Conventionally, engineers use positive numbers to denote tensile loads and negative numbers for compressive loads. The most commonly used test is tension and here there is generally no problem, as everything is positive. However, setting a limit for a compressive load often needs to include a negative sign. It sounds trivial but is easily overlooked and many students have stood watching the machine crush their specimen wondering why the machine has not stopped! Only after hitting the emergency stop button have they realized they omitted the negative sign in front of the load limit they had set. There is often no clear end point for failure in compression, unlike for tension, and determining when to stop the test has to be decided beforehand. In our studies we have decided that any reduction in stiffness—that is a reduction in the slope of the load–displacement curve—is a sign of the beginning of failure. As we usually wish to do further analysis on the specimens and minimize the damage caused by the test, we watch the load–displacement curve (which is plotted on the computer monitor during the test) carefully during the test, and stop the test as soon as it becomes obvious that the slope of the curve is decreasing.

8. Calculating intrinsic properties of bone from bending tests: Equations have been derived to calculate intrinsic properties from these data but are fraught with diffi-

culties when testing whole bones because of the asymmetric cross section of the bone. It is not recommended to use these without expert advice.

References

1. Aspden, R. M. (1990) Constraining the lateral dimensions of uniaxially loaded materials increases the calculated strength and stiffness: application to muscle and bone. *J. Mater. Sci. Mater. Med.* **1**, 100–104.
2. Bryce, R., Aspden, R. M., and Wytch, R. (1995) Stiffening effects of cortical bone on vertebral cancellous bone *in situ. Spine* **20**, 999–1003.
3. Gibson, L. J. (1985) The mechanical behaviour of cancellous bone. *J. Biomech.* **18**, 317–328.
4. Gibson, L. J. and Ashby, M. F. (1988) *Cellular Solids*. Pergamon Press, Oxford.
5. Cowin, S .C. (2001) *Bone Mechanics Handbook*. CRC Press, Boca Raton, FL.
6. Keaveny, T. M., Guo, X. E., Wachtel, E. F., McMahon, T. A., and Hayes, W. C. (1994) Trabecular bone exhibits fully linear elastic behavior and yields at low strains. *J. Biomech.* **27**, 1127–1136.
7. Li, B. and Aspden, R. M. (1997) Composition and mechanical properties of cancellous bone from the femoral head of patients with osteoporosis or osteoarthritis. *J. Bone Miner. Res.* **12**, 641–651.
8. Turner, C. H. and Burr, D. B. (2001) Experimental techniques for bone mechanics, in *Bone Mechanics Handbook* (Cowin, S. C., ed.), CRC Press, Boca Raton, FL, pp. 7-1–7-35.
9. Spatz, H. C., Oleary, E. J., and Vincent, J. F. V. (1996) Young's moduli and shear moduli in cortical bone. *Proc. R. Soc.* **B263**, 287–294.

28

Bone Cell Responses to Fluid Flow

Hazel Y. Stevens and John A. Frangos

1. Introduction

The relationship between mechanical loading and bone formation has long been documented *(1)*. However, the identity of the transductory mechanism, conveying loading signals to bone cells, remains elusive. Mechanical strain, interstitial fluid flow, and streaming potentials are all likely candidates but the separate investigation of these factors has proven difficult. Studies in our laboratory and others have shown fluid shear stress to be influential in bone modeling and remodeling *(2–4)*. The characteristics of the flow causing this bone formation and probable inhibition of resorption have been more difficult to determine.

In the absence of loading, interstitial fluid, originating from leaky venous sinusoids in the intramedullary cavity, is driven radially outward through intracortical pores, the direction being dictated by a transmural pressure gradient between the endosteal vasculature and the lymphatic drainage at the periosteal surface *(5)*. Load-induced compression or bending of bone generates localized pressure gradients, which cause rapid fluid flow from areas of compression to areas where tension builds. After a loading event there is an associated relaxation phase, hence a pulsatile flow ensues. Changes in interstitial flow may be responsible for the induction of bone formation in regions of elevated intraosseous pressure, for example, hypertension whereas normal pressures may serve to maintain normal bone architecture *(6)*.

The attainment of high fluid shear stresses within a short space of time, that is, temporal gradients in shear (TGS) are typically seen in high-impact exercise such as running and jumping (high amplitude but fairly infrequent strains) whereas posture maintenance involves a large number and high frequency of low-amplitude strains. Ramped flow is typified by the attainment of high shear

stress over a longer period of time. Given that impulse flow contains only tem-poral gradients and ramped flow involves only steady shear components with negligible temporal gradients, it is possible to subject cells to these different flow profiles and compare their responses. McAllister and Frangos *(7)* identi-fied two different mechanochemical transduction pathways in osteoblasts, depending on whether the stimulus was rapid onset of shear or steady shear. Preliminary data in our laboratory suggest that UMR-106 osteoblasts respond to transients in flow with increased cell proliferation and ERK phosphoryla-tion yet ramped flow appears inhibitory to ERK activation *(8)*.

This concurs with our studies on human endothelial cells *(9)*. We have hypothesized that transients in shear mediate bone formation and deposi-tion by activating mitogenic factors whereas steady flow provides suffi-cient nitric oxide (NO) release to inhibit resorptive processes in localized bone remodeling. All bone cell types respond directly or indirectly to inter-stitial fluid flow. The signalling moieties include: inositol triphosphate (IP3; *[10]*; cyclic adenosine monophosphate (cAMP; *[2]*); transforming growth factor-β (TGF-β; *[11]*); cellular fos proto-oncogene (c-fos *[12]*) and intracellular calcium in osteoblasts *(13,14)*; prostaglandin E_2 (PGE_2) and prostacyclin (PGI_2) in osteoblasts and osteocytes *(15)* and nitric oxide (NO) in osteoblasts *(3,16)* and osteocytes *(17)*. Preosteoclast-like cells are stimu-lated by fluid shear stress to release autocrine factors such as NO and PGE_2 *(18)*, which can regulate localized resorption in vivo *(19)*. Many of these responses are G-protein-dependent *(20)* with the exception of steady shear production of NO *(7)* (*see* **Fig. 1**).

The study of flow in vitro is complicated by the use of a range of different substrates, flow chambers, rates, characteristics of flow, as well as differences in preparation of cells (serum starvation, nutrients, confluency, etc). Although primary cells from mammalian donors are physiologically the most relevant cell types, they are difficult to isolate and characterize, therefore use of cell lines (e.g., UMR-106) has its place in such studies. In our laboratory, flow systems have been developed to test the responses of anchorage-dependent cells to a range of steady and pulsatile shear stresses under well-defined condi-tions. This chapter describes methods for using cultured cells to study effects of fluid flow in bone.

2. Materials
2.1. Tissue Culture Medium (UMR-106), Cell Line, and Substrate

1. Dulbecco's modified Eagle's minimal essential medium (DMEM) with phenol red, ATP-free (Gibco, Grand Island, NY), supplemented to a final concentration of 10% with heat-inactivated fetal calf serum (FCS), 2 mmol/L of L-glutamine, 50 U/mL of penicillin, and 50 μg/mL of streptomycin for the maintenance of the UMR-106 rat osteosarcoma cell line.

Fig. 1. Proposed scheme for G-protein signaling in the osteoblast. Fluid shear stress causes an increase in membrane fluidity leading to direct activation of G-proteins. NO production is G-protein and calcium insensitive under steady shear and is pertussis toxin (PTx)-insensitive G-protein mediated with rapid onset of shear (TGS). Prostaglandin E_2 release is G-protein (partial PTx sensitive) mediated for both types of shear. α,β,γ, subunits of G-protein; Cav, caveolin; DAG, diacylglycerol; eNOS, endothelial nitric oxide synthase; ERK, extracellular signal regulated kinase; GDP, guanosine diphosphate; GTP, guanosine triphosphate; IP_3, inositol triphosphate; MEK, ERK kinase; PGE_2, prostaglandin E_2; PKC, protein kinase C; PLA_2, phospholipase A_2; PLC, phospholipase C.

2. Serum-free DMEM supplemented with 0.1% bovine serum albumin (BSA) Fraction V cell culture tested (Sigma) and stored at 4°C; L-glutamine; penicillin; and streptomycin for the starving of monolayers before and during the flow experiment.
3. Hanks' balanced salt solution (HBSS) without calcium and magnesium (Gibco) for the washing of cell monolayers.
4. Trypsin–EDTA (0.25% trypsin, 1 m*M* tetrasodiumethylenediaminetetraacetic acid (EDTA.4Na) for the detachment of cells from tissue culture flasks.
5. Fibronectin-like engineered protein polymer (1 mL of diluent and 1 mg of powder combine to give a stock of 1 mg/mL; Sigma) stored at room temperature (RT).
6. UMR-106 rat osteosarcoma osteoblast cell line (cat. no. CRL-1661, American Type Culture Collection [ATCC], Rockville, MD).

2.2. Tissue Culture Medium (Primary Calvarial Osteoblast-Like Cells)

1. M199 (Modified medium 199, with phenol red; Gibco) supplemented with 10% FCS, 1% penicillin–streptomycin, and 1% L-glutamine for the isolation and maintenance of rat calvarial osteoblasts (complete medium).
2. M199, ATP-free (custom made from Gibco), serum-free for the incubation of calvaria and the shear experiments.
3. Fibronectin-like engineered polymer (*see* **Subheading 2.1.**, **item 5**).
4. 300–500-μm Glass chips.
5. Collagenase A (Roche Diagnostics, Berkeley, CA) stock, 1 mg/mL in HBSS stored in aliquots at -20°C.

2.3. Equipment

2.3.1 Flow Chamber Apparatus

The apparatus is shown diagrammatically in **Figs. 2–4**.

1. The flow chamber (Cytodyne.net, La Jolla, CA) is a polycarbonate plate (Rohm and Haas, Philadelphia, PA), custom machine milled with a vacuum channel on one face. Laminar parallel flow is provided in a flow channel formed by a rectangular size 0.020-inch Silastic gasket (Dow Corning, Midland, MI) and a glass slide with adherent cell monolayer. Standard luer female fittings are at fluid inlet/outlet and vacuum ports. Interconnecting tubing (1/8-inch inner diameter) of polytetrafluoroethylene (PTFE, Teflon) (Cole Parmer, Chicago, IL) is fitted with luer male connectors. The relatively inert and gas impermeable tubing prevents water and gas loss and minimizes absorption of metabolites.
2. Syringe pump (pump 44, Harvard Apparatus, Holliston, MA), syringes (100-mL gas-tight borosilicate glass with PTFE [Teflon] plunger and luer lock; Scientific Glass Engineering Inc, Austin, TX and 30-mL glass syringe; Becton Dickinson, Franklin Lakes, NJ).
3. 37°C Air box, with a high-throughput blower to provide heating and a thermostatic regulator.
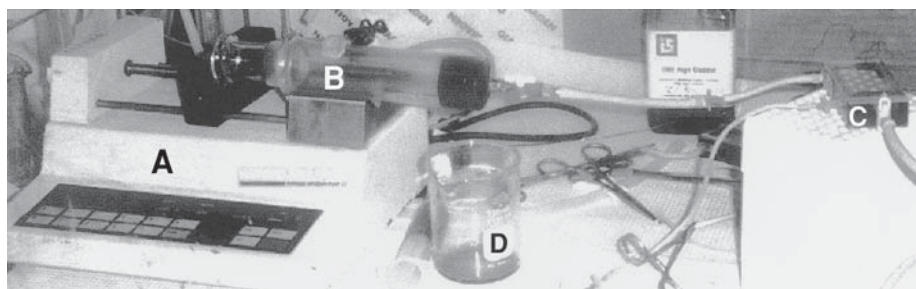
Fig. 2. Flow chamber apparatus for short-term experiments: *A*, computer-controlled syringe pump; *B*, syringe; *C*, flow chamber; and *D*, collector of perfusate.
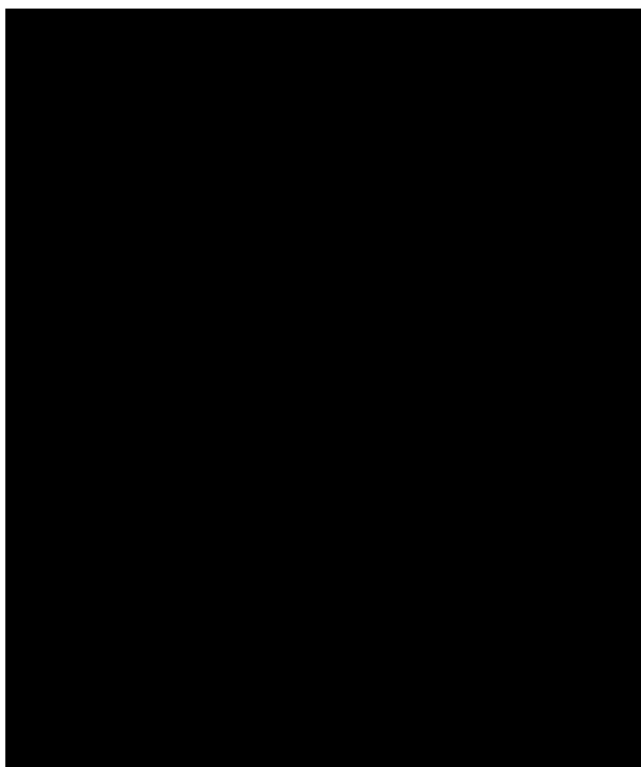

Fig. 3. Parallel plate flow chamber. The polycarbonate plate, the gasket (*G*), and the glass slide (*H*) with the attached cells are held together by a vacuum (*C*), forming a channel of parallel plate geometry. Medium enters at entry port (*A*), through slit (*E*), into the channel, and exits through slit (*F*), and exit port (*B*). Entry port (*A*) also serves as a trap for bubbles, which can be removed through valve (*D*). (From: Frangos, J. A., McIntire, L. V., and Eskin, S. G. (1988) Shear stress induced stimulation of mammalian cell metabolism. *Biotechnol. Bioeng.* **32**, 1053–1060. Copyright ©1988. Reprinted by permission of Wiley-Liss, Inc., a subsidiary of John Wiley & Sons, Inc.)
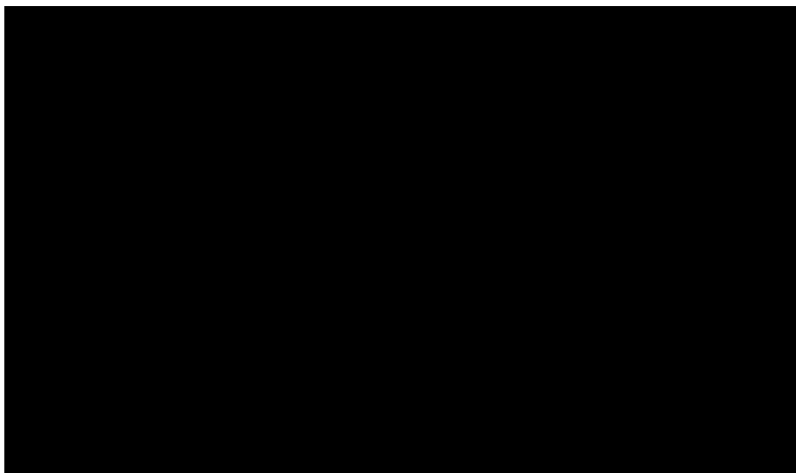
Fig. 4. Pulsatile flow loop. An offset cam **(A)** driven by an electric motor drives syringe plunger **(B)** through one-way check valves **(C)**, forcing flow through chamber **(D)**, recirculating into the reservoir. Media samples may be drawn aseptically from valve **(E)** (Hillsley MS Thesis 1990). (From Hillsley et al., *Calcified Tissue International* 1997; **60**, 48–53, with permission of Springer-Verlag New York, Inc.)

4. 38 × 75 mm Glass microscope slides, thickness 0.90–1.10 mm (Corning Inc, Acton, MA).
5. Offset cam driven by a stepper motor (Anaheim Automation, Anaheim, CA; 23A 108C with smc40x driver/indexer) and syringe.

2.3.2. Glass Reservoir for Fluid Loop

1. One-way check valves (Becton Dickinson).
2. Optional electromagnetic flow probe (Zepeda Instruments, Seattle, WA).

2.3.3. Flow Loop (see **Fig. 5**)

1. Upper and lower glass reservoirs (Cytodyne.net), roller pump (Becton Dickinson). PTFE tubing (0.125-inch outer diameter, Cole Parmer) except for section through roller pump which is silicone (Masterflex, Cole Parmer). Silicone collars join the reservoirs to the manifold and tubing.
3. Overflow glass manifold (19-mm outer diameter, Pyrex, Corning Glass Works, Corning, NY).

2.4. Cell Assays

1. Dextran (2,000,000 mol wt; Sigma).
2. Chemiluminescent flow analyzer, Radical Purger (ASM 03296) and Nitrate Chemical Kit (ASK 14400-01) (Sievers Instruments, Boulder, CO).
3. Bradford protein assay (Bio-Rad, Hercules, CA).

Fig. 5. Drawing of small volume flow loop: (1) upper reservoir, (2) lower reservoir, (3) overflow manifold, (4) filtered humidified 95% air + 5% CO_2 input, (5) gas outlet, (6) flow chamber, (7) gasket, (8) slide with cell monolayer, (9) microscope objective, (10) vacuum, (11) sampling port, (12) roller pump, (13) PFA teflon tubing, (14) constant pressure head, and (15) flow probe. (From: Frangos, J. A., McIntire, L. V., and Eskin, S. G. (1988) Shear stress induced stimulation of mammalian cell metabolism. *Biotechnol. Bioeng.* **32**, 1053–1060. Copyright (c) 1988. Reprinted by permission of Wiley-Liss, Inc., a subsidiary of John Wiley & Sons, Inc.)

4. Aminoguanidine (AG; Alexis Biochemicals, San Diego, CA) and N^G-amino L-arginine (L-NAA; Alexis).
5. Alkaline phosphatase 86-C kit (Sigma).
6. GDPβS, GTPγS (Calbiochem), pertussis toxin (Sigma).

3. Methods

3.1. Preparation of UMR-106 Cells for Flow Experiments

1. Prepare rectangular glass microscope slides (38 × 75 mm) for cell seeding by fibronectin coating. Place autoclaved slides into 100-mm Ø Petri dishes and dilute fibronectin polymer stock to 10 μg/mL with sterile phosphate-buffered saline (PBS; Irvine Scientific, Santa Ana, CA) before using 1 mL to coat each slide. Leave the slides for 5 min at RT before removing the excess, rinsing twice in PBS and leaving the slides to air-dry in the flow hood (class II laminar flow hood) for at least 1 h.

2. Aspirate medium from a 75-cm^2 flask of cells and wash the cells in HBSS. Add 1 mL of trypsin and incubate the flask for approx 10 min at 37°C, after which time the cells should have become detached. Add 9 mL of DMEM containing 10% FCS to the flask in stages and pool the washes. Introduce 20 μL into a hemocytometer to determine cell count and centrifuge the rest at 240g for 5 min.

3. Resuspend the cells in sufficient DMEM with 10% FCS for seeding 0.7 mL of cells onto the slides at 0.8×10^6 cells/mL and let them grow to confluence for 2–3 d in a humidified incubator at 5% CO$_2$–95% air at 37°C. Before exposure to shear, place a negative template of the gasket underneath each Petri dish and scrape the cells from this region to avoid the inclusion of cells squashed by the gasket. Serum starve the confluent cell monolayers for 24 h in 0.1% BSA–DMEM before subjecting them to flow. Dissolve the BSA powder in medium and then sterilize by passing it through a 0.2-μm filter.

3.2. Preparation of Newborn Rat Calvarial Osteoblast-Like Cells for Flow Experiments

This method employs culture techniques adapted from Ecarot-Charrier et al. *(21)*, the premise being the selective migration of osteoblasts onto glass chips *(22)*. The protocol, described in detail by Reich et al. *(2)*, uses the calvaria from 3–6-d-old Sprague–Dawley rat pups.

1. Remove the calvaria aseptically and place them into M199 with no additives. Strip the periosteum carefully from both sides using watchmakers' forceps and place the bone into Petri dishes.

2. Place glass chips on the endocranial surface of the calvaria and add complete medium.

3. After 4–6 d, dislodge the glass chips from the calvaria by irrigation with complete medium and incubate the glass chips for an additional 7–10 d before use, replacing the medium every 3–4 d.

4. Remove the cells from the glass chips by collagenase digestion (30 min, 0.2 mg/mL in HBSS) and resuspend the cells in complete medium. Allow cells to grow until confluent in culture flasks.

5. Trypsinize the cells as in **Subheading 3.1.** and seed 1 mL of the cells onto glass slides coated with fibronectin until they reach confluence, in complete medium. Differentiation of osteoblastic precursor cells is encouraged by the addition of 50 μg/mL of ascorbic acid and 5 m*M* β-glycerophosphate to the medium. The cells are characterized morphologically and functionally by their alkaline phos-

phatase (AP) activity and their ability to form mineralized nodules (*see* **Note 1**).

3.3. Flow Experiments (see Note 2)

3.3.1. Apparatus for Computer Driven Syringe Pump Model (Short-Term Experiments)

The entire flow device is housed in a 37°C air box (*see* **Fig 2.**). The fluid used to shear the cells is the same as the incubation medium prior to shear. The parallel plate flow chamber is perfused by a syringe pump. The channel base area is 13 cm^2 and the channel depth is nominally 230 μm (*see* **Fig. 3**). Perfusion medium is equilibrated with 5% CO_2, 37°C and the apparatus is allowed to equilibrate to 37°C.

1. Fill 100-mL and 30-mL glass syringes with 37°C medium and expel any bubbles (*see* **Note 3**). Prime all the tubing, including the exit slit and port. Introduce medium into the chamber by means of the pump so that the medium fills the area to be occupied by the slide. Invert the first slide over the flooded chamber by gently placing one edge near the inlet port and lowering it gently to avoid any air bubbles. Once the slide is positioned on the chamber, apply uniform pressure and attach the vacuum line to the vacuum port to keep the slide in place and to ensure uniform channel depth. Excess medium will flow out so it is advisable to cover the chamber support with absorbent material. The outlet port tubing can be placed into a beaker to collect perfusate as long as all tubes entering and exiting the chamber are maintained at the same elevation. At all times the chamber must be handled carefully to minimize shear and to avoid temporal gradients in particular. The entry port is larger than the exit port to serve as a bubble trap and once the vacuum is applied, the whole chamber can be inverted and bubbles removed via the septum port. Trapped air bubbles can interfere with the fluid flow and change its characteristics (*see* **Note 3**).

2. The syringe pump is programmed to generate a range of different flow profiles, the flow rate (*see* **Note 4**) being changed in 80-ms microsteps. The fluid dynamics of the chamber are described in greater detail in *(23)* (*see* also **Note 4**). Four well-defined laminar flow profiles are used to separate the effects of different flow stimuli in bone cells (*see* **Fig. 6**).

   a. Stepped flow (instantaneous [100 ms] shear stress increase from 0 to 16 dyn/cm^2 followed by steady shear for 10 min).

   b. Ramp flow (shear stress smoothly transitioned from 0 to 16 dyn/cm^2 over 30 sec, sustained for 9 min before ramping down over 30 sec).

   c. Impulse flow (a 500-ms to 3-sec impulse of 16 dyn/cm^2 with cells maintained on the flow chamber at 0.016 dyn/cm^2 for 10 min).

   d. Pulsatile flow (multiple flow impulses with 3-sec intervals). Slides are maintained on the flow chamber for the same overall amount of time. The inclusion of time-matched stationary (in Petri dishes) and sham controls (placed on the chamber but not subjected to shear, only the vacuum) is important in defining the response of cells to fluid flow alone.

1. Stepped flow

2. Ramped flow

3. Impulse flow
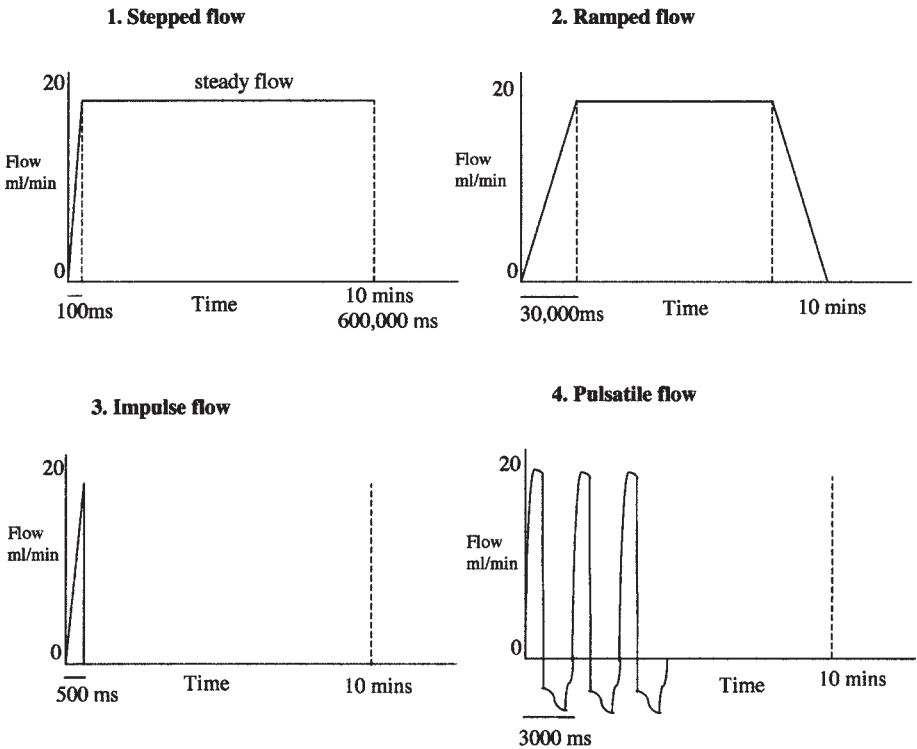

4. Pulsatile flow

Fig. 6. Flow profiles for the experiments detailed in **Subheading 3.3.**

3.3.2. Apparatus for Pulsatile Flow Loop Model

Longer term studies on pulsatile flow require the apparatus shown in **Fig. 4**.

1. Fill the syringe and release any trapped air bubbles. Fill the tubing until there is no air in the system.
2. Attach the syringe to the offset cam and motor. The syringe will draw in medium from the reservoir through a one-way valve and force it out through another one-way check valve to the chamber.
3. Adjust the flow rate by changing the frequency of pulsation of the syringe and the stroke volume. Experiments can be run for 15 min to 24 h (*see* **Note 5**).

3.3.3. Apparatus for Steady Flow Loop Model

Longer term steady flow studies on bone cells require the apparatus shown in **Fig. 5**. The flow loop consists of two reservoirs, situated one above the other with the flow chamber between them. Flow is maintained by the hydrostatic pressure head created by the vertical distance between the two reservoirs. The continuous pumping of the culture medium from the lower to the upper reser-

voir, at rates greater than those through of the chamber, maintains the pressure head. As the excess fluid drains down the glass overflow manifold it meets the incoming $5\%CO_2$–95% humidified air, which facilitates gas exchange with the medium.

1. Add medium to the top reservoir (10–20 mL), filling the lower reservoir as well and flooding the chamber.
2. Add the slide as before and adjust the fluid shear stress by changing the column height in the loop. Recirculation allows for the quantitation of cumulative NO production. In the PGE_2 studies, it is advisable to add serum to the medium to ensure that arachidonic acids, necessary for the response, are not rate limiting. Using this model Johnson et al. *(16)* demonstrated the rapid and continuous release of NO in primary rat calvarial osteoblasts.

3.4. Assays (see *Note 6*)

The practical applications of these fluid flow models are numerous, as they allow for *in situ* studies of perfusate and cells as well as production of lysates and immunocytochemistry. A popular application in our laboratory has been their use to investigate signaling mechanisms in fluid shear. A brief description of some of these techniques, to study G-protein-regulated pathways, follows.

3.4.1. Viscosity and Shear Rate Experiments

The role of viscosity is investigated by addition of high molecular weight, neutral dextran to the perfusion medium (2 g/100 mL, viscosity $\mu = 3.9$ mPa·s. [The viscosity of water at 20°C $\cong 1$ mPa·s]). Normal viscosity of the medium is therefore assumed to be 1 mPa·s $\equiv 0.01$ dyn s/cm^2. Using the equation for viscosity (*see* **Note 4**), the viscosity and shear rate can be varied independently. Three or more profiles can be used:

1. Wall shear stress $(\tau_1) = 26$ dyn/cm^2 where viscosity $(\mu) = 0.01$ and shear rate $(\gamma) = 2600$ s^{-1}.
2. $\tau_2 = 26$ dyn/cm^2, $\mu = 0.039$ (dextran added) and $\gamma = 660$ s^{-1}.
3. $\tau_3 = 6$ dyn/cm^2, $\mu = 0.01$, and $\gamma = 600$ s^{-1}.

In calvarial osteoblasts the rate of NO production increases with shear stress magnitude (0.25–26 dyn/cm^2) within the postulated physiological shear stress range (**Fig. 7**) *(7)*. For a given viscosity (with wall shear stress τ_1 and τ_3) the increase in shear rate is associated with an increase in NO release and for similar shear rates (wall shear stress τ_2 and τ_3) the increased viscosity stimulates increased NO production (**Fig. 8**) *(7,24)*. At equal flow rate the streaming potentials and mass transport are not affected by increasing the viscosity but the wall shear stress is directly proportional to viscosity. Therefore wall shear stress is the main mechanotransductory factor in NO production.
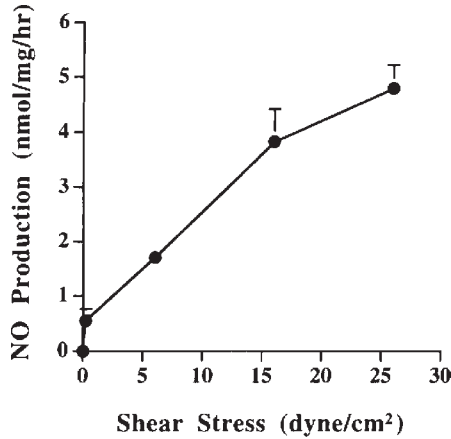
Fig. 7. NO production rates (0–6 h) in primary rat calvarial osteoblasts demonstrate a dose response across the range of physiological shear stress. (Reproduced from *J. Bone Miner. Res.* 1999; **14**, 930–936 with permission of the American Society for Bone and Mineral Research.)
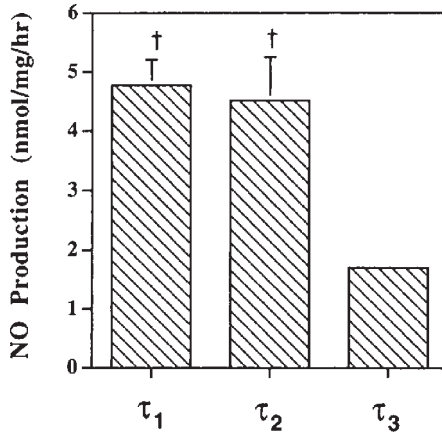

Fig. 8. Viscosity (μ) and shear rate (γ) were varied independently to investigate the role of viscosity and wall shear stress (τ). NO production rates (0–6 h) are plotted for three cases: $\tau_1 = 26$ dynes/cm^2 where $\mu = 1.0$ and $\gamma = 2600$; $\tau_2 = 26$ dynes/cm^2 where $\mu = 3.9$ and $\gamma = 660$; $\tau_3 = 6$ dynes/cm^2 where $\mu = 1.0$ and $\gamma = 600$. † τ_1 and τ_2 were significantly different from τ_3 ($p < 0.05$). (Reproduced from *J. Bone Miner. Res.* 1999; **14**, 930–936, with permission of the American Society for Bone and Mineral Research.)

3.4.2. NO Release Measurement

1. Draw 500-μL samples from the perfusate (from the outflow in the computerized flow apparatus and from the valve at the base of the reservoir in the flow loop apparatus).

2. Reduce the nitrite and nitrate in the sample to NO using a vanadium chloride reaction vessel (Radical Purger and Nitrate Chemical Kit [Sievers]). In brief, vanadium (III) chloride in hydrochloric acid converts nitrate to NO and it also converts nitrite and *S*-nitroso compounds to NO. The reaction takes place at 90°C for high conversion efficiency with 5 mL of reducing agent for 20–50 samples.

3. Quantify NO content using a chemiluminescent NO analyzer. Samples are compared with standard curves, then normalized to total cellular protein using the Bradford protein assay. Controls without cells are included to account for nitrates leeching from the loop apparatus or sampling equipment.

3.4.3. Measurement of NO Synthase Inhibition

1. Conduct flow studies with UMR-106 cells pretreated with the nitric oxide synthase (NOS) inhibitors aminoguanidine (AG) at 100 μ*M* and L-NAA at 100 μ*M* prior to flow and during flow, for example, for 6 h at 12 dyn/cm^2.

2. L-NAA is stable at RT but has poor solubility in water so a stock in HCl is diluted further in culture medium.

3. AG is a selective inhibitor of iNOS (NOS II), and L-NAA inhibits both constitutive and inducible NOS.

4. In UMR-106 cells the iNOS inhibitor does not attenuate NO production whereas the general inhibitor of NOS significantly inhibits the flow-induced response (**Fig. 9**) *(7)*. The form of NOS activated by shear is constitutive and is likely to be NOS III (eNOS) demonstrated to be present in osteoblasts *(25)*.

3.4.4. The Role of G-Proteins in NO Production

1. Conduct flow studies with UMR-106 cells and primary calvarial osteoblasts preincubated with G-protein inhibitors GDPβS (300–900 μ*M*) for 2 h, pertussis toxin 1 μg/mL, 1 h.

2. Incubate static cultures of osteoblasts on glass slides with or without G-protein activator GTPγS (300–900 μ*M*) for 2 h.

3. NO production with flow is biphasic, with a point of inflection at 30 min. The rate of production of NO from 0 to 30 min is about fourfold that of the sustained response. Static cultures treated with GTPγS showed a dose dependent increase in NO production rates. In sheared cultures the inhibitor GDPβS blocks the initial burst of NO but does not affect the sustained production (**Fig. 10**). Pertussis toxin, inhibitory for G_i/G_o class of G-proteins did not significantly affect either phase of NO production.

4. Notes

1. For AP staining follow the manufacturer's instructions (Sigma kit 86-C). In brief, the kit comprises a naphthol AS–BI phosphate alkaline solution and a Fast Blue BB salt. The AP enzyme cleaves the phosphate from the ASBI salt, which in turn reacts with Fast Blue to give a blue pigment. Discrete granular deposits of pigment can be seen microscopically and reflect areas of AP activity. The primary osteoblast-like cells stain for AP activity, usually in patches. Cells grown in the
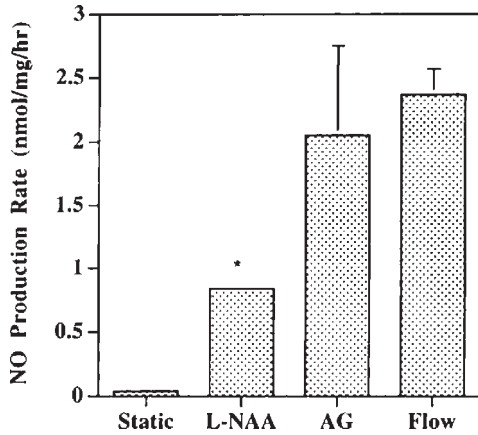
Fig. 9. Cumulative NO production for flow at 12 dyn/cm^2, flow + AG, flow + L-NAA, and static controls in UMR-106 cells. *L-NAA significantly inhibited NO release ($p < 0.05$). (Reproduced from *J. Bone Miner. Res.* 1999; **14**, 930–936, with permission of the American Society for Bone and Mineral Research.)
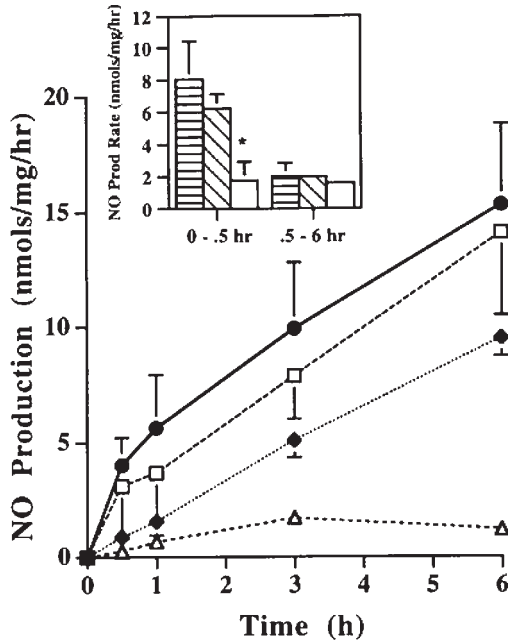

Fig. 10. Cumulative NO production for flow at 16 dyn/cm^2 (*filled circle*), flow + GDPβS (*filled diamond*), flow + PTx (open square), and static controls (*open triangle*) in primary rat calvarial osteoblasts. *Inset*: Short- and long-term production rates are shown for flow (*horizontal hatching*), flow + PTx (*diagonal hatching*), and flow +

presence of ascorbic acid and β-glycerophosphate form mineralized nodules as determined by von Kossa staining (*see* the chapter by Scutt et al., *this volume*, for details on procedure). The cells show a threefold increase in cAMP in response to 15 min parathyroid hormone stimulation, which is characteristic of osteoblasts and they produce osteocalcin *(2)*. In our experience cell viability, assessed by trypan blue staining, is >98% in all experiments.

2. Studies on cell metabolism usually require minimal flow volume (loop fluid) and maximum cell surface area, and the design of this flow chamber gives a high cell to volume ratio (10^6 cells/10 mL), suitable for the study of metabolite production. The slide area is also sufficient for the collection of lysates and the processing of samples for immunoblotting. A flow chamber with slightly reduced proportions can be mounted on an inverted microscope, allowing for time lapse photography of the cells. Several groups have used a cone and plate viscometer, which gives a smaller cell to volume ratio, does not allow for continuous sampling of the perfusate, and suffers from substantial evaporation of the tissue culture medium. Some alternative fluid flow loops require large amounts of medium (in excess of 100 mL) for perfusion and have a relatively small cell surface area ($1 \ cm^2$); hence they are not so reliable for metabolic studies.

3. In our experience, the computer-controlled syringe pump is essential for the delivery of rapid yet precisely controlled bursts of flow. The cells, if grown to confluence on coated/alkali etched slides, do not lose adherence during the flow cycle. However, a stray air bubble in the flow loop can easily tear cells from the slide and occasionally, on application of the vacuum, there is an air leak between the gasket and the chamber which will lead to a much greater volume of fluid being evacuated from the slide. To prevent these problems it is important to check for air bubbles before each flow experiment and to pass medium through to release any bubbles. In addition, the silastic gasket must be fully flush with the chamber and sealed with a little vacuum grease. It is advisable to set up a few extra slides in case one of the slides fails owing to these problems. Glass syringes are superior to plastic syringes as they respond more quickly to the action of the syringe pump owing to low compliance and are necessary for the correct delivery of short impulse flow. The chamber should be protected from scratches and chips as this will affect the flow characteristics. The length of the outlet should be kept to a minimum to avoid resistance to flow and at the same elevation as the chamber outlet to avoid suction or back pressures.

4. The shear stresses of 0–16 dyn/cm^2 (1 dyn/cm^2 = 0.1 Pa) are calculated from the velocity of flow, medium viscosity and dimensions of the chamber. The chamber is engineered to give flow rate and shear stress a linear relationship. The wall shear stress on the cell monolayer can be calculated using the momentum balance for a Newtonian fluid and assuming parallel plate geometry:

Fig. 10. *(continued)* GDPβS (*white*). GDPβS significantly inhibited short-term NO production ($p < 0.05$). (Reproduced from *J. Bone Miner. Res.* 1999; **14**, 930–936, with permission of the American Society for Bone and Mineral Research.)

$$\tau = (6Q\mu)/(bh^2)$$

where Q is the flow rate (mL/s); μ is the viscosity (~ 0.01 dyn s/cm^2 at 25°C); h is the channel height (0.023 cm); b is the slit width (2.35 cm); and τ is the wall shear stress (dyn/cm^2). Therefore for a shear stress of 16 dyn/cm^2 the flow rate in mL/sec is: Q = 0.332 mL/s = 19.89 mL/min for one syringe (9.94 mL/min for two syringes).

The Reynolds number for flow through the chamber is 0–20 for shear stresses up to 24 dyn/cm.^{2} The transition to turbulent flow starts at 1000–8000 Reynolds so the flow can be considered laminar. The entrance length for this flow chamber is 0.018 cm (length required before the channel flow is truly laminar), and as the chamber is in effect approx 6.4 cm in length, the region at the top of the chamber where flow is nonlaminar is negligible.

The wall shear stress (τ) in dynes per square centimeter is defined as :

$$\tau = \gamma\mu$$

where γ = shear rate s^{-1} and μ = dynamic viscosity (dyn s/cm^2).

5. Flow can be monitored by the introduction of a flow sensor to the system. The flow pattern generated by this system is essentially a half sine wave. One cycle of the cam constitutes a half-sinusoidal positive flow and then a period of no flow. The peak flow rate and therefore peak shear stress is $\pi \times$ the average flow rate, the average flow rate being calculated through an entire cycle. As shear stresses on osteocytes are calculated to be in the range 8–30 dyn/cm^2 *(26)*, an average pulsatile shear stress of 5 dyn/cm^2 is used (giving a maximum shear stress of 5 × π =15 dyn/cm^2).

6. Most experimental time is taken up with the passaging of cells and preparation of slides ready for the flow experiments. Depending on the conditions used, the flow experiments are relatively short and the most time is expended in heating the medium, air hood, and apparatus to 37°C. The perfusion medium can be left overnight gassing in CO_2, as it is important to maintain the correct pH during the flow study and the medium rapidly loses CO_2 in the air hood. Fresh medium can be taken from the closed gassed bottle for each new experiment. Owing to the biohazardous nature of the waste from this experiment all syringes, plastic tubing, and flow chamber are washed in Tergazyme (Alconox Inc., New York, NY) and then rinsed in distilled H_2O before air drying. The silastic gasket does not retain its shape after autoclaving but can be subjected to ultraviolet light in a flow hood. For short term experiments sterility is not an issue. However, for long-term experiments it is advisable to autoclave the respective parts of the apparatus and assemble them in a laminar flow hood.

Acknowledgment

References

1. Wolff, J. (1892) *Das Gesetz der Transformation der Knochen*. Hirschwald, Berlin.
2. Reich, K. M., Gay, C. V., and Frangos, J. A. (1990) Fluid shear stress as a mediator of osteoblast cyclic adenosine monophosphate production. *J. Cell. Physiol.* **143**, 100–104.
3. Smalt, R., Mitchell, F. T., Howard, R. L., and Chambers, T. J. (1997) Induction of NO and prostaglandin E2 in osteoblasts by wall-shear stress but not mechanical strain. *Am. J. Physiol.* **273**, E751–E758.
4. Bergula, A. P., Huang, W., and Frangos, J. A. (1999) Femoral vein ligation increases bone mass in the hindlimb suspended rat. *Bone* **24**, 171–177.
5. McAllister, T. N. and Frangos, J. A. (1998) Nitric oxide and mechanical factors: fluid shear stress, in *Nitric Oxide in Arthritis and Osteoporosis* (Hukkanen, M. V. J., Polak, J. M., and Hughes, S. P. F., eds.), Cambridge University Press, Cambridge, UK, pp. 141–150.
6. Hillsley, M. V. and Frangos, J. A. (1994) Review: bone tissue engineering: The role of interstitial fluid flow. *Biotechnol. Bioeng.* **43**, 573–581.
7. McAllister, T. N. and Frangos, J. A. (1999) Steady and transient fluid shear stress stimulate NO release in osteoblasts through distinct biochemical pathways. *J. Bone Miner. Res.* **14**, 930–936.
8. Jiang, G. L., White, C. R., Stevens, H. Y., and Frangos, J. A. (2002) Temporal gradients in shear stimulate oseoblastic proliferation via ERK1/2 and retinoblastoma protein. *Am. J. Physiol. Endocrinol. Metab.* **283,** E383–E389.
9. Bao, X., Clark, C. B., and Frangos, J. A. (2000) Temporal gradient in shear-induced signaling pathway: involvement of MAP kinase, c-fos, and connexin 43. *Am. J. Physiol. Heart Circulat. Physiol.* **278**, H1598–H1605.
10. Reich, K. M. and Frangos, J. A. (1991) Effect of flow on prostaglandin E2 and inositol trisphosphate levels in osteoblasts. *Am. J. Physiol.* **261**, C428–C432.
11. Sakai, K., Mohtai, M., and Iwamoto, Y. (1998) Fluid shear stress increases transforming growth factor beta 1 expression in human osteoblast-like cells: modulation by cation channel blockades. *Calcif. Tissue Int.* **63**, 515–520.
12. Pavalko, F. M., Chen, N. X., Turner, C. H., et al. (1998) Fluid shear-induced mechanical signaling in MC3T3-E1 osteoblasts requires cytoskeleton-integrin interactions. *Am. J. Physiol.* **275**, C1591–C1601.
13. Hung, C. T., Pollack, S. R., Reilly, T. M., and Brighton, C. T. (1995) Real-time calcium response of cultured bone cells to fluid flow. *Clin. Orthopaed. Relat. Res.* **313**, 256–259.
14. McDonald, F., Somasundaram, B., McCann, T. J., Mason, W. T., and Meikle, M. C. (1996) Calcium waves in fluid flow stimulated osteoblasts are G protein mediated. *Arch. Biochem. Biophys.* **326**, 31–38.
15. Klein-Nulend, J., van der Plas, A., Semeins, C. M., et al. (1995) Sensitivity of osteocytes to biomechanical stress in vitro. *FASEB J.* **9**, 441–445.
16. Johnson, D. L., McAllister, T. N., and Frangos, J. A. (1996) Fluid flow stimulates rapid and continuous release of nitric oxide in osteoblasts. *Am. J. Physiol.* **271**, E205–E208.

17. Klein-Nulend, J., Semeins, C. M., Ajubi, N. E., Nijweide, P. J., and Burger, E. H. (1995) Pulsating fluid flow increases nitric oxide (NO) synthesis by osteocytes but not periosteal fibroblasts—correlation with prostaglandin upregulation. *Biochem. Biophys. Res. Commun.* **217**, 640–648.

18. McAllister, T. N., Du, T., and Frangos, J. A. (2000) Fluid shear stress stimulates prostaglandin and nitric oxide release in bone marrow-derived preosteoclast-like cells. *Biochem. Biophys. Res. Commun.* **270**, 643–8.

19. Kasten, T. P., Collin Osdoby, P., Patel, N., et al. (1994) Potentiation of osteoclast bone-resorption activity by inhibition of nitric oxide synthase. *Proc. Natl. Acad. Sci. USA* **91**, 3569–3573.

20. Reich, K. M., McAllister, T. N., Gudi, S., and Frangos, J. A. (1997) Activation of G proteins mediates flow-induced prostaglandin E2 production in osteoblasts. *Endocrinology* **138**, 1014–1018.

21. Ecarot-Charrier, B., Glorieux, F. H., van der Rest, M., and Pereira, G. (1983) Osteoblasts isolated from mouse calvaria initiate matrix mineralization in culture. *J. Cell Biol.* **96**, 639–643.

22. Jones, S. J. and Boyde, A. (1977) The migration of osteoblasts. *Cell Tissue Res.* **184**, 179–193.

23. Frangos, J. A., McIntire, L. V., and Eskin, S. G. (1988) Shear stress induced stimulation of mammalian cell metabolism. *Biotechnol. Bioeng.* **32**, 1053–1060.

24. Bakker, A. D., Soejima, K., Klein-Nulend, J., and Burger, E. H. (2001) The production of nitric oxide and prostaglandin E(2) by primary bone cells is shear stress dependent. *J. Biomech.* **34**, 671–677.

25. Helfrich, M. H., Evans, D. E., Grabowski, P. S., Pollock, J. S., Ohshima, H., and Ralston, S. H. (1997) Expression of nitric oxide synthase isoforms in bone and bone cell cultures. *J. Bone Miner. Res.* **12**, 1108–1115.

26. Weinbaum, S., Cowin, S. C., and Zeng, Y. (1994) A model for the excitation of osteocytes by mechanical loading-induced bone fluid shear stresses. *J. Biomech.* **27,** 339–360.

29

Methods for Analyzing Bone Cell Responses to Mechanical Loading Using In Vitro Monolayer and Organ Culture Models

Andrew A. Pitsillides, Victoria Das-Gupta, Dominic Simon, and Simon C. F. Rawlinson

1. Introduction

As bone's primary function is mechanical, it is not surprising that almost all studies using intact bone concern its morphology. Such histomorphometric studies have been used to provide insights into how bone responds, as an organ, to mechanical loading. However, despite the fact that the cellular basis for "sensing" mechanical stimuli or "communicating" their influence to coordinate any loading-induced changes that they engender is not known, studies in intact bone are rarely used to establish the direct links with any changes in bone cell biochemistry. It is also evident that most studies aimed at defining these mechanisms currently use bone cells grown in vitro, and that this has produced rapid advances in our understanding of the factors that might be involved in regulating bone cell responses to loading-induced stimuli. It is clear that such in vitro studies facilitate the final mechanistic deciphering and constitute a useful initial approach. However, it is also evident that they generally take little regard of the influence that might be provided by cell–cell and cell–matrix interactions within a bone's complex environment and architecture *(1)*. It is therefore imperative to attempt to bridge the gap between the cell biology of bone's response to loading on the one hand and the morphological approach to this same problem on the other.

In this chapter, we concentrate on techniques by which the cellular responses to mechanical stimulation can be examined in cell monolayer and in organ culture. We provide details on a wide range of devices that can be used to generate precise, measurable mechanical strains in these preparations and give

details of those devices that we have used extensively in both organ and cell culture. We hope that this provides a basis upon which new investigators into this field can decide how to approach their own particular set of questions. In our opinion, as such experiments take into account the essential load-bearing role of skeletal tissues, they should become a key aspect of any investigation into bone cell biology. Thus, it may be considered appropriate that studies into the effects on nonmechanical factors should ideally also be conducted in an environment in which skeletal tissues (or indeed other load-bearing connective tissues), and cells derived from these tissues experience their normal physiological range of mechanical stimuli.

We first address some of the aspects of in vitro culture that need to be considered during the interpretation of results derived from experiments investigating the cellular responses to mechanical stimuli, with respect to their in vivo relevance. We then describe model cell culture systems for investigating the response of isolated bone cells to mechanical strain, and finally we describe methods for loading bone explants in culture.

1.1. Limitations of In Vitro Organ and In Vitro Cell Culture Strain Application Models

Organ culture, the maintenance of tissue explants in vitro, is an attempt to bridge the gap between cell culture and in vivo models. Many tissues including cartilage, tendon, and bone have been studied in organ culture *(2–6)*. This offers, as a major advantage, the maintenance of an intact extracellular matrix (ECM). ECMs are the product of resident cells, are structurally unique, and are specialized according to local requirements. For example, mineralization is important for bone rigidity and type I collagen endows it with mechanical strength *(7,8)*. Retention of the ECM is important as it maintains normal cell attachment sites and spatial relationship between cells in a tissue. By retaining the tissue's architectural organization, it is also likely that the relationship between distinct mechanical sequelae of loading, such as strain, fluid shear stress, and streaming potentials, will be conserved. Both organ and monolayer cell cultures allow the responses to be investigated without the complication of systemic factors. Yet at the same time it is possible, indeed probable, that some of these responses to mechanical stimulus will be complicated by the consequence of tissue or cell isolation and maintenance in culture.

Connective tissues, including bone, play major structural roles; for example, the skeleton must support body weight, facilitate movement, and protect internal organs. In such tissues, the ECM and not the resident cells, fulfils such roles; thus its preservation in culture may be considered appropriate in experiments that are aimed at establishing the basis of the tissue's response to load-bearing. Bones undergo an adaptive response to dynamic loading in vivo; with

very low cycle numbers capable of inducing changes in bone architecture and mass *(9–11)*. Indeed, an osteogenic/antiresorptive regimen of 36 loading cycles at 0.5 Hz is sufficient to produce a maximal response *(9)*. The brief duration (72 sec) of this mechanical stimulation, required to activate a full osteogenic response in vivo, makes the study of the preceding "preosteogenic" events feasible. Thus, similar loading regimens have been used in organ culture and in "strain models" in cell culture to investigate loading-induced responses *(5,6,12)*. Because strain, fluid shear stress, and streaming potentials have all been reported to influence bone cell metabolism, it is important to appreciate that the ECM may modify both the signals to which resident cells respond, as well as the specific cellular reaction that such signals generate *(9–11,13–15)*.

Many bone ECM molecules contain integrin-binding Arg-Gly-Asp (RGD) sequences and in vivo changes in integrin expression profoundly affect bone metabolism *(16–19)*. This is important, as any lack of integrin-binding sites in cell monolayer culture may also lead to changes in integrin expression. ECM molecules are known to influence cell behavior. Indeed, osteoblasts that bind preferentially to fibronectin in vitro, also exhibit a faster rate of proliferation on this substrate than when seeded onto poly-L-lysine *(20,21)*. Differential integrin expression has been shown in osteoclasts seeded on bone sialoprotein-coated glass compared to plastic *(22)*. It is therefore pertinent, at least in the short term, that organ culture maintains normal cell–ECM attachment sites, retains cell–cell associations and their three-dimensional relationships. In contrast, cell cultures are usually two-dimensional monolayers in which there is little control of such relationships.

A feature of bone explant culture is that it retains the relative positions of osteocytes, osteoblasts, and osteoclasts. These might be important for maintaining signaling gradients, for example, all bone cells produce nitric oxide and its release may establish local concentration gradients that regulate behavior *(23)*. It is unlikely that such gradients are produced in cell culture models. Further, osteocytes and osteoblasts can communicate via gap junctions found at the termini of cell processes stretching through the canaliculi *(24)*. Despite the fact that these are observed in cell culture *(25)*, any positional information that they may confer will be lost as their expression patterns are altered as a consequence of their two-dimensional organization. These arguments may be particularly pertinent for the terminally differentiated osteocytes, which are normally embedded in the bone ECM and are difficult to isolate and grow in cell culture. Although an osteocyte-like cell line has recently been produced, at present there is only one well-established method for isolating primary osteocytes for cell culture *(26)* (*see* the chapter by Nijweide et al., *this volume*). It may also be relevant that as well as maintaining the relative position of bone cell types, organ culture models also conserve their normal cell ratios. Thus,

organ culture models can be used to examine potential cellular crosstalk, which may occur during the tissue's response to mechanical stimuli. In contrast, cell culture can only partially achieve this through the use of coculture systems in which cell ratios and positional relationships will only approximate to those in vivo.

1.2. The Effects of Loading: Mechanical Strain, Fluid Shear, and Streaming Potentials

Retention of structural integrity in organ culture allows the response to applied loads that are capable of generating physiological levels of mechanical strain to be investigated. Ideally, cell culture would complement this by allowing for particular responses to a specific single component, uniaxial strains, applied to large numbers of uniform cells, to be determined. However, logistical problems and the fact that substrates stretched along one axis will inevitably contract at 90° to this principle strain axis (subject to Poisson's ratio) mean that such "ideals" are not readily achievable. As this ratio is fixed for any single material, but can vary between different materials, direct comparison between studies in which substrates differ should be made only with care. Currently, such considerations are unavoidable. With appropriate loading, cells in explants can probably experience physiological levels of strain at their given location. However, despite precise loading regimens, cells within explants will experience a range of strain magnitudes in either compression or tension and these location-specific variations should ideally be taken into account during experimental design and interpretation.

Another consideration involves the fact that the lacuna–canalicular network of bone is filled with tissue fluid, and that although this network is retained in organ culture models, its contents are replaced by culture media. When this fluid flows over, or through the ECM, fluid shear forces are generated. Application of shear forces in vitro has been shown to induce a response in endothelial cells, chondrocytes, and bone cells *(13,14,27,28)*. In bone, fluid shear forces are generated as a result of a mechanical load-induced shift in tissue fluid, and thus mechanical strain cannot be investigated independently of fluid shear in vivo or in organ culture models. It is possible to investigate the independent effects of fluid shear application in cell culture systems (*see* the chapter by Stevens and Frangos et al., *this volume*). Nevertheless, it is also clear that the ECM modifies fluid shear rate and magnitude in a way that it is practically impossible to reproduce currently in cell culture models.

A further complication is introduced by the contribution of the flow of charged tissue fluid over the surface of bone's charged ECM, which results in electrical, streaming potential, currents. Media bathing lacuna–canalicular networks in bone explants contain many charged molecules, including amino acids

and proteins. Thus, both the media and the surface of the tissue show a net charge, and any potential difference created at this site of contact results in an electrostatically charged layer around the tissue. In intact bone, cyclical mechanical loading creates fluid flow and establishes a streaming potential. Removal of bone from an animal isolates it from the load it normally experiences and results in fluid shifts. It is therefore important to acknowledge the disturbance to these streaming potentials that are an unavoidable consequence in both organ and monolayer cultures.

Cell cultures have as their main advantage that they are universally established, easy, and reproducible (*see* Parts I and II).

The media, cell number, percentage confluence and differentiation state can all be defined and controlled, making it possible to reproduce experiments in different laboratories. Similar standardization is not yet achieved in organ cultures, but should be achievable in the future by use of the same culture media, explants of similar size, origin, age, sex, hormonal status, and so forth. In contrast with cell cultures, it is almost impossible to control cell content, tissue architecture or sample heterogeneity in organ cultures, and the responses within any one cell type is likely to be subject to paracrine controlling influences. Although recent developments have been made (*see* **Subheading 3.5.**), another current drawback of organ culture models is the limited time that explants can retain viability ex vivo. Finally, loadable organ cultures are clearly not appropriate for the application of all techniques. For instance, mechanically stimulated increases in intracellular free calcium are impossible to monitor in organ culture, but can be relatively easily observed in cell monolayer culture.

2. In Vitro Cell Culture Loading Models

Before describing any specific methods (*see* **Note 1**), we emphasize that the history of the cell-straining techniques has, for the most part, relied on custom-built devices that remained relatively unique to individual investigators. To some extent this may have been due to a desire for progressive augmentation in the system's efficiency in delivering a specific component of the mechanical loading environment. This is clearly a desirable objective. Nonetheless, it does not negate the contribution to our understanding made by systems in which the precise nature of the stimulus to which cells are exposed remains largely undefined. It is, however, surprising, in our opinion, that few if any of these studies have attempted to relate zonal variations in the applied stimulus to any differences in the cell's biochemical response at the level of an individual cell. To do this, the investigator would simply need to measure some response, at the level of an individual cell, and relate this to the magnitude of the mechanical stimulus to which that cell was exposed.

In an attempt to delineate the defining character of straining techniques, it is important that a number of principles are considered:

1. A mechanical strain (often tensional) is applied by substrate deformation.
2. A known strain magnitude is generated in the substrate onto which the cells are seeded.
3. The substrate is able to support cell growth and differentiation.
4. Cells must attach to the substrate and not detach as a consequence of deformation.
5. The substrate should have perfect elastic properties.
6. Adequate access for observation, extraction, and other processing is possible.
7. During experiments, the apparatus should be housed in a controlled gaseous and thermostatic environment.
8. Techniques should aim to subject all cells to equal levels of mechanical strain, or, as a minimum, ensure that their levels are accurately measured or estimated and described.

The extrinsic mechanical stimulus to which bones respond may be a change in tension, compression, gravitation, vibration, or hydrostatic pressure. Herein, we outline different techniques that have been developed to study the response of cultured cells to tension in culture, by stretching (or bending) the substrate onto which the cells have adhered. Thereafter, we will describe in detail one such four-point straining device that we have used extensively.

2.1. Biaxial Straining

In "dish-deforming" cell culture models, the imposed biaxial substrate deformation provides a nonhomogeneous strain on cells. Commonly, dishes are intermittently deformed over a template to produce a 5% change in surface area *(29,30)*, such that cells near the center of the dish would be strained in excess of those at the periphery. Several systems have been developed (single- and multiple-dish versions) that control the input strains by varying the curvature of the template. In these systems, estimates of the template's arc length of spherical distension provide a basis for calculating average strains *(31)*.

Numerous other platen-driven devices for applying biaxial strain have been developed for cells grown in culture dishes with a flexible membrane, instead of rigid tissue culture plastic, bottoms. Examples of such techniques include: upward or downward "tenting" of membranes using vertically pulsating ball-ended prongs *(32,33)*, electrocylinder-driven pulsations of spherical watchglass sectors to indent culture dishes *(34)*, and upward indentation of Petri dishes with flat-ended circular pistons *(35)*.

In 1985, flexible-bottomed circular, cell culture plates were specifically designed that could be interfaced with a computer-controlled vacuum manifold system *(36)*. Vacuum application to the culture well undersurface stretched it

downward in a manner that could be controlled by varying vacuum magnitude, waveform, frequency, and number. Another differential pressure, flexible-substrate system used positive, solenoid valve-mediated, pressure to deform circular, peripherally clamped, 100-μm polyurethane–urea membranes *(37)*.

A common problem with such devices is that the deformation can result in nonuniform strains of the substrate. It is clear that these will also be subject to variations in the strain applied to cells at various positions across their diameter. This is an important consideration, as it has been predicted that biaxial straining is at least twice as potent as uniaxial strains *(38)*. Thus, unless one was going to investigate a particular response in a single cell of known location and strain, then it would be necessary to appreciate that any results may represent an aggregate of total inhomogeneous cellular responses to the applied range of strains. One might also consider the effect of "puddling"; that is, as the substrate is drawn downwards by the vacuum, the overlying medium will collect at the lowest point. The effect of this fluid movement has not been tested.

Another method that aims to apply uniform biaxial strain involves using a square elastic substrate that is stretched on four sides, over the rim of a platen. As increasing amounts of the original (flat) membrane slip radially, outward over an axially advancing platen rim (its area increasing as it does), the portion of the membrane remaining directly over the platen theoretically experiences homogeneous biaxial strain. Brighton et al. found that when straining cultured osteoblasts in this way, they could detect a physiological response at strains as low as 300 με *(39)*.

2.2. Uniaxial Straining

These experiments purport to investigate the effect of uniaxial strains, however, it is important to note that they nonetheless are subject to the restrictions imposed by Poisson's ratio (a substrate stretched along one axis will inevitably contract at 90° to this principle strain). Most of these devices have relied on four-point bending, but a three-point bending technique was designed by Hasegawa et al. *(30)*. Whilst this successfully applied uniaxial strains, their magnitude over the plate's surface will have been unequal.

2.2.1. Stretching of Substrates

Uniaxial straining devices have been developed in which a strip of silicone (*see* **Note 2**) is placed in a trough and anchored at one end, a magnet attached at the strip's free end and another magnet outside the culture system, operated by hand or via a motor-driven cam, is used to stretch the substrate. Other methods using silicone as a substrate require film spools to create the length change *(38)*. Using derivatives of such systems, in which cells are seeded onto

prestretched membranes, it is possible to observe cells during their response to compression as well as tension.

Recently, cell culture chambers attached with silicone sealant to the surface of polycarbonate sheets have been used to subject adherent cells to mechanical strain *(40)*. This system, based on a design originally described by Murray and Rushton *(41)*, uses strips of polycarbonate that are adapted into cell culture chambers, by attaching lids removed from four-well slides with silicone sealant. Cell straining is achieved using a device consisting of two platens that run on dry linear bearings, driven by a servo-controlled pneumatic ram. The actuator and compressor are housed outside the incubator and the former is controlled from a computer supplied with feedback from a linear variable displacement transducer. The polycarbonate strips, with adherent wells and cells, are clamped across the two platens. Controls consist of strips clamped across "static" platens as well as strips that are clamped across a moving platen that will generate medium perturbation equivalent to that experienced by strips subjected to strain stimuli *(40)*. This device is capable (determined by appropriate strain gauge measurements) of applying controlled cyclical strains between 100 and 200,000 µε, at strain rates from 100 to 1,000,000 µε/sec and in this system, strains have been applied as a ramped square wave pattern.

Similar systems for applying uniaxial strain using a polyurethane substrate have also been developed by Grabner et al. *(42)*, in which a motor-driven linear stage was used for the application of a cyclical tension. These devices appear to represent a key to addressing questions that relate to the differential effects of mechanical strain and fluid flow.

2.2.2 Four-Point Bending of Substrates

Four-point bending of a plate requires a pair of lateral forces acting outside two fulcra. This produces an even curve at both the tension (convex) and compression (concave) surfaces, and the curve makes up a segment of a circle, between the fulcra. Several four-point bending systems have been designed, and in the simplest terms these differ in the manner by which loads are applied, and the culture substrates compounds that are used. One such system, which uses rectangular culture plates (polycarbonate or glass), was recently devised in which culture plates are suspended within a common 40 × 40 mm silicone rubber well *(43)*. By allowing both sides of the substrate to act as the surface onto which cells can be seeded, the device elegantly permits the cell's response to either tensile or compressive strains to be examined. It also includes scope for direct strain gauge readout to monitor the parameters of strain to which cells are exposed. Another powerful feature of this device is that it permits the use of a range of culture

substrate materials, with different Young's moduli, thus facilitating application of a broad range of strain magnitudes.

2.3. An Example of Four-Point Bending of Monolayers of Cells on Plastic Strips

A four-point bending system that is able to engender low-strain levels has been used *(5,44–48)*, in which tensional strain is applied to plastic strips containing adherent monolayer bone cell cultures in a custom-designed loading apparatus (**Fig. 1**). This four-point bending system was designed to deliver strain levels of several hundred to several thousand $\mu\varepsilon$, which are within the physiological range recorded for bone cells in vivo (*see* **Note 3**). It should be noted that this system is also capable of delivering compressive strain. The method is as follows:

1. Passage cells onto presterilized plastic strips for at least 24 h (this time depends upon initial seeding density) and maintain cells for 24 h and throughout the experimental application of mechanical strain in a humidified atmosphere of 95% air–5% CO_2 in serum-free medium (*see* **Note 2**).
2. Transfer the strips (n = 5 for each variable) to the loading apparatus under sterile conditions. To do this, separate the loading apparatus into its two component parts: a base for the strained strips and an upper portion with the cam, platen, and flow chambers. Remove strips from the dishes in which they have been preincubated, and position into individual chambers with the requisite volume of medium (10 mL) added.
3. Reconstruct the whole apparatus, place back into the humidified incubator, and allow for equilibration. Keep disturbance of the medium minimal at all times.
4. Apply a load generating mechanical strain of 3400 $\mu\varepsilon$ at 1 Hz for 600 cycles to cells adherent on the strips (*see* **Note 3**).
5. Subject similar strips with cells attached to cyclic perturbation of the medium (flow controls) without applied loads, and subject others only to identical changes of the medium without any mechanical perturbation to serve as "static" controls (*see* **Note 4**).
6. Following strain application, remove strips from loading apparatus and return to dishes for various times post-straining, depending on response to be investigated.

2.4. Alternative Methods for Applying Strain

Magnets are used to provide a high degree of control in devices capable of stretching a substrate, and such magnetostrictive actuators have been used in order to generate up to 22,000 $\mu\varepsilon$ on particular substrates. The electromagnetic elements placed at either end of the substrate are attached to clamps mounted on a guide plate that ensures unidirectional travel. It is an aspect of these devices that they generate powerful electromagnetic fields that may directly affect cell behavior, and shielding from these fields should always be used.
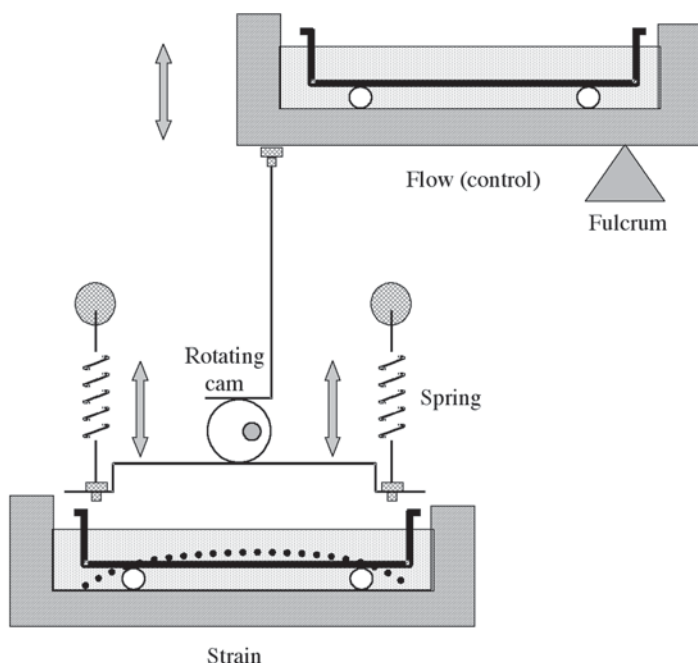
Fig. 1. Schematic diagram of the custom-built apparatus used for straining cells by subjecting plastic strips to four-point bending. As the eccentric cam rotates it presses the loading platen onto the vertical edges of the plastic strips and causes their deformation (to the *dotted* position) in an arc around the paired fulcra underlying the strips (*white*). The platen is returned to the unloaded position by the spring. The rotation of the cam also acts to rock the chamber into which strips to be subjected to flow "control" are placed. For dose–response experiments, peak strain magnitudes can be altered by vertical displacement of the base unit by using a range of washers (with different thickness, placed between base and upper units; *see* **Fig. 4**), and frequency altered with rheostat control of cam revolution rate. This unfortunately affects the waveform produced. However, a novel device has recently been designed (yet untried), in which the platen's vertical displacement is governed by a screw mechanism that is computer controlled. This offers greater flexibility in the waveforms that can be generated, such that on/off dwell times and the "on" as well as "off" strain rates can be varied independently (*see* **Fig. 5**; Stromberg et al., *personal communication*). In addition this model utilizes commercially available cell culture strips (of equivalent size to microscope slides) that do not possess the end walls.

As an alternative, piezoelectric extension may be used to provide the displacement. This allows accurate control, however, like magnetostrictive actuators, generates high electrical fields. Such actuators have been used in vitro to apply strains of controlled magnitude (200–40,000 με), frequency (up to 100 Hz),

and waveform, which adequately cover the range experienced by bone cells in vivo. The cells are mechanically strained by moving a plunger, connected to the center of an actuator, both ends of which are inserted into grooves on an acrylic resin frame, thus generating maximum actuator displacement. Cultured cells are seeded on, or in, a collagen gel block between plungers made of a non-conductive acrylic resin material, and the gel block anchored by stainless-steel wire meshes (lattice size; 0.4 × 0.4 mm) fixed to the plunger-ends *(49)*.

3. In Vitro Organ Culture Loading Models

Culturing bone as a tissue allows for the preservation of normal cell–matrix attachments as well as cell–cell attachments between resident cells. Preservation of the structural, load-bearing, mineralized compartment means that loading of segments in vitro can be controlled so that the extent of bending produced, engenders levels of strain (measured directly in loaded segments using attached strain gauges) identical to those measured at the same site during normal physiological activity in vivo (*see* **Note 3**). Providing disruption is kept to a minimum, it is also likely that in vitro loading of bone segments will reproduce other associated phenomena of loading (fluid shear/streaming potentials). On the other hand, such isolation will result in many unavoidable changes, including loss of blood flow, a potential restriction on the ability of nutrients to reach cells, and changes in the relationship between bone and its marrow. Nonetheless, this approach allows attempts at bridging the gap between the morphological disciplines and those of the cell biologist, in determining the mechanisms of bone's response to loading (*see* **Note 4**).

The in vivo loadable avian ulna model developed by Lanyon and Rubin *(9,50)* determined that dynamic mechanical loads applied to a functionally isolated portion of bone could result in an increase in bone formation. The extent of new bone produced, was dependent on the magnitude and the rate at which the strains were engendered *(51)*. Further studies indicated that only 36 cycles (over a period of 72 sec) per day of applied load were sufficient to produce a maximal formative response *(9)*. That all the information needed to produce new bone was contained in only a short period of time, provided the rationale for generating organ culture models to investigate other early loading-related responses that might contribute to controlling the osteogenic response.

The in vitro loadable models, which have been developed in Lanyon's laboratory, include adult canine cancellous bone cores, rat cortical ulnar bones, rat parietal bones, and embryonic chick tibiotarsi. All of these have used the aforementioned in vivo studies and have, as a consequence, used similar strain regimens as the mechanical stimulus. Further models from other groups include a loadable bovine cancellous bone core system *(52)* and a human bone core model *(53)*. Each system requires that attendant soft tissues and marrow (where pos-

sible) are removed, to leave exclusively bone tissue with resident bone cells and associated internal vasculature. To generate results that are likely to have in vivo relevance, it is imperative that these organ culture systems are calibrated. Thus, prior to loading bone in vitro, the amount of force required to generate those levels of strain that are engendered by normal activity in vivo, should be defined (*see* **Notes 3**, **5**, and **6**). In the following subheading we describe several models of loadable bone organ cultures that have been defined in this way.

3.1. Loading of Adult Canine Cancellous Bone Cores

3.1.1. Reagents

1. Culture medium: Minimum essential medium (MEM) + Hanks' salts and 25 m*M N*-2-hydroxyethylpiperazine-*N*'-2-ethanesulfonic acid (HEPES) (Gibco) supplemented with 2.0 m*M* L-glutamine (Gibco), 0.1% bovine serum albumin (Sigma), 100 IU/mL of penicillin, and 100 µg/mL of streptomycin (Gibco). Perform all cultures at 37°C in an air incubator.

3.1.2. Preparation of Bone Cores

1. Euthanize the animal with an overdose of barbiturate, flex the stifle, and make an incision longitudinally in the skin.
2. Deflect the kneecap to expose the trochlear groove of the distal femur. Using a trephine with a nonretractable pointed insert (slightly proud of the cutting edge), make a circular groove in the articular cartilage surface. Remove the pointed insert and take a full-depth cartilage and bone plug from the epiphysis of both left and right limbs.
3. Place each core into a cutting rig, and trim to a uniform length (1 cm).
4. Introduce the core into a syringe barrel with the nozzle portion and end removed. Flush sterile, warm phosphate-buffered saline (PBS) through the core to remove marrow from between the bony trabeculae.
5. Store cores individually in culture medium in sterile bottles at 37°C until all cores required for an experiment have been collected.

3.1.3. Loading of Bone Cores

1. Within separate flexible collars of silicone tubing (*see* **Note 7**), support each of the bone cores between a pair of milled Perspex supports, which have been drilled to allow the passage of culture medium through them and the core (*see* **Note 5**). Make sure the end face of each support is cut to be of equal diameter to the core. To create a seal between the supports and to surround the core, the internal bore of the silicone tubing should be equal to the core diameter. Hold the control channels in place on a backboard with clips.
2. Place cores into the loading apparatus (**Fig. 2**). To do this, mount the lower Perspex support onto a rigid, nonflexible, bar attached to the backboard. Connect the upper support to a pneumatically operated actuator, fixed to the backboard,
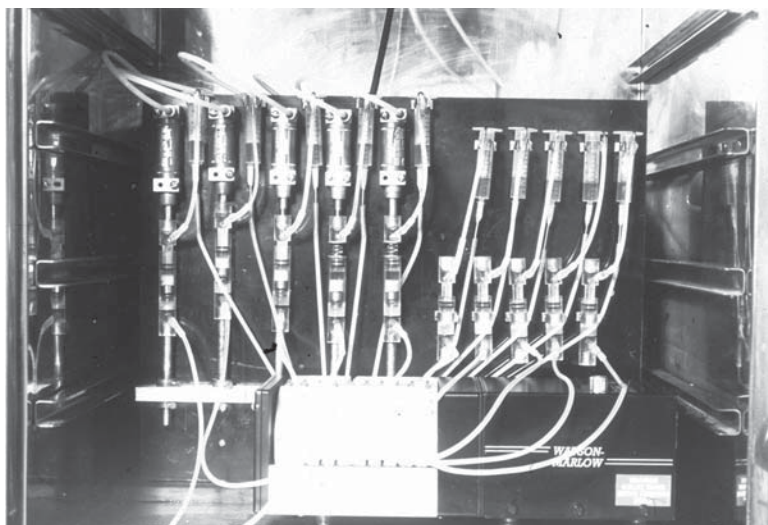
Fig. 2. Loading apparatus for bone cores.

which is operated by an air compressor unit. Introduce recirculating medium into the reservoir syringe above each core and draw through the silicone tubing, by a peristaltic pump, back to the reservoir syringe above the core (one lane per core). Controls comprise cores housed similarly in silicone tubing and Perspex supports, which are attached to the backboard with clips but remain unloaded.

3. Prior to loading, preincubate all cores for 4–5 h in a recirculating system, in which culture medium is delivered at a flow rate of 0.3 mL/min. Following this preincubation period, convert the recirculating system to single-passage perfusate mode. Refill all reservoirs and replenish continually for the remainder of the experiment for any "real time" analyses. Alternatively, retain the recirculating system as appropriate.

4. To load bone cores, regulate air pressure to deliver the same force that generates a bulk strain of 5000 $\mu\varepsilon$ in separate cores, at a loading frequency of 1 Hz.

3.2. Rat Ulnae Organ Cultures (see Note 6)

3.2.1. Reagents

1. Culture medium: Dulbecco's modified Eagle medium (DMEM) plus 10% charcoal–dextran extracted fetal calf serum, supplemented with 2.0 m*M* L-glutamine (Gibco), 100 IU/mL of penicillin, and 100 μg/mL of streptomycin (Gibco). Perform all cultures at 37°C in a humidified incubator in 5% CO_2 at 37°C. The culture medium used in these experiments depends on the conditions employed during the application of loading (*see* **Subheading 3.2.3.**).

3.2.2. Preparation of Bones for Loading

1. Dissect ulnae and clear of attendant soft tissue. Cut ulnae to equal length and remove marrow.
2. Preincubate on hand-milled polytetrafluoroethylene (PTFE) supports at the air–medium interface for 6 h in 12-well culture plates in a humidified atmosphere of 95% air–5% CO_2 at 37°C.
3. Place into one of two different loading devices (weight lifting, or pneumatic actuator; *see* **Subheading 3.2.3.** and **3.2.4.**). Following loading, remove bones from the loading apparatus and return to PTFE supports in 12-well plates for various times post-loading, depending on the response to be investigated.

3.2.3. Loading of Bones in Weight-Lifting Model

1. Ulnae are loaded in individual chambers with medium recirculating around the cortical shaft. This loading apparatus is maintained in an air incubator, so during the loading period, the culture medium is supplemented with 25 m*M* HEPES buffer.
2. Each bone is held vertically between two cups. The lower cup is connected to an eccentric cam, while the upper cup is connected to a weight-carrying platform that rests on a ledge. As the cam rotates, the bone is raised and lowered. On the up stroke, the bone acts as the sole support for the weight-carrying platform and on the down stroke the weight returns to rest upon the ledge. The amount of weight on the platform can be altered, thus permitting different levels of mechanical strain to be engendered *(12,54,55)*.
3. Following loading, remove bones from the loading apparatus and return to 12-well plates for various times post-loading, depending on the response to be investigated. Controls comprise ulnar segments, treated identically, that do not lift weights.

3.2.4. Loading of Bones in the Pneumatic Model

1. This rat ulna organ culture model maintains the tissue in a fixed volume of medium (*see* **Fig. 3**). The device consists of a milled polycarbonate block containing 10 chambers, in which five are customized to permit loading and five serve as controls; loads are applied by pneumatic actuators.
2. The bone shafts are removed from the preincubation medium and introduced into the holding cups of the loading apparatus, either in loading or control chambers each containing 4 mL of culture medium.
3. After 5 min equilibration time, bone explants are loaded axially to generate mechanical strains levels on the lateral mid-shaft, similar to those generated in vivo. Control bone shafts are not loaded.
4. After the loading period, bone shafts are transferred back to 12-well plates and cultured for various periods of time, depending on the response to be investigated *(6,44,56,57)*.

3.3. Loadable Rat Calvariae Organ Cultures

3.3.1. Materials

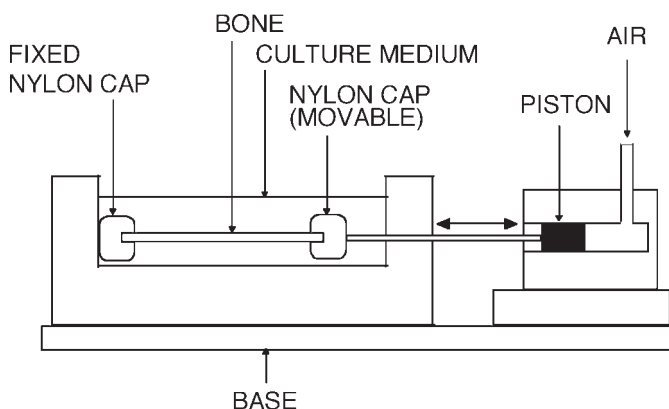The culture medium is as given in **Subheading 3.2.**

Fig. 3. Diagram of organ culture loading apparatus, showing the bone segment held between nylon caps immersed in culture medium. Oscillating air pressure in the pneumatically operated cylinders applies a dynamic load to the tissues.

3.3.2. Method

Essentially the method used is identical to that described under **Subheading 3.2.**, but an adaptation is made in the caps that hold the tissue within the apparatus *(6)*. The caps retain bones to limit uncontrolled translation. For the ulnar bone shafts these nylon caps are fashioned into cups, whereas for the parietal bone (calvariae) explants, the caps have a shallow, narrow rebate engineered to accommodate the thin, plate-like architecture of these bones.

1. Cut the parietal bones into rectangular explants and culture as described in **Subheading 3.2.**
2. To apply loads, first locate the rostral and caudal ends of the bones into the "cap" rebates, thus allowing axial loading without scope for slip.
3. Perform loading using the pneumatic actuator device (*see* **Subheading 3.2.** and **Notes 6** and **8**).
4. After the loading period, bone expalnts are transferred back to 12-well plates and cultured for various periods of time, depending on the response to be investigated.

3.4. Loading of the Chick Tibio-Tarsus (see Note 9)

3.4.1. Materials

1. Culture medium: Fitton–Jackson's modification of BGJb medium containing 2 m*M* L-glutamine, 100 IU/mL of penicillin, 100 μg/mL of streptomycin, 50 ug/mL of L-ascorbic acid, and 2% heat-inactivated fetal calf serum. Culture bone at 37°C in a humidified 5% CO_2 incubator (*see* **Subheading 3.2.**).

3.4.2. Method

3.4.2.1. PREPARATION OF BONE SEGMENTS

1. Euthanize 18-d-old embryonic White Leghorn chicks using an approved method and remove the tibiotarsi.
2. Remove adherent soft tissues and fibula, and both cartilaginous ends to leave a 9-mm bone shaft segment.
3. Aspirate the marrow, but leave the periosteum intact.
4. Wash briefly in PBS.
5. Culture bone segments at the air–medium interface on PTFE supports for 5 h.

3.4.2.2. LOADING OF BONE SEGMENTS

1. Hold the embryonic tibial bone shafts at either end by polypropylene caps, in chambers milled into a Perspex block.
2. Both "weight lifting" and "pneumatic" actuator devices *(58)* have been used to load these bones (**Subheading 3.2.**). Each device is calibrated to generate the required strain levels (*see* **Note 2**).
3. For weight-bearing induced loading, an eccentric cam (rotating at 1 Hz) is employed to raise and lower an L-shaped cradle holding the weights. The force is transferred to the bones via a pivot positioned at the right angle of the L-shaped cradle, and thus when the cradle is lowered, the tibia supports the weight of the cradle *(59,60)*. As in other models, the level of engendered strain can be altered by changing the amount of weight that is "lifted."

3.5. Long-Term Perfusion Loading Model

A recently described long-term model system designed to overcome the limited viability of previous organ explant models *(53)* may soon make significant advances in our understanding of loading-related bone formation. This system involves perfusion of trabecular bone cores, includes the marrow, and extends the lifetime of the tissue to 72 d in vitro (*see* **ref. *61***). Preliminary studies using the incorporation of fluorescent labels into newly mineralized surfaces, to provide a direct measurement of bone formation rate, have shown that these bone cores can retain their in vivo rates of bone formation for up to 20 d in vitro *(52)*. Along with the loadability of such explants in vitro, it is possible that such models will provide a means by which the cellular basis for "sensing" mechanical stimuli or "communicating" their influence to coordinate loading-induced changes in bone remodeling can be elucidated.

4. Notes

1. We highlight in **Subheading 2.** that systems for applying mechanical strain are currently, for the most part, unique to individual laboratories. This makes a detailed description of a generic device impossible. For this reason, we have given a broad account of some of the many, and various, "models" that have been used

to apply mechanical strain to isolated bone cells in vitro (*see* **Subheading 2.**). We have also tried to give some insights into their strengths and weaknesses, the materials used and the methods employed, and some of the considerations that should be taken into account when deciding which model might be chosen (*see* **Subheading 1.**). This choice clearly depends on the hypothesis that each investigator has selected to address, and is one that must take into account which mechanical consequence of loading (strain, flow, streaming potential) is being examined. Although each of these can be accurately defined, each also exhibits many components that can vary. For example, magnitude, frequency, and rate of change can be varied during mechanical strain application, and it is vital that each of these is considered prior to selecting a "model" in which bone cell responses to are to be examined. Perhaps the most obvious and pertinent of these deliberations is whether the applied stimulus falls within the physiological range. This can only be reflected upon if the variable in question has been measured directly in vivo.

2. A vital consideration for cell culture experiments is that both the substrate and culture wells should be made from biocompatible materials. Indeed, it has been found that "biocompatibility" of material positively correlates with the amount of noncollagenous matrix protein produced by cultured bone cell monolayers *(62)*. Medical grade silicone, with its high biocompatibility, is therefore a rational choice of substrate. Aclar-33C (Allied Chemical Co.) is a clear, biocompatible material that may be sectioned for electron microscopy, transmits UV light with little attenuation or scatter, and is also useful in such devices.

3. Load-strain relationships have to be determined in any new model of in vitro strain application by prior calibration. Thus, for example, plastic strips identical to those that will be used experimentally must previously have had strain gauges attached to them and loaded in a controlled manner. During load application to these substrates in vitro (and indeed loading of bone segments in organ culture), the correct force must be delivered to produce the required level (physiological or if required nonphysiological) of mechanical strain. Strain gauges cannot be attached to samples that will be used for experimental investigation; therefore it is necessary before each new device is used to establish the relationship between applied load, which can be monitored and adjusted directly, and the resultant strain, which cannot. To calculate the relationship between strain and load for plastic strips (and bone explants; *see* **Figs. 4** and **5**, *[11]*) use single-element microminiature strain gauges. Bond gauges to the test substance (or bone surface) with cyanoacrylate adhesive, ensuring that that the prewired strain gauge will detect strains along the substrate's principal strain axis. Connect gauges to a strain gauge conditioner and amplifier, in a quarter bridge configuration, and record the output voltage on a personal computer equipped with an analog to digital (A/D board) converter. Convert to strain values using a 1000 µε calibration shunt resistance built into the conditioner units. Use the recorded strain data files to assess peak strain magnitude and strain rate and determine frequency of a loading cycle.
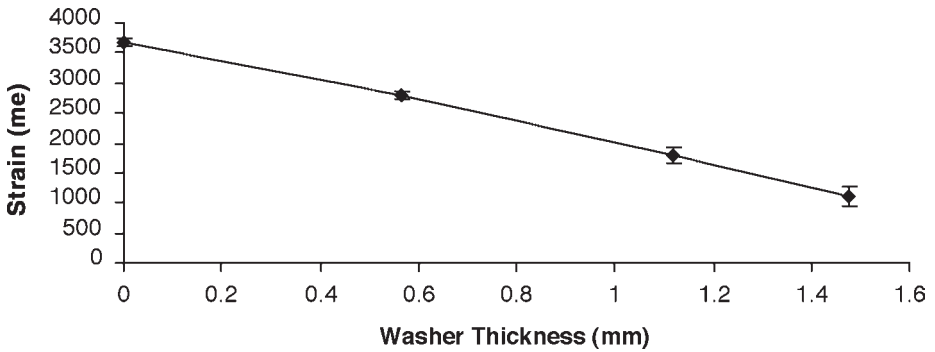
Fig. 4. Peak strain magnitude in plastic strips can be altered by changing the difference in height between the lower and upper base units in the four-point loading device.
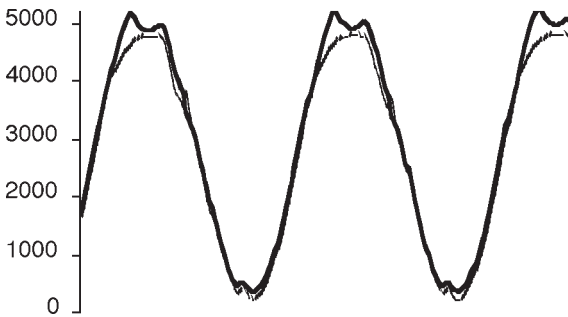

Fig. 5. Waveform of the loading generated strains in two strain gauges attached to one strip in the loading apparatus (Stromberg et al., *personal communication*).

4. Mechanical strain application results in the exposure of cells to both tensional strains, via bending of their substrate, and perturbation of their medium as a consequence of the cyclical displacement of these strips vertically through their medium. As a precaution, devices are therefore designed with flow "controls," which are included to allow identification of both flow-related and non-flow-related responses in the cells that have been exposed to mechanical strain. Examination of the cellular responses to such flow stimulation (medium perturbation) has made it clear that this often includes components of the cell's response to strain application, but that it also often induces a range of responses that are particular and specific to the application of flow itself **(45)**. Thus, it is vital that controls are included that have been subjected to similar "preparatory" changes in the medium, but that are not subjected to any form of further medium perturbation or substrate deformation (i.e., "static" controls). An essential caveat, however, in the flow "controls" included is that the precise nature of the flow

stimulus to which the cells are exposed remains, unlike in other studies (*see* the chapter by Stevens and Frangos, *this volume*), ill defined. Many other cell culture variables may also affect the cellular response to strain application. These are likely to include: the effects of changing the medium, serum deprivation, cell density, growth rate, differentiation status, and so forth. Although most devices allow the investigator to sample medium at various times after strain application, the investigations are often limited by the fact that large volumes of medium are required in such studies and by the fact it is very difficult to make direct microscopic observations in vitro.

5. Cell viability should be tested in preliminary experiments by measuring intracellular lactate dehydrogenase activity and the ability to produce cAMP in response to parathyroid hormone. (*See* chapter by Nobel and Stevens, *this volume*.) In addition, the detection of a difference between loaded and control bones indicates that the cells present in the cultures are still viable *(44,63–65)*.

6. In these experiments, medium can be supplemented with exogenous factors, such as enzyme inhibitors/activators, and their effects on the response to loading investigated. It is also possible using these systems to measure the accumulation of soluble metabolites in the medium conditioning each individual culture *(6,44,56,57)*. An important strength of such models is that they allow detailed investigation of the specific changes associated with individual cells within bone tissue. Thus, appropriate treatment (e.g., chilling tissue and preparing cryostat sections) of individual bone segments, at various times after loading, allows for the analysis of specific components of the strain response to be examined at the individual cell level by *in situ* analyses.

7. When rigid Perspex is used to surround the core, "barreling" of the core is prevented and no loading-related responses are measurable. When silicone tubing is used instead, 'barreling' of the core is allowed when loads are applied and changes in biochemical activity in the loaded compared with nonloaded cores are detected.

8. In our published studies, we first applied a 100 µε loading episode. This equates to strains that are higher than those determined in vivo, as the loading apparatus was not sensitive enough to lower the strains to physiological levels. In later experiments, loads that generated 1000 µε were applied. Although this level of strain is approx 30 times greater than physiological, the bone did not fracture, reflecting the high safety factor in such bones *(6)*.

9. This model was initially established to ascertain whether embryonic bone responded similarly to adult bone. In some experiments, the periosteum was removed to elucidate the contribution from the periosteal cells *(58)*.

Acknowledgments

F. R.). We would also like to thank Dr. Gul Zaman for his constructive and critical comments.

References

1. Bradbeer, J. N. (1992). Cell biology of bone remodelling, in *Recent Advances in Endocrinology and Metabolism* (Edwards, C. R. E. and Lincoln, D. W., eds.), Churchhill Livingstone, pp. 95–113.

2. Bonassar, L. J., Grodzinsky, A. J., Srinivasan, A., Davila, S. G., and Trippel, S. B. (2000) Mechanical and physicochemical regulation of the action of insulin-like growth factor-I on articular cartilage. *Arch. Biochem. Biophys.* **379**, 57–63.

3. Bayliss, M. T., Howat, S., Davidson, C., and Dudhia, J. (2000) The organization of aggrecan in human articular cartilage. Evidence for age-related changes in the rate of aggregation of newly synthesized molecules. *J. Biol. Chem.* **275**, 6321–6327.

4. Packer, D. L., Dombi, G. W., Yu, P. Y., Zidel, P., and Sullivan, W. G. (1994) An in vitro model of fibroblast activity and adhesion formation during flexor tendon healing. *J. Hand Surg. [Am.]* **19**, 769–776.

5. Zaman, G., Pitsillides, A. A., Rawlinson, S. C. F., et al. (1999) Mechanical strain stimulates nitric oxide production by rapid activation of endothelial nitric oxide synthase in osteocytes. *J. Bone Miner. Res.* **14**, 1123–1131.

6. Rawlinson, S. C. F., Mosley, J. R., Suswillo, R. F., Pitsillides, A. A., and Lanyon, L. E. (1995) Calvarial and limb bone cells in organ and monolayer culture do not show the same early responses to dynamic mechanical strain. *J. Bone Miner. Res.* **10**, 1225–1232.

7. Currey, J. D. (1979) Mechanical properties of bone tissues with greatly differing functions. *J. Biomech* **12**, 313–319.

8. Riggs, C. M., Lanyon, L. E., and Boyde, A. (1993) Functional associations between collagen fibre orientation and locomotor strain direction in cortical bone of the equine radius. *Anat. Embryol. (Berl.)* **187**, 231–238.

9. Rubin, C. T. and Lanyon, L. E. (1984) Regulation of bone formation by applied dynamic loads. *J. Bone Joint Surg. Am.* **66**, 397–402.

10. Turner, C. H., Akhter, M. P., Raab, D. M., Kimmel, D. B., and Recker, R. R. (1991) A noninvasive, in vivo model for studying strain adaptive bone modeling. *Bone* **12**, 73–79.

11. Mosley, J. R., March, B. M., Lynch, J., and Lanyon, L. E. (1997) Strain magnitude related changes in whole bone architecture in growing rats. *Bone* **20**, 191–198.

12. Cheng, M. Z., Zaman, G., and Lanyon, L. E. (1994) Estrogen enhances the stimulation of bone collagen synthesis by loading and exogenous prostacyclin, but not prostaglandin E2, in organ cultures of rat ulnae. *J. Bone Miner. Res.* **9**, 805–816.

13. Reich, K. M., Gay, C. V., and Frangos, J. A. (1990) Fluid shear stress as a mediator of osteoblast cyclic adenosine monophosphate production. *J. Cell Physiol.* **143**, 100–104.

14. Reich, K. M. and Frangos, J. A. (1993) Protein kinase C mediates flow-induced prostaglandin E2 production in osteoblasts. *Calcif. Tissue Int.* **52**, 62–66.

15. MacGinitie, L. A., Wu, D. D., and Cochran, G. V. (1993) Streaming potentials in healing, remodeling, and intact cortical bone. *J. Bone Miner. Res.* **8**, 1323–1335.

16. Ruoslahti, E. and Pierschbacher, M. D. (1987) New perspectives in cell adhesion: RGD and integrins. *Science* **238**, 491–497.

17. Oldberg, A., Franzen, A., and Heinegard, D. (1986) Cloning and sequence analysis of rat bone sialoprotein (osteopontin) cDNA reveals an Arg-Gly-Asp cell-binding sequence. *Proc. Natl. Acad. Sci. USA* **83**, 8819–8823.

18. Oldberg, A., Franzen, A., and Heinegard, D. (1988) The primary structure of a cell-binding bone sialoprotein. *J. Biol. Chem.* **263**, 19430–19432.

19. Zimmerman, D., Jin, F., Leboy, P., Hardy, S., and Damsky, C. (2000) Impaired bone formation in transgenic mice resulting from altered integrin function in osteoblasts. *Dev. Biol.* **220**, 2–15.

20. Gronthos, S., Stewart, K., Graves, S. E., Hay, S., and Simmons, P. J. (1997) Integrin expression and function on human osteoblast-like cells. *J. Bone Miner. Res.* **12**, 1189–1197.

21. Cowles, E. A., Brailey, L. L., and Gronowicz, G. A. (2000) Integrin-mediated signaling regulates AP-1 transcription factors and proliferation in osteoblasts. *J. Biomed. Mater. Res.* **52**, 725–737.

22. Flores, M. E., Heinegard, D., Reinholt, F. P., and Andersson, G. (1996) Bone sialoprotein coated on glass and plastic surfaces is recognized by different beta 3 integrins. *Exp. Cell Res.* **227**, 40–46.

23. Collin-Osdoby, P., Nickols, G. A., and Osdoby, P. (1995) Bone cell function, regulation, and communication: a role for nitric oxide. *J. Cell Biochem.* **57**, 399–408.

24. Doty, S. B. (1981) Morphological evidence of gap junctions between bone cells. *Calcif. Tissue Int.* **33**, 509–512.

25. Schiller, P. C., Ippolito, G., Balkan, W., Roos, B. A., and Howard, G. A. (2001) Gap-junctional communication is required for the maturation process of osteoblastic cells in culture. *Bone* **28**, 362–369.

26. Aarden, E. M., Nijweide, P. J., van der Plas, A., et al. (1996) Adhesive properties of isolated chick osteocytes in vitro. *Bone* **18**, 305–313.

27. Garcia-Cardena, G., Fan, R., Shah, V., et al. (1998) Dynamic activation of endothelial nitric oxide synthase by Hsp90. *Nature* **392**, 821–824.

28. Das, P., Schurman, D. J., and Smith, R. L. (1997) Nitric oxide and G proteins mediate the response of bovine articular chondrocytes to fluid-induced shear. *J. Orthop. Res.* **15**, 87–93.

29. Binderman, I., Shimshoni, Z., and Somjen, D. (1984) Biochemical pathways involved in the translation of physical stimulus into biological message. *Calcif. Tissue Int.* **36** (Suppl. 10, S82–S85.

30. Hasegawa, S., Sato, S., Saito, S., Suzuki, Y., and Brunette, D. M. (1985) Mechanical stretching increases the number of cultured bone cells synthesizing DNA and alters their pattern of protein synthesis. *Calcif. Tissue Int.* **37**, 431–436.

31. Basdra, E. K., Kohl, A., and Komposch, G. (1996) Mechanical stretching of periodontal ligament fibroblasts—a study on cytoskeletal involvement. *J. Orofac. Orthop.* **57**, 24–30.

32. Vandenburgh, H. H. (1988) A computerized mechanical cell stimulator for tissue culture: effects on skeletal muscle organogenesis. *In Vitro Cell Dev. Biol.* **24**, 609–619.

33. Soma, S., Matsumoto, S., and Yamamoto, T. (1997) Enhancement by conditioned

medium of stretched calvarial bone cells of the osteoclast-like cell formation induced by parathyroid hormone in mouse bone marrow cultures. *Arch. Oral Biol.* **42**, 205–211.

34. Andersen, K. L. and Norton, L. A. (1991) A device for the application of known simulated orthodontic forces to human cells in vitro. *J. Biomech.* **24**, 649–654.

35. Matsuo, T., Uchida, H., and Matsuo, N. (1996) Bovine and porcine trabecular cells produce prostaglandin F2 alpha in response to cyclic mechanical stretching. *Jpn. J. Ophthalmol.* **40**, 289–296.

36. Banes, A. J., Gilbert, J., Taylor, D., and Monbureau, O. (1985) A new vacuum-operated stress-providing instrument that applies static or variable duration cyclic tension or compression to cells in vitro. *J. Cell Sci.* **75**, 35–42.

37. Winston, F. K., Macarak, E. J., Gorfien, S. F., and Thibault, L. E. (1989) A system to reproduce and quantify the biomechanical environment of the cell. *J. Appl. Physiol.* **67**, 397–405.

38. Jones, D. B., Leivseth, G., Sawada, Y., van der Sloten, J., and Bingmann, D. (1994). Application of homogenous, Defined strains to cell cultures, in *Biomechanics and Cells* (Lyall, R. and El-Haj, A. J., eds.), Cambridge University Press, Cambridge, UK, pp. 197–219.

39. Brighton, C. T., Strafford, B., Gross, S. B., Leatherwood, D. F., Williams, J. L., and Pollack, S. R. (1991) The proliferative and synthetic response of isolated calvarial bone cells of rats to cyclic biaxial mechanical strain. *J. Bone Joint Surg. Am.* **73**, 320–331.

40. Fermor, B., Gundle, R., Evans, M., Emerton, M., Pocock, A., and Murray, D. (1998) Primary human osteoblast proliferation and prostaglandin E2 release in response to mechanical strain in vitro. *Bone* **22**, 637–643.

41. Murray, D. W. and Rushton, N. (1990) The effect of strain on bone cell prostaglandin E2 release: a new experimental method. *Calcif. Tissue Int.* **47**, 35–39.

42. Grabner, B., Varga, F., Glantschnig, H., et al. (1999) A new in vitro system for applying uniaxial strain on cell cultures. *Calcif. Tissue Int.* **64** (Suppl. 1), S114.

43. Jones, D. B., Nolte, H., Scholubbers, J. G., Turner, E., and Veltel, D. (1991) Biochemical signal transduction of mechanical strain in osteoblast-like cells. *Biomaterials* **12**, 101–110.

44. Pitsillides, A. A., Rawlinson, S. C. F., Suswillo, R. F., Bourrin, S., Zaman, G., and Lanyon, L. E. (1995) Mechanical strain-induced NO production by bone cells: a possible role in adaptive bone (re)modeling? *FASEB J.* **9**, 1614–1622.

45. Jessop, H. L., Sjoberg, M., Cheng, M. Z., Zaman, G., Wheeler-Jones, C. P., and Lanyon, L. E. (2001) Mechanical strain and estrogen activate estrogen receptor alpha in bone cells. *J. Bone Miner. Res.* **16**, 1045–1055.

46. Zaman, G., Cheng, M. Z., Jessop, H. L., White, R., and Lanyon, L. E. (2000) Mechanical strain activates estrogen response elements in bone cells. *Bone* **27**, 233–239.

47. Cheng, M. Z., Zaman, G., Rawlinson, S. C. F., Mohan, S., Baylink, D. J., and Lanyon, L. E. (1999) Mechanical strain stimulates ROS cell proliferation through IGF-II and estrogen through IGF-I. *J. Bone Miner. Res.* **14**, 1742–1750.

48. Zaman, G., Suswillo, R. F., Cheng, M. Z., Tavares, I. A., and Lanyon, L. E. (1997) Early responses to dynamic strain change and prostaglandins in bone-derived cells in culture. *J. Bone Miner. Res.* **12**, 769–777.

49. Tanaka, S. M. (1999) A new mechanical stimulator for cultured bone cells using piezoelectric actuator. *J. Biomech.* **32**, 427–430.

50. Lanyon, L. E. and Rubin, C. T. (1984) Static vs dynamic loads as an influence on bone remodelling. *J. Biomech.* **17**, 897–905.

51. Rubin, C. T. and Lanyon, L. E. (1985) Regulation of bone mass by mechanical strain magnitude. *Calcif. Tissue Int.* **37**, 411–417.

52. Smith, E. L., Martens, F., Koller, K., Clark, W., and Jones, D. B. (2000) The effects of 20 days of mechanical loading plus PTH on the E-modulus of cow trabecular bone. *J. Bone Miner. Res.* **15** (Suppl. 1), S247.

53. Walker, L. M., Preston, M. R., Magnay, J. L., Thomas, P. B., and El-Haj, A. J. (2001) Nicotinic regulation of c-fos and osteopontin expression in human-derived osteoblast-like cells and human trabecular bone organ culture. *Bone* **28**, 603–608.

54. Cheng, M. Z., Zaman, G., Rawlinson, S. C. F., Pitsillides, A. A., Suswillo, R. F., and Lanyon, L. E. (1997) Enhancement by sex hormones of the osteoregulatory effects of mechanical loading and prostaglandins in explants of rat ulnae. *J. Bone Miner. Res.* **12**, 1424–1430.

55. Cheng, M. Z., Zaman, G., Rawlinson, S. C. F., Suswillo, R. F., and Lanyon, L. E. (1996) Mechanical loading and sex hormone interactions in organ cultures of rat ulna. *J. Bone Miner. Res.* **11**, 502–511.

56. Rawlinson, S. C. F., Pitsillides, A. A., and Lanyon, L. E. (1996) Involvement of different ion channels in osteoblasts' and osteocytes' early responses to mechanical strain. *Bone* **19**, 609–614.

57. Rawlinson, S. C. F., Wheeler-Jones, C. P., and Lanyon, L. E. (2000) Arachidonic acid for loading induced prostacyclin and prostaglandin E(2) release from osteoblasts and osteocytes is derived from the activities of different forms of phospholipase A(2). *Bone* **27**, 241–247.

58. Pitsillides, A. A., Rawlinson, S. C. F., Mosley, J. R., and Lanyon, L. E. (1999) Bone's early responses to mechanical loading differ in distinct genetic strains of chick: selection for enhanced growth reduces skeletal adaptability. *J. Bone Miner. Res.* **14**, 980–987.

59. Dallas, S. L., Zaman, G., Pead, M. J., and Lanyon, L. E. (1993) Early strain-related changes in cultured embryonic chick tibiotarsi parallel those associated with adaptive modeling in vivo. *J. Bone Miner. Res.* **8**, 251–259.

60. Zaman, G., Dallas, S. L., and Lanyon, L. E. (1992) Cultured embryonic bone shafts show osteogenic responses to mechanical loading. *Calcif. Tissue Int.* **51**, 132–136.

61. http://www.med.uni-marburg.de/eobm/redbaron.html

62. Jones, D. B. and Scholubbers, J. G. (1987) Evidence that phospholipase C mediates the mechanical stress effect in bone. *Calcif. Tissue Int.* **41**, 4.

63. El-Haj, A. J., Minter, S. L., Rawlinson, S. C. F., Suswillo, R. F. L., and Lanyon, L. E. (1990) Cellular responses to mechanical loading in vitro. *J. Bone Miner. Res.* **5**, 923–932.

64. Rawlinson, S. C. F., El-Haj, A. J., Minter, S. L., Tavares, I. A., Bennett, A., and Lanyon, L. E. (1991) Loading-related increases in prostaglandin production in cores of adult canine cancellous bone in vitro: a role for prostacyclin in adaptive bone remodeling? *J. Bone Miner. Res.* **6**, 1345–1351.

65. Rawlinson, S. C. F., Mohan, S., Baylink, D. J., and Lanyon, L. E. (1993) Exogenous prostacyclin, but not prostaglandin E2, produces similar responses in both G6PD activity and RNA production as mechanical loading, and increases IGF-II release, in adult cancellous bone in culture. *Calcif. Tissue Int.* **53**, 324–329.

30

Extraction of Nucleic Acids from Bone

Tracy L. Stewart and Val Mann

1. Introduction

Nucleic acids can be extracted from bone for the analysis of gene expression, to look for somatic mutations in analysis of tumors or other pathological tissue, or for genotyping archive material when other sources of DNA are not available. Several methods have been described for the extraction of DNA and RNA from tissues *(1–4)*, and several kits based on these methods are currently available from biotech companies. If you are extracting DNA from a large number samples, however, it is probably cost effective to use a homemade method as described here. Successful extraction of nucleic acids from tissue is based on four procedures: disrupting the tissue so that extraction reagents can reach the cells; disrupting the cell membranes so that nucleic acids are liberated; separation of the nucleic acid from other cellular components; and precipitation and solubilization of the nucleic acid.

2. Materials (*see* Note 1)
2.1. Equipment

1. Cryogenic mill to pulverize bone samples (Glen Creston, Middlesex, UK).
2. Sterile scalpels, scissors, and bone cutters.
3. Sterile 35-mm tissue culture plates.

2.2. For DNA Extraction

1. DNA extraction buffer: Add 17.6 mL of 0.75 M sodium citrate, pH 7.0, 26.4 mL of 10% sodium lauryl sarkosyl, and 250 g of guanidinium isothiocyanate to 293 mL of distilled water and mix well. Add 7.2 µL of β-mercaptoethanol/mL of lysis buffer on the day of use (*see* **Note 2**).

2. Fumed silica: Required for DNA extraction from dried or embedded bone (*see* **Subheading 3.3.**).

   a. Suspend 50 g of unfumed silica (Sigma) in 100 mL of double-distilled water. Stir for 1 h and allow to settle under gravity for 1 h.
   b. Aspirate the supernatant and centrifuge at 6000g for 10 min to pellet the glass. Resuspend the pellet in 25–30 mL of double-distilled H_2O.
   c. Add concentrated nitric acid to 50%. Bring to a boil in a fume hood and allow to cool.
   d. Pellet the silica by centrifugation at 6000*g* for 10 min.
   e. Wash the pellet with double-distilled water until the pH of the supernatant is 7.0.
   f. Store the pellet as 50% slurry in double-distilled H_2O (*see* **Note 3**).

3. Silica wash buffer: Add 157.6 mg of Tris-HCl and 70.92 g of guanidinium isothiocyanate to 100 mL of distilled water.

2.3. For RNA Extraction

1. Tris-saturated phenol, pH 7.8–8.0 (Sigma).
2. Hoechst 33258. For DNA quantitation.
3. RNA extraction buffer: RNAzolB™ (AMS Biotechnology).

2.4. General Reagents

1. Diethylpyrocarbonate (DEPC)-treated water: Add DEPC to distilled water to a final concentration of 0.1% and incubate at 37°C for 12 h; inactivate the DEPC by autoclaving.
2. Ethidium bromide (10 mg/mL) Dissolve 100 mg ethidium bromide in 10 mL of distilled water. Store at room temperature in a bijoux or universal container and protect from light by wrapping in aluminum foil.
3. Chloroform.
4. Ethanol, 75% and 100%.
5. Isopropanol, 100%.
6. 0.5 *M* ETDA: Add 93.05 g of EDTA to 300 mL of distilled water and add 10 *N* NaOH to pH 8.0. Make up to 500 mL. Autoclave.
7. 1 *M* Tris: Add 212 g of Tris base to 800 mL of distilled water. Adjust to pH 8.0 with concentrated HCl. Make up to 1 L with distilled water. Autoclave.
8. Tris–EDTA: Add 1 mL of 1 *M* Tris to 200 µL of 0.5 *M* EDTA. Make up to 100 mL with distilled water.
9. 3 *M* Sodium acetate, pH 5.2: Add 401.8 g of sodium acetate to 800 mL of distilled water. Adjust pH to 5.1 with glacial acetic acid. Make up to 1 L with distilled water. Autoclave.

3. Methods

3.1. DNA Extraction from Fresh Bone

The method detailed below enables extraction of genomic DNA fragments (up to 80 Kb) from fresh or freshly frozen bone that contains marrow, and the

majority of DNA will actually be derived from the marrow cells. Since all genomic DNA is equal this is only a problem if a somatic mutation in bone cells is investigated.

1. Collect the bone sample in a sterile container containing phosphate-buffered saline (PBS) and transport to the laboratory within 1–2 h (*see* **Note 4**).
2. Place the bone tissue in a clean glass Petri dish. Using bone cutters or a strong sharp pair of scissors, isolate a piece of bone measuring about 1 cm^3 and transfer to a clean 5-mL bijoux container.
3. Add 1 mL of DNA extraction buffer and homogenize the tissue with the scissors until a slurry is obtained.
4. Transfer 500 µL aliquots of slurry into screw-capped conical-bottomed 1.5-mL Eppendorf tubes.
5. Add one volume of Tris-saturated phenol, followed by one volume of chloroform per tube. Mix well by inverting the tubes a few times or by shaking. Do not vortex (*see* **Note 5**).
6. Centrifuge the tubes at 10,000*g* for 20 min to separate the phases.
7. Transfer the upper layer to a fresh centrifuge tube (taking note of the volume), being careful not to disturb the milky layer at the interface. Repeat **steps 5–7** if the interface is disturbed.
8. Add one volume of ice-cold isopropanol and 0.1 volumes of 3 *M* sodium acetate to the supernatant. Mix well and allow to stand for 15 min on ice.
9. Centrifuge the tubes at 10,000*g* for 20 min to pellet the DNA (*see* **Note 6**).
10. Aspirate and discard the supernatant, taking care not to disturb the pellet. Wash the sample with 1.75 mL of ice-cold ethanol and centrifuge at 10,000*g* for 5 min. Aspirate and discard the supernatant and then repeat the wash.
11. Dissolve the DNA pellets in 10–50 µL of water or Tris–EDTA buffer (you can pool DNA from the same sample at this stage) and quantitate by spectrophotometry or with Hoechst 33258 (*see* **Note 7**).
12. Store the sample frozen at –20°C or below.

3.2. DNA Extraction from Cultured Cells

Extraction of DNA from a cultured cell layer does not require a homogenized step since the cells will be lysed by the salt and detergent in the lysis buffer.

1. Remove the medium from the cultured cells and discard.
2. Wash the cell layer with sterile PBS, aspirate, and discard. Repeat once.
3. Add 1 mL of DNA extraction buffer per T-75 flask of cells. Swirl the lysis buffer around the flask so that all cells are coated. Leave for 1 min, and detach the cells using a cell scraper.
4. Transfer the extracted cell layer into screw-capped conical-bottomed 1.5-mL Eppendorf tubes in 500-µL aliquots. Pipet the mixture up and down to break up the cells.
5. Follow **steps 5–12** of the extraction procedure described in **Subheading 3.1.**

3.3. DNA Extraction from Dried or Embedded Bone

Dried bone, e.g., archeological samples, contain little cellular material and the following method is more suitable for these specimens. Be aware that the majority of DNA obtained will be mitochondrial DNA. The technique relies on the propensity of nucleic acids to adsorb to silica *(5)*. Kits based upon this methodology are available, e.g., Silica Adsorption Kit (Roche, East Sussex, UK).

1. Homogenize the bone sample with a liquid nitrogen cooled powder mill or manually by cooling the specimen with liquid nitrogen and then grinding to a fine powder in a mortar and pestle or an electric food grinder. *See also* Fig. 3 in the chapter by Ireland, *this volume*.
2. Add 500 µL of DNA extraction buffer to a clean Eppendorf tube and place on ice. Carefully add 100–500 mg of bone powder to the extraction buffer, ensuring that it moistens all the powder.
3. Place the sample on an end-over-end rotator in a cold room for 24 h.
4. Centrifuge the sample at 10,000*g* for 5 min in a microcentrifuge to pellet the bone powder. Collect the supernatant, containing the DNA, and pipet into a fresh Eppendorf tube.
5. Add 50 µL of fumed silica to the supernatant. Place on an end-over-end rotator in a cold room for 1 h.
6. Pellet the silica (which contains the adsorbed DNA *[5]*) by centrifugation at 6000*g* for 5 min and discard the supernatant (*see* **Note 8**).
7. Add 1 mL of silica wash buffer to the pellet and invert a couple of times to resuspend the silica. Centrifuge at 6000*g* for 5 min and discard the supernatant.
8. Resuspend the pellet in 95% ethanol (to remove salt contamination) and mix by inverting two or three times (*see* **Note 9**). Centrifuge at 6000*g* for 5 min and discard the supernatant.
9. Repeat **step 8**.
10. Elute the DNA from the silica by resuspending the pellet in up to 100 µL of either 10 m*M* Tris HCl, pH 8.0, or distilled deionized water, pH >7.5 *see* **Note 10**).
11. Incubate the sample at 56°C for 10 min. Centrifuge at 6000*g* for 5 min to pellet the silica and aspirate the supernatant (which contains the DNA) into a fresh tube and store frozen at –70°C or below.

3.4. RNA Extraction from Fresh Bone

The method given here uses RNAzolB™ reagent, but the same method can be used with TRIzol® reagent, allowing isolation of both RNA and DNA from the same sample (*see also* the chapter by Ireland, *this volume*).

1. Collect the bone sample in a sterile container containing PBS and transport to the laboratory within 30 min (*see* **Note 11**).
2. Wearing gloves, place a 1-cm^3 sample of bone tissue into a 35-mm sterile Petri dish using sterile forceps (*see* **Note 12**).

3. Add 1.5–1.75 mL of RNAzolB solution to the sample and chop the tissue up into a coarse slurry using bone cutters or scissors. Using a sterile scalpel, finely divide the sample further until it forms a smooth homogenate.

4. Carefully transfer up to 1.5 mL/tube of homogenate into a 2-mL screw-cap Eppendorf tube and place on ice.

5. Add 0.1 volume of chloroform per tube and shake vigorously for 15 sec. Place on ice for 5 min.

6. Centrifuge at 10,000*g* for 20 min at 4°C.

7. Carefully aspirate the upper layer (taking note of the volume) into a fresh 1.5-mL conical bottom screw-top Eppendorf tube, taking care not to disturb the interface (*see* **Note 13**).

8. Add one volume of ice-cold isopropanol and mix gently by inverting the tube five or six times.

9. Place the sample on ice for 15 min to precipitate the RNA (*see* **Note 14**).

10. Centrifuge at 10,000*g* for 15 min at 4°C to pellet the RNA (*see* **Note 15**). Aspirate and discard the supernatant.

11. Wash the pellet with 1 mL of ice-cold 75% ethanol and centrifuge at 10,000*g* for 5 min at 4°C. Aspirate and discard the supernatant.

12. Repeat **step 11**.

13. Allow the pellet to air-dry (3–5 min). Do not over-dry the pellet.

14. Dissolve the RNA in 50 μL DEPC-treated distilled water (adjust volume according to sample size).

15. Quantitate and assess purity of the RNA by spectrophotometry and/or gel electrophoresis (*see* **Note 16** and **Fig. 1**). Typical yields of RNA from cells and tissues are shown in **Table 1**.

16. Store the RNA at –70°C until use.

3.5. Extraction of RNA from Frozen Bone

If the sample has been stored at –70°C it can be ground to a fine powder prior to the extraction protocol, either in a cryogenic mill (Glen Creston, Middlesex, UK) or by mortar and pestle (*see also* Fig. 3 in the chapter by Ireland, *this volume*).

1. Pulverize the sample to a fine powder using a cryogenic mill or mortar and pestle (*see* **Note 17**).

2. Transfer the powder into a 2-mL Eppendorf tube, add 1.5–1.75 mL of RNAzolB, mix well by shaking the tube vigorously, and place on ice.

3. Proceed through **steps 5–16** of the RNA extraction procedure described in **Subheading 3.4.**

3.6. Extraction of RNA from Cultured Cells

1. Aspirate the medium from the cell culture and discard.

2. Wash the cells with 10 mL of sterile PBS and discard.

3. Add 1.5 mL of RNAzolB per T-75 flask of cells and allow to spread over the cell layer. For cells in suspension, *see* **Note 18**.
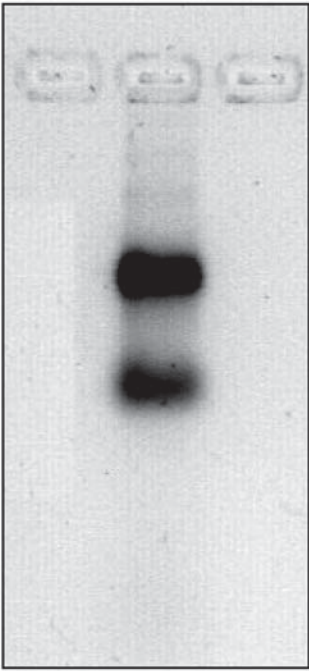
Fig. 1. Gel electrophoresis of RNA extracted from bone. bands corresponding to the 285S and 185S units of ribosomal RNA should be clearly visible.

Table 1
Typical Yields of Total RNA Extracted Using the Described
Method from Either Tissue or In Vitro Cell Cultures

Sample	OD $_{260\,nm}$	OD $_{280\,nm}$	Ratio $_{260/280}$	RNA (μg)
1 cm^3 Bone biopsy	0.0374	0.0197	1.89	37.4
Confluent T75 flask	0.253	0.147	1.76	39

4. Scrape cells using a cell scraper and aspirate the resulting slurry into a 2.0-mL Eppendorf tube.
5. Pipet the slurry up and down through a p1000 to lyse the cells.
6. Proceed through **steps 5–15** of the RNA extraction procedure described in **Subheading 3.4.**

4. Notes

1. Safety: The methods described involve use of mercaptoethanol, chloroform, and phenol and should be carried out in a fume hood to minimize exposure to these solvents. DEPC is a suspected carcinogen and appropriate precautions in han-

dling it should be taken. We recommend purchase of ethidium bromide in liquid to minimize exposure to this mutagen.

2. All chemicals should be of molecular biology grade. The solutions can be stored at 4°C for up to 3 mo.

3. Working stocks can be stored for up to 1 wk at 4°C. Store stocks frozen at –70°C.

4. If the DNA extraction is not initiated immediately, freeze the sample at –20°C or below for later use.

5. Vortex-mixing causes long strands of DNA to shear.

6. Orientate the Eppendorf tube so that you can identify where the DNA pellet lies. A pellet should be visible the bottom of the tube.

7. Dilute the sample 1:200 for DNA and 1:100 for RNA in distilled water and read the absorbance at 260 nm and 280 nm using a quartz cuvette in a UV spectrophotometer. Hoechst 33258 is a DNA-specific dye that can be used to quantitate DNA. Quantification is achieved by setting up a standard curve of DNA at known concentrations (purchase stock with known concentrations) and analyzing the test samples in a fluorimeter at an excitation wavelength of 350–363 nm and a detection wavelength of 410–480 nm. Another dye useful for high-throughput applications is PicoGreen®. The integrity of DNA and RNA can be checked by PCR for a housekeeping gene.

8. You may wish to keep the supernatant in a fresh tube until you are confident that the extraction has been successful.

9. Do not simply add the ethanol and immediately decant it off again; the pellet needs to be well mixed so that the ethanol can penetrate the sample and dissolve the salt.

10. The pH must be above 7.5 to elute the DNA from the silica.

11. A major challenge in extracting RNA from any tissue bone is to isolate the nucleic acid in an intact state before it is degraded. If it is impractical to begin the extraction within 30 min, the bone should be snap frozen in liquid nitrogen immediately and stored at -70°C or below until use.

12. All procedures should be carried out wherever possible in an RNase-free environment. Gloves should be worn at all times when handling samples and frequently changed after handling samples, and all solutions should be prepared to ensure that they are free of RNases. This involves making up the solutions for RNA use with DEPC-treated water using glassware, stirrers and spatulas that have been oven baked for 2 h to inactivate RNases. If possible a separate room or area within the laboratory should be dedicated to RNA work and dedicated sets of pipets purchased. Surfaces should be routinely cleaned with RNase-inactivation reagents such as RNase-Away™ (Fisher Scientific, Leicestershire, UK). The use of RNase-free disposable plasticware and filtertips is recommended. Further details can be found in Sambrook's text *(6)*.

13. The upper (clear) aqueous layer contains the RNA and is separated from lower (blue) phase containing debris and DNA by a white layer containing protein and lipids.

14. The samples can be stored overnight at –20°C at this point. Addition of glycogen (20 µg/tube; Boeringer Mannheim) can improve precipitation of small amounts of RNA and help in identification of the pellet (*see* **Note 15**).

15. It is a good idea to mark the side of the Eppendorf tube so you can identify where the RNA pellet lies.

16. If the RNA is pure, the optical density reading at 260 nm/280 nm should be 1.8 or greater. If spectrophotometry readings indicate that the RNA is not of the desired purity add 1.5 mL of RNAzolB to the RNA solution, mix well, and reextract by repeating **steps 5–15**. We perform such double extractions routinely on bone biopsies. DNase treatment can be performed to remove any contaminating genomic DNA prior to RT-PCR. We use DNase I amplification grade (Invitrogen). Follow manufacturer's instructions.

17. A small amount of liquid nitrogen can be poured into the pestle to maintain low temperature.

18. For cells in suspension, pellet the cells by centrifugation at 400g for 10 min, aspirate the medium, and discard. Suspend the pellet in 1.5 mL of RNAzolB, by aspirating up and down using a p1000 pipet tip and proceed through **steps 5–15** of the extraction described in **Subheading 3.4.**

References

1. Chomczynski, P. and Sacchi, N. (1987) Single step method of RNA isolation by acid guanidinium thiocyanate-phenol-chloroform extraction. *Analyt. Biochem.* **162**, 156–159.

2. Blin, N. and Stafford, D. W. (1976) A general method for isolation of high molecular weight DNA from eukaryotes. *Nucl. Acid Res.* **3**, 2303–2308.

3. Kupiec, J. J., Giron, M. L., Vilette, D., Jeltsch, J. M., and Emanoil-Ravier, R. (1987) Isolation of high molecular weight DNA from eukaryotic cells by formamide treatment and dialysis. *Analyt. Biochem.* **164**, 53–59.

4. Bowtell, D. D. L. (1987) Rapid isolation of eukaryotic DNA. *Analyt. Biochem.* **162**, 463–465.

5. Vogelstein, B. and Gillespie, D. (1979) Preparative and analytical purification of DNA from agarose. *Proc. Natl. Acad. Sci. USA* **76**, 615–619.

6. Sambrook, J., Fritsch, E. F., and Maniatis, T. (2000) *Molecular Cloning: A Laboratory Manual*, 3rd edit. Cold Spring Harbor Laboratory Press, Cold Spring Harbor, NY.

31

Analysis of Gene Expression in Bone by Quantitative RT-PCR

Deborah Ireland

1. Introduction

1.1. RNA Isolation

The isolation of undegraded RNA, free from inhibitors of reverse transcription-polymerase chain reaction (RT-PCR), is a major technical challenge in the analysis of gene expression in the skeleton. Bone is a mineralized tissue containing an abundant matrix, which makes RNA isolation difficult. On the positive side, however, frozen bone is quite brittle and can be ground to a powder, thus releasing the cell contents. Reno and colleagues *(1)* evaluated 12 different protocols for isolating total RNA from small amounts of rabbit ligament, cartilage, and tendon using phenol–guanidinium-based reagents. Like bone, these tissues contain few cells in an abundant organic matrix. Absence of ribosomal bands, nondetection of glyceraldehyde-3-phosphate dehydrogenase (GAPDH) mRNA on Northern blotting, presence of DNA and/or protein contamination, and insoluble RNA pellets generated by these procedures led to the development of the Trispin method, based on a combination of two commercially available kits *(2)*. In this procedure, the tissue is powdered in a stainless steel ball mill vessel that is cooled in liquid nitrogen. We have used a ball mill and modified Trispin method to extract high-quality, RT-PCR-ready RNA from bone samples.

1.2. Quantitation of Gene Expression

The small quantities of RNA that can be obtained from bone biopsies make quantitative RT-PCR an appropriate technique for gene expression studies. Several quantification strategies can be used but real-time fluorescence-based RT-PCR has the advantage that it allows measurements to be performed over a
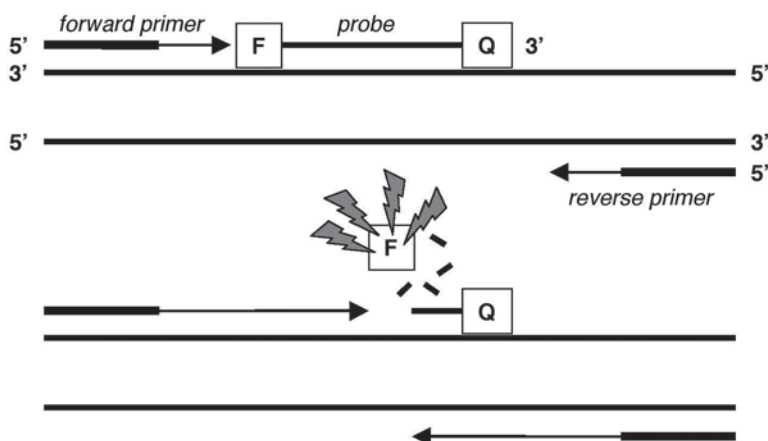
Fig. 1. Generation of reporter fluorescence by the 5' nuclease activity of *Taq* polymerase on a TaqMan® probe during DNA amplification. The reporter dye is released from the annealed probe during extension of the forward primer. Fluorescence is measured during each PCR cycle.

wide range of RNA concentrations with no post-amplification steps. Reaction mixtures contain amplification primers and an internal probe, which is labeled at the 5' end with a reporter dye and at the 3' end with a quencher molecule that suppresses reporter fluorescence in the intact probe. The 3' end of the probe is blocked to prevent extension during PCR. The 5' exonuclease activity of *Taq* DNA polymerase cleaves the reporter dye from the annealed probe during amplification primer extension, resulting in increased fluorescence (**Fig. 1**). Fluorescence is measured at each PCR cycle and the number of cycles needed to reach a threshold level (C_t) determined. Dilutions of standard RNA are used to generate a standard curve by plotting C_t against log standard RNA concentration (**Fig. 2**). Relative or absolute concentrations of sample RNAs can then be calculated from the curve.

2. Materials
2.1. RNA Extraction and Solubilization (see Note 1)

1. Mikro-Dismembrator S ball mill (B. Braun Biotech International, Melsungen, Germany) for grinding frozen bone samples.
2. A 5-mL stainless steel ball mill vessel containing a 10-mm steel/chrome grinding ball.
3. Stainless steel tray.
4. Two small dishes suitable for holding liquid nitrogen.
5. Small stainless steel hammer for crushing bone.
6. Aluminum foil.
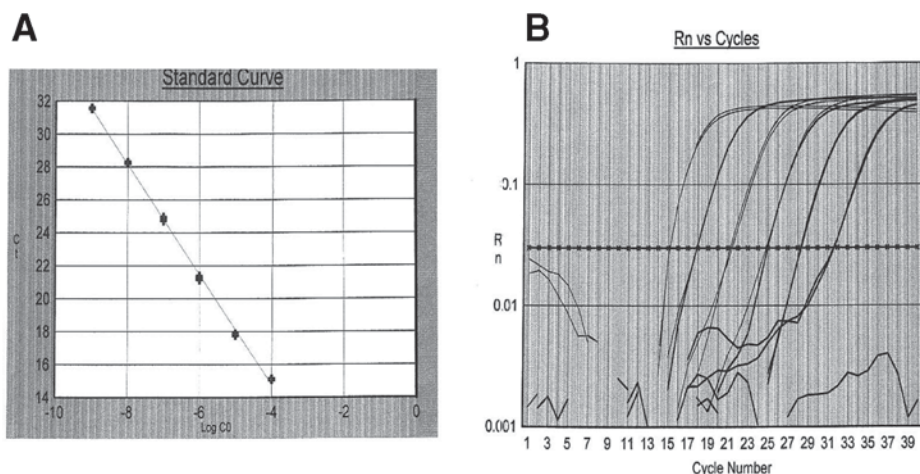7. Forceps for handling the bone and bone fragments.

Fig. 2. TaqMan® plots of log fluorescence against cycle number for 10-fold dilutions of in vitro transcribed mRNA (**A**) and threshold cycle number (C_t) against log RNA concentration (**B**). The threshold level is chosen to be in the middle of the linear range.

8. TRIZOL® (Invitrogen, Paisley, Scotland) or a homemade monophasic reagent (PIG-B) prepared according to Weber et al. *(2)* for solubilizing total RNA from powdered bone.
9. Liquid nitrogen for freezing the bone sample.

2.2. RNA Purification and Quantitation

1. Chloroform (Analar grade).
2. SV Total RNA isolation kit (Promega, Southampton, UK).
3. NAP-5 columns containing Sephadex G-25 (Amersham Pharmacia Biotech UK Ltd., Little Chalfont) for removing RT-PCR inhibitors.
4. 2 *M* Sodium acetate solution, pH 4.5.
5. Ethanol: 95% and 75%.
6. Spectrophotometer to check optical density readings.
7. RiboGreen reagent (Molecular Probes, Inc.).

2.3. Primer Design

1. Primer Express™ software package (Applied Biosystems, Warrington, UK), for primer and probe design.

2.4. Preparation of In Vitro Transcribed RNA Standards

1. Thermal cycler for generating PCR products.
2. Custom oligonucleotide primers.
3. TA cloning kit (pCR®II TOPO—Invitrogen, Paisley, Scotland) for cloning PCR products for in vitro transcription.

4. Wizard Plus SV Minipreps DNA purification system.
5. SP6/T7 RNA polymerases for making mRNA standards.
6. Microspin S-300 HR columns (Amersham Pharmacia Biotech UK Ltd., Little Chalfont) for purifying in vitro transcribed mRNA.
7. Molecular Probes RiboGreen™ kit (Cambridge Bioscience, Cambridge, UK) for quantifying RNA.

2.5. Real-Time Fluorescence-Based Quantitative RT-PCR

1. Gene Amp® 5700 Sequence Detection System (Applied Biosystems, Warrington, UK).
2. Custom oligonucleotide primers (Invitrogen, Paisley, Scotland).
3. Labeled probes (Applied Biosystems, Warrington, UK).
4. TaqMan® One-Step RT-PCR Master Mix Reagents Kit (Applied Biosystems, Warrington, UK).

3. Methods
3.1. Pulverizing the Bone Sample

An overview of the procedure is depicted in **Fig. 3**.

1. Assemble the apparatus and cool the ball mill vessel and bone sample for several min by placing in a dish containing liquid nitrogen (*see* **Note 1**).
2. Wrap the bone sample in foil and hammer until flat, taking care not to pierce the foil, and refreeze in the liquid nitrogen (*see* **Note 2**).
3. Quickly and carefully transfer the frozen bone fragments to the Mikro-Dismembrator vessel.
4. Shake for 2 min at maximum speed.
5. Carefully open the vessel and add 5 mL of TRIZOL® or PIG-B reagent to the bone powder (*see* **Note 3**).
6. Transfer the TRIZOL/bone suspension to microcentrifuge tubes and briefly centrifuge at 12,000g in a centrifuge for 15 min to pellet the insoluble material.

3.2. RNA Extraction

1. Transfer 800 µl of supernatants to individual microcentrifuge tubes each containing 0.25 volumes (200 µL) of chloroform, and shake vigorously for 15 sec.
2. Incubate for 3 min, then centrifuge for 15 min at 10,000g to separate the phases.
3. Transfer the aqueous phase (approx 500 µL) to microcentrifuge tubes containing 0.4 volumes (200 µL) of 95% ethanol and mix by pipetting three to four times.
4. Transfer the contents of the microcentrifuge tubes to spin columns and continue with RNA purification according to the manufacturer's instructions, using 100 µL of nuclease-free water to elute RNA from each spin column.
5. Combine the eluates from each spin column in a single microcentrifuge tube.
6. Add the RNA solution to an NAP-5 column preequilibrated with 10 mL of nuclease-free water. When all solution has entered the gel bed, elute the RNA with 1 mL of nuclease-free water, collecting 100 µL fractions.
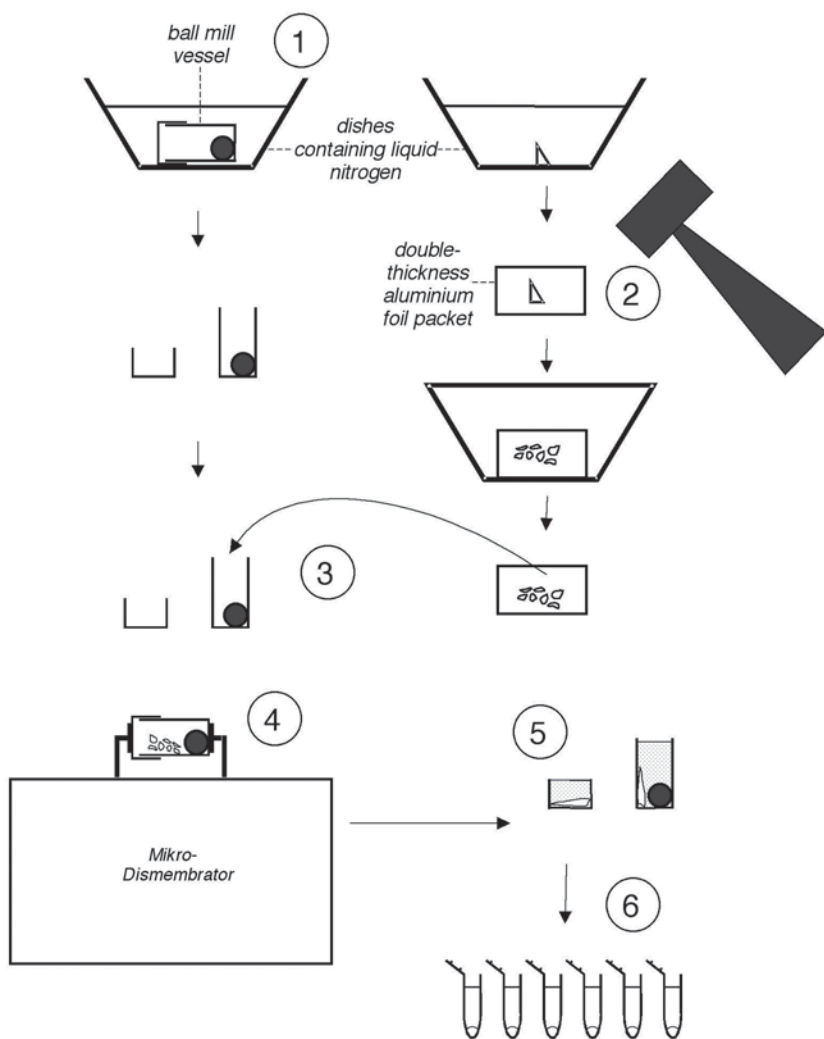
Fig. 3. Overview of RNA extraction from bone.

7. Determine RNA concentration and purity of fractions by measuring absorbance at 260/280 nm (*see* **Note 4**). Integrity of the RNA can also be checked by gel electrophoresis (**Fig. 4**).
8. Combine fractions containing RNA and precipitate using 1/10 volume of 3 *M* sodium acetate solution, pH 4.5, and 2.5 volumes 95% ethanol. Leave on ice for 10 min or at –20°C overnight.
9. Centrifuge at 10,000–12,000*g* for 15 min to pellet RNA.
10. Carefully wash pellet with 75% ethanol and air-dry.
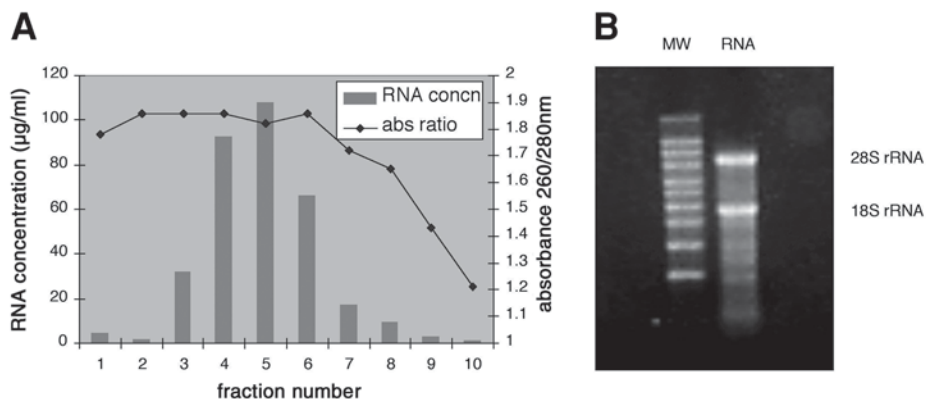11. Resuspend RNA in nuclease-free water and store at –80°C.

Fig. 4. (**A**) Yield and OD$_{260/280}$ ratios of total RNA purified from 500 mg of frozen iliac crest biopsy using the Tripsin method described. The RNA was eluted as 100-μL fractions using 1 mL of nuclease-free water. The integrity of the RNA is apparent on electrophoresis of an aliquot through a 1.2% formaldehyde–agarose gel.

3.3. Primer Selection for Cloning and RT-PCR

1. Fetch the cDNA sequence of interest from the Embl or Genbank data bases.
2. Obtain the corresponding gene sequence and mark the exon–exon boundaries onto a copy of the cDNA sequence.
3. Export the cDNA sequence onto the sequence page in the Primer Express file TaqMan™ probe and primer design.
4. Mark the exon–exon boundaries using the program junction tool.
5. Using the probe tool, select a probe sequence that is centred on an exon–exon boundary and has a T_m of 70°C. Follow the manufacturer's instructions and make sure that the probe has more Cs than Gs and that it does not have a G at the 5' end. The probe can be complementary to either strand of the PCR product.
6. Using the default parameters, allow the program to select suitable amplification primers. Disregard any that have fewer than three A/Ts among the five bases at the 3' end.
7. If a satisfactory result is not obtained in **step 5**, repeat **steps 4** and **5** with a different exon–exon boundary.
8. Design cloning primers that will give a 300–500-basepair PCR product that includes the TaqMan amplicon. A suitable restriction enzyme recognition site can be added to one of the primers to allow insert orientation if a TA cloning vector is used.

3.4. Generating an Internal Control RNA Molecule

1. Generate the template for in vitro transcription of the target RNA by PCR.
2. Clone the product into the pCRII–TOPO vector and check orientation of insert (*see* **Note 5**).

3. Linearize the plasmid.
4. Transcribe using RNA polymerase.
5. Treat the transcription reaction with DNase and remove any free nucleotides on a spin column.
6. Quantify RNA using RiboGreen™ reagent.

3.5. Real-Time Fluorescence-Based Quantitative RT-PCR

1. Create a new file with the desired plate layout and instrument control using the Gene Amp® 5700 Sequence Detection System software. Relative or absolute quantities must be assigned to the standards (*see* **Note 6**).
2. Prepare dilutions of the appropriate in vitro transcribed mRNA in nuclease-free water.
3. Prepare enough diluted TaqMan® One-Step RT-PCR master mix containing probe and primers for the desired number of replicates of both control and sample reactions (*see* **Note 7**).
4. Add control and sample RNA to the diluted master mix and plate out into a 96-well PCR plate according to the chosen layout.
5. Cap the wells of the plate with optical caps, insert the plate into the thermal cycler, and run the assay.
6. When the run is completed, look at the amplification plot showing fluorescence signals against cycle number and set a baseline. Change the *y*-axis to a log scale and choose a threshold value in the middle of the linear range.
7. Edit the standards to include only those dilutions that give a linear standard curve (*see* **Note 8**).
8. Use the program to generate a report of the assay.
9. Assay the same samples for an internal control RNA (*see* **Note 9**).
10. Normalize the amounts of specific mRNA in the samples by dividing by the amounts of internal control RNA.
11. Calculate the standard deviations of the quotients according to the formula

$$CV = \sqrt{CV_1^2 + CV_2^2}$$

where CV = standard deviation (mean value.
12. Express amounts of mRNA in the samples as *x*-fold differences from the amount in the experimental control or calibrator *(3)*.
13. Assess the significance of the differences between sample means using the approximate test for unequal variances based on the *t* distribution *(4)*.

4. Notes

1. Preparation of apparatus: It is important that all the apparatus is wrapped in aluminum foil before use and heated at 180°C for 8 h to sterilize it and to destroy ribonucleases.
2. Size of bone sample: The bone sample should be <500 mg.
3. Pulverizing the tissue: Make sure that the bone is completely powdered—if not, carefully replace the vessel lid, cool the vessel and contents in liquid nitrogen,

remount them on the Mikro-Dismembrator, and shake at maximum speed for 2 min. Note that when the TRIZOL® or PIG-B reagent is added to the vessel, the reagent may freeze. If this happens it should be allowed to thaw at room temperature and then incubated for a further 5 min at room temperature to ensure that nucleoprotein complexes are dissociated.

4. Spectrophotometry of fractions from NAP columns: The ratio of absorbance at 260/280 nm of fractions containing purified RNA should be 1.8–2.0.

5. Cloning products for internal mRNA control: We use the pCRII–TOPO vector, but many alternative cloning vectors and other PCR-based strategies can be used to generate in vitro transcribed mRNA. Orientation of the insert can be checked by DNA sequencing or restriction enzyme analysis.

6. Setting up standard curve on Gene Amp 5700: Quantities must be assigned to the standards so that a standard curve can be generated.

7. Avoiding PCR contamination: Remember to include no-template controls to check for contamination. It is important to avoid contamination in all PCR experiments: we recommend using a laminar flow cabinet for the preparation of the reactions. The number of identical and experimental replicates must be decided according to the expected differences in mRNA levels. Identical replicates will give an idea of the precision of the assay.

8. Screening for PCR inhibitors: Because RNA isolated from bone samples can contain RT-PCR inhibitors, it is important to prepare dilutions of such samples to check for inhibition.

9. Choice of internal control RNA: The internal control is usually a housekeeping gene such as glyceraldehyde-3-phosphate dehydrogenase or β-actin or a ribosomal RNA.

References

1. Reno, C., Marchuk, L., Sciore, P., Frank, C. B., and Hart, D. A. 1997. Rapid isolation of total RNA from small samples of hypocellular, dense connective tissues. *BioTechniques* **22**, 1082–1086.

2. Weber, K., Bolander, M. E., and Sarkar, G. (1998) PIG-B: a homemade monophasic cocktail for the extraction of RNA. *Mol. Biotechnol.* **6**, 73–77.

3. Perkin-Elmer Corporation (1997) User Bulletin No. 2. *ABI PRISM 7700 Sequence Detection System. Relative Quantitation of Gene Expression.*

4. Armitage, P. and Berry, G. (1994) *Statistical Methods in Medical Research.* Blackwell Science, Boston, pp. 111–113.